VOLUME 38 JUNE 1960 NUMBER 6

Canadian Journal of Chemistry

Published by THE NATIONAL RESEARCH COUNCIL

OTTAWA CANADA

Canadian Journal of Chemistry

Under the authority of the Chairman of the Committee of the Privy Council on Scientific and Industrial Research, the National Research Council issues THE CANADIAN JOURNAL OF CHEMISTRY and five other journals devoted to the publication, in English or French, of the results of original scientific research. Matters of general policy concerning these journals are the responsibility of a joint Editorial Board consisting of: members representing the National Research Council of Canada; the Editors of the Journals, and members representing the Royal Society of Canada and four other scientific societies.

The Chemical Institute of Canada has chosen the Canadian Journal of Chemistry as its medium of publication for scientific papers.

Manuscripts for publication should be submitted to Dr. Léo Marion, Editor-in-Chief, Canadian Journal of Chemistry, National Research Council, Ottawa 2, Canada.
(For instructions on preparation of copy, see **Notes to Contributors** (inside back cover).)

Proof, correspondence concerning proof, and orders for reprints should be sent to the Manager, Editorial Office (Research Journals), Division of Administration and Awards, National Research Council, Ottawa 2, Canada.

Subscriptions, renewals, requests for single or back numbers, and all remittances should be sent to Division of Administration and Awards, National Research Council, Ottawa 2, Canada. Remittances should be made payable to the Receiver General of Canada, credit National Research Council.

The journals published, frequency of publication, and subscription prices are:

Canadian Journal of Biochemistry and Physiology	Monthly	$9.00 a year
Canadian Journal of Botany	Bimonthly	$6.00 a year
Canadian Journal of Chemistry	Monthly	$12.00 a year
Canadian Journal of Microbiology	Bimonthly	$6.00 a year
Canadian Journal of Physics	Monthly	$9.00 a year
Canadian Journal of Zoology	Bimonthly	$5.00 a year

The price of regular single numbers of all journals is $2.00.

CORRECTIONS

Volume 37, 1959

Page 2093, line 7. The statement that "unsubstituted $\Delta^{\alpha\beta}$-butenolide (I, R = H) has not been previously synthesized" should be deleted.

Volume 38, 1960

Pages 128, 129. The illustration that appears above the caption for Figure 1 on p. 128 is in fact Figure 2 and should be inserted on p. 129. Likewise the illustration above the caption for Figure 2 on p. 129 is Figure 1 and should appear on p. 128.

Canadian Journal of Chemistry

Issued by THE NATIONAL RESEARCH COUNCIL OF CANADA

VOLUME 38 JUNE 1960 NUMBER 6

SYNTHESIS OF SUGARS FROM SMALLER FRAGMENTS

PART XII. SYNTHESIS OF D-GLYCERO-D-ALTRO-, L-GLYCERO-L-GALACTO-, D-GLYCERO-L-GLUCO-, AND D-GLYCERO-L-GALACTO-OCTULOSE[1]

J. K. N. JONES AND H. H. SEPHTON[2]

ABSTRACT

1,3-Dihydroxy-2-propanone phosphate condenses with D-ribose, L-arabinose, D-lyxose, and D-xylose in the presence of rabbit muscle aldolase to yield octulose phosphates from which the octuloses named in the title were prepared.

Previous publications (1, 2, 3) have demonstrated that 1,3-dihydroxy-2-propanone phosphate (dihydroxyacetone phosphate) will combine with aldehydes, in the presence of the enzyme aldolase, to yield 2-keto-sugars in which the hydroxyl groups on C_3 and C_4 have the D-threo-configuration. Thus, with glycolaldehyde a D-threo-pentulose is produced, L-lactaldehyde yields 6-deoxy-L-sorbose, and D-erythrose gives rise to D-altro-heptulose. It was of interest to see whether aldolase would cause dihydroxyacetone phosphate to condense with pentoses and thus form octuloses. At about the time that we had obtained paper chromatographic evidence that such a reaction was taking place, albeit in very small yield, Dr. N. K. Richtmyer informed us that he and Dr. A. J. Charlson had isolated an octulose from the avocado (4). This octulose was the first found in nature and was shown to have the D-glycero-D-manno-configuration. It has subsequently also been isolated from a species of the *Sedum* plant (5). We have prepared four octuloses by the aldolase-catalyzed condensation of dihydroxyacetone phosphate with D-ribose, L-arabinose, D-lyxose, and D-xylose. The first three products have been shown to be D-glycero-D-altro- (I), L-glycero-L-galacto- (II), and D-glycero-L-gluco-octulose (III) respectively. These octuloses are syrups (glasses) and were characterized as their crystalline 2,5-dichlorophenylhydrazones (from I and II) and as the phenylosazones (from II and III). The fourth product (from D-xylose) appears to be D-glycero-L-galacto-octulose (VI). All these sugars possess the D-threo-configuration of hydroxyl groups on C_3 and C_4. They give a characteristic color reaction on paper chromatograms when sprayed with the orcinol spray reagent for ketoses (6) and heated at 110°, viz. crimson that fades to grey. D-Glycero-L-gluco-octulose has also previously been obtained from the corresponding heptonyl chloride by Wolfrom and Cooper by diazomethane synthesis (7).

The products were identified in the following manner: D-glycero-D-altro-octulose (I) was oxidized with oxygen in alkaline solution (8) and yielded the known crystalline D-glycero-D-altro-heptono-γ-lactone (IV); its configuration was thus proved. L-Glycero-L-galacto-octulose (II) was identified with its known enantiomorph (9) by optical rotation

[1]*Manuscript received January 6, 1960.*
Contribution from the Department of Chemistry, Queen's University, Kingston, Ontario. A summary of this work was given at the Atlantic City Meeting of the American Chemical Society, September, 1959.
[2]*Present address: Laboratory of Chemistry, NIAMD, National Institutes of Health, Bethesda 14, Maryland, U.S.A.*

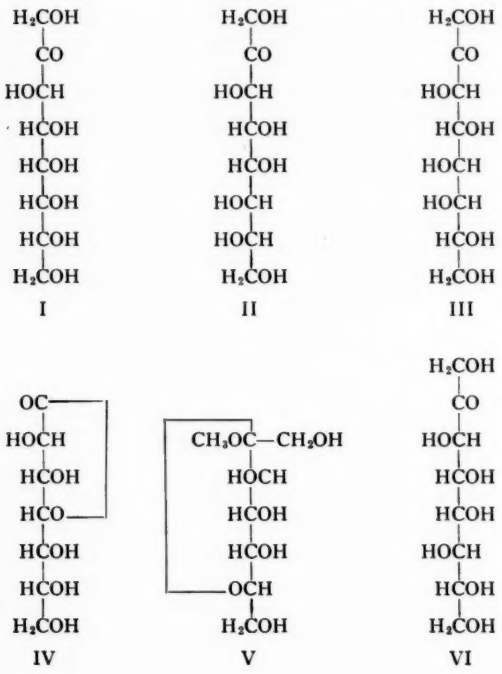

data and by infrared absorption and melting point data on the 2,5-dichlorophenylhydrazone derivatives of the enantiomorphs. The methyl glycoside of the second octulose (II) was oxidized with 1 mole of periodate and the product reduced with sodium borohydride. The resulting heptuloside (V) was hydrolyzed and found to behave like L-galacto-heptulose on a paper chromatogram (orcinol spray test). This observation is in accord with the expected high susceptibility to periodate attack of the C_7—C_8 bond of the octuloside in the pyranose form. The third octulose (III) when heated in aqueous solution with phenylhydrazine acetate yielded D-glycero-L-gluco-octose phenylosazone, which was found to be identical with a phenylosazone prepared from a specimen of the known synthetic D-glycero-L-gluco-octulose (7). The small quantity of the fourth octulose (VI) obtained precluded its positive identification. It was oxidized with oxygen in alkaline medium (8) and the lactone produced was found to behave like D-glycero-L-galacto-heptonic lactone (10) on a paper chromatogram. The methyl glycoside of this octulose (VI) was oxidized with 1 mole of periodate and the product reduced with potassium borohydride and hydrolyzed. The reducing compound thus obtained moved at the same rate as L-galacto-heptulose on a paper chromatogram.

When L-arabinose-1C^{14} was used as a substrate, a radioactive octulose 1-phosphate was produced. This on hydrolysis with acid gave an octulose which was indistinguishable chromatographically from L-glycero-L-galacto-octulose. The radiogram also indicated that a faster-moving material, probably an anhydro octulose (orcinol spray test), had also been formed. A similar product was also readily obtained upon acid hydrolysis of either the 1-phosphate or the methyl glycoside of D-glycero-D-altro-octulose. To avoid as far as possible the formation of anhydro octulose derivatives, phosphate groups were

removed from the octulose phosphate preparations by means of the enzyme phosphatase. All condensations were carried out at pH 6.7 to avoid non-enzymic-type condensation. The aldolase was prepared from rabbit muscle and was twice recrystallized. Two other enzymic syntheses of an octulose have been recorded: an octulose 8-phosphate was prepared from the action of transaldolase on a mixture of D-ribose 5-phosphate and D-fructose 6-phosphate (11), and in a footnote to this publication reference is made to the preparation of an octulose 1,8-diphosphate, which was prepared by Dische from ribose 5-phosphate, dihydroxyacetone phosphate, and muscle aldolase. These products were not characterized and their probable configurations (D-glycero-D-altro-octulose) were not discussed.

The stereospecificity of the aldolase condensation as illustrated above precludes it as the mechanism by which D-glycero-D-manno-octulose (4) is formed in nature unless the latter arises from D-glycero-D-altro-octulose phosphate by the action of an epimerase on C_4.

EXPERIMENTAL

General Methods

Distilled aqueous 1-butanol was used to elute cellulose column chromatograms. Materials to be chromatographed were dissolved in methanol, cellulose powder was added, and the solvent subsequently removed under vacuum from the suspension to precipitate the material onto the cellulose powder. The latter was resuspended in 1-butanol and allowed to settle under gravity in the form of a horizontal band on top of the packed cellulose column before elution was begun. Individual fractions from the columns were examined by paper chromatography using 1-butanol – ethanol – water (3:1:1) by the descending method. Sugars were detected by the silver nitrate spray in acetone followed by the ethanolic sodium hydroxide spray reagent (12) and ketoses by the orcinol and trichloroacetic acid in tertiary butanol spray reagent (6). Octuloses and anhydro octuloses were found to give a characteristic color reaction upon heating at 110° with the latter reagent, viz. a bright crimson which upon further heating fades to a more or less stable grey. Individual fractions were reduced to small volume by evaporation under vacuum in a rotary evaporator with a bath temperature of less than 50°.

Rabbit Muscle Aldolase

One fully grown female rabbit was anesthetized by intravenous injection of Nembutal and most of the blood drained through one of the jugular veins. The carcass was rapidly skinned and the main skeletal muscles cut out. Subsequent operations were carried out at 4° following the procedure described by Taylor (13). The microcrystalline enzyme obtained was kept as a suspension in 50% ammonium sulphate solution (1500 ml) at 4°. Under these conditions no appreciable loss in enzyme activity was observed after 5 months' storage.

Preparation of Substrates

Barium D-fructose 1,6-diphosphate (Nutritional Biochemicals Corp.), a biochemical source of dihydroxyacetone phosphate, was purified by reprecipitation and washing according to the method detailed by Dounce and Beyer (14). Substrates were prepared by stirring the barium salt in a small volume of distilled water to which Amberlite IR-120 resin was added as required to effect solution. Decationization was completed (negative test for barium) by passing the solution through a column of this resin. The pH of the fructose diphosphate solution obtained was adjusted to 6.7 by the addition of 2 *N* sodium hydroxide.

Preparation of D-*Glycero*-D-*altro-octulose* (I)

A substrate (pH 6.6) of disodium fructose diphosphate was prepared from purified barium fructose diphosphate (7 g) and D-ribose (4.5 g) was added. Rabbit muscle aldolase was collected from the ammonium sulphate suspension preparation (200 ml) by filtration and washed through the filter paper into the substrate with distilled water. The pH of the medium (500 ml) was readjusted to 6.7 and toluene (2 drops) was added. The flask was covered with aluminum foil and placed in an incubator at 32° for 4 days, during which time the pH of the medium dropped to 6.4. The enzyme protein was coagulated by heating the reaction mixture to 80° on the boiling-water bath and removed by filtration. Amberlite IR-120 resin was cautiously added to the cooled filtrate to adjust the pH to 4.3 and immediately removed by filtration. Acid phosphatase (Nutritional Biochemicals Corp.) (0.3 g) was added to the filtrate; the flask was covered and left in the incubator at 32° for 2 days. The protein was coagulated by heating the substrate to 80° on the boiling-water bath and the solids were removed by filtration. The cooled filtrate was completely deionized by passage through columns of Amberlite IR-120 and Duolite A-4 resins respectively and evaporated to a syrup (4.37 g). Paper chromatograms indicated the presence of D-ribose (R_f, 0.26), D-fructose (R_f, 0.18), and an octulose (R_f, 0.10) (orcinol spray). The syrup was separated by chromatography on a column of packed cellulose powder (4.5×25 cm) and eluted with aqueous 1-butanol. Three distinct fractions were obtained but the octulose (third) fraction (0.120 g) was slightly contaminated with D-ribose as a result of relative overloading of the column with respect to the latter constituent. The contaminating D-ribose was removed by rechromatographing the octulose fraction on a cellulose column (2.5×25 cm). The product (86 mg) had $[\alpha]_D^{22}$ +7.9° (*c*, 3.3 in methanol). Two additional batches of the octulose were prepared by similar procedures.* One had $[\alpha]_D^{26}$ +8.0° (*c*, 2.5 in methanol) with $[\alpha]_D^{26}$ +2.9° (*c*, 1.4 in water, inaccurate) and the other $[\alpha]_D^{27}$ +8.4° (*c*, 5.5 in methanol) (no mutarotation observed). These products were obtained (in 3.1%, 2.1%, and 1.1% yields respectively, based on fructose diphosphate, FDP) as hygroscopic amorphous solid foams upon removal of solvents under vacuum. When acid hydrolysis (pH 1 at 50° for 6 hours) was employed in another experiment to split the phosphate esters, an octulose, chromatographically identical with the above products, was obtained. In addition, the presence of an anhydro octulose in the acid hydrolyzate was indicated by paper chromatography (R_f, 0.28; orcinol spray reagent). This product was also readily formed upon acid hydrolysis of the pure octulose methyl glycoside.

D-*Glycero*-D-*altro-octulose 2,5-Dichlorophenylhydrazone*

The octulose (0.070 g) was treated with an equal weight of 2,5-dichlorophenylhydrazine in dry methanol (2.5 ml) under reflux for 2 hours. The solvent was removed under vacuum, the solid residue washed with ether by decantation to remove excess reagent, and the product recrystallized from a small volume of methanol, m.p. 169.5–170.5° (decomp.) (Kofler microstage, corrected). $C_{14}H_{20}Cl_2N_2O_7$ requires: C, 42.2; H, 5.0; Cl, 17.8; N, 7.0. Found: C, 42.3; H, 5.2; Cl, 18.0; N, 6.9.

Oxidative Degradation of D-*Glycero*-D-*altro-octulose to* D-*Glycero*-D-*altro-heptono-γ-lactone*

The octulose (0.049 g) was shaken with *N* potassium hydroxide (1.5 ml) in a small flask filled with oxygen and connected to an oxygen burette, at room temperature (28.5°) and atmospheric pressure. The volume of oxygen absorbed was measured after

**The conditions used were not necessarily the optimum conditions nor were the yields obtained necessarily the opitmum yields.*

suitable time intervals (4.0 ml; 4 hours) until it remained constant (7.5 ml; overnight). The alkaline solution was decationized with Amberlite IR-120 resin, filtered, and the volatile acidic products removed by evaporating the aqueous solution to dryness several times. The syrupy product (0.030 g) was examined by paper chromatography. The presence of at least six reducing components was revealed by alkaline silver nitrate spray reagent; the main component (R_f, 0.23) moved with the same speed as authentic D-glycero-D-altro-heptono-γ-lactone (kindly provided by Dr. N. K. Richtmyer). This component was isolated on Whatman No. 3 mm paper and obtained as a clear syrup (0.010 g) which crystallized upon nucleating with authentic D-glycero-D-altro-heptono-γ-lactone. The syrup had $[\alpha]_D^{30}$ +22.2° (*c*, 0.9 in water) (no mutarotation observed). The crystals, washed with methanol, had m.p. 122–123.5°, undepressed by mixing with authentic D-glycero-D-altro-heptono-γ-lactone.

Preparation of L-*Glycero*-L-*galacto-octulose* (II)

A substrate was prepared as described above from purified barium fructose 1,6-diphosphate (16 g) and adjusted to pH 6.7 (450 ml). Muscle aldolase was collected from the enzyme preparation (280 ml) by filtration and washed through the filter into the substrate with distilled water (150 ml). The pH of the preparation was readjusted to 6.7 and L-arabinose (12 g) added, followed by toluene (2 drops). The preparation was incubated at 32° for 4 days. The protein in the solution (pH 6.4) was coagulated by heating it to 80° on a boiling-water bath and the precipitate removed by filtration. The filtrate was adjusted to pH 4.3 by careful addition of Amberlite IR-120 resin and filtration. Acid phosphatase (1.0 g) was added to the filtrate and the solution was left in the incubator (32°) for 2 days. The enzyme was denatured by heating the solution to 75° on the boiling-water bath and removed by filtration. The filtrate was deionized by passage through columns of Amberlite IR-120 and Duolite A-4 and concentrated to a syrup. The octulose (0.318 g) was obtained from the syrup after chromatographing twice on cellulose columns as described for the previous octulose preparation (yield: 5.1% based on FDP). The product was obtained as a clear amorphous hygroscopic glassy foam after removal of all solvents under vacuum; $[\alpha]_D^{25}$ −62° (*c*, 0.105 in water) (no mutarotation observed). A second reducing product was eluted from the cellulose column following closely on the octulose. This material did not give the typical octulose color reaction. It was rechromatographed and a homogeneous product (0.085 g) obtained having $[\alpha]_D^{25}$ −20° (*c*, 0.8 in methanol). This material was not investigated.

L-*Glycero*-L-*galacto-octulose Phenylosazone*

The octulose (0.0095 g) was heated in a 10-ml test tube with water (0.5 ml), phenylhydrazine (0.05 ml, redistilled), and acetic acid (0.05 ml) for 7 minutes in a steam bath. The osazone started to crystallize at this stage and the solution was allowed to cool slowly to room temperature. The crystalline phenylosazone was collected by filtration on a small Büchner funnel, washed with water and methanol, and dried in vacuum over P_2O_5. The product (0.005 g) had m.p. 202–206° (decomp.). $C_{20}H_{26}N_4O_6$ requires: N, 13.4. Found: N, 13.0.

L-*Glycero*-L-*galacto-octulose 2,5-Dichlorophenylhydrazone*

The octulose (0.040 g) was heated with an equal weight of 2,5-dichlorophenylhydrazine in methanol (3 ml) under reflux for 2 hours. The solvent was removed under vacuum and the solid residue washed with ether by decantation. The residue was recrystallized from a small volume of methanol. Thrice-recrystallized material (12 mg) had m.p.

194–195° (decomp. corrected). $C_{14}H_{20}Cl_2N_2O_7$ requires: C, 42.2; H, 5.0; Cl, 17.8; N, 7.0. Found: C, 41.9; H, 5.3; Cl, 16.5; N, 6.8. The 2,5-dichlorophenylhydrazone prepared as above from D-glycero-D-galacto-octulose (0.018 g) (kindly provided by Professor M. L. Wolfrom) had m.p. 196–197° (decomp. corrected). $C_{14}H_{20}Cl_2N_2O_7$ requires: C, 42.2; H, 5.0; Cl, 17.8; N, 7.0. Found: C, 42.5; H, 5.3; Cl, 16.5; N, 6.6. The mixed melting points of these two substances lay between those of the individual constituents. The infrared spectra of these materials (0.8% in KBr) were recorded and were found to have closely corresponding absorption peaks throughout.

Periodate Oxidation of Methyl L-*Glycero*-L-*galacto-octuloside*

The octulose (0.004 g) was treated with 2% methanolic hydrogen chloride (3 ml) under reflux for 3 hours. The solution was neutralized to pH 7.8 (dilute sodium hydroxide) and the methanol removed under vacuum. The remaining aqueous solution (10 ml) was filtered and a 25% aliquot (2.5 ml) used for the oxidation. Sodium metaperiodate (0.46 ml 0.01 *N*) (1 mole) was added and the solution left at room temperature (27°) for 12 minutes. Excess sodium borohydride was added and the solution was left at room temperature for 3 hours. The solution was rendered acidic by the addition of Amberlite IR-120 resin and filtered. The methyl glycosides were hydrolyzed by heating the solution on the boiling-water bath for 1 hour. The solution was evaporated to dryness under vacuum and this was repeated several times after addition of methanol (5 ml) to remove methyl borate. The residue was taken up in water and deionized on Duolite A-4 resin. The neutral solution was evaporated to a syrup and chromatographed on Whatman No. 1 filter paper. The orcinol – trichloroacetic acid spray reagent indicated the presence of a heptulose (intense blue spot) which had an R_f value similar to that of L-galacto-heptulose.

Preparation of D-*Glycero*-L-*gluco-octulose* (III)

The substrate was prepared as detailed above using barium fructose 1,6-diphosphate (12 g) and D-lyxose (10 g) in water (500 ml) at pH 6.7 with muscle aldolase from the above enzyme preparation (190 ml). The mixture was incubated at 32° for 5 days and worked up as in the previous case, using acid phosphatase (0.3 g) to hydrolyze the phosphate esters. After removal of the protein the deionized solution was evaporated to a syrup, dissolved in methanol (10 ml), and nucleated with D-lyxose. Crystalline D-lyxose (7 g) was removed by filtration and the octulose isolated from the mother liquors by chromatography on a cellulose column. The product (0.186 g) was obtained as a hygroscopic solid glassy foam (yield 4.0% based on FDP); $[\alpha]_D^{27}$ −46.9° (*c*, 2.73 in water) (no mutarotation observed).

The phenylosazone, prepared from the octulose (0.0098 g) as described above, had m.p. 199–202° (decomp. corrected). A similar osazone, prepared from D-glycero-L-gluco-octulose obtained from Professor Wolfrom (7) had m.p. 199–204° (decomp.). The mixed melting point of these two derivatives was 199–202° (decomp.). The infrared spectra of these two osazones were obtained (0.6% in KBr) and were found to be closely similar.

Preparation of D-*Glycero*-L-*galacto-octulose* (VI)

The substrate was prepared as previously described using disodium fructose 1,6-diphosphate (0.4 g) and D-xylose (1 g) in water (50 ml) at pH 6.7 and muscle aldolase from the enzyme preparation (20 ml) was added. After incubation at 32° for 108 hours the enzyme was precipitated by heating the solution on the water bath to 80° and was removed by filtration. The filtrate was rendered acidic (pH 1–2) by decationizing with

Amberlite IR-120 and warmed overnight at 55° to hydrolyze the phosphate esters. The cooled solution was deacidified (Duolite A-4) and evaporated to a syrup. The octulose (0.006 g) was isolated from the syrup by chromatography on thick filter paper and by exhaustively extracting the appropriate area with methanol; $[\alpha]_D^{28}$ −43.4° → −13.4° (3 hours, *c*, 0.6 in water).

Degradation of D-*Glycero*-L-*galacto-octulose*

Spengler–Pfannenstiel Oxidation

The octulose (3 mg) was oxidized overnight in *N* potassium hydroxide (0.5 ml) under an oxygen atmosphere as described previously. The solution was diluted with water and decationized on Amberlite IR-120 resin. The effluent was repeatedly concentrated to a syrup after addition of water (3 ml) to remove the volatile acids. The residue was examined on paper chromatograms sprayed with the silver oxide (12) and with the lactone spray reagents (15). Both results indicated that the lactone produced was chromatographically indistinguishable from authentic D-glycero-L-galacto-heptonic lactone (10) provided by Dr. N. K. Richtmyer.

Periodate Oxidation

The octulose (1.5 mg) was treated under reflux with methanolic hydrogen chloride for 4 hours. The solution was neutralized to pH 7.8 with 0.1 *N* aqueous sodium hydroxide and the methanol removed under vacuum. Sodium metaperiodate (1.3 mg) was added and the solution left at room temperature for 12 minutes. Excess potassium borohydride was now added and the solution left at room temperature for 6 hours. The solution was rendered acidic by decationizing (IR-120 resin) and the methyl esters hydrolyzed by heating under reflux for 1 hour. The solution was evaporated several times with methanol (5 ml) to remove methyl borate. The residue was deionized and examined by paper chromatography. Three components were indicated; the main component moved at the same rate as authentic L-galacto-heptulose (silver oxide spray reagent).

Preparation of Isotopically Labelled L-*Glycero*-L-*galacto-octulose*

The substrate was prepared as previously described using barium fructose 1,6-diphosphate (0.6 g) and L-arabinose (0.14 g) to which was added L-arabinose-1C^{14} (1.42 mg containing 5 μc activity) in water (50 ml) at pH 6.7. Muscle aldolase from the preparation (20 ml) was added and the solution incubated at 32° for 108 hours. The enzyme was precipitated by warming the solution to 80° and removed by filtration. The cooled solution was decationized with Amberlite IR-120 resin and the acidic solution (pH 1–2) warmed overnight at 55° to hydrolyze phosphate esters. The cooled solution was deacidified (Duolite A-4) and evaporated to a syrup. The syrup was dissolved in methanol (5 ml) and nucleated with L-arabinose. The crystalline L-arabinose was removed by filtration and the mother liquors concentrated to a syrup and chromatographed on thick filter paper. A radiogram was obtained (14 days exposure) on X-ray film showing the presence of radioactive octulose and anhydro octulose (by crimson color reactions with orcinol spray reagent on the paper chromatogram).

ACKNOWLEDGMENTS

The authors thank the National Research Council of Canada for financial assistance. This work was carried out during the tenure of a Postdoctoral Fellowship (awarded to H. H. S.).

REFERENCES

1. L. HOUGH and J. K. N. JONES. J. Chem. Soc. 4047 (1952).
2. L. HOUGH and J. K. N. JONES. J. Chem. Soc. 4052 (1952).
3. L. HOUGH and J. K. N. JONES. J. Chem. Soc. 342 (1953).
4. A. J. CHARLSON and N. K. RICHTMYER. J. Am. Chem. Soc. **81**, 1512 (1959).
5. A. J. CHARLSON and N. K. RICHTMYER. J. Am. Chem. Soc. In press.
6. R. KLEVSTRAND and A. NORDAL. Acta Chem. Scand. **4**, 1320 (1950).
7. M. L. WOLFROM and P. W. COOPER. J. Am. Chem. Soc. **71**, 2668 (1949).
8. O. SPENGLER and A. PFANNENSTIEL. Z. Wirtschaftsgruppe Zuckerind. **85**, Tech. Tl. 547 (1935).
9. M. L. WOLFROM and P. W. COOPER. J. Am. Chem. Soc. **72**, 1345 (1950).
10. A. T. MERRILL, W. T. HASKINS, R. M. HANN, and C. S. HUDSON. J. Am. Chem. Soc. **69**, 70 (1947).
11. E. RACKER and E. SCHROEDER. Arch. Biochem. Biophys. **66**, 241 (1957).
12. W. E. TREVELYAN, D. P. PROCTOR, and J. S. HARRISON. Nature, **166**, 444 (1950).
13. J. F. TAYLOR. Biochem. Preparations, **5**, 12 (1957).
14. A. L. DOUNCE and G. T. BEYER. J. Biol. Chem. **173**, 159 (1948).
15. M. ABDEL-AKHER and F. SMITH. J. Am. Chem. Soc. **73**, 5859 (1951).

ARYLPYRIDINES

PART I. ORIENTATION IN THE REACTION OF PHENYLLITHIUM WITH SOME 3-SUBSTITUTED PYRIDINES[1]

R. A. Abramovitch, Giam Choo Seng, and A. D. Notation

ABSTRACT

The orientation of the entering phenyl substituent in the addition of phenyllithium to 3-picoline and nicotine has been studied. In the first case the main product was 3-methyl-2-phenylpyridine together with a small amount of 5-methyl-2-phenylpyridine, the ratio of the isomers being 19:1. The structure of the isomers was established by oxidation to the corresponding phenylnicotinic acids, by infrared and n.m.r. spectroscopy. Quantitative analysis of the crude mixture of isomers was effected by vapor phase chromatography. Phenylation of nicotine gave 2-phenyl- and 6-phenyl-nicotine in the ratio of 1:1. Separation of the isomers was effected by preparative vapor phase chromatography and their orientation established as above. Evidence that the 3-substituent exerts an appreciable steric effect in the end product of the addition is presented. The results are taken to mean that addition of phenyllithium, and probably of other nucleophilic reagents, to 3-substituted pyridines occurs preferentially at the 2-position but the 3-substituent, if sufficiently bulky, may exert a steric effect resulting in appreciable addition at the 6-position also.

The reaction of lithium alkyls and aryls with dry pyridine is well known (1, 2). An intermediate (I) is probably first formed and this on heating loses lithium hydride to give the 2-substituted pyridine.

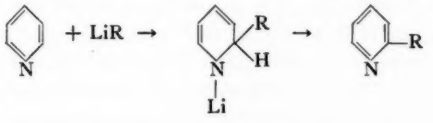

I

The formation of a 4-substituted pyridine has not been reported in such reactions. It is clear, therefore, that the addition of 1 mole of phenyllithium to a 2- or a 4-substituted pyridine can only lead to the formation of one compound. On the other hand, addition to a 3-substituted pyridine may lead to one, or a mixture, of two isomers. Very little is known about the directive effect of such a 3-substituent upon the entering phenyl group.

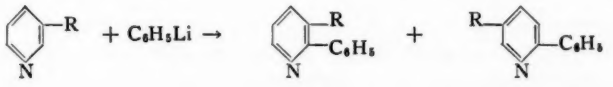

II III IV

Miller, Osuch, Goldberg, and Levine (3) claimed that the reaction of 3-picoline (II, R = CH_3) with phenyllithium gave 5-methyl-2-phenylpyridine (IV, R = CH_3) exclusively. Similarly, Wiley, Jarboe, Callahan, and Nielsen (4) reported that the reaction of 3-phenylpyridine (II, R = C_6H_5) with phenyllithium gave 2,5-diphenylpyridine (IV, R = C_6H_5) as the only isomer isolated. On the other hand, the reaction of 3-substituted pyridines with other nucleophilic reagents has yielded different results. Plazek, Marcinikow, and Stammer (5), for example, established the preferential formation of 2-amino-3-methylpyridine in the reaction of 3-picoline with sodamide while Seide reported the

[1]*Manuscript received January 14, 1960.*
Contribution from the Department of Chemistry, University of Saskatchewan, Saskatoon, Saskatchewan.

Can. J. Chem. Vol. 38 (1960)

exclusive formation of this isomer when potassium amide was used (6). Hardegger and Nikles studied the amination of 3-*n*-butylpyridine (II, R = *n*-Bu) with sodamide; the product, obtained in 50% yield, was a mixture containing 80% of the 2,3-isomer and 20% of the 2,5-isomer (7). Similarly, Leonard and Ryder found that the reaction of butyllithium with 3-picoline produced predominantly 2-butyl-3-methylpyridine (8).

The various observations recorded above appear to be contradictory. It was therefore of interest to establish conclusively the orientation in the addition of phenyllithium to 3-substituted pyridines and to this end it was proposed to study in the first instance the reaction with 3-picoline. This reaction was carried out in the usual way, the addition of the picoline to phenyllithium being carried out in ether solution and the temperature eventually raised to ca. 110° by the replacement of the ether by toluene. The product (42.4% yield) consisted mainly of a mixture of the two phenylated 3-picolines. Preliminary attempts at separating the mixture by vapor phase chromatography were unsuccessful. The isomers were eventually separated by fractional distillation using a spinning band column, and were obtained in the ratio of 8:1 by weight. The major product was characterized as 3-methyl-2-phenylpyridine (III, R = CH_3) as follows:

(i) Oxidation with neutral aqueous potassium permanganate gave 2-phenylpyridine-3-carboxylic acid (III, R = CO_2H), m.p. 167–169°. Ishiguro, Morita, and Ikushima (9) report m.p. 168–169° for this acid whereas Benary and Psille (10) give m.p. 229° for 2-phenylpyridine-5-carboxylic acid. The acid (III, R = CO_2H) was converted into its acid chloride which was then treated with aluminum chloride in benzene, when it failed to undergo the expected intramolecular acylation but gave instead a product $C_{18}H_{13}ON$ exhibiting a strong band at 1663 cm^{-1} characteristic of an aromatic ketone and two strong bands at 742 and 690 cm^{-1} characteristic of a monosubstituted phenyl group, thus showing the product to be 3-benzoyl-2-phenylpyridine (V). The intramolecular acylation was achieved by carrying out the reaction in light petroleum as the solvent instead of benzene. 4-Azafluorenone (VI), m.p. 139.5–141.5°, was thus obtained, identical with the

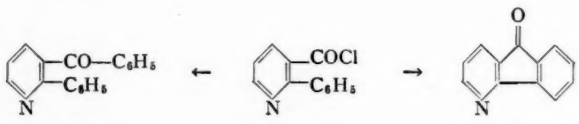

V VI

product described by Skraup and Cobenzl (11) (infrared bands at 1725 and 745 cm^{-1}).

(ii) The n.m.r. spectrum was measured through the courtesy of Mr. LeRoy Johnson of Varian Associates, who interpreted the following data as being only compatible with the 2,3-isomer, and not with a 2,5-disubstituted pyridine. This is in agreement with the findings of Schneider, Bernstein, and Pople (11*a*) for pyridine, and of Bernstein and Schneider (11*b*) and Anet and Eves (11*c*) for substituted pyridines. The signal at 506 c.p.s. is due to the α-proton which must be adjacent to a β-proton as indicated by the magnitude of the ortho-coupling constant $J_{5,6} = 5$ c.p.s. (for pyridine $J_{2,3} = 5.5$ and $J_{2,4} = 1.9$ c.p.s. (11*a*)). This supports the 2,3- and not the 2,5-orientation for this disubstituted pyridine.

(iii) The infrared spectrum of the major product exhibited a band at 1579 cm^{-1} characteristic of a 2,3-disubstituted pyridine derivative (12). No band was observed above this one in the 6 μ region. The minor product had a band at 1604 cm^{-1} characteristic of 2,5-disubstituted pyridines (12).

TABLE I

N.m.r. spectrum of 3-methyl-2-phenylpyridine in carbon tetrachloride solution with tetramethylsilane as an internal reference standard

Ring position	C.p.s. from $SiMe_4$ (approximately)	Spin–spin coupling observed
4	438–447	$J_{4,5}$ = ca. 7 c.p.s.; $J_{4,6}$ = 1 c.p.s.
5	416–431	$J_{4,5}$ = 7 c.p.s.; $J_{5,6}$ = 5 c.p.s.
6	495–513	$J_{5,6}$ = 5 c.p.s.; $J_{4,6}$ = 1 c.p.s.

NOTE: Frequency 60 Mc/sec.

(iv) While this work was in progress Ishiguro, Morita, and Ikushima reported an unambiguous synthesis of 3-methyl-2-phenylpyridine involving the condensation of allyl alcohol and 1-phenyl-1-propanone with ammonia over a high-temperature catalytic bed (9). Dr. Ishiguro kindly supplied us with an authentic sample of this base and of its picrate. Comparison of the infrared absorption spectra of the bases and their picrates as well as a mixed melting point of the picrates established the identity of the major product obtained from the phenyllithium reaction with 3-methyl-2-phenylpyridine.

The minor fraction from the distillation proved to be somewhat impure 5-methyl-2-phenylpyridine (IV, R = CH_3). This was shown by oxidation of the base with neutral permanganate to 2-phenylpyridine-5-carboxylic acid, m.p. 232° (molecular formula $C_{12}H_9O_2N$), and by its infrared spectrum, which exhibited a band at 1600 cm^{-1} characteristic of 2,5-disubstituted pyridines (12).

It was subsequently found that the mixture of phenylpicolines could be resolved quite easily by vapor phase chromatography using an Apiezon "N" column, the retention time of the 2,5-isomer being appreciably greater than that of the 2,3-isomer under the conditions used. This permitted a much more accurate quantitative measurement of the isomer ratio, the determination being carried out on the crude mixture of bases. In this way it was found that the ratio 2,3/2,5 was 95:5, and not 8:1 as previously estimated by fractional distillation.

In view of this result the procedure described by Miller *et al.* (3) for the obtention of 5-methyl-2-phenylpyridine was reinvestigated. This method involved adding 3-picoline to an ethereal solution of phenyllithium, the total addition time being 10 minutes; the ether solution was then boiled under reflux (temperature below 50°) for ½ hour and the mixture was then hydrolyzed with water. None of the phenylpicolines were obtained under these conditions; instead, an oil, b.p. 120–215°/0.32 mm, was obtained whose infrared spectrum did not show any bands characteristic of a pyridine ring in the 800 cm^{-1} region. The conditions of the reaction appear to be too mild to lead to the elimination of lithium hydride. After hydrolysis the dihydro derivative may have been obtained, which might account for the absence of the characteristic pyridine bands in the infrared. It may be possible to oxidize this to the required phenylpyridine but this was not investigated.

In one of the runs during the preparation of the phenylpicolines a small amount of high boiling material was obtained. This appeared to be a mixture since several peaks appeared in a gas chromatographic analysis using a silicone-on-celite column at 220°. A pure picrate, m.p. 204–206°, could be obtained from this material and the analytical figures for this derivative fitted those of a dipicrate of a base $C_{12}H_{12}N_2$, which corresponds to the molecular formula of a dimethyldipyridyl. There was insufficient material for a molecular weight determination so that as a working hypothesis the by-product was assumed to be

a dipicolyl. Stoehr and Wagner (13) obtained 3,3′-dimethyl-4,4′-dipyridyl by the action of metallic sodium on 3-picoline, and a product presumed to be 6,6′-di-*tert*-butyl-2,2′-dipyridyl has been obtained by the action of methyllithium on 2-*tert*-butylpyridine (14).

The picrate of the base obtained above depressed the melting point of 3,3′-dimethyl-4,4′-dipyridyl picrate (m.p. 231°) prepared from 3-picoline and sodium (13). 3,3′-Dimethyl-2,2′-dipyridyl was prepared from 2-amino-3-picoline via 2-bromo-3-picoline using Case's procedure (15) but again its dipicrate, m.p. 191–192°, proved different from that of the unknown base. A similar method was used to synthesize 5,5′-dimethyl-2,2′-dipyridyl from 2-amino-5-methylpyridine. This base formed a monopicrate, m.p. 175.5–176.5°, which was clearly different from that of the unknown base. No further work was done at this stage to attempt to identify this compound.

In view of the results of Wiley *et al.* (4) the possible steric effect of the 3-substituent upon the orientation of the entering phenyl group was investigated. Nicotine (VII) was chosen because of its ready availability and the fact that the 2-*N*-methylpyrrolidyl group is appreciably larger than the methyl group. The reaction was carried out as for 3-picoline

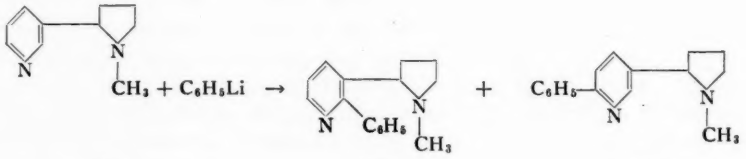

VII VIII IX

to give a 34% yield of product, b.p. 120–200°/0.1 mm. This was shown by vapor phase chromatography on a silicone-on-firebrick (1:4) column to be a mixture of two compounds, assumed to be 2-phenylnicotine (VIII) and 6-phenylnicotine (IX) in the ratio of 1:1 by weight. These findings are qualitatively similar to those of Tschitschibabin and Kirssanow (16), who obtained a mixture of 2- and 6-substituted nicotines on treatment of nicotine with sodamide in xylene at 140°. The isomers were then separated by preparative vapor phase chromatography using a 1/2-in. preparative column packed with silicone-on-celite to give one base, b.p. 145°/0.75 mm, and the other with a longer retention time, b.p. 165°/0.6 mm. Each of these gave analytical results compatible with the molecular formula $C_{16}H_{18}N_2$, confirming the assumption that they were the isomeric phenylnicotines.

The base eluted first had a band at 1588 cm^{-1} in the infrared and was, therefore, tentatively assigned the 2,3-orientation (12) whereas the second one had a band at 1600 cm^{-1} and was assumed to be the 2,5-isomer (IX). This latter assignment (and therefore the former as well) could be confirmed by oxidation of the more slowly eluted base with potassium permanganate to give 2-phenylpyridine-5-carboxylic acid identical with that obtained from 5-methyl-2-phenylpyridine.

Further confirmatory evidence for the structures assigned to these isomers was obtained from their n.m.r. spectra which were measured by Varian Associates through the courtesy of Mr. L. Johnson. Mr. Johnson also kindly interpreted the spectra and his report reads as follows: "The NMR spectrum for the first sample fits the structure of 2-phenylnicotine. The signal from the proton on the carbon in ring position 6 appears 506 c.p.s. from the tetramethylsilane and shows five cycle ortho coupling to the proton on C5 and two cycle meta coupling to the proton on C4. Likewise the signal around 478 from the proton on C4

exhibits an eight cycle coupling to the proton on C5 and again a two cycle coupling to the proton on C6. Finally, the proton on C5 at 432 shows the five and eight cycle coupling to the other two protons on this ring. The benzene ring protons are all very nearly equivalent and produce a single sharp line at 440.

The NMR spectrum of the second sample is quite different in that the protons on the benzene ring are separated into two groups; one from two of the protons in the benzene ring at 478, the other group from the three remaining protons centered around 440. This case is similar to that of acetophenone . . . . The proton α- to the nitrogen produces a signal at 506 and in this case is a close-spaced triplet due to spin coupling to the protons at C4 and C5. Coincidentally the signals from the protons on C4 and C5 appear at exactly the same field position, 460 c.p.s from tetramethylsilane, and show the spin coupling to the C2 proton of about 1.5 c.p.s. In an attempt to shift the C4 and C5 proton signals we dissolved the sample in dioxane; however, this unfortunately did not shift these signals relative to each other . . . . This is convincing evidence for assigning the 6-phenylnicotine structure to the second sample." Once again the signal at 506 c.p.s. in the case of the first compound is at the expected field position for an α-proton and consists essentially of a quartet as required for ortho- and meta-coupling. The $J_{5,6}$ and $J_{4,6}$ values are of the correct order of magnitude confirming the assignment of the 2,3-disubstituted orientation for this compound. In the case of the second sample the magnitude of the spin–spin coupling constants for the α-proton at 506 c.p.s. is small as would be expected for meta- and para-coupling (11*a*), but not for ortho-coupling.

The isomer ratio in the phenylation of nicotine as compared with 3-picoline clearly shows the presence of a steric effect of the 3-substituent upon the orientation of the product obtained. This effect is being studied in greater detail and the results obtained on changing the size of the 3-substituent systematically will be reported soon. It was of interest, however, to try and see whether even a small group such as methyl did exert any appreciable steric interference. To this end the ultraviolet absorption spectra of 2-phenylpyridine, 3-methyl-2-phenylpyridine, 5-methyl-2-phenylpyridine, 2-phenylnicotine, and 6-phenylnicotine in ethanol were compared. The results are shown in Fig. 1 where it can be seen that the spectra of 2-phenylpyridine, 5-methyl-2-phenylpyridine, and 6-phenylnicotine are very similar and only show slight intensity variations. On the other hand, the spectra of 3-methyl-2-phenylpyridine and 2-phenylnicotine formed a separate group. The maxima exhibited a hypsochromic shift and a decrease in intensity compared with the first three curves. This indicated that in these latter two compounds the 3-substituent was exerting an appreciable steric effect resulting in the non-coplanarity of the two rings. It should be pointed out, however, that such a steric effect as is evidenced here was observed in the *final product*; this does not necessarily mean that the same effect is in operation *in the transition state* also, though there can be little reason to doubt that such an effect, though smaller, would also be exerted in this instance. No such steric effect should be present in the phenylation at the 6-position so that the latter mode of reaction would be the more probable one if steric considerations were the sole factors involved.

The above results seem to indicate that in spite of a moderate steric effect nucleophilic addition takes place preferentially at the 2-position though the 3-substituent, if sufficiently bulky, may direct appreciable addition to the 6-position also. The exclusive formation of 2,5-diphenylpyridine (4) might be attributed to steric inhibition of coplanarity in the transition state (e.g. X) in the formation of the 2,3-isomer, whereas no such inhibition exists in the transition state for the 2,5-isomer (e.g. XI). Other factors may

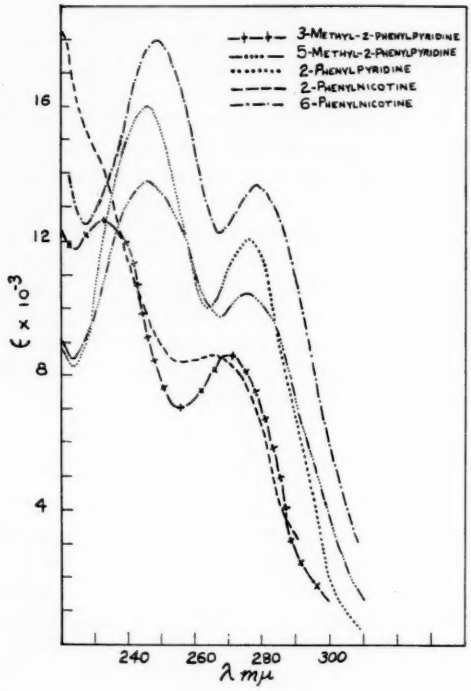

FIG. 1.

very well be involved also. Similar results concerning the preferential formation of the 2,3-isomer have been obtained by Professor H. C. Brown from a study of the addition of methyllithium to 3-substituted pyridines (14).

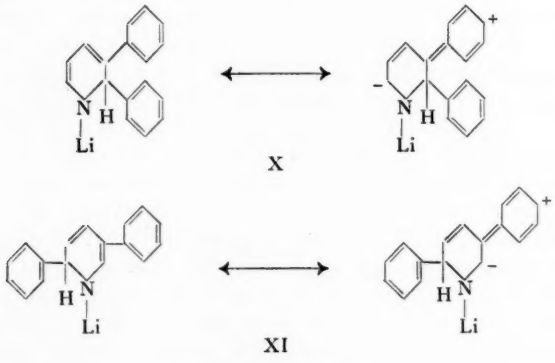

EXPERIMENTAL

Melting points are uncorrected. Infrared spectra were measured using a Perkin–Elmer Model 21 instrument using sodium chloride optics. Ultraviolet absorption spectra were

measured on a Beckman DK-2 recording spectrophotometer. The vapor phase chromatographic work was carried out using a Beckman GC-2 unit with helium as the carrier gas.

Reaction of Phenyllithium with 3-Picoline

(i) Phenyllithium was prepared from lithium (14 g) and bromobenzene (156 g) in anhydrous ether under dry nitrogen. 3-Picoline (110 ml) in anhydrous ether (110 ml) was added dropwise with stirring at such a rate as to maintain gentle boiling under reflux. When the addition was complete the ether was distilled off and simultaneously replaced by dry toluene (210 ml) in order that the temperature of the solution might be raised to ca. 110°. The reaction mixture was stirred under dry nitrogen and boiled under reflux for 7½ hours. Water was then cautiously added to the cooled solution with stirring, the toluene layer separated, and the aqueous layer ether extracted repeatedly. The combined ether and toluene layers were dried (KOH pellets), filtered, and distilled up to 130° at atmospheric pressure. The residue was distilled under vacuum using a Podbielniak Mini-Cal spinning band fractional distillation column (Series 3400). Fractions, b.p. 107–119°/0.3 mm, consisted of slightly impure 3-methyl-2-phenylpyridine; those boiling at 119–133°/0.3 mm consisted of impure 5-methyl-2-phenylpyridine. The over-all yield based on bromobenzene was 42.4%. The isomers were obtained in the ratio of 8:1 by weight respectively. After three fractional distillations pure 3-methyl-2-phenylpyridine had b.p. 159–160°/31 mm. Calc. for $C_{12}H_{11}N$: C, 85.17; H, 6.55. Found: C, 84.94; H, 6.99. I.R. spectrum (liquid film) (main peaks only): 1589 (s), 1573 (s), 800 (s), 788 (s), 750 (s), 703 cm^{-1} (s). λ_{max} 232, 272 mμ, $\epsilon \times 10^{-3}$ 12.56, 8.67 (in ethanol). The picrate, on recrystallization from ethanol, had m.p. 164–166°, undepressed on admixture with an authentic sample. Ishiguro, Morita, and Ikushima (9) report m.p. 163.5–165.5° for this picrate. Calc. for $C_{12}H_{11}N,C_6H_3O_7N_3$: C, 54.27; H, 3.54. Found: C, 54.62; H, 3.49.

Several fractional distillations of 5-methyl-2-phenylpyridine, b.p. 164–166°/16 mm, failed to give a completely pure analytical sample. Vapor phase chromatography indicated the presence of some contaminant. A pure sample was obtained by vapor phase chromatography using the conditions described below and the eluted fraction collected in a dry ice – acetone trap. One further distillation under vacuum gave the required pure isomer. Found: C, 84.65; H, 6.49. I.R. spectrum (liquid film) (main peaks only): 1604 (m), 1566 (m), 835 (m), 775 (s), 736 (s), 693 cm^{-1} (s). λ_{max} 245, 275 mμ. $\epsilon \times 10^{-3}$ 13.8, 10.59 (in ethanol). After several recrystallizations from ethanol the picrate had m.p. 182–183°. Found: C, 54.10; H, 3.76.

In a previous run, a fraction, b.p. 155–180°/9 mm, was forced over. Gas chromatographic analysis of a sample of this material on a 2-ft silicone-on-celite (1:4) column with an inlet pressure of helium of 30 p.s.i. and operated at 220° gave rise to several poorly resolved peaks, indicating that this fraction was a mixture of compounds. A picrate could be prepared which, on recrystallization from ethanol, had m.p. 204–206° (decomp.). Calc. for $C_{12}H_{12}N_2,2C_6H_3O_7N_3$: C, 44.87; H, 2.82. Found: C, 44.68; H, 2.91. On subsequent similar reactions this product could not be isolated again.

Quantitative Analysis.—This was effected by vapor phase chromatography using the following conditions: 5½ ft × ¼ in. copper tubing column packed with Apiezon "N" on "Embacel" Kieselguhr (May and Baker) (1:4 by weight); column temperature 220°; inlet temperature 235°; helium inlet pressure 30 p.s.i. Under these conditions the retention time was found to vary with the sample volume; the 'emergence time' (i.e. the time at which the compound began to emerge from the column, or the foot of the peak) was constant, however, and independent of sample size. The 'emergence time' for 3-methyl-2-

phenylpyridine was 11 minutes whereas that of 5-methyl-2-phenylpyridine was 16 minutes 20 seconds. In both cases the area under the curve was proportional to the sample size. For the analysis the reaction was carried out as described above but the combined ether and toluene layers were extracted with dilute hydrochloric acid (leaving any diphenyl behind in the organic phase). The acid extract was shaken several times with small quantities of ether, made strongly alkaline, and extracted continuously with ether. The ether extract of the bases was dried (KOH pellets), the solvent evaporated, and the residue used directly for the quantitative estimation. The ratio of 2,3/2,5 isomers was thus found to be 95:5 or 19:1.

(ii) The reaction was repeated using the procedure of Miller, Asuch, Goldberg, and Levine (3). To a solution of phenyllithium (from 2.8 g of lithium and 21 ml of bromobenzene) in dry ether (250 ml) was added 3-picoline (18.6 ml) with stirring under nitrogen over 10 minutes. The mixture was then boiled under reflux for 30 minutes, water (75 ml) added carefully, and the mixture then poured onto ice (500 g) and 6 *N* hydrochloric acid (100 ml). The ether layer was separated and extracted several times with 6 *N* hydrochloric acid. The combined acid extracts were treated with 20% aqueous sodium hydroxide until the mixture was only slightly acid. Solid sodium carbonate was then added to make the mixture slightly basic. The suspension was repeatedly extracted with ether leaving behind a copious amount of light orange resinous material. The combined ether extracts were dried ($MgSO_4$), filtered, and evaporated on a water bath. The residue was distilled under vacuum giving a fraction with a boiling point up to 190°/0.32 mm (2.5 g) and then one having a boiling point 190–215°/0.32 mm (1.5 g). A pure picrate could not be isolated from any of the fractions. I.R. spectrum of the second fraction (liquid film) (main peaks only): 2870 (s) (broad), 1600 (w), 1577 (w), 1560 (w), 865 (m), 745 (s) (broad), 698 cm^{-1} (s). Miller *et al.* (3) reported a yield of 30.8% of a product, b.p. 241–245°/2 mm, to which they assigned the structure of 5-methyl-2-phenylpyridine.

2-Phenylpyridine-3-carboxylic Acid

3-Methyl-2-phenylpyridine (6 g) was boiled under reflux with a solution of potassium permanganate (11.2 g) in water (400 ml) until the solution was decolorized; more solid potassium permanganate was then added in small portions and heating continued, the process being repeated until no more oily material appeared in the reflux condenser. The excess permanganate was destroyed by adding a few drops of methanol and heating, the hot mixture was filtered, the solid residue washed three times with hot water, and the combined filtrates evaporated down to ca. 40 ml. The solution was made just acid by adding a slight excess of acetic acid, and a saturated solution of copper acetate (70 ml) was stirred into the mixture, which was warmed for a few minutes and then allowed to stand while precipitation of the copper salt occurred. This was filtered, washed with cold water, slurried in water, and decomposed with hydrogen sulphide. The mixture was boiled to remove the excess hydrogen sulphide, filtered hot, the black sulphide precipitate washed with hot water, and the combined filtrates evaporated to give 2-phenylpyridine-3-carboxylic acid (2.85 g), m.p. 167–169°. Ishiguro, Morita, and Ikushima (9) report m.p. 168–169° for this acid.

2-Phenylpyridine-5-carboxylic Acid

5-Methyl-2-phenylpyridine was oxidized as described above for the 3-isomer to give the carboxylic acid, which, after recrystallization from aqueous ethanol, had m.p. 232°. Benary and Psille (10) report a melting point of 229° for this acid. Calc. for $C_{12}H_9O_2N$:

C, 72.51; H, 4.44. Found: C, 72.55; H, 4.55. I.R. spectrum (Nujol mull) (main peaks only): 1678 (s) (broad), 1602 (s), 749 (s), 720 (w), 678 cm^{-1} (m).

2-Phenylpyridine

This compound was prepared according to the procedure of Evans and Allen (2). It had λ_{max} 223, 245, 275 mμ. $\epsilon \times 10^{-3}$ 8.27, 16.08, 12.12 (in ethanol).

3,3'-Dimethyl-2,2'-dipyridyl

This was prepared from 2-bromo-3-methylpyridine by Case's method (15). The dipicrate (from ethanol) had m.p. 191–192.5°, depressed on admixture with the unknown dipyridyl dipicrate. Case reports a melting point of 188–189° for this dipicrate.

5,5'-Dimethyl-2,2'-dipyridyl

2-Bromo-5-methylpyridine (2 g) and copper powder (3.2 g) were mixed and heated to 220°; the temperature was gradually increased to 240° over a period of ¾ hour. When the mixture had cooled it was extracted with dilute hydrochloric acid, the combined extracts basified, extracted with ether, and the ether extracts dried (Na_2SO_4). Evaporation of the solvent gave 5,5'-dimethyl-2,2'-dipyridyl which was converted directly to the picrate. A monopicrate was formed which, on recrystallization from ethanol, had m.p. 175.5–176.5°. Calc. for $C_{12}H_{12}N_2,C_6H_3O_7N_3$: C, 52.30; H, 3.66. Found: C, 52.10; H, 3.66.

3,3'-Dimethyl-4,4'-dipyridyl

This compound was obtained in 20% yield from 3-picoline and sodium according to the procedure of Stoehr and Wagner (13). The base, b.p. 300°/720 mm, gave a picrate, m.p. 231°, depressed to 190° (decomp.) on admixture with the unidentified picrate. Stoehr and Wagner report a boiling point of 300° for the free base and melting point of 231° for its picrate. I.R. spectrum of the free base (liquid film) (main peaks only): 1587 (s), 853 (w), 806 (m), 800 (w), 710 cm^{-1} (m).

3-Benzoyl-2-phenylpyridine

2-Phenylpyridine-3-carboxylic acid (1 g) was allowed to stand with thionyl chloride (10 ml) at room temperature for 1½ hours. The excess thionyl chloride was removed under vacuum and the residue treated with dry benzene. The benzene was evaporated to dryness and the process repeated. The residue was taken up in anhydrous benzene (30 ml) and stirred while anhydrous aluminum chloride (2 g) was slowly added. A dark-colored complex formed which, after ¾ hour, turned a dark greenish-grey. The complex was decomposed with ice, the mixture basified with aqueous sodium hydroxide, the benzene layer separated, and the aqueous layer extracted with ether. The extracts (which exhibited a slight green fluorescence) were combined, dried (Na_2SO_4), and evaporated. Distillation of the residue (1.03 g) gave 3-benzoyl-2-phenylpyridine, b.p. 167°/0.45 mm. Calc. for $C_{18}H_{13}ON$: C, 83.37; H, 5.05. Found: C, 82.26; H, 5.20. I.R. spectrum (liquid film) (main peaks only): 1663 (s), 1598 (w), 1579 (m), 1556 (w), 923 (s), 790 (w), 742 (s), 690 cm^{-1} (s). In view of the poor value for the carbon analysis the compound was further characterized as its picrate which, after recrystallization from alcohol, had m.p. 137.5–138.5° (after sintering at 135.5°). Calc. for $C_{18}H_{13}ON,C_6H_3O_7N_3$: C, 59.02; H, 3.30. Found: C, 58.98; H, 3.26.

4-Azafluorenone

2-Phenylpyridine-3-carboxylic acid (0.1 g) was allowed to stand with an excess of thionyl chloride (2 ml) and worked up as described above. The acid chloride was stirred in dry light petroleum (b.p. 40–60°) (20 ml) and an excess of anhydrous aluminum

chloride (0.5 g) slowly added. Stirring was continued for 2 hours when a red complex had formed on the sides of the flask. Ice was added to decompose the complex, the mixture was made alkaline with aqueous sodium hydroxide, the petroleum ether layer separated, and the aqueous layer extracted with ether. The combined extracts were dried (Na_2SO_4) and evaporated to yield a solid residue which, on recrystallization from ethanol, gave 4-azafluorenone (0.086 g), m.p. 139.5–141.5°. Skraup and Cobenzl (11) reported m.p. 141° for this compound. Calc. for $C_{12}H_7ON$: C, 79.55; H, 3.98. Found: C, 79.58; H, 3.91. I.R. spectrum (Nujol mull) (main peaks only): 1725 (s) (broad), 1615 (w), 1600 (m), 1569 (w), 918 (m), 742 cm^{-1} (s).

Reaction of Phenyllithium with Nicotine

Nicotine (12 g) in anhydrous ether (30 ml) was added dropwise to a solution of phenyllithium (prepared from lithium (1.0 g) and bromobenzene (12 ml) in dry ether (130 ml) under nitrogen) at such a rate as to maintain gentle boiling of the ether. The ether was then evaporated and simultaneously replaced by dry toluene (50 ml) and the temperature raised to ca. 110°. Stirring and heating under nitrogen was then continued for 8 hours. The reaction mixture was cooled, carefully treated with water, and the toluene layer separated. The aqueous layer was extracted with ether and the organic phases combined and extracted with 10% hydrochloric acid. The aqueous acid extracts were made alkaline and extracted with ether, the ether extracts combined, dried (KOH pellets), and evaporated. Vacuum distillation of the residue gave the following fractions:

(i) up to 120°/0.09 mm	1.1 g pale yellow liquid;
(ii) 120–200°/0.09 mm	5.5 g deep yellow liquid;
(iii) 200°/0.15 mm–326°/0.67 mm	4.3 g deep red resin.

Fraction (ii) was found to consist of a mixture of 2- and 6-phenylnicotine (48% yield).

The ratio of the two isomers was found to be close to 1:1. The analysis was performed by vapor phase chromatography of the crude reaction product before distillation. A 1 ft × ¼ in. copper tubing column packed with silicone-on-firebrick (1:4) was used. The samples were run in ether solution. At 220° and with a helium inlet pressure of 30 p.s.i. the retention time for 2-phenylnicotine was 6¾ minutes and that for 6-phenylnicotine was 12⅔ minutes, whereas at 190° these were 16⅓ minutes and 38 minutes respectively. The areas under the peaks were found to be proportional to the concentration of each isomer. The results were as follows:

2-phenylnicotine	49.4%	6-phenylnicotine	50.6%
	49.8%		50.2%

Separation of the two isomers was effected by preparative vapor phase chromatography using an injection cell preheater and a fraction collector. Fraction (ii) from the distillation was used. The column was a 2-ft preparative column (½-in. diameter) packed with Embacel (May and Baker, 60–100 mesh) and silicone oil (4:1), and was operated at 190° with a helium inlet pressure of 30 p.s.i. The first fraction collected proved to be 2-phenylnicotine which, after redistillation, had b.p. 145°/0.5 mm. Calc. for $C_{16}H_{18}N_2$: C, 80.63; H, 7.61. Found: C, 80.05; H, 7.67. I.R. spectrum (liquid film) (main peaks only): 1578, 1569, 805, 791, 750, and 696 cm^{-1}. λ_{max} 264 mμ; λ_{infl} 225, 255 mμ. $\epsilon \times 10^{-3}$ 8.57, 15.76, 8.45. 2-Phenylnicotine dipicrate was recrystallized from alcohol and had m.p. 211–213°. Calc. for $C_{16}H_{18}N_2,2C_6H_3O_7N_3$: C, 48.28; H, 3.74. Found: C, 48.62; H, 3.98. The second fraction proved to be 6-phenylnicotine, which was redistilled and had a boiling point of 165°/0.6 mm. Found: C, 80.33; H, 7.20. I.R. spectrum (liquid film) (main

peaks only): 1600, 1567, 841, 779, 740, 691 cm^{-1}. λ_{max} 249, 279 mμ. $\epsilon \times 10^{-3}$ 17.97, 13.66. The picrate had m.p. 166–167°.

Oxidation of 6-Phenylnicotine to 2-Phenylpyridine-5-carboxylic Acid

6-Phenylnicotine (0.2 g) was boiled under reflux in water (50 ml) while small amounts of potassium permanganate were added as long as the solution was decolorized and oily material appeared in the reflux condenser. The mixture was then decolorized by the addition of a few drops of methanol to the hot solution and the carboxylic acid isolated as described for 2-phenylpyridine-3-carboxylic acid. The crude 2-phenylpyridine-5-carboxylic acid (20 mg) was recrystallized from water to give colorless crystals, m.p. 230–233° (decomp.), undepressed on admixture with an authentic sample.

ACKNOWLEDGMENTS

The authors are grateful to Dr. L. Vining for the use of a recording ultraviolet spectrophotometer and to Mr. LeRoy Johnson of the Applications Laboratory of Varian Associates for kindly determining and interpreting the n.m.r. spectra reported in this paper. They would also like to thank Dr. Ishiguro for a sample of 3-methyl-2-phenylpyridine and its picrate, Dr. H. C. Brown for communicating to us some of his results before publication, and the University of Saskatchewan for the award of the Thorvaldson Scholarship to one of us (A. D. N.). This work was supported by a grant from the National Research Council.

REFERENCES

1. K. Ziegler and H. Zeiser. Ber. **63**, 1847 (1930).
2. J. C. W. Evans and C. F. H. Allen. Org. Syntheses, Collective Vol. II, 517 (1943).
3. A. D. Miller, C. Osuch, N. N. Goldberg, and R. Levine. J. Am. Chem. Soc. **78**, 674 (1956).
4. R. H. Wiley, C. H. Jarboe, P. X. Callahan, and N. J. Nielsen. J. Org. Chem. **23**, 780 (1958).
5. E. Plazek, A. Marcinikow, and Ch. Stammer. Roczniki Chem. **15**, 505 (1935); Chem. Abstr. **30**, 1377 (1936).
6. O. Seide. Ber. **57**, 1802 (1924).
7. E. Hardegger and E. Nikles. Helv. Chim. Acta, **39**, 505 (1956).
8. N. J. Leonard and B. L. Ryder. J. Org. Chem. **18**, 598 (1953).
9. T. Ishiguro, Y. Morita, and K. Ikushima. Yakugaku Zasshi, **78**, 220 (1958); Chem. Abstr. **52**, 11846g (1958).
10. E. Benary and H. Psille. Ber. **57**, 828 (1924).
11. Z. Skraup and A. Cobenzl. Monatsh. **4**, 436 (1883).
11. (*a*) W. G. Schneider, H. J. Bernstein, and J. A. Pople. Ann. N.Y. Acad. Sci. **70**, 806 (1958).
11. (*b*) H. J. Bernstein and W. G. Schneider. J. Chem. Phys. **24**, 499 (1956); H. J. Bernstein, J. A. Pople, and W. G. Schneider. Can. J. Chem. **35**, 65 (1957).
11. (*c*) F. A. L. Anet and C. R. Eves. Can. J. Chem. **36**, 902 (1958).
12. R. A. Abramovitch, Giam Choo Seng, and A. D. Notation. Can. J. Chem. **38**, 624 (1960).
13. C. Stoehr and M. Wagner. J. prakt. Chem. **48**, 1 (1893).
14. H. C. Brown. Personal communication.
15. F. H. Case. J. Am. Chem. Soc. **78**, 2574 (1946).
16. A. E. Tschitschibabin and A. W. Kirssanow. Ber. **57**, 1163 (1924).

THE INFRARED SPECTRA OF SOME URANYL COMPOUNDS[1]

G. L. CALDOW,[2] A. B. VAN CLEAVE, AND R. L. EAGER

ABSTRACT

The infrared spectra for the di- and hexa-hydrates of uranyl nitrate, for anhydrous uranyl acetate, and for sodium zinc uranyl acetate hexahydrate have been obtained using the potassium bromide pressed disk technique. Where possible, samples were prepared by freeze-drying aqueous solutions of the appropriate compound and potassium bromide. The uranyl nitrate hydrates gave spectra with peaks characteristic of both nitrate and nitrato groups. For uranyl acetate the type of spectra obtained depended upon the ratio of uranyl acetate to potassium bromide in the freeze-dried mixture. It is postulated that, for relatively large ratios of uranyl acetate to potassium bromide, the carbonyl oxygen atoms of the acetate groups are chelated to the uranium atom. The spectrum of sodium zinc uranyl acetate hexahydrate is quite similar to that reported by Jones for sodium uranyl acetate. Using the 933 cm^{-1} peak, the Beer–Lambert law was obeyed for samples prepared by freeze-drying solutions containing uranyl nitrate and potassium bromide.

INTRODUCTION

The authors have been interested in the infrared spectra of uranyl compounds and in the possible application to a quantitative determination of uranium by infrared spectrophotometry. Various investigations have been made of the infrared spectra of uranium compounds (1, 2, 3, 4, 5, 6, 7). The repeated occurrence in the infrared spectra of uranyl compounds of a strong absorption band at 10.87 μ (920 cm^{-1}) led to the suggestion by Lecompte and Freymann (2) that this band could be used for the identification of uranyl ions. For water-soluble substances the potassium bromide disk technique (8, 9), combined with the freeze-drying of aqueous solutions containing both the substance whose spectrum is being investigated and potassium bromide, gives good quantitative results (10).

EXPERIMENTAL

Apparatus and Reagents

The spectra were recorded with a Perkin–Elmer model 21 double-beam infrared spectrophotometer equipped with a sodium chloride prism.

The sample chamber of the freeze-drying apparatus was a 250-mm vacuum desiccator from which the ground-glass sleeve had been removed. The desiccator was connected to a 1-liter trap by means of a 55/40 standard taper ground-glass joint and 40-mm I.D. glass tubing. A length of rubber tubing and a 18/7 ball and socket joint were used to connect the trap to a high vacuum system. A freezing mixture of dry ice – acetone was used to cool the trap.

The die used to prepare the potassium bromide disks was of the type described by Bauer, Epp, and Lemieux (11). The disk holder is removable and fits into an adapter which can be inserted into the standard sample slide on the spectrophotometer. A 20-ton hydraulic press was used to apply pressure to the die.

Reagent grade chemicals were used. Sodium zinc uranyl acetate was prepared from zinc uranyl acetate and sodium chloride solutions using the method of Barber and Kolthoff (12).

Sample Preparation

The freeze-dried mixtures were prepared by mixing together, in Erlenmeyer flasks,

[1]*Manuscript received January 7, 1960.*
Contribution from the Department of Chemistry, University of Saskatchewan, Saskatoon, Saskatchewan, with financial assistance from the National Research Council of Canada. Presented in part at the 40th Annual Conference of the Chemical Institute of Canada, Vancouver, B.C., June 3–5, 1957.
[2]*Present address: Oxford University, Oxford, England.*

appropriate quantities of aqueous solutions of the substance whose spectrum was being determined and potassium bromide. The mixtures were frozen rapidly by immersing the Erlenmeyer flasks in a dry ice – acetone mixture and swirling their contents. The Erlenmeyer flasks of a given run were left in the dry ice – acetone mixture until all the samples were prepared, after which they were placed in the sample chamber of the freeze-drying apparatus. The apparatus was immediately evacuated, and the samples left for approximately 24 hours. The product was a very fine fluffy powder (10).

Some of the uranyl salt – potassium bromide mixtures were prepared by mixing the dry solids in a small plastic vial attached to a vibrating tool. Freeze-dried potassium bromide was used in all of these preparations in order to ensure small particle size (10). Freeze-dried uranyl salts were used except in the case of uranyl nitrate hexahydrate, which was ground in a mortar until the crystals would pass through a 200-mesh screen.

Approximately 0.5 g of the uranyl salt – potassium bromide mixture was placed in the partly assembled die, care being taken to distribute the sample evenly in the disk holder. The powder was tamped down using the flattened end of a glass rod. The assembled die was then placed in the hydraulic press and evacuated, by means of a mechanical oil vacuum pump, for 1 minute. While still evacuated the die was subjected to a pressure of 99,000 pounds per square inch for 1 minute. After the pressure had been released, air was allowed to leak slowly into the die. The resulting transparent window was cleaned of loose powder.

Recording the Spectra

For a qualitative survey of the infrared spectra of uranyl compounds the spectrophotometer was operated essentially as recommended by the manufacturer using slit schedule 4 (13). It was found that the noise level was lowered if a gain of 5.5 was used, instead of the recommended 6.5–7, and if zero suppression was used, instead of the recommended 2. For quantitative work the recommended slit schedule 2 was used. It was found that better results were obtained in the quantitative work when a potassium bromide blank was used in the reference beam. However, a blank was not necessary in order to obtain good qualitative spectra.

RESULTS AND DISCUSSION

Preparation of Lower Hydrates of Uranyl Compounds by Freeze-Drying

Uranyl nitrate hexahydrate and uranyl acetate dihydrate were used to prepare the mixtures for freeze-drying. Since other hydrates of these salts can exist, it was of interest to determine the degree of hydration of the products when aqueous solutions of either uranyl nitrate or of uranyl acetate were freeze-dried. The freeze-dried samples were analyzed for their uranium content by the method of Kolthoff and Lingane (14). The results shown in Table I indicate the formation of anhydrous uranyl acetate and of

TABLE I

Analysis of freeze-dried uranyl compounds

Sample	Uranium, %	Deviation from theoretical value
Freeze-dried uranyl acetate	61.26	0.07
Theoretical for $UO_2(C_2H_3O_2)_2$	61.33	
Freeze-dried uranyl nitrate	55.14	0.21
	55.28*	0.07
Theoretical for $UO_2(NO_3)_2 \cdot 2H_2O$	55.35	

*The trap was cooled with liquid nitrogen in this experiment.

uranyl nitrate dihydrate. It was assumed in the subsequent work that the same compounds would be formed whether or not potassium bromide was present during the freeze-drying process. The fact that uranyl nitrate dihydrate was formed, and not the monohydrate or the anhydrous salt, is interesting since all of the many attempts to prepare these salts have been unsuccessful (15, 16).

The results indicate that the freeze-drying technique may be a convenient and relatively simple method for preparing the lower hydrates for substances which form more than one hydrate. The method eliminates the use of elevated temperatures which have been used in the preparation of many hydrates, and which often results in undesired decomposition reactions.

It should be noted that the product obtained from freeze-drying a solution of uranyl nitrate and potassium bromide will not necessarily be only a mixture of these two compounds. It is quite possible that uranyl bromide and potassium nitrate will also be present, perhaps even in relatively large quantities, since bromide ions and potassium ions were originally present in large excess. However, when a solution prepared by dissolving uranyl acetate and potassium bromide in water is freeze-dried, it is likely that the product will be largely uranyl acetate and potassium bromide. This follows from the fact that there is good evidence (17, 18, 19) that in aqueous solution, the tendency for covalent bond formation between acetate and uranyl ions is large.

Spectra

In general, all the spectra could be interpreted as consisting of the spectra of the anion present and of the uranyl ion. The spectra of all samples show strong absorption in the 930 cm^{-1} region, which has been assigned to the antisymmetrical normal vibration, ν_3, of the uranyl ion (1). In a few of the samples of uranyl nitrate dihydrate, prepared by freeze-drying an aqueous solution of uranyl nitrate and potassium bromide, there is a definite, but quite weak, absorption at 856 cm^{-1}. This absorption at 856 cm^{-1} could be the 860 cm^{-1} band, which has been assigned to the symmetrical normal vibration, ν_1, of the uranyl ion (1) and which, for the free gaseous ion, would be infrared inactive.

(*a*) *Uranyl Nitrate Hydrates*

The spectra of uranyl nitrate hexahydrate mixed with potassium bromide by the vibration technique, of freeze-dried uranyl nitrate dihyrate mixed with potassium bromide by the vibration technique, and of uranyl nitrate dihydrate mixed with potassium bromide by the freeze-drying technique are shown in Figs. 1, 2, and 3 respectively. The frequencies of the observed maxima are given in Table II. The close similarity of the spectra of the dihydrate and of the hexahydrate is contrary to the results of Sevchenko and Stepanov (3), of Tridot (6), and of Gatehouse and Comyns (7). The above authors used the solid hydrate samples, which were either pressed between fluorite plates (3), suspended in carbon tetrachloride (6), or mulled with Nujol (7). These authors found, for example, that a peak at 1390 cm^{-1} was present in the spectra of the hexahydrate but was not in the spectra of the dihydrate, whereas peaks present in the 1300 cm^{-1} and 1550 cm^{-1} regions of the spectra of the dihydrate were not present in the spectra of the hexahydrate. In contrast, all three peaks were observed in the spectra of both the hexahydrate and the dihydrate in the present work. Gatehouse and Comyns (7) have made the most detailed assignment of the bands in the infrared spectrum of the uranyl nitrate hydrates by the use of compounds enriched in N^{15}. They reached the conclusion that co-ordinated nitrato groups are present in the dihydrate (and also in the trihydrate), whereas ionic nitrate

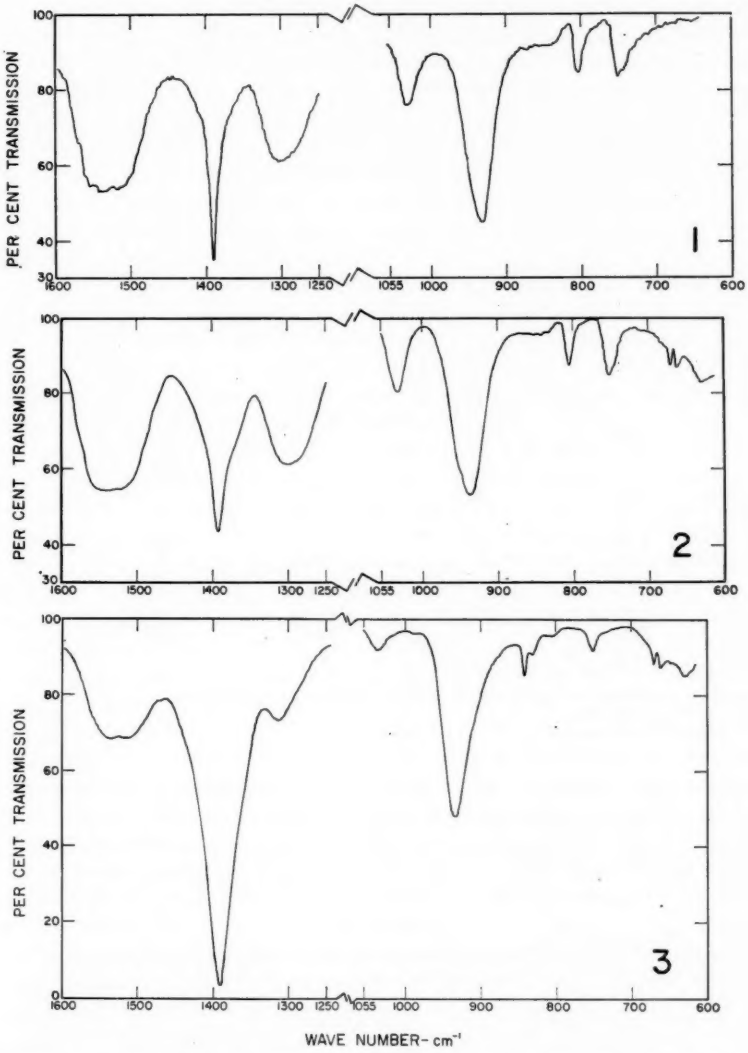

FIG. 1. Infrared spectrum of uranyl nitrate hexahydrate mixed with potassium bromide by vibration.
FIG. 2. Infrared spectrum of uranyl nitrate dihydrate mixed with potassium bromide by vibration.
FIG. 3. Infrared spectrum of uranyl nitrate dihydrate mixed with potassium bromide by freeze-drying.

groups are present in the hexahydrate. Their results for the dihydrate and for the hexahydrate, both containing natural nitrogen, are also given in Table II. The symbols of the nitrate vibrations are designated by an asterisk in Table II.

The symmetry of the nitrate ion is D_{3h} whereas that for the co-ordinated nitrato group is C_{2v}, hence for the nitrato group the doubly degenerate vibrations, ν_3 and ν_4, of the

TABLE II

Infrared spectra of uranyl nitrate hydrates (frequencies in cm^{-1})

Assignments	Dihydrate			Hexahydrate	
	Vib. mixed with KBr	Freeze-dried with KBr	Gatehouse and Comyns (7)	Vib. mixed with KBr	Gatehouse and Comyns (7)
ν_5[a]	662 670	662 670	706		
ν_3[a]	745 (vw, sh) 752	752	743 748 (sh)		
ν_4*				745 (vw, sh) 752	748
ν_2*				804	803 835
ν_6	805	805 (vw)	801		
ν_2* (KNO_3)		830 842	811[b] 826		
ν_3 (UO_2^{++})	937	933	951	933	941
ν_1*				1032	1030
ν_2	1032	1035	1026 1044		
ν_1	1298 (bd)	1312	1280 1311	1300	
ν_3*	1392	1392		1392	1366
ν_4	1520 1535	1515 1537	1515 1547	1515 1531	
Unassigned	630	630			

[a]The assignment of the lower frequency to ν_5 and of the higher frequency to ν_3 is arbitrary (7).
[b]These results are from Decius (22).
*Denotes vibrations of the nitrate ion.

nitrate ion are both split (20). The conventions for numbering the vibrations of the nitrate ion (21) differ from those used for the co-ordinated nitrato group (20). To avoid confusion in the following discussion a summary of the relations between these two conventions is given in Table III (7). It was observed by Gatehouse and Comyns (7) that

TABLE III

Summary of designation of vibrations for the nitrate ion and the nitrato group (7)

	ν_1	ν_2	ν_3		ν_4	
NO_3^-	NO stretch	Out of plane	NO_2 stretch		NO_2 bend	
	ν_2	ν_6	ν_1	ν_4	ν_3	ν_5
O_2NO	NO stretch	Out of plane	NO_2 stretch sym	NO_2 stretch antisym	NO_2 bend sym	NO_2 bend antisym

some of the vibrations for both the nitrate and the nitrato group were split. It was concluded that this splitting was the result of the in-phase and the out-of-phase vibrations of adjacent nitrate, or nitrato, groups having slightly different frequencies.

Considering first the spectra of the dihydrates, it is seen from Figs. 2 and 3 and Table II that the spectra obtained in the present work are similar in most respects to the spectra obtained by Gatehouse and Comyns. Hence it appears that nitrato groups, co-ordinated to the uranyl ion, are present in these samples. However, the intense peak at 1392 cm^{-1} is

undoubtedly due to the normal vibration ν_3 of the nitrate ion, which was not observed by Gatehouse and Comyns for the dihydrate. For the sample prepared by freeze-drying an aqueous solution of uranyl nitrate and potassium bromide this peak is extremely intense, as shown in Fig. 3. It seems likely, as suggested earlier, that in the freeze-drying step, some potassium nitrate was formed. By comparing Figs. 2 and 3 it is seen that the intensities of the peaks assigned to the nitrato group are weaker in Fig. 3 than in Fig. 2, indicating that in the sample prepared entirely by freeze-drying, an appreciable amount of the original nitrate appeared as such in the final product. The presence of nitrate in the sample mixed by vibration, Fig. 2, can be explained by the observation (20) that some compounds with co-ordinated nitrato groups react with sodium chloride windows and that the products give the spectrum of the nitrate ion. Possibly a similiar reaction could occur with potassium bromide. The presence of potassium nitrate in the sample mixed with potassium bromide by freeze-drying would also explain a feature of the spectrum of this sample which differs from that for the sample mixed with potassium bromide by vibration. In the spectrum, Fig. 2, of the latter sample there is a peak at 805 cm^{-1} which has been assigned by Gatehouse and Comyns (7) to the out-of-plane vibration of the nitrato group. This peak is only faintly evident in the spectrum, Fig. 3, of the sample mixed with potassium bromide by freeze-drying. There is, however, in the spectrum of the latter a weak peak at 830 cm^{-1} and a relatively stronger one at 842 cm^{-1}. Decius (22) observed that in potassium nitrate, the out-of-plane vibration of the nitrate ion, ν_2, is split to give a weak peak at 811 cm^{-1} and a strong one at 826 cm^{-1}. The splitting observed by him is 15 cm^{-1} while that shown in Fig. 3 is 12 cm^{-1}.

The remainder of the spectrum for both dihydrate samples is quite similar to that observed by Gatehouse and Comyns (7) except for the splitting of some of the peaks. A splitting of 8 cm^{-1} was observed in the present work for ν_5 whereas Gatehouse and Comyns (7) observed only a single peak. A splitting of 5 cm^{-1} (708 and 713 cm^{-1}) was observed by Dieke and Duncan (23) for a sample of $CsUO_2(NO_3)_3$. No shoulder is evident on the low frequency side of the 752 cm^{-1} peak for the freeze-dried sample, indicating that the frequency ν_3 was not split. However, the intensity of this peak is low and it would be difficult to observe a shoulder. Neither ν_2 nor ν_1 shows splitting in the present work, although in the sample mixed by vibration the 1298 cm^{-1} peak is broad and some splitting may be present. Gatehouse and Comyns (7) observed a splitting for both of these vibrations. No assignment is offered for the weak 630 cm^{-1} peak observed in the spectra of both of the dihydrate samples.

The spectrum of the hexahydrate, Fig. 1, shows more resemblance to those of the dihydrates, Figs. 2 and 3, than it does to the one obtained by Gatehouse and Comyns for the hexahydrate (7). It is particularly similar to the spectrum obtained for the dihydrate sample mixed with potassium bromide by vibration, Fig. 2. The only difference is in the 600 to 700 cm^{-1} region. In this region the hexahydrate has negligible absorption whereas the dihydrate has moderate absorption with peaks at 662, 670, and 630 cm^{-1}. The spectrum does have the strong peak at 1392 cm^{-1}, characteristic of nitrates, but it also has strong peaks in the 1300 and 1500 cm^{-1} regions which were not observed for the hexahydrate by Gatehouse and Comyns (7). The presence of these latter peaks suggests that the symmetry of the nitrate ion has been lowered from that of D_{3h} and consequently the ν_3 vibration of the nitrate ion has been split.

Why the symmetry of the nitrate ion should change is not immediately obvious. It is conceivable that a deformation of the crystal structure occurred as a result of subjecting the sample to the high pressures used in forming the disk. This deformation might cause

a lowering of the symmetry of the nitrate ion. Another possibility is that at the high pressures used, and in the presence of a large excess of potassium bromide, the hexahydrate was partially dehydrated. With the loss of water molecules the uranyl ion would then perhaps react with nitrate ions to form co-ordinated nitrato groups.

(*b*) *Uranyl Acetate*

In earlier work (1, 2, 3) the samples used appear to have been hydrates of uranyl acetate, although this is not always definitely stated. In the present work freeze-dried uranyl acetate was used, hence, as indicated by the results shown in Table I, the samples contained anhydrous uranyl acetate. Preliminary experiments, using samples obtained by freeze-drying aqueous solutions of uranyl acetate and potassium bromide, indicated that the type of spectra obtained depended upon the ratio of uranyl acetate to potassium bromide. To investigate this effect further a series of solutions containing uranyl acetate and potassium bromide in varying porportions were freeze-dried. The freeze-dried mixtures were next mixed by vibration with additional freeze-dried potassium bromide to give sufficient material for pressing into disks. There was always approximately the same amount of uranyl ion present in each disk. In Figs. 4 and 5 are shown portions of the

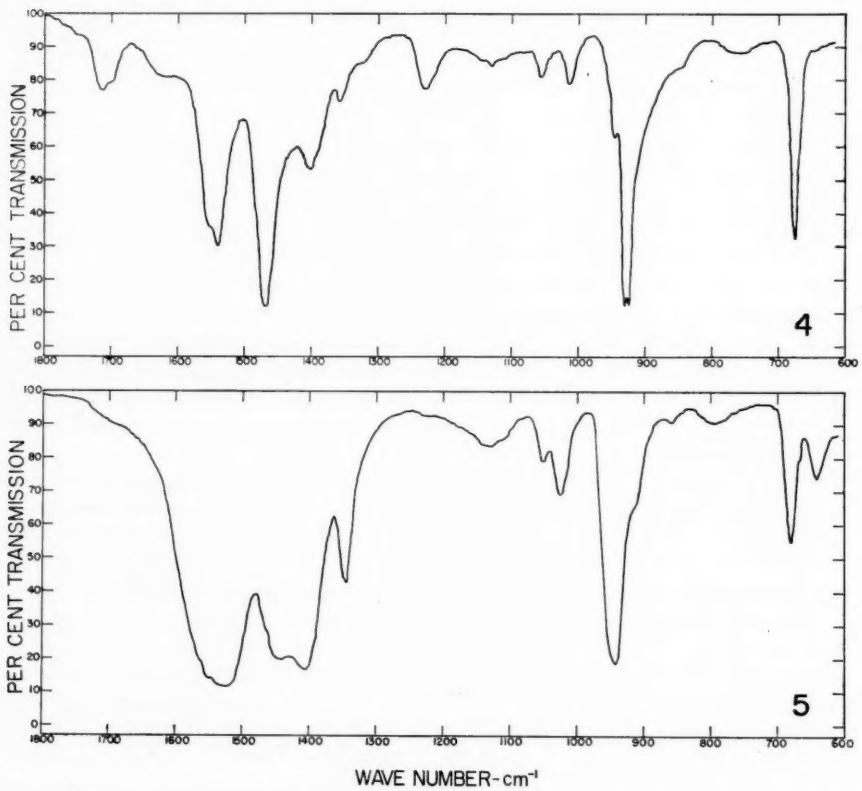

FIG. 4. Infrared spectrum of uranyl acetate mixed with potassium bromide by freeze-drying. Molar ratio of uranyl acetate to potassium bromide 0.1 to 1.

FIG. 5. Infrared spectrum of uranyl acetate mixed with potassium bromide by freeze-drying. Molar ratio of uranyl acetate to potassium bromide 1000 to 1.

spectra of samples in which the molar ratio of uranyl acetate to potassium bromide during the freeze-drying process was 0.1 to 1 and 1000 to 1 respectively. The type of spectra obtained showed a smooth transition from that shown in Fig. 4 to that shown in Fig. 5 as the molar ratio was varied between the above limits. In the following discussion spectra of the type shown in Fig. 4, i.e. from samples where a small molar ratio of uranyl acetate to potassium bromide was present during freeze-drying, will be designated as type I spectra, whereas spectra of the type shown in Fig. 5, i.e. from samples where a large molar ratio of uranyl acetate to potassium bromide was present during freeze-drying, will be designated as type II spectra.

The strong peak in the neighborhood of 930 cm^{-1} is undoubtedly due to the asymmetric normal vibration, ν_3, of the uranyl ion. In type I spectra there is a strong double peak at 924 and 930 cm^{-1} together with a shoulder at 945 cm^{-1}. In type II spectra the intense peak is at 942 cm^{-1} with a shoulder on the low wave number side.

The strong absorption at 676 cm^{-1} may arise as the result of the acetate groups being attached to the uranyl group by covalent bonds. There is considerable evidence (17, 18, 19) which indicates that in aqueous solution the tendency for covalent bond formation between the acetate group and the uranyl group is large. Hence it seems reasonable to expect that in solid uranyl acetate the acetate groups are attached, as indicated in formula I, by covalent bonds. The force constants for C=O, C=C, C=N, and N=O

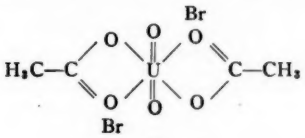

I

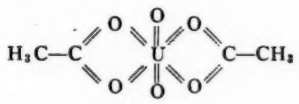

II

bonds are approximately double those of the corresponding C—O, C—C, C—N, and N—O bonds (24). If the assumption is made that this relationship also holds for U=O and U—O bonds then a peak due to the U—O bond might be expected in the region 927 $cm^{-1}/\sqrt{2}$ = 655 cm^{-1}. This calculation assumes the vibration to be harmonic, which is probably not true for the solid state. Thus, considering also the approximation made concerning the bond strength, the agreement with the observed peak at 676 cm^{-1} is as good as could be expected. A peak at 678 cm^{-1} has been reported for $NaUO_2(C_2H_3O_2)_3$ (5). This peak was assigned (5) to a CO_2 deformation vibration by comparison with the similar assignment of a peak at 645 cm^{-1} observed for sodium acetate (25). However, there is good evidence that in $NaUO_2(C_2H_3O_2)_3$ the uranyl and acetate ions are present as the complex anion $UO_2(C_2H_3O_2)_3^-$ (27). Considering the large tendency for covalent bond formation between the acetate and uranyl groups (17, 18, 19), it is unlikely that any appreciable amount of free acetate ions is present. Hence a CO_2 deformation vibration is not very likely and the assignment of the 676 cm^{-1} peak to a C—O bond appears to be reasonable.

The peaks at 1713 and 1230 cm^{-1}, which are present in type I spectra but which are absent in type II spectra, are probably due to the C=O and C—O stretching vibrations of the acetate group (24, 26). It would ordinarily be expected that the intensities of these peaks, especially the 1713 cm^{-1} peak (24) would be greater than those observed in type I spectra.

In type II spectra a peak is present at 642 cm^{-1} which is absent in type I spectra. The intensity of this peak progressively increases as the ratio of uranyl acetate to potassium bromide is increased.

A tentative explanation for the change in the spectra from type I to type II as the ratio of uranyl acetate to potassium bromide is increased is that the uranium atom of the uranyl group becomes chelated to the carbonyl oxygen atom of the acetate groups instead of being bonded to bromide ions. There is strong evidence that the uranium atom in the uranyl ion has a tendency for a co-ordination number greater than six (17, 18). Hence it is possible that besides the co-ordinate covalent bonds formed with the oxygen atoms of the two C—O groups, the uranium atom will show a tendency to form co-ordinate covalent bonds with other atoms, such as possibly bromide ions or the oxygen atoms of water molecules. Thus in uranyl acetate dihydrate the water molecules are perhaps attached to the uranium atom by co-ordinate covalent bonds. When uranyl acetate is freeze-dried, water molecules are no longer available and if a relatively large excess of potassium bromide is present it is possible that two, or perhaps more, bromide ions are bound to the uranium atom by co-ordinate covalent bonds, giving the compound represented by formula I. In the presence of a relatively small amount of potassium bromide, however, it is possible that the tendency of the uranium atom to form additional co-ordinate covalent bonds may be satisfied by chelation with the carbonyl oxygen atoms of the acetate groups giving a compound represented by formula II. In the resulting compound it is likely that the two oxygen atoms of each of the acetate groups will be equivalent.

Chelation of the carbonyl group often results in a considerable lowering in frequency of the band in the 1700 cm^{-1} region (26) and this effect could account for the disappearance of the 1713 cm^{-1} peak together with the increase in intensity and the broadening of the bands in the 1500 cm^{-1} region. The disappearance of the 1230 cm^{-1} band would also be expected. The shift of the asymmetrical normal vibration, ν_3, of the uranyl group from the 927 cm^{-1} region, type I spectra, to 942 cm^{-1}, type II spectra, could be the result of the changes which have occurred in the neighborhood of the uranium atom.

The 642 cm^{-1} peak which is present in type II spectra may be due to some vibration of the  group. This would account for the appearance of this peak as the ratio of uranyl acetate to potassium bromide increases. The low intensity, mentioned earlier, of the 1713 and 1230 cm^{-1} bands of the carbonyl group in type I spectra suggests that some chelation with the carbonyl oxygen atoms of the acetate groups has already occurred, even at a low uranyl acetate to potassium bromide ratio. Hence type I spectra probably results from the presence in the sample of a mixture of compounds I and II rather than from the presence of compound I alone.

In the above discussion intermolecular chelation has been postulated. It is conceivable that intramolecular chelation is either partially, or wholly, responsible for the changes observed in the spectrum as the uranyl acetate to potassium bromide ratio is varied.

(*c*) *Sodium Zinc Uranyl Acetate*, $NaZn(UO_2)_3(C_2H_3O_2)_9.6H_2O$

The spectrum was obtained from a sample prepared by mixing the compound with freeze-dried potassium bromide by vibration. The spectrum is very similar to that obtained by Jones (5) for $NaUO_2(C_2H_3O_2)_3$. A peak of moderate intensity which was not observed for $NaUO_2(C_2H_3O_2)_3$ was found in the present work at 1355 cm^{-1}. A very broad peak was observed at 3380 cm^{-1}. This region was not investigated by Jones (5). It is possible that this latter peak is due to the water of crystallization. As mentioned earlier for $NaUO_2(C_2H_3O_2)_3$, there is good evidence (27) that in $NaZn(UO_2)_3(C_2H_3O_2)_9.6H_2O$ the uranyl and acetate ions are present as the complex anion $UO_2(C_2H_3O_2)_3^-$. Hence it is not surprising that the infrared spectrum of these two compounds are quite similar. For

the same reasons as presented earlier in the discussion of the spectrum of uranyl acetate, it is believed that the intense peak observed at 680 cm^{-1} for $NaZn(UO_2)_3(C_2H_3O_2)_9.6H_2O$ is due to a C—O bond vibration rather than to a CO_2 deformation vibration as postulated by Jones for $NaUO_2(C_2H_3O_2)_3$ (5).

Infrared Spectrophotometric Determination of Uranyl Ion

An examination of the spectra of samples prepared by freeze-drying aqueous solutions of uranyl salts and potassium bromide indicated that the 923 cm^{-1} peak of uranyl nitrate might be suitable for the infrared spectrophotometric determination of the uranyl ion. This peak is relatively intense and sharp, and there is little interference from neighboring bands.

Solutions of known compositions were prepared by adding various volumes of a standard uranyl nitrate solution to known volumes of a standard potassium solution. The amount of potassium bromide used for each sample was 0.2 g. After freeze-drying, the samples were pressed into disks and their spectra recorded. The weight of the disk, which could not be removed from the die, was found by taking the difference between the weight of the die plus the disk after the excess material had been removed and the weight of the clean die. From a knowledge of the proportion of uranyl nitrate to potassium bromide used, the weight of uranyl ion present in the disk could be calculated. If the Beer–Lambert law is obeyed a plot of the optical density against the weight of uranyl ion present in the disk should give a straight line. The baseline optical density method of Heigl, Bell, and White (28) was used to determined the optical density. A potassium bromide blank was used in the reference beam. In Fig. 6 the optical density is plotted against the weight, in milli-

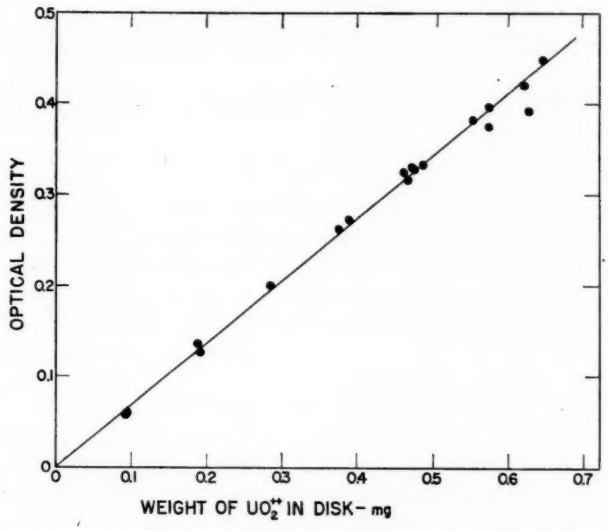

FIG. 6. Beer–Lambert's law plot for uranyl ion. Uranyl nitrate and potassium bromide mixed by freeze-drying. Wave number, 923 cm^{-1}.

grams, of uranyl ion present in the disk. The results indicate that with samples of uranyl nitrate prepared by the above technique and for the concentration range used, the Beer–Lambert law is obeyed.

ACKNOWLEDGMENTS

In the interpretation of the spectra of the uranyl acetate samples we wish to acknowledge the helpful suggestions made by Dr. R. A. Abramovitch. We are indebted to Mr. E. C. Bailey for the preparation of the sodium zinc uranyl acetate. One of us (G. L. C.) wishes to thank the National Research Council of Canada for financial assistance in the form of a Bursary and a Studentship.

REFERENCES

1. G. K. T. Conn and C. K. Wu. Trans. Faraday Soc. **34**, 1483 (1938).
2. J. Lecompte and R. Freymann. Bull. soc. chim. **8**, 622 (1941).
3. A. N. Sevchenko and B. I. Stepanov. Zhur. Eksp. i Teoret. Fiz. **19**, 1113 (1949).
4. L. H. Jones and R. A. Penneman. J. Chem. Phys. **21**, 542 (1953).
5. L. H. Jones. J. Chem. Phys. **23**, 2105 (1955).
6. G. Tridot. Ann. chim. (Paris), **10**, 225 (1955).
7. B. M. Gatehouse and A. E. Comyns. J. Chem. Soc. 3965 (1958).
8. N. M. Stimson and M. J. O'Donnell. J. Am. Chem. Soc. **74**, 1805 (1952).
9. U. Schiedt and H. Reinwein. Z. Naturforsch. **7**(*b*), 270 (1952).
10. U. Schiedt, as reported by H. Hausdorff. Appl. Spectroscopy, **7**, 75 (1953).
11. H. F. Bauer, A. Epp, and R. U. Lemieux. The mounting of samples in potassium bromide for infrared spectroscopy. Prairie Regional Laboratory, National Research Council of Canada, Saskatoon, Sask.
12. H. H. Barber and I. M. Kolthoff. J. Am. Chem. Soc. **50**, 1625 (1928).
13. Instruction Manual, Volume 3B. Model 21 infrared spectrophotometer operating and maintenance instructions. The Perkin-Elmer Corp., Norwalk, Connecticut. 1952.
14. I. M. Kolthoff and J. J. Lingane. J. Am. Chem. Soc. **55**, 1871 (1933).
15. J. J. Katz and G. T. Seaborg. The chemistry of the actinide elements. Methuen and Co., Ltd., London. 1957. p. 193.
16. H. R. Hoekstra and J. J. Katz. *In* The actinide elements. National Nuclear Energy Series. Vol. IV-14A. *Edited by* G. T. Seaborg and J. J. Katz. McGraw-Hill Book Co., Inc., New York. 1954. p. 146.
17. L. Sacconi and G. Giannoni. J. Chem. Soc. 2368 (1954).
18. L. Sacconi and G. Giannoni. J. Chem. Soc. 2751 (1954).
19. G. H. Tishkoff. *In* Pharmacology and toxicology of uranium compounds. National Nuclear Energy Series. Vol. VI-1. *Edited by* C. Voegtlin and H. C. Hodge. McGraw-Hill Book Co., Inc., New York. 1949. Chap. 1, Appendix B. pp. 125–146.
20. B. M. Gatehouse, S. E. Livingstone, and R. S. Nyholn. J. Chem. Soc. 4222 (1957).
21. G. Herzberg. Infrared and raman spectra of polyatomic molecules. Van Nostrand, New York. 1945. p. 178.
22. J. C. Decius. J. Chem. Phys. **23**, 1290 (1955).
23. G. H. Dieke and A. B. F. Duncan. Spectroscopic properties of uranium compounds. McGraw-Hill Book Co., Inc., New York. 1949.
24. R. N. Jones and C. Sandorfy. *In* Technique of organic chemistry. Vol. IX. *Edited by* A. Weissberger. Interscience Publishers, Inc., New York. 1956. pp. 334, 443, 453, 476.
25. H. L. Jones and E. McLaren. J. Chem. Phys. **22**, 1796 (1954).
26. L. J. Bellamy. The infra-red spectra of complex molecules. John Wiley and Sons, Inc., New York. 1954. pp. 123, 153.
27. H. Brintzinger *et al.* As reported in reference (16). p. 169.
28. J. J. Heigl, M. F. Bell, and J. U. White. Ind. Eng. Chem. Anal. Ed. **19**, 293 (1947).

EFFECT OF MEAN PORE SIZE ON THE LOW-TEMPERATURE ADSORPTION OF NITROGEN ON ALUMINA[1]

J. L. BLUMENTHAL, S. SOURIRAJAN, AND KEN NOBE

ABSTRACT

The effect of mean pore size on the low-temperature adsorption of nitrogen on two samples of alumina has been studied. The mean pore radius of one sample of alumina was 37 Å, and that of the other was 3100 Å. The two adsorption isotherms at −195.8° C have been plotted in terms of the volume of gas adsorbed per square meter of surface area vs. relative pressure ratio. The data have been found to fall into three distinct regions. In the first region extending up to the relative pressure ratio of 0.3, the two isotherms are nearly identical. In the second region extending from the relative pressure ratio of 0.3 to 0.75, the isotherm for the small mean pore size alumina lies above that for the large mean pore size sample. In the third region extending from the relative pressure ratio of 0.75 up to saturation, the isotherm for the small mean pore size sample tends to level off whereas that for the large mean pore size sample rises rapidly with increase in the relative pressure ratio. The above experimental observations have been explained on the basis of capillary condensation.

INTRODUCTION

The object of this investigation was to determine experimentally the effect of the mean pore size on the nitrogen adsorption isotherms of two samples of porous solids having the same chemical composition. This paper reports the results of a study of the low-temperature adsorption of nitrogen gas on two samples of alumina having widely different surface areas and mean pore radii.

EXPERIMENTAL

The apparatus used in this study for the determination of the gas adsorption isotherms and the total pore volume of the alumina samples was similar to the one described by Joyner (1). Pure dry nitrogen gas was used for adsorption, and helium gas was used to determine the dead space volumes. The sample bulb was immersed in a constant-temperature liquid nitrogen bath at −195.8° C during the experiment. Adsorption measurements were taken from relative pressures of 0.02 up to the saturation pressure. The surface area of the alumina samples were determined by the B.E.T. method (2). The total pore volumes of the samples were determined by the helium–mercury method by measuring the difference between the helium dead space and mercury dead space in a bulb containing the alumina sample (3). The mean radius of the pores in each of the samples was then calculated from the known surface area and pore volume data assuming the pores to be cylindrical.

RESULTS AND DISCUSSION

Alumina sample I had a surface area of 272 sq. meters per gram, and a mean pore radius of 37 Å. Alumina sample II had a surface area of 1.3 sq. meters per gram, and a mean pore radius of 3100 Å. The experimental adsorption data of nitrogen gas on the above alumina samples are given in Tables I and II respectively. In order to compare the two adsorption isotherms on a common basis, the data are plotted in Fig. 1 in terms of the volume of gas adsorbed per unit (sq. meter) of surface area vs. relative pressure ratio.

[1]*Manuscript received February 12, 1960.*
Contribution from the Department of Engineering, University of California, Los Angeles 24, California.

Can. J. Chem. Vol. 38 (1960)

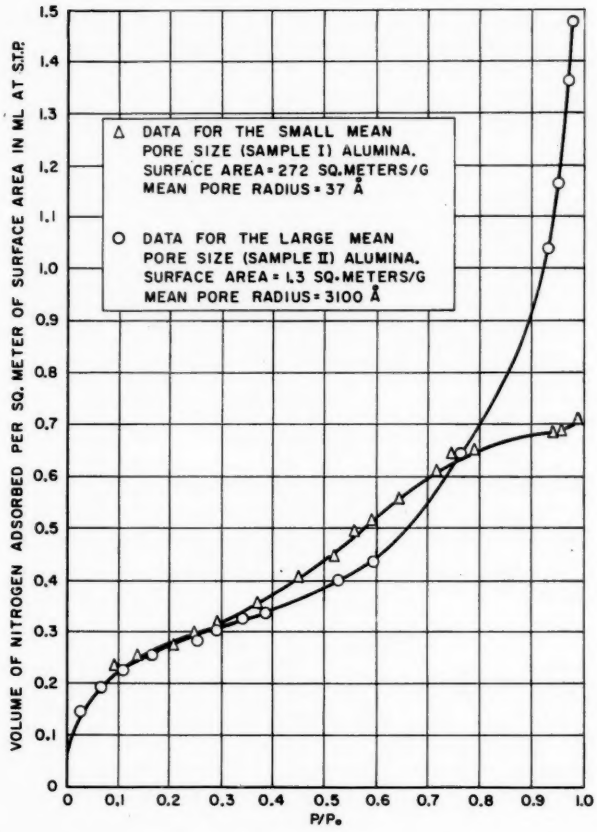

FIG. 1. Adsorption isotherms for the small mean pore size and the large mean pore size alumina samples.

From Fig. 1, it is seen that the data fall into three distinct regions. In the first region, which extends up to a relative pressure ratio of 0.3, the curves for both the small mean pore size (high surface area) alumina, and the large mean pore size (low surface area) alumina are nearly identical. This is the part of the isotherm which is useful for the B.E.T. plot. In the second region, which extends from the relative pressure ratio of 0.3 up to 0.75, the adsorption isotherm for the small mean pore size alumina lies above that for the large mean pore size sample. In the third region, which extends from the relative pressure ratio of 0.75 up to saturation, the isotherm for the small mean pore size sample almost levels off, whereas that for the large mean pore size sample rises very rapidly with increase in the relative pressure ratio. The above experimental observations can be explained as being due to the predominant effect of capillary condensation of nitrogen in the pores of the samples in the second and third regions. According to the well-known Kelvin equation (4), the relative pressure at which capillary condensation can take place increases exponentially with increase in pore size. Hence, a given amount of capillary condensation can take place at a lower relative pressure in the case of the

TABLE I

Nitrogen gas adsorption data for sample I alumina

Volume of gas adsorbed at S.T.P. in ml	Relative pressure ratio, P/P_0	Volume of gas adsorbed at S.T.P. per sq. meter of surface area, in ml
15.5	0.091	0.237
16.7	0.137	0.255
18.3	0.205	0.279
20.3	0.247	0.310
21.0	0.290	0.321
23.5	0.363	0.359
26.7	0.443	0.407
29.4	0.515	0.448
32.6	0.552	0.497
33.6	0.588	0.513
36.2	0.647	0.553
39.9	0.715	0.610
42.2	0.742	0.643
42.8	0.790	0.650
44.8	0.938	0.683
45.1	0.953	0.687
47.0	0.985	0.717

NOTE: Weight of sample: 0.2401 gram.
Surface area: 272 sq. meters/gram.
Total pore volume: 0.51 ml/gram.
Mean pore radius: 37 Å.
Adsorption temperature: −195.8° C.
P = adsorption pressure.
P_0 = vapor pressure of nitrogen at its normal boiling point.

TABLE II

Nitrogen gas adsorption data for sample II alumina

Volume of gas adsorbed at S.T.P. in ml	Relative pressure ratio, P/P_0	Volume of gas adsorbed at S.T.P. per sq. meter of surface area, in ml
2.11	0.022	0.134
3.09	0.062	0.195
3.52	0.108	0.223
3.97	0.165	0.252
4.49	0.251	0.284
4.74	0.292	0.300
5.27	0.384	0.334
6.31	0.522	0.400
6.93	0.591	0.438
10.2	0.760	0.645
16.4	0.930	1.04
18.5	0.948	1.17
21.7	0.970	1.37
23.4	0.978	1.48

NOTE: Weight of sample: 12.20 grams.
Surface area: 1.3 sq. meters/gram.
Total pore volume: 0.21 ml/gram.
Mean pore radius: 3100 Å.
Adsorption temperature: −195.8° C.

small mean pore size alumina than in the case of the large mean pore size sample. This explains the relative positions of the adsorption isotherms in the region 2. At the close of the region 2, it is reasonable to assume that most of the pores in the small mean pore size sample are already filled, whereas most of the pores in the large mean pore size

sample are yet to be filled. Hence in the region 3, at relative pressures above 0.75, the adsorption isotherm for the small mean pore size alumina tends to level off, whereas that for the large mean pore size sample rises rapidly with increase in the relative pressure ratio.

ACKNOWLEDGMENTS

This investigation forms part of the catalysis studies in the Air Pollution Research program of the Department of Engineering, University of California at Los Angeles. The authors are grateful to Professor L. M. K. Boelter and Professor W. C. Hurty for their support and encouragement of this work.

REFERENCES

1. L. G. JOYNER. Gas adsorption apparatus for measuring surface areas. *In* Scientific and industrial glass blowing and laboratory techniques. W. E. Barr and Victor J. Anhorn. Instruments Publishing Co., Pittsburg. 1949. p. 257.
2. S. BRUNAUER, P. H. EMMETT, and E. TELLER. J. Am. Chem. Soc. **60**, 309 (1938).
3. P. H. EMMETT. Catalysis. Vol. II. Reinhold Publ. Corp., New York. 1955. Chap. 2.
4. P. H. EMMETT. Catalysis. Vol. I. Reinhold Publ. Corp., New York. 1954. Chap. 1.

REARRANGEMENT STUDIES WITH C^{14}

IX. THE FORMOLYSIS OF METHYL-C^{14}-ISOPROPYLCARBINYL *p*-TOLUENESULPHONATE

A. J. FINLAYSON[2] AND C. C. LEE

ABSTRACT

Formolysis of methyl-C^{14}-isopropylcarbinyl *p*-toluenesulphonate (I) at reflux temperature gave a mixture of 2-methyl-2-butene (II), 2-methyl-1-butene (III), and 3-methyl-1-butene (IV). The relative amounts of olefins II, III, IV were measured by gas–liquid chromatography to be 88%, 11%, and 1%, respectively. When the formolysis was carried out at 50° C, besides olefins II, III, and IV, some *t*-amyl formate was obtained indicating a substitution reaction with neighboring hydrogen participation. Degradation of the mixture of olefins from formolysis gave, among other compounds, radioactive acetone, indicating an isotope position rearrangement in the chief product, 2-methyl-2-butene (II). This rearrangement may be attributed to a 1,2-methyl shift in one of the processes that gave rise to olefin II. A comparison of the data from the acetolysis and the formolysis of I showed that in the E_1 reactions, neighboring hydrogen participation is predominant in either solvent. For a change of solvent from acetic acid to the more ionizing formic acid, it was demonstrated that there is a greater degree of neighboring methyl participation while the process involving no neighboring group participation assumes less importance.

The acetolysis of methyl-C^{14}-isopropylcarbinyl *p*-toluenesulphonate (I) at reflux temperature gave only olefinic products while at 50° C, a small amount of *t*-amyl acetate was obtained besides the olefins (1). The elimination reactions were found to involve processes with no neighboring group participation, and with neighboring hydrogen and neighboring methyl participation, the hydrogen participation being predominant (1). In kinetic studies, a change of solvent from acetic to formic acid may help to disclose driving force due to participation by allowing neighboring group participation to displace nucleophilic assistance by solvent and by making the rate of solvolysis of a reference substance less assisted by nucleophilic driving force (2). Thus Winstein and Marshall (2) have studied the formolysis rates of a series of secondary alkyl *p*-bromobenzenesulphonates and have concluded that there is some assistance to ionization from neighboring hydrogen and/or carbon during solvolysis of methylisopropylcarbinyl derivatives. In the present work, solvolysis of methyl-C^{14}-isopropylcarbinyl *p*-toluenesulphonate (I) was carried out in formic acid and the results compared with those reported for the acetolysis of I (1).

RESULTS AND DISCUSSIONS

As in the acetolysis, the formolysis of I at reflux temperature gave a mixture of 2-methyl-2-butene (II), 2-methyl-1-butene (III), and 3-methyl-1-butene (IV) with no isolatable amount of substitution product. At 50° C, a yield of about 10% crude *t*-amyl formate and 42% of the mixture of olefins II, III, and IV were obtained. The relative amounts of II, III, and IV, as measured by gas–liquid chromatography, are tabulated in Table I. For comparison, the olefin composition in the products of acetolysis is also given in Table I.

Degradation of the mixture of olefins II, III, and IV by treatment with performic acid followed by cleavage with sodium metaperiodate yielded a mixture of formaldehyde, acetaldehyde, isobutyraldehyde, acetone, and methyl ethyl ketone. Separation of these carbonyl compounds as their 2,4-dinitrophenylhydrazones was effected by adsorption

[1]*Manuscript received January 4, 1960.*
Contribution from the Department of Chemistry, University of Saskatchewan, Saskatoon, Sask. For paper VIII, see Lee, C. C., Tkachuk, R., and Slater, G. P. Tetrahedron, 7, 206 (1959).
[2]*Present address: Prairie Regional Laboratory, National Research Council, Saskatoon, Saskatchewan.*

TABLE I

Relative amounts of olefins from solvolyses of methyl-C^{14}-isopropylcarbinyl *p*-toluenesulphonate

Reaction temperature	Olefin	% composition in formolysis products			% composition in acetolysis products[a]
		Analyzed by gas chromatography	Analyzed by radioactivity		Analyzed by gas chromatography
			Run 1	Run 2	
Reflux	2-Methyl-2-butene	88	83	84	80
	2-Methyl-1-butene	11			18
	3-Methyl-1-butene	1			2
50° C	2-Methyl-2-butene	91	88	93	83
	2-Methyl-1-butene	9			16
	3-Methyl-1-butene	trace			1

[a]Data from reference 1.

chromatography in a silicic acid – celite column as described previously (1). The 2,4-dinitrophenylhydrazones of acetaldehyde and acetone, which were derived from degradation of the chief product, 2-methyl-2-butene (II), were recovered and their radioactivity

TABLE II

Radioactivity data from formolyses of methyl-C^{14}-isopropylcarbinyl *p*-toluenesulphonate

Reaction temperature	Compound assayed	Specific activity (c.p.m. on a molar basis)		% of total activity		% rearrangement in 2-methyl-2-butene		% rearrangement in 2-methyl-2-butene from acetolysis[c]	
		Run 1	Run 2	Run 1	Run 2	Run 1	Run 2	Run 1	Run 2
Reflux	Glycol mixture from olefins II, III, and IV	20500	13020	100	100				
	CH_3CHO[a]	16100	10250	78.6	78.8				
	CH_3COCH_3[a]	885	646	4.3	5.0	5.2	5.8	2.6	2.4
	CBr_4[b]	1065	835	5.2	6.4				
50° C	Glycol mixture from olefins II, III, and IV	17000	15750	100	100				
	CH_3CHO[a]	14660	14300	86.3	90.8				
	CH_3COCH_3[a]	312	329	1.8	2.2	2.1	2.3	0.9	0.9
	CBr_4[b]	334	330	1.9	2.2				

[a]As the 2.4-dinitrophenylhydrazone.
[b]From reaction of ketonic degradation products with bromine and sodium hydroxide.
[c]Data from reference 1.

determined. The results are given in Table II. The sum of the activities of acetaldehyde and acetone is a measure of the amount of olefin II in the mixture of II, III, and IV. This serves as a check on the gas chromatographic analysis of II given in Table I.

The presence of C^{14} activity in the acetone indicated that there was some isotope position rearrangement in the chief olefinic product, 2-methyl-2-butene (II). For the formolysis at reflux temperature run No. 1, this rearrangement amounted to

$$\{885/(16100+885)\} \times 100 = 5.2\%.$$

Such rearrangement data are included in Table II. For comparison, the degrees of

isotope position rearrangement in 2-methyl-2-butene obtained from acetolysis are also presented in Table II.

The interpretations of the results summarized in Tables I and II may be made in a way exactly analogous to the interpretations of the results from acetolysis of I (1). The *t*-amyl formate obtained from formolysis at 50° C indicates that the substitution reaction involves neighboring hydrogen participation resulting in a 1,2-hydrogen shift. The elimination reactions may be discussed in terms of reaction sequences 1, 2, and 3, representing processes without neighboring group participation, with neighboring hydrogen participation, and with neighboring methyl participation, respectively.

According to Saytzeff's rule, each of these three processes is expected to give a greater amount of the chief product, 2-methyl-2-butene (II or II_r). The presence of only very small amounts of 3-methyl-1-butene (IV or IV_r), as shown in Table I, indicates that reaction sequence 1 makes a relatively minor contribution to the over-all elimination reactions. It is even possible that all or a large part of the 3-methyl-1-butene detected by gas chromatography may have been due to reaction sequence 3, which results in the production of some isotopically rearranged olefin IV_r. By analogy with findings from acetolysis studies (1, 3) and from the presence of fairly large quantities of 2-methyl-1-butene (III) in the olefinic products of formolysis, it is reasonable to conclude that reaction sequence 2 depicts the predominant elimination process. The participation of neighboring methyl group (reaction sequence 3) results in the formation of isotopically rearranged 2-methyl-2-butene (II_r), the degradation of which gave radioactive acetone. The degree of this isotope position rearrangement in the 2-methyl-2-butene from formolysis is greater than the corresponding rearrangement after acetolysis by a factor of about 2 (Table II). This indicates a greater extent of neighboring methyl participation in formolysis than in acetolysis.

The location of C^{14} in the methyl group, and not in the carbonyl group, of acetone is required by reaction sequence 3. This was shown to be the case in the following way. After degradation of the mixed olefins II, III, and IV, the carbonyl compounds obtained were treated with neutral potassium permanganate to destroy all aldehydes (4). The remaining acetone and methyl ethyl ketone, recovered as an aqueous solution by distillation, were treated with bromine and sodium hydroxide to give carbon tetrabromide. If much of the C^{14} activity were present in the carbonyl group of acetone, the activity of the carbon tetrabromide would be lower than that of acetone and this was not observed (Table II). Actually, in the formolysis at 50° C, the C^{14} activity of acetone and of carbon tetrabromide was about equal. For the formolysis at reflux temperature, the carbon tetrabromide activity was even somewhat higher than the activity of acetone. Possibly, this difference may be due to some C^{14} located in the methyl group of methyl ethyl ketone. Results similar to this were noted in the acetolysis of I and it was suggested that the location of C^{14} in the methyl group of methyl ethyl ketone may be explained by a process involving first a 1,2-methyl shift followed by a 1,2-hydrogen shift before the formation of olefins (1).

In conclusion, it is evident that the formolysis of I involves processes similar to those operating in the acetolysis of I. The isolated substitution product results only from neighboring hydrogen participation. In the E_1 reactions, hydrogen participation also predominates. Comparing the data from formolysis and acetolysis, the greater degrees of isotope position rearrangement in 2-methyl-2-butene, coupled with the smaller amount of 3-methyl-1-butene in the over-all olefinic products, indicate a greater extent of

[1]
[2]
[3]
I
II
III
IV
II,
IV,

neighboring group participation and a lesser importance of the process without participation for the formolysis. This is in agreement with expectation that a change of solvent from acetic acid to the more ionizing formic acid would enhance the degree of participation by neighboring groups in E_1 as well as S_N1 reactions.

EXPERIMENTAL

Procedures for the synthesis of methyl-C^{14}-isopropylcarbinyl *p*-toluenesulphonate (I), and for the analysis and degradation of the products of solvolyses, have been described previously (1).

Formolysis at Reflux Temperature

A solution of I (5.80 g, 0.024 mole) in 45 ml of anhydrous formic acid, m.p. 8.2–8.3° C (lit. (5) m.p. 8.4° C), containing 2.3 g (0.027 mole) of anhydrous potassium formate was gently refluxed for 2.5 hours. During the reflux period, the olefins formed were swept out by a stream of dry nitrogen and collected in a dry-ice-cooled trap.

After the refluxing, the reaction mixture was cooled, poured into 200 ml of ice and water containing 50 g of dissolved sodium chloride, and then repeatedly extracted with a 1:3 solution of ether – petroleum ether. The extracts were washed free of acid by a 5% solution of sodium carbonate and dried over anhydrous magnesium sulphate. Removal of the solvent, however, left no residue, indicating no recoverable quantity of substitution product.

The mixture of olefins collected in the dry-ice-cooled trap weighed 1.25 g (75%). It was distilled once, b.p. 35–38° C, before being used for degradation and gas chromatographic analysis.

Formolysis at 50° C

Methyl-C^{14}-isopropylcarbinyl *p*-toluenesulphonate (I) (10.0 g, 0.041 mole) was dissolved in 70 ml of anhydrous formic acid containing 3.7 g (0.044 mole) of anhydrous potassium formate. The solution was stirred mechanically in a bath maintained at 50±1° C for 3 hours. During the heating period, the olefins formed were swept out by dry nitrogen and collected in a dry-ice-cooled trap.

The reaction mixture was poured into 300 ml of ice and water containing 60 g of dissolved sodium chloride and then worked up as described under formolysis at reflux temperature. The removal of the ether – petroleum ether solvent left a colorless residue from which 0.5 g of material, b.p. 110–112° C, distilled and 1.0 g of unreacted I was recovered. The liquid product was redistilled at 112–113° C (lit. (6) b.p. of *t*-amyl formate, 113° C). Infrared and gas chromatographic analysis indicated that it was *t*-amyl formate contaminated with a small amount of *t*-amyl alcohol. The yield of this crude *t*-amyl formate was about 10% based on the 9.0 g of I used up in the reaction.

The mixture of olefins collected in the dry-ice-cooled trap weighed 1.10 g (42% based on 9.0 g of I). It was distilled once and then utilized for degradation and analysis.

ACKNOWLEDGMENTS

Sincere thanks are extended to Dr. J. Bardwell for the use of his apparatus for gas–liquid chromatography and to the National Research Council of Canada for generous financial support.

REFERENCES

1. A. J. FINLAYSON and C. C. LEE. Can. J. Chem. **37**, 940 (1959).
2. S. WINSTEIN and H. MARSHALL. J. Am. Chem. Soc. **74**, 1120 (1952).
3. S. WINSTEIN and J. TAKAHASHI. Tetrahedron, **2**, 316 (1958).
4. J. D. ROBERTS, R. E. MCMAHON, and J. S. HINE. J. Am. Chem. Soc. **72**, 4237 (1950).
5. L. C. BATEMAN and E. D. HUGHES. J. Chem. Soc. 1187 (1937).
6. BEILSTEIN'S HANDBUCH DER ORGANISCHEN CHEMIE. Vol. II. 4th ed. Julius Springer, Berlin. 1920. p. 22.

CONSTITUTION OF A GLUCOMANNAN FROM JACK PINE (PINUS BANKSIANA, LAMB)[1]

C. T. BISHOP AND F. P. COOPER

ABSTRACT

A hemicellulose fraction from jack pine wood has been shown to contain D-mannose, D-glucose, and D-galactose in a molar ratio of 49:17:2. The glucomannan was electrophoretically homogeneous and showed a degree of polymerization of 18–21 by three different methods of end group analysis. Methylation and hydrolysis yielded the following *O*-methyl ethers: 2,3,4,6-tetra-*O*-methyl-D-glucose (2.8 moles); 2,3,4,6-tetra-*O*-methyl-D-galactose (1 mole); 2,3,6-tri-*O*-methyl-D-mannose (52 moles); 2,3,6-tri-*O*-methyl-D-glucose (15.3 moles); di-*O*-methyl-D-glucose (1 mole); di-*O*-methyl-D-galactose (2 moles). Lack of survival of any monosaccharides in the periodate-oxidized glucomannan showed that there was no branching through C_2 or C_3 of any of the units. Gas–liquid partition chromatography was used to analyze products from methylation and hydrolysis and from periodate oxidation and reduction of the polysaccharides. The results showed that the glucomannan from jack pine was composed of $1 \rightarrow 4$ linked β-D-mannose and β-D-glucose residues with D-galactose residues present as non-reducing terminal units. Branching, if any, must occur through C_6 of units making up the polysaccharide. This structure is compared with those of glucomannans found in other soft woods.

It has been known for a long time that a large percentage of the non-cellulosic polysaccharides in soft woods give rise to D-mannose on hydrolysis (1, 2, 3). However, reports on the isolation of mannose-containing polysaccharides and studies of the mode of linkage of the mannose residues are of much more recent date (4–19). It was apparent from the earliest of these reports (4, 5) that at least some of the mannose residues in slash pine α-cellulose were joined to glucose units. Subsequent publications described the isolation of glucomannans from western hemlock (6), white spruce (7, 8), loblolly pine (9), Norwegian spruce (10), and a Mitscherlich pulp (11) and showed with reasonable certainty, by fractionation and fragmentation analysis, that these polysaccharides were true glucomannans and not mixtures of mannans, glucans, and glucomannans. These results have been supported by recent structural studies on glucomannans from loblolly pine (12, 13), Sitka spruce (14, 15), Norwegian spruce (16), western hemlock (17), western red cedar (18), and Scots pine (19). All of these glucomannans possessed the main structural feature of a linear chain of $1 \rightarrow 4$ linked residues of β-D-mannose and β-D-glucose. However, there were smaller but significant differences which involved the question of branching in the polysaccharide and the presence or absence of D-galactose units as an integral part of the molecule.

This paper reports the isolation and structural study of a glucomannan from jack pine (*Pinus banksiana*, Lamb) and forms a further contribution to the general chemistry of this class of polysaccharides. A previous report (20) described a water-soluble arabogalactan isolated from the same wood and therefore the present work also provides further information about the carbohydrates in a single biological species.

The isolation of polysaccharides from jack pine wood is shown schematically in Fig. 1. The sugars listed are those which were released by acid hydrolysis of the various polysaccharide fractions and detected chromatographically. Polysaccharides containing glucose, mannose, and galactose could be obtained from the first two alkaline extracts by repeated complexing with copper but yields were low, presumably because of interference

[1]*Manuscript received February 5, 1960.*
Contribution from the Division of Applied Biology, National Research Council of Canada, Ottawa, Canada. Presented at the 136th meeting of the American Chemical Society, Atlantic City, N.J., September, 1959. Issued as N.R.C. No. 5644.

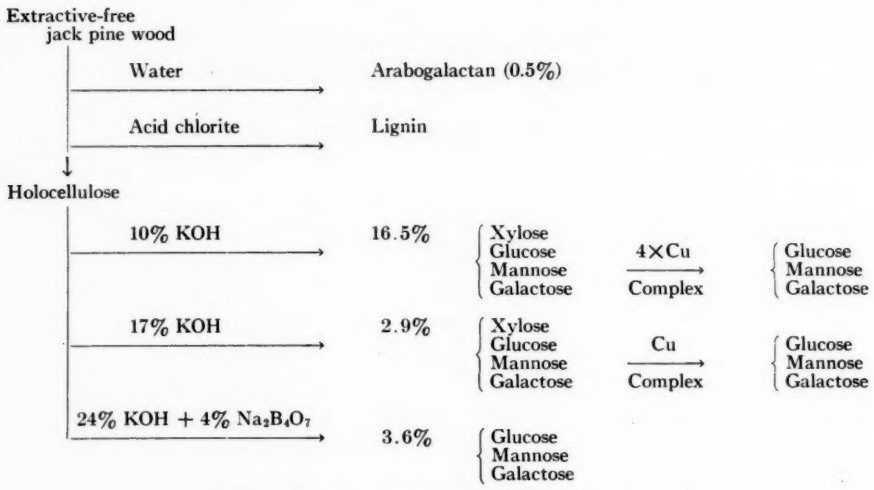

FIG. 1. Isolation of polysaccharides from jack pine wood.

by the large amounts of xylan present in these extracts. Structural studies were therefore carried out on the polysaccharide which were extracted by alkali and borate (21) and which yielded on hydrolysis glucose, mannose, and galactose as the only products detectable by paper chromatography. The monosaccharide composition of this material (mannose:glucose:galactose, 49:17:2, molar ratio) was unchanged by repeated complexing with copper. The significance of the persistent galactose component will be referred to later in comparing the structure of the present polysaccharide with those of other glucomannans.

The glucomannan isolated from the alkaline borate extraction showed a single sharp peak on electrophoresis (Fig. 2; the first, non-mobile, peak has been shown to be a false

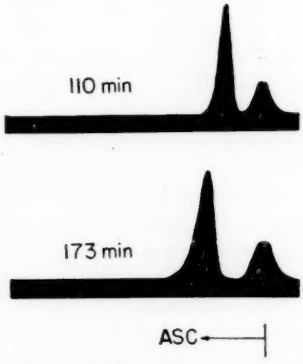

FIG. 2. Electrophoresis of glucomannan from jack pine.

boundary, see experimental) and had a specific rotation of $-26°$ indicative of β-glycosidic linkages. The observation that the polysaccharide was not hydrolyzed in hot dilute oxalic

acid showed that no terminal furanoside ring forms were present. On periodate oxidation the polysaccharide consumed 1.11 moles of oxidant per mole anhydrohexose with production of 0.10 mole of formic acid per mole anhydrohexose. The oxidized polysaccharide was examined by the procedure developed by Smith and his co-workers (22) with an innovation that utilized the unique analytical powers of gas–liquid partition chromatography (23, 24). The sequence of reactions is outlined in Fig. 3 and consisted of oxidation,

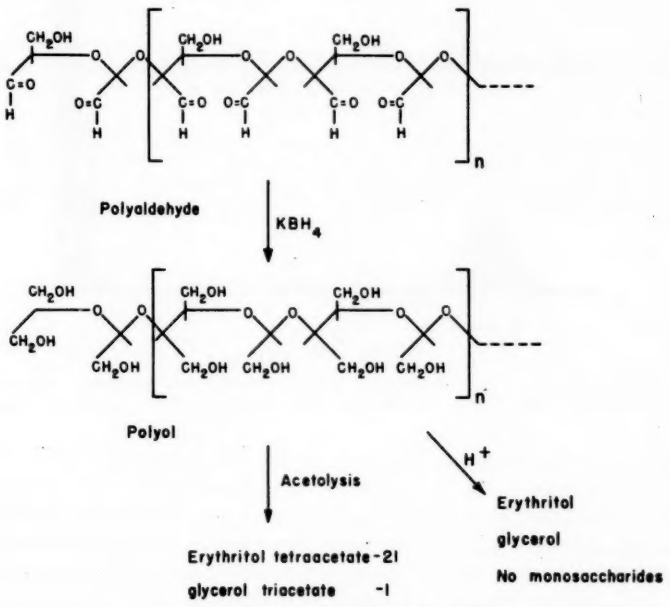

FIG. 3. Smith degradation of 1 → 4 linked hexosan.

reduction, and hydrolysis of the polysaccharide to yield erythritol and glycerol as the only products detectable by paper chromatography. The polyol was also subjected to acetolysis and the products were analyzed by gas–liquid partition chromatography (Fig. 4) giving a ratio of erythritol to glycerol of 20.8:1.0. This procedure also permitted the unequivocal identification of erythritol as its crystalline tetraacetate. The erythritol and glycerol found by this sequence of reactions must have arisen from 1 → 4 linked units and non-reducing terminal residues respectively and the ratio between them is a measure of degree of polymerization for a linear polysaccharide (22). The amount of formic acid produced in periodate oxidation of a linear polysaccharide can also be used as a measure of degree of polymerization. Under the conditions of periodate oxidation (pH 4.37) and formic acid estimation (release of iodine from potassium iodide in the presence of iodate) used here it is likely that C_1 of the reducing unit would remain attached as a formyl ester and hence would not be detected in the estimation. The polysaccharide would therefore liberate only 2 moles of formic acid and the amount found (0.10 mole per mole anhydrohexose) would give a degree of polymerization of 20, in good agreement with the value of 21 found by the erythritol:glycerol ratio. A linear chain of twenty 1 → 4 linked residues would consume 22 moles of periodate or 1.10 moles per mole anhydrohexose, a

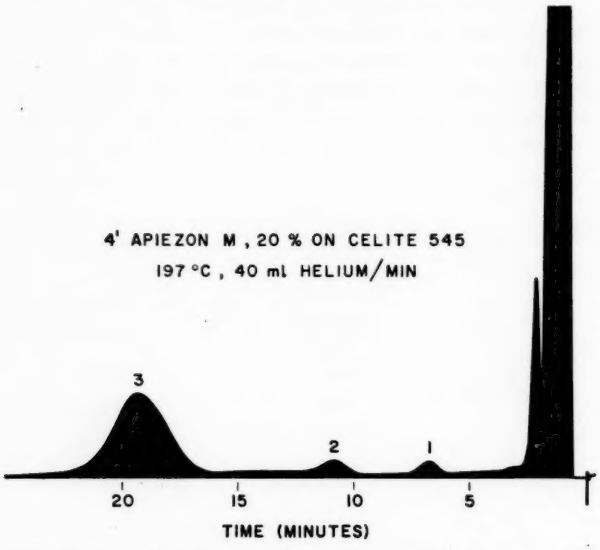

FIG. 4. Gas–liquid partition chromatogram of acetolysate from oxidized, reduced glucomannan. (1) Glycerol triacetate. (2) Not identified, possibly acetate of glycolic aldehyde. (3) Erythritol tetraacetate.

value which agrees with the periodate consumption (1.11 moles per mole anhydrohexose) determined experimentally. In a $1 \rightarrow 4$ linked polysaccharide any branching through C_2 or C_3 results in the unit forming the branch point being resistant to periodate oxidation because of a lack of vicinal hydroxyl groups. The absence of any monosaccharides in the hydrolyzate of the oxidized, reduced glucomannan showed that there was no branching through C_2 or C_3 of any of the monosaccharide units in the chain. Branching, if any, must have been through C_6.

The glucomannan was methylated and the hydrolysis products were separated, as their methyl glycosides, by gas–liquid partition chromatography (23, 24). The separations are shown in Figs. 5 and 6 and the quantitative data, obtained from measurements of areas under these peaks, is given in Table I. Component 6, Table I, was clearly evident

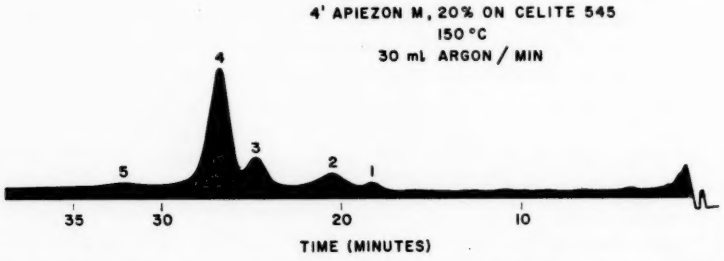

FIG. 5. Gas–liquid partition chromatogram of methanolysis products from methylated glucomannan. (1) Methyl 2,3,4,6-tetra-*O*-methyl α- and β-D-glucopyranoside. (2) Methyl 2,3,4,6-tetra-*O*-methyl α- and β-D-galactopyranoside and methyl 2,3,6-tri-*O*-methyl-β-D-glucopyranoside. (3) Methyl 2,3,6-tri-*O*-methyl-α-D-glucopyranoside. (4) Methyl 2,3,6-tri-*O*-methyl-α-D-mannopyranoside. (5) Methyl-di-*O*-methyl (α,β?)-D-galactoside.

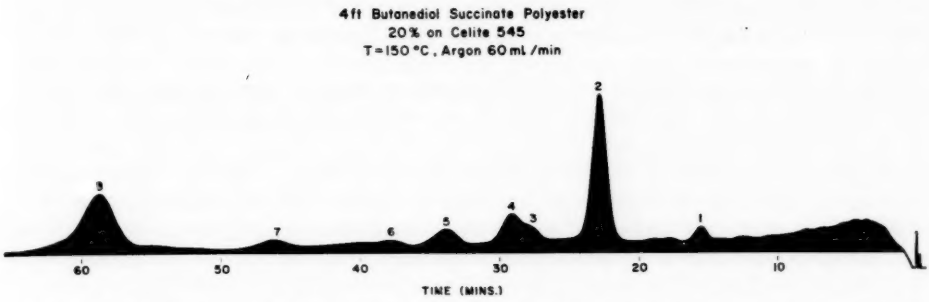

FIG. 6. Gas–liquid partition chromatogram of peaks 1 and 2, Fig. 5. (1) Methyl 2,3,4,6-tetra-*O*-methyl-β-D-glucopyranoside. (2) Methyl 2,3,4,6-tetra-*O*-methyl-α-D-glucopyranoside. (3) Methyl 2,3,4,6-tetra-*O*-methyl-β-D-galactopyranoside. (4) Methyl 2,3,4,6-tetra-*O*-methyl-α-D-galactopyranoside. (5, 6, 7) Not identified; probably methyl-di-*O*-methyl pentosides. (8) Methyl 2,3,6-tri-*O*-methyl-β-D-glucopyranoside.

TABLE I

Hydrolysis products from methylated glucomannan

	Molar ratio
(1) 2,3,4,6-Tetra-*O*-methyl-D-glucose	2.8
(2) 2,3,4,6-Tetra-*O*-methyl-D-galactose	1
(3) 2,3,6-Tri-*O*-methyl-D-mannose	52
(4) 2,3,6-Tri-*O*-methyl-D-glucose	15.3
(5) Di-*O*-methyl galactose	2
(6) Di-*O*-methyl glucose	1

in the gas–liquid partition chromatograms but had such a large retention volume that space did not permit its inclusion in Fig. 5. The peaks in Figs. 5 and 6 were identified by comparison with authentic samples on the gas–liquid partition chromatogram. These identities were confirmed by collection of samples from the effluent gas stream of a semi-preparative apparatus and isolation of crystalline derivatives. There were not sufficient amounts of components 5 and 6, Table I, to permit complete identification; it was only possible to establish the parent sugar by demethylation and chromatography. In Table I components 1 and 2 represent the non-reducing terminal units and components 3 and 4 must have originated from a series of 1 → 4 linked D-mannose and D-glucose units. The structural significance of components 5 and 6 is rather more difficult to assess. Hydrolysis products of the periodate-oxidized, reduced glucomannan showed that any branch points in the polysaccharide must be through C_6 and therefore, to be structurally significant, these di-*O*-methyl hexoses must be the 2,3-di-*O*-methyl isomers. Unfortunately it was not possible to make positive identifications which would decide this point. It is possible, of course, that the di-*O*-methyl hexoses were products of incomplete methylation or of demethylation during hydrolysis. However, it was noteworthy that none of the major monosaccharide component (D-mannose) in the polysaccharide showed up as a di-*O*-methyl derivative. It may be that different monosaccharides are methylated or demethylated to different extents depending perhaps on their position in the polysaccharide and on the spatial disposition (conformation) of their hydroxyl groups. These are points which seem worthy of investigation and until they are clarified the authors are reluctant to assign a branch point to the polysaccharide. It is worth mentioning that the di-*O*-methyl hexoses were barely detectable by paper chromatography and almost certainly would

have been dismissed as trace amounts in any quantitative estimation by that technique. The more accurate data available from gas–liquid partition chromatography would appear to necessitate a reassessment of the methylation technique for studying polysaccharides. The ratio of tetra- to tri-*O*-methyl ethers from the methylated glucomannan was 1:17.7, a value in reasonable agreement with the degrees of polymerization of 20 and 21 found respectively by formic acid production during periodate oxidation and by the erythritol:glycerol ratio in the hydrolyzate of the oxidized, reduced polysaccharide. Because of this agreement a linear structure is favored for the polysaccharide. The observations that the polysaccharide was electrophoretically homogeneous, that D-galactose persisted as a component sugar through repeated copper complexing, and that 50% of the D-galactose showed up in the methylated polysaccharide as non-reducing terminal units showed that D-galactose was an integral part of the polysaccharide and was not present in a contaminant.

Two structures are possible for the glucomannan from jack pine: (*a*) linear chains of $1 \rightarrow 4$ linked β-D-glucose and β-D-mannose units some of which are terminated by glucose and others by galactose units, (*b*) the same linear chains but with a proportion of the molecules (approximately 1 in 2.8) containing D-galactose units attached as single unit side chains. It is not possible to decide between these alternatives from the evidence available at the present time. The presence of D-galactose in glucomannans has been observed before but it has not always been considered to be an integral part of the polysaccharide. Loblolly pine contains a polysaccharide made up of D-glucose, D-mannose, and D-galactose residues (12, 13). In the first investigation (12) of this material all of the D-galactose was found as non-reducing terminal units and was considered to have arisen from a galactomannan present in admixture with the glucomannan. In a later investigation (13) of the same hemicelluloses, D-galactose was present as non-reducing terminal unit and there were two such units (one of mannose and one of galactose) per chain of 27–33 residues. Hamilton and Partlow (18) found di-*O*-methyl- and 2,3,4,6-tetra-*O*-methyl-D-galactose in the methylated glucomannan from western red cedar and attributed these results to the presence of a contaminating galactoglucomannan. Dutton and Hunt (15) found D-galactose as a non-reducing terminal unit in one fraction of a glucomannan from Sitka spruce. They concluded that it was part of a low molecular weight polysaccharide because dialysis of another fraction of the same material yielded a product which contained no D-galactose. Glucomannan fractions from Scots pine (19) contained D-galactose and D-xylose but both of these sugars were removed by further delignification of the polysaccharides. From this result it was postulated that several polysaccharides might be joined to the same lignin molecule and their separation prevented thereby. D-Galactose was not found as a constituent sugar in glucomannans from western hemlock (17), Norwegian spruce (16), and in another investigation of Sitka spruce (14).

Other differences between glucomannans from various sources are in the non-reducing terminal units, other than D-galactose, and in the results of periodate oxidation. In the present work D-glucose formed the only non-reducing terminal units other than D-galactose. It is certain that no 2,3,4,6-tetra-*O*-methyl-D-mannose was present because it would have been separated from 2,3,4,6-tetra-*O*-methyl glucose by gas–liquid partition chromatography and would have emerged before peak 1, Fig. 5. Similar results have been obtained from the glucomannan of western red cedar (18) but those of western hemlock (17) and Scots pine (19) contained non-reducing terminal units of both D-glucose and D-mannose. On the other hand glucomannans from loblolly pine (12, 13), Sitka spruce (14, 15), and Norwegian spruce (16) had non-reducing terminal units of D-mannose and

none of D-glucose. It is possible that some of these differences have been caused by the difficulty in separating the 2,3,4,6-tetra-*O*-methyl ethers of D-glucose and D-mannose from each other (14).

Only the glucomannans of western hemlock (6), Norwegian spruce (16), and Scots pine (19) have been examined by the Smith degradation (22). All of these yielded D-glucose plus a trace of D-mannose in hydrolyzates of the periodate-oxidized, reduced polysaccharides and the results were interpreted as indicative of branching through C_2 or C_3 of the glucose units. No D-glucose or D-mannose was found in the present work after the same sequence of reactions had been applied to the glucomannan from jack pine. This difference may have been caused by the different times allowed for oxidation. The glucomannans from western hemlock (6), Norwegian spruce (16), and Scots pine (19) were oxidized for 432, 350, and 174 hours respectively while that from jack pine was oxidized for 552 hours. It has been shown (25) that sugar units are resistant to oxidation by periodate if the hydroxyls on C_2 and C_3 are in *trans* position in a rigid conformation. Although little is known about the conformation of sugar units in polysaccharides it is possible that the above conditions could obtain for a chain of $1 \rightarrow 4$ linked D-glucose units. This would account for the presence in the periodate-oxidized glucomannans of more D-glucose than D-mannose which has its C_2 and C_3 hydroxyls in *cis* orientation. Hamilton and Smith (26) have stressed the importance of prolonged oxidation if this technique is to be used to detect branch points.

Clearly, further work is necessary to ascertain the structural significance of the D-galactose residues in glucomannans, and to decide whether branch points are present or absent. One possible approach to these questions, fragmentation analysis by enzyme hydrolysis, is now in progress in this laboratory.

EXPERIMENTAL

Paper chromatograms were run by the descending method using the following solvent systems (v/v):

(A) butan-1-ol:pyridine:water, 6:4:3;
(B) ethyl acetate:acetic acid:water, 4:1:4;
(C) butan-1-ol:ethanol:water, 3:1:1.

Reducing sugars were detected on paper chromatograms by the *p*-anisidine hydrochloride spray reagent (27); non-reducing components were detected by silver nitrate and sodium hydroxide sprays (28). Evaporations were carried out in a rotary film evaporator under diminished pressure at 35° C or less. Melting points are corrected and rotations are equilibrium values unless otherwise stated.

Isolation of Glucomannan

The sequence of extractions is shown in Fig. 1. Extractive-free jack pine wood was extracted with water which removed an arabogalactan (0.5%) (20). The residue from this extraction was delignified by acid chlorite (29) and then extracted successively with 10% and 17% potassium hydroxide and finally with 24% potassium hydroxide containing 4% of sodium tetraborate (21). Three extractions, each of 24-hour duration, were made at each alkali concentration. Each extract was neutralized with acetic acid, dialyzed to remove inorganic salts, and the non-dialyzables were freeze-dried to yield the crude polysaccharides.

Figure 1 shows the order of the above extractions and the component sugars in the polysaccharides as detected by paper chromatography (solvents A and B) after hydrolysis

for 12 hours at 97° C by *N* hydrochloric acid. Yields of polysaccharides in the alkaline extractions were based on holocellulose. The 10% potassium hydroxide removed mainly xylan as shown by the predominance of xylose in the hydrolyzate from this polysaccharide mixture. The 17% potassium hydroxide extraction yielded roughly equal quantities of pentosan and hexosan; the final extraction with 24% potassium hydroxide and 4% sodium tetraborate yielded a polysaccharide which contained only glucose, mannose, and galactose. The polysaccharides in the 10% and 17% potassium hydroxide extracts were precipitated as their copper complexes. The precipitates were washed thoroughly with water, dissolved in cold *N* hydrochloric acid, and poured into 4 volumes of ethanol to reprecipitate the polysaccharides which were then examined by hydrolysis and chromatography as described above. Four precipitations of the copper complex were required to yield a glucomannan from the polysaccharides extracted by 10% potassium hydroxide. One such treatment sufficed to give the same result with the polysaccharides extracted by 17% potassium hydroxide. However, yields of glucomannan from these fractions were low (ca. 1% of the fraction) and the remainder of the work was carried out on the polysaccharide extracted by 24% potassium hydroxide and 4% sodium tetraborate.

The polysaccharide showed a single sharp peak (Fig. 2) ($\mu = 9.86 \times 10^{-5}$ cm^2, volts^{-1}, sec^{-1}) on moving boundary electrophoresis in 0.05 *M* borate buffer carried out in a Spinco Model H Tiselius-type apparatus. Electrophoretic patterns at two time intervals are included in Fig. 2 to show that the first peak did not migrate and is in fact a false boundary. This has been proved by Adams (30), who has isolated material responsible for this peak, which always occurs in electrophoresis in borate, and showed that it yielded no sugars on hydrolysis. The monosaccharide composition, mannose:glucose:galactose, 49:17:2, determined by the phenol–sulphuric acid method (31), was unchanged by repeated fractionation of the polysaccharide as its copper complex. The glucomannan had $[\alpha]_D^{27} = -26°$ (*c*, 1% in *N* sodium hydroxide) and did not yield any sugars detectable by paper chromatography when heated at 97° C with 0.025 *N* oxalic acid for 3 hours.

Periodate Oxidation of Glucomannan

Sodium metaperiodate (6.47 g) was dissolved in water (150 ml) and *N* sodium hydroxide was added to adjust the solution to pH 4.37. This reagent (30 ml) was added to duplicate samples (121 mg) of the polysaccharide suspended in water (120 ml). Reagent blanks were also prepared and the oxidations were allowed to proceed in the absence of light and with continuous shaking. At the intervals noted below samples were removed for estimation of periodate consumption and formic acid production.

For estimation of formic acid, 2,3-butanediol (6 drops) was added to the sample (20 ml), which was then kept in the dark for 30 minutes. A few crystals of potassium iodide were then added and the liberated iodine was titrated to a starch end point with 0.01 *N* sodium thiosulphate.

Periodate was estimated by the excess arsenite method of Fleury and Lange (32, 33). Results of these two estimations in moles per mole anhydrohexose at various time intervals were as follows:

Time (hours)	21	45	47	69	71	93	95	167	170	552
Formic acid	0.067	0.077	—	0.086	—	0.088	—	0.098	—	0.106
Periodate	—	—	0.087	—	0.85	—	0.85	—	0.88	1.11

In a separate experiment (Fig. 3) (22) the glucomannan (1.0 g) was oxidized by 0.4 *M* sodium metaperiodate (50 ml) at 21° C for 23 days. Iodate and excess periodate were

precipitated by addition of 0.5 *M* barium acetate and the precipitate was filtered. The filtrate was deionized by Amberlite ion exchange resins IR-45 and IR-120 and potassium borohydride (1.0 g) was then added. After 48 hours the solution was neutralized with acetic acid and deionized by Amberlite IR-45 and IR-120. The solution was then evaporated to dryness and last traces of borate were removed from the residue by repeated evaporation with methanol. The residue was dissolved in water (50 ml) and an aliquot (1 ml) was hydrolyzed by *N* hydrochloric acid (1 ml) at 97° C for 6 hours. Paper chromatograms (solvents A and B) showed the presence of two components that were identical with authentic samples of erythritol and glycerol run on the same paper strips. No component corresponding to a monosaccharide could be found, even on heavily loaded chromatograms. Another aliquot of the polyol solution (5 ml) was evaporated to dryness and the residue, dried *in vacuo*, was heated at 80° C for 20 hours in a solution (20 ml) of acetic anhydride containing 2% of sulphuric acid. The acetolysate was examined directly by gas–liquid partition chromatography (23, 24) and the separation curve is shown in Fig. 4. Authentic samples of glycerol triacetate and erythritol tetraacetate gave the same retention volumes as peaks 1 and 3, Fig. 4, respectively, either when run separately or when added to the unknown mixture. The compound giving peak 3 was collected from the effluent gas stream and the product crystallized spontaneously. Recrystallization from ether: petroleum ether (30–60° C) gave a compound with a melting point of 84–85° C. A mixed melting point with authentic erythritol tetraacetate was 84–86° C. The compound giving peak 1 was also collected but glycerol triacetate is liquid at room temperature and there was not sufficient material to permit deacetylation and formation of another derivative.

The ratio of erythritol to glycerol was 20.8:1 as determined from the relative areas under peaks 3 and 1 (24).

Methylation of Glucomannan

The glucomannan (1.5 g) was acetylated with acetic anhydride (30 ml) in pyridine (45 ml). The mixture was poured into water and the precipitated polysaccharide acetate was centrifuged, washed with water, and dried *in vacuo*; yield, 1.3 g. This product was dissolved in tetrahydrofuran (25 ml), sodium hydroxide (17 g) was added, and the mixture was stirred during dropwise addition of dimethyl sulphate (20 ml) (34). A second addition of reagents was made and the mixture was then refluxed for 1 hour. A further 10 additions of the same quantities of sodium hydroxide and dimethyl sulphate were made over a period of 4 days with continuous stirring and occasional addition of tetrahydrofuran to maintain fluidity. The solution was refluxed for 1 hour, cooled, and filtered. The filtrate and the residual solids (dissolved in water) were extracted continuously with chloroform for 24 hours. The aqueous phases from the two extractions were evaporated to dryness and the residues were extracted with chloroform and methanol. All extracts were combined, dried, and evaporated to yield a product (1.12 g) with a methoxyl content of 38.0%. This product was methylated six times with Purdie's reagents using the same amounts of methyl iodide (25 ml) and silver oxide (5 g) for each methylation. The product (0.76 g) from these methylations had a methoxyl content of 42.2% and showed no hydroxyl absorption in the infrared.

Hydrolysis of Methylated Glucomannan

The methylated glucomannan (0.72 g) was hydrolyzed by formic acid according to the procedure of Jones and Wilkie (35). The hydrolyzate was examined by paper chromatography (solvent C) and showed a major component which corresponded to 2,3,6-tri-*O*-

methyl-D-mannose; minor components were chromatographically identical with 2,3,4,6-tetra-*O*-methyl-D-glucose; 2,3,4,6-tetra-*O*-methyl-D-galactose; and 2,3,6-tri-*O*-methyl-D-glucose. Trace amounts of two di-*O*-methyl hexoses were also present.

The mixture of sugars was refluxed with 5% methanolic hydrogen chloride and the resulting mixture of glycosides was analyzed by gas–liquid partition chromatography (23, 24). Figure 5 shows the separation of the total mixture on a liquid phase of Apiezon M. In addition to the components shown there was another di-*O*-methyl hexose, present in half the quantity of peak 5, Fig. 5, which had a much larger retention volume and could not be included in the diagram. Identities of the peaks were established by comparison with authentic samples of the compounds listed and were confirmed by isolation of crystalline derivatives as described below. Because it was known that several methylated sugars had the same retention volumes of peaks 1 and 2, Fig. 5, under the conditions used, the compounds giving these two peaks were collected as one fraction from the effluent gas stream and were re-run using butanediol succinate polyester as the liquid phase. The separation, shown in Fig. 6, illustrated clearly that the major component of peak 2, Fig. 5, was the β-methyl glycoside of 2,3,6-tri-*O*-methyl-D-glucose. Figure 6 also shows that no tetra-*O*-methyl-D-mannose was present because it would have appeared between the anomeric methyl glycosides of 2,3,4,6-tetra-*O*-methyl-D-glucose. Peaks 5, 6, and 7, Fig. 6, were not identified conclusively but were probably di-*O*-methyl pentoses arising from a small amount of pentosan present as impurity in the glucomannan. The detection of these components serves to illustrate the sensitivity of gas–liquid partition chromatography because no pentoses could be detected by paper chromatography in hydrolyzates of the polysaccharide or of its methyl ether.

The quantitative data given in Table I were obtained directly from the curves shown in Figs. 5 and 6 by measurement of the areas under the peaks. Areas of peaks representing anomeric glycosides of the same sugar were, of course, added together.

Identification of O-Methyl Ethers

Semipreparative gas–liquid partition chromatography of the mixture of methyl glycosides was carried out at 180° C on an 8-ft column (6-mm I.D.) containing 20% Apiezon M on Celite 545. The apparatus used (23) permitted collection of 1–15 mg of each component.

2,3,4,6-Tetra-O-methyl-D-glucose

This component was collected from the effluent gas stream as its liquid α-methyl glycoside. The glycoside (1 mg) was hydrolyzed at 97° C in *N* hydrochloric acid (0.5 ml) for 6 hours and the hydrolyzate was evaporated to dryness. Ethanol (0.2 ml) and freshly distilled aniline (1 drop) were added, the solution was refluxed for 20 minutes, and then cooled at 5° C for 20 hours. The fine, white needles that separated had a melting point of 115–120° C. Recrystallization from ethanol:water gave a product with a melting point of 134–135° C, and a mixed melting point with an authentic sample of *N*-phenyl 2,3,4,6-tetra-*O*-methyl-D-glucosylamine was 134–136° C. Reported (36): m.p. 135° C.

2,3,4,6-Tetra-O-methyl-D-galactose

This component was collected from the effluent gas stream as a mixture of its anomeric methyl glycosides. These were hydrolyzed and anilide formation was carried out as just described. The crystalline product had a melting point of 192° C, undepressed by admixture with an authentic sample of *N*-phenyl-2,3,4,6-tetra-*O*-methyl-D-galactosylamine. Reported (37): m.p. 192° C.

*2,3,6-Tri-O-methyl-*D*-glucose*

The anomeric methyl glycosides of this component were widely separated by gas–liquid partition chromatography and were collected separately. Methyl 2,3,6-tri-*O*-methyl-β-D-glucopyranoside crystallized in the collection tube and was recrystallized from ether: petroleum ether (30–60° C), m.p. 59° C and mixed m.p. 59–60° C with an authentic sample of methyl-2,3,6-tri-*O*-methyl-β-D-glucopyranoside. Reported (38): m.p. 58–60° C.

The α-methyl glycoside was hydrolyzed with *N* hydrochloric acid at 97° C for 6 hours. The hydrolyzate was neutralized with Amberlite IR-45 ion exchange resin and evaporated to dryness in a desiccator. The residue crystallized, m.p. 115–120° C, and was recrystallized from ether to yield a product with m.p. 121–122° C, undepressed by admixture with authentic 2,3,6-tri-*O*-methyl-D-glucose. Reported (39): m.p. 121–123° C.

*2,3,6-Tri-O-methyl-*D*-mannose*

This component was collected as its sirupy α-methyl glycoside (15 mg) which was then hydrolyzed by *N* hydrochloric acid at 97° C for 6 hours. The hydrolyzate was evaporated to dryness and anilide formation was carried out as described for 2,3,4,6-tetra-*O*-methyl-D-glucose. The product was recrystallized from ether:petroleum ether (30–60° C) to m.p. 128° C, undepressed by admixture with an authentic sample of *N* phenyl-2,3,6-tri-*O*-methyl-D-mannosylamine. Reported (40): m.p. 127–128° C.

Di-O-methyl Hexoses

Peak 5, Fig. 5, and the other di-*O*-methyl-hexose which had too large a retention volume to be included in Fig. 5 were collected separately and were hydrolyzed and demethylated simultaneously by 48% hydrobromic acid at 97° C in a sealed tube for 20 minutes. The solutions were neutralized (silver carbonate), concentrated, and the total samples were examined by paper chromatography (solvent A). Galactose was obtained from peak 5, Fig. 5, by this procedure while the other di-*O*-methyl hexose yielded glucose.

ACKNOWLEDGMENTS

The authors wish to thank Dr. T. E. Timell, who generously donated samples of 2,3,6-tri-*O*-methyl ethers of D-glucose and D-mannose. Analyses were done by Mr. A. E. Castagne.

REFERENCES

1. G. Bertrand. Compt. rend. **129**, 1025 (1899).
2. K. Hess and M. Ludtke. Ann. **466**, 18 (1928).
3. E. Husemann. J. prakt. chem. **155**, 13 (1940).
4. J. G. Leech. Tappi, **35**, 249 (1952).
5. A. Anthis. Tappi, **39**, 401 (1956).
6. J. K. Hamilton, H. W. Kircher, and N. S. Thompson. J. Am. Chem. Soc. **78**, 2508 (1956).
7. T. E. Timell and A. Tyminski. Tappi, **40**, 519 (1957).
8. G. A. Adams. Tappi, **40**, 721 (1957).
9. J. K. N. Jones and T. J. Painter. J. Chem. Soc. 669 (1957).
10. B. Lindberg and H. Meier. Svensk. Papperstidn. **60**, 785 (1957).
11. E. Merler and L. E. Wise. Tappi, **41**, 80 (1958).
12. D. H. Ball, J. K. N. Jones, W. H. Nicholson, and T. J. Painter. Tappi, **39**, 438 (1956).
13. J. K. N. Jones and T. J. Painter. J. Chem. Soc. 573 (1959).
14. G. O. Aspinall, R. A. Laidlaw, and R. B. Rashbrook. J. Chem. Soc. 4444 (1957).
15. G. G. S. Dutton and K. Hunt. J. Am. Chem. Soc. **80**, 5697 (1958).
16. I. Croon and B. Lindberg. Acta Chem. Scand. **12**, 453 (1958).
17. J. K. Hamilton and H. W. Kircher. J. Am. Chem. Soc. **80**, 4703 (1958).
18. J. K. Hamilton and E. V. Partlow. J. Am. Chem. Soc. **80**, 4880 (1958).
19. I. Croon, B. Lindberg, and H. Meier. Acta Chem. Scand. **13**, 1299 (1959).
20. C. T. Bishop. Can. J. Chem. **35**, 1010 (1957).
21. J. K. N. Jones, L. E. Wise, and J. P. Jappe. Tappi, **39**, 139 (1956).
22. M. Abdel-Akher, J. K. Hamilton, R. Montgomery, and F. Smith. J. Am. Chem. Soc. **74**, 4970 (1952).

23. A. G. McINNES, D. H. BALL, F. P. COOPER, and C. T. BISHOP. J. Chromato. **1**, 556 (1958).
24. C. T. BISHOP and F. P. COOPER. Can. J. Chem. **38**, 388 (1960).
25. B. H. ALEXANDER, R. J. DIMLER, and C. L. MEHLTRETTER. J. Am. Chem. Soc. **73**, 4658 (1951).
26. J. K. HAMILTON and F. SMITH. J. Am. Chem. Soc. **78**, 5910 (1956).
27. L. HOUGH, J. K. N. JONES, and W. H. WADMAN. J. Chem. Soc. 1702 (1950).
28. W. E. TREVELYAN, D. P. PROCTER, and J. S. HARRISON. Nature, **166**, 444 (1950).
29. L. E. WISE, M. MURPHY, and A. A. D'ADDIECO. Paper Trade J. **122**, 35 (1946).
30. G. A. ADAMS. Unpublished results.
31. M. DUBOIS, K. A. GILLES, J. K. HAMILTON, P. A. REBERS, and F. SMITH. Anal. Chem. **28**, 350 (1956).
32. P. P. FLEURY and J. LANGE. J. pharm. chim. **17**, 107 (1933).
33. D. H. GRANGAARD, E. K. GLADDING, and C. B. PURVES. Paper Trade J. **115**, 41 (1942).
34. E. L. FALCONER and G. A. ADAMS. Can. J. Chem. **34**, 338 (1956).
35. J. K. N. JONES and K. C. B. WILKIE. Can. J. Biochem. and Physiol. **37**, 377 (1959).
36. J. C. IRVINE and A. M. MOODIE. J. Chem. Soc. 93, 95 (1908).
37. J. C. IRVINE and D. MCNICOLL. J. Chem. Soc. 97, 1449 (1910).
38. J. C. IRVINE and I. M. A. BLACK. J. Chem. Soc. 862 (1926).
39. J. C. IRVINE and E. L. HIRST. J. Chem. Soc. 121, 1213 (1922).
40. W. N. HAWORTH, E. L. HIRST, and H. R. L. STREIGHT. J. Chem. Soc. 1349 (1931).

11-OCTADECENOIC ACID AND OTHER FATTY ACIDS OF ASCLEPIAS SYRIACA SEED OIL[1]

MARY J. CHISHOLM AND C. Y. HOPKINS

ABSTRACT

The seed oil of *Asclepias syriaca* L., family Asclepidaceae, was examined by gas chromatography and distillation of the methyl esters. The fatty acids were found to include a considerable proportion of *cis*-11-octadecenoic acid, which has not been observed previously in seed oils. It was obtained as a concentrate ($\simeq 80\%$) by low-temperature crystallization of the C18 acids and identified as 11,12-dihydroxystearic acid. The amount of 11-octadecenoic acid in the oil was determined by oxidative splitting of the total fatty acids and estimation of the resulting azelaic and undecanedioic acids by gas chromatography.

The C16 acids included 9,12-hexadecadienoic acid, which is rare in seed oils, and an unusually large proportion of 9-hexadecenoic acid. The percentage composition of the fatty acids was estimated from the data as follows: palmitic 4,9-hexadecenoic 10, 9,12-hexadecadienoic 2, stearic <1, oleic 15, 11-octadecenoic 15, linoleic 53, linolenic <1. The unsaturated acids have the *cis* configuration.

INTRODUCTION

In preparation for a study of the development of oil in a maturing seed, it was desired to know the normal composition of the seed oil of *Asclepias syriaca* L. (common milkweed), family Asclepidaceae. The oil of this species has been examined by a number of workers in the past and the fatty acids have been reported for the most part as consisting of the ordinary oleic, linoleic, and saturated acids (1, 2, 3). However, there are some indications in these reports of the presence of less common constituents.

In the present work, the seed oil of *Asclepias syriaca* L. was examined by distillation of the methyl esters, followed by low-temperature crystallization and gas chromatography of the fractions. The identity of the individual acids was determined with certainty by orthodox procedures.

The results show that the oil has by no means a simple palmitic–oleic–linoleic composition. A novel constituent is 11-octadecenoic acid, reported here for the first time in a seed oil. The amount is substantial and is estimated to be 15% of the total fatty acids. Ordinary oleic acid is present also.

The composition of the C16 acids is distinctly different from that of the common seed oils. The major C16 acid is 9-hexadecenoic and the ratio of 9-hexadecenoic acid to palmitic acid is 2:1 or greater. There is an appreciable amount of 9,12-hexadecadienoic acid, which is known in only one other seed oil (4).

The presence of an isomer of oleic acid (other than the well-known petroselinic acid) in seed oils has been suspected from time to time. As early as 1927, Hilditch, Riley, and Vidyarthi reviewed the claims for the existence of such an isomer in rapeseed oil and examined a number of Cruciferae oils (5). They found strong evidence of a possible 1 or 2% of isomers of oleic acid in rapeseed and mustard-seed oils but did not succeed in identifying them. Millican and Brown noticed similar indications of an isomer or isomers in rapeseed and soybean oils (6).

The present investigation establishes the occurrence of *cis*-11-octadecenoic acid* in the glycerides of *Asclepias syriaca* seed oil. No evidence was found of any other octadecenoic acid except the ordinary oleic acid.

[1]*Manuscript received February 15, 1960.*
Contribution from the Division of Pure Chemistry, National Research Council, Ottawa, Canada. Presented at the meeting of the American Chemical Society, Cleveland, Ohio, April, 1960.
Issued as N.R.C. No. 5646.

**If a trivial name is desired, it is suggested that cis-11-octadecenoic acid be called "asclepic acid".*

EXPERIMENTAL

Seed pods of *Asclepias syriaca* L. were collected in late September, 1959, from a stand of wild plants near Ottawa. The seed was removed from the pods by hand, dried, ground, and extracted with petroleum ether. The following data were recorded: moisture in seeds as harvested, 39.6%; mean weight of seeds (moisture-free) per pod, 0.82 g; weight of 100 seeds (moisture-free), 0.57 g; oil content of seeds (moisture-free basis), 19.4%. Constants of the oil are shown in Table I.

TABLE I

Properties of the oil

Iodine value	127.2	Acetyl value	0
Acid value	1.5	Refractive index, 25°	1.4748
Unsaponifiable matter, %	2.2	Equiv. wt. of mixed fatty acids	279.0

Separation of the Fatty Acids

The oil was converted to methyl esters by methanolysis with dry hydrogen chloride catalyst and the esters were examined by gas–liquid chromatography, using a polyester liquid phase. The detector was a thermistor type of thermal conductivity cell. Column length was 1 meter, temperature 190°, and helium flow rate 95 ml/minute, at an inlet pressure of 12.5 p.s.i. The chromatogram is shown in Fig. 1.

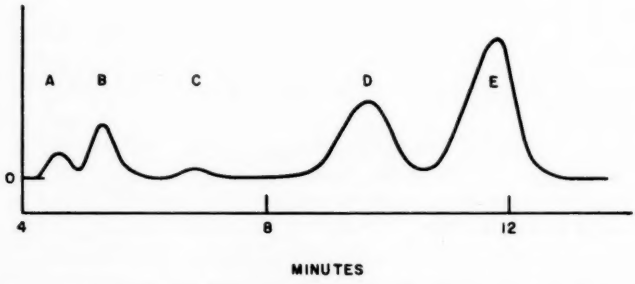

FIG. 1. Main portion of the gas chromatogram of the methyl esters. The peaks represent esters of the following acids: A, palmitic; B, hexadecenoic; C, hexadecadienoic; D, octadecenoic; E, linoleic. A small peak at 15.4 minutes (not shown) is assigned to linolenic acid.

Tentative identification of peaks A, D, and E was made by comparing emergence times with those of authentic samples. The identity of all of the main components was established after distillation of the esters as described below. The chromatogram also indicated the presence of traces of stearic and linolenic acids (less than 1% of each) but no C20 acids.

The main portion of the methyl esters was distilled through a spinning band column at 0.5 mm pressure in order to collect the C16 acids. Distillation data are given in Table II.

Examination of the distilled portions by gas chromatography showed that fraction 1 consisted of three acids in the C16 range, presumably palmitic, hexadecenoic, and hexadecadienoic. The intermediate fraction 2 contained these in lesser amounts along with octadecenoic and octadecadienoic acids. Fraction 3 consisted almost entirely of C18 acids.

TABLE II

Distillation of methyl esters

Fraction	Temp., °C (0.5 mm)	Weight, g	Predominant chain length	Iodine value	Refractive index, 25°
1	120–122	9.1	C16	76.9	1.4472
2	122–131	0.9	—	104.4	1.4517
3	131–133	9.8	C18	145.1	1.4571
R	Residue				

THE C16 ACIDS

Fraction 1 was estimated by gas chromatography to contain 14% of hexadecadienoate. Ultraviolet absorption analysis after alkali isomerization (45 minutes at 180° in glycerol–air) gave a value of 16.3% for dienoic ester, calculated as hexadecadienoate. A portion of fraction 1 (8 g) was subjected to fractional crystallization from acetone at low temperature (Table III). When examined by gas chromatography, the portion recovered from the final filtrate was found to consist of equal parts of hexadecenoate and hexadecadienoate.

TABLE III

Fractional crystallization of C16 methyl esters

Fraction	Crystallizing temp., °C	Yield, g	Refractive index, $n_D^{25°}$
1	−12	1.55	Solid at 25°
2	−60	0.80	Solid at 25°
3	−65*	3.05	1.4493
4	Filtrate	1.78	1.4548

*Crystallizing temperature after removing half of the solvent.

Palmitic Acid

Fraction 1 (Table III) was methyl palmitate. On saponification it gave pure palmitic acid directly, m.p. 62–62.5° alone and mixed with an authentic sample.

9-Hexadecenoic Acid

Fraction 3 (Table III) was almost entirely methyl hexadecenoate. It was identified by hydroxylation with alkaline permanganate (7). The product, when recrystallized from ethyl acetate, melted at 125–126° and did not lower the melting point of a known sample of erythro-9,10-dihydroxy-palmitic acid. The original acid was therefore *cis*-9-hexadecenoic acid.

9,12-Hexadecadienoic Acid

Fraction 4 (Table III) was hydroxylated in the same way and the dihydroxy acid was removed from the product by leaching with warm ethyl acetate. The remaining tetrahydroxy acid was recrystallized from a large volume of ethyl acetate. It melted at 163–164°. Calculated for tetrahydroxypalmitic acid, $C_{16}H_{32}O_6$: C, 59.98; H, 10.07. Found: C, 59.79; H, 9.92. This substance has not been reported hitherto.

In order to determine the position of the original double bonds, a portion of fraction 4 was subjected to oxidative splitting by periodate–permanganate (8). At the end of the reaction, the excess of reagents was destroyed by sodium bisulphite and the products

were extracted with ether. The ether solution was made alkaline to prevent loss of volatile acids and it was taken to dryness. *n*-Butanol containing an excess of dry hydrogen chloride was added and the mixture was refluxed to convert all of the acids to butyl esters. The excess butanol was allowed to remain and the mixture was examined by gas chromatography at a column temperature of 80°.

Since fraction 4 contained both monoenoic and dienoic acids, the products of splitting would include heptanoic and azelaic acids arising from 9-hexadecenoic acid, as well as those from the dienoic acid. The chromatogram showed peaks corresponding to two monobasic acids, butyric and heptanoic, in approximately equal amounts (as butyl esters). It is apparent that the heptanoic acid came from oxidation of the hexadecenoic acid since it has already been shown that its double bond is Δ^9. The butyric acid must have come from the dienoic acid. Thus, one double bond in the dienoic acid is situated between the fourth and fifth carbon atoms, counting from the methyl end of the chain. The chromatogram also showed traces of pentanoic and hexanoic acids, which may have arisen from minor proportions of isomeric monoene or diene acids.

The mixture of butyl esters was then chromatographed at a column temperature of 190°. Azelaic acid was the only dibasic acid detected. Thus both the monoenoic and dienoic acids gave azelaic acid. The corresponding double bond of the diene acid is therefore in the 9,10 position, counting from the carboxyl end of the chain and the acid is 9,12-hexadecadienoic acid. The tetrahydroxy acid (described above) must be erythro, erythro-9,10,12,13-tetrahydroxypalmitic acid, since permanganate oxidation of *cis* double bonds gives the erythro structure. The infrared spectrum of the C16 methyl esters (fraction 1, Table II) showed no *trans* absorption (965 cm^{-1}), hence both the monoene and diene acids are considered to have *cis* unsaturation.

THE C18 ACIDS

Examination of the esters of C16 and C18 acids is summarized in the following diagram, which shows in parentheses the acids identified in the various fractions from the ester distillation (Table II). The separation of the C18 acids is described below.

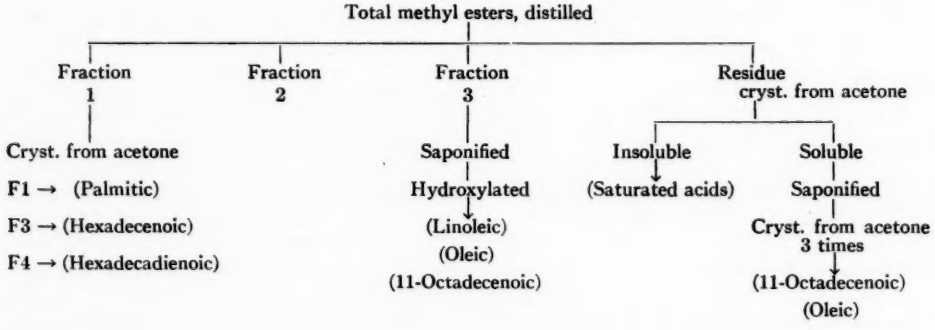

Linoleic Acid

A portion of fraction 3 of the distilled methyl esters (Table II) was saponified and the acids were hydroxylated by alkaline permanganate (7). Upon fractional crystallization from ethyl acetate, the most insoluble part of the product melted sharply at 171–172° and was identified by mixed melting point as erythro, erythro-tetrahydroxystearic acid, from ordinary linoleic acid.

Octadecenoic Acids

The more soluble portion, presumably dihydroxystearic acid, melted at 114–115°, unchanged on further recrystallization. It was evidently not the ordinary erythro-9,10-dihydroxystearic acid which melts when pure at 132°. The equivalent weight of the substance was 318.1 (dihydroxystearic acid 316.5).

It was subjected to splitting by permanganate–periodate (8). At the end of the reaction the acidic products were extracted with ether and the ether solution was made alkaline and evaporated to dryness. Methanol containing excess hydrogen chloride was added and refluxed gently. The mixture was poured into water and the methyl esters were extracted with cyclohexane, washed with a little aqueous sodium bicarbonate and water, and dried. The cyclohexane solution was submitted to gas chromatography at 80° and 130°. Monobasic acids were represented by two major peaks, corresponding in emergence times to heptanoate and nonoate, with a very small peak corresponding to hexanoate. There was no indication of octanoate or decanoate. It was concluded that the substance with a melting point of 114–115° must be a mixture of 9,10- and 11,12-dihydroxystearic acids, formed from oleic acid and 11-octadecenoic acid. The ratio of nonoate (from oleic) to heptanoate (from 11-octadecenoic), determined from the area of the peaks, was 5:4.

The hexanoate was probably formed from a little tetrahydroxystearic acid (from linoleic acid) present in the dihydroxy acid mixture. It amounted to 6% of the total of the C6–C9 acids by peak area measurement.

When the mixture of methyl esters was chromatographed at 170°, peaks corresponding to azelate and undecanedioate appeared. There was no evidence of sebacate. This confirms the presence of 9,10- and 11,12-dihydroxystearic acids in the original mixture. The undecanedioate could not have arisen from eicosenoic acid since the chromatogram of the total esters of the oil showed that no C20 acids were present. The ratio of azelate to undecanedioate was 5:4.

Identification of 11-Octadecenoic Acid

Confirmatory evidence of the presence of 11-octadecenoic acid was sought. The residue from the distillation of methyl esters (Table II) (46.0 g) was crystallized from 400 ml of acetone at −30°. The crystals (4.1 g) were saponified and recrystallized twice from ethanol, giving 1.1 g of solid acid(s) melting at 66–68°. It depressed the melting point of pure stearic acid and is judged to contain some higher saturated acid(s).

The filtrate from the crystallization of the esters was evaporated, the esters saponified, the unsaponifiable matter removed, and the acids recovered (38.0 g). These acids (largely linoleic acid) were crystallized successively from 380 ml of acetone at −45° and from 50 ml of acetone at −35°, giving 4.3 g of acids of refractive index $\alpha_D^{25°}$ 1.4595 (oleic acid, 1.4581). This product was crystallized fractionally from 40 ml of acetone as follows:

Fraction	Temp. of crystallization, °C	Yield, g	Iodine value	$\alpha_D^{25°}$
1	−22	1.3	78.3	Semisolid
2	−40	1.3	89.6	1.4591
3	Filtrate	1.3		1.4645

Fraction 1 probably contained a little stearic acid and fraction 3 some linoleic acid. The fraction of iodine value 78.3 was hydroxylated by alkaline permanganate for 15 minutes at 10°, yielding a dihydroxystearic acid, m.p. 128–128.5° after three crystallizations from

ethyl acetate, and washing with petroleum ether (yield 0.62 g). The equivalent weight was 315.8 (calculated for dihydroxystearic acid, 316.5). On mixing with erythro-9,10-dihydroxystearic acid (from oleic acid), it melted at 116–122°.

It was identified as erythro-11,12-dihydroxystearic acid by comparison with an authentic sample, kindly furnished by Dr. F. D. Gunstone. There was no depression of melting point in admixture with this sample. The melting point of erythro-11,12-dihydroxystearic acid from synthetic 11-octadecenoic acid is given by Ahmad (9) as 127–128° and by Huber (10) as 129–130°. Thus fraction 1 (iodine value 78.3) was mainly 11-octadecenoic acid.

To confirm the identification, the dihydroxy acid with a melting point of 128–128.5° was subjected to oxidative splitting by permanganate–periodate. The reaction mixture, when acidified, gave a precipitate with a melting point of 107–108°, raised to 109–110° by one crystallization from ethyl acetate. This proved to be undecanedioic acid. The equivalent weight was 109.2 (calc. 108.1). Its melting point was unchanged in admixture with an authentic sample prepared by oxidative splitting of 11,12-dihydroxyarachidic acid made from jojoba oil.

The filtrate from the oxidation was treated as before to convert the monobasic acids to methyl esters without loss. The mixture of esters was chromatographed at 80° and 130°. It gave only one peak in the region of medium chain length and that had the correct emergence time for methyl heptanoate, by comparison with an authentic sample. There was no evidence of monobasic acids of chain length C8–C12. The hydroxylated acid is therefore erythro-11,12-dihydroxystearic acid and the original acid in the oil is *cis*-11-octadecenoic acid.

The second fraction of the octadecenoic acids (I.V. 89.6) was submitted to oxidative splitting and the fragments were esterified and chromatographed at 80° and 170°. Peaks corresponding in emergence time to nonoate and azelate (from oleic acid) and to heptanoate and undecanedioate (from 11-octadecenoic acid) were recorded. There were no peaks in the regions corresponding to hexanoate, octanoate, suberate, and sebacate. The ratio of oleic acid to 11-octadecenoic acid in this fraction was estimated from the area of the peaks to be 28:72.

Total Composition

The fatty acid composition of the oil was estimated from the entire data, including the measurement of the peak areas in the gas chromatography of the methyl esters, the results of examination of the distilled ester fractions, and analysis of certain fractions by ultraviolet absorption. Calculated in this manner, the content of octadecenoic acids is 30% of the total fatty acids of the oil and the percentages of the other acids are as shown in Table IV.

TABLE IV

Estimated fatty acid composition (% of total fatty acids)

Acid	%	Acid	%
Palmitic	4	Stearic*	<1
9-Hexadecenoic	10	Oleic	15
9,12-Hexadecadienoic	2	11-Octadecenoic	15
		Linoleic	53
		Linolenic*	<1

*Identified by its emergence time under gas chromatography.

The content of 11-octadecenoic acid was determined by treating a sample of the total fatty acids of the oil with permanganate–periodate and determining the ratio of the resulting dibasic acids by gas chromatography at 170° (as methyl esters). In this reaction 11-octadecenoic acid yields undecanedioic acid while each of the other unsaturated acids of this oil gives azelaic acid. The ratio of undecanedioic acid to azelaic acid (w/w) was 16.5:83.5 (mean ratio of peak areas from triplicate samples). Allowing for the approximately 5% of saturated acids and taking into account the stoichiometric yield of the two dibasic acids from the various original unsaturated acids, the content of 11-octadecenoic acid is calculated to be 15% of the total fatty acids. Since the total octadecenoic acids are estimated at 30%, the content of oleic acid, by difference, is also 15% of the total fatty acids. The fatty acid composition is summarized in Table IV.

Other Samples

Samples of seed harvested in 1952 and 1958 were also examined. The oil content of these was 21.5% and 22.7% respectively (moisture free basis). The 1958 oil had iodine value 127.5, acid value 1.1, unsaponifiable matter 1.8%, and equivalent weight of the fatty acids 279.4. The oil from both lots was analyzed by gas chromatography and the 1952 sample was also treated by fractional distillation of its methyl esters and examination of the fractions. However, the ratio of oleic to 11-octadecenoic acid was not determined. The estimated percentages of fatty acids in the 1952 and 1958 oils were respectively: palmitic 5, 5; hexadecenoic 11, 12; hexadecadienoic 1.3, 1.7; octadecenoic acids 30, 33; linoleic acid 52, 47.

DISCUSSION

The oil is unusual in respect to the composition of both the C16 and C18 acids. One other seed oil of the family Asclepidaceae has been studied, viz. *Cryptostegia grandiflora* R. Br. (11). It was reported to be composed of the ordinary oleic, linoleic, and saturated fatty acids.

The occurrence of 11-octadecenoic acid in *Asclepias* oil was unexpected. An isomer of oleic acid was indicated when the erythro-dihydroxystearic acid was found to melt at 114–115° instead of the usual 132°. Apparently an equilibrium mixture was formed with the ordinary 9,10-dihydroxystearic acid which was not separable by ordinary crystallization from solvents. A similar anomalous melting point was observed by Watson and Levitin (12) when the oil of the *pods* of *Asclepias syriaca* was examined. Their dihydroxystearic acid melted at 116° but was not investigated further. Hilditch and co-workers obtained repeatedly a dihydroxy acid or mixture of acids, melting at 117–118°, from the C18 fractions of rapeseed and mustard-seed oils (5). A similar product was obtained by one of us (13) from the seed oil of *Conringia orientalis* L. (Cruciferae). On the basis of the present results, it seems likely that all of these consisted of mixtures of two or more position isomers of dihydroxystearic acid.

The possibility that 11-octadecenoic acid was formed by isomerization of oleic acid or ester during treatment is considered very unlikely. Similar treatment of many oils in this laboratory did not give evidence of such isomerization. The temperature reached in the distillation of the methyl esters in the present instance was lower than usual because only one-third of the esters was distilled off. It is also considered very unlikely that isomerization (shift of the double bond) occurred during the hydroxylation by alkaline permanganate or during the oxidative splitting by permanganate–periodate. Simple olefinic acids do not undergo a double-bond shift in these reactions to our knowledge.

11-Octadecenoic acid has been observed previously in the fat of bacteria, fish, and animals (14). The *trans* form is most common in animal fats and is thought to originate by bacterial action in the digestive process. Thus 11-octadecenoic acid may be to some extent characteristic of the lower forms of living matter. If so, its occurrence in *Asclepias*, along with the unusually large amount of unsaturated C16 acids, may give an indication of the place of this genus in the scale of evolution of plants.

11-Octadecenoic acid differs from most natural unsaturated fatty acids in having the double bond at the seventh carbon atom from the methyl end of the chain. In this respect, it is the same as 9-hexadecenoic acid which accompanies it in similar amount in this oil.

The unusually high content of 9-hexadecenoic acid and an appreciable content of 9,12-hexadecadienoic acid are noteworthy. The amount of hexadecenoic acid is exceeded in one other seed oil, viz. *Macadamia ternifolia* (Proteaceae) (15). Hexadecadienoic acid has been found in one other seed oil, viz. *Acacia giraffae* (Leguminosae) (4). The estimated amounts of C16 acids in these oils are as follows:

	C16 acids in total fatty acids, wt.%		
Species	Palmitic	Hexadecenoic	Hexadecadienoic
Asclepias syriaca	4	10	2
Macadamia ternifolia (15)	8	20	0 (16)
Acacia giraffae (4)	13	7	1

ACKNOWLEDGMENTS

The authors are grateful to Dr. R. W. Watson and Dr. H. A. Senn for assistance in procuring seed and to Mr. R. Lauzon for determination of infrared spectra.

REFERENCES

1. E. W. Eckey and L. P. Miller. Vegetable fats and oils. Reinhold Publishing Corp., New York. 1954. p. 727.
2. H. J. Lanson, D. Habib, and P. E. Spoerri. Ind. Eng. Chem. **37**, 179 (1945).
3. I. K. Matzurevich. J. Appl. Chem. (U.S.S.R.), **9**, 509 (1936); Chem. Abstr. **30**, 7887 (1936).
4. G. S. Harrison and F. Hawke. J. S. African Chem. Inst. **5**, 1, 23 (1952).
5. T. P. Hilditch, T. Riley, and N. L. Vidyarthi. J. Soc. Chem. Ind. (London), **46**, 462 T (1927).
6. R. C. Millican and J. B. Brown. J. Biol. Chem. **154**, 437 (1944).
7. A. Lapworth and E. N. Mottram. J. Chem. Soc. **127**, 1628 (1925).
8. R. U. Lemieux and E. von Rudloff. Can. J. Chem. **33**, 1701 (1955).
9. K. Ahmad, F. M. Bumpus, and F. M. Strong. J. Am. Chem. Soc. **70**, 3391 (1948).
10. W. F. Huber. J. Am. Chem. Soc. **73**, 2730 (1951).
11. R. H. Siddiqui and S. A. Warsi. Indian J. Pharm. **7**, 75, 88 (1945).
12. R. W. Watson and N. Levitin. Can. J. Research, F, **24**, 95 (1946).
13. C. Y. Hopkins. Can. J. Research, B, **24**, 211 (1946).
14. T. P. Hilditch. Chemical constitution of natural fats. 3rd ed. Chapman & Hall Ltd., London. 1956. p. 524.
15. R. E. Bridge and T. P. Hilditch. J. Chem. Soc. 2396 (1950).
16. C. Y. Hopkins. To be published.

EQUILIBRIUM DECOMPOSITION PRESSURES OF K_2TiCl_6[1]

S. N. Flengas and T. R. Ingraham

ABSTRACT

The equilibrium decomposition pressures of K_2TiCl_6 were measured at temperatures between 370° and 530° C, using a glass-bellows mercury manometer.

The pressure–temperature relationship was found to obey the equation

$$\log_{10} P(\text{cm of Hg}) = -\{(5.774\times10^3)/T\} + 9.120$$

and the heat of the reaction

$$K_2TiCl_{6(s)} \rightleftharpoons 2KCl_{(s)} + TiCl_{4(g)}$$

was found to be

$$\Delta H = +26.4\pm1.3 \text{ kcal/mole.}$$

INTRODUCTION

Because of its relatively high degree of stability at room temperature, the compound K_2TiCl_6 offers interesting possibilities as a source of $TiCl_4$ for the electrolytic preparation of titanium in fused salt baths. Indeed, K_2TiCl_6 may be an intermediate in the chain of chemical reactions proceeding in electrolytic cells which are supplied with gaseous $TiCl_4$ and contain KCl as a constituent of the bath.

K_2TiCl_6 has been prepared by wet chemical methods involving the dissolution of the mineral ilmenite ($FeO.TiO_2$) in aqueous sulphuric acid, and the salting out of K_2TiCl_6 by HCl in the presence of KCl (1) at 0° C. Unsuccessful attempts have been made to prepare the compound in an autoclave at about 300° C, by the direct reaction of KCl with $TiCl_4$ (2).

At higher temperatures, the direct reaction of KCl with $TiCl_4$ has been used successfully in these laboratories to prepare K_2TiCl_6 for use in studies of the potentials of the various titanium ions in molten salt solutions. In this preparation, which was reported in a previous paper (3), the experiments were done at temperatures from 230° to 500° C. It was observed that the rate of reaction was relatively slow at temperatures up to about 300° C, and attained a maximum rate at about 410° C. At temperatures substantially above 400° C, at which the rate of reaction might have been expected to increase, the rate of reaction decreased. It seemed probable that the compound K_2TiCl_6 was becoming increasingly unstable as the temperature was increased.

To confirm these implications, and to establish some of the thermodynamic properties of K_2TiCl_6 which might be of interest in evaluating it as a possible source of titanium tetrachloride for electrowinning cells, it was decided to study the equilibrium decomposition pressures of titanium tetrachloride over the compound.

Since our previous experience in preparing the compound had suggested that this solid–gas state reaction was relatively slow to establish equilibrium, a static method, rather than a dynamic method, of measuring the decomposition pressure was selected.

EXPERIMENTAL

The compound K_2TiCl_6 was prepared in a 1-in. diameter tube, bent in a right angle, and sealed at one end. Purified titanium tetrachloride was introduced into the closed vertical arm and was frozen with liquid air. A silica boat containing potassium chloride

[1]*Manuscript received February 10, 1960.*
Contribution from the Extraction Metallurgy Division, Mines Branch, Department of Mines and Technical Surveys, Ottawa, Ontario.

powder of a particle size less than 325 mesh was then placed in the horizontal arm and the tube was evacuated and sealed. By heating the titanium tetrachloride to a temperature between 130 and 134° C, and the potassium chloride to a temperature of about 400° C, for 12 hours, K_2TiCl_6 was formed quantitatively. When prepared by this method, the compound contained a small excess of adsorbed titanium tetrachloride. To prevent attack by moisture, the samples were transferred in a dry box to airtight glass containers.

The equilibrium decomposition pressures were measured in the apparatus shown diagrammatically in Fig. 1. The most important feature of the apparatus is the glass-

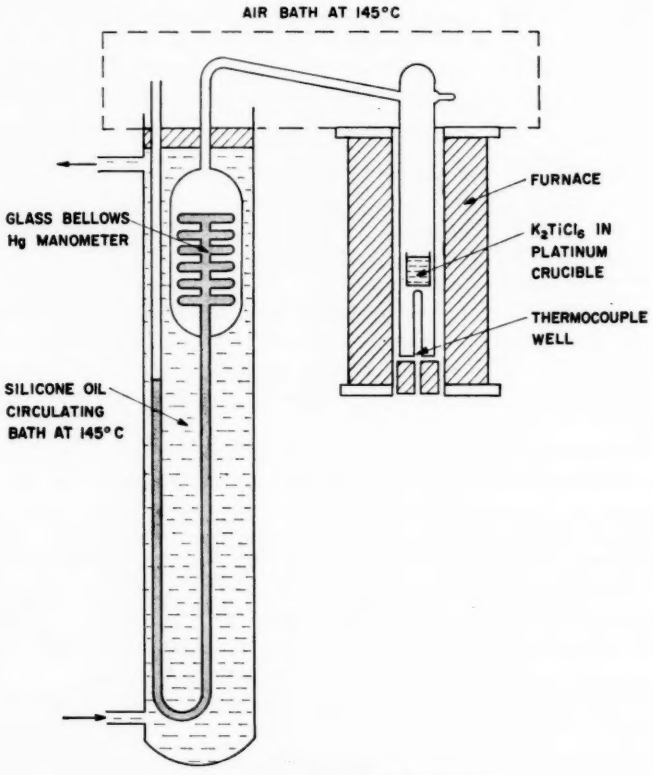

FIG. 1. Pressure measuring apparatus.

bellows mercury manometer, originally designed by Spence (4). It was modified for use in these experiments. This type of manometer is well suited to studies of equilibrium pressures in systems in which the decomposition product is a highly corrosive gas, which would be likely to attack conventional manometric liquids.

The manometer was calibrated at various pressures, and the relationship between the height of the mercury column of the manometer and the pressure was found to be linear over the pressure range between 1.2 and 76 cm. A deflection of 1.000 cm Hg was equivalent to a 1.540 cm of Hg pressure change. Pressure changes were observed with a cathetometer and were corrected for barometric fluctuations.

The reaction cell was constructed from Pyrex and Vycor. The Vycor section extended

out of the hot zone of the furnace, where it was joined, through a graded seal, to the Pyrex part of the apparatus. To avoid the condensation of titanium tetrachloride (b.p. 136.4° C), the bellows manometer was thermostatically controlled at a temperature of 145.0±0.1° C, using silicone oil (Dow Corning 550 fluid) as the heat transfer medium in a circulating bath. The connecting tube between the reaction cell and the manometer was also maintained at a temperature of 145.0±0.5° C by means of a thermostatically controlled air bath.

The reaction cell was heated in a tubular furnace, the temperature of which was kept constant, within ±1° C, by a thermocouple set in a well just below the sample and connected with a Kelwyn–Hughes phototransistor proportional temperature controller, type MIK IV.

To begin an experiment, about 10 grams of K_2TiCl_6 was transferred to a platinum crucible and the crucible was placed just above the thermocouple well. The open end of the reaction tube was then sealed and the apparatus was evacuated through a side arm for about 20 hours to remove excess titanium tetrachloride adsorbed on the K_2TiCl_6 powder. After evacuation was complete, the apparatus was sealed under vacuum and the furnace was heated to a predetermined temperature. Readings of the pressure were made at 2-hour intervals and equilibrium was considered to have been established when the pressure remained unchanged for a period of 12 hours. In the initial runs, it was observed that, at low temperatures, the same equilibrium pressure was not obtained readily when the temperature was approached from above and below. It was found that in spite of the 20-hour evacuation period, a small excess of $TiCl_4$ remained adsorbed on the sample. The $TiCl_4$ was removable by evacuation at higher temperatures, but it was found more convenient to mix excess KCl with the K_2TiCl_6 before beginning the run. When this was done, the same equilibrium pressures could be established readily on either an increasing or a decreasing temperature cycle.

RESULTS

The results obtained in three typical runs are shown in Table I.

TABLE I

Equilibrium decomposition pressures of K_2TiCl_6

Temperature (°C)	P (cm of Hg)		
	Run 1, using K_2TiCl_6	Run 2, using K_2TiCl_6	Run 3, using K_2TiCl_6 + KCl
On heating			
373	—	—	1.89
432	—	—	8.44
456	—	21.52	—
469	22.33	—	—
485	—	—	29.33
489	—	36.77	—
494	—	39.16	—
506	—	48.47	48.75
515	—	—	55.65
518	—	65.32	—
525	52.84	—	—
529	66.44	—	72.67
On cooling			
512	—	53.40	—
509	—	51.86	—
432	—	—	8.58
374	—	—	1.83

From Table I it may be seen that the decomposition of K_2TiCl_6 begins at a temperature of about 350° C, and that the decomposition pressure of $TiCl_4$ at about 530° C is 1 atm.

The equilibrium constant for the decomposition of K_2TiCl_6,

$$K_2TiCl_{6(s)} \rightleftharpoons 2KCl_{(s)} + TiCl_{4(g)},$$

is given by the equation

$$K_p = P_{TiCl_4}.$$

The results shown in Table I were used to calculate log K_p and $1/T$, and when these were plotted, the straight-line relationship shown in Fig. 2 was obtained by applying the least-squares method. It is evident from Fig. 2 that the linear relationship holds

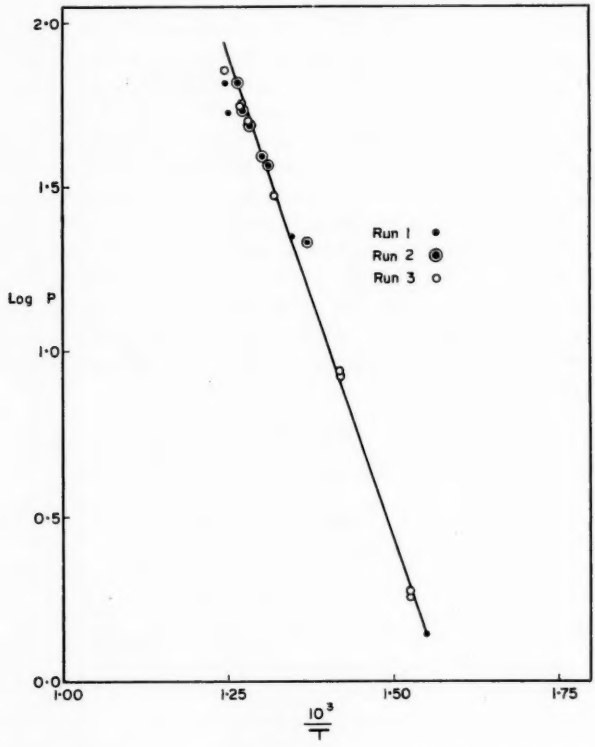

FIG. 2. The variation of log P with the reciprocal of the absolute temperature.

reasonably well for pressures between 2 and 76 cm. From Fig. 2, the variation of pressure with temperature corresponds with the equation

$$\log_{10} P(\text{cm of Hg}) = -\{(5.774\times10^3)/T\} + 9.120.$$

The average error, a, of a single observation, as calculated by the least-squares method, is

$$\log a = \pm 0.045.$$

The heat of reaction was calculated from the slope of the straight line in Fig. 2 in accordance with the van't Hoff equation

$$\Delta H = +26.4 \pm 1.3 \text{ kcal/mole.}$$

This is in good agreement with +27 kcal/mole obtained by Ehrlich and Framm (2) from their experiments using the isoteniscope method.

Free energy and entropy changes for the decomposition were calculated at selected temperatures. The results are shown in Table II.

TABLE II

Thermodynamic functions for the reaction

$K_2TiCl_{6(s)} \rightleftharpoons 2KCl_{(s)} + TiCl_{4(g)}$

Temp. (°C)	K_p (atm)	ΔH (kcal/mole)	ΔF (kcal/mole)	ΔS (e.u.)
350	9.36×10^{-3}	+26.40	+5.77	33.6
400	4.56×10^{-2}	+26.40	+3.88	33.4
450	1.79×10^{-1}	+26.40	+2.52	33.0
500	5.88×10^{-1}	+26.40	+0.81	33.1

CONCLUSIONS

Since the reaction

$$K_2TiCl_{6(s)} \rightleftharpoons 2KCl_{(s)} + TiCl_{4(g)}$$

is endothermic, the formation of the compound is promoted at lower temperatures. However, from kinetic considerations (3) it appears that the rate of reaction at temperatures below 300° C is slow; this would explain the inability of Ehrlich and Framm (2) to prepare K_2TiCl_6 in an autoclave at 300° C.

Furthermore, the thermal stability of K_2TiCl_6 in the temperature range of 300–400° C indicates that the compound might be used as a constituent of a low-melting-point fused salt bath, e.g. KCl + LiCl, for the production of titanium metal by electrolysis. Indeed, it appears that the accepted practice of using fused salt baths at high temperatures, e.g. KCl + NaCl at 700° C, would hinder the introduction of gaseous titanium tetrachloride into the melt, under circumstances where the introduction depended upon the formation of K_2TiCl_6.

ACKNOWLEDGMENT

The authors wish to thank Mr. George Ensell, National Research Council of Canada glass blower, for constructing the glass-bellows mercury manometer.

REFERENCES

1. F. V. SCHOSSBERGER. Ind. Eng. Chem. **51** (5), 669 (1959).
2. B. EHRLICH and E. FRAMM. Z. Naturforsch. **9b**, 326 (1954).
3. S. N. FLENGAS. Solubilities of titanium tetrachloride in mixtures of potassium and sodium chlorides, and the electrode potentials of the titanium chlorides in 1/1 mole KCl + NaCl solutions. Paper presented at the New York Academy of Science, April, 1959.
4. R. SPENCE. Trans. Faraday Soc. **36**, 417 (1940).

ELECTRON CORRELATION AND MOLECULAR SHAPE[1]

R. J. GILLESPIE

ABSTRACT

It is proposed that the arrangements of the electron pairs in the valency shell of a central atom of a polyatomic molecule can be predicted by considering the equilibrium arrangements of similar particles on the surface of a sphere with an appropriate law of force between the particles. The arrangements resulting from an inverse square law of force, corresponding to electrostatic repulsions, and a force which is proportional to $1/r^n$ where n is large, corresponding to Pauli forces, are considered specifically. It is shown that the arrangements predicted agree with those found experimentally for molecules containing only non-transitional elements. The possible arrangements for seven, eight, and nine pairs of electrons in a valency shell are discussed in detail. A method is suggested for predicting the arrangements of electron pairs in valency shells containing lone pairs which can occupy alternative non-equivalent positions. The effect of the interactions of electron pairs on bond lengths in certain molecules is discussed. The extension of the same principles to molecules containing transitional elements is briefly outlined.

It was shown recently by Gillespie and Nyholm (1) that the shapes of a wide range of molecules can be correctly predicted by means of the simple rule that the electron pairs, including both shared (i.e. bonding) pairs and unshared (i.e. lone) pairs, of the valency shell of a central atom of a polyatomic molecule adopt certain definite arrangements which depend only on their total number as shown in Table I.

TABLE I

Predicted arrangements of electron pairs in valency shells (1)

Number of electron pairs	Arrangement
2	Linear
3	Equilateral triangle
4	Tetrahedron
5	Trigonal bipyramid
6	Octahedron

These arrangements are a consequence of the mutual interactions of the valency shell electrons due to

(i) electrostatic repulsions, and to

(ii) the operation of the Pauli exclusion principle, as a consequence of which electrons of the same spin tend to keep as far apart as possible while electrons of opposite spin tend to be drawn together (2).

The interaction arising from the Pauli exclusion principle is in general more important than that arising from electrostatic repulsions and the arrangements of electron pairs given in Table I can be deduced from a consideration of this interaction alone ignoring electrostatic repulsions. It has been shown by several authors (2–10) that, by assigning the electrons to appropriate s, p, and d atomic orbitals, writing the complete antisym-

[1]*Manuscript received January 22, 1960.*
Contribution from the Department of Chemistry, McMaster University, Hamilton, Ontario.

metric wave function for these electrons, thereby taking account of the Pauli exclusion principle, and then calculating the most probable distribution of the electrons, the arrangements of electron pairs that are obtained are identical with those given in Table I. The same results can be obtained in a simple qualitative manner as follows. As a consequence of its kinetic energy, an electron will tend to occupy as much as possible of the space in which it is confined and as a consequence of the Pauli exclusion principle will tend to keep all other electrons having the same spin out of this space. Thus one electron in the central force field of a single nucleus will spread out to occupy a spherical region of space around the nucleus; it is said to occupy an *s* orbital. A second electron of opposite spin can also independently occupy the same region of space, i.e. the same orbital, but a second electron of the same spin will tend to keep as far as possible from the first electron and they will share the available spherical volume; each electron thus effectively occupies a hemispherical region on either side of the nucleus (digonal *sp* orbitals). The most probable distribution of these two electrons will be that in which the angle between the two electrons and the nucleus has a value of 180°. For a total of four electrons, two of one spin and two of opposite spin, the tendency of electrons of opposite spin to keep apart and for electrons of the same spin to come together causes the most probable arrangement of the electrons to be that in which there are two pairs making an angle of 180° with the nucleus, or in other words a pair of opposite spin in each of two equivalent digonal orbitals. Three electrons of the same spin or three pairs of opposite spin will each tend to occupy one-third of the available spherical space and their most probable distribution will be at the corners of an equilateral triangle making angles of 120° with the nucleus. We say that the electrons occupy a set of three equivalent trigonal sp^2 orbitals. For four electrons of the same spin or four pairs of opposite spin the most probable arrangement, i.e. that which maximizes their distance apart or gives them equivalent segments of the available spherical space, is the tetrahedral arrangement (8). Four electrons of the same spin or four pairs of opposite spin may be regarded as occupying four equivalent tetrahedrally directed segments of the available spherical volume, i.e. a set of four equivalent tetrahedral sp^3 orbitals. The same result may be obtained by constructing a set of equivalent hybrid orbitals from the available atomic orbitals. Because such hybrid orbitals are so constructed that they overlap only slightly, the electron distribution that would be obtained if these orbitals were independently occupied by electron pairs differs only slightly from that obtained from the complete antisymmetrical wave function and in particular the positions of maximum probability for the electron pairs coincides with the directions of the maxima of the hybrid orbitals (1, 3, 6, 11).

The most probable arrangements for five or more single electrons of the same spin or pairs of opposite spin is not, perhaps, immediately obvious. If these cases are treated by assigning the electrons to appropriate atomic orbitals and then calculating the most probable distribution of the electrons from the antisymmetrized wave function, a problem arises because of the non-equivalence of the various *d* orbitals that may be used. Some examples are given in Table II where it may be seen that different combinations of one *s* and three *p* orbitals with the various *d* orbitals give different most probable arrangements of electron pairs. It is therefore not possible to unambiguously predict by this method the shapes of molecules whose central atom has a valency shell containing five or more electron pairs. One can only find which shapes are possible, i.e. are compatible with the available atomic orbitals, but one cannot decide which of the possible shapes will be adopted in any particular case.

TABLE II

Most probable arrangements of electron pairs for various orbital combinations*

Number of electron pairs	Occupied orbitals	Arrangement	References
2	sp	Linear	1, 6
3	sp^2	Equilateral triangle	1, 6
4	sp^3	Tetrahedron	6, 7, 8
5	$sp^3d_{x^2-y^2}$	Square prism	10
	$sp^3d_{z^2}$	Trigonal bipyramid	10, 12
6	$sp^3d_{x^2-y^2}d_{z^2}$	Octahedron	10
	$sp^3d_{xz}d_{yz}$	Trigonal prism	10, 13
7	$sp^3d_{x^2-y^2}d_{z^2}d_{xy}$	Pentagonal bipyramid	14
	$sp^3d_{xy}d_{xz}d_{yz}$	†	15
8	$sp^3d_{x^2-y^2}d_{xy}d_{xz}d_{yz}$	Square antiprism	16
	$sp^3d_{z^2}d_{xy}d_{xz}d_{yz}$	Dodecahedron	10, 16
9	sp^3d^5	"Tripyramid"‡	15

*This table is not intended to be complete but only to illustrate some of the probable arrangements of electron pairs that correspond to the occupation of different combinations of atomic orbitals. It does not, for example, include any arrangements based on the partial use of two or more d orbitals, or any arrangement based on the use of d orbitals in preference to p orbitals.
†This polyhedron is obtained by adding one extra point over the center of one rectangular face of a trigonal prism.
‡This polyhedron is obtained by adding an extra point over the center of each of the rectangular faces of a trigonal prism.

Arrangements of Similar Particles on a Spherical Surface

One method of determining which of the possible arrangements of a given number of electron pairs is the most probable is to consider the possible arrangements of similar particles on the surface of a sphere under the action of some appropriate force law. If we assume that the electron pairs in a valency shell are all at the same average distance from the nucleus, which will in fact be the case for two, three, four, and six electron pairs bonding the central atom to a set of identical atoms and will almost certainly be a reasonably good approximation in other cases, then the problem of determining the most probable arrangement of these electron pairs is the same as that of determining the arrangement of a set of particles on the surface of a sphere under the action of an appropriate force law. Since the Pauli exclusion principle causes electrons of the same spin to avoid one another they behave as if there was a force between them. This force has been called a Pauli force or an exchange force (18). The magnitude of this force increases rapidly with the increasing overlap of the orbitals of two electrons with the same spin and therefore can be represented by an inverse function of some large power of the interelectron distance. The arrangement of particles on the surface of a sphere under such a force law is the same as that which is obtained by maximizing the least distance between any two particles (19) and this problem has been treated by Shutte and van der Waerden (20), who obtained the results given in Fig. 1. The arrangement of particles on the surface of a sphere under the action of an inverse square law of force, which would be appropriate if the arrangement of electrons were determined only by electrostatic forces, has been studied by Foppl (21), whose results are given in Table III. In all cases except that of seven particles the two force laws lead to the same arrangements and it seems reasonable to conclude that these will also therefore be the arrangements of these numbers of equivalent pairs of electrons in the valency shell of a central atom. The case of seven electron pairs is further discussed below. For any number of electron pairs up to six these are also the arrangements given by Gillespie and Nyholm (1) which, they point out, lead, without exception, to the correct prediction of the shapes of molecules

Number of particles	2	3	4	5
Arrangement	Linear	Equilateral triangle	Tetrahedron	Trigonal bypiramid

Number of particles	6	7	8	9
Arrangement	Octahedron	"1:3:3"	Square antiprism	"Tripyramid"

FIG. 1. Arrangements of similar particles on the surface of a sphere obtained by maximizing the least distance between any two particles.

TABLE III

Equilibrium arrangements of similar particles on the surface of a sphere under the action of an inverse square law of force

Number of particles	Arrangement
2	Linear
3	Equilateral triangle
4	Tetrahedron
5	Trigonal bipyramid
6	Octahedron
7	Pentagonal bipyramid
8	Square antiprism

containing only non-transitional elements even if not all the electron pairs are equivalent because they are forming bonds to different atoms or are lone pairs. Although Gillespie and Nyholm (1) discussed the shapes of some molecules involving seven, eight, and nine electron pairs in the valency shell of the central atom, they were not able to satisfactorily extend their rules to cover these cases which will therefore be discussed in more detail now.

Seven Electron Pairs

Figure 2 shows that for an interparticle force that is proportional to $1/r^n$, where n is large, the arrangement of seven particles is at the corners of an irregular octahedron

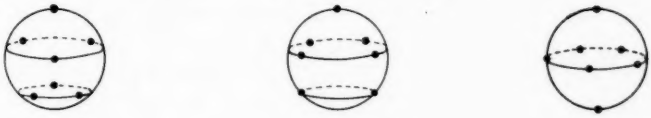

Force law	(I) $1/r^n$	(II) $1/r^m$ $(2 < m < n)$	(III) $1/r^2$
Arrangement	"1:3:3" Octahedron plus extra particle opposite one face	"1:4:2" Trigonal prism plus extra particle opposite one face	"1:5:1" Pentagonal bipyramid

FIG. 2. Arrangements of seven particles on the surface of a sphere.

with an additional particle opposite the middle of one of its faces, i.e. a "1:3:3" arrangement (I), while for an inverse square law the equilibrium arrangement of seven particles is the pentagonal bipyramid, i.e. a "1:5:1" arrangement (III). It seems reasonable to suppose that as the exponent n is decreased the equilibrium arrangement will pass from I to III through the intermediate II, which is an irregular trigonal prism with an additional particle opposite one of its rectangular faces, i.e. a "1:4:2" arrangement. Iodine heptafluoride IF_7(22–25), the ions UF_7^{3-} and $UO_2F_5^{3-}$ (25), and probably ZrF_7^{3-} (26) have the pentagonal bipyramid structure III* while the ions TaF_7^{2-}, NbF_7^{2-}, and $NbOF_6^{2-}$ have the distorted trigonal prism structure II (25). In the A-modification oxides of the X_2O_3 of La, Ce, Pr, and Nd the metal atom is seven-co-ordinated and the oxygen atoms have the arrangement I (27). The antimony atom in the ion $SbBr_6^{2-}$ has a valency shell containing seven electron pairs, one of which is a lone pair. This ion has been reported to have an octahedral structure (25): if this is in fact a not quite regular octahedral structure it would indicate that the arrangement of the seven electron pairs is as in I with the lone pair at one pole, i.e. opposite one face of the distorted octahedron. Since lone pairs exert greater repulsions than bond pairs (1) the arrangement of seven electron pairs including one lone pair is likely to be that in which the lone pair has a minimum number of nearest neighbors and this is structure III. The three structures I, II, and III probably have rather similar energies, and which structure is adopted in any particular case presumably depends on factors such as the size of the central atom, the electronegativities of the ligands, and the non-equivalence of one or more of the electron pairs.

Eight Electron Pairs

For a valency shell containing eight equivalent electron pairs the predicted arrangement is the square antiprism IV and this is indeed the structure that has been found for TaF_8^{3-} (25) and for thorium acetylacetonate $Th(C_5H_7O_2)_4$ (28). The only other arrangement of eight bonds around a central atom that has been observed is the dodecahedral arrangement V (Fig. 3) found in the complex $Mo(CN)_8^{4-}$ ion of the transition metal

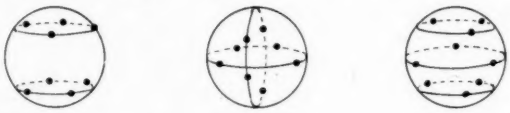

	(IV)	(V)	(VI)
Number of particles	8	8	9
Arrangement	Square antiprism	Dodecahedron $Mo(CN)_8^{4-}$	"Tripyramid"

FIG. 3. Arrangements of eight and nine particles on the surface of a sphere.

molybdenum. There are, however, actually nine electron pairs in the valency shell of the molybdenum atom in this ion, one of which is a lone pair. In transition metal complexes unshared pairs do not necessarily have such an important stereochemical effect as in compounds of non-transition elements (see below) and it is difficult to predict the effect of the single lone pair in this case although it may be said with certainty that if it does have any effect the arrangement of the eight bonds will not be the antiprism. The cube has been suggested (29) as a possible structure for eight-co-ordinated atoms but it is evident that for eight particles (e.g. electron pairs) that repel each other with a force that is proportional to any inverse power of their distance apart the cubic arrangement will always be less stable than the antiprism.

**It is possible that in the crystal the molecule of* IF_7 *has a slightly distorted pentagonal bipyramid structure (23, 24).*

Nine Electron Pairs

For nine electron pairs the predicted arrangement is the trigonal prism arrangement of six pairs with an additional electron pair opposite each rectangular faces, i.e. a "tripyramid" (Fig. 1), and this is indeed the arrangement of the nine bonds around a central atom found in a number of crystalline compounds such as UCl_3, $LaCl_3$, NH_4CdCl_3, $Nd(BrO_3)_3 9H_2O$, and $SrCl_2 6H_2O$ (26). Although the degree of covalent character of the bonds concerned here is uncertain it is interesting that they all do have the predicted arrangement and that this is in fact the only arrangement that has been observed for nine co-ordination.

We may summarize by saying that the predicted arrangements of two, three, four, five, and six electron pairs in a valency shell are as given in Table I. These are found experimentally for all molecules of non-transitional elements even when some of the electron pairs are not equivalent either because they bond different ligands or because one or more are lone pairs. The preferred arrangement for eight equivalent pairs is the antiprism. For nine equivalent pairs the most probable arrangement is the "tripyramid" (Fig. 1). For seven equivalent pairs the three different arrangements I, II, and III seem to be possible.

Valency Shells Containing Lone Pairs

In order to be able to decide between possible alternative locations of lone pairs in valency shells it is necessary to take account of the fact that repulsions exerted by lone pairs are greater than those exerted by bond pairs (1). The orbital associated with a bonding electron pair which is under the influence of two nuclei is smaller, or more localized, than the orbital of a lone pair which, being under the influence of only one nucleus, is able to spread out more and take up more of the available space than the bond pairs (9, 30). Thus bond pairs can approach more closely to each other than lone pairs before appreciable overlap of their orbitals occurs. This is equivalent to saying that bond pairs repel each other less than lone pairs. Alternatively one can say that lone pairs which are under the influence of a single nucleus will be at a slightly smaller average distance from the central nucleus than will the bond pairs which are also under the influence of the ligand nucleus, hence, if all the electron pairs had a symmetrical angular arrangement, the lone pairs would be closer together than the bond pairs and therefore they would repel each other more than the bond pairs. Hence bond pair – bond pair (b–b) repulsions are smaller than bond pair – lone pair (b–l) repulsions which are in turn smaller than lone pair – lone pair (l–l) repulsions. The reality of these differences in the repulsions between lone pairs and bond pairs is borne out by the bond angles in a series of molecules such as CH_4, NH_3, and H_2O. The introduction of one lone pair in NH_3 causes a decrease in the bond angle to 106.6° from the tetrahedral angle in CH_4 and the introduction of a second lone pair in H_2O causes a further reduction in the bond angle to 104.5° (25).

Since Pauli forces play the dominant role in the electron interactions that we have been considering and since these fall off rapidly with distance it seems reasonable to consider only the interactions between a given electron pair and its nearest neighbors in predicting the shapes of molecules with one or more lone pairs in the valency shell of a central atom. Thus in structures based on the trigonal bipyramid we need only consider interactions between electron pairs that make angles of 90° at the nucleus; interactions between electron pairs that make angles of 120° and 180° at the nucleus will be much smaller and can be ignored at least to a first approximation. Thus for ClF_3, BrF_3, and $C_6H_5ICl_2$, which each have three bonding pairs and two lone pairs in the valency shell of the central

atom and may be described as AX_3L_2 molecules where X stands for a ligand atom and L for a lone pair of electrons, the three structures VII, VIII, and IX (Fig. 4) are possible.

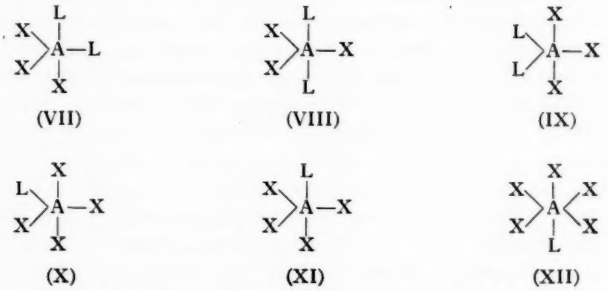

FIG. 4. Possible structures of AX_3L_2, AX_4L, and AX_5L molecules.

Considering only interactions of electron pairs making angles of 90° with the nucleus, VII has one l–l repulsion, three b–l repulsions, and two b–b repulsions, VIII has six b–l repulsions, while IX has four b–l and two b–b repulsions; thus IX will be more stable than either VII or VIII in agreement with the results of experimental determinations of the structures of these molecules (25, 31). For SeF_4, $TeCl_4$, $(CH_3.C_6H_4)_2SeCl_2$, and $(CH_3.C_6H_4)_2SeBr_2$, which may be described as AX_4L molecules, the structures X and XI (Fig. 4) are possible. In X there are two b–l and four b–b repulsions while in XI there are three b–l and three b–b repulsions; evidently X will be the more stable. This is consistent with the experimentally determined structures of these molecules (25). It is interesting to note that the bond angles in ClF_3 are only 87.5° (25), and in BrF_3 only 86.2° (31); this can be attributed to the strong repulsions exerted by the two equatorial lone pairs. Similar small bond angles of less than 90° have been found in BrF_5 (32) and this can be attributed to the strong repulsions exerted by a lone pair in an octahedral arrangement of six pairs (XII).

Bond Lengths

In the tetrahedral and octahedral arrangements of four and six electron pairs respectively, all the pairs have equivalent positions with respect to each other but in the trigonal bipyramidal arrangement of five electron pairs this is not the case; thus the pairs at the poles each have three nearest neighbors with which they make angles of 90° at the nucleus while the equatorial pairs have only two nearest neighbors at 90° and two more further away at 120°. Thus if all the electron pairs are at the same distance from the nucleus the repulsions between the polar electrons and those at the equator will be greater than the repulsions between the equatorial electrons. It may therefore be expected that the distances of the electron pairs from the nucleus will adjust themselves slightly so as to attempt to equalize these repulsions; this will lead to the polar electron pairs being at a slightly greater distance from the nucleus than the equatorial pairs and hence the axial bonds will be slightly longer than the equatorial bonds. The equatorial and axial bond lengths are respectively 2.04 Å and 2.19 Å in PCl_5, 2.31 Å and 2.43 Å in $SbCl_5$, 1.598 Å and 1.698 Å in ClF_3, and 1.721 Å and 1.810 Å in BrF_3 (25, 31). It is therefore not necessary to postulate that the bond to the equatorial fluorine atom has a double-bond character in order to account for the bond lengths in ClF_3 and BrF_3 (33). Similar effects can occur in octahedral arrangements of six electron pairs including one lone

pair which gives rise to square pyramidal molecules such as BrF_5 and IF_5 and ions such as SbF_5^{--} and $SbCl_5^{--}$ (XII). The four electron pairs at the base of the pyramid are not equivalent to the pair at the apex and as a consequence the corresponding bonds might be expected to differ in length. It seems difficult to predict which bonds would be the longest. The equatorial and axial bonds respectively have lengths of 1.68 Å and 1.79 Å in BrF_5 (30) and 2.02 Å and 2.08 Å in SbF_5^{--} (25), i.e. the equatorial bonds are shorter than the apical bond, but in $SbCl_5^{--}$ the reverse is the case (equatorial 2.62 Å, apical 2.36 Å) (25). The reason for this difference is not clear. Similarly in IF_7 the bond lengths would be expected to differ: experimentally it has been found that the equatorial bonds have a length of 1.83 Å while the axial bonds have a length of 1.94 Å although the accuracy of these values seems uncertain (23, 24).

Transitional Elements

In the preceding discussion it has been assumed that all the electron pairs occupy localized (i.e. hybrid) orbitals. This will necessarily be the case for bonding pairs but not for unshared or lone pairs of electrons. For the non-transitional elements for which all the valency electrons *s*, *p*, and *d* belong to the same quantum shell there appear to be no exceptions to the rule that the unshared pairs occupy localized orbitals and have an equally important effect in determining the stereochemistry of an atom as do the bonding pairs (1). However, for the transitional elements in which the valency electrons are in general associated with two quantum shells, electron interactions may lead to most probable configurations in which some or all of the non-bonding electrons occupy non-localized (i.e. atomic or "unhybridized") *d* orbitals and are at a somewhat smaller average distance from the nucleus than the bonding electrons. Such non-localized non-bonding electrons may have only a relatively small influence on the arrangement of the bonding electrons and therefore on the stereochemistry. Thus six-co-ordinated complex ions of the transitional metals are in general octahedral irrespective of whether or not they have additional unshared electrons in the valency shell (1). The six bonding pairs of electrons have the same octahedral arrangement that they would have if no non-bonding electrons were present and they may be conveniently described as occupying octahedral d^2sp^3 or sp^3d^2 equivalent hybrid orbitals. Up to six non-bonding electrons can occupy one or more of the set of equivalent $d_{xy}d_{xz}d_{yz}$ orbitals which each have four maxima between the directions of the octahedral orbitals and in which they have a somewhat smaller average distance from the nucleus than the bonding electrons. Electrons in these orbitals will have little or no effect on the octahedral arrangement of the six bonding pairs of electrons. Thus, for example, TiF_6^{3-}, VF_6^{3-}, $Cr(NH_3)_6^{3+}$, $Fe(CN)_6^{3-}$, and $Co(CN)_6^{3-}$ have one, two, three, five, and six non-bonding *d* electrons respectively and they all have regular octahedral structures. However, if there are more than six non-bonding *d* electrons these must go into the d_{z^2} and $d_{x^2-y^2}$ orbitals, which have their maxima along the octahedral directions of the bonding pairs, and they may therefore exert repulsions on these bonding pairs that are sufficient to distort the shape of the octahedron. The configurations d_{z^2}, $d_{z^2}^2$, and $d_{z^2}^2d_{x^2-y^2}$ may by virtue of the repulsions that they exert on the bonding pairs cause two trans bonds to be longer than the other four. If the repulsions are sufficiently strong they may cause two trans ligands to be lost completely leaving a square planar complex. Thus depending on the strength of the interaction between the bonding electron pairs and the non-bonding *d* electrons the structure of a six-co-ordinated transition metal complex molecule or ion may be an octahedron, or a distorted octahedron with two long bonds, and in some cases as a

result of strong repulsions two trans ligands may be lost giving a four-co-ordinated square planar complex. For example, the ions $Co(NH_3)_6^{3+}$ and $Ni(NH_3)_6^{3+}$ with seven and eight non-bonding d electrons respectively have regular octahedral structures but Pd(diarsine)$_2$ I_2 with eight non-bonding d electrons has a distorted octahedral structure with two unusually long Pd—I bonds (11). The complex compounds of Cu(II), which has nine non-bonding d electrons, are generally square planar, e.g. $Cu(H_2O)_4^{2+}$ and $Cu(NH_3)_4^{2+}$, but in the crystal these ions often attach two further ligands at longer distances to form irregular octahedral complexes (26). When there are 10 d electrons the d shell is complete and symmetrical and the arrangement of six bonding pairs will again be that of a regular octahedron.

Four pairs of electrons in the absence of any non-bonding electrons are arranged tetrahedrally. In a transitional metal complex up to four non-bonding d electrons can be accommodated in the d_{z^2} and $d_{x^2-y^2}$ orbitals, whose maxima lie between the direction of the tetrahedral orbitals occupied by the bonding pairs. Further d electrons must go into the $d_{xy}d_{yz}d_{zx}$ orbitals in which they may exert considerable repulsions on the bonding pairs and may cause the tetrahedral arrangement to be less stable than the square planar arrangement. Thus, for example, VCl_4 with one d electron and $FeCl_4^-$ with five d electrons are tetrahedral but $PtCl_4^-$ and $Cu(NH_3)_4^{2+}$ with eight and nine non-bonding d electrons respectively are square planar.

ACKNOWLEDGMENT

The author is indebted to Dr. J. Leech for helpful correspondence.

REFERENCES

1. R. J. Gillespie and R. S. Nyholm. Quart. Revs. **9**, 339 (1957).
2. P. G. Dickens and J. W. Linnett. Quart. Revs. **9**, 291 (1957).
3. Sir John Lennard-Jones. Proc. Roy. Soc. A, **198**, 14 (1949).
4. Sir John Lennard-Jones. J. Chem. Phys. **20**, 1024 (1952).
5. Sir John Lennard-Jones. Advance of Sci. **51**, 136 (1954).
6. Sir John Lennard-Jones and J. A. Pople. Proc. Roy. Soc. A, **202**, 166 (1950).
7. A. Brickstock and J. A. Pople. Phil. Mag. **43**, 581, 1090 (1953); **44**, 697, 705 (1954).
8. H. K. Zimmerman and P. Van Rysselberghe. J. Chem. Phys. **17**, 598 (1949).
9. J. W. Linnett and A. J. Poe. Trans. Faraday Soc. **47**, 1033 (1951).
10. J. W. Linnett and C. E. Mellish. Trans. Faraday Soc. **50**, 657 (1954).
11. R. J. Gillespie and R. S. Nyholm. Progress in stereochemistry. Academic Press, New York. 1958. p. 261.
12. G. H. Duffey. J. Chem. Phys. **17**, 196 (1949).
13. G. H. Duffey. J. Chem Phys. **17**, 1328 (1949).
14. G. H. Duffey. J. Chem. Phys. **18**, 943 (1950).
15. G. H. Duffey. J. Chem. Phys. **19**, 553 (1951).
16. G. H. Duffey. J. Chem. Phys. **18**, 746 (1950).
17. G. H. Duffey. J. Chem. Phys. **18**, 1444 (1950).
18. W. Kauzmann. Quantum chemistry. Academic Press, New York. 1957. p. 319.
19. J. Leech. Math. Gazette, **41**, 81 (1957).
20. K. Shutte and B. L. van der Waerden. Math. Ann. **123**, 96 (1951). See also L. L. Whyte. American Math. Monthly, **59**, 606 (1952).
21. L. Foppl. J. reine angew. Math. **141**, 251 (1912).
22. R. D. Burbank and F. N. Bensey. J. Chem. Phys. **27**, 981 (1957).
23. J. Donohue. J. Chem. Phys. **30**, 1618 (1959).
24. R. D. Burbank. J. Chem. Phys. **30**, 1619 (1959).
25. Interatomic Distances. Chem. Soc. Special Publication. No. 11. 1958.
26. W. H. Zachariasen. Acta Cryst. **7**, 792 (1954).
27. A. F. Wells. Structural inorganic chemistry. Oxford University Press. 1950.
28. D. Grdenic and B. Matokovic. Nature, **182**, 465 (1958).
29. L. E. Marchi, W. C. Fernelius, and J. P. McReynolds. J. Am. Chem. Soc. **65**, 329 (1943).
30. A. W. Searcy. J. Chem. Phys. **31**, 1 (1959).
31. D. W. Magnusson. J. Chem. Phys. **27**, 223 (1957).
32. R. D. Burbank and F. N. Bensey. J. Chem. Phys. **27**, 982 (1957).
33. R. D. Burbank and F. N. Bensey. J. Chem. Phys. **21**, 642 (1953).

THE PYROLYSIS OF DIALLYL (1,5-HEXADIENE)[1]

D. J. Ruzicka and W. A. Bryce

ABSTRACT

The mechanism of decomposition of diallyl has been studied in a static system in the temperature range 460–520° C. The principal gaseous products (room temperature) were propylene, methane, ethylene, and 1-butene, and the liquid products were cyclopentene, cyclopentadiene, 1-hexene, and benzene. The over-all activation energy of decomposition was 31.3±1.0 kcal/mole for an A factor of 10^7 sec^{-1}. A mechanism of decomposition based on hydrogen abstraction by allyl and the addition of allyl to olefinic double bonds is proposed. Some decomposition by a non-radical mechanism may also occur.

INTRODUCTION

A recent study of the pyrolysis of 1-butene (1) has provided evidence that allyl radicals play an important part in the mechanism. The primary step in the decomposition is, almost certainly,

$$CH_3—CH_2—CH=CH_2 \rightarrow CH_3 + CH_2—CH=CH_2.$$

Propylene, one of the major decomposition products, is presumably formed by hydrogen abstraction by allyl from unreacted 1-butene. Bryce and Kebarle (1) postulated also that the formation of substantial amounts of various cyclic unsaturated hydrocarbons occurred through the addition of allyl to the double bond of 1-butene and propylene.

The amount of information in the literature on the reactivity of the allyl radical is very limited. The inhibiting power of propylene in certain hydrocarbon decompositions has been said to be due to the formation of allyl radicals by abstraction of hydrogen from propylene. The resonance-stabilized allyl radical has been assumed to be relatively unreactive and not capable of acting as a chain carrier (2). In a recent review of relative radical reactivities Semenov (3) calculates a value of −21.5 kcal/mole for the heat of reaction of the allyl radical in a series of reactions for which the reactivities of the vinyl, methyl, and benzyl radicals are +9.4, 0, and −17.4 kcal/mole respectively. The low reactivity of allyl is presumably a reflection of the electron delocalization that occurs on formation of the radical. The resonance or delocalization energy of allyl has been estimated by Coulson (4) to be 15.4 kcal/mole and by Bolland and Gee (5) to be 18.7 kcal/mole.

The formation of the allyl radical has been proposed (6) for the primary step in the pyrolysis of propylene studied with a flow system in the temperature range 680–870° C.

$$CH_2=CH—CH_3 \rightarrow CH_2=CH—CH_2 + H$$

The formation of allene as a major pyrolysis product led to the conclusion that allyl disappeared principally by the reaction

$$CH_2=CH—CH_2 \rightarrow CH_2=C=CH_2 + H.$$

No allene was detected, however, among the products in the pyrolysis of 1-butene in a static system at temperatures near 500° C (1).

Abstraction of hydrogen atoms by allyl has been proposed as a reaction in the pyrolysis of isobutene (7). McNesby and Gordon (8) have shown recently that very little abstraction by allyl occurs at 381° C in the pyrolysis of cyclopentane–acetone mixtures. Most of the

[1]*Manuscript received in original form July 3, 1959, and, as revised, March 3, 1960.*
Contribution from the Department of Chemistry, University of British Columbia, Vancouver 8, B.C. From a thesis presented by D. J. R. in partial fulfillment of the requirements for the degree of Master of Science.

allyl formed combines with methyl to form 1-butene. At 453° C 1-butene is still formed but hydrogen abstraction occurs from both cyclopentane and acetone. Allyl appears to abstract hydrogen extensively at temperatures above 500° C, a result supported by the conclusions of Bryce and Kebarle.

Lossing and his co-workers (9) found allyl to be the main radical product of the pyrolysis of 1,5-hexadiene (diallyl) in a flow reactor attached to a mass spectrometer for the temperature range 690–890° C. It seems reasonable to assume therefore that the pyrolysis of diallyl in a static system at lower temperatures should involve the production of allyl in the primary step

$$CH_2{=}CH{-}CH_2{-}CH_2{-}CH{=}CH_2 \rightarrow 2CH_2{=}CH{-}CH_2. \qquad [1]$$

The present study of the decomposition of diallyl was undertaken in the hope that it would reveal something of the properties of the allyl radical. This compound has also been used as a source of allyl in studying reactions between allyl and other hydrocarbons (10) with a view to gaining additional information about the mechanism of decomposition of olefins, and about the role of propylene as an inhibitor in hydrocarbon decompositions.

EXPERIMENTAL

The diallyl used was a standard sample (99.9% pure) obtained from the American Petroleum Institute, Pittsburgh. The pyrolyses were done in a quartz vessel of 300-ml capacity attached to a conventional static vacuum system. Rapid admission to the reaction vessel of the sample to be pyrolysed was achieved through the use of a calibrated pre-expansion volume. Samples for gas chromatographic analysis were obtained by expansion of the reaction products through a heated sampling line into evacuated pipettes equipped with metal–teflon taps. Standard gas chromatographic techniques were used for the qualitative and quantitative determination of the decomposition products. Individual compounds were identified, when necessary, by trapping them as they emerged from the column and introducing the sample into a mass spectrometer.

Decomposition Products

The principal products formed in the pyrolysis of 70 mm of diallyl at 521° C are shown in the chromatogram presented in Fig. 1. This separation was achieved on a 6-ft alumina column using the technique of increasing the column temperature progressively

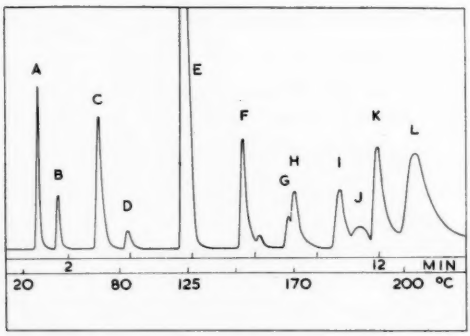

FIG. 1. Chromatogram showing principal products of decomposition of diallyl: A, methane; B, ethane; C, ethylene; D, propane; E, propylene; F, 1-butene; G, cyclopentene; H, cyclopentadiene; I, 1-hexene; J, cyclohexene plus methylcyclopentene; K, diallyl; L, benzene.

to speed up the elution of the less volatile sample constituents. The diallyl was approximately 90% decomposed in this particular analysis but essentially the same products were found in samples in which the decomposition was only approximately 5%. No definite evidence as to the extent of formation of C_6 cyclic products was obtained since at this low conversion the large peak of the undecomposed diallyl covered the region of the chromatogram presumably occupied by these compounds.

The sensitivity of the apparatus to the components of the reaction mixture was determined by calibration with a synthetic mixture of methane, ethane, propylene, 1-butene, cyclopentene, 1,5-hexadiene, and benzene in proportions corresponding approximately to those found in the reaction mixture under standard conditions. The sensitivities of compounds for which no internal standards were available were assumed to be equal to those of the available standards with the closest retention volumes under comparable conditions. Peak areas were taken as the measure of amount of compound.

Analytical Results

Analytical results for the products of pyrolysis of 70 mm of diallyl in the temperature range 460–521° C are given in Table I. The values shown are expressed as mole% of the

TABLE I

Products of 1,5-hexadiene pyrolysis at various temperatures

	Temp., ° C							
	460	470.5	480	490	501	506	510	521
Products	Concentrations expressed as mole%							
Hydrogen	1.0	2.0	3.3	4.5	6.3	6.5	7.0	7.8
Methane	1.4	1.5	2.6	4.6	4.1	6.3	5.4	7.7
Ethane	0.9	0.8	1.5	2.2	2.0	3.4	2.3	2.7
Ethylene	4.7	4.2	6.7	9.2	9.2	9.2	8.4	10.3
Propane	0.11	0.17	0.28	0.8	0.6	1.3	1.1	1.3
Propylene	18.2	16.6	26.8	35.3	35.6	36.7	31.0	35.3
1-Butene	3.2	2.9	4.4	5.7	5.3	5.3	4.5	5.1
Cyclopentene	1.7	1.3	1.3	2.3	0.9	0.8	0.85	1.0
Cyclopentadiene	3.2	2.6	4.5	5.4	3.9	3.1	2.6	2.5
1-Hexene	1.7	1.5	2.4	2.7	2.2	1.6	1.9	2.2
Cyclohexene and methylcyclopentene	1.4	1.4	1.6	2.1	0.7	1.0	0.6	0.7
1,5-Hexadiene	43.5	36.2	16.8	11.2	5.3	4.2	3.2	3.2
Benzene	2.4	2.9	4.6	7.7	6.4	8.7	6.9	8.8
Total mole%	75.4	74.1	76.8	93.7	82.5	89.1	75.8	88.6

NOTE: Reaction time, 5 minutes; P_{init} = 70 mm.

sample withdrawn. It can be seen that the analysis has accounted for an average of 85% of the volatile reaction products. The failure to achieve a complete mass balance may be a consequence of the irreversible adsorption on the chromatographic column of the reaction products with molecular weights greater than benzene. Furthermore, reliable sensitivities were known for only half the reaction products. It can be seen that higher recoveries of products were attained at higher temperatures. Polymerization reactions leading to less volatile products are thus apparently more important at lower temperatures. The supposition that such polymeric products are formed in the present system, in which the concentrations of large relatively stable radicals may be fairly high, is supported by the observation that in subsequent work the reactions of allyl with ethylene and propylene (10) identical analytical techniques were used and complete mass balances were obtained.

Kinetic Results

The decomposition was found to be first order for low conversions at a given temperature but the order rose to higher values as more extensive reaction occurred. An Arrhenius plot (Fig. 2) of first-order rate constants based on gas chromatographic analysis for diallyl

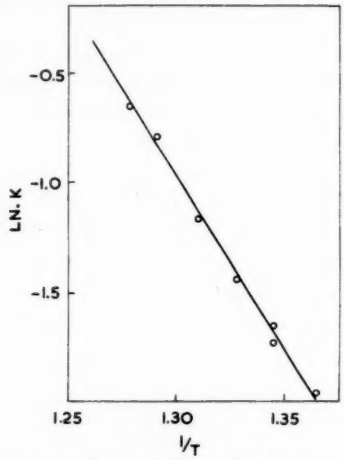

FIG. 2. Arrhenius plot for diallyl decomposition.

consumed gave a value of 31.3 ± 1.0 kcal/mole for the over-all activation energy. The corresponding A factor was 10^7 sec^{-1}.

The variation with time in the concentrations of the light hydrocarbon products for the pyrolysis of 70 mm of diallyl at 501° C is given in Fig. 3. The concentrations of the

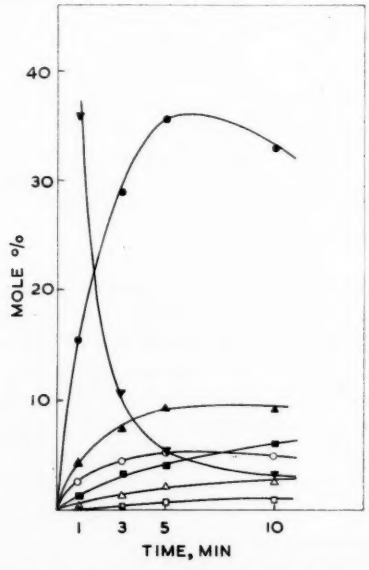

FIG. 3. Variation with time of light hydrocarbon products at 501° C: ●, propylene; ▲, ethylene; ■, methane; ○, 1-butene; ▼, 1,5-hexadiene; △, ethane; □, propane.

unsaturated products (propylene, ethylene, and 1-butene) level off as the hexadiene disappears from the system. The concentrations of the saturated products (methane, ethane, propane) show a progressive increase with time. The concentrations of the higher hydrocarbon products (Fig. 4), largely unsaturated cyclic compounds, go through maxima

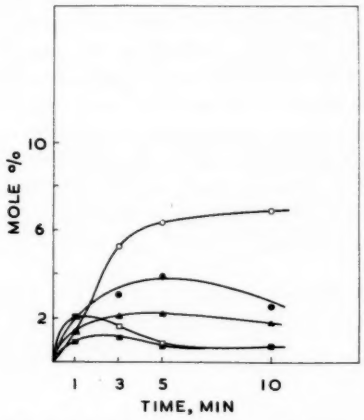

FIG. 4. Variation with time of cyclic products at 501° C. ○, benzene; ●, cyclopentadiene; ▲, 1-hexene; ■, cyclopentene; □, cyclohexene, methylcyclopentene.

as the reaction proceeds, with the exception of benzene. Results very similar to those shown in Fig. 4 are obtained if concentration is plotted against temperature for constant reaction time, i.e. the relative concentrations of saturated hydrocarbons and hydrogen increase with temperature while the concentrations of unsaturated hydrocarbons, excepting benzene, go through maxima.

DISCUSSION

The change from first to higher orders with extent of reaction indicates the increasing complexity of the mechanism as secondary reactions become important. The value of 31.3 ± 1.0 kcal/mole obtained for the over-all activation energy is significantly less than the estimate of 42 kcal/mole which has been made for the dissociation energy of the allyl–allyl bond (6). The apparent activation energy for a reaction involving chain propagation is given (11) by the expression

$$E_A = E_P + (1/w)(E_i - E_t)$$

where E_p, E_i, and E_t are the activation energies for propagation, initiation, and termination respectively, and w is the order of the chain-terminating step. Hence the apparent activation energy, E_A, may well be smaller than E_i either because of a non-zero value for E_t or because of a second-order chain-breaking process. The activation energy for recombination of two allyl radicals or for the disappearance of allyl by some other radical capture process may be greater than zero. Unfortunately no data are available from which this energy, nor E_p, the activation energy for propagation by allyl, can be calculated with any certainty.

Mechanism of the Reaction

The wide variety of products produced in the pyrolysis of diallyl suggest very strongly the operation of a complex free radical mechanism. The observation (9) that at a high

temperature (690–890° C) the molecule decomposes in the primary step by splitting the central bond provides evidence that initiation of the reaction at the temperatures used in the present study occurs in the same way. No evidence has been obtained in the present study as to whether this initiation is homogeneous or heterogeneous. It has also been shown (10) that diallyl present in 5 mole% concentration can serve to initiate the decomposition of hydrocarbons such as 1-butene, propylene, ethylene, and *n*-butane, and that the rate of initiation is linearly related to the square root of the diallyl concentration. Such a dependence is consistent with a primary dissociation of diallyl into two radicals, each capable of initiating further decomposition of the substrate molecules. The present results will therefore be interpreted principally in terms of a free radical mechanism, although the possibility exists that a significant portion of the decomposition occurs by a molecular, non-radical, mechanism. Such a mechanism could account for the occurrence of appreciable amounts of ethylene in the decomposition products

$$CH_2{=}CH{-}CH_2{-}CH_2{-}CH{=}CH_2 \rightarrow CH_2{=}CH_2 + CH_2{=}CH{-}CH{=}CH_2.$$

The butadiene that would be formed simultaneously in a molecular decomposition of this type was not found in the gas chromatographic analysis. Its concentration could have been kept low, however, by rapid reaction with various radicals formed in the system.

Reactions of the Allyl Radical

The allyl radical produced in the primary decomposition would be expected to be relatively stable at low temperatures because of its high delocalization energy. The observation that propylene is a major pyrolysis product of both 1-butene and diallyl at temperatures around 500° C provides direct evidence that hydrogen abstraction by allyl occurs readily under these conditions, an observation which confirms the work of other investigators. The most probable reaction would be

$$CH_2{=}CH{-}CH_2 + CH_2{=}CH{-}CH_2{-}CH_2{-}CH{=}CH_2 \rightarrow CH_2{=}CH{-}CH_3 + CH_2{=}CH{-}CH{-}CH_2{-}CH{=}CH_2. \quad [2]$$

Hydrogen abstraction by allyl from products formed in the decomposition of the hexadienyl radical would occur in later stages of the reaction as the concentrations of these products became appreciable. The observation that the concentrations of a number of these products go through maxima with both time and temperature suggest that they undergo secondary reactions with radicals such as allyl.

The formation of cyclopentene, cyclopentadiene, and methylcyclopentene can best be explained on the basis of the addition of allyl to the double bonds of the parent molecule followed by intramolecular addition:

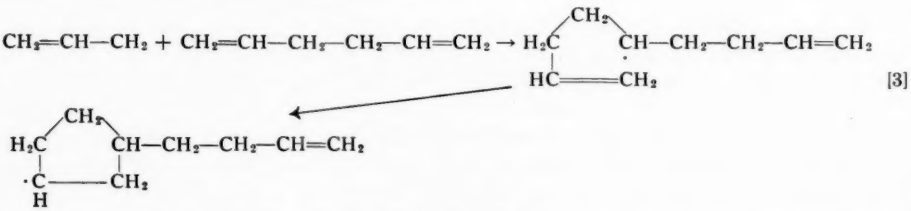

[3]

The product radical would most probably split off its side group and undergo an H-atom shift to form cyclopentene. It could undergo a further hydrogen abstraction from the ring to produce a 1-butenyl-substituted cyclopentene which could react in a variety of ways to produce some of the observed reaction products:

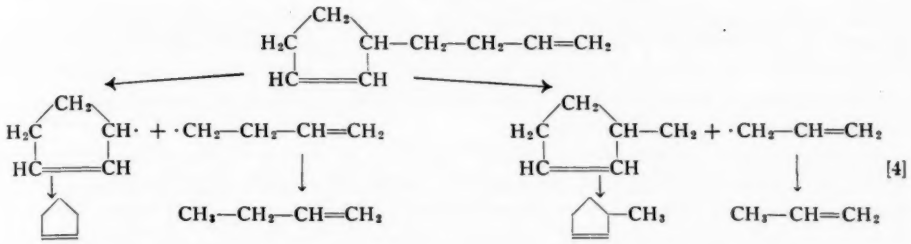

[4]

The radical formed by the addition to the non-terminal carbon of the double bond would either be identical with that produced in reaction [3], or would lead to the formation of a substituted six-membered ring, depending on the mode of ring closure.

Addition of allyl to the double bond of propylene, the major decomposition product, could proceed as follows:

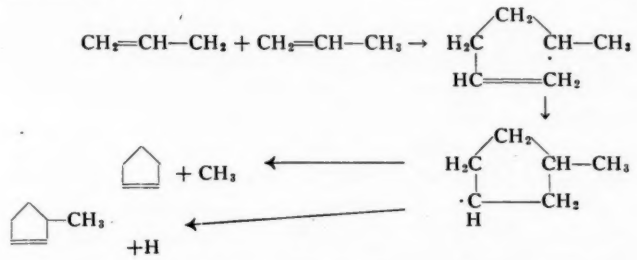

[5]

Cyclopentadiene is assumed to be formed by further dehydrogenation of the cyclopentene formed in reactions [4] and [5].

The occurrence of ethylene as a substantial product cannot involve the pyrolyses of the allyl radical to vinyl and methylene because of the high endothermicity (120–130 kcal) of this reaction. Its formation may occur as a result of a molecular decomposition of diallyl as has been mentioned earlier.

The Fate of the 1,5-Hexadienyl Radical

The concentration of the hexadienyl radical in the early stages of the reaction is presumably fairly high because of its formation by hydrogen abstraction. It can be considered to disappear from the system by rearrangement to the alternate canonical form followed by intramolecular addition:

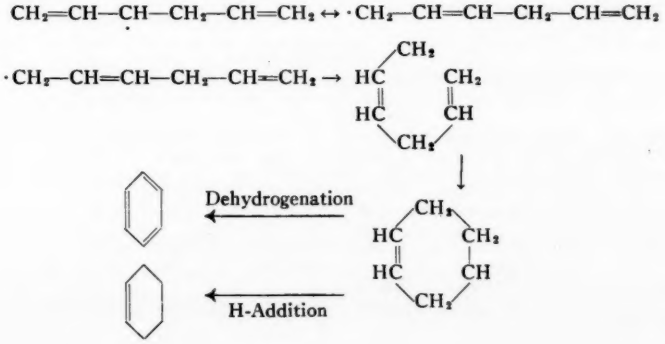

[6]

The failure to observe cyclohexadiene as an intermediate in the dehydrogenation process may be a consequence of the high degree of resonance stabilization which the radical formed by hydrogen abstraction from the diene would have. The conversion of cyclohexadiene to benzene would, of course, be favored because of the over-all enthalpy decrease accompanying the reaction.

Decomposition of the radical with the formation of allyl and allene may occur. The failure to observe allene among the pyrolysis products of diallyl may be because of the slowness of the pyrolysis of the stabilized radical or because of the high reactivity which allene would exhibit towards all radicals present in the system. The 1,5-hexadienyl radicals would also be expected to disappear by combination with other radicals producing compounds adsorbed irreversibly on the gas chromatographic column. Since the steady-state concentration of this radical is presumably quite high the amounts of such addition products may have been appreciable. These compounds may be responsible for the failure to achieve a complete mass balance in the gas chromatographic analysis.

Other Radical Reactions

In the above discussion mechanisms for the formation of the following reaction products were suggested: propylene, ethylene, 1-butene, cyclopentene, cyclopentadiene, cyclohexene, methylcyclopentene, benzene. The formation of the remaining reaction products is assumed to proceed largely by the following reactions:

Methane: $CH_3 + RH \rightarrow CH_4 + R$

Ethane: $CH_3 + CH_3 \rightarrow C_2H_6$

$CH_2{=}CH_2 + H \rightarrow C_2H_5$

$C_2H_5 + RH \rightarrow C_2H_6 + R$

Propane: $CH_2{=}CH{-}CH_3 + H \rightarrow CH_2{-}CH_2{-}CH_3$

$CH_2{-}CH_2{-}CH_3 + RH \rightarrow C_3H_8 + R$

1-Hexene: $CH_2{=}CH{-}CH_2{-}CH_2{-}CH{=}CH_2 + H \rightarrow C_6H_{11}$

$C_6H_{11} + RH \rightarrow C_6H_{12} + R$

Hydrogen: $H + RH \rightarrow H_2 + R$

The activation energies of all these reactions are sufficiently low to permit them to occur rapidly at the temperatures used in the present work.

ACKNOWLEDGMENTS

We are indebted to Dr. S. A. Ryce for advice in connection with the gas chromatographic analysis and to Mr. E. C. W. Clarke for the mass spectrometric identification. This investigation was supported by the Defence Research Board (DRB44-50-01-10), to whom we express our thanks. One of us (D. J. R.) is indebted to the B. C. Sugar Refining Company for a scholarship.

REFERENCES

1. W. A. Bryce and P. Kebarle. Trans. Faraday Soc. **54**, 1660 (1958).
2. E. W. R. Steacie. Atomic and free radical reactions. Reinhold Publishing Corp., New York. 1954. p. 125.
3. N. N. Semenov. Some problems of chemical kinetics and reactivity. Vol. I. Pergamon Press, London. 1958. p. 37.
4. C. A. Coulson. Proc. Roy. Soc. A, **164**, 383 (1938).
5. J. L. Bolland and G. Gee. Trans. Faraday Soc. **42**, 244 (1946).
6. M. Szwarc. J. Chem. Phys. **17**, 284 (1949).
7. M. J. Molera and J. F. Stubbs. J. Chem. Soc. 381 (1952).
8. J. R. McNesby and A. S. Gordon. J. Am. Chem. Soc. **79**, 4593 (1957).
9. F. P. Lossing, K. U. Ingold, and I. H. S. Henderson. J. Chem. Phys. **22**, 621 (1954).
10. W. A. Bryce and D. J. Ruzicka. This issue.
11. A. A. Frost and R. G. Pearson. Kinetics and mechanism. John Wiley & Sons, Inc., New York. 1953. p. 232.

REACTIONS OF ALLYL RADICALS WITH OLEFINS[1]

W. A. Bryce and D. J. Ruzicka

ABSTRACT

A study has been made of the mechanisms of the reactions of allyl radicals, produced thermally from diallyl, with various hydrocarbons in the temperature range 460–506° C. The allyl radical is capable of abstracting hydrogen from certain hydrocarbons and of adding to olefinic double bonds at these temperatures. The rates of formation of the principal products in the reactions between allyl and 1-butene, propylene, and ethylene are linearly related to the square root of the diallyl concentration. Mechanisms are proposed to account for the reaction products formed. In addition to reacting readily with olefins the allyl radical is observed to sensitize the decomposition of *n*-butane at 506° C. The implications of the present results with respect to inhibition in pyrolysis of hydrocarbons are discussed briefly.

INTRODUCTION

The information available in the literature on the reactivity of the allyl radical has been reviewed briefly in an earlier paper (1). The formation of allyl has been proposed as the primary step in the pyrolysis of diallyl (1), propylene (2), allyl bromide (3, 4), isobutene (5), and 1-butene (6). The action of propylene as an inhibitor for certain organic decompositions has been commonly ascribed to the formation of allyl by hydrogen abstraction from the propylene by active radicals like methyl and ethyl. It has been fairly generally assumed that in the temperature range in which pyrolyses in static systems normally occur the allyl radical has sufficient resonance stabilization to render it incapable of propagating reaction chains (7, p. 126). The resonance stabilization energy has been estimated by Coulson (8) to be 15.4 kcal/mole and by Bolland and Gee (9) to be 18.7 kcal/mole. Semenov (10) ascribes to the allyl radical a reactivity less than that of benzyl and a delocalization energy of 23 kcal/mole.

The formation of allyl has been observed directly in the pyrolysis of allyl iodide and of diallyl using a mass spectrometer with a flow system at temperatures between 690 and 890° C (11). The mechanism of decomposition of this latter compound in a static system at temperatures between 460 and 520° C can best be understood (1) on the assumption that the primary step involves a split into two allyl radicals which can subsequently abstract hydrogen to form propylene or add to olefinic double bonds to form the cyclic unsaturated products which are formed in substantial amounts. The conclusion that allyl abstracts hydrogen readily under these conditions is in agreement with recent results of McNesby and Gordon (12).

The present study was undertaken to demonstrate more clearly the nature of allyl reactivity and to gain further insight into the mechanism of its reaction with unsaturated hydrocarbons. Reactions with 1-butene were of particular interest because of work done previously in this laboratory on the pyrolysis of this compound (6), the results of which provided strong evidence for reactions between it and the allyl radical.

EXPERIMENTAL

The substance used as a thermal source of allyl radicals was diallyl (1,5-hexadiene) obtained from the American Petroleum Institute, Pittsburgh (99.9 mole% pure). Other hydrocarbons used were all Research Grade (Philips Petroleum Co., Bartlesville, Okla.).

The experimental techniques used were similar to those described earlier (1). Diallyl

[1]*Manuscript received in original form July 3, 1959, and, as revised, March 3, 1960.*
Contribution from the Department of Chemistry, University of British Columbia, Vancouver 8, B.C. From a thesis presented by D. J. R. in partial fulfillment of the requirements for the degree of Master of Science.

and the substrate hydrocarbon were premixed and then admitted rapidly to the reaction vessel. Extensive decomposition of diallyl occurred in nearly all cases at temperatures well below those at which decomposition of the substrate hydrocarbon normally occurred. Analyses were done by gas chromatography supplemented by mass spectrometry where necessary.

RESULTS AND DISCUSSION

The Decomposition of 1-Butene – Diallyl Mixtures

The pyrolysis of 1-butene by itself and of 1-butene containing 5% by volume of diallyl was studied at 506° C with a total pressure of 200 mm Hg. The variation in pressure with time (Fig. 1) provides a measure of the effect of diallyl on the rate of decomposition

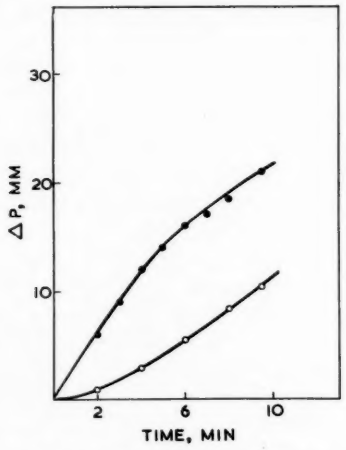

FIG. 1. Pressure–time curves showing effect of 5% diallyl on the rate of decomposition of 1-butene. Open circles, butene alone.

of 1-butene. A value of 6.5 was obtained for the relative rates of pyrolysis of 1-butene with and without diallyl for a reaction time of 1 minute.

The dissociation of diallyl, R_2, would yield allyl radicals, R, which could undergo reaction with the substrate olefin, M, leading to the formation of the products observed. If termination of the chains occurs by bimolecular radical recombination processes of the types

$$2R \rightarrow R_2$$

$$RM. + R \rightarrow RMR$$

and if the rate constant for the decomposition of diallyl is very much less than the propagation and termination rate constants, the rate of the over-all reaction will be given by

$$-d[M]/dt = k[R_2]^{\frac{1}{2}}[M].$$

The concentration of products resulting from the reaction between allyl and olefin ought therefore to be linearly related to the square root of the diallyl concentration for a constant reaction time.

The effect of varying the initial diallyl concentration on the rates of formation of

reaction products was studied with diallyl concentrations ranging from 0 to 11.4% for a total pressure of 200 mm Hg. The reaction time was 5 minutes at 506° C. Earlier experiments (1) had shown that decomposition of the diallyl under these conditions would be 95% complete. The concentrations of the principal decomposition products of 1-butene are plotted against the square root of the diallyl concentration in Fig. 2. An approximately

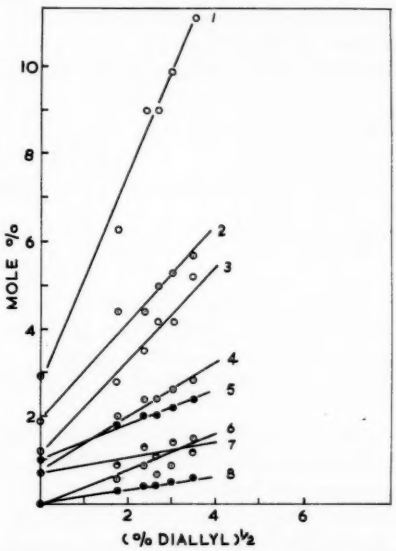

FIG. 2. Concentrations of principal decomposition products of 1-butene versus square root of diallyl concentration; 1, propylene; 2, methane; 3, ethylene; 4, ethane; 5, cyclopentadiene; 6, benzene; 7, cyclopentene; 8, cyclohexene plus methylcyclohexene.

linear dependence is obtained for each product. The decomposition of 1-butene by itself at this temperature could contribute to each product an amount given by the ordinate at zero diallyl concentration. A significant amount of the increased yield of propylene with increasing diallyl concentration would result of course from the increase in diallyl itself. However, it is not possible to account for the increase in propylene by assuming that the diallyl and 1-butene decompose independently, i.e. the increase in propylene is very much greater than can be accounted for by the diallyl present. The possible contribution of diallyl to the concentrations of all other products is at most a few per cent of the amount of diallyl present and hence can be neglected. The three compounds whose concentrations are most affected by increasing the diallyl concentration (propylene, methane, and ethylene) are the chief products formed in the decomposition of 1-butene.

The allyl radical can react with 1-butene in two ways: by abstraction of hydrogen to form propylene and the butenyl radical, or by addition to the double bond. The reaction sequences proposed for these two processes are given below.

Hydrogen Abstraction

$$CH_2{=}CH{-}\dot{C}H_2 + CH_2{=}CH{-}CH_2{-}CH_3 \rightarrow CH_2{=}CH{-}CH_3 + CH_2{=}CH{-}\dot{C}H{-}CH_3$$

Kinetic evidence (6) favors the abstraction of the allylic hydrogen from 1-butene but

the butenyl radical thus formed can be represented as existing in two alternative canonical forms,

$$CH_2{=}CH{-}\dot{C}H{-}CH_3 \leftrightarrow \cdot CH_2{-}CH{=}CH{-}CH_3.$$

The extensive isomerization of 1-butene to 2-butene that occurs in the temperature range 450–520° C if methyl radicals are added to 1-butene (13) provides convincing evidence that the butenyl radical can be considered to react in the 2-butenyl form to a substantial degree. This radical may be removed by hydrogen abstraction or by addition to the double bond of 1-butene followed by intramolecular addition to form various cyclic unsaturated products:

$$\cdot CH_2{-}CH{=}CH{-}CH_3 + CH_2{=}CH{-}CH_2{-}CH_3 \rightarrow H_2C{-}\dot{C}H{-}CH_2{-}CH_3$$

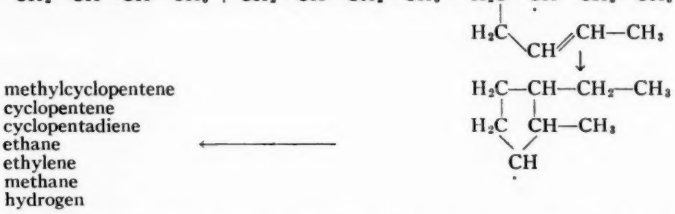

An H-atom shift is required for the formation of cyclopentene in the dissociation of the cyclic radical shown.

The formation of both methane and ethylene is markedly increased by the addition of allyl radicals to the system. The increase is considerably greater than that for the cyclic compounds and hence ethylene and methane cannot be assumed to be formed primarily from the cyclization reaction given above although the ethyl and methyl radicals eliminated in the formation of the cyclic compounds could lead to ethane, ethylene, and methane as follows:

$$C_2H_5 \rightarrow C_2H_4 + H,$$
$$C_2H_5 + C_2H_5 \rightarrow C_2H_4 + C_2H_6,$$
$$CH_3 + RH \rightarrow CH_4 + R.$$

The increased formation of ethylene and methane must be a consequence of pyrolysis of higher radicals. Their formation as a result of the decomposition of the butenyl radical,

$$CH_2{=}CH{-}\dot{C}H{-}CH_3 \rightarrow CH_2{=}CH{-}\dot{C}H \cdot + CH_3,$$
$$CH_2{=}CH{-}\dot{C}H{-}CH_3 \rightarrow CH_2{=}\dot{C}H + CH_2{=}CH_2,$$

seems improbable because of the relatively high endothermicities of these reactions. Butenyl might be expected to stabilize itself under the present conditions by hydrogen loss,

$$CH_2{=}CH{-}\dot{C}H{-}CH_3 \rightarrow CH_2{=}CH{-}CH{=}CH_2 + H,$$

or by disproportionation with allyl,

$$CH_2{=}\dot{C}H{-}CH_2 + CH_2{=}CH{-}\dot{C}H{-}CH_3 \rightarrow CH_2{=}CH{-}CH_3 + CH_2{=}CH{-}CH{=}CH_2.$$

Butadiene was not observed in the reaction products although the gas chromatographic column used may have retained it because of its high degree of unsaturation. Similarly any allene formed by allyl decomposition,

$$CH_2{=}CH{-}\dot{C}H_2 \rightarrow CH_2{=}C{=}CH_2 + H,$$

would also tend to be retained in the chromatographic column. Furthermore both compounds would most probably disappear from the system rapidly through reaction with the variety of radicals present. It is not possible to decide, therefore, whether or not such reactions are important in the present study.

Addition to the Double Bond

The mechanism proposed for this reaction is similar to that suggested for the decomposition of diallyl (1):

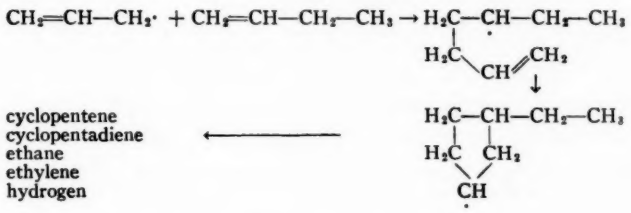

Ethane and ethylene could be formed from the elimination of the ethyl group and hydrogen from the conversion of the cyclopentene to cyclopentadiene. The results for the pyrolysis of 1-butene (6) provide evidence that such radical elimination reactions are an effective method of dehydrogenation of the cyclic addition products.

The Decomposition of Ethylene–Diallyl Mixtures

A series of experiments was done in which diallyl in proportions ranging from 0 to 10.1% by volume was mixed with ethylene and decomposed for 5 minutes at a temperature of 506° C. The total initial pressure in each case was again 200 mm Hg. No reaction of the ethylene occurred in the absence of diallyl but reaction was observed to occur when diallyl was present. The pressure change in the system was negative indicating that products of molecular weight greater than ethylene were being formed. The analytical results, given in Table I, show that a satisfactory mass balance was obtained in all cases.

TABLE I

Analytical results for pyrolysis of ethylene–diallyl mixtures for 5 minutes at 506° C

	Mole % diallyl				
	2.9	5.2	6.7	8.9	10.1
Product	Mole %				
Hydrogen	0.22	0.35	0.47	0.65	0.71
Methane	0.06	0.35	0.50	0.47	0.67
Ethane	0.51	1.1	1.3	1.4	1.6
Ethylene	92	93	89	88	86.5
Propylene	2.2	2.8	3.7	4.4	4.6
1-Butene	0.40	0.65	1.0	1.1	1.1
Cyclopentene + 1,4-pentadiene	1.8	2.7	3.8	4.3	4.7
Diallyl	0	0.06	0.07	0.31	0.40
Total	97.2	100.0	99.8	100.6	100.3

Propylene is again a major product, formed by the hydrogen abstraction reactions of allyl. The variation of the amount of propylene with the square root of the diallyl concentration is linear (Fig. 3). The abstraction of hydrogen by allyl from ethylene

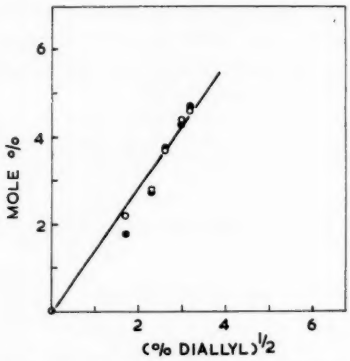

FIG. 3. Variation of propylene (open circles) and of cyclopentene plus 1,4-pentadiene with diallyl concentration in the reaction with ethylene.

would be endothermic by some 30 kcal and therefore seems unlikely. The most probable reaction between allyl and ethylene is addition to form the pentenyl radical

$$CH_2{=}CH{-}CH_2 + CH_2{=}CH_2 \rightarrow H_2C(\cdot){-}CH_2{-}CH_2{-}CH{=}CH_2 \quad [1]$$

which could undergo intramolecular addition to form the cyclopentyl radical

$$H_2C(\cdot){-}CH_2{-}CH_2{-}CH{=}CH_2 \rightarrow \text{cyclopentyl radical} \quad [2]$$

In view of the high allyl concentration the following reactions are probable:

$$CH_2{=}CH{-}CH_2 + H_2C(\cdot){-}CH_2{-}CH_2{-}CH{=}CH_2 \rightarrow HC{\equiv}CH_2{-}CH_2{-}CH{=}CH_2 + CH_2{=}CH{-}CH_3 \quad [3]$$

$$CH_2{=}CH{-}CH_2 + H_2C(\cdot){-}CH_2{-}CH_2{-}CH{=}CH_2 \rightarrow CH_2{=}CH{-}CH_3 + \text{cyclopentene} \quad [4]$$

Cyclopentene and 1,4-pentadiene are formed as significant products of the reaction between allyl and ethylene. Cyclopentene is formed in only trace amounts in the decomposition of diallyl and 1,4-pentadiene is not formed at all (1). They thus provide a direct measure of the extent of the allyl–ethylene reaction. They were not separated from each other in the analyses given in Table I but their identification was achieved by mass spectrometry.

The results presented in Fig. 3 show that the rate of formation of 1,4-pentadiene plus cyclopentene is numerically equal to the rate formation of propylene, an observation which is explained by reactions [3] and [4] above. A quantitative separation was achieved in the analysis of the reaction mixture for a single experiment, using a squalane–pelletex column at 0° C. The initial diallyl concentration in this experiment was 6.7%. The analytical result obtained gave the ratio

$$\text{1,4-pentadiene/cyclopentene} = 11/20.$$

This ratio is presumably a measure of the relative rates of reactions [3] and [4].

Other reactions which presumably occur in this system include

$$\cdot CH_2{-}CH{=}CH_2 + CH_3 \rightarrow CH_3{-}CH_2{-}CH{=}CH_2,$$

$$CH_2{=}CH{-}CH_2{-}CH_3 \rightarrow CH_2{=}CH{-}CH_2\cdot + CH_4,$$

$$CH_3 + RH \rightarrow CH_4 + R,$$

$$CH_3 + CH_3 \rightarrow CH_3CH_3,$$

$$H + RH \rightarrow H_2 + R.$$

The Decomposition of a Propylene–Diallyl Mixture

Propylene containing 5.3% diallyl was decomposed for 5 minutes at 506° C and an initial total pressure of 200 mm Hg. At this temperature propylene by itself is quite stable. A slight pressure increase occurred. The composition of the reaction mixture is given in Table II.

TABLE II

Analytical results for pyrolysis of 5.3% diallyl in propylene for 5 minutes at 506° C

Hydrogen	0.37 mole%
Methane	1.17
Ethane	0.16
Ethylene	2.29
Propane	0.73
Propylene	92.0
1-Butene	1.11
Cyclopentene	0.94
1-Hexene	0.94
Methylcyclopentene	0.28
Diallyl	0.50
Total	100.2

The range of products formed is very similar to that obtained in the pyrolysis of diallyl itself but the amounts formed in nearly all cases are very much greater than can be accounted for by decomposition of the diallyl only. For example the pyrolysis of diallyl at 506° C yields 9.2% ethylene (1). Hence the maximum possible contribution of diallyl to the ethylene yield given in Table II, assuming an independent decomposition, would be 0.5%. Thus most, if not all, of the ethylene formed in the diallyl–propylene system is produced by the decomposition of propylene initiated by the added allyl radicals.

The only primary reaction of allyl with propylene that is of interest is addition to the double bond; the hydrogen abstraction reaction is trivial. The mechanism proposed for the addition reaction is as follows:

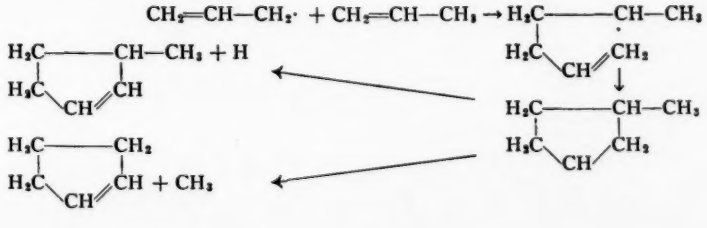

The only two cyclic products are thus accounted for by two alternative modes of reaction of the addition product. The analytical results indicate that the decomposition to cyclopentene and the methyl radical has approximately the same probability as the dehydrogenation to methylcyclopentene. Two isomeric methylcyclopentenes appear to be formed.

The 1-butene may be formed by the combination of allyl and methyl

$$CH_2{=}CH{-}CH_2\cdot + CH_3 \rightarrow CH_2{=}CH{-}CH_2{-}CH_3.$$

The high yield of ethylene indicates again that decomposition of a higher radical must occur readily at these temperatures. One possibility is the pyrolysis of allyl,

$$CH_2{=}CH{-}CH_2\cdot \rightarrow CH_2{=}CH\cdot + \cdot CH_2.$$

However, the relatively high endothermicity of this process makes it rather improbable under the present conditions. Propane is presumably formed by the addition of hydrogen atoms to propylene.

$$H + CH_2{=}CH{-}CH_3 \rightarrow C_3H_7$$
$$C_3H_7 + RH \rightarrow C_3H_8$$

The Decomposition of an n-Butane – Diallyl Mixture

In order to compare the reactivity of allyl with olefins and paraffins the pyrolysis of a *n*-butane – diallyl mixture was studied in one experiment. The results for a system containing 5% diallyl at 506° C (200 mm total pressure) are given in Table III.

TABLE III

Analytical results for the pyrolysis of 5% diallyl in *n*-butane for 5 minutes at 506° C

	Non-sensitized mole%	Sensitized mole%	Sensitized / Non-sensitized
Methane	2.0	4.9	2.5
Ethane	0.9	2.0	2.2
Ethylene	0.9	3.4	3.8
Propylene			3.5
1-Butene	Negligible	1.7	
1-Pentene	—	0.85	
Benzene	—	Negligible	

The principal products from the pyrolysis of *n*-butane alone are propylene methane, ethane, and ethylene. Since the yield of each of the latter three compounds in the complete pyrolysis of diallyl by itself is less than 10% of the diallyl decomposed it is apparent that the allyl radicals have initiated the decomposition of *n*-butane to a significant extent. The concentration ratios for these three products in the sensitized and non-sensitized experiments provides a measure of the accelerating effect of the allyl radicals. The analytical results for propylene were inconclusive because of the difficulty in separating propylene and *n*-butane completely on the alumina column used for these analyses.

Substantial amounts of both 1-butene and 1-pentene were formed in the allyl-sensitized reaction, presumably by the following processes:

$$CH_2{=}CH{-}CH_2\cdot + CH_3 \rightarrow CH_2{=}CH{-}CH_2{-}CH_3,$$
$$CH_2{=}CH{-}CH_2\cdot + \cdot CH_2{-}CH_3 \rightarrow CH_2{=}CH{-}CH_2{-}CH_2{-}CH_3.$$

The formation of both methyl and ethyl radicals has been proposed as primary steps in the pyrolysis of *n*-butane (7, p. 153). Both of these radicals could, of course, come from the pyrolysis of the butyl radical formed in the primary reaction between *n*-butane and allyl.

$$CH_2{=}CH{-}CH_2\cdot + CH_3CH_2CH_2CH_3 \rightarrow CH_2{=}CH{-}CH_3 + CH_3CH_2\dot{C}HCH_3$$

$$CH_3CH_2\dot{C}HCH_3 \rightarrow CH_3 + CH_2{=}CH{-}CH_3$$

$$\rightarrow CH_3CH_2 + CH_2{=}CH_2$$

Inhibition in Decomposition Reactions

The results obtained in the present study have shown that in the temperature region around 500° C allyl radicals can not only add to olefinic double bonds but are sufficiently reactive to abstract hydrogen from a variety of positions in hydrocarbons. This reactivity makes it difficult to assume that the residual reaction in hydrocarbon decomposition inhibited by the addition of propylene does not involve free radical mechanisms, as it is apparent that the allyl radicals formed under the present conditions are capable of propagating radical chains. The residual reactions in hydrocarbon decomposition fully inhibited by propylene may therefore be processes in which chains are propagated by less effective radicals like allyl, the concentration of the highly reactive alkyl radicals being kept at very low values by reaction with propylene. This idea is in accordance with suggestions made many years ago (16) that thermal decomposition of certain organic compounds may involve more than one type of chain mechanism, not all of which are suppressed by the addition of an inhibitor.

Chain propagation by stabilized radicals has been proposed for the decomposition of 1-butene (6), a system believed to be fully self-inhibited. The reaction of such radicals with substrate hydrocarbon in the propylene-inhibited pyrolysis of paraffins could maintain the propagation process and would result in the formation of products from the decomposition of the paraffinic radicals not greatly different from those obtained in normal pyrolyses.

In the inhibition of hydrocarbon pyrolysis by nitric oxide a similar mechanism may operate. The efficiency of nitric oxide as an inhibitor, roughly 12 times that of propylene (17), is very much less than might be expected assuming that both inhibitors operate by the removal of radicals like methyl from the system. The rate of reaction of methyl with nitric oxide is 400 times the rate of its reaction with propylene (18). However, nitric oxide may be capable only of removing active propagators like methyl and ethyl by converting them fairly rapidly into stable products. The reaction between nitric oxide and electronically stabilized radicals like allyl may be ineffective because of the weakness of the bond formed. Hence the residual reaction in nitric-oxide-inhibited pyrolyses of paraffins may be, to a considerable extent at least, a short-chain process propagated by stabilized radicals formed by H-abstraction from decomposition products like propylene and butene. Propylene may have an inhibition efficiency relative to nitric oxide greater than that expected from their relative rates of reaction with methyl because it can remove radicals by addition reactions as well as by serving as a source of hydrogen for abstractions.

The position of nitric oxide as an inhibitor is confused by the observation that in some systems it is unable to inhibit processes which seem fairly clearly to involve methyl radicals while in other systems it appears to function as a chain initiator (18). A more definitive study of the role played by both nitric oxide and propylene in various reaction

systems, based on a study of the rate at which they are removed and on the nature of the products formed, would be valuable in endeavoring to understand their function as inhibitors.

ACKNOWLEDGMENTS

We are indebted to Dr. S. A. Ryce for advice in connection with the gas chromatographic analyses and to Mr. E. C. W. Clarke for the mass spectrometric identifications. This work was supported by the Defence Research Board (DRB44-50-01-10), to whom we express our thanks. One of us (D. J. R.) is indebted to the B. C. Sugar Refining Company for a scholarship.

REFERENCES

1. D. J. Ruzicka and W. A. Bryce. Can. J. Chem. This issue.
2. M. Szwarc. J. Chem. Phys. **17**, 284 (1949).
3. M. Szwarc, B. N. Ghosh, and A. H. Sehon. J. Chem. Phys. **18**, 1142 (1950).
4. A. Maccoll. J. Chem. Phys. **17**, 1350 (1949).
5. M. J. Molera and J. F. Stubbs. J. Chem. Soc. 381 (1952).
6. W. A. Bryce and P. Kebarle. Trans. Faraday Soc. **54**, 1660 (1958).
7. E. W. R. Steacie. Atomic and free radical reactions. Reinhold Publishing Corp., New York. 1954.
8. C. A. Coulson. Proc. Roy. Soc. A, **164**, 383 (1938).
9. J. L. Bolland and G. Gee. Trans. Faraday Soc. **42**, 244 (1946).
10. N. N. Semenov. Some problems of chemical kinetics and reactivity. Vol. I. Pergamon Press, London. 1958.
11. F. P. Lossing, K. N. Ingold, and I. H. S. Henderson. J. Chem. Phys. **22**, 621 (1954).
12. J. R. McNesby and A. S. Gordon. J. Am. Chem. Soc. **79**, 4593 (1957).
13. W. A. Bryce and S. A. Ryce. To be published.
14. M. Szwarc. Chem. Rev. **47**, 75 (1950).
15. J. S. Roberts and H. A. Skinner. Trans. Faraday Soc. **45**, 339 (1945).
16. C. N. Hinshelwood. Kinetics of chemical change. Oxford. 1940.
17. F. J. Stubbs and C. N. Hinshelwood. Proc. Roy. Soc. (London), A, **200**, 458 (1950).
18. A. F. Trotman-Dickenson. Gas kinetics. Butterworths, London. 1955. p. 156.

THE AQUEOUS BENZOATE SYSTEM AS A SENSITIVE DOSIMETER FOR IONIZING RADIATIONS[1]

W. A. Armstrong and D. W. Grant

ABSTRACT

The aqueous benzoate system, as typified by $6\times10^{-4}M$ calcium benzoate, meets many of the requirements for a sensitive chemical dosimeter. The concentration of salicylic acid, determined spectrophotofluorometrically, increases linearly with radiation dose in the range 5 to 5000 rads and is independent of temperature from 15 to 45° C, of energy from 160 kev to 3 Mev, and of dose rate from 4 to about 1000 rads/minute. The decrease in sensitivity with increasing dose rate from 1000 to 85,000 rads/minute is reported.

INTRODUCTION

The ideal chemical dosimeter should be easy to prepare and stable indefinitely under ordinary storage conditions. The concentration of radiolytic product should be proportional to radiation dose, and independent of radiation intensity (dose rate), radiation energy, and temperature. There should be no postirradiation change in the concentration of that radiolytic product. The method of analysis for the product should be simple, accurate, and precise throughout the range of product concentrations corresponding to the dose range of the dosimeter.

For radiobiological work, a number of additional characteristics are desirable. In particular the system should be tissue-equivalent. This means that the radiation dose absorbed in the dosimeter system should be the same as that absorbed in an identical volume of tissue exposed under identical conditions. This condition is approximately satisfied if the system is water-based. In addition, the system should be sensitive to radiation doses in the range 1 rad (100 ergs/g) to a few thousand rads and be able to discriminate between neutrons and electromagnetic radiation.

Although many radiation-induced chemical reactions have been studied, no system has been developed which meets all of the above requirements. All proposed water-based systems have responses which depend to varying degrees on the radiation energy and at present it seems likely that more than one type of system will have to be exposed simultaneously for dosimetry of mixed neutron–gamma fields.

The two main factors which determine the lowest dose measurable by a given dosimeter are the yield (the amount of product P formed per unit of radiation dose, usually designated as G_P = number of molecules of P formed per 100 ev of energy absorbed) and the sensitivity of the analytical method for P. In general, a G_P greater than 20 indicates that the radiation-induced reaction involves some chain mechanism and, therefore, a dosimeter based on such a system will be dose rate dependent (1). If G_P is small an extremely sensitive analytical method is required. For example, if $G_P = 1$ a dose of 100 rads will produce approximately 10^{-7} moles of P per liter, a concentration barely detectable by even the most sensitive colorimetric methods. A dosimeter based on the oxidation of a leuco base to a dye by the radiolysis products of water and having a G_{dye} approximately equal to 1 has been developed (2, 3). However, it is not sufficiently sensitive for accurate use in the very low dose range.

The simplest analytical method capable of accurate measurements at such high dilutions is spectrophotofluorometry. Thus an extremely sensitive dosimeter might be based on the radiation-induced formation of a fluorescent species from a non-fluorescent

[1]*Manuscript received February 11, 1960.*
Contribution from Defence Research Board, Defence Research Chemical Laboratories, Ottawa, Ontario.
Issued as D.R.C.L. Report No. 306.

precursor. Such a system is the benzoate ion in aqueous solution, which on irradiation undergoes partial conversion to the salicylate ion (4). In a preliminary communication (5), the authors have shown that doses down to 5 rads produce accurately measurable amounts of salicylate ion in aqueous calcium benzoate solutions. The present paper describes the results of the experiments undertaken to determine how well a benzoate system meets the requirements for a chemical dosimeter.

EXPERIMENTAL

Materials

Water from a Barnsted still was redistilled from alkaline $KMnO_4$ in an all Pyrex apparatus which incorporated a splash column. Calcium benzoate as the monohydrate (judged by weight loss on heating) was prepared by mixing solutions of reagent grade calcium chloride and benzoic acid dissolved in dilute sodium hydroxide, followed by repeated recrystallizations of the calcium benzoate from aqueous solution. The salicylic acid was reagent grade material recrystallized from aqueous solution and dried. All other materials were reagent grade and were used without further purification.

All glass equipment was vigorously cleaned with fresh chromic acid followed by repeated washings with redistilled water. Steam from boiling dilute alkaline permanganate was then passed through the Pyrex irradiation vessels and the flasks used for storing solutions.

Radiations

The following radiations were used: γ-rays from 2 curies of Cs^{137} and 200 curies of Co^{60}; X rays from a 3-Mev Van de Graaff generator. All dose rates were determined using the Fricke dosimeter (6), assuming $G_{Fe(III)}$ to be 15.5 for all radiations employed. The usual corrections were made for the decreased energy absorption in water.

The 2-curie Cs^{137} source has been described previously (3). The 200-curie Co^{60} source is housed in a facility similar to the one described by Schwarz and Allen (7). The cobalt is located in a pipe 1 in. by 4 in. welded to the center of the bottom of a cylindrical tank 7 ft high and 1 ft in diameter. The tank is sunk about 6 feet in the ground and filled with water. The earth and water provide adequate shielding. Samples were irradiated at dose rates of 70 to 1500 rads/minute in a jig designed to fit over the source.

The 3-Mev Van de Graaff generator, a High-Voltage Corp. horizontal model, was used for high dose rate studies. Samples were dropped through a lucite tube into the X-ray beam for a period of time controlled by an interval timer. With this arrangement, it was possible to irradiate samples with doses of a few thousand rads at dose rates up to 85,000 rads/minute.

Analysis

Fluorescence measurements were made with a Bowman–Aminco spectrophotofluorometer normally using 1-cm quartz cells, although microcells requiring as little as 0.1 ml have been used successfully. The salicylic acid formed on irradiation was determined by comparing the fluorescence of the irradiated sample at 400 mμ when activated with light of 295 mμ, with that of a standard salicylic acid solution. As fluorescent measurements may be affected by the presence of non-fluorescent species, all standards were prepared by adding the desired amount of salicylic acid to a solution of the same composition as the solution to be irradiated. In the concentration range investigated ($<10^{-5}$ M) and with the pH between 4 and 8, neither quenching effects nor interference from other products were encountered.

RESULTS

1. *Dose*

From Fig. 1 it is seen that for a benzoate ion concentration of 1.2×10^{-3} M, the amount

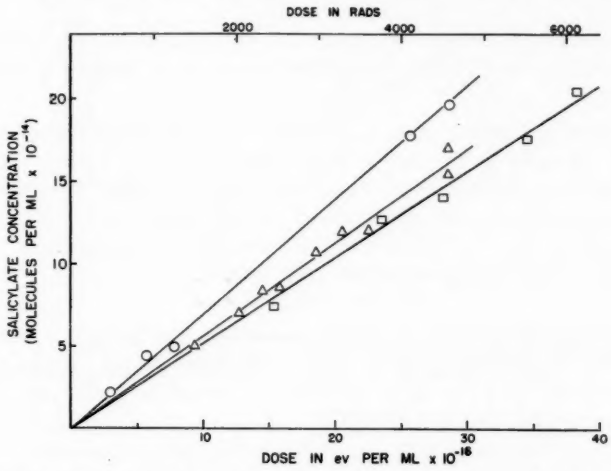

Fig. 1. Effect of dose rate on the formation of salicylic acid in aqueous solutions $1.2\times10^{-3}M$ in benzoate ion: ○ 4 rads/minute (Cs^{137} γ-rays), △ 18,000 rads/minute (3-Mev X rays), □ 85,000 rads/minute (3-Mev X rays).

of salicylic acid produced is a linear function of dose up to about 5000 rads. As the system was studied primarily for the measurement of doses of radiobiological interest (0–1000 rads), few measurements were taken at higher doses. However, there is an indication (not shown) that at high dose rates (18,000 rads/minute), the yield of salicylic acid tends to fall off slightly above 6000 rads even with benzoate ion concentrations as high as 1.2×10^{-2} M. At low benzoate ion concentrations (2.4×10^{-4} M) the product yield appears to decrease when the dose exceeds 1500 rads.

2. *Concentration of Benzoate Ion*

As shown in Fig. 2, the yield of salicylic acid, G_{Sal} (the number of molecules of

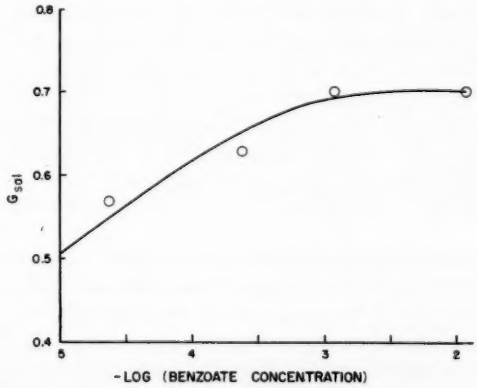

FIG. 2. Effect of benzoate ion concentration on G_{Sal}. Calcium benzoate solutions were irradiated with Cs^{137} γ-rays at 4 rads/minute.

salicylic acid formed per 100 ev of energy absorbed), increases with increasing benzoate ion concentration from 0.57 for 2.4×10^{-5} M to a limiting value of 0.70 at about 10^{-3} M benzoate ion.

3. Radiation Energy

It has been reported previously (5) that G_{Sal} is independent of radiation energy over the range 1.25 Mev to 0.16 Mev but is 20% lower at an energy of 0.05 Mev.

4. Dose Rate

G_{Sal} decreases with increasing dose rate. The results of irradiations of 6×10^{-4} M calcium benzoate solutions at three dose rates, plotted in Fig. 1, give G_{Sal} = 0.70 at 4 rads/minute, 0.59 at 18,000 rads/minute, and 0.53 at 85,000 rads/minute. Intermediate values were obtained using dose rates of 70, 3000, 5000, and 10,000 rads/minute. These are not listed as they lie within the experimental error ($\pm5\%$) of those values obtained for either 4 rads/minute or 18,000 rads/minute.

5. Temperature

Samples of 1.2×10^{-4} M calcium benzoate, thermostatted to within 0.5° C as previously described (3), were irradiated at a rate of 4 rads/minute with Cs^{137} γ-rays. Changes in temperature over the range 15–45° C were found to have no detectable effect on the radiation-induced reaction.

6. pH

The effect of pH on the fluorescence of salicylic acid and *m*-hydroxybenzoic acid has been described by Thommes and Leininger (8). The fluorescence of salicylic acid is due to the salicylate ion and is independent of pH in the range 4–13. However, *m*-hydroxybenzoic acid, which has been identified as a primary product of the radiolysis of benzoate solutions (9), exhibits fluorescence in solutions of pH greater than 8. Thus salicylic acid can best be determined fluorometrically in solutions of pH 4 to 8.

Unbuffered 6×10^{-4} M calcium benzoate solutions having a pH of about 6.3 were used almost exclusively in the radiation studies. Unbuffered 10^{-3} M benzoic acid solutions having a pH of about 3.6 were used successfully with irradiations at low dose rates by comparing the fluorescence of irradiated samples with that of standard salicylic solutions made up in 10^{-3} M benzoic acid. However, such a procedure is not recommended as small changes in pH produce large changes in fluorescence.

The results of the irradiation of alkaline benzoate solutions (pH 11.8) are shown in Fig. 3. The amount of salicylic acid plotted is not the true amount as it was calculated by comparing the total fluorescence due to the salicylic acid and the *m*-hydroxybenzoic acid in irradiated samples with that of a salicylic acid standard. From Fig. 3 the apparent G_{Sal} = 1.08 for Co^{60} γ-rays at 70 rads/minute and 0.87 for 3-Mev X rays at 18,000 rads/minute. This decrease in sensitivity with increasing dose rate is similar to that found in neutral solutions. As the sensitivity of neutral solutions is considered adequate, alkaline solutions were not further investigated.

7. Other Effects

Although benzoate solutions decarboxylate to some extent on prolonged standing, no effect attributable to this was found during any irradiation. No salicylate was detected in solutions which had been stored for many weeks in Pyrex flasks.

No detectable postirradiation effect was observed over a period of 24 hours. This was noted for samples receiving doses of about 100 rads at a dose rate of 4 rads/minute and also for samples receiving doses of about 2000 rads at a dose rate of 18,000 rads/minute.

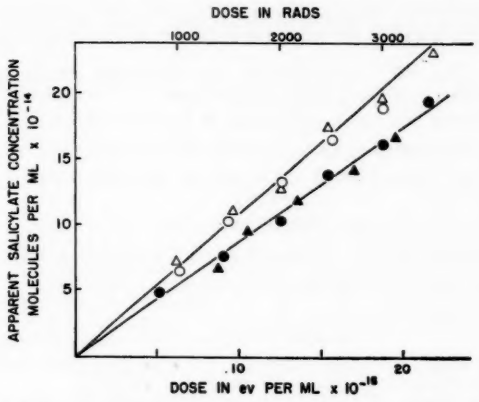

FIG. 3. Results of the irradiation of benzoate solutions 0.01 M in sodium hydroxide: ○ 6×10^{-4} M calcium benzoate, △ 10^{-3} M benzoic acid. Open symbols indicate irradiation with Co^{60} γ-rays at 70 rads/minute, darkened symbols irradiation with 3-Mev X rays at 18,000 rads/minute.

Calcium benzoate was used almost exclusively in this investigation primarily because it can be easily purified by repeated crystallizations from water. Samples of sodium and potassium benzoate as well as benzoic acid available at the outset of the investigation contained traces of salicylic acid and other impurities. The traces of salicylic acid caused high blank fluorescences and made the solutions unsuitable for the measurement of low doses. The other impurities caused some postirradiation changes. At a later date pure potassium benzoate was obtained and shown to give results identical with those obtained with calcium benzoate. Zone-refined PVS benzoic acid was also investigated briefly. As has been mentioned, millimolar benzoic acid solutions are too acidic for the accurate measurement of salicylate fluorescence. However, as shown in Fig. 3, the irradiation of alkaline benzoic acid and alkaline calcium benzoate gave similar results.

DISCUSSION

The results indicate that the aqueous benzoate system, as typified by 6×10^{-4} M calcium benzoate, meets many of the requirements for a sensitive chemical dosimeter. It is stable, easy to prepare, and exhibits no postirradiation change. The concentration of salicylic acid increases linearly with radiation dose in the range 5 to 5000 rads and is independent (within the estimated experimental error of $\pm5\%$) of temperature from 15 to 45° C, of energy from 160 kev to 3 Mev, and of dose rate from 4 to about 1000 rads/minute. With radiation energies lower than 160 kev, the response decreases with decreasing photon energy and at 50 kev is 17% lower (5). The indicated dose, on the basis of $G_{Sal} = 0.70$, will be lower than the actual dose by 5 to 15% with dose rates of 1000 to 18,000 rads/minute and by 16 to 24% with dose rates of 18,000 to 85,000 rads/minute.

It must be stressed that the sensitivity of this system as a dosimeter depends on the method of analysis. The ultimate sensitivity of any dosimeter which is based on fluorescence measurements is dependent on the ratio of the intensities of fluorescent and scattered light at a given wavelength λ, $(I_f/I_s)_\lambda$. In the Bowman–Aminco instrument, a high I_f is obtained by the use of a high intensity light source while I_s is kept to a minimum by the use of diffraction grating monochromators and excellent optical design.

However, it should be possible to adapt for accurate salicylate analysis any fluorometer which is equipped with an ultraviolet light source by the use of appropriate optical filters.

A discussion of the results reported here in terms of a mechanism for the radiation-induced reactions in aqueous benzoate solutions is beyond the scope of this paper. A report describing the formation of products other than salicylic acid and discussing the theoretical aspects of the benzoate system will be published soon.

ACKNOWLEDGMENTS

The authors wish to thank Mr. F. A. Bury for his assistance with the experiments which required the use of the Van de Graaff generator.

REFERENCES

1. G. J. HINE and G. L. BROWNELL. Radiation dosimetry. Academic Press Inc. 1956. Chap. 8.
2. W. A. ARMSTRONG and G. A. GRANT. Radiation Research, **8**, 375 (1958).
3. W. A. ARMSTRONG and G. A. GRANT. Can. J. Chem. **36**, 1398 (1958).
4. M. J. DAY and G. STEIN. Nature, **164**, 671 (1949).
5. W. A. ARMSTRONG and D. W. GRANT. Nature, **182**, 747 (1958).
6. J. WEISS, A. O. ALLEN, and H. A. SCHWARZ. Proceedings of the International Conference on the Peaceful Uses of Atomic Energy, Geneva, **14**, 179 (1955).
7. H. A. SCHWARZ and A. O. ALLEN. Nucleonics, **12** (2), 58 (1954).
8. G. A. THOMMES and E. LEININGER. Anal. Chem. **30**, 1361 (1958).
9. H. LOEBL, G. STEIN, and J. WEISS. J. Chem. Soc. 405 (1951).

RADIATION CHEMISTRY OF CYCLOHEXANE

II. DOSE RATE EFFECTS ON THE FORMATION AND DESTRUCTION OF CYCLOHEXENE[1]

P. J. DYNE AND J. W. FLETCHER

ABSTRACT

Prolonged radiolysis of cyclohexane leads to a steady-state concentration of cyclohexene where G(cyclohexene) = 0. At concentrations greater than this steady concentration, cyclohexene is destroyed. It is shown that this steady-state concentration is a function of dose rate, varying approximately as the fourth root of the radiation intensity. A discussion of these and other observations indicates that dose rate and L.E.T. effects are observed in cyclohexane only if radical scavengers are present and that cyclohexene, a product of radiolysis, acts as a radical scavenger in irradiated cyclohexane.

INTRODUCTION

Cyclohexene and bicyclohexyl are the two major high molecular weight products formed in the radiolysis of cyclohexane. Dewhurst and Schuler (1) have shown that the initial G values (molecules formed/100 ev absorbed) for cyclohexene and bicyclohexyl are independent of the L.E.T. (Linear Energy Transfer)* of the irradiation. Dewhurst (2) showed that G(cyclohexene) decreases with dose (i.e. with increasing cyclohexene concentration) and, further, that in concentrated solution (5×10^{-4} moles/g), cyclohexene is destroyed. It follows that prolonged irradiation of cyclohexane or of solutions of cyclohexene in cyclohexane leads to a "steady-state" concentration of cyclohexene where G(cyclohexene) = 0. Dewhurst and Schuler (1) found some evidence that G(cyclohexene) fell off more rapidly with cyclohexene concentration at low dose rates, using a Co^{60} γ-ray source, than at the higher dose rates obtained with electron and particle beams.

We have studied the formation and destruction of cyclohexene as a function of the dose rate, using Co^{60} γ-rays and have shown that the "steady-state" concentration increases slowly with the dose rate. The dependence is less than a proportionality to the square root of radiation intensity and approximates to a fourth root dependence.

EXPERIMENTAL

Samples of cyclohexane (spectroscopic grade from various manufacturers) were irradiated in sealed glass vessels. The liquids were degassed by freezing, pumping, and thawing five times. Two Co^{60} sources were used (3) having dose rates of 1.4×10^{19} ev/g hr and 9.6×10^{17} ev/g hr. These dose rates were established using the Fricke dosimeter, $G(Fe^{3+})$ = 15.5 ions/100 ev. Analysis for cyclohexene was done by infrared spectrophotometry of the 640 cm^{-1} band of cyclohexene using a Perkin–Elmer, model 21, spectrometer. Path lengths of 0.2–4.0 mm were used with compensating cells containing pure cyclohexane for the thicker cells. The irradiations were made over an extended period of time (irradiations of up to 1400 hours at the low dose rate). The solutions were stored after irradiation and were all analyzed at one time together with a series of standard solutions of known concentration. The concentrations were determined by graphical interpolation from the measurements of the standard spectra. At the low

[1]*Manuscript received February 2, 1960.*
Contribution from the Research Chemistry Branch, Atomic Energy of Canada Limited, Chalk River, Ontario. Issued as A.E.C.L. No. 1005.
**Equivalent to the ionization density along the track.*

dose rates the range of the experiments was increased by irradiating solutions that already contained cyclohexene. These results fitted smoothly into the curves obtained in the irradiation of pure cyclohexane.

RESULTS

Most of the experimental results for the high and low dose rates are shown in Figs. 1 and 2 respectively. It should first be noted that at the lower dose rate cyclohexene is

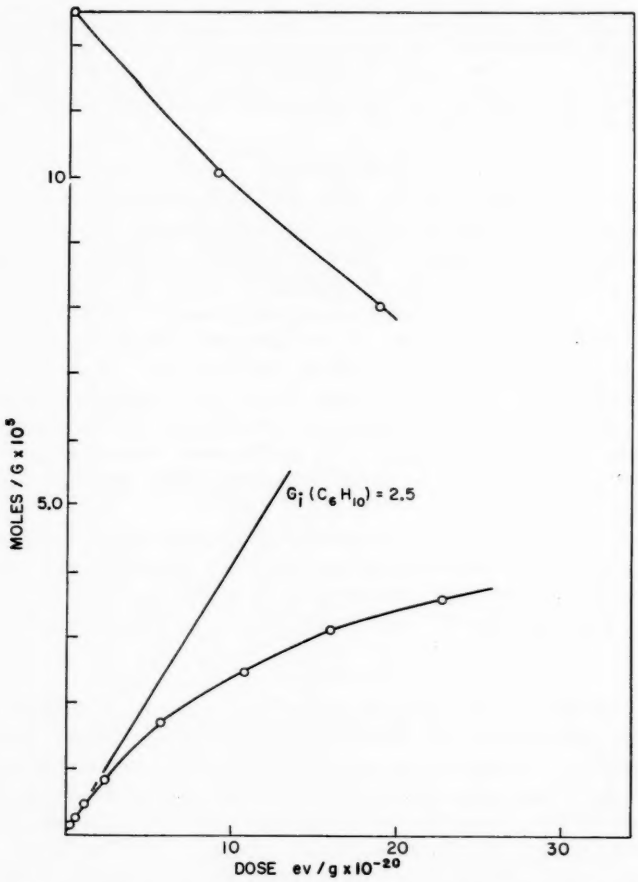

FIG. 1. Formation and destruction of cyclohexene at a dose rate of 1.4×10^{19} ev/g hr.

destroyed at concentrations such as 3.0×10^{-5} moles/g where it is still being formed at the higher dose rate. A similar comparison can be made between our high dose rate results, where decomposition occurs at concentrations greater than 4.5×10^{-5} moles/g, and Dewhurst's results with an electron beam (1), where net decomposition is observed only at concentrations greater than 4.0×10^{-4} moles/g.

We have drawn an initial slope, equivalent to $G(C_6H_{10}) = 2.5$, equal to Dewhurst's

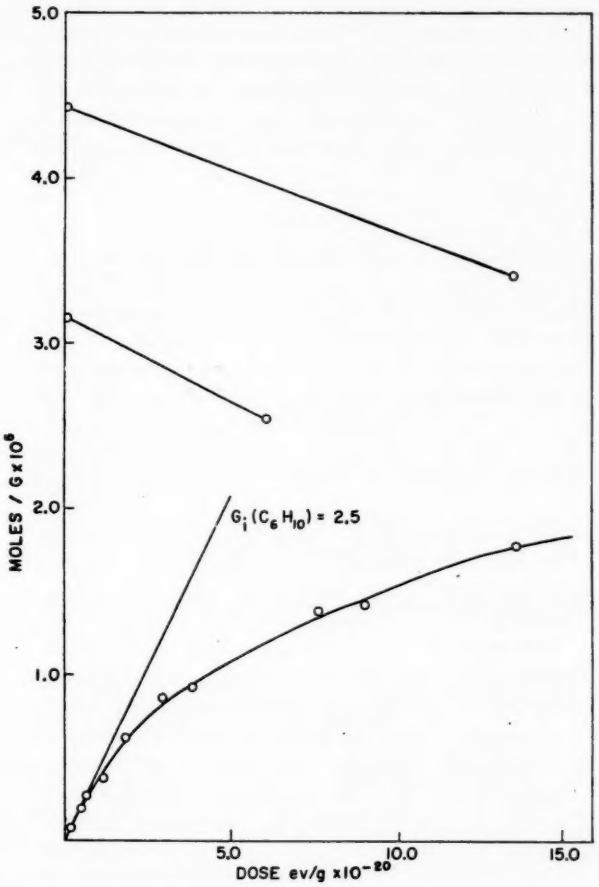

FIG. 2. Formation and destruction of cyclohexene at a dose rate of 9.6×10^{17} ev/g hr.

value, on both Figs. 1 and 2. It can be seen that there is no significant change in the initial *G*-value with dose rate. The *G*-value indicated by the first point (at the lowest cyclohexene concentration) in Fig. 1 and in Dewhurst's Fig. 1 are between 3.0 and 3.2. The value of 2.5 must be regarded as a minimum value; it is possible that the true limiting *G*-value is 3.0 or higher.

We have calculated *G*-values for each successive pair of experimental points in Figs. 1 and 2 and for Dewhurst's experimental results. In Fig. 3 the *G*-values are plotted against the concentration of the first point, i.e. the one with lower concentration where *G*-cyclohexene is positive and the one with the higher concentration when *G*-cyclohexene is negative. This procedure is, we feel, preferable to drawing a smooth curve through the experimental points and measuring graphically the slopes of a series of tangents. Due to the fairly steep curvature of the plots of $G(C_6H_{10})$ vs. cyclohexene concentration this is a plot of minimum *G*-values ($G(C_6H_{10})$ and $G(-C_6H_{10})$ both having positive signs). The high initial points, $G = 3.0$–3.2 mentioned in the previous paragraph, are seen on the

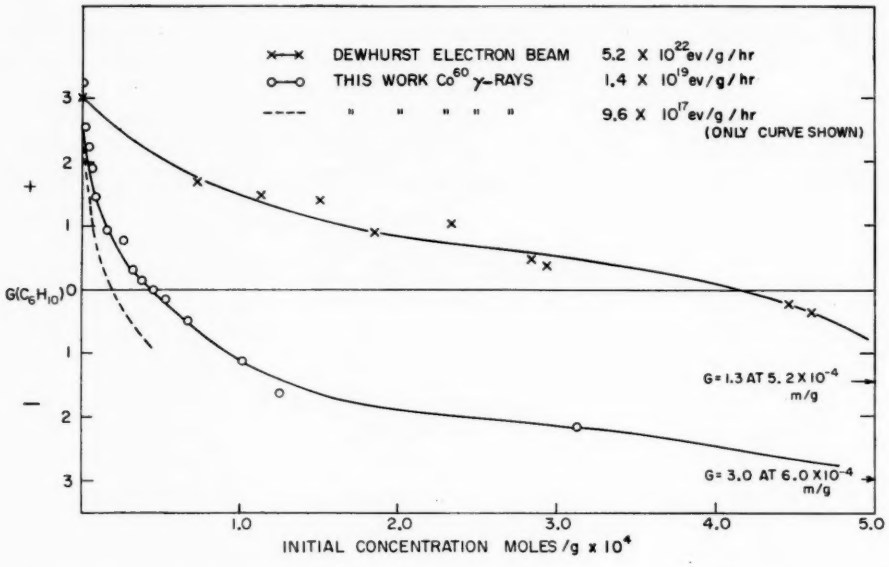

FIG. 3. *G*-values for formation and destruction of cyclohexene as a function of cyclohexene concentration. See text for method of calculation.

graph. The locus of $G(C_6H_{10})$ vs. C_6H_{10} for the lower dose rate (9.6×10^{17} ev/g hr) experiments is also shown in Fig. 3. At this low dose rate $G(C_6H_{10}) = 0$ at a cyclohexene concentration of 2×10^{-5} moles/g and the largest observed value of $G(-C_6H_{10})$ is 1.6 at 6.1×10^{-4} moles/g. The largest observed value of $G(-C_6H_{10})$ at our higher dose rate of 1.4×10^{19} ev/g hr was 3.0 at 6.0×10^{-4} moles/g. Dewhurst reports a value of $G(-C_6H_{10}) = 2.3$ at 5.2×10^{-4} moles/g at the high dose rate obtained with the electron beam. This value is greater than that shown in Fig. 3 as it was derived from the initial slope of a smoothed curve.

The steady-state concentrations determined from Fig. 3 are given in Table I, which includes the relative concentrations and dose rates and shows that the steady-state concentration varies approximately as the fourth root of the dose rate. The term steady state is, perhaps, somewhat unfortunate as it implies that this concentration will never change. With very long irradiations, 10 or more times the highest doses used here, further reactions must be expected. The term refers only to the dose range of the present experiments.

TABLE I

Variation of steady-state concentration with dose rate

Dose rate, ev/g hr	Steady-state concn., moles/g	Relative dose rate	Relative concn.	(Relative dose rate)$^{1/2}$	(Relative dose rate)$^{1/4}$
9.6×10^{17}	2.0×10^{-5}	1.0	1.0	1.0	1.0
1.4×10^{19}	4.5×10^{-5}	14.5	2.25	3.80	1.94
5.2×10^{22}	4.2×10^{-4}	5.4×10^{4}	21.0	2.32×10^{2}	15.2

Irradiation of cyclohexane in a spent fuel-element γ-ray source, reported by Nixon and Thorpe (4), gave a concentration of 2.7×10^{-5} moles/g cyclohexene at a dose of 4.8×10^{21} ev/g, equivalent to G(cyclohexene) = 0.34. When compared with the initial G(cyclohexene) = 2.5 this low G-value indicates that the system was approaching a steady state. The steady-state concentration at their dose rate ($\sim4\times10^{19}$ ev/g hr or perhaps somewhat less) (5) is, by interpolation from the data in Table I, $\sim6\times10^{-5}$ moles/g.

DISCUSSION

Two different, but closely related, effects have to be explained; the invariance of initial yields with L.E.T. and with dose rate, and the variation of yields with dose rate in the presence of cyclohexene. It is well known that both L.E.T. and dose rate effects are generally due to a competition between reactions $R + R \rightarrow$ products, P_1 involving two precursors (free radicals) and reactions $R + S \rightarrow$ products, P_2 involving one precursor and a stable molecule S present in macro quantities. The products P_1 and P_2 may consist of more than one species. Variations in yield with L.E.T. occur because the balance of the competition is largely determined by the initial distribution of the precursor R. The chief features of the radiation chemistry of water are explicable in these terms.

Variations of yields with dose rate occur, in general, because the steady-state concentration of precursors is determined by functions involving the dose rate and the square root of the dose rate: the square root arising from the bimolecular removal of precursors in a reaction $R + R \rightarrow P_1$. This situation occurs if the precursors are reacting homogeneously, track effects being absent (as in photochemistry).

The chief experimental observations to be correlated and explained are:

1. The initial yield of hydrogen from cyclohexane is independent of L.E.T. and dose rate. This was demonstrated by Schuler and Allen (6).

2. The initial yield of cyclohexene is also independent of dose rate and L.E.T. This may be stated, using E for cyclohexene, as $(dE/dt)\ (E \rightarrow 0) = k_1 I$, where I is the dose rate. This also expresses the fact that dose rate and/or L.E.T. effects are observed only in the presence of cyclohexene.

3. The yield of cyclohexene from unimolecular processes $C_6H_{12} \rightarrow C_6H_{10} + H_2$ has a G-value less than 1.0; the major fraction of the yield ($\sim2/3$) is produced by bimolecular processes, probably the disproportionation of cyclohexyl radicals, $2C_6H_{11} \rightarrow C_6H_{10} + C_6H_{12}$. This conclusion was reached by Dewhurst (2) from studies of the yield of cyclohexene in the presence of oxygen (1) and is in agreement with the measurements made by Dyne and Jenkinson (7) of the yield of deuterium produced in unimolecular processes from C_6D_{12}.

4. The steady-state concentration of cyclohexene varies slowly with radiation intensity, approximately as the fourth root of I, i.e. $E_s \simeq k_2 I^{1/4}$.

5. The yield of cyclohexene drops very sharply with cyclohexene concentration at the lower dose rates. Cyclohexene inhibits its own formation very effectively, more effectively than it reduces the yield of molecular hydrogen.

The invariance of the hydrogen yield with L.E.T. can be simply explained. Hydrogen is presumably formed by $H + C_6H_{12} \rightarrow H_2 + C_6H_{11}$; this is essentially the scavenging reaction $R + S \rightarrow$ products, where S is present at a very high concentration—so high that the probability of the recombination reaction $H + H \rightarrow H_2$ is very small. It should also be noted that the scavenging reaction gives one molecule H_2 for one hydrogen atom

while the recombination reaction gives one molecule H_2 for two hydrogen atoms. If the two reactions rates were comparable then the hydrogen yield would *decrease* with increasing L.E.T. as the probability of bimolecular recombination would increase.

The invariance of the initial yield of cyclohexene with L.E.T. may arise from the opposite circumstance; all the precursors of cyclohexene react $R + R \rightarrow$ products (e.g. cyclohexene) and the scavenging reaction is non-existent. Scavengers (cyclohexene itself, for instance) may be formed during the radiolysis. Changes in yield with L.E.T. would then be observed in solutions containing cyclohexene but not in pure cyclohexane. This is in agreement with experiment. The variation in yield of bicyclohexyl with dose rate, which is similar to the behavior of cyclohexene observed by Dewhurst and Schuler (1), would be explained similarly.

With reference to the steady-state concentration, it is not possible to distinguish properly between L.E.T. and dose rate effects. The dose rate variation has been observed with Co^{60} γ-rays. No α-particle or proton beam experiments have been reported in which the total dose rate was varied or in which the irradiation was carried to a sufficiently high dose rate for the observation of the radiation steady state.

Dose rate effects in γ-ray irradiations can occur only when radicals (or precursors) have an appreciable probability of escaping from the spur in which they were formed and of reacting with radicals produced in other spurs. Homogeneous kinetics, as in photochemistry, are then applicable. A competition between $R + R \rightarrow P_1$ reactions (second order in R) and $R + S \rightarrow P_2$ reactions (first order in R) will give rise to dose rate dependence of the yields of P_1 and P_2 and of the disappearance of S. The present evidence suggests that cyclohexene is the scavenger S as its presence generates the dose rate effects. The effectiveness of cyclohexene in the inhibition of its own formation suggests, also, that in the $R + R \rightarrow P_1$ reactions, P_1 includes cyclohexene. Cyclohexene is destroyed in the scavenging reactions and in some of these same reactions it destroys its own precursors. As G(cyclohexene) falls more rapidly than $G(H_2)$ with cyclohexene concentration (i.e. the reduction in $G(H_2)$ is not equivalent to the reduction in G(cyclohexene)), cyclohexene must presumably be reacting with other precursors as well as with hydrogen atoms.*

Schuler (8), using a variety of ionizing radiations, measured the disappearance of iodine in cyclohexane solutions and equated this yield with the total radical yield. The radical yield obtained with 33-Mev helium ions is about 30% less than that found in electron beam irradiations. Compared with the effects in water this is a small change in yield with L.E.T. Under the particular experimental conditions used (dose rate, scavenger concentration, etc.) the scavenging reaction is dominating the recombination reaction over the whole L.E.T. range. Detailed studies of scavenging, similar to those done by Charlesby and Lloyd (9) on anthracene are needed to put this and other observations (such as those presented in this paper on cyclohexene) on a quantitative basis.

The relations $dE/dt.(E \rightarrow 0) = k_1 I$ and $E_s \simeq k_2 I^{1/4}$ are reduced, approximate forms of the general rate equation $dE/dt = F - D$ where F is the rate function for all processes forming cyclohexene and D the rate function for all processes destroying cyclohexene. Both these rates F and D are likely to be functions of E and I. We may speculate on the form of F and D, as follows. The $I^{1/4}$ function is probably derived from the $I^{1/2}$ dependence found in many radical chain mechanisms. The relation $E_s \simeq k_2 I^{1/4}$ is possibly

**This conclusion is contrary to the argument given by Dewhurst, who equates the change in hydrogen yield with the value of $G(-C_6H_{10})$ at a concentration of 5.2×10^{-4} moles/g. The correct value for the comparison is $[G_{\text{initial}}(C_6H_{10}) + G(-C_6H_{10})]$ and this is greater than the reduction in hydrogen yield.*

a simplification of $E_s^2 \simeq k_2^2 I^{1/2}$. This equation is a reduced form of the relation $D = F$ when $E = E_s$. Now F, the processes of formation, are likely to be proportional to I; they are certainly so when $E = 0$. The process of destruction is likely to be a reaction of cyclohexene with a reactive intermediate with a rate governed by $k.E.R$ where R is the steady-state concentration of this intermediate. If this is the intensity-dependent process, it may have the form $k''EI^{1/2}$. The relation $E_s^2 \simeq k_2^2 I^{1/2}$ can be rearranged to $E_s I^{1/2} \simeq k_2^2 I/E_s$ which we identify with $D = F$. Now F cannot be inversely proportional to E as $E \to 0$—it must have a form of the type: $k_2^2 I/(k_3+E)$, in which k_3 is sufficiently small that E quickly becomes the dominating term in the denominator.

The true rate equations must be more complex than this. We know that there are two processes, one unimolecular, the other bimolecular, forming cyclohexene, i.e. $F = F_1+F_2$, each presumably having a different dependence on E and I. There may again be more than one process destroying cyclohexene. The sum of all destruction $\Sigma_1 D_1$ and formation processes are related by $\Sigma_1 D_1 = F_1+F_2$ at the steady state. The relation $E_s I^{1/2} \simeq k_2^2 I/(k_3+E)$ is a simplification of this relation which is observed over a possibly limited range of values of E and I.

In summary, the chief conclusion of this study is that, in liquid cyclohexane, scavengers must be present before dose rate and L.E.T. effects are observed and that a major product of the radiolysis, cyclohexene, acts as a scavenger.

ACKNOWLEDGMENTS

It is a pleasure to acknowledge the helpful and critical interest Dr. R. H. Betts has shown in this work.

REFERENCES

1. H. A. DEWHURST and R. H. SCHULER. J. Am. Chem. Soc. **81**, 3210 (1959).
2. H. A. DEWHURST. J. Phys. Chem. **63**, 813 (1959).
3. P. B. AITKEN, P. J. DYNE, and E. C. TRAPP. Nucleonics, **15**, 100 (1957).
4. A. C. NIXON and R. E. THORPE. J. Chem. Phys. **28**, 1004 (1958).
5. A. C. NIXON. Private communication.
6. R. H. SCHULER and A. O. ALLEN. J. Am. Chem. Soc. **77**, 507 (1955).
7. P. J. DYNE and W. M. JENKINSON. Can. J. Chem. **38**, 539 (1960).
8. R. H. SCHULER. J. Phys. Chem. **63**, 925 (1959).
9. A. CHARLESBY and D. G. LLOYD. Proc. Roy. Soc. A, **249**, 51 (1958).

THE DECOMPOSITION OF METHANE BY LOW-ENERGY ELECTRONS[1]

J. E. MANTON[2] AND A. W. TICKNER

ABSTRACT

The decomposition of methane by a beam of electrons having energies between 15 and 100 ev has been studied using methane pressures between 10^{-4} and 10^{-3} mm of mercury. The products were frozen out on a surface cooled to about −220° C and situated approximately 5 millimeters from the electron beam.

Ethane, ethylene, and acetylene were found to be the main products along with smaller amounts of saturated and unsaturated higher hydrocarbons. The results provide some evidence that under these experimental conditions ions do not play a major part in the decomposition and a free radical mechanism has been proposed to explain the formation of the main products.

INTRODUCTION

Recently the authors have become interested in the study of chemical reactions in the electric discharge. For many years, the interpretation of the results of such studies was based largely on the reactions of free radicals, ionic reactions not being considered of importance. During the last few years, however, it has been observed, initially by Stevenson (1), that ions frequently have enhanced cross sections for reaction. This has led to a reappraisal of the role played by ions in radiation and discharge chemistry.

As an aid to understanding the decomposition of methane in a discharge, the experimental conditions have been simplified in such a way that many of the experimental parameters could be separately controlled. In addition, an effort has been made to reduce the extent to which secondary reactions occur by providing for the rapid removal of the products from the reaction zone. In this way, it was hoped to obtain some information concerning the primary products of the discharge reaction.

EXPERIMENTAL

A conventional vacuum system, capable of maintaining a background pressure of less than 10^{-6} mm Hg, was used. The essential details of the apparatus are shown in Figs. 1 and 2.

An electrically heated (a-c.) tungsten ribbon filament was the source of electrons, the filament being enclosed in a housing with its own pumping for the removal of pyrolysis products. The beam of electrons was defined by apertures 1.5 mm in diameter in a series of Chromel A plates. Further alignment and collimation of the beam were obtained by the use of a permanent magnet which provided a uniform field strength of 870 gauss over an area about 4 centimeters in diameter at the center of the gap. Onto the final collimator (collimator 2) was soldered a hollow brass cone, A, which fitted into the glass tube surrounding the reaction zone. This arrangement caused the major pressure drop to be across the defining aperture in the center of the collimator. The collector served to monitor the electron beam. The collector grid, about 1 mm in front of it, consisted of 90% transparent tungsten mesh and was maintained at the same potential as the final collimator, thus creating a field free reaction zone 4.5 centimeters in length.

The various potentials were obtained from a regulated d-c. supply and were chosen to give the maximum beam current consistent with stability and reasonable filament

[1]*Manuscript received January 27, 1960.*
Contribution from the Division of Applied Chemistry, National Research Council, Ottawa, Canada. Presented in part at the Annual Conference of the Chemical Institute of Canada, May, 1959.
Issued as N.R.C. No. 5668.
[2]*N.R.C. Postdoctorate Fellow. Present address: Royal Military College, Kingston, Ontario, Canada.*

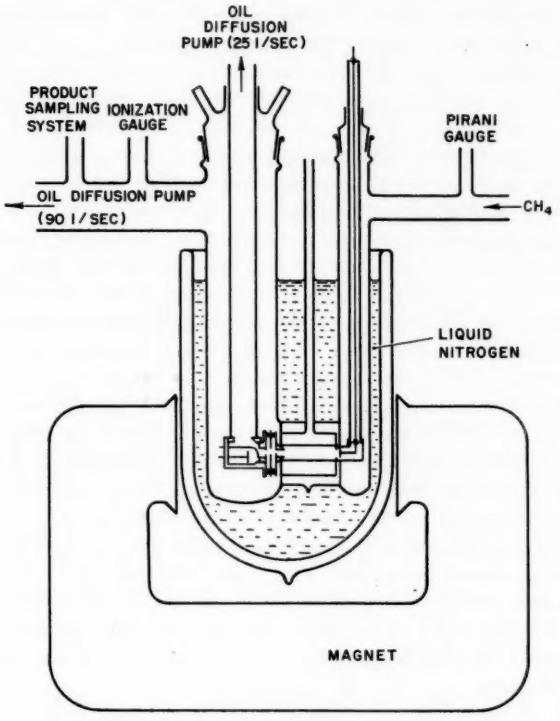

FIG. 1. Apparatus.

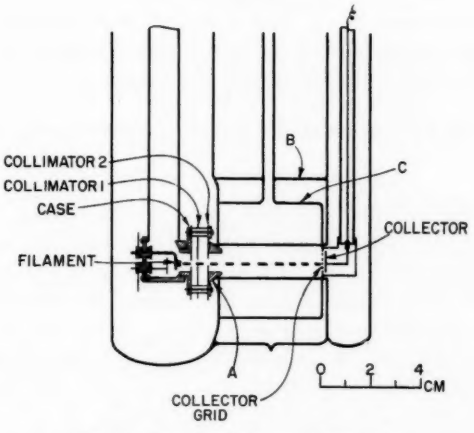

FIG. 2. Details of electron beam tube.

life. The filament housing was maintained at +25 v and collimator 1 at +10 v to +15 v, all potentials being established with respect to the center of the filament. Collimator 2 and the collector grid were set at the electron energy required for the experiment and

the collector was maintained about 25 volts more positive. The electron beam current was controlled manually by adjusting the filament current.

The path of the electron beam through the methane could be observed, in a darkened room, as a faint bluish column, approximately the diameter of the defining apertures and extending the whole length of the reaction zone. After the initial experiments, the inside surface of the glass tube surrounding the reaction zone was gold-coated by evaporation in order to prevent charge accumulation on the walls. A spring contact connected the gold layer electrically to the collector grid.

The reaction products were expected to be mixtures of the lower hydrocarbons similar to those obtained in the decomposition of methane in the d-c. glow discharge at low temperatures (2, 3). The estimated rates of formation, based on the low-temperature discharge work, together with values of the vapor pressures of the C_2 hydrocarbons, obtained by extrapolation of the data of Tickner and Lossing (4), indicated that a temperature of about $-215°$ C would be necessary to freeze out the reaction products quantitatively. The refrigerant used was solid nitrogen, obtained by reducing the pressure above liquid nitrogen. The solid nitrogen was in chamber C in Fig. 2, this being surrounded by the evacuated chamber B, and the whole immersed in liquid nitrogen. In this way, the walls of the tube surrounding the reaction zone could be cooled to slightly below $-220°$ C, as indicated by the vapor pressure of methane.

The methane used was Matheson C.P. grade and was purified by fractional distillation before admission to the storage reservoir. From this reservoir, the methane was admitted to the reaction system via a needle valve, which controlled the flow rate, and a trap maintained at the freezing point of nitrogen, $-210°$ C for final purification. The methane pressure was measured with a Pirani gauge, which had been calibrated, *in situ*, against a standard McLeod gauge.

In carrying out an experiment, a steady flow of methane was established and the electron beam turned on for the required time. The length of a run, about 20 minutes, was chosen in order to obtain the maximum quantity of products consistent with maintaining sufficient solid nitrogen in the jacket for efficient trapping. At the end of an experiment, the methane was turned off and the system pumped briefly to a low pressure and then isolated. After the reaction system had warmed up, the products were quantitatively transferred to a gas burette by means of a Toepler pump and the volume measured. A sample was then taken and analyzed on the mass spectrometer.

EXPERIMENTAL RESULTS

In order to determine the contributions of materials formed by pyrolysis on the filament, blank runs at 5×10^{-3} mm and 10×10^{-3} mm pressure of methane were performed. The experimental conditions, including the filament current, were the same as those used in the other runs except that no d-c. potentials were applied to the system. Small amounts of the C_2 hydrocarbons were found, which did not exceed 2% of the amounts formed during any of the experiments. In addition, propylene was found in amounts up to 5% and butene in amounts up to 25% of the quantities obtained as products in subsequent runs. The quantity of pentene found in the blank corresponded to between 25% and 50% of the amounts recovered in subsequent experiments. Since in almost every case, the corrections would be small compared with the other uncertainties involved, no corrections have been made for the presence of pyrolysis products among the reaction products.

The variation of the reaction products with electron energy is shown in Fig. 3. The

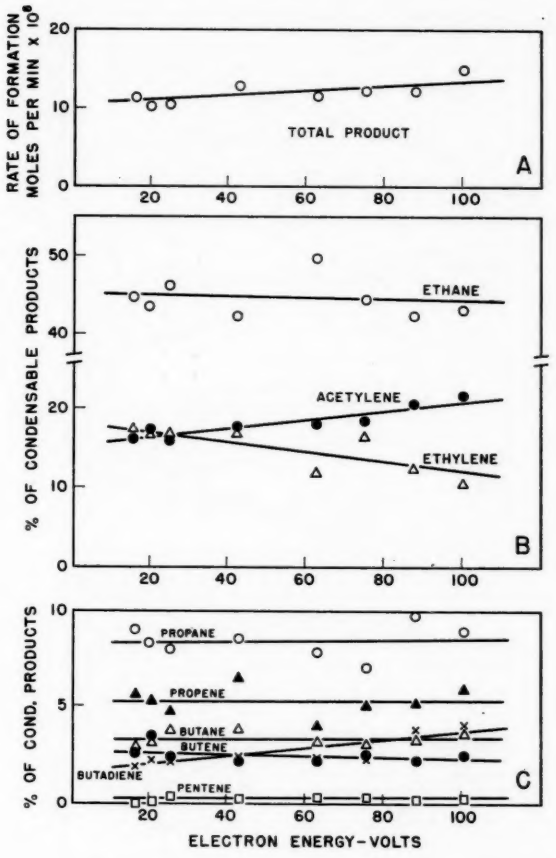

FIG. 3. Variation of products with electron energy.

values were obtained at a pressure of 5.2×10^{-3} mm of methane and collector currents of $250(\pm5)$ μa. It was not found possible to extend the measurements to lower voltages because the electron beam became unstable below about 15 volts. At 50 ev the extent of decomposition was about 3% and in all cases the contact time was estimated to be about 0.02 second.

The effect of pressure on the reaction products is shown in Fig. 4. These experiments were carried out with collector currents of $230(\pm10)$ μa and at an electron energy of 50 ev. At the temperature used to trap the products ($-220°$ C) the maximum pressure of methane which could be used is the vapor pressure (about 10^{-2} mm). The lower limit to the pressure range was set by the fact that the rate of formation of products decreased as the pressure was lowered. Consequently, the more volatile products could not be recovered quantitatively below about 2×10^{-3} millimeters.

Figure 5 shows the effect of collector current on the products, using 50-v electrons and a pressure of 5.2×10^{-3} mm of methane. The lower limit of 100 μa was again

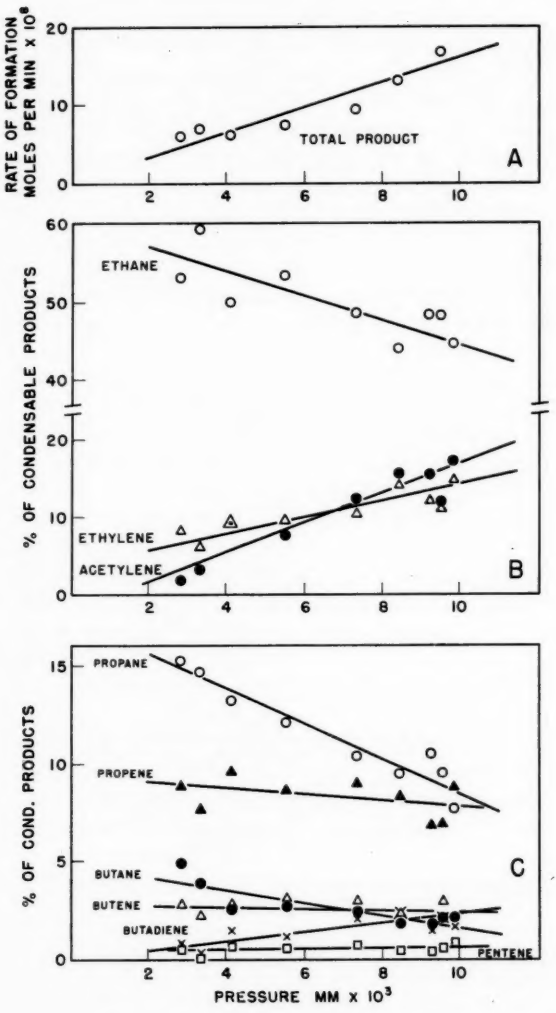

FIG. 4. Variation of products with pressure.

determined by the vapor pressures of the products and the efficiency with which they could be trapped.

No analyses were made for the hydrogen which was presumably formed in the decomposition. Such an analysis would have been difficult to perform accurately since the concentration of hydrogen in the reacted gas would have been less than 3% and the total gas pressure downstream from the reaction zone was less than 10^{-4} mm of mercury. A study of the decomposition of methane in the negative glow of a d-c. discharge (3) has shown that under comparable conditions the products are very similar to those reported here. In the discharge experiments, which could be carried to higher con-

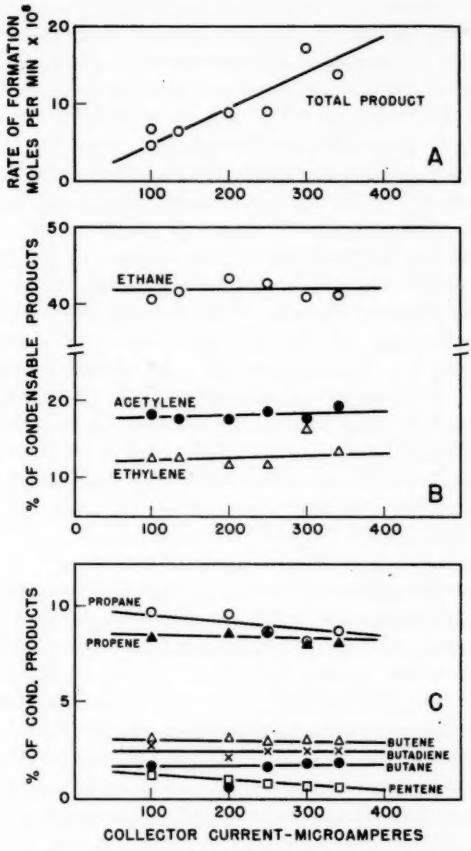

FIG. 5. Variation of products with collector current.

versions and in which the gas could be sampled at much higher pressures, analysis of the reacted gas showed that the theoretical amount of hydrogen was in fact produced.

The experimental conditions made it difficult to study the effect of the reaction products on the over-all reaction, except for hydrogen. Experiments with up to 10% hydrogen in the methane showed no significant change in either the percentage composition or the rate of formation of the products. Similarly, in an experiment with 2% of deuterium in the methane, no deuteration of the products was detected.

The values of the methane pressure given throughout this report are those measured on the calibrated Pirani gauge. The true pressures in the reaction zone were undoubtedly somewhat lower than the measured values due to the existence of a small pressure gradient. In addition, it was difficult to fit the brass cone on the final collimator reproducibly into the end of the glass tube surrounding the reaction zone. Since it was necessary to disturb the alignment of the cone each time the filament was replaced (about once in 10 runs), each filament had associated with it a different pressure gradient and hence a different relationship between the measured value of the pressure and the true value.

The experimental points in each figure were obtained using a single setting of the collimator but the values of the pressure given in different figures are not directly comparable. From a comparison of the results obtained with a number of different collimator settings we believe that all of the values of the pressure given agree with the true value within a factor of 2.

In general the results show a considerable amount of scatter due to the small amount of product formed and the uncertainties involved in working out the composition from the mass spectrum of such a complex mixture. Straight lines have been drawn through the points in all cases for the purpose of indicating trends.

In two cases there is some ambiguity in the identification of the products. The mass spectra provide some evidence that the substance appearing at $m/e = 42$ may consist of cyclopropane as well as propene. Because of the overlapping of the spectra and the small amounts involved it was not possible to distinguish quantitatively between these two compounds and in reporting the experimental results this product has simply been called propene. Similarly, the product appearing at $m/e = 54$ could, on the basis of the mass spectra, be either butadiene or butyne. Because propyne, for which there was qualitative evidence but which could not be determined accurately, was present only in smaller amounts, this compound has been designated butadiene.

DISCUSSION

The results in Fig. 3A indicate that the rate of formation of products varies only slightly with electron energy from 100 v to within a few volts of the ionization potential of methane. If the products were formed mainly by a process depending on the formation of ions, it would be expected that the rate of formation would fall off rapidly below about 50 ev in accordance with Tozer's values (5) for the ionization cross section of methane. Thus, although ions are undoubtedly formed, there seems to be no evidence that they play an important role in the formation of the products.

This conclusion is in agreement with that of Williams (6), who has studied the decomposition of methane using photoelectrons which are accelerated through the gas. Although the work he reports was carried out at much higher pressures and in the presence of an electric field, the products he obtained are similar to those obtained in this work. The absence of unsaturated hydrocarbons among his reaction products seems reasonable since his experiments were carried out in a static system for relatively long periods at room temperature. Thus, the more reactive unsaturated hydrocarbons which might have formed initially could have reacted to form saturated hydrocarbons or polymers. Since in this work the products were trapped within a few mean free paths of the reaction zone it is evident that they were removed from the reaction at a much earlier stage.

Although their work is not entirely comparable it is interesting to note that recently Yang and Manno (7), using nitric oxide as an inhibitor, have determined the free radical contribution to the various products formed in the γ-radiolysis of methane. They estimated the free radical contribution to the formation of ethane, propane, butane, and pentene, which together make up nearly all of their hydrocarbon products and which constitute most of ours, to be 85% or greater.

Figure 4A shows that the quantity of product increases linearly with methane pressure. Although the composition of the product changes as the pressure is raised the changes, to a large extent, offset the effect of one another on the carbon balance. Thus, the amount of methane decomposed is approximately proportional to the pressure over the range studied.

The experiments recorded in Fig. 5A indicate that the amount of product formed is directly proportional to the electron current. Since the composition of the product changes little over the range of currents studied, the products apparently arise in each case as the result of a single collision of an electron with a methane molecule. Secondary collisions between the product molecules and other electrons do not appear to play an important part.

If the electron efficiency is defined as the number of molecules of methane decomposed per electronic charge passed through the system, then our results yield a value of 1.8 for 50 ev electrons and a methane pressure of 5×10^{-3} mm. This assumes that all of the methane decomposed is recovered as volatile hydrocarbon products; if additional involatile products are formed, the electron efficiency would be correspondingly greater. Experiments utilizing the negative glow of a d-c. discharge under comparable conditions have led to electron efficiencies of about 10 (2, 3). The difference in the values seems reasonable since the discharge experiments were carried out at higher pressures and our results show that the electron efficiency increases with pressure. In addition, the electron multiplication and recombination which occur in a discharge would tend to increase the value of the electron efficiency as calculated on the above basis. Williams (6) has reported values of the electron efficiency which vary with pressure and with the voltage gradient and which lie within the range 0 to 10.

Because the products do not appear to depend to any large extent on ions for their formation, the discussion of mechanism will be limited to a consideration of the manner in which the products might be formed by free radical processes. A further restriction upon the possible reactions to be considered is imposed by the low temperature at which the experiments were carried out. This restricts the reactions to those having very low activation energies or those involving excited species.

The chemical effects of the high-energy irradiation of methane have been attributed largely to the action of secondary electrons having energies of the same order as the electrons used in this work (8). Thus it seems reasonable to expect that free radicals which have been detected in the radiolysis of methane may also play a part in the decomposition of methane under the conditions of our experiments. Gevantman and Williams (9), using iodine as a free radical scavenger, concluded that methyl, methylene, and ethyl radicals were important in the decomposition of methane by high-energy X rays and electrons. More recently, Meisels, Hamill, and Williams (10) studied the irradiation of methane in mixtures with argon and krypton and concluded that methyl and ethyl radicals and ethylene were significant intermediates. Because no ketene was formed in the radiolysis of mixtures of argon, methane, and carbon monoxide, they concluded that CH_2 was not formed.

There is also a great similarity between the results reported here for the decomposition of methane in a beam of electrons and the decomposition of methane in an electric discharge. This is especially true for the negative glow of a d-c. discharge when small currents are used and the discharge tube is cooled to low temperatures. Under these conditions the products are almost identical with those reported here (2, 3). Jen, Foner, Cochran, and Bowers (11), using electron spin resonance, have detected methyl radicals in the products of a low-power discharge in methane when the products were frozen out rapidly at 4.2° K. Under conditions of high-power input and high conversion, as used by Wiener and Burton (12), the main hydrocarbon product of the discharge decomposition of methane is acetylene. In their work they consider that both methyl and methylene radicals contribute to the over-all reaction.

In view of the above evidence and our experimental results it seems reasonable to assume that in our experiments methane decomposes according to reaction 1. The main product, ethane, would then be formed by reaction 2 which may occur to a large extent on the wall.

$$CH_4 \xrightarrow{e} CH_3 + H \quad [1]$$

$$2CH_3 \longrightarrow C_2H_6 \quad [2]$$

It would be difficult, however, to account for the complex product obtained solely on the basis of the reactions of methyl radicals, even allowing for the possible subsequent formation of other saturated radicals. During the last few years a considerable amount of chemical evidence has been obtained for the existence of excited methylene radicals (13) and recently the existence of the methylene radical in an excited state has been confirmed spectroscopically (14). Burton and Magee (15) have suggested that excited methylene radicals play an important part in the discharge decomposition of methane.

The data in Figs. 4A and 5A indicate that the rate of decomposition of methane increases linearly with both current and pressure, presumably due to the increase in the number of collisions between electrons and methane molecules. However, the amounts of ethylene and acetylene formed increase more rapidly with pressure than that of ethane, whereas the relative amounts of these products do not change with increasing current. This can be accounted for by assuming that, in addition to reaction 1, methane can decompose to yield another species which is capable of reacting with methane at the low temperature of the experiment. Thus, a reaction such as reaction 3 is indicated, where * designates an excited species. This would then be followed by reactions such as 4, 5, 6, and 7. Reaction 6 may occur to a large extent on the wall.

$$CH_4 \xrightarrow{e} CH_2^* + H_2 \quad [3]$$

$$CH_2^* + CH_4 \longrightarrow [C_2H_6]^* \quad [4]$$

$$[C_2H_6]^* \longrightarrow C_2H_4^* + H_2 \quad [5]$$

$$C_2H_4^* \xrightarrow{M} C_2H_4 \quad [6]$$

$$C_2H_4^* \longrightarrow C_2H_2 + H_2 \quad [7]$$

It has been reported (16) that energy-rich ethylene molecules may stabilize by deactivation as in reaction 6 or by decomposition as in reaction 7. If the excited state of ethylene involved in this work is different from that encountered in the mercury-photosensitized decomposition, it is possible that reactions 5 and 7 may involve as intermediates ethyl and vinyl radicals, with the resulting formation of hydrogen atoms. From the fact that the experiments with methane containing up to 10% hydrogen showed no appreciable change in the products, it seems probable that hydrogen atoms do not play a major part in the over-all reaction scheme.

Assuming that most of the methyl radicals combine to form ethane as in reaction 2, it follows that the rate of formation of ethane should increase linearly with both pressure and current, which is approximately the case. The rates of formation of ethylene and acetylene should increase linearly with current but, because of the dependence of reaction 4 on methane concentration, should increase more rapidly than that of ethane as the methane pressure is increased.

The increase in the rate of formation of acetylene, at the apparent expense of ethylene, with increasing electron energy (Fig. 3B) might be explained on the basis of the inter-

dependence of reactions 6 and 7. If the energy imparted to the methylene radical increases as the electron energy is increased this might result in an ethylene molecule possessing increasing amounts of energy and therefore in an increase in the rate of its decomposition (reaction 7) at the expense of deactivation (reaction 6).

Although the over-all extent of methane decomposition is small, most of the decomposition occurs within the electron beam giving locally a relatively high concentration of radicals and product molecules. As a result, radical–radical and radical–product reactions might be expected to occur. There is thus the possibility of forming other radicals by reactions such as 8 and 9.

$$CH_2^* + CH_3 \longrightarrow C_2H_5^* \quad [8]$$

$$C_2H_5^* \longrightarrow C_2H_3 + H_2 \quad [9]$$

The formation of the hydrocarbons of higher molecular weight may be accounted for in a general way as being due to further reactions of the free radicals present. Some of them may arise by simple radical combination reactions such as 10 and 11.

$$CH_3 + C_2H_5 \longrightarrow C_3H_8 \quad [10]$$

$$2C_2H_5 \longrightarrow C_4H_{10} \quad [11]$$

Others may be formed by reactions between radicals and product molecules. Vanpee and Grard (17) have suggested that higher hydrocarbons can be formed stepwise by reactions like 12 and 13.

$$CH_2 + C_2H_4 \longrightarrow C_3H_6 \quad [12]$$

$$CH_2 + C_2H_6 \longrightarrow C_3H_8 \quad [13]$$

Their suggestion has been confirmed by much recent work (13, 18). In addition, Gordon and McNesby (19) have shown that the polymerization of ethylene by methyl radicals results in the formation of many of the higher hydrocarbons found here.

One of the higher products, butadiene, seems to deserve individual consideration. The curves giving the variation in the percentage of this compound are not consistent with those of the other C_4 hydrocarbons but instead parallel those of acetylene. There is thus evidence that butadiene is formed by some species associated with the formation of acetylene. One possibility is given by reaction 14.

$$2C_2H_2 \longrightarrow C_4H_6 \quad [14]$$

The narrow limits within which the experiments could be carried out and the large amount of scatter in the experimental points make it difficult to arrive at a definite mechanism for the formation of most of the C_3 and C_4 products. The reactions occurring may involve highly excited species and therefore may not be comparable with the work referred to in the preceding paragraphs. Nevertheless, it seems to follow from Fig. 4 that the slopes of the lines representing the saturated hydrocarbon products are similar to one another, and that the olefins behave as another group. It is tempting to relate this to a stepwise process for the formation of the higher hydrocarbons as suggested by Vanpee and Grard (17).

ACKNOWLEDGMENTS

The authors wish to express their appreciation to Dr. R. J. Cvetanović for several helpful discussions, to Mr. S. Tong for assistance with the experimental work, and to Mr. R. Sander, who carried out the mass spectrometer analyses.

REFERENCES

1. D. P. STEVENSON and D. O. SCHISSLER. J. Chem. Phys. **23**, 1353 (1955).
2. L. M. YEDDANAPALLI. J. Chem. Phys. **10**, 249 (1942).
3. A. W. TICKNER. To be published.
4. A. W. TICKNER and F. P. LOSSING. J. Phys. Chem. **55**, 733 (1951).
5. B. A. TOZER. J. Electronics and Control, **4**, 149 (1958).
6. R. R. WILLIAMS. J. Phys. Chem. **63**, 776 (1959).
7. K. YANG and P. J. MANNO. J. Am. Chem. Soc. **81**, 3507 (1959).
8. RADIATION BIOLOGY. Vol. I. High energy radiation. *Edited by* A. Hollaender. McGraw-Hill Book Co. Inc., New York. 1954.
9. L. H. GEVANTMAN and R. R. WILLIAMS. J. Phys. Chem. **56**, 569 (1952).
10. G. G. MEISELS, W. H. HAMILL, and R. R. WILLIAMS. J. Phys. Chem. **61**, 1456 (1957).
11. C. K. JEN, S. N. FONER, E. L. COCHRAN, and V. A. BOWERS. Phys. Rev. **112**, 1169 (1958).
12. H. WIENER and M. BURTON. J. Am. Chem. Soc. **75**, 5815 (1953).
13. H. M. FREY and G. B. KISTIAKOWSKY. J. Am. Chem. Soc. **79**, 6373 (1957).
    H. M. FREY. Proc. Roy. Soc. A, **250**, 409 (1959); A, **251**, 575 (1959).
14. G. HERZBERG and J. SHOOSMITH. Nature, **183**, 1801 (1959).
15. M. BURTON and J. L. MAGEE. J. Chem. Phys. **23**, 2195 (1955).
16. D. J. LEROY and E. W. R. STEACIE. J. Chem. Phys. **9**, 829 (1941).
    A. B. CALLEAR and R. J. CVETANOVIĆ. J. Chem. Phys. **24**, 873 (1956).
17. M. VANPEE and F. GRARD. Ann. mines Belg. **49**, 701 (1950).
18. W. VON E. DOERING and H. PRINZBACH. Tetrahedron, **6**, 24 (1959).
19. A. S. GORDON and J. R. MCNESBY. J. Chem. Phys. **31**, 853 (1959).

THE CELL WALL POLYSACCHARIDES OF CANDIDA ALBICANS: GLUCAN, MANNAN, AND CHITIN[1]

C. T. BISHOP, F. BLANK,[2] AND P. E. GARDNER[3]

ABSTRACT

Cells of *Candida albicans*, a pathogenic yeast, have been shown to contain, in addition to chitin, a glucan ($[\alpha]_D$ −30°) and a mannan ($[\alpha]_D$ +78°) in the approximate ratio of 1.00:0.64. The two polysaccharides were easily distinguishable by moving boundary electrophoresis in borate buffer and were separated from each other by fractionation of their copper complexes. Methylation and hydrolysis of the glucan yielded the following *O*-methyl ethers of D-glucose: 2,3,4,6-tetra-*O*-methyl (7 moles); 2,3,4-tri-*O*-methyl (13 moles); 2,4,6-tri-*O*-methyl (trace); 2,4-di-*O*-methyl (6 moles); and 2-*O*-methyl (1 mole). It was concluded that the glucan was a highly branched polysaccharide containing β 1 → 6 and β 1 → 3 linked residues. Periodate oxidation of the glucan supported this conclusion.

Methylation and hydrolysis of the mannan yielded the following *O*-methyl ethers of D-mannose: 2,3,4,6-tetra-*O*-methyl (1.65 moles); 3,4,6-tri-*O*-methyl (1.00 mole); 2,3,6-tri-*O*-methyl (0.18 mole); 3,4-di-*O*-methyl (1.90 moles). The mannan was therefore a highly branched polysaccharide with short chains of α 1 → 2 linked mannose residues joined together by α 1 → 6 linkages. Results of periodate oxidation agreed with this structure.

The differences between these two polysaccharides and glucans and mannans found in other yeasts are discussed.

Structural investigations of polysaccharide components of yeasts have been limited, with only one exception, to those in bakers' yeast (*Saccharomyces cerevisiae*) and there are a number of reports dealing with the glucan (1–4) and mannan (5–7) that occur in this species. The only report dealing with structures of polysaccharides from other yeast species appears to be that by Gorin and Perlin (8) which described a mannan produced by *Saccharomyces rouxii*. There have been other publications on the composition of cell walls of yeasts (9–18) and some of these (13–18) have dealt with species other than *Saccharomyces cerevisiae*. However, these papers were concerned primarily with examination of fractions of yeast cell walls by X-ray diffraction, electrophoresis, and chromatography of hydrolyzates; structures of polysaccharides were not investigated and constituent sugars were identified only by paper chromatography. The identification of D-arabinose as a constituent of polysaccharides found in *Nocardia asteroides* (19) and *Mycobacterium tuberculosis* (20) has shown that sugars can occur in unusual configurations in microorganisms. For this reason the distinction of enantiomorphic forms of naturally occurring sugars is of considerable significance and such distinction cannot be made by paper chromatography. It was therefore of interest to examine the polysaccharides of another species of yeast, *C. albicans*, to see if they differed in structure or constituent sugars from the polysaccharides of bakers' yeast. In addition to this a report that the polysaccharides of *C. albicans*, a pathogenic yeast, are serologically active (21) indicated that elucidation of their structures could be of immunological significance.

Isolation of Glucan and Mannan from C. albicans

Crude polysaccharides were isolated from powdered cells of *C. albicans* by the procedure given in the Experimental section. The product contained no nitrogen and hence was free from any proteinaceous material. Examination of this crude preparation by moving

[1]*Manuscript received January 29, 1960.*
Contribution from the Division of Applied Biology, National Research Council, Ottawa, and the Department of Bacteriology and Immunology, McGill University, Montreal, Que. Presented in part at the Annual Conference of the Chemical Institute of Canada, Halifax, June 1959.
Issued as N.R.C. No. 5662.
[2]*Department of Bacteriology and Immunology, McGill University, Montreal, Que.*
[3]*National Research Council Postdoctorate Fellow 1957–1959.*

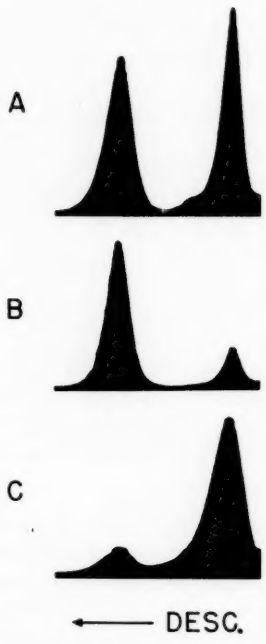

FIG. 1. Moving boundary electrophoresis of (A) crude polysaccharides, (B) mannan + trace of glucan, (C) glucan + trace of mannan.

boundary electrophoresis in borate buffer gave the separation pattern shown in Fig. 1A. The result clearly indicated two components; these were present in an approximate ratio of 0.61–0.67:1.00. Hydrolysis and chromatography of the crude polysaccharide preparation revealed the presence of mannose and glucose in a molar ratio of 0.50:1.00. The reasonable agreement between this ratio and the ratio of the two components found by electrophoresis indicated that these two components were a glucan and a mannan. This conclusion was confirmed by the isolation of a glucan and a mannan by fractionation with Fehling's solution. Fractions in which each polysaccharide still contained traces of the other were used to identify the two peaks in the electrophoretic separation. Figure 1B is the electrophoretic pattern given by the mannan-rich fraction and Fig. 1C is that given by the glucan-rich fraction. All three separations shown in Fig. 1 were photographed after the same time interval; the results show clearly that the component of greater mobility was the mannan, and the one with lower mobility the glucan. Electrophoretic mobilities of the two components were the same after fractionation as before, an indication that the separation procedure had not altered the polysaccharides.

Isolation of a glucan and a mannan from *C. albicans* has not been reported before. Jonsen *et al.* (15) isolated a polysaccharide preparation from the same organism and identified glucose and mannose by paper chromatography after hydrolysis. However, these authors obtained a single peak on electrophoresis of the polysaccharide in acetate buffer and accepted this as indicative of homogeneity. Polysaccharides, unless they contain acidic groups, would be expected to have very similar mass:charge ratios and hence would not be separable by electrophoresis in acetate buffer. The electrophoretic

separations reported in the present communication depended on the polysaccharides being complexed to different extents with borate (22) thereby acquiring different mass: charge ratios which permitted their separation. More recently Kessler and Nickerson (18) have reported the isolation of glucomannan–protein and glucan–protein complexes from three strains of *C. albicans*. However, the fractionation procedure used, alkali extraction and ammonium sulphate precipitation, was not designed to separate the polysaccharides nor was any criterion of homogeneity of the fractions reported. It is very likely, in view of the present work, that the glucomannans reported (15, 18) in *C. albicans* were mixtures of a glucan and mannan.

The glucan and mannan found in *Saccharomyces cerevisiae* have been established as components of the cell wall (9); this is also thought to be true for the glucan and mannan from *C. albicans* because an isolated cell wall preparation yielded glucose and mannose on hydrolysis.

A small amount of chitin was isolated from the cell wall of *C. albicans* and identified by X-ray diffraction. These results agree with those of other workers (12, 13, 14) who have reported the presence of chitin in small and variable amounts in the cell walls of a number of yeast species, including *C. albicans*.

Glucan from C. albicans

The glucan gave a number average degree of polymerization of 30 ± 2. On acid hydrolysis it yielded D-glucose, characterized as the *p*-nitroanilide and by specific rotation, as the only detectable sugar. Its negative rotation ($[\alpha]_D$ $-30°$) indicated that a high proportion of β-glycosidic bonds were present and its stability to hot dilute oxalic acid showed that furanose ring forms were absent.

When oxidized by periodate the glucan consumed 1.60 moles of oxidant and yielded 0.72 mole of formic acid per mole anhydroglucose. The latter value indicated that about 70% of the D-glucose units were non-reducing terminal units or were joined to adjacent units by $1 \rightarrow 6$ linkages. The very small amount of oxidant not accounted for by formic acid production indicated that most, if not all, of the remaining 28% of glucose units were substituted so that they were resistant to oxidation by periodate. This conclusion was confirmed by reduction and hydrolysis of the periodate-oxidized polysaccharide (23) which yielded glycerol and glucose as the only products detectable by paper chromatography. The glycerol arose from C_4, C_5, and C_6 of those glucose units which were terminal or 1,6-disubstituted and the glucose represented those units in the glucan that were not oxidized. No erythritol could be found in the hydrolyzate of the oxidized, reduced polysaccharide and therefore no $1 \rightarrow 4$ linkages were present in the glucan (23). The above results showed that in the glucan 72% of the glucose units were non-reducing terminal units or were joined by $1 \rightarrow 6$ linkages, the remainder being $1 \rightarrow 3$ linked or highly substituted in a branched structure.

The glucan was methylated and hydrolyzed to give the methyl ethers listed in Table I.

TABLE I

Hydrolysis products of methylated glucan

2,3,4,6-Tetra-*O*-methyl-D-glucose	(7 moles)
2,3,4-Tri-*O*-methyl-D-glucose	(13 moles)
2,4,6-Tri-*O*-methyl-D-glucose	(Trace)
2,4-Di-*O*-methyl-D-glucose	(6 moles)
2-*O*-Methyl-D-glucose	(1 mole)

The main products shown here must have arisen from the following structural units in the polysaccharide:

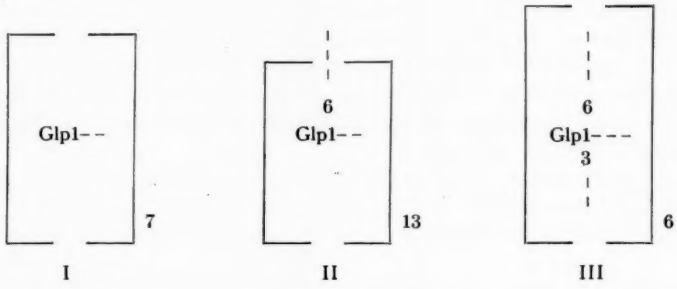

Thus 2,3,4,6-tetra-*O*-methyl-D-glucose represented non-reducing terminal units substituted only in position 1 (I); 2,3,4-tri-*O*-methyl-D-glucose came from units that were joined through positions 1 and 6 (II); 2,4-di-*O*-methyl-D-glucose arose from units that were linked through positions 1, 3, and 6 (III). The significance of the 2,4,6-tri-*O*-methyl-D-glucose and the 2-*O*-methyl-D-glucose is difficult to assess because of the small amounts found and because the methylated glucan, methylated to constant methoxyl and showing no hydroxyl absorption in the infrared, still contained only 40.5% methoxyl (calc. 45.6%). It is possible that the polysaccharide contained an impurity other than protein (e.g. lipid) which caused this low methoxyl. A glucan, containing the above three structural units in the amounts indicated, would consume 1.54 moles of periodate per mole anhydroglucose with production of 0.77 mole of formic acid per mole anhydroglucose. These are in good agreement with the values of 1.60 and 0.72 that were found for periodate consumption and formic acid production respectively in the purified glucan. If there was an impurity in the glucan which caused the low methoxyl then it must have consumed periodate, otherwise these values would be lower than theoretical. The results of the methylation study therefore confirmed the conclusions based on periodate oxidation and showed clearly that the glucan from *C. albicans* was a highly branched polysaccharide formed from β 1 $\rightarrow$ 6 and β 1 $\rightarrow$ 3 linked glucose residues. This structure is quite different from those proposed by various workers (1, 2, 3, 4) for the glucan from *Saccharomyces cerevisiae*. Hassid *et al.* (1) found 2,4,6-tri-*O*-methyl-D-glucose as the only product from methylation and hydrolysis of that glucan and therefore proposed a straight chain, β 1 $\rightarrow$ 3 linked structure. On the other hand, Bell and Northcote (2) reported similar experiments in which the products from methylation and hydrolysis showed that the glucan was branched with chains of β 1 $\rightarrow$ 3 linked units being joined by 1 $\rightarrow$ 2 interchain links. Peat *et al.* (3) have shown by fragmentation analysis that the glucan from *Saccharomyces cerevisiae* was a linear polysaccharide formed by β 1 $\rightarrow$ 3 and β 1 $\rightarrow$ 6 glycosidic linkages. A succeeding report (4) showed that some 10–20% of the linkages were β 1 $\rightarrow$ 6. The glucan from *C. albicans* differs from these three structures reported for the glucan from *Saccharomyces cerevisiae* in being much more highly branched and having a preponderance (73%) of β 1 $\rightarrow$ 6 linkages.

Mannan from C. albicans

The mannan showed a number average degree of polymerization of 41$\pm$2 and had a

specific rotation of $+78°\pm2°$. Mannose was the only sugar detectable by paper chromatography and electrophoresis after acid hydrolysis and it was proved to be D-mannose by the specific rotation ($+13°\pm2°$) and by isolation of its crystalline phenylhydrazone. The decrease in rotation after hydrolysis indicated that α-glycosidic bonds were predominant. The mannan was stable to hot, dilute oxalic acid showing that no furanose ring forms were present.

On methylation and hydrolysis the mannan yielded the components shown in Fig. 2.

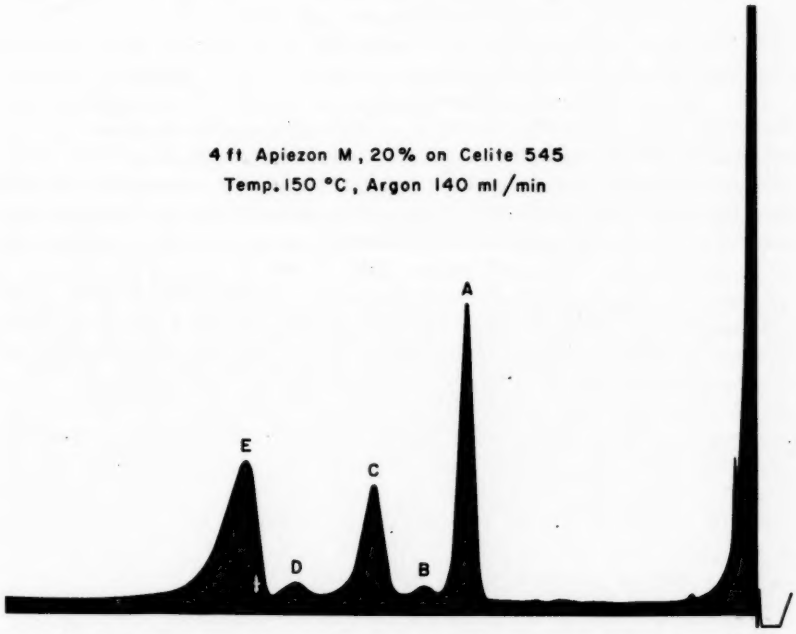

FIG. 2. Separation of methanolysis products from methylated mannan by gas–liquid partition chromatography.

		Molar ratio
(A)	Methyl-2,3,4,6-tetra-*O*-methyl-α-D-mannopyranoside	1.65
(B)	Unknown	0.13
(C)	Methyl-3,4,6-tri-*O*-methyl-α-D-mannopyranoside	1.00
(D)	Methyl-2,3,6-tri-*O*-methyl-α-D-mannopyranoside	0.18
(E)	Methyl-3,4-di-*O*-methyl-α-D-mannopyranoside	1.90

This is a reproduction of the separation curve from gas–liquid partition chromatography of the methanolysis products from the methylated mannan. This technique was developed only recently (24, 25) and was not available for use when the glucan from *C. albicans* was being investigated. Components A, C, and E were identified by isolation of crystalline derivatives and represented the main structural units of the mannan. The quantities of components B and D were too small to permit unequivocal identifications but component D was identical on gas–liquid partition chromatograms with an authentic sample of methyl-2,3,6-tri-*O*-methyl-α-D-mannopyranoside. The main structural features of the mannan could therefore be represented by the following units.

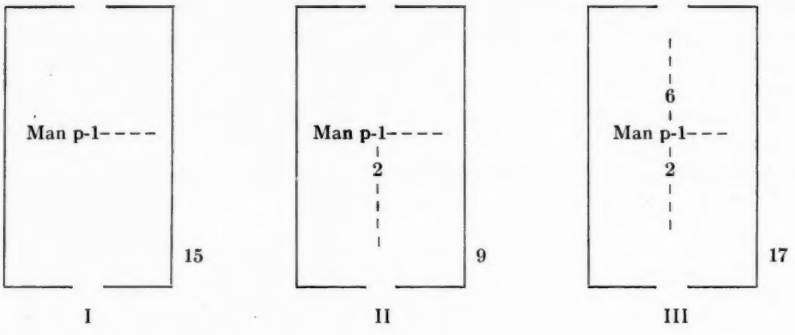

Thus components A, C, and E in Fig. 2 represented structural units I, II, and III respectively. The significance of components B and D in Fig. 4 is uncertain because of the possibility that they were products of incomplete methylation or of demethylation on hydrolysis. The amount of non-reducing terminal end groups (I) is slightly less than required to account for the branch points (III). A loss of 13% of the 2,3,4,6-tetra-*O*-methyl-D-mannose during evaporations of the formic acid hydrolyzate could account for this. It is possible that such discrepancies have not been detected previously because of the lack of accurate quantitative data as supplied by gas–liquid partition chromatography. A polysaccharide composed of structural units I, II, and III should consume 1.37 moles of periodate per mole anhydromannose with production of 0.37 mole of formic acid per mole anhydromannose. The values actually found, 1.13 and 0.27 moles per mole anhydromannose, respectively, were slightly lower and could have been caused by an impurity present in the mannan during periodate oxidation but removed during methylation, or again could be a result of greater accuracy of the gas–liquid partition chromatography data as compared with the periodate oxidation data. After periodate oxidation the resulting polyaldehyde was reduced and hydrolyzed (23). Glycerol was the only polyol detectable in the hydrolyzate, in agreement with the finding from methylation that only $1 \rightarrow 2$ and $1 \rightarrow 6$ bonds were present. It was clear from the foregoing data that the mannan possessed a highly branched structure in which relatively short chains of $\alpha\ 1 \rightarrow 2$ linked mannose units were joined together by $\alpha\ 1 \rightarrow 6$ linkages. The mannan from *C. albicans* is therefore somewhat different from the mannan isolated from bakers' yeast (*Saccharomyces cerevisiae*) (5, 6, 7) and more closely resembles that found in *Saccharomyces rouxii* (8). All of these mannans exhibited high positive specific rotations, which indicated the presence of α-glycosidic linkages, and this has been confirmed unequivocally (8) for the $1 \rightarrow 2$ linkage in the mannan from *Saccharomyces rouxii*. The difference lies in the tri-*O*-methyl-D-mannoses found after hydrolysis of the methylated mannans. The methylated mannans from bakers' yeast (5, 6, 7) yielded equimolar amounts of 2,4,6- and 3,4,6-tri-*O*-methyl-D-mannose indicative of an equal number of $1 \rightarrow 3$ and $1 \rightarrow 2$ linkages in the unbranched portion of the polysaccharide. On the other hand, the methylated mannan from *Saccharomyces rouxii* (8) yielded 2,4,6- and 3,4,6-tri-*O*-methyl-D-mannose in a ratio of 2:7 indicating that $1 \rightarrow 2$ linkages predominated over $1 \rightarrow 3$. The mannan from *C. albicans* yielded no 2,4,6-tri-*O*-methyl-D-mannose after methylation and hydrolysis and therefore could not have contained any $1 \rightarrow 3$ linkages. This conclusion was substantiated by the absence of mannose in the hydrolyzate of the periodate-oxidized mannan because any $1 \rightarrow 3$ linked mannose residues would have survived the oxidation. This

absence of 1 → 3 linkages and the high degree of branching constitute the main differences between the mannan from *C. albicans* and those so far examined from other yeasts.

EXPERIMENTAL

Paper chromatograms were run by the descending method using the following solvent systems (v/v ratio):

(A) butan-1-ol:pyridine:water, 6:4:3;
(B) butan-1-ol:ethanol:water, 9:3:3;
(C) 2-butanone:water, azeotrope.

Paper electrophoreses were done on Whatman 3 MM paper in 0.1 *M* borate buffer (22) using a potential gradient of 25 v/cm for 1 hour. Sugars were detected on chromatograms and electrophorograms by the *p*-anisidine hydrochloride spray reagent (26). Non-reducing compounds were detected on chromatograms by silver nitrate : sodium hydroxide sprays (27). Moving boundary electrophoreses were carried out in 0.05 *M* borate buffer in a Tiselius-type, Spinco Model H apparatus. Evaporations were carried out under diminished pressure at 35° C or less on a rotary film evaporator. Melting points are corrected and specific rotations are equilibrium values unless stated otherwise.

Isolation of Crude Polysaccharides

C. albicans was cultured in a liquid medium containing the following nutrients: 4% cerelose (crude glucose), 2% neopeptone "Difco", 0.05% yeast extract, 0.001% thiamin, 0.005% inositol. After incubation at 37° C for 5–12 days the cultures were autoclaved at 121° C for 20 minutes; cells were then separated in a continuous centrifuge, freeze-dried, and ground in a ball mill for 16 hours. Extraction with petroleum ether (30–60° C) removed lipid, and digestion with trypsin destroyed protein. The residue from these two treatments was then extracted with boiling 3% aqueous sodium hydroxide to solubilize the polysaccharides, which were freed from low molecular weight impurities by dialysis and precipitation with ethanol. The polysaccharide preparation thus obtained (6.3% of the dried, powdered cells) was a light tan powder which contained no nitrogen as shown by microanalysis. A sample of this material was hydrolyzed by *N* hydrochloric acid at 97° C in a sealed tube for 16 hours. Paper chromatography (solvent A) and paper electrophoresis of the hydrolyzate showed two components which were identical with samples of glucose and mannose run on the same paper strips. Another sample (150 mg) of the polysaccharide preparation was dissolved in 0.05 *M* sodium tetraborate, equilibrated with the buffer by dialysis, and examined by moving boundary electrophoresis. Figure 1A shows the complete separation of two components that was obtained by this procedure. The electrophoretic mobilities (μ) of these two components were respectively 4.38 and 9.34×10^{-5} cm^2 v^{-1} sec^{-1}. Areas under the two peaks were measured from diagrams obtained at two different times and gave ratios of the two components of 0.61:1.00 and 0.67:1.00. The molar ratio of mannose to glucose in the hydrolyzate of the polysaccharide mixture was 0.50:1.00 as determined by the densitometer method of Martin (28).

Separation of Glucan and Mannan

The crude polysaccharides (8.0 g) were stirred vigorously in water (1200 ml) for 3 hours. Insoluble material was removed by centrifugation and dried by solvent exchange with ethanol and ether (yield, 0.9 g). Paper electrophoresis of a hydrolyzate of a sample from this fraction showed that glucose was the only component sugar present. Hydrolysis and paper electrophoresis of the material in solution showed the presence of both glucose and mannose. An attempt was made to separate the mixture of polysaccharides in aqueous

solution by fractional precipitation with ethanol (29) but the fractions obtained showed no variation in glucose and mannose composition. These fractions were therefore combined, redissolved in water, and the polysaccharides were precipitated as copper complexes by addition of Fehling's solution. This method was used successfully by Haworth *et al.* (5) to isolate a mannan from bakers' yeast. The precipitated copper complex was washed repeatedly with water and at the sixth washing the precipitate dissolved. This solution was poured into 5 volumes of 10% methanolic hydrogen chloride to precipitate the polysaccharide which was dried by solvent exchange with ethanol and ether (yield, 2.13 g). Paper electrophoresis of a hydrolyzate of a sample from this fraction showed that mannose was the only component sugar present. The washings from the precipitated copper complex were combined and the polysaccharides were recovered by precipitation with acidified ethanol. This material was then recomplexed with copper and washed with water in the same way as before. Four repetitions of this procedure yielded two more polysaccharide fractions, one yielding mainly mannose but with a trace of glucose on hydrolysis and the other yielding mainly glucose with a trace of mannose. To preserve the chemically pure glucan and mannan for structural studies these impure fractions were used to determine the identities of the two peaks found in electrophoresis. The electrophoretic diagram shown in Fig. 1B is that given by the fraction yielding mainly mannose on hydrolysis but with a trace of glucose. Figure 1C shows the electrophoretic pattern given by the fraction yielding glucose on hydrolysis with only a trace of mannose. Fractionation in the same way of another 6.0 g of crude polysaccharides provided further quantities of pure glucan (0.60 g) and mannan (1.5 g).

Properties of Purified Glucan and Mannan

Glucan

This polysaccharide had $[\alpha]_D^{26} = -30° \pm 2°$ (*c*, 1.0% in *N* sodium hydroxide) changing to $[\alpha]_D^{26} = +53° \pm 2°$ (*c*, 2.0% in *N* hydrochloric acid) after hydrolysis in *N* hydrochloric acid at 97° C for 16 hours. The hydrolyzate was neutralized (Amberlite IR-45 ion exchange resin), evaporated to dryness, and the residue was heated with *p*-nitroaniline in methanol solution for 40 minutes. The solution was cooled and the crystals which separated were recrystallized from methanol to yield *N*-*p*-nitrophenyl-D-glucopyranosylamine dihydrate (30), m.p. 183–184° C, $[\alpha]_D^{25} = -199° \pm 1°$ (*c*, 1.0% in pyridine). Attempted partial hydrolysis of the glucan by 0.025 *N* oxalic acid at 97° C for 3 hours released no cleavage products detectable by paper chromatography. The degree of polymerization of the glucan was 30 ± 2 as determined by hypoiodite oxidation of the reducing end group in phosphate buffer (31).

Mannan

This polysaccharide had $[\alpha]_D^{26} = +78 \pm 2°$ (*c*, 1.1% in water) changing to $[\alpha]_D^{26} = +13° \pm 2°$ (*c*, 2.0% in *N* hydrochloric acid) after hydrolysis in *N* hydrochloric acid at 97° C for 16 hours. The hydrolyzate was neutralized (Amberlite IR-45 ion exchange resin), mixed with an equal volume of an aqueous solution of phenylhydrazine acetate, and allowed to stand at 25° C for 20 hours. The crystals which formed were recrystallized twice from water:ethanol to yield mannose phenylhydrazone (32), m.p. 198–199° C (d), $[\alpha]_D^{24} = +25° \pm 2°$ (*c*, 1.0% in pyridine). Like the glucan, the mannan showed no evidence of partial hydrolysis when heated with 0.025 *N* oxalic acid at 97° C for 3 hours. The degree of polymerization of the mannan, estimated in the same way as for the glucan, was 41 ± 2.

Periodate Oxidations

The glucan (111.2 mg, 0.66 mmole) and mannan (122.3 mg, 0.75 mmole) were dissolved separately in water (125 ml) and 0.25 *M* sodium periodate (25 ml) was added to each. Reagent blanks were also prepared and oxidations were carried out at 25° C in the absence of light. At the intervals noted below samples were removed for estimation of formic acid and periodate. For estimation of formic acid the excess periodate in a 10-ml aliquot was destroyed by 2,3-butanediol, a few crystals of potassium iodide were added and the liberated iodine was titrated to a starch end point with 0.01 *N* thiosulphate. For periodate estimations (33, 34) sodium bicarbonate (1.7 g), 0.1 *N* sodium arsenite (5 ml), and a few crystals of potassium iodide were added to 10-ml aliquots from the oxidations. The solutions were stored in the dark for 30 minutes and were then titrated with 0.022 *N* iodine solution to a starch end point. The results, given in moles per anhydrohexose unit were as follows:

Time, hours	Glucan		Mannan	
	Formic	Periodate	Formic	Periodate
24	0.68	1.60	0.21	1.10
44	0.71	1.58	0.26	1.10
70	0.72	1.61	0.27	1.13

After the oxidations were complete excess periodate was destroyed by 2,3-butanediol and salts and acetaldehyde were removed by dialysis. The oxidized polysaccharides were then reduced by potassium borohydride, hydrolyzed by *N* hydrochloric acid at 97° C for 3 hours and the hydrolyzates were examined by paper chromatography (solvent B, silver nitrate : sodium hydroxide sprays) (23). By this sequence of reactions the glucan yielded glycerol and glucose while the mannan gave only glycerol. Erythritol was not found in either hydrolyzate.

Methylation of Glucan and Mannan

Glucan

The glucan (893 mg) was methylated five times for 24 hours in 30% sodium hydroxide (20 ml) and dimethyl sulphate (10 ml). The product was isolated by extraction into chloroform and was treated for 24 hours in that solvent (10 ml) with methyl iodide (6 ml) and silver oxide (3.0 g). After three further methylations with methyl iodide and silver oxide, the methylated polysaccharide was precipitated as a white powder (1.0 g, methoxyl = 40.5%) from chloroform solution by addition of petroleum ether (30–60° C). The methoxyl content of this product was not increased by another methylation and an infrared spectrum showed only a trace of hydroxyl absorption. The powdery product was extracted with petroleum ether and then successively with petroleum ether containing increasing amounts of chloroform. All fractions showed identical hydrolysis products on paper chromatograms and the main portion of the product dissolved in petroleum ether : chloroform mixtures of 6:4, 5:5, and 4:6. These three fractions were combined and reprecipitated to give a white powder (660 mg, methoxyl 40.5%) showing no hydroxyl absorption in the infrared.

Mannan

The mannan (2.14 g) was methylated five times with 30% sodium hydroxide

(5×100 ml) and dimethyl sulphate (5×50 ml) in the same way as described for the glucan. The product (2.29 g) showed distinct hydroxyl absorption in the infrared so it was methylated again, this time in tetrahydrofuran (30 ml) with sodium hydroxide (10 g) and dimethyl sulphate (15.5 ml) (35). The product still showed hydroxyl absorption in the infrared and had methoxyl equal to 39.7% so it was methylated again in tetrahydrofuran as before. This methylation gave a product (2.20 g) having no hydroxyl absorption in the infrared and with methoxyl equal to 40.4%, unchanged by another methylation. The methylated polysaccharide was extracted with boiling petroleum ether (30–60° C). The extract was removed by decantation and evaporated to yield an oily product (methoxyl = 29%) which was discarded. The residue from this extraction was stirred in ether and the insoluble portion was removed by centrifugation. The ethereal supernatant was evaporated to yield the methylated mannan (1.56 g, methoxyl = 43.2%), which showed no hydroxyl absorption in the infrared.

Hydrolysis Products from Methylated Glucan

The methylated glucan (650 mg) was hydrolyzed by formic acid according to the procedure described by Jones and Wilkie (36). Qualitative and quantitative (37) paper chromatography gave approximate molar ratios of the methyl ethers of glucose shown in Table I.

The mixture of methylated sugars (645 mg) was resolved on a cellulose column (2.3×28 cm) using solvent C to give four fractions. *Fraction 1* (73.5 mg) contained only 2,3,4,6-tetra-*O*-methyl-D-glucose; *fraction 2* (126.4 mg) contained 2,3,4,6-tetra-*O*-methyl-D-glucose and 2,3,4-tri-*O*-methyl-D-glucose; *fraction 3* (236.8 mg) contained 2,3,4-tri-*O*-methyl-D-glucose and a trace of 2,4,6-tri-*O*-methyl-D-glucose; *fraction 4* (126.7 mg) contained 2,4-di-*O*-methyl-D-glucose with a trace of 2-*O*-methyl-D-glucose (recovery) = 563.4 mg, 87.4%). Those fractions which were mixtures were resolved further by preparative paper chromatography on Whatman 3 MM paper using solvent C, and individual components were identified as described below.

2,3,4,6-Tetra-O-methyl-D-glucose

The unknown showed the same chromatographic mobility in solvents A, B, and C as an authentic sample of 2,3,4,6-tetra-*O*-methyl-D-glucose. The product crystallized from petroleum ether (30–60° C) and was recrystallized from *N*-hexane to give a compound with a melting point of 88–89° C and $[\alpha]_D^{24} = +82° \pm 2°$ (*c*, 0.16% in water). The melting point was unchanged by admixture with an authentic sample of 2,3,4,6-tetra-*O*-methyl-D-glucose.

2,3,4-Tri-O-methyl-D-glucose

The sirupy unknown had R_g values of 0.90 and 0.75 in solvents B and C respectively. Authentic samples of tri-*O*-methyl-D-glucoses showed the following R_g values in the same solvents: 2,3,4—0.90, 0.75; 2,4,6—0.85, 0.62; 2,3,6—0.88, 0.70. The unknown (97.3 mg) was refluxed for 1½ hours with aniline (41.0 mg) in ethanol (2 ml). The solvent was evaporated and the crystalline residue was recrystallized from ether to give a product having a melting point of 144.5–145.5° C and $[\alpha]_D^{26} = +70° \pm 1°$ (*c*, 0.83% in ethanol). Peat *et al.* (38) report a melting point of 145–146° C for *N*-phenyl-2,3,4-tri-*O*-methyl-D-glucosylamine. Mother liquors from the above crystallization yielded a product having a melting point of 137–138° C unchanged by repeated recrystallization. The analysis and infrared spectrum of this material were identical with those of the product melting at 144.5–145.5° C and it appeared to be another crystalline form of the same compound. Analysis: Calc. for $C_{15}H_{23}O_5N$: C, 60.59%; H, 7.74%. Found: C, 60.61%, H, 7.42%.

2,4,6-Tri-O-methyl-D-glucose

Only a trace of this compound was present. It gave the same color reaction with *p*-anisidine hydrochloride on paper chromatograms and had the same R_g values (0.85, 0.62) in solvents B and C as an authentic sample of 2,4,6-tri-*O*-methyl-D-glucose.

2,4-Di-O-methyl-D-glucose

The unknown sample gave the same color reaction with *p*-anisidine hydrochloride on paper chromatograms as 2,4-di-*O*-methyl-D-glucose. In solvents A, B, and C it had R_g values of 0.81, 0.67, and 0.31 respectively. Authentic samples of di-*O*-methyl-D-glucoses had the following R_g values in the same solvents: 2,4—0.81, 0.67, 0.31; 2,3—0.83, 0.72, 0.36; 3,6—0.79, 0.66, 0.28. The unknown product (96.6 mg) was dissolved in ethanol (3 ml) to which *p*-nitroaniline (80 mg) and glacial acetic acid (2 drops) were added. The solution was kept at 25° C for 1½ hours, heated on a steam bath for 2 hours and stored at room temperature overnight. A brown precipitate was filtered and washed with ethanol and ethyl acetate which removed much of the color. It was found that the light tan residue, consisting of microcrystals, could be purified by sublimation at 0.01 mm pressure at 200° C (bath temperature) to give *N*-*p*-nitrophenyl-2,4-di-*O*-methyl-D-glucosylamine, m.p. 250–251° C (*d*) (39).

2-O-Methyl-D-glucose

The unknown sample had the same R_g value (0.55) in solvent A as 2-*O*-methyl-D-glucose and gave the same color reaction with *p*-anisidine. R_g values of mono-*O*-methyl glucoses in solvent A were as follows: 2-*O*-methyl-, 0.55; 3-*O*-methyl-, 0.57; 4-*O*-methyl-, 0.51; 6-*O*-methyl-, 0.49. Attempts to isolate the compound in crystalline form or to prepare a crystalline derivative were unsuccessful because of insufficient material.

Hydrolysis Products from Methylated Mannan

The methylated mannan (1.54 g) was hydrolyzed by the formic acid procedure of Jones and Wilkie (36). A portion (100 mg) of the hydrolyzate was refluxed with 4% methanolic hydrogen chloride for 16 hours. The resulting mixture of methyl glycosides was resolved by gas–liquid partition chromatography (24, 25), which gave the separation and quantitative data shown in Fig. 2. To identify the constituents of the mixture the remainder (1.44 g) of the hydrolyzate was fractionated on a cellulose column using solvent C to give five fractions:

Fraction 1, tetra-*O*-methyl-D-mannose (0.150 g).
Fraction 2, tetra- and tri-*O*-methyl-D-mannoses (0.692 g).
Fraction 3, tri-*O*-methyl-D-mannose (0.065 g).
Fraction 4, tri- and di-*O*-methyl-D-mannoses (0.241 g).
Fraction 5, di-*O*-methyl-D-mannose (0.207 g).
Recovery = 1.355 (94.1%).

The major components in these fractions were identified as follows:

2,3,4,6-Tetra-O-methyl-D-mannose

On paper chromatograms fraction 1 showed only one component having R_g values of 0.99 and 0.98 in solvents B and C respectively. The specific rotation was $[\alpha]_D^{28} = +30° \pm 1°$ (*c*, 3.0% in methanol) and the product yielded a crystalline anilide, m.p. 144–145° C, $[\alpha]_D^{26} = +42° \rightarrow 8°$ (*c*, 0.72% in methanol). These values are in agreement with those reported for 2,3,4,6-tetra-*O*-methyl-D-mannose (40) and its anilide (41). After methanolysis fraction 1 showed one peak, corresponding to peak A, Fig. 2, on gas–liquid partition chromatography.

*3,4,6-Tri-O-methyl-*D*-mannose*

On paper chromatograms fraction 3 was identical with 3,4,6-tri-*O*-methyl-D-mannose and had R_g values of 0.90 and 0.76 in solvents B and C respectively. The product crystallized when nucleated with an authentic sample of 3,4,6-tri-*O*-methyl-D-mannose. Recrystallization from ether:hexane yielded a product with a melting point of 102–104° C and $[\alpha]_D^{28} = +33° \pm 3°$ (*c*, 3.2% in methanol), which are in agreement with the reported values (42). This compound showed only one peak, corresponding to peak C, Fig. 2, on gas–liquid partition chromatography after methanolysis.

*3,4-Di-O-methyl-*D*-mannose*

R_g values of fraction 5 on paper chromatograms were 0.74 and 0.44 in solvents B and C respectively, identical with those given by authentic 3,4-di-*O*-methyl-D-mannose. The product crystallized when nucleated with an authentic sample and recrystallization from ethyl acetate yielded a product with a melting point of 70–73° C (8, 43), and $[\alpha]_D^{28} = +32 \pm 1°$ (*c*, 2.0% in methanol) (6). This compound was methanolyzed and the methyl glycoside gave one peak, corresponding to peak E, Fig. 2, on gas–liquid partition chromatography.

Isolation of Chitin from C. albicans

Chitin was isolated from dried *C. albicans* cells (9.0 g) by the procedure of Scholl (44), which involved exhaustive extraction with boiling 10% potassium hydroxide, oxidation with 1% aqueous potassium permanganate, and removal of manganese dioxide by dilute (0.8%) hydrochloric acid. The residue from these reactions was dried with ethanol and ether to yield a product (545 mg, 6.05%) which was shown by X-ray diffraction to contain chitin and traces of corundum.

Isolation and Hydrolysis of Cell Walls from C. albicans

Cells of *C. albicans* were extracted with petroleum ether to remove lipid, incubated with trypsin to destroy protein, and suspended in water at a concentration of 1%. This suspension was shaken with fine glass beads for 45 minutes in a Mickle disintegrator (45). The glass beads were then removed by filtration on sintered glass and the turbid filtrate was centrifuged for 1 minute at 1000 r.p.m. Microscopic examination of the precipitate revealed the presence of many whole cells but further centrifugation of 1 minute at 1000 r.p.m. yielded a precipitate in which no intact cells could be detected. Hydrolysis and paper chromatography of this precipitate revealed the presence of glucose and mannose. The supernatant liquid from the second precipitate was centrifuged for 15 minutes at 15,000 r.p.m. to yield a creamy precipitate which yielded neither glucose nor mannose after hydrolysis.

ACKNOWLEDGMENTS

The authors gratefully acknowledge the careful technical assistance of Mr. F. P. Cooper (National Research Council) and Mr. A. A. Strachan (Department of Bacteriology and Immunology, McGill University). Authentic samples of *O*-methyl ethers of D-glucose were kindly donated by Dr. T. E. Timell, Division of Cellulose Chemistry, McGill University; authentic samples of *O*-methyl ethers of mannose were obtained from Dr. G. A. Adams, Division of Applied Biology, National Research Council. Analyses were done by Mr. A. E. Castagne and the X-ray diffraction diagram was done by the Eidgenossische Materialprufungs-und Versuchsanstalt, Zürich, Switzerland.

REFERENCES

1. W. Z. Hassid, M. A. Joslyn, and R. M. McCready. J. Am. Chem. Soc. **63**, 295 (1941).
2. D. J. Bell and D. H. Northcote. J. Chem. Soc. 1944 (1950).
3. S. Peat, W. J. Whelan, and T. E. Edwards. J. Chem. Soc. 3862 (1958).
4. S. Peat, J. R. Turvey, and J. M. Evans. J. Chem. Soc. 3868 (1958).
5. W. N. Haworth, E. L. Hirst, and F. A. Isherwood. J. Chem. Soc. 784 (1937).
6. W. N. Haworth, R. L. Heath, and S. Peat. J. Chem. Soc. 833 (1941).
7. J. A. Cifonelli and F. Smith. J. Am. Chem. Soc. **77**, 5682 (1955).
8. P. A. J. Gorin and A. S. Perlin. Can. J. Chem. **34**, 1796 (1956).
9. D. H. Northcote and R. W. Horne. Biochem. J. **51**, 232 (1952).
10. W. E. Trevelyan and J. S. Harrison. Biochem. J. **50**, 298 (1952).
11. P. A. Roelofsen. Biochim. et Biophys. Acta, **10**, 477 (1953).
12. A. L. Houwink and D. R. Kreger. Antonie van Leeuwenhoek. J. Microbiol. Serol. **19**, 1 (1953).
13. P. A. Roelofsen and I. Hoette. Antonie van Leeuwenhoek. J. Microbiol. Serol. **17**, 297 (1951).
14. D. R. Kreger. Biochim. et Biophys. Acta, **13**, 1 (1954).
15. J. Jonsen, S. Rasch, and A. Strand. Acta Pathol. Microbiol. Scand. **37**, 449 (1955).
16. M. W. Miller and H. J. Phaff. Antonie van Leeuwenhoek. J. Microbiol. Serol. **24**, 225 (1958).
17. M. Shifrine and H. J. Phaff. Antonie van Leeuwenhoek. J. Microbiol. Serol. **24**, 274 (1958).
18. G. Kessler and W. J. Nickerson. J. Biol. Chem. **234**, 2281 (1959).
19. C. T. Bishop and F. Blank. Can. J. Microbiol. **4**, 35 (1958).
20. N. Haworth, P. W. Kent, and M. Stacey. J. Chem. Soc. 1211 (1948).
21. J. Jonsen, S. Rasch, and A. Strand. Acta Pathol. Microbiol. Scand. **37**, 449 (1955).
22. A. B. Foster. Advances in Carbohydrate Chem. **12**, 81 (1957).
23. M. Abdel-Akher, J. K. Hamilton, R. Montgomery, and F. Smith. J. Am. Chem. Soc. **74**, 4970 (1952).
24. A. G. McInnes, D. H. Ball, F. P. Cooper, and C. T. Bishop. J. Chromatog. **1**, 556 (1958).
25. C. T. Bishop and F. P. Cooper. Can. J. Chem. **38**, 388 (1960).
26. L. Hough, J. K. N. Jones, and W. H. Wadman. J. Chem Soc. 1702 (1950).
27. W. E. Trevelyan, D. P. Procter, and J. S. Harrison. Nature, **166**, 444 (1950).
28. S. M. Martin. Chem. & Ind. (London), 823 (1957).
29. R. L. Whistler and J. N. BeMiller. J. Am. Chem. Soc. **78**, 1163 (1956).
30. S. A. Barker, A. B. Foster, I. R. Siddiqui, and M. Stacey. J. Chem. Soc. 2358 (1958).
31. S. K. Chanda, E. L. Hirst, J. K. N. Jones, and E. G. V. Percival. J. Chem. Soc. 1289 (1950).
32. E. Fischer. Ber. **20**, 821 (1887).
33. P. P. Fleury and J. Lange. J. pharm. chim. **17**, 107 (1933).
34. D. H. Grangaard, E. K. Gladding, and C. B. Purves. Paper Trade J. **115**, 41 (1942)
35. E. L. Falconer and G. A. Adams. Can. J. Chem. **34**, 338 (1956).
36. J. K. N. Jones and K. C. B. Wilkie. Can. J. Biochem. and Physiol. **37**, 377 (1959).
37. H. D. Fowler. Nature, **168**, 1123 (1951).
38. S. Peat, E. Schlüchterer, and M. Stacey. J. Chem. Soc. 581 (1939).
39. J. W. Van Cleve and W. C. Schaefer. J. Am. Chem. Soc. **77**, 5341 (1955).
40. R. D. Greene and W. L. Lewis. Science, **64**, 206 (1926).
41. J. C. Irvine and D. McNicoll. J. Chem. Soc. **97**, 1449 (1910).
42. H. G. Bott, W. N. Haworth, and E. L. Hirst. J. Chem. Soc. 1395 (1930).
43. D. H. Ball and G. A. Adams. Can. J. Chem. **37**, 1012 (1959).
44. E. Scholl. Monatsh. Chem. **29**, 1023 (1908).
45. M. R. J. Salton and R. W. Horne. Biochim. et Biophys. Acta, **7**, 177 (1951).

ALIPHATIC CHEMISTRY OF FLUORENE

PART II. AN UNUSUAL GRIGNARD REACTION[1]

P. M. G. BAVIN[2]

ABSTRACT

The reaction between methyl 9-methylfluorene-9-carboxylate and phenyl magnesium iodide gave 9,9′-dimethyl-9,9′-difluorenyl in almost quantitative yield. Evidence is presented which shows that 9-methylfluorene anion is an intermediate. The probable intervention of elemental iodine is discussed.

9-Methyl-9,9′-difluorenyl and 9,9′-dimethyl-9,9′-difluorenyl have been synthesized. A convenient preparation of 9,9′-difluorenylidene is described.

Some years ago we were interested in the reaction between phosphorus pentoxide and tertiary alcohols having structure I, where R is not hydrogen (1). We succeeded in preparing only two alcohols of the desired structure (I, $R_1 = R_2 = R_3$ = methyl or ethyl) by the reaction between methyl 9-methyl or ethylfluorene-9-carboxylate and the corresponding alkyl magnesium halide. The similar reaction between methyl 9-methylfluorene-9-carboxylate and phenyl magnesium bromide gave an easily crystallized hydrocarbon of melting point 209–210°, which has now been identified as 9,9′-dimethyl-9,9′-difluorenyl (II*b*). Although this hydrocarbon has been reported previously (2, 3, 4) identity has been established by the following unambiguous syntheses.

9-Bromofluorene reacted rapidly with methyl fluorene-9-carboxylate anion to give methyl 9-(9′-fluorenyl)-fluorene-9-carboxylate (the ethyl ester has been prepared previously from 9,9′-difluorenyl (5)), which was saponified and decarboxylated to 9,9′-difluorenyl. Methylation with methyl lithium and methyl iodide gave finally 9,9′-dimethyl-9,9′-difluorenyl (II*b*).

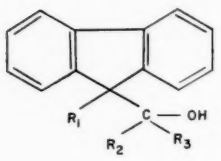

(I)

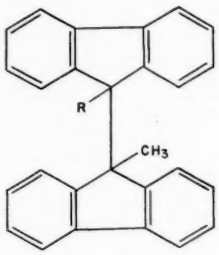

(II)

(a) R = H
(b) R = CH_3

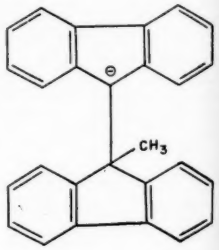

(III)

In the second synthesis, the anion (III) was prepared by the addition of methyl lithium to 9,9′-difluorenylidene. The further reaction with methyl iodide gave 9,9′-dimethyl-9,9′-difluorenyl. The preparation of 9-methyl-9,9′-difluorenyl (II*a*) by hydrolysis of the anion (III) with water proved unexpectedly difficult, residual methyl iodide giving

[1]*Manuscript received December 1, 1959.*
Contribution from the Chemistry Department, the University, Hull, East Yorkshire, England.
[2]*I.C.I. Fellow.*

instead dimethyldifluorenyl (II*b*). After removing the last traces of methyl iodide with magnesium, 9-methyl-9,9′-difluorenyl was obtained in 80–90% yield.

The yield of the hydrocarbon (II*b*) in the Grignard reaction was almost quantitative when phenyl magnesium iodide was used, from which it was inferred that the tertiary alkoxide (IV) was formed in the usual way. By analogy with certain tertiary aliphatic alkoxides recently investigated by Zook (6), decomposition should lead to 9-methylfluorene anion (V) and benzophenone, as shown in the annexed scheme (Fig. 1). The

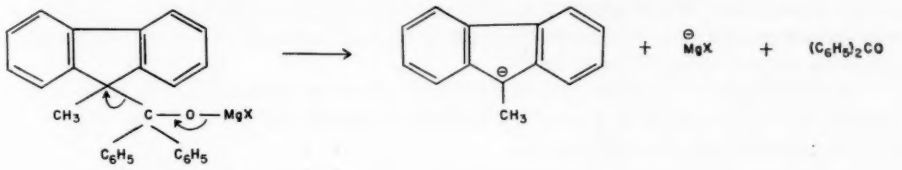

(IV) (V)

FIG. 1.

necessary driving force for the decomposition is supplied by the mesomeric nature of the ion (V) (cf. the facile base-induced cleavage of 9-methyl-9-benzoylfluorene (7)), which accounts for the unusually low reaction temperature (cf. (6)).*

The use of organic iodides in the preparation of Grignard reagents, or of a crystal of iodine to initiate their formation, may often result in the presence of traces of free iodine in such reactions, probably owing their formation to aerial oxidation. It is well known that iodine brings about the dimerization of many esters in the presence of strong base (e.g. phenylacetic ester (8)) and, by analogy, it might be expected to bring about dimerization of the anion (V) to dimethyldifluorenyl (II*b*).

Evidence is presented below which supports the postulated decomposition of the tertiary alkoxide (IV) and the participation of iodine in the formation of the hydrocarbon (II*b*).

Evidence for the Formation of the 9-Methylfluorene Anion (V)

The most convincing evidence for the formation of the anion (V) came from a study of the reactions of 9-methyl-9-benzoylfluorene, which has recently been prepared for the first time (7). The ketone reacted with ethereal methyl or phenyl lithium and with ethereal phenyl magnesium bromide to produce a deep red color, which was fully developed in a few minutes. In order to demonstrate the presence of the anion (V), methyl iodide was added. 9,9-Dimethylfluorene could then be isolated from amongst the products. Triphenylmethanol could be isolated from the products of reaction with phenyl lithium or the corresponding Grignard reagent, thereby accounting for the benzophenone formed in the decomposition of the tertiary alkoxide (IV). Prolonged reaction times favored formation of the hydrocarbon (II*b*). Other experiments showed that methyl 9-methylfluorene-9-carboxylate gave the same products under the same conditions.

It is probable that the formation of the anion (V) from the ketone proceeds by way of the tertiary alkoxide (IV), but it may equally well involve base-induced cleavage of the non-enolizable ketone (7), with methyl or phenyl anion acting as base. Similar

*Zook (6) has emphasized that the decompositions are the reversal of addition of an organometallic reagent to a ketone.

mechanisms can account for the formation of acetophenone and triphenylmethane from the reaction between benzopinacolin and methyl magnesium bromide (reference 3 quoted in 6). In both cases the direction of cleavage is controlled by formation of the mesomeric ions (V) and the triphenylmethyl anion. Differentiation between the decomposition and cleavage mechanisms might be possible by kinetic studies.

The Role of Iodine

The importance of iodine may be judged from the following experimental results.

(i) The yield of the hydrocarbon (II*b*) from methyl 9-methyl-fluorene-9-carboxylate was almost quantitative when phenyl magnesium iodide was used, but was considerably less with phenyl magnesium bromide.

(ii) The anion (V), generated from 9-methylfluorene with phenyl lithium, reacted rapidly with iodine to give a good yield of the hydrocarbon (II*b*). Under similar conditions fluorene gave 9,9′-difluorenyl.

(iii) The reaction between 9-methylfluorene, ethyl lithium, and ethyl iodide produced 10% of the hydrocarbon (II*b*). The similar reaction using ethyl bromide and ethyl lithium prepared from ethyl bromide gave only 9-ethyl-9-methylfluorene.

Since many Grignard reagents react with iodine to give good yields of iodides (9, pp. 1332–1335) the tertiary iodide (VI) has to be considered as a possible intermediate in the formation of the hydrocarbon (II*b*) by reaction with the anion (V). Evidence for the formation of a reactive iodo compound in the dimerization of phenylacetic ester has already been reported (8, footnote on page 446; see also 10), and it has now been observed that traces of unstable iodo compounds are present in the products of the dimerization of fluorene or 9-methylfluorene with iodine and phenyl lithium.

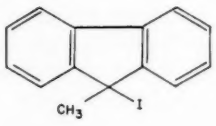

(VI)

Tertiary halides do not as a general rule give C-alkylation products with organic anions. However, methyl fluorene-9-carboxylate anion has been shown to be exceptional in this respect (11, 12). It has now been found that methyl 9-bromofluorene-9-carboxylate reacts rapidly with methyl fluorene-9-carboxylate anion to give dimethyl 9,9′-difluorenyl-9,9′-dicarboxylate, at a rate comparable with that observed for the iodine-induced dimerization of the anion. These results suggest the feasibility of the anion (V) reacting with the iodide (VI) to give II*b*.

Comparable experiments with 9-bromo-9-methylfluorene and methyl fluorene-9-carboxylate anion have been unsuccessful. Crude preparations of the bromide, difficult to obtain pure (30), gave a low yield of what is probably methyl 9-(9′-fluorenylmethyl)-fluorene-9-carboxylate as the product of Michael addition of methyl fluorene-9-carboxylate anion to 9-methylenefluorene. Experiments with the corresponding chloride, which has not been obtained pure (13, 30), gave similar results.

Alternative mechanisms for the formation of the hydrocarbon (II*b*) obviously cannot be ruled out. For example, oxidation of the anion (V) by iodine might give the radical,

leading by dimerization to II*b*. In addition, trace amounts of certain metals are known to bring about oxidative coupling of organic anions (9).

Summing up the available evidence, it is clear that formation of dimethyldifluorenyl (II*b*) in the reaction between methyl 9-methylfluorene-9-carboxylate and a phenyl Grignard reagent proceeds through 9-methylfluorene anion (V), formed either by decomposition of the tertiary alkoxide (IV) or by basic cleavage of 9-methyl-9-benzoylfluorene. Iodine seems to play an essential part but its exact role is uncertain.

The formation of 9,9′-difluorenyl by the reaction between Grignard reagents and 9-chlorofluorene (14) may very well be related to its formation from fluorene, phenyl lithium, and iodine, mentioned above. The annexed scheme (Fig. 2) shows the reactions

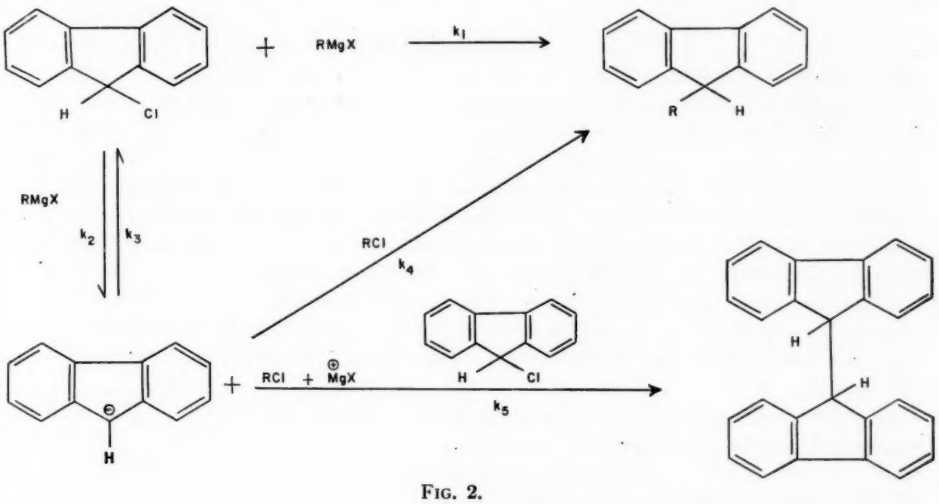

FIG. 2.

likely to be involved. It will be seen that an essential postulated reaction is a Grignard exchange having forward rate k_2. The existence of at least two such reactions has been convincingly demonstrated (15, 16) but it has been claimed that 9-chlorofluorene does not exchange with methyl magnesium bromide (17) because fluorene-9-carboxylic acid was not isolated from amongst the products of carbonation. These workers seem to have been unaware of the earlier paper by Bachmann (14); neglect to report on the neutral products obviously invalidates their work. The reaction between 9-bromofluorene and methyl magnesium iodide has been found to give 9,9′-difluorenyl in more than 90% yield, even in the presence of added methyl iodide. This observation confirms Bachmann's results (14).

Bachmann's efforts to explain his results (14), particularly the infrequent formation of 9-alkylfluorenes, in terms of the structure of the Grignard reagent are almost certainly invalid in view of recent studies with the ^{28}Mg isotope (18). The alternative scheme shown in Fig. 2 may provide a complete explanation. The rate k_1 is likely to be small compared with k_2 so that *the products formed will depend on the reactivities of 9-chlorofluorene and the halide RCl towards fluorene anion*, the reactivities being measured by k_5 and k_4.

An outstanding property of fluorene anions is the speed with which they react with a very wide range of alkyl halides (7, 11, 12). It has now been demonstrated that the anions from fluorene, 9-methylfluorene, and 9-phenylfluorene react almost instantaneously

with methyl iodide, providing convenient preparations of 9,9-dimethylfluorene and 9-methyl-9-phenylfluorene. The relative reactivities of various alkyl halides to methyl fluorene-9-carboxylate anion are being measured by competition and will be reported later. The formation of difluorenyl from the reaction between 9-bromofluorene and methyl Grignard in the presence of methyl iodide suggests that the fluorene halide is the more reactive.

The reaction between 9-bromofluorene and sodium *t*-butoxide has been found to give 9,9′-difluorenylidene in 85% yield, representing a considerable improvement in both yield and convenience over published preparations (20, 21).

The existence (19) has been confirmed of two polymorphic forms of 9,9-dimethylfluorene.

EXPERIMENTAL

9,9′-Dimethyl-9,9′-difluorenyl (II*b*)

(i) Methyl 9-methylfluorene-9-carboxylate (2.24 g, 0.01 mole) was boiled under reflux for 4 hours with ethereal phenyl magnesium iodide (from iodobenzene, 12 g, 0.06 mole). The complex was decomposed with ice and ammonium chloride and the product crystallized from heptane to give pale yellow prisms, m.p. 186–190° (1.76 g, almost quantitative yield). Two further crystallizations yielded colorless well-defined rhombs (1.6 g), m.p. 209–210°. Found for two samples: C, 93.71, 93.97; H, 6.29, 6.19%. Calculated for $C_{28}H_{22}$: C, 93.81; H, 6.19% (lit. m.p.: 209° corr. (2), 209–210° (3), 205° (4)).

Phenyl magnesium bromide was used in earlier experiments, formation of the Grignard reagent being assisted by the addition of a crystal of iodine. The hydrocarbon (II*b*) was obtained in 45% yield only after 24 hours. In the absence of iodine the hydrocarbon was not formed.

(ii) 9-Bromofluorene (22), prepared by Bolton, reacted rapidly at 30–35° with one equivalent of methanolic methyl fluorene-9-carboxylate anion. *Methyl 9-(9′-fluorenyl)-fluorene-9-carboxylate*, isolated in the usual way, formed well-defined rhombs (76%) from benzene–hexane, m.p. 215–216°. Found: C, 86.11; H, 5.18%. Calculated for $C_{28}H_{20}O_2$: C, 86.57; H, 5.19%.

The ester was boiled under reflux for 2 hours with twice its weight of potassium hydroxide in ethylene glycol. Cooling and diluting with water precipitated 9,9′-difluorenyl, which crystallized as slender colorless needles (94%) from benzene–hexane, m.p. 248–249°.

9,9′-Difluorenyl (2 g) in benzene (200 ml) was added to ethereal phenyl lithium (from bromobenzene, 20 g) to give a deep red solution, the color of which was almost instantly discharged on addition of methyl iodide (8 g). The *hydrocarbon* crystallized as rhombs (1.4 g) from benzene–hexane, m.p. 209–210°. Identity with the product from (i) was established by mixed melting point determination and comparison of infrared spectra.

(iii) 9-Methylfluorene (1 g) was added to ethereal phenyl lithium (from bromobenzene, 5 g) followed by crystals of iodine until the color of the latter persisted. The product (0.8 g) had a melting point of 207–209° and was identical with that obtained from (i).

Under similar conditions fluorene (1 g) gave 9,9′-difluorenyl (0.7 g), m.p. and mixed m.p. 245–246°.

The crude products from both preparations were washed with a solution of sodium metabisulphite to remove iodine, but traces of the latter were always formed during crystallization.

(iv) 9,9′-Difluorenylidene (1 g) was boiled under reflux for 30 minutes with ethereal methyl lithium (from methyl iodide, 10 g) and methyl iodide (10 g). The product crystal-

lized from heptane as small colorless prisms (0.9 g), m.p. 208–210°, and was identical with the product from (i).

9,9′-Difluorenylidene

A hot solution of sodium *t*-butoxide (from sodium, 7 g) in *t*-butanol (500 ml) was added to 9-bromofluorene (25 g) and the mixture boiled under reflux for 15 minutes. Most of the solvent was recovered by distillation and the residue poured into dilute hydrochloric acid (500 ml). The reddish-orange solid was collected, washed with water, dried, and crystallized from carbon tetrachloride – ethanol, which was the best solvent system found. Difluorenylidene was obtained as beautiful red needles (14.2 g, 85%, in two crops), m.p. 187–189° (lit. m.p. 185–187° (20, 21)).

9-Methyl-9,9′-difluorenyl

Ethereal methyl lithium was prepared from methyl iodide (28 g) and lithium (3 g). When the reaction was apparently complete, magnesium (5 g) was added and the mixture boiled gently under reflux for 30 minutes. Residual solids were removed by decantation through a plug of glass wool to give a solution of methyl lithium in ether free from methyl iodide.

Difluorenylidene (1 g) was warmed for 15 minutes with an excess of the above methyl lithium reagent. The ether layer was washed with water, dried, and evaporated, leaving the product as a yellow solid. The product was purified by passing a hexane solution through a column of activated alumina, crystallization of the eluted material from heptane yielding small colorless prisms (0.85 g), m.p. 169–170° (lit. m.p. 172° (4)). Found: C, 94.25; H, 5.89%. Calculated for $C_{27}H_{20}$: C, 94.15; H, 5.85%.

A mixed melting point determination with dimethyldifluorenyl was 151–179°.

9-Ethyl-9-methylfluorene

(i) 9-Methylfluorene (1 g) was added to ethereal ethyl lithium (from ethyl bromide, 4 g), followed by ethyl bromide (4 g). The product crystallized readily from methanol as white needles (0.8 g), m.p. 59–60.5° (lit. m.p. 61–62° (23)).

(ii) Ethyl iodide replaced ethyl bromide in (i). Crystallization of the product from heptane gave small colorless prisms (0.1 g), m.p. 204–207°, identified as 9,9′-dimethyl-9,9′-difluorenyl. The mother liquors contained impure ethylmethylfluorene.

9,9-Dimethylfluorene

(i) Fluorene (16.6 g, 0.1 mole) was added to ethereal methyl lithium (from methyl iodide, 43 g, 0.3 mole). Methyl iodide was added dropwise until the solution became colorless. The product crystallized from methanol as colorless prismatic needles (17.3 g, 89%), m.p. 90–93°, raised to 95–96° by a further crystallization.

Phenyl lithium gave less satisfactory yields unless the product was distilled at 1 to 2 mm prior to crystallization.

(ii) Methylation of 9-methylfluorene with methyl lithium – methyl iodide gave, in the same way, 9,9-dimethylfluorene in 92%.

Two melting points have been recorded for 9,9-dimethylfluorene: 71° (19) and 69–70° (24), 95–96° (19, 25) and 96° (23). Through the kindness of Dr. C. C. Barker, his original sample (24) has been examined after a lapse of several years and found to have a melting point of 81–92°, raised to 95–96° by one crystallization from methanol. Attempts by Emmerson (24) to obtain the higher melting form had been unsuccessful but the present author has been unable to obtain the lower melting form. The existence of the two crystalline forms reported earlier (19) is thus confirmed.

9-Methyl-9-phenylfluorene

Methylation of 9-phenylfluorene as described for fluorene gave methylphenylfluorene in 87% yield, crystallizing as colorless lustrous plates from methanol, m.p. 86–86.5° (lit. m.p. 84–85° (26), 86–87° (27)). Found: C, 93.97; H, 6.19%. Calculated for $C_{20}H_{16}$: C, 93.71; H, 6.29%.

Experiments with 9-Methyl-9-benzoylfluorene

(i) 9-Methyl-9-benzoylfluorene (2 g) in dry ether (100 ml) was added to ethereal phenyl lithium (from bromobenzene, 5 g). The solution immediately assumed a deep red color, similar to that produced by adding 9-methylfluorene to phenyl lithium. The color was rapidly discharged by the addition of methyl iodide (2 g). The product crystallized from methanol as colorless prismatic needles (0.9 g), m.p. 94–96°, identified as 9,9-dimethylfluorene. Found: C, 92.46; H, 7.04%. Calculated for $C_{15}H_{14}$: C, 92.74; H, 7.26%.

(ii) The experiment was performed as in (i) but without the addition of methyl iodide. The product crystallized as long needles (0.17 g) from methanol, m.p. 163–164°, after several crystallizations. Found: C, 87.43; H, 6.13%. Calculated for $C_{19}H_{16}O$: C, 87.66; H, 6.20%. Identity with triphenylmethanol was established by mixed melting point determination and comparison of infrared spectra. The oily residues were not examined.

In other experiments, methyl 9-methylfluorene-9-carboxylate satisfactorily replaced the ketone, and methyl lithium replaced phenyl lithium, although attempts were not made to isolate methyldiphenylmethanol.

9,9'-Difluorenyl

Ethereal methyl magnesium iodide (from methyl iodide, 4 g) was decanted from magnesium and added dropwise to a solution of 9-bromofluorene (2.4 g) and methyl iodide (2 g) in ether. After 10 minutes, the complex was decomposed with ice and ammonium chloride. The product was crystallized from heptane to give, in two crops, difluorenyl (1.5 g), m.p. and mixed m.p. 244–246°.

Dimethyl 9,9'-difluorenyl-9,9'-dicarboxylate

Methyl 9-bromofluorene-9-carboxylate (1.3 g) was added to a solution of methyl fluorene-9-carboxylate (1 g) in methanol containing sodium methoxide (from sodium, 0.2 g) and the suspension was warmed for 10 minutes. The product crystallized as small prisms (1.1 g) from benzene–hexane, m.p. 238–240°, identical with a sample prepared by the reaction between methyl fluorene-9-carboxylate anion and iodine (cf. 29) (lit. m.p. 237° (28)).

Methyl 9-(9'-fluorenylmethyl)-fluorene-9-carboxylate (?)

9-Methyl-9-fluorenol (1 g) was warmed for a few minutes with dry ether (30 ml) and acetyl bromide (1 ml). The solvent was evaporated below 30° and to the residual oil was added a solution of methyl fluorene-9-carboxylate (1.1 g) in methanol (30 ml) containing sodium methoxide (from sodium, 0.2 g). Polymeric material was removed by filtration, after which the clear yellow filtrate was warmed for 30 minutes. Careful dilution with water and scratching induced crystallization. After two crystallizations from heptane the colorless prisms (0.2 g) had a melting point of 173–174°. Found: C, 85.97; H, 6.16%. Calculated for $C_{29}H_{22}O_2$: C, 86.54; H, 5.51%.

Saponification in ethylene glycol was incomplete after 2 hours and yielded an unresolved mixture from which 9-methyl-9,9'-difluorenyl was not obtained by seeding, although a careful comparison of infrared spectra suggested its presence.

ACKNOWLEDGMENTS

The author is indebted to Professor N. B. Chapman for his interest and encouragement, to Doctors K. Clarke and J. Parrick for commenting on the manuscript, and to Dr. G. W. Gray and Miss A. Stephenson for the infrared spectra. Mr. R. Bolton kindly provided details of unpublished work on the 9-halo-9-methylfluorenes.

REFERENCES

1. F. A. L. Anet and P. M. G. Bavin. Can. J. Chem. **36**, 763 (1958).
2. A. Wanschiedt and B. Moldavskii. Ber. **64**, 917 (1931).
3. E. J. Greenhow, E. N. White, and D. McNeil. J. Chem. Soc. 3099 (1953).
4. O. Exner. Chem. listy, **47**, 869 (1953).
5. S. Wawzonek and E. Dufek. J. Am. Chem. Soc. **78**, 3530 (1956).
6. H. D. Zook, J. March, and D. F. Smith. J. Am. Chem. Soc. **81**, 1617 (1959).
7. P. M. G. Bavin. Can. J. Chem. **37**, 2023 (1959).
8. H. Wren and C. J. Still. J. Chem. Soc. **107**, 444 (1915).
9. M. S. Kharasch and O. Reinmuth. Grignard reactions of non-metallic substances. Prentice-Hall, Inc., New York. 1954.
10. A. McKenzie, H. D. K. Drew, and G. H. Martin. J. Chem. Soc. **107**, 26 (1915).
11. F. A. L. Anet and P. M. G. Bavin. Can. J. Chem. **34**, 991 (1956).
12. P. M. G. Bavin. Anal. Chem. In press.
13. Beilstein's handbuch der organischen chemie. Vol. V, 2nd Suppl. p. 551.
14. H. F. Miller and G. B. Bachmann. J. Am. Chem. Soc. **57**, 766 (1935).
15. M. S. Kharasch, F. L. Lambert, and W. H. Urry. J. Org. Chem. **10**, 298 (1945).
16. C. D. Hurd and K. Wilkinson. J. Am. Chem. Soc. **70**, 739 (1948).
17. M. S. Kharasch and C. F. Fuchs. J. Org. Chem. **10**, 292 (1945).
18. R. E. Dessy, G. S. Handler, J. H. Wotiz, and C. A. Hollingsworth. J. Am. Chem. Soc. **79**, 3476 (1957).
19. M. Anchell and A. H. Blatt. J. Am. Chem. Soc. **63**, 1948 (1941).
20. J. R. Sampey and E. E. Read. J. Am. Chem. Soc. **69**, 234 (1947).
21. C. R. Hauser *et al.* J. Am. Chem. Soc. **78**, 1653 (1956).
22. N. Buu-Hoi and J. Lecocq. Compt. rend. **226**, 87 (1948).
23. E. J. Greenhow and D. McNeil. J. Chem. Soc. 3204 (1956).
24. R. G. Emmerson. Thesis. London. 1955.
25. P. LeBeau and M. Picon. Compt. rend. **173**, 84 (1921).
26. E. Bergmann and A. Bondi. Ber. **64**, 1455 (1931).
27. J. R. Dice, T. E. Watkins, and H. L. Schuman. J. Am. Chem. Soc. **72**, 1738 (1950).
28. R. Stollé and F. Wolf. Ber. **46**, 2251 (1913).
29. W. Wislicenus and W. Mocker. Ber. **46**, 2778 (1913).
30. R. Bolton. Unpublished experiments.

SOME OPEN-CHAIN DERIVATIVES OF GLUCOSE AND MANNOSE[1]

E. J. C. CURTIS AND J. K. N. JONES

ABSTRACT

The dimethyl thioacetals of D-glucose and D-mannose have been condensed with acetone. Mannose dimethyl thioacetal forms a crystalline 3,4:5,6-di-*O*-isopropylidene derivative while glucose forms a mixture of the crystalline 3,4:5,6-di-*O*-isopropylidene and syrupy 2,3:5,6-di-*O*-isopropylidene isomers. These three di-*O*-isopropylidene dimethyl thioacetals have been converted via crystalline intermediates into the corresponding di-*O*-isopropylidene dimethyl acetals. These derivatives are suitable open-chain compounds for use in Koenigs–Knorr syntheses and provide (*a*) mannose with the C_2 hydroxyl free, (*b*) glucose with the C_2 hydroxyl free, and (*c*) glucose with the C_4 hydroxyl free.

INTRODUCTION

It has already been shown (1) that in Koenigs–Knorr syntheses of disaccharides much greater yields may be obtained by the use of an open-chain hydroxyl reactant rather than the more generally used ring-form derivatives. This is presumably because there is less steric hindrance to reaction in the case of the open-chain compound. In the synthesis of lactose, however (1), the hydroxyl reactant used (syrupy 2,3:5,6-di-*O*-isopropylidene-D-glucose dimethyl acetal) contained small amounts of other di-*O*-isopropylidene isomers due to the method of synthesis. This, of course, resulted in an impure product from the Koenigs–Knorr reaction, there being small amounts of other disaccharides present in addition to lactose. In the present work syntheses are described of open-chain derivatives of (*a*) mannose with the C_2 hydroxyl group free, (*b*) glucose with the C_2 hydroxyl group free, and (*c*) glucose with the C_4 hydroxyl group free. All of these have been made via pure crystalline intermediates and should prove very useful in Koenigs–Knorr syntheses.

Schinle (2) condensed D-glucose dibenzyl thioacetal with acetone in the presence of anhydrous copper sulphate and obtained a syrupy mixture of mono- and di-*O*-isopropylidene derivatives. There was at first some doubt as to the structure of the di-*O*-isopropylidene material but Munro and Percival (3) later showed this to be a mixture of 2,3:5,6- and 3,4:5,6-di-*O*-isopropylidene isomers of D-glucose dibenzyl thioacetal. Condensation of D-glucose diethyl thioacetal with acetone (1) gives a syrupy mixture which consists largely of the 2,3:5,6-di-*O*-isopropylidene derivative.

Pacsu and Trister (4) condensed D-mannose dibenzyl thioacetal with acetone and obtained a syrupy di-*O*-isopropylidene derivative which was shown to be mainly the 3,4:5,6 isomer. Condensation of D-mannose diethyl thioacetal with acetone yields a syrupy product which has been shown to be largely the 3,4:5,6-di-*O*-isopropylidene derivative (5).

In the present work condensation of D-mannose dimethyl thioacetal with acetone in the normal way resulted in a crystalline di-*O*-isopropylidene derivative in high yield. This compound was shown by methylation experiments to be 3,4:5,6-di-*O*-isopropylidene-D-mannose dimethyl thioacetal. The compound formed a crystalline benzoate which then was converted into 2-*O*-benzoyl-3,4:5,6-di-*O*-isopropylidene-D-mannose dimethyl acetal using a modification of the method of Wolfrom (6). Debenzoylation yielded 3,4:5,6-di-*O*-isopropylidene-D-mannose dimethyl acetal.

Condensation of D-glucose dimethyl thioacetal with acetone resulted in a syrupy product which partially crystallized on standing. The crystalline portion (19% yield)

[1]*Manuscript received February 18, 1960.*
Contribution from the Department of Chemistry, Queen's University, Kingston, Ontario.

was shown by methylation experiments to be 3,4:5,6-di-*O*-isopropylidene-D-glucose dimethyl thioacetal, while methylation of the syrupy portion (76% yield) showed this to be mainly the 2,3:5,6-di-*O*-isopropylidene isomer. Both isomers formed benzoates. 2-*O*-Benzoyl-3,4:5,6-di-*O*-isopropylidene-D-glucose dimethyl thioacetal was converted into the dimethyl acetal, which on debenzoylation yielded 3,4:5,6-di-*O*-iso-propylidene-D-glucose dimethyl acetal. By a similar route, 2,3:5,6-di-*O*-isopropylidene-D-glucose dimethyl acetal was also formed. 3,4:5,6-Di-*O*-isopropylidene-D-glucose dimethyl acetal formed a crystalline toluene-*p*-sulphonyl derivative.

EXPERIMENTAL

Optical rotations were measured in water at 21°±2° C unless otherwise stated. Solutions were concentrated under reduced pressure at 40° C. The following solvent systems (v/v) were used to separate sugars on paper chromatograms: (A) ethyl acetate:acetic acid:water, 9:2:2; (B) *n*-butanol:ethanol:water, 3:1:1. Sugars were detected using the *p*-anisidine hydrochloride spray (7). Infrared absorptions were measured as solutions in chloroform or as a powder suspended in a potassium bromide pellet on a Perkin–Elmer Model 21 spectrophotometer.

Preparation of Di-O-isopropylidene-D-mannose Dimethyl Thioacetal

Mannose dimethyl thioacetal (22 g) was added to a mixture of dry acetone (400 ml), anhydrous copper sulphate (12 g), and concentrated sulphuric acid (2 ml), and the resulting mixture was shaken at room temperature for 24 hours. The solution was neutralized with concentrated ammonium hydroxide solution and filtered. The precipitate was washed with acetone and filtrate and washings were evaporated to a colorless syrup. This was diluted with chloroform (200 ml) and extracted once with water. The chloroform solution was dried ($MgSO_4$), filtered, and evaporated to a syrup (23 g) which crystallized completely on standing. After recrystallization from light petroleum the material weighed 21.8 g (76% yield) and had a melting point of 58–59° C and $[\alpha]_D$ +5.0° (*c*, 7.6, chloroform). Anal. Calc. for $C_{14}H_{26}O_5S_2$: C, 49.70; H, 7.69; S, 18.94. Found: C, 49.87; H, 7.78; S, 18.99.

Methylation of Di-O-isopropylidene-D-mannose Dimethyl Thioacetal

Di-*O*-isopropylidene-D-mannose dimethyl thioacetal (2 g) was dissolved in methyl iodide (20 ml). Silver oxide (3.6 g) plus Drierite (2 g) were added to the solution which was then shaken in the dark at room temperature for 24 hours. Filtration and subsequent evaporation yielded a brown syrup (1.5 g). Isopropylidene and thioacetal groupings were removed by refluxing for 5 hours with aqueous ethanol (20%) containing hydrochloric acid (5%). The solution was neutralized by passage through a column of Duolite A-4 resin (OH form) and concentrated to a syrup (0.9 g). Chromatographic examination of this (solvent A) showed mainly a spot at $R_{mannose}$ 2.15, with smaller spots corresponding to mannose and arabinose. Part of this syrup (200 mg) was separated by chromatography on sheets of Whatman No. 1 filter paper using solvent B as eluent. Guide strips were cut and sprayed and the fraction $R_{mannose}$ 2.15 was cut out and eluted with acetone. The acetone solution was evaporated to dryness. The residue was diluted with a little ethanol, warmed with charcoal, and filtered. Evaporation of the filtrate yielded a syrup (77 mg) which crystallized on dilution with a little ethanol.

After recrystallization from methanol/ether the material had a melting point of 134–136° C and $[\alpha]_D$ +5.2° (constant) (*c*, 1.2). It formed a phenylhydrazone which had a melting point of 161–163° C and $[\alpha]$ −60.5° (constant) (*c*, 0.38, pyridine). Authentic

2-*O*-methyl-α-D-mannose has a melting point of 136–137° C and $[\alpha]_D$ +7.0° → +4.5° (constant) and forms a phenylhydrazone with a melting point of 163° C and $[\alpha]_D$ −49.1° → −60.7° (pyridine, constant) (4).

*2-O-Benzoyl-di-O-isopropylidene-*D*-mannose Dimethyl Thioacetal*

Di-*O*-isopropylidene-D-mannose dimethyl thioacetal (17.2 g) was dissolved in dry pyridine (180 ml). The solution was stirred mechanically and cooled externally. The temperature was kept at −5° C while a solution of benzoyl chloride (18 g) in pyridine (30 ml) was added dropwise. Cooling was continued at −5° C (30 minutes) and then at 0° C (7 hours), and the solution was finally stored at room temperature (14 hours). The product was precipitated by slowly pouring the solution into ice plus water (700 ml). After 30 minutes at room temperature, the crude crystalline material was filtered and washed with water. It was recrystallized from methanol and weighed 19.3 g (86% yield). It had a melting point of 83–84° C and $[\alpha]_D$ +7.8° (*c*, 1.0, methanol). Anal. Calc. for $C_{21}H_{30}O_6S_2$: S, 14.48. Found: S, 14.68.

*2-O-Benzoyl-di-O-isopropylidene-*D*-mannose Dimethyl Acetal* (ref. 6)

2-*O*-Benzoyl-di-*O*-isopropylidene-D-mannose dimethyl thioacetal (10 g) was dissolved in dry methanol (300 ml). Cadmium carbonate (87 g) was added to the solution and a solution of mercuric chloride (87 g) in methanol (100 ml) was then added portionwise with vigorous stirring at room temperature. After completion of the addition (5 hours), stirring was continued for a further 15 hours at room temperature, and the solution was then boiled under reflux for 15 minutes. The cooled solution was filtered through a Celite pad and the precipitate was washed with methanol. Filtrate and washings were concentrated to ca. 150 ml and this solution was poured into 200 ml each of chloroform and water. The chloroform layer was extracted with water until chloride-free, dried ($MgSO_4$), filtered, and evaporated to a syrup (7.5 g) which crystallized on standing overnight. Recrystallization from methanol yielded 6.5 g of product (70%). After further recrystallizations from methanol and from light petroleum the material had a melting point of 73.5–74° C and $[\alpha]_D$ −1.6° (*c*, 3.5, chloroform). Anal. Calc. for $C_{21}H_{30}O_8$: C, 61.43; H, 7.37. Found: C, 61.35; H, 7.53.

*3,4:5,6-Di-O-isopropylidene-*D*-mannose Dimethyl Acetal*

2-*O*-Benzoyl-di-*O*-isopropylidene-D-mannose dimethyl acetal (0.67 g) was dissolved in 50% aqueous ethanol (30 ml) containing potassium hydroxide (0.12 g) and the solution was warmed at 70° C (4 hours). The solution was concentrated to a small volume to remove ethanol and then extracted with chloroform. The chloroform solution was extracted three times with water, dried ($MgSO_4$), filtered, and evaporated to a syrup (0.49 g, 98%). Infrared analysis showed no absorption for carbonyl group (1700–1750 cm^{-1}). The material had $[\alpha]_D$ −1.3° (*c*, 1.6, methanol).

*Preparation of a Mixture of Di-O-isopropylidene-*D*-glucose Dimethyl Thioacetals*

Glucose dimethyl thioacetal (20 g) was added to a mixture of dry acetone (400 ml), anhydrous copper sulphate (12 g), and concentrated sulphuric acid (2 ml) and the resulting solution was shaken at room temperature for 24 hours. The solution was neutralized with concentrated ammonium hydroxide solution, filtered, and the precipitate was washed with acetone. Filtrate and washings were evaporated to a syrup which was diluted with chloroform (150 ml) and extracted once with water. The chloroform solution was dried ($MgSO_4$), filtered, and evaporated to a syrup (26 g). This partially crystallized on standing. The mixture of crystals and syrup was diluted with light

petroleum and refrigerated. Subsequent filtration yielded 3.1 g crystalline material. Concentration of the filtrate followed by seeding produced a further 2.0 g crystals; total yield of crystalline product 5.1 g (19%). This was recrystallized from light petroleum and had a melting point of 92–94° C and $[\alpha]_D$ −1.0° (*c*, 9.8, chloroform). Anal. Calc. for $C_{14}H_{26}O_5S_2$: C, 49.70; H, 7.69; S, 18.94. Found: C, 49.64; H, 7.52; S, 18.86.

When all the above crystalline material had been removed from the reaction product there remained 20.6 g (76%) syrup which could not be crystallized. It had $[\alpha]_D$ −92.4° (*c*, 1.2, chloroform). Anal. Calc. for $C_{14}H_{26}O_5S_2$: S, 18.94. Found: S, 18.72, 18.64.

Methylation of Crystalline Di-O-isopropylidene-D-glucose Dimethyl Thioacetal

Crystalline di-*O*-isopropylidene-D-glucose dimethyl thioacetal (0.93 g) was dissolved in dry tetrahydrofuran (20 ml). Small pieces of clean sodium were then added to the solution until no further reaction took place. Methyl iodide (0.5 ml) was added to the solution which was stored in a darkened, stoppered flask at room temperature for 24 hours, further small quantities of sodium and methyl iodide being added at intervals. The solution was filtered and the precipitate was washed with tetrahydrofuran. Filtrate and washings were evaporated to dryness and the residue was dissolved in chloroform and washed with water until free from iodide. The solution was dried (Na_2SO_4), filtered, and evaporated to a syrup (0.91 g). Infrared examination of this indicated only a very small amount of free hydroxyl group present. Thioacetal groupings were removed by the method of Wolfrom (8), using mercuric chloride in the presence of cadmium carbonate in aqueous ethanol and isopropylidene groupings were subsequently hydrolyzed by warming the product in sulphuric acid (0.5 *N*) solution. The solution was deionized by passage through a column of Amberlite IR-120 (H form) and Duolite A-4 (OH form) resins in series and the neutral eluate was concentrated to a syrup (0.50 g). Chromatography of this (solvent A) showed mainly a spot at $R_{glucose}$ 2.61, with much smaller spots at $R_{glucose}$ 1.01, 3.92, and 7.30, these latter two being presumably due to unhydrolyzed isopropylidene derivatives.

The syrup was stored in a stoppered flask at room temperature and after 6 weeks it was found that a crystal nucleus had developed. When this was mixed with the syrup the mass crystallized. Part of the crude material (200 mg) was transferred to a porous tile and the crystals were cleaned by rapidly washing them with methanol. This material (110 mg) was recrystallized from methanol/ether. Chromatography in solvent A showed a single spot at $R_{glucose}$ 2.61. It had a melting point of 156–158° C and $[\alpha]_D$ +26.3° → +67.8° (constant) (*c*, 2.3). It formed a tetrabenzoate which had a melting point of 167°–168° C and $[\alpha]_D$ −8.4° (*c*, 0.6, chloroform). 2-*O*-Methyl-β-D-glucose has a melting point of 157–159° C and $[\alpha]_D$ +12.0 → +66.0 (constant) (9) and forms a tetrabenzoate with a melting point of 169°–170° C and $[\alpha]_D$ −6.2° (10). Under drastic conditions the material formed an osazone whose infrared spectrum was identical with that of authentic D-glucosazone.

Methylation of Syrupy Di-O-isopropylidene-D-glucose Dimethyl Thioacetal

Syrupy di-*O*-isopropylidene-D-glucose dimethyl thioacetal (5 g) was methylated using silver oxide and methyl iodide in the same way as described for di-*O*-isopropylidene-D-mannose dimethyl thioacetal. After removal of thioacetal and isopropylidene groupings and deionization, a clear syrup (1.9 g) was obtained. Chromatography of this (solvent A) showed spots at $R_{glucose}$ 1.00 and 2.56 with much smaller spots at 2.65, 3.40, and 4.45. The spot at $R_{glucose}$ 2.65 was presumably due to 2-*O*-methyl-D-glucose, formed from traces of the 3,4:5,6-di-*O*-isopropylidene isomer not removed by crystallization.

The spots at 3.40 and 4.45 were due either to unhydrolyzed isopropylidene residues or to methylation of mono-isopropylidene materials. Part of the syrup (1.4 g) was separated by chromatography on a column of powdered cellulose using solvent A as eluent. A fraction (0.73 g) was collected which showed a single spot at $R_{glucose}$ 2.56 in solvent A. The material had $[\alpha]_D$ +52.1° (*c*, 2.4). It did not crystallize. Authentic 4-*O*-methyl-D-glucose has $[\alpha]_D$ +53° (3). It formed an osazone which had a melting point of 157–159° C and $[\alpha]_D$ −17.4° (constant) (*c*, 0.6, pyridine). Anal. Calc. for $C_{19}H_{24}O_4N_4$: OMe, 8.35. Found: OMe, 8.15. 4-*O*-Methyl-D-glucose phenylosazone has a melting point of 158–160° C and $[\alpha]_D$ −32.6° → −15.5° (constant) (3).

Part of the syrup was converted into 4-*O*-methyl-D-glucose methyl glucoside by refluxing it for 3 hours with hydrochloric acid in methanol (2%). The solution was neutralized (Ag_2CO_3) and filtered, and the filtrate was evaporated to a clear syrup. This crystallized after it was diluted with a drop of ethyl acetate and nucleated with authentic 4-*O*-methyl-D-glucose methyl-α-D-glucoside. The material was washed on a porous tile with ethyl acetate and dried. It showed an infrared spectrum identical with that of 4-*O*-methyl-D-glucose methyl-α-D-glucoside.

*2-O-Benzoyl-di-O-isopropylidene-*D*-glucose Dimethyl Thioacetal*

3,4:5,6-Di-*O*-isopropylidene-D-glucose dimethyl thioacetal (3.1 g) was dissolved in dry pyridine (30 ml). The solution was stirred mechanically and cooled to −5° C while a solution of benzoyl chloride (2 g) in pyridine (10 ml) was added dropwise, after which the temperature was kept at −5° C (30 minutes) and then at 0° C (4 hours). The solution was finally stored at room temperature (20 hours). It was poured slowly into ice plus water (200 ml) when the product separated as an oil which did not crystallize on standing. The solution was extracted with chloroform (4×40 ml) and the combined extracts were washed successively with solutions of dilute sulphuric acid, sodium bicarbonate, and water. The solution was dried ($MgSO_4$), filtered, and evaporated to a syrup (3.9 g). This proved difficult to crystallize. However, seed crystals were obtained by dissolving part of the syrup in methanol and cooling this in an acetone/Dry Ice bath, and at the same time scratching the side of the vessel with a glass rod. The syrup crystallized completely on subsequent seeding. Recrystallization from methanol yielded 3.8 g (93%). The material had a melting point of 85–86° C and $[\alpha]_D$ −15.5° (*c*, 1.0, methanol). Anal. Calc. for $C_{21}H_{30}O_6S_2$: S, 14.48. Found: S, 14.66.

*2-O-Benzoyl-di-O-isopropylidene-*D*-glucose Dimethyl Acetal*

2-*O*-Benzoyl-di-*O*-isopropylidene-D-glucose dimethyl thioacetal (3 g) was converted to the acetal using the method described above for the preparation of 2-*O*-benzoyl-di-*O*-isopropylidene-D-mannose dimethyl acetal. A syrup (2.7 g) was obtained which crystallized on standing. Recrystallization from aqueous methanol yielded 2.5 g material (90%). After further recrystallizations from methanol and from light petroleum it had a melting point of 71–72.5° C and $[\alpha]_D$ −40.8° (*c*, 2.0, chloroform). Anal. Calc. for $C_{21}H_{30}O_8$: C, 61.43; H, 7.37. Found: C, 61.39; H, 7.34.

*3,4:5,6-Di-O-isopropylidene-*D*-glucose Dimethyl Acetal*

2-*O*-Benzoyl-di-*O*-isopropylidene-D-glucose dimethyl acetal (1.11 g) was dissolved in 50% aqueous ethanol (40 ml) containing potassium hydroxide (0.17 g) and the solution was warmed at 70° C (5 hours). The product was worked up as described above for the corresponding mannose derivative. A syrup (0.77 g, 93%) was obtained which crystallized on standing in a vacuum desiccator. After recrystallization from light petroleum it had

a melting point of 88–89° C and $[\alpha]_D$ −9.0° (*c*, 4.2, methanol). Infrared analysis showed no absorption for the carbonyl group (1700–1750 cm^{-1}).

2-O-Tosyl-di-O-isopropylidene-D-glucose Dimethyl Acetal

3,4:5,6-Di-*O*-isopropylidene-D-glucose dimethyl acetal (0.113 g) was dissolved in dry pyridine (1 ml) and toluene *p*-sulphonyl chloride (0.098 g) was added to the solution. Moisture was excluded from the solution, which was kept at room temperature (18 hours) and then warmed to 70° C on a water bath (30 minutes). The product was isolated in the usual way, a syrup (0.116 g, 68%) being obtained which crystallized immediately. After recrystallization from light petroleum the material had a melting point of 109–111° C and $[\alpha]_D$ +10.4° (*c*, 2.5, chloroform). Anal. Calc. for $C_{21}H_{32}O_9S$: S, 6.96. Found: S, 6.82.

Benzoylation of Syrupy Di-O-isopropylidene-D-glucose Dimethyl Thioacetal

Syrupy di-*O*-isopropylidene-D-glucose dimethyl thioacetal (14.3 g) was benzoylated as described above. A clear syrup (21 g) was obtained which showed no absorption for hydroxyl group (3500–3600 cm^{-1}) on infrared analysis. It had $[\alpha]_D$ +34.0° (*c*, 1.05, methanol).

4-O-Benzoyl-di-O-isopropylidene-D-glucose Dimethyl Acetal

Syrupy 4-*O*-benzoyl-di-*O*-isopropylidene-D-glucose dimethyl thioacetal (9.3 g) was converted to the dimethyl acetal in the usual way. A syrup (7.7 g) was obtained which crystallized on standing. Recrystallization from methanol yielded 4.9 g (56%). After further recrystallization from light petroleum the material had a melting point of 101.5–102° C and $[\alpha]_D$ −5.8° (*c*, 1.85, chloroform). Anal. Calc. for $C_{21}H_{30}O_8$: C, 61.43; H, 7.35. Found: C, 61.47; H, 7.38.

2,3:5,6-Di-O-isopropylidene-D-glucose Dimethyl Acetal

4-*O*-Benzoyl-di-*O*-isopropylidene-D-glucose dimethyl acetal (2.73 g) was dissolved in 50% aqueous methanol (100 ml) containing sodium hydroxide (0.27 g) and the solution was warmed at 70° C (4 hours). Following the usual method of isolation a syrup (1.92 g, 95%) was obtained. This had $[\alpha]_D$ −15.9° (*c*, 3.5, methanol). Infrared analysis showed no absorption for carbonyl peak.

The authors wish to thank the National Research Council for grants which made this work possible.

REFERENCES

1. E. J. C. Curtis and J. K. N. Jones. Can. J. Chem. **37**, 358 (1959).
2. R. Schinle. Ber. **65** B, 315 (1932).
3. J. Munro and E. G. V. Percival. J. Chem. Soc. 873 (1935).
4. E. Pacsu and S. M. Trister. J. Am. Chem. Soc. **63**, 925 (1941).
5. Unpublished results.
6. M. L. Wolfrom, L. T. Tanghe, R. W. George, and S. W. Waisbrot. J. Am. Chem. Soc. **60**, 1932 (1938).
7. L. Hough, J. K. N. Jones, and W. H. Wadman. J. Chem. Soc. 1702 (1950).
8. M. L. Wolfrom. J. Am. Chem. Soc. **51**, 2188 (1929).
9. J. W. H. Oldham and J. K. Rutherford. J. Am. Chem. Soc. **54**, 1086 (1932).
10. J. W. H. Oldham. J. Am. Chem. Soc. **56**, 1360 (1934).

THE STUDY OF HYDROGEN BONDING AND RELATED PHENOMENA BY ULTRAVIOLET LIGHT ABSORPTION

PART IV. INTERMOLECULAR HYDROGEN BONDING IN ANILINES AND PHENOLS[1]

J. C. DEARDEN[2] AND W. F. FORBES[3]

ABSTRACT

Intermolecular hydrogen bonding in anilines and phenols can be subdivided into bonding involving solute molecules only, and into bonding involving both solute and solvent molecules. Interactions which do not involve hydrogen bonding are also possible between solute and solvent molecules. Spectral effects which may be associated with each of these interactions are described and discussed for anilines and phenols. By noting the effects of substituents on the various interactions, tentative conclusions can be deduced concerning the nature of these interactions.

INTRODUCTION

Intermolecular hydrogen bonding is a well-known phenomenon in a number of phenols and anilines, since the changes caused by the bonding can be detected by the changes in a number of physical properties such as melting points, solubilities, dipole moments, spectral effects, and other properties. The spectral changes caused by intermolecular hydrogen bonding in substituted benzoic acids have been discussed in previous parts of this series (1). The purpose of the present paper is to extend this investigation to anilines and phenols.

HYDROGEN BONDING BETWEEN SOLUTE MOLECULES ONLY

Von Keussler (2) has shown that an increase of the solute concentration beyond the more readily accessible concentration range (i.e. solute concentration greater than ca. 10^{-2} moles/liter) causes a concentration dependence in the *C*-band of the ultraviolet spectrum for solutions of phenol in cyclohexane. (For band nomenclature used, see previous parts of this series.) We have verified von Keussler's results and have also investigated the corresponding spectral changes in both the *B*-band and the *C*-band for a number of phenols, and for anisole. The relevant data are listed in Table I. Table I and also Ito's recently obtained values for the *C*-bands of phenol and anisole (3) show that only phenol and certain alkyl-substituted phenols give rise to appreciable spectral changes in the *C*-band and this suggests that the spectral changes are caused by intermolecular hydrogen bonding between phenol molecules. The relevant spectral curves are shown in Fig. 1. The ultraviolet data in this way confirm the well-known fact that phenol forms an intermolecular hydrogen bond with other phenol molecules, and incidentally that this bond is weaker than the intermolecular hydrogen bond between benzoic acid molecules since greater solute concentrations are required for the phenol solutions before a concentration dependence is observed. This conclusion has frequently been deduced from other spectral data which indicate that phenol molecules associate by means of hydrogen bonding to form dimers, trimers, and even polymers with the degree of association

[1]*Manuscript received February 16, 1960.*
Contribution from the Memorial University of Newfoundland, St. John's, Newfoundland, and from the Division of Protein Chemistry, C.S.I.R.O., Melbourne, Australia. Presented in part at the meetings of the Chemical Institute of Canada, Halifax, Nova Scotia, May, 1959.
[2]*Present address: "Shell" Research Limited, P.O. Box 1, Chester, England.*
[3]*Present address: Division of Protein Chemistry, C.S.I.R.O., 343 Royal Parade, Parkville, N.2, Melbourne, Victoria, Australia. (All correspondence should be addressed to this author.)*

TABLE I

Concentration dependence data in cyclohexane solution for phenol, aniline, and related compounds*

	B-Band			*C*-Band		
	Concn. (molar)	λ_{max}	ϵ_{max}	Concn. (molar)	λ_{max}	ϵ_{max}
Phenol	2.88×10^{-2}	211	5,800	0.104	265	1,400
					271	1,940
					278	1,770
	0.499	210	5,300	2.44	ca. *265*	*1,230*
					270	1,600
					276	1,320
Anisole	3.14×10^{-2}	219	7,850	0.137	266	1,480
					272	2,150
					278	2,120
	0.470	219	6,250	1.46	266	1,290
					272	1,830
					278	1,680
o-Cresol	3.52×10^{-2}	212–213	7,170	0.146	272	1,860
					278	1,720
	0.374	212	7,500	1.16	271	1,400
					277	1,230
m-Cresol	5.33×10^{-2}	214	6,580	0.107	273	1,600
					279	1,640
	0.580	214–215	5,800	0.958	272–273	1,500
					278	1,500
p-Cresol	4.83×10^{-2}	220	6,080	9.65×10^{-2}	271	1,420
					274	1,620
					277	1,860
					279	1,950
					285.5	1,730
	0.437	220	5,150	0.873	277–278	1,680
					283	1,390
2,6(t.Bu)$_2$-phenol	3.49×10^{-2}	213	8,050	6.98×10^{-2}	270–271	1,920
					277–278	1,950
	0.175	214	7,070	0.349	270–271	1,770
					277–278	1,750
Aniline	4.25×10^{-2}	233	8,850	0.127	281	1,700
					284–285	1,850
					287–288	1,880
					ca. *291*	*1,720*
	0.319	233	8,500	1.28	287	1,430
N,N-Dimethylaniline	1.61×10^{-2}	251	15,800	8.06×10^{-2}	297–298	2,380
	0.250	251	13,700	1.25	297	2,300

NOTE: Wavelengths are corrected in this and subsequent tables. Values in italics represent inflections.
*Two cell thicknesses were used throughout. 25.1 μ for concentrations ca. 10^{-2}–10^{-1} molar, and 2.91 μ for concentrations ca. 0.1–2 molar.

apparently being proportional to concentration, and also that appreciable hydrogen bonding does *not* occur below a solute concentration of about 0.01 mole/liter (see refs. 4, 5 and compare also, for example, refs. 6, 7, 8, which suggest that the related alcohols also do not associate appreciably below a solute concentration of ca. 0.005 mole/liter).*

**Neither the ultraviolet spectrum of aniline within the concentration range 1.00×10^{-2} to 3.36×10^{-4} moles/liter in cyclohexane solution (9), nor the ultraviolet spectrum of phenol within the concentration range 2.88×10^{-2} to 0.92×10^{-4} moles/liter in cyclohexane solution (this paper) shows any appreciable concentration dependence. Since under these conditions the benzoic acid spectrum shows a concentration dependence which has been ascribed to intermolecular hydrogen bonding (1), this again supports the hypothesis that within this same concentration range aniline and phenol do not associate appreciably.*

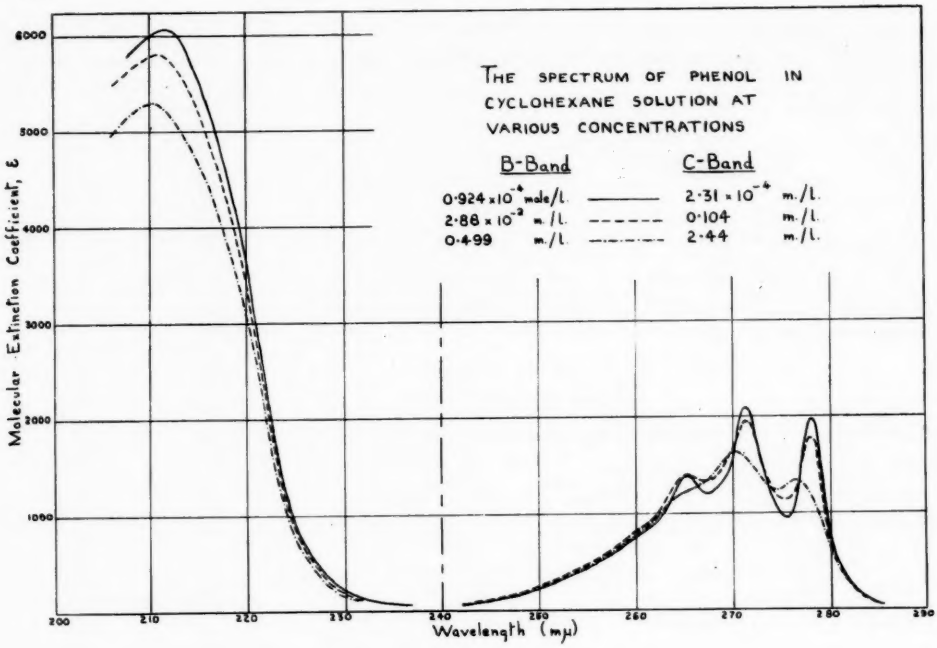

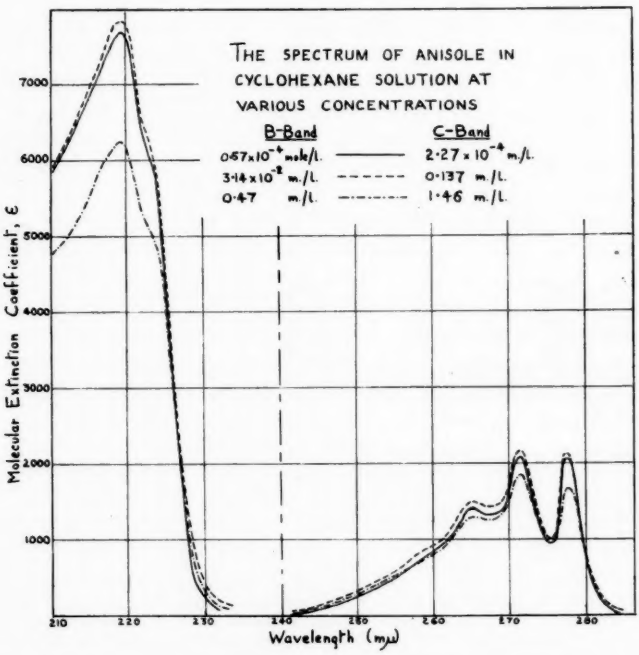

FIG. 1. The spectra of (A) phenol and (B) anisole in cyclohexane solution.

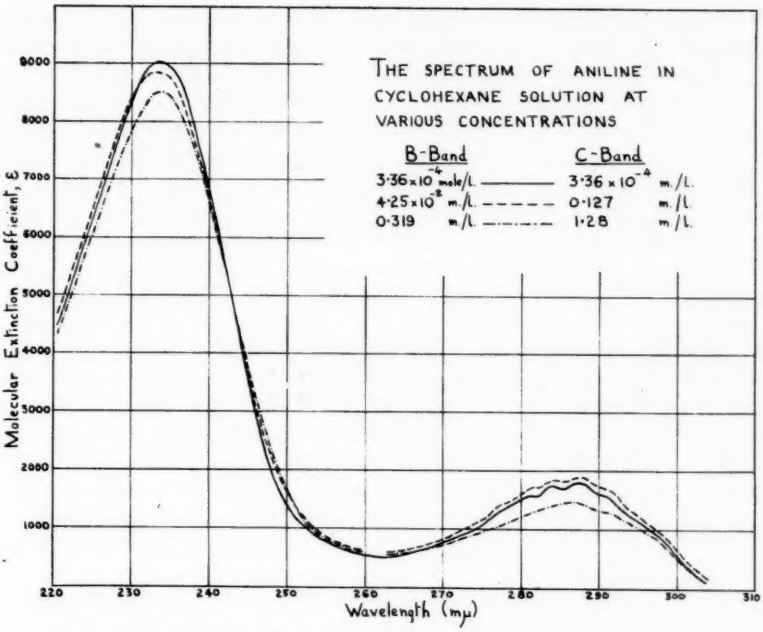

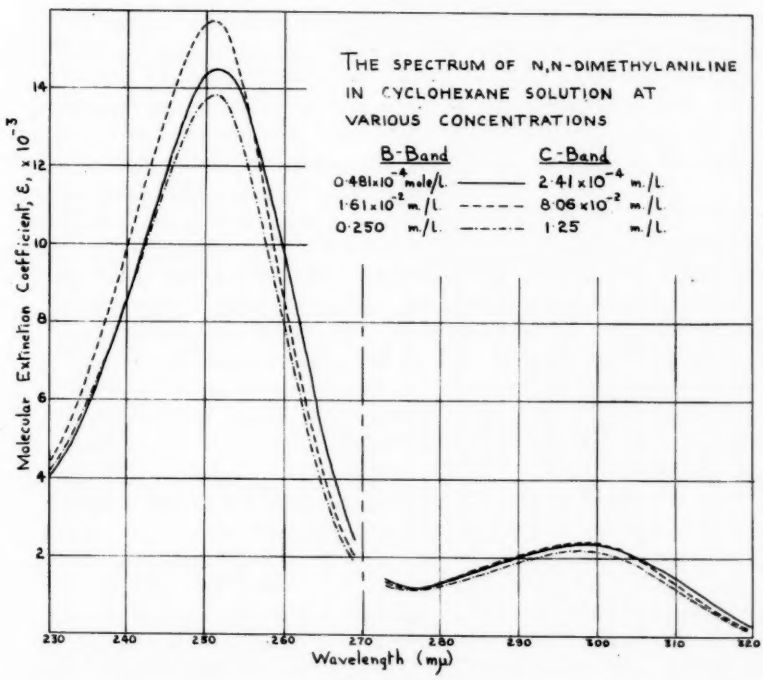

FIG. 2. The spectra of (A) aniline and (B) N,N-dimethylaniline in cyclohexane solution.

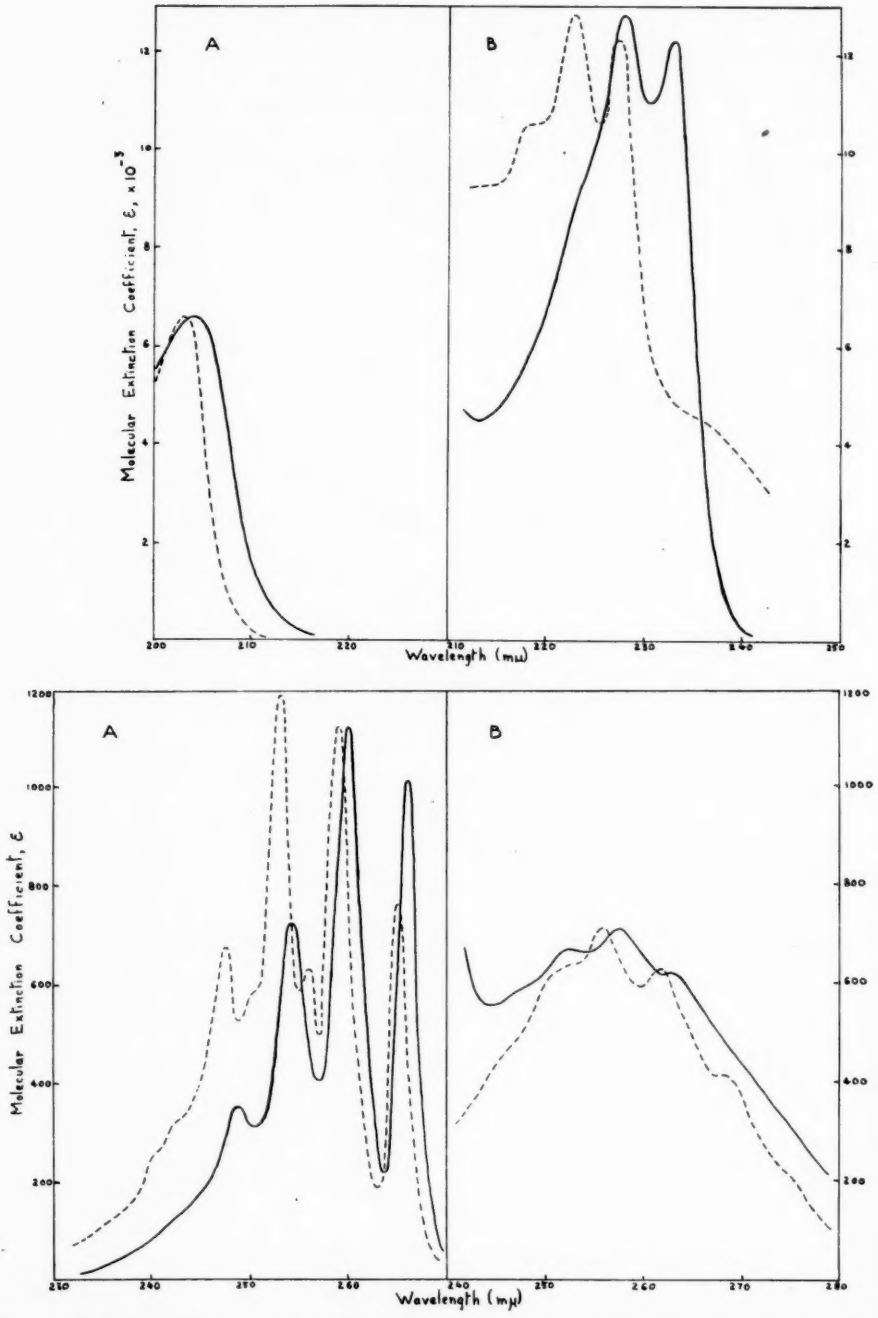

FIG. 3. The *B*-bands (above) and the *C*-bands (below) of (A) fluorobenzene and (B) iodobenzene in the vapor phase (- - -) and in cyclohexane solution (——). (ε values in the vapor phase are arbitrarily chosen.)

Our own data for the infrared hydroxyl band of phenol solutions in cyclohexane are as follows: at a solute concentration of 1.0 mole/liter, $\nu_{max} = 3613$ cm^{-1} for what is assumed to be the unassociated hydroxyl band, the absorption being weak compared with the absorption ascribed to associated hydroxyl bands; at a solute concentration of 0.1 mole/liter, $\nu_{max} = 3622$ cm^{-1}, and this band associated with free hydroxyl absorption is now considerably more intense than the other hydroxyl absorption.

The observed concentration dependences for the ultraviolet spectra of aniline and N,N-dimethylaniline are shown in Fig. 2. As might be anticipated from the *C*-band spectral changes observed for phenol and for the methyl-substituted analogue anisole, the *C*-band of aniline shows a decreased fine structure with increase of solute concentration. N,N-Dimethylaniline shows no fine structure even at the lowest concentrations.

From theoretical considerations it might be expected that an O—H...O hydrogen bond is energetically more favorable than an N—H . . . N hydrogen bond for the molecules under consideration, and this indication is again supported by the infrared data (see ref. 5 and cf. also refs. 10, 11). Our own data for the infrared N—H stretching bands of aniline solutions in cyclohexane are as follows: at a solute concentration of 1.00 mole/liter, $\nu_{max} = 3358$ and 3449 cm^{-1} whereas at a solute concentration of 0.20 mole/liter, $\nu_{max} = 3366$ and 3456 cm^{-1}. It is also noteworthy that these bands are still intense in a solution of aniline in cyclohexane containing 4% ether.

SOLUTE-SOLVENT INTERACTIONS INVOLVING ONLY SOLUTE AND INERT SOLVENT

If the ultraviolet absorption spectra of phenol or aniline are determined in the vapor phase and in an inert solvent it is found that a wavelength displacement occurs for each compound. This displacement cannot be caused exclusively by intermolecular X—H...Y hydrogen bonding because similar wavelength displacements are observed for anisole, and comparable wavelength displacements are also observed for a number of other compounds in which intermolecular hydrogen bonding is unlikely to occur to any marked extent. These observations are illustrated in Table II and the spectral curves for fluorobenzene and iodobenzene are also recorded in Fig. 3.

The data in Table II show that the main absorption bands of a number of aromatic conjugated compounds tend to be bathochromically displaced on passing from the vapor phase spectrum to the spectrum in cyclohexane solution, an observation which has previously been noted by Bayliss and McRae (15). Also, the observed fine structure appears to decrease in cyclohexane solution (see Fig. 3). The displacement appears to be qualitatively related to the dipole moment of the solute, since it is generally larger for compounds possessing an appreciable dipole moment such as nitrobenzene, and larger still for compounds like *p*-iodonitrobenzene (see Table II). Further, altering the temperature does not appreciably affect the wavelength of maximal absorption of some of the compounds in the vapor phase (14), and the spectra of some of these compounds are, moreover, similar in hexane and cyclohexane solution (see "Experimental").

It may further be noted that this somewhat unexpected solvent effect is not confined to the ultraviolet spectra since a "general" solvent effect is also observed in the infrared spectra; for example, the locations of the maximal frequencies of the two infrared NH absorptions for aniline and related compounds are appreciably displaced to lower frequency, i.e. to longer wavelength, in carbon tetrachloride solution, compared with the vapor phase spectrum (see ref. 16, and cf. also refs. 7, 17, 18). The most probable explanation is to associate this solvent effect with oriented solvent molecules which, by virtue of an induced dipole, facilitate the absorption.

TABLE II

Wavelength displacements between vapor phase spectra and spectra in cyclohexane solution

Absorption band		λ_{max}(mμ) (vapor)	λ_{max}(mμ)* (in cyclohexane)	Wavelength displacement (mμ)	Source
Aniline	*B*-band	230	234.5	4.5	Ref. 9
Aniline	*C*-band	ca. 283	289	6	Ref. 9
Phenol	*B*-band	205	210	5	Ref. 12
Phenol	*C*-band	264 267 269.5 ca. *273* 276	266 272 279	ca. 2	Ref. 12
Anisole	*B*-band	214.5	220	5.5	Ref. 13
Anisole	*C*-band	ca. *256* ca. *262* 264 269 270 275.5	ca. *268* 273 279	ca. 7	Ref. 13
Fluorobenzene	*B*-band	203	204	1	*
Fluorobenzene	*C*-band	249.5 255 258 261 267	251 256 262 268	ca. 1	*
Iodobenzene	*B*-band	ca. *219* 224 228	ca. *225* 229 234	ca. 6	*
Iodobenzene	*C*-band	ca. *254* 258 264	255 259.5 265	ca. 1	*
Nitrobenzene	*B*-band	239.1	253	13.9	Ref. 14
p-Fluoronitrobenzene	*B*-band	245.1	256	10.9	Ref. 14
p-Chloronitrobenzene	*B*-band	251.3	264.7	13.4	Ref. 14
p-Bromonitrobenzene	*B*-band	254.6	269	14.4	Ref. 14
p-Iodonitrobenzene	*B*-band	264.1	287.6	23.5	Ref. 14

*This paper.

SOLUTE-SOLVENT INTERACTIONS INVOLVING HYDROGEN BONDING IN SOLUTIONS OF ANILINES AND PHENOLS

Apart from the general solvent effect discussed in the previous section we can discern spectral effects which are ascribed to intermolecular hydrogen bonding between solute and solvent. For example, ether frequently causes a bathochromic wavelength displacement in the *B*-band which is ascribed to intermolecular hydrogen bonding of type I or II, because replacement of the relevant hydrogen atom by a methyl group tends to destroy this effect (see Fig. 4 and cf. ref. 19), and also because parallel effects may be deduced from *C*-band and dipole moment data (20, cf. also 21).

Figure 4 shows that the spectral change ascribed to hydrogen bonding is greater for

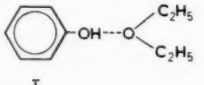

I

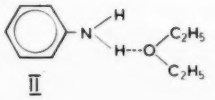

II

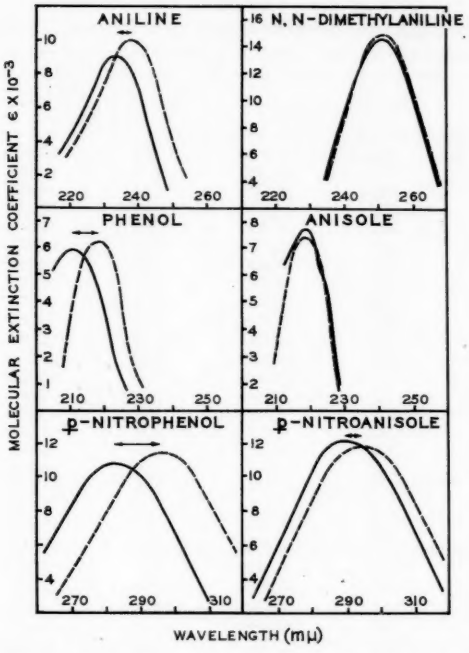

FIG. 4. *B*-Bands of anilines, phenol, and *p*-nitrophenol, and methyl-substituted analogues in cyclohexane (full lines) and in ether (dotted lines).

phenol than for aniline, which supports the previously noted hypothesis that an O—H...X hydrogen bond is energetically more favored than an N—H...X hydrogen bond for the molecules under consideration. A fuller list of spectra of phenols, aromatic amines, and their O- and N-methyl derivatives in cyclohexane and ether solutions is provided in Table III.

Table III indicates that for a number of *p*- or *m*-substituted compounds, where the relevant spectra are available, the observed wavelength displacements are similar to those in the parent compounds, phenol or aniline. That is, the bathochromic wavelength displacement, ascribed to the intermolecular hydrogen bond, is comparable for compounds like *p*-nitrophenol and for phenol, remembering that part of the observed wavelength displacement also occurs in *p*-nitroanisole or nitrobenzene and is therefore not caused by the same intermolecular hydrogen bonding involving the phenol group (see Fig. 4 and Table III). Moreover, since the total displacement, if expressed in wave numbers, for *p*-nitrophenol is only slightly smaller than the sum of the effects in phenol and nitrobenzene, this suggests that interactions which can be represented by resonance structures of type III do not appreciably affect the intermolecular hydrogen bond.

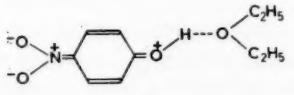

III

TABLE III

Bathochromic wavelength displacements ($\Delta\lambda$ in mμ and $\Delta\nu$ in cm^{-1}) between *B*-bands in cyclohexane (non-bonded species) and ether (hydrogen-bonded species) solutions

Solute	λ_{max}(mμ) (in cyclohexane)	ϵ_{max}	λ_{max}(mμ) (in ether)	ϵ_{max}	$\Delta\lambda$ (in mμ)	$\Delta\nu$ (in cm^{-1})
Aniline	234.5	9,000	238	10,000	3.5	600
N,N-Dimethylaniline	251	14,500	251.5	14,800	(0.5)	100
Phenol	210	6,000	218	6,400	8	1,700
Anisole	220	7,500	219	7,400	(−1)	−200
p-Nitrophenol	286	10,800	299	11,400	13	1,500
p-Nitroanisole	294	12,100	298	11,800	(4)	450
Nitrobenzene	253	9,000	256	8,500	(3)	500
p-Fluorophenol	210–211	4,200	217	4,000	6.5	1,400
p-Fluoroanisole	217	5,400	217.5	5,200	(0.5)	100
p-Chlorophenol	225	8,800	228	10,000	3	600
p-Chloroanisole	228	11,700	228	12,400	(0)	0
p-Bromophenol	225	10,250	226	11,300	1	200
p-Bromoanisole	227	12,500	227	13,000	(0)	0
p-Aminoanisole	237	9,100	239	9,500	(2)	400
p-Cresol	221	5,900	223	6,600	2	400
p-Methoxyphenol	225	7,000	225	7,250	0	0
p-Methoxyanisole	227	9,700	226	9,500	(−1)	−200
m-Nitrophenol	222	10,200	226	10,000	4	800
m-Nitroanisole	224	13,000	225	11,500	(1)	200
m-Cresol	214	6,100	221	5,600	7	1,450
m-Nitroaniline	234 ca. *263–264*	15,500 *4,000*	234 ca. *274*	18,500 *4,000*	0 ca. *10.5*	0
m-Hydroxyacetophenone	242.5 *248*	8,650 *7,250*	247 ca. *253*	9,300 *7,250*	4.5	750
m-Hydroxybenzaldehyde	245 251	10,000 9,500	250 *255*	9,800 *9,200*	5	800
o-Hydroxyacetophenone	248.5 255	9,000 8,700	249 ca. *253*	9,000 *8,500*	(−0.5)	−100
o-Hydroxybenzaldehyde	251 258	11,000 11,700	ca. *251* 255.5	*10,400* 10,700	(−1)	−150
o-Nitrophenol	269	7,350	268–269	6,900	−0.5	−100
o-Nitroanisole	248–249	3,400	250–251	3,050	(2)	300
o-Fluorophenol	212	5,800	216	5,500	4	900
o-Fluoroanisole	218	7,100	219	7,000	(1)	200
o-Chlorophenol	212	6,450	217	6,200	5	1,100
o-Chloroanisole	219 223	7,500 7,400	219 222	7,500 7,500	(0)	0
o-Bromophenol	212	8,700	219	7,000	7	1,550
o-Bromoanisole	ca. *219*	*8,300*	219	8,800	(0)	0
o-Cresol	213	7,500	218	5,350	5	1,100
o-Methoxyphenol	216	6,200	220	6,200	4	800
o-Aminoanisole	237	8,500	239	9,000	2	350

Other *p*-substituents, such as —Cl, —CH_3, etc., appear to have a similar effect and also tend to weaken slightly the intermolecular hydrogen bond as judged by the observed frequency displacements (see Table III). A *m*-substituent again sometimes appears to reduce the strength of the hydrogen bond, as indicated by the reduced frequency displacements (see Table III). A possible explanation is that a *m*- or *p*-substituent tends to interact with the π-electrons of the benzene ring, and that this interaction is competitive in as much as it reduces the benzene ring—OH group interaction which facilitates intermolecular hydrogen bonding.

o-Substituted compounds are evidently less satisfactory for comparison purposes since steric interactions *and* intramolecular hydrogen bonding would be expected to interfere with the conformations of the molecule and with the solvent–solute interactions. However, it may be noted as shown in Fig. 5 that the spectra of some intramolecularly bonded molecules such as *o*-hydroxyacetophenone are almost identical in ether and cyclohexane

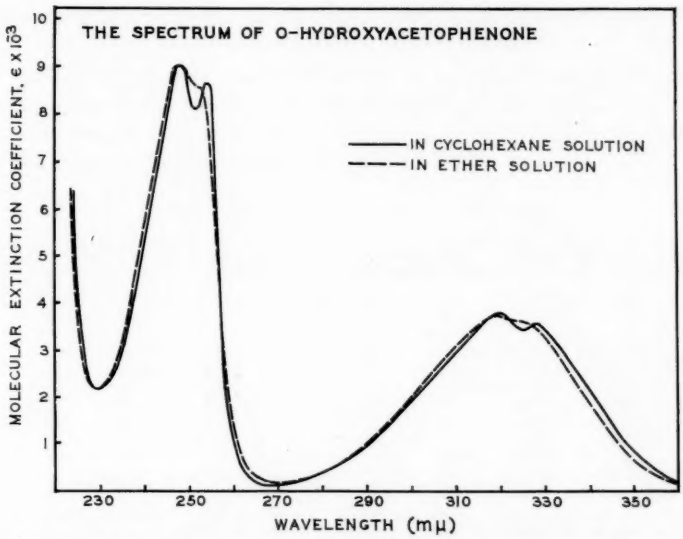

FIG. 5. The ultraviolet spectrum of *o*-hydroxyacetophenone in cyclohexane (full line) and ether (dotted line) solution.

solution (see also Table III for the *B*-bands of *o*-hydroxyacetophenone and *o*-hydroxybenzaldehyde and relevant reference compounds), and this is assumed to show that an intramolecular hydrogen bond prevents the formation of an intermolecular hydrogen bond, since intermolecular hydrogen bonding normally gives rise to spectral changes. *o*-Fluorophenol, however, does give rise to an appreciable wavelength displacement (cf. ref. 1 for the spectrum of *o*-fluorobenzoic acid, which also indicates the absence of a strong intramolecular hydrogen bond for the latter *o*-fluoro compound).

The data in Figs. 6 and 7 for phenol and *p*-nitrophenol in cyclohexane–ether solvent mixtures show that only small amounts of ether are necessary to cause the appearance of the absorption characteristic of the hydrogen-bonded structures. Support for this hypothesis is also received from the infrared spectrum of phenol. This shows that at a concentration of 0.1 mole/liter, i.e. at a concentration at which in cyclohexane solution the free hydroxyl band at 3622 cm^{-1} predominates, addition of 1% of ether to the solution considerably decreases the intensity of this band at the expense of a band at 3331 cm^{-1}, which is ascribed to associated hydroxyl absorption. In cyclohexane solution containing 2% ether the band at 3622 cm^{-1} occurs at 3618 cm^{-1} with yet further decreased absorption intensity and the hydroxyl absorption associated with hydrogen-bonded structures of type I at 3331 cm^{-1} accounts almost completely for the observed hydroxyl absorption. This again suggests that a relatively strong hydrogen bond is formed between the phenolic OH group and the ether molecules, a bond which may be regarded almost as a stoichiometric linkage (cf. also ref. 20 for the effect of small quantities of dioxane on the ultraviolet *C*-band of phenol). Previously determined data, on the other hand, indicated that small amounts of ether do *not* appreciably alter the typical aniline spectrum (see Table I in ref. 9), and this must be taken as evidence against the formation of a "stable stoichiometric" hydrogen bond between aniline and ether molecules under the conditions of the experiment. That is, the data again suggest that the N—H...X bond is weaker than the O—H...X hydrogen bond.

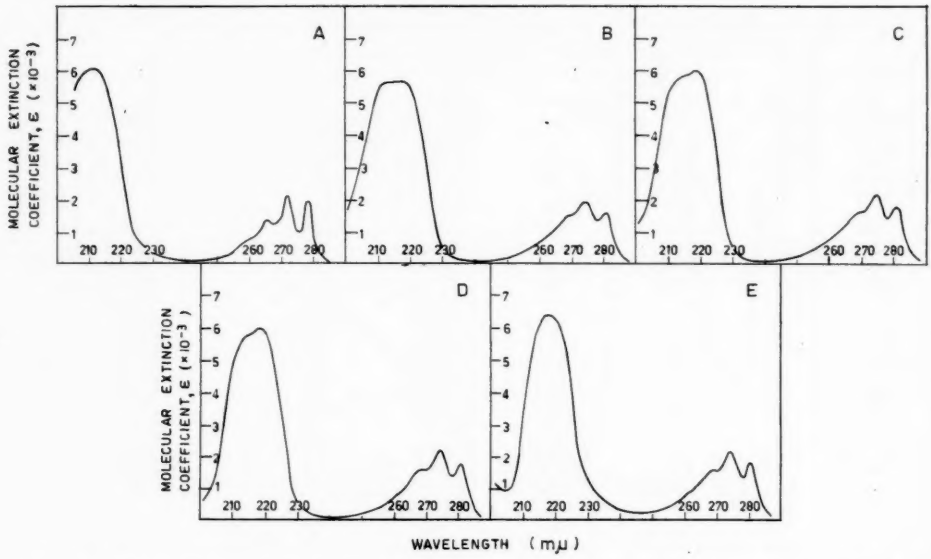

FIG. 6. The spectrum of phenol in (A) cyclohexane; (B) cyclohexane containing ca. 2% ether; (C) ether, cyclohexane volume ratio 1:9; (D) ether, cyclohexane volume ratio 1:3; and (E) ether.

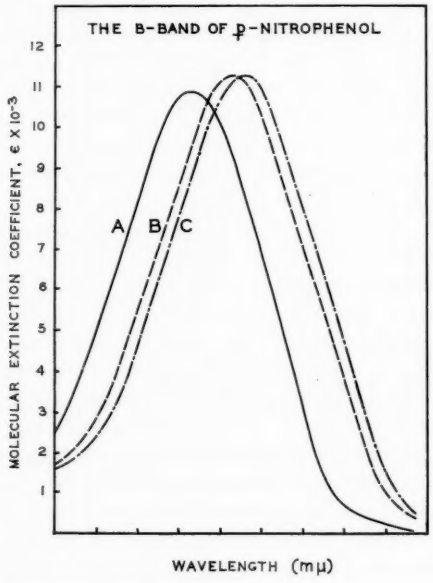

FIG. 7. The spectrum of *p*-nitrophenol in (A) cyclohexane solution (——); (B) cyclohexane solution containing ca. 1% ether (– – –); and (C) ether solution (— — — —).

SOLUTE-SOLVENT INTERACTIONS INVOLVING THE OXYGEN OR NITROGEN ATOMS OF PHENOLS AND ANILINES

Another spectral effect which may be caused by intermolecular hydrogen bonding is the observed hypsochromic wavelength displacement in the *B*-bands of aniline, N,N-dimethylaniline, phenol, and anisole on changing the solvent from cyclohexane or ethanol to water. A selection of the relevant data is listed in Table IV.

TABLE IV

Wavelength displacements ($\Delta\lambda$ in mμ) between *B*-bands in cyclohexane (non-bonded species) and ethanol or aqueous solutions

Solute	λ_{max}(mμ) (in cyclohexane)	ϵ_{max}	λ_{max}(mμ) (in ethanol)	ϵ_{max}	$\Delta\lambda$ relative to cyclohexane	λ_{max}(mμ) (in water)	ϵ_{max}	$\Delta\lambda$ relative to cyclohexane	Source
Aniline	234.5	9,000	235.5	8,000	1	231	8,000	−3.5	Ref. 9
N,N-Dimethylaniline	251	14,500	251	12,900	0	244	8,700	−7	Ref. 22
Phenol	210*	6,000	219	6,000	—	210	6,000	−9⊕	Ref. 12
Anisole	220	7,500	219.5	7,000	−0.5	217.5	4,300	2.5	Ref. 13
p-Aminoacetophenone	284	19,500§	319	20,000	35	311–312	16,500	27.5	Ref. 9
p-Hydroxyacetophone	258	12,600§	278	15,300	20	278	11,000	20	Ref. 23, †
p-Methoxyacetophenone	264	18,000	272	16,400‡	8				Ref. 13, †
p-Nitroaniline	322	14,600	371	15,500	49	380	13,000	58	Refs. 9, 25
p-Nitrophenol	286	10,800	314	13,000	28	317	9,300	31	Refs. 12, 24
p-Nitroanisole	294	12,100	305	13,000	11	316	10,500	22	Refs. 13, 24
p-Aminoanisole	237	9,100	234	9,000	−3				Ref. 13, †
p-Fluorophenol	210–211	4,200	216	3,800	5.5	207	4,500	−3.5	Ref. 12, †
p-Fluoroanisole	217	5,400	217	5,100	0	213	3,600	−4	Ref. 13, †
p-Chlorophenol	225	8,800	228	9,400	3	225	8,600	0	Ref. 12, †
p-Chloroanisole	228	11,700	228	11,200	0	226	9,000	−2	Ref. 13, †
p-Bromophenol	225	10,250	227	10,600	2	224	9,300	−1	Ref. 12, †
o-Bromoanisole	ca. *219* ca. *224*	*8,300* *7,400*	ca. *213.5* ca. *218* ca. *221*	*8,200* *7,900* *7,200*	ca. −2	ca. *213* ca. *219*	*7,600* *6,500*	ca. −5	Ref. 13, †

*This value is believed to be caused preferentially by transitions involving locally excited states and hence the absorption is considered anomalous (see ref. 12).

⊕Relative to ethanol.

†This paper.

‡W. G. Douben and J. W. Collette (J. Am. Chem. Soc. **81**, 967 (1959)) report an ϵ_{max} value of 6600 for this compound, but this ϵ value is almost certainly too low.

§Values in *n*-heptane (see ref. 23).

Table IV shows that definite wavelength displacements now occur also for the methyl analogues, anisole, and N,N-dimethylaniline, and hence the wavelength displacements cannot be caused exclusively by hydrogen-bonded structures of type I or II. The wavelength displacements in Table IV can, however, be associated—at least partly—with hydrogen-bonded structures of type IV and V, since structures of this type can be imagined to decrease the electronic interaction between the nitrogen or oxygen atoms and the benzene ring, and so cause the *hypsochromic* wavelength displacement (cf. 19,

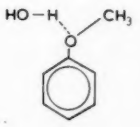

IV

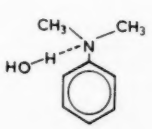

V

20, 22), and incidentally the frequently observed decreased absorption intensity in the ultraviolet region for spectra of this type in aqueous media.*

However, while the above is probably a contributing factor it is evidently not the sole contributing factor, since, for example, the previously mentioned interactions will also contribute to the observed spectral changes. Therefore, a variety of spectral changes would be expected and are, in fact, observed. For example, in the spectra of compounds like *p*-nitroanisole or *p*-nitrophenol, water or ethanol molecules can attach themselves to the nitro group and this presumably accounts partly for the observed *bathochromic* wavelength displacement between cyclohexane, ethanol, and aqueous solutions (see Table IV). Moreover, dipole–dipole interactions would also be expected to cause *bathochromic* wavelength displacements, which may again hide any *hypsochromic* wavelength displacement caused by the solute–solvent interaction under discussion, and hydrogen bonding involving the hydrogen atoms of a phenolic OH group would be expected to have a similar effect. Hence wavelength displacements appear to be of doubtful diagnostic value. It is, however, significant that for a number of compounds of this type a characteristic intensity decrease is observed if the spectra are determined in aqueous solution (see Table IV).

Next, the solvent changes in the spectra of phenol for solutions containing various ethanol–water solvent mixtures are shown in Fig. 8. Figure 8 indicates a gradual change

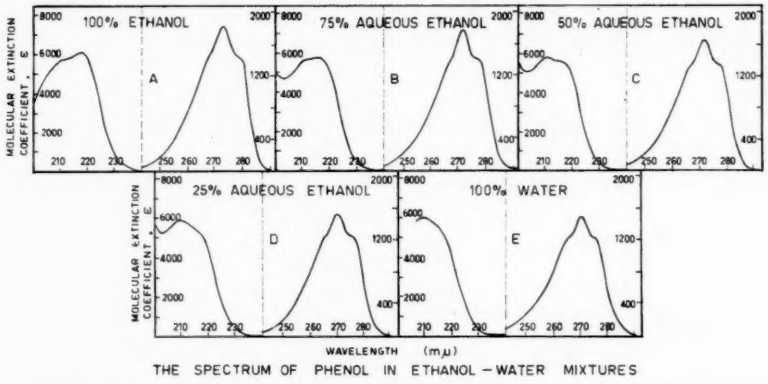

FIG. 8. The spectrum of phenol in (A) ethanol; (B) 75% aqueous ethanol; (C) 50% aqueous ethanol; (D) 25% aqueous ethanol; and (E) water.

in the spectrum of phenol on replacing ethanol by water as the solvent, and this suggests the absence of a stable predominating hydrogen bond between phenol and water. This follows because the spectral changes shown in Figs. 6 and 8 are different, and consequently the hydrogen bond between phenol and ether molecules probably differs from the solute–

More precisely, this decreased interaction between the π-electrons of the benzene ring and the p-electrons of the nitrogen or oxygen atom may be caused in two ways; either the hydrogen bond directly removes electrons from the nitrogen or oxygen atoms, or because the hydrogen-bonded structure increases the effective size of the oxygen- or nitrogen-substituted group and a consequent twisting of the group out of the plane of the benzene ring may cause the observed hypsochromic wavelength displacement. There is, in fact, some evidence for the operation of steric factors because steric interactions have previously been noted to be able to prevent the formation of intermolecular hydrogen bonding (cf. the discussion of the spectra of o-substituted phenols in ref. 12). Moreover, the postulate of steric interactions can be used to rationalize the greater effectiveness of the water molecule in forming this type of hydrogen bond, since a larger solvent molecule such as ethanol might be expected to have greater difficulty in approaching the oxygen or nitrogen atoms (see, for example, the spectra of N,N-dimethylaniline and anisole in Table IV).

solvent interaction involving the oxygen or nitrogen atoms in solutions of phenols or anilines. If phenol were to form a considerably stronger hydrogen bond with water than with ethanol it would be expected that only small quantities of water were necessary to produce a spectrum similar to the spectrum of phenol in water. A probable explanation of the above spectral changes is that *both* water and ethanol are continually forming and reforming hydrogen bonds with the phenol molecules (cf. ref. 1). According to this view the difference between the spectral changes in Fig. 6 and Fig. 8 can be explained because for solutions of phenol in cyclohexane–ether mixtures any hydrogen bonds competing with phenol–ether hydrogen bonds are likely to be insignificant, while for solutions of phenol in ethanol–water mixtures hydrogen bonds competing with phenol–water hydrogen bonds are probably important.

Apart from the wavelength displacements observed in Fig. 8 it may be noted that the change to the more polar solvent (water) decreases the fine structure of the phenolic *B*-band. A decreased fine structure in the *C*-band of phenol and anisole has previously (12, 13) been associated with hydrogen bonding or other solvent–solute interactions, and this view also receives support from the *B*-band of benzaldehydes (26) and of other compounds (27) where the characteristic fine structure is markedly decreased in the presence of ethanol or ether.

EXPERIMENTAL

The ultraviolet absorption spectra were determined by standard methods using a Unicam SP500 spectrophotometer. For each compound at least two independent sets of observations were made. The accuracy of λ_{max} values is estimated to be ± 1 mμ, and the precision of ϵ_{max} values $\pm 5\%$ or better. Values were reproducible in most cases to $\pm 2\%$. Vapor spectra were obtained by allowing specially designed 1-cm cells (Research and Industrial Instruments Co., Brixton, London, S.W.9, England) to remain in an atmosphere of the relevant compound until the optical density was within the permissible limits, and the cells were then sealed (see also footnote of Table I).

Some of the spectra have previously been described by other workers but whenever convenient the spectra were redetermined to ensure identical conditions for all the recorded spectra. The spectrum of *m*-iodobenzaldehyde was determined in both hexane and cyclohexane solution, and the determinations were found to be identical within experimental error.

The infrared spectra were determined on a Unicam SP100 instrument, using a NaCl prism.

The compounds under investigation were mostly commercial materials, purified by distillation or recrystallization until their boiling points and refractive indices or melting points showed them to be sufficiently pure. The solvents used were spectroanalyzed cyclohexane (Fisher), *n*-hexane specially prepared for spectroscopy (BDH), ethyl ether (Spectro Grade, Eastman), commercially available absolute ethanol suitable for spectroscopy, and freshly distilled water.

ACKNOWLEDGMENTS

The authors are greatly indebted to Miss N. Joan Smith for very competent technical assistance in the spectral determination of some of the compounds, and thanks are due to Mr. D. L. Coffen for determining the infrared spectra.

They also wish to thank the Fisheries Research Board of Canada for financial support, since part of this work was carried out under a contract between the Fisheries Research

Board of Canada and the Memorial University of Newfoundland. The authors further gratefully acknowledge the general assistance of the National Research Council in support of these studies.

REFERENCES

1. W. F. FORBES, A. R. KNIGHT, and D. L. COFFEN. Can. J. Chem **38**, 728 (1960); W. F. Forbes and A. R. Knight. **37**, 334 (1959).
2. V. VON KEUSSLER. Z. Elektrochem. **58**, 136 (1954).
3. M. ITO. J. Mol. Spectroscopy, **4**, 125 (1960).
4. C. M. HUGGINS, G. C. PIMENTEL, and J. N. SHOOLERY. J. Phys. Chem. **60**, 1311 (1956).
5. N. FUSON, M-L. JOSIEN, R. L. POWELL, and E. UTTERBACK. J. Chem. Phys. **20**, 145 (1952).
6. M. SAUNDERS and J. B. HYNE. J. Chem. Phys. **29**, 1319 (1958).
7. U. LIDDEL and E. D. BECKER. Spectrochim. Acta, **10**, 70 (1957).
8. W. C. COBURN JR. and E. GRUNWALD. J. Am. Chem. Soc. **80**, 1318 (1958).
9. W. F. FORBES and I. R. LECKIE. Can. J. Chem. **36**, 1371 (1958).
10. H. RICHTERING. Z. Phys. Chem. **9**, 393 (1956).
11. L. J. BELLAMY and R. L. WILLIAMS. Spectrochim. Acta, **9**, 341 (1957).
12. J. C. DEARDEN and W. F. FORBES. Can. J. Chem. **37**, 1294 (1959).
13. J. C. DEARDEN and W. F. FORBES. Can. J. Chem. **37**, 1305 (1959).
14. W. M. SCHUBERT, J. M. CRAVEN, and H. STEADLY. J. Am. Chem. Soc. **81**, 2696 (1959).
15. N. S. BAYLISS and E. G. MCRAE. J. Phys. Chem. **58**, 1002 (1954).
16. W. J. ORVILLE-THOMAS, A. E. PARSONS, and C. P. OGDEN. J. Chem. Soc. 1047 (1958).
17. C. G. CANNON. Spectrochim. Acta, **10**, 341 (1958).
18. U. LIDDEL and E. D. BECKER. J. Chem. Phys. **25**, 173 (1956).
19. T. MASAMUNE. J. Am. Chem. Soc. **79**, 4418 (1957).
20. S. NAGAKURA and H. BABA. J. Am. Chem. Soc. **74**, 5693 (1952).
21. J. W. SMITH and S. M. WALSHAW. J. Chem. Soc. 3217 (1957).
22. H. E. UNGNADE. J. Am. Chem. Soc. **75**, 432 (1953).
23. J. TANAKA, S. NAGAKURA, and M. KOBAYASHI. J. Chem. Phys. **24**, 311 (1956).
24. A. BURAWOY and J. T. CHAMBERLAIN. J. Chem. Soc. 2310 (1952).
25. C. J. TIMMONS. J. Chem. Soc. 2613 (1957).
26. J. C. DEARDEN and W. F. FORBES. Can. J. Chem. **36**, 1362 (1958).
27. J. DERKOSCH and W. KALTENEGGER. Monatsh. **88**, 778 (1957).

ALIPHATIC CHEMISTRY OF FLUORENE

PART III. SOME DERIVATIVES OF FLUORENE AND PHENANTHRENE[1]

P. M. G. Bavin

ABSTRACT

Methyl fluorene-9-carboxylate and 9-methyl-9-acetylfluorene have been nitrated and the products converted to 2-nitrophenanthrene and 2-nitro-9,10-dimethylphenanthrene, respectively.

Acetylation of 9,10-dimethylphenanthrene has given only one ketone, probably the 3-isomer. 4-Nitrofluorenone has been synthesized by a convenient route.

All five mononitrophenanthrenes have been synthesized (1) but only the 2-isomer is readily accessible (1, 2). Another closely related route to 2-nitrophenanthrene has now been found. Methyl 2-nitrofluorene-9-carboxylate (II), prepared by nitrating the ester (I), was reduced with lithium borohydride and the crude carbinol heated with polyphosphoric acid to give 2-nitrophenanthrene in 45% yield. In a similar way, 2-nitro-9,10-dimethylphenanthrene (VI) was prepared from 9-methyl-9-acetylfluorene (III) via the nitro-ketone (IV).

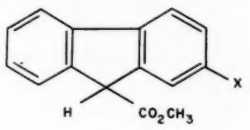

I, X = H
II, X = NO_2

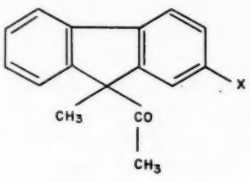

III, X = H
IV, X = NO_2

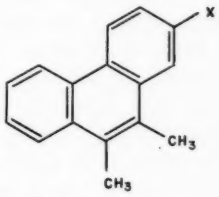

V, X = H
VI, X = NO_2
VII, X = NH_2
VIII, X = $NH \cdot CO \cdot CH_3$

During the isolation of the nitro-ester (II), it was noted that washing a chloroform solution of the nitration products with 2% sodium hydroxide solution resulted in the formation of a deep purple color, most easily observed by dissolving the pure nitro-ester in methanol containing sodium methoxide. Under the latter conditions, the color was rapidly discharged by methyl iodide with formation of what is considered to be the C-methyl derivative (IX) (cf. the alkylation of I (3)). The deep purple color was attributed to the anion (X) (cf. methyl fluorene-9-carboxylate anion (3)). These observations led directly to investigations of several aspects of the chemistry of fluorene (3, 4, 5) which are still in progress.

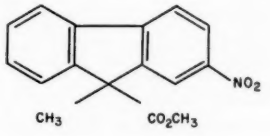

IX

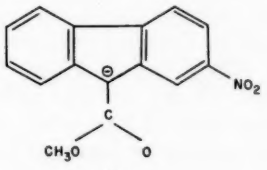

X

[1]*Manuscript received February 5, 1960.*
Contribution from the Chemistry Department, the University, Hull, East Yorkshire, England.

4-Nitrofluorenone (XIV) has been synthesized by the cyclization of the nitro-acid (XI) (cf. the acids XII and XIII which gave XV and XVI (6, 7)), but its conversion to 4-nitrofluorene, a desirable intermediate for the synthesis of the very inaccessible 4-nitrophenanthrene, was not achieved.

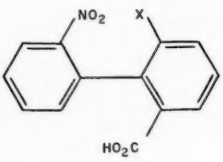

XI, X = H
XII, X = NO_2
XIII, X = CO_2H

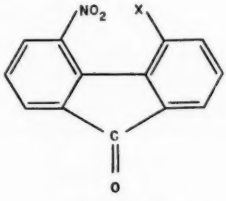

XIV, X = H
XV, X = NO_2
XVI, X = CO_2H

The use of methyl fluorene-9-carboxylate as a synthetic tool has made several otherwise inaccessible hydrocarbons readily available (3, 8). One of these, 9,10-dimethylphenanthrene, has now been acetylated. Under homogeneous conditions in nitrobenzene at room temperature, only one ketone was isolated in 75–85% yield after reaction times of either 12 hours or 14 days. Prolonged efforts to degrade the ketone to the amine or carboxylic acid have failed. Attempts to synthesize reference compounds other than the amine (VII) have been unsuccessful but are reported in the Experimental section. The orientation of the *x*-acetyl-9,10-dimethylphenanthrene remains unestablished, but it is probably the 3-isomer by analogy with the acetylation of phenanthrene (9, 10 but see also Gore (11)).

9,10-Dimethylphenanthrene has been oxidized by aqueous sodium dichromate at 250° to phenanthrene-9,10-dicarboxylic acid (94%), 2-methyltriphenylene yielding the corresponding acid in 98% yield.* This technique should prove of great value in the preparation of derivatives of polycyclic hydrocarbons.

EXPERIMENTAL

2-Nitrophenanthrene

Methyl fluorene-9-carboxylate (2 g) was nitrated as described for 9-fluorenylmethyl acetate (1). *Methyl 2-nitrofluorene-9-carboxylate* crystallized from xylene–pentane as pale yellow needles (0.8 g), m.p. 178–179°. Found: C, 67.0; H, 4.31; N, 5.21%. Calc. for $C_{15}H_{11}NO_4$: C, 66.91; H, 4.12; N, 5.20%. Less satisfactorily, 2-nitrofluorene-9-carboxylic acid (13) was esterified with methanolic hydrogen chloride.

The nitro-ester dissolved in methanol containing sodium methoxide to give a black solution, purple at high dilution. The color was rapidly discharged by methyl iodide with formation of *methyl 9-methyl-2-nitrofluorene-9-carboxylate*, pale yellow prisms from heptane, m.p. 122–123°. Found: C, 67.73; H, 4.19%. Calc. for $C_{16}H_{13}NO_4$: C, 67.84; H, 4.63%.

The nitro-ester (II) was reduced with lithium borohydride in tetrahydrofuran (14, 15) to give an orange resin. A part of the resin was acetylated with isopropenyl acetate (1) and the product purified by passing a hexane solution of it through a column of activated

**The author is indebted to Dr. D. Fishel of the State University of South Dakota for these experiments (12, p. 22P).*

alumina. The eluted material crystallized as pale yellow prisms (22%) from hexane, m.p. 123–125°, not depressed by authentic 2-nitro-9-fluorenylmethyl acetate (1).

The other part of the resin was heated with polyphosphoric acid as described for 9-fluorenylmethyl acetate (1) to give 2-nitrophenanthrene as yellow needles from heptane (45%), m.p. 118–119°, not depressed by an authentic sample (1). Oxidation with periodic acid in boiling acetic acid gave 2-nitrophenanthraquinone, orange plates from acetic acid, m.p. 270–272°, not depressed by an authentic specimen (16). Found: C, 65.79; H, 2.60%. Calc. for $C_{14}H_7NO_4$: C, 66.41; H, 2.79%.

2-Nitro-9,10-dimethylphenanthrene

Pure 9-methyl-9-acetylfluorene (8) was nitrated as described for 9-fluorenylmethyl acetate (1). *2-Nitro-9-methyl-9-acetylfluorene* (70%) formed pale yellow prisms from methanol, m.p. 136–138°, raised to 138–139° by two further crystallizations. Found: C, 71.99; H, 5.19%. Calc. for $C_{16}H_{13}NO_3$: C, 71.90; H, 4.90%.

The *carbinol*, obtained as an oil by reducing the nitro-ketone with methanolic sodium borohydride, was esterified with *p*-toluenesulphonyl chloride in pyridine (3). The crude *tosylate* was boiled under reflux for 12 hours with 94% formic acid, *2-nitro-9,10-dimethylphenanthrene* crystallizing on cooling. Purification by passing a hexane solution of it through a column of activated alumina and concentration of the eluant gave bright yellow needles (74% based on nitro-ketone), m.p. 163–164°. Found: C, 76.75; H, 5.31%. Calc. for $C_{16}H_{13}NO_2$: C, 76.47; H, 5.57%.

2-Amino-9,10-dimethylphenanthrene, prepared by reducing the nitro compound with hydrazine and palladized charcoal (17), crystallized as white needles from ethanol, m.p. 141–142°. The *N-acetyl* derivative crystallized from toluene as small white needles, m.p. 256–257°. A sample was sublimed at 220°/10^{-3} mm for analysis. Found: C, 82.16; H, 6.86%. Calc. for $C_{18}H_{17}NO$: C, 82.10; H, 6.51%.

4-Nitrofluorenone

2′-Nitrodiphenyl-2-carboxylic acid (18) (1.2 g) was maintained for 20 minutes at 115° with concentrated sulphuric acid (40 ml). Pouring onto ice precipitated a yellow solid, which crystallized from methanol (Norite) as long yellow needles (0.98 g), m.p. 173–174° (lit. m.p. 173–174° (19)).

9,10-Dimethylphenanthrene

Crude 9-acetylfluorene (20) (1 mole) was methylated with methyl iodide (2.1 moles) in methanol containing sodium methoxide (2 moles), the reaction being complete after 6 hours at room temperature. The crude ketone (96%, m.p. 82–84°) (lit. m.p. 85–86° (8)) was reduced with ethereal lithium aluminum hydride to 1′-(9-methyl-9-fluorenyl)-ethanol (98%, m.p. 77–80°) (lit. m.p. 81° (8)). The *tosylate*, prepared in the usual way (3), formed colorless prisms from chloroform–hexane, m.p. 88–90° with decomposition to 9,10-dimethylphenanthrene. Found: S, 8.62%. Calc. for $C_{23}H_{22}O_3S$: S, 8.47%.

9,10-Dimethylphenanthrene was prepared either by boiling the crude tosylate with 94% formic acid, or by boiling the carbinol with its own weight of phosphorus pentoxide in xylene for 2 hours. It formed long white needles (85–91%) from toluene–hexane, m.p. 143–144° (lit. m.p. 143–144° (8)).

Phenanthrene-9,10-dicarboxylic acid

9,10-Dimethylphenanthrene was oxidized by aqueous sodium dichromate solution at 250° (12), giving crude phenanthrene-9,10-dicarboxylic acid in 94% yield. The anhydride

4-Nitrofluorenone (XIV) has been synthesized by the cyclization of the nitro-acid (XI) (cf. the acids XII and XIII which gave XV and XVI (6, 7)), but its conversion to 4-nitrofluorene, a desirable intermediate for the synthesis of the very inaccessible 4-nitrophenanthrene, was not achieved.

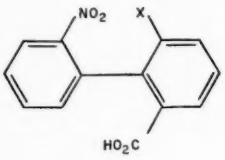

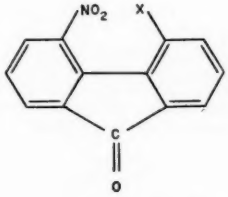

XI, X = H
XII, X = NO_2
XIII, X = CO_2H

XIV, X = H
XV, X = NO_2
XVI, X = CO_2H

The use of methyl fluorene-9-carboxylate as a synthetic tool has made several otherwise inaccessible hydrocarbons readily available (3, 8). One of these, 9,10-dimethylphenanthrene, has now been acetylated. Under homogeneous conditions in nitrobenzene at room temperature, only one ketone was isolated in 75–85% yield after reaction times of either 12 hours or 14 days. Prolonged efforts to degrade the ketone to the amine or carboxylic acid have failed. Attempts to synthesize reference compounds other than the amine (VII) have been unsuccessful but are reported in the Experimental section. The orientation of the *x*-acetyl-9,10-dimethylphenanthrene remains unestablished, but it is probably the 3-isomer by analogy with the acetylation of phenanthrene (9, 10 but see also Gore (11)).

9,10-Dimethylphenanthrene has been oxidized by aqueous sodium dichromate at 250° to phenanthrene-9,10-dicarboxylic acid (94%), 2-methyltriphenylene yielding the corresponding acid in 98% yield.* This technique should prove of great value in the preparation of derivatives of polycyclic hydrocarbons.

EXPERIMENTAL

2-Nitrophenanthrene

Methyl fluorene-9-carboxylate (2 g) was nitrated as described for 9-fluorenylmethyl acetate (1). *Methyl 2-nitrofluorene-9-carboxylate* crystallized from xylene–pentane as pale yellow needles (0.8 g), m.p. 178–179°. Found: C, 67.0; H, 4.31; N, 5.21%. Calc. for $C_{15}H_{11}NO_4$: C, 66.91; H, 4.12; N, 5.20%. Less satisfactorily, 2-nitrofluorene-9-carboxylic acid (13) was esterified with methanolic hydrogen chloride.

The nitro-ester dissolved in methanol containing sodium methoxide to give a black solution, purple at high dilution. The color was rapidly discharged by methyl iodide with formation of *methyl 9-methyl-2-nitrofluorene-9-carboxylate*, pale yellow prisms from heptane, m.p. 122–123°. Found: C, 67.73; H, 4.19%. Calc. for $C_{16}H_{13}NO_4$: C, 67.84; H, 4.63%.

The nitro-ester (II) was reduced with lithium borohydride in tetrahydrofuran (14, 15) to give an orange resin. A part of the resin was acetylated with isopropenyl acetate (1) and the product purified by passing a hexane solution of it through a column of activated

**The author is indebted to Dr. D. Fishel of the State University of South Dakota for these experiments (12, p. 22P).*

alumina. The eluted material crystallized as pale yellow prisms (22%) from hexane, m.p. 123–125°, not depressed by authentic 2-nitro-9-fluorenylmethyl acetate (1).

The other part of the resin was heated with polyphosphoric acid as described for 9-fluorenylmethyl acetate (1) to give 2-nitrophenanthrene as yellow needles from heptane (45%), m.p. 118–119°, not depressed by an authentic sample (1). Oxidation with periodic acid in boiling acetic acid gave 2-nitrophenanthraquinone, orange plates from acetic acid, m.p. 270–272°, not depressed by an authentic specimen (16). Found: C, 65.79; H, 2.60%. Calc. for $C_{14}H_7NO_4$: C, 66.41; H, 2.79%.

2-Nitro-9,10-dimethylphenanthrene

Pure 9-methyl-9-acetylfluorene (8) was nitrated as described for 9-fluorenylmethyl acetate (1). *2-Nitro-9-methyl-9-acetylfluorene* (70%) formed pale yellow prisms from methanol, m.p. 136–138°, raised to 138–139° by two further crystallizations. Found: C, 71.99; H, 5.19%. Calc. for $C_{16}H_{13}NO_3$: C, 71.90; H, 4.90%.

The *carbinol*, obtained as an oil by reducing the nitro-ketone with methanolic sodium borohydride, was esterified with *p*-toluenesulphonyl chloride in pyridine (3). The crude *tosylate* was boiled under reflux for 12 hours with 94% formic acid, *2-nitro-9,10-dimethylphenanthrene* crystallizing on cooling. Purification by passing a hexane solution of it through a column of activated alumina and concentration of the eluant gave bright yellow needles (74% based on nitro-ketone), m.p. 163–164°. Found: C, 76.75; H, 5.31%. Calc. for $C_{16}H_{13}NO_2$: C, 76.47; H, 5.57%.

2-Amino-9,10-dimethylphenanthrene, prepared by reducing the nitro compound with hydrazine and palladized charcoal (17), crystallized as white needles from ethanol, m.p. 141–142°. The *N-acetyl* derivative crystallized from toluene as small white needles, m.p. 256–257°. A sample was sublimed at 220°/10^{-3} mm for analysis. Found: C, 82.16; H, 6.86%. Calc. for $C_{18}H_{17}NO$: C, 82.10; H, 6.51%.

4-Nitrofluorenone

2′-Nitrodiphenyl-2-carboxylic acid (18) (1.2 g) was maintained for 20 minutes at 115° with concentrated sulphuric acid (40 ml). Pouring onto ice precipitated a yellow solid, which crystallized from methanol (Norite) as long yellow needles (0.98 g), m.p. 173–174° (lit. m.p. 173–174° (19)).

9,10-Dimethylphenanthrene

Crude 9-acetylfluorene (20) (1 mole) was methylated with methyl iodide (2.1 moles) in methanol containing sodium methoxide (2 moles), the reaction being complete after 6 hours at room temperature. The crude ketone (96%, m.p. 82–84°) (lit. m.p. 85–86° (8)) was reduced with ethereal lithium aluminum hydride to 1′-(9-methyl-9-fluorenyl)-ethanol (98%, m.p. 77–80°) (lit. m.p. 81° (8)). The *tosylate*, prepared in the usual way (3), formed colorless prisms from chloroform–hexane, m.p. 88–90° with decomposition to 9,10-dimethylphenanthrene. Found: S, 8.62%. Calc. for $C_{23}H_{22}O_3S$: S, 8.47%.

9,10-Dimethylphenanthrene was prepared either by boiling the crude tosylate with 94% formic acid, or by boiling the carbinol with its own weight of phosphorus pentoxide in xylene for 2 hours. It formed long white needles (85–91%) from toluene–hexane, m.p. 143–144° (lit. m.p. 143–144° (8)).

Phenanthrene-9,10-dicarboxylic acid

9,10-Dimethylphenanthrene was oxidized by aqueous sodium dichromate solution at 250° (12), giving crude phenanthrene-9,10-dicarboxylic acid in 94% yield. The anhydride

crystallized from acetic anhydride as pale yellow needles, m.p. 322–324°, not depressed by an authentic specimen (21).* The dimethyl ester formed pale yellow needles from benzene, m.p. 132–133° (lit. m.p. 131° (21)).

Triphenylene-2-carboxylic Acid

2-Methyltriphenylene (22), oxidized as above, gave triphenylene-2-carboxylic acid in 98% yield. The methyl ester crystallized as colorless needles from toluene, m.p. 129–130°. Found: C, 83.81, 84.01; H, 5.26, 5.34%. Calc. for $C_{20}H_{14}O_2$; C, 83.90; H, 4.93% (lit. m.p. 122–124° (23)).

x-Acetyl-9,10-dimethylphenanthrene

Anhydrous aluminum chloride (43 g, 2.2 moles) was dissolved in dry nitrobenzene (150 ml) and the solution cooled to 0°. 9,10-Dimethylphenanthrene (29.8 g, 1 mole) was added, followed by freshly distilled acetyl chloride (16 g, 1.4 moles). The mixture was left at room temperature for 14 days with exclusion of moisture. The complex was decomposed with ice and hydrochloric acid and the nitrobenzene removed by distillation with steam. Distillation of the residue at 1–2 mm gave the ketone as an almost colorless oil, which soon crystallized. One crystallization from acetone–methanol gave very pale yellow prisms (26 g, 73%), m.p. 108–110°. Fractional crystallization gave a further 4.5 g of ketone of the same melting point. A second ketone was not found.

The first crop of ketone was recrystallized once from methanol–acetone and twice from toluene–heptane to give colorless prisms (20 g, 56%), m.p. 111.5–112°. This melting point was not raised by further crystallizations. Found: C, 86.94; H, 6.55%. Calc. for $C_{18}H_{16}O$: C, 87.06; H, 6.50%.

The *oxime*, prepared in pyridine–ethanol, crystallized as white needles from toluene–heptane, m.p. 209–210°. OH stretching band (CS_2 solution) 3586 cm^{-1}. Found: C, 82.13; H, 6.65%. Calc. for $C_{18}H_{17}NO$: C, 82.11; H, 6.51%.

The *azine*, prepared by warming the ketone with hydrazine in ethanol, separated from xylene as golden-yellow plates, m.p. 280–281°. Found: C, 87.82; H, 6.41; N, 5.80%. Calc. for $C_{36}H_{32}N_2$: C, 87.77; H, 6.55; N, 5.69%.

x-Ethyl-9,10-dimethylphenanthrene was prepared by boiling the ketone (1 g) under reflux for 6 hours with hydrazine hydrate (10 ml) and diethylene glycol (100 ml). The purified hydrocarbon, obtained by passing a hexane solution of it through a column of activated alumina, crystallized from methanol as long white needles, m.p. 45.5–46°. Found: C, 92.32; H, 5.72%. Calc. for $C_{18}H_{18}$: C, 92.26; H, 5.74%. The 1,3,5-trinitrobenzene complex crystallized from methanol as bright yellow needles, m.p. 164–166°.

Numerous attempts to oxidize the ketone using aqueous sodium hypochlorite and pyridine or dioxane as diluent gave tars and only traces of acidic material. Reaction with sodium azide in acetic acid (24) also failed to yield useful products.

Reaction between the pure oxime and phosphorus pentachloride – benzene, hydrogen chloride – acetic acid or polyphosphoric acid gave uniformly low yields of mixtures, from which traces of an amine were obtained by hydrolysis with ethanolic hydrogen chloride. The amine rapidly turned red in air, behavior similar to that of 3-aminophenanthrene, and had an infrared spectrum markedly different from that of 2-amino-9,10-dimethylphenanthrene.

3-Ethylphenanthrene-9-carboxylic acid

3-Acetyl-9-bromophenanthrene (55 g, m.p. 151–153°) (lit. m.p. 150–151° (25)) was

*The author is indebted to I. Ungar of the Battelle Memorial Institute for this sample.

boiled under reflux for 4 hours with cuprous cyanide (20 g) and dimethylformamide (150 ml) containing 2 drops of pyridine. After cooling, the mixture was poured into concentrated aqueous ammonia and the precipitated solid crystallized from toluene, 3-acetyl-9-cyanophenanthrene (50 g) separating as yellow needles, m.p. 226–227° (lit. m.p. 220–221° (25)).

The nitrile (49 g) was boiled under reflux with hydrazine hydrate (40 ml) and diethylene glycol (300 ml). After 1 hour a solution of potassium hydroxide (40 g) in water (60 ml) was added dropwise. The mixture was distilled until a distillate temperature of 195° was reached. After a further 4 hours, the mixture was cooled and poured into excess dilute hydrochloric acid. The *acid* was collected, washed, and dissolved in 5% aqueous potassium carbonate solution and the solution filtered into dilute hydrochloric acid. The purified acid was dried and converted to the methyl ester by successive reactions with thionyl chloride and methanol. After distillation at 200–210° and 1–2 mm, the colorless ester was saponified, giving the acid as an oil which crystallized during several days. The yield was 20 g. Two crystallizations from methanol–acetone gave almost colorless needles, m.p. 180–182°, with previous sintering. Found: C, 82.30, 82.20; H, 5.57, 5.68%. Calc. for $C_{17}H_{14}O_2$: C, 81.58; H, 5.64%.

3-Ethyl-9,10-phenanthraquinone

3-Acetylphenanthrene (9) was reduced to 3-ethylphenanthrene using hydrazine and diethylene glycol. The hydrocarbon, which has not been obtained crystalline (26), was distilled and purified through the picrate, which crystallized from methanol as orange needles, m.p. 120–121°. Oxidation with chromic oxide in acetic acid gave 3-ethylphenanthraquinone, slender orange needles from ethanol, m.p. 173–174° (lit. m.p. 168–170° (26)). Heating the quinone with potassium hydroxide in water or aqueous alcohol gave tars and only traces of acidic material.

3-Methylfluorene

Benzyl *p*-tolyl ketone (218 g, 55%) was prepared from phenylacetyl chloride (2 moles) and toluene, as described for benzyl phenyl ketone (27, p. 156). It formed plates from methanol, m.p. 109–110° (lit. m.p. 110–110.5° (28)). Found: C, 85.57; H, 6.88%. Calc. for $C_{15}H_{14}O$: C, 85.68; H, 6.71%. The *2,4-dinitrophenylhydrazone* formed irregular red prisms from benzene, m.p. 213–214°. Found: C, 64.45; H, 4.47%. Calc. for $C_{21}H_{18}N_4O_4$: C, 64.60; H, 4.65%.

The preceding desoxybenzoin was converted to 4-methylbenzoin* by a general procedure (29, p. 296) involving successively photobromination, reaction with sodium ethoxide, and hydrolysis with dilute hydrochloric acid. It crystallized from aqueous ethanol as long colorless needles (65%), m.p. 112–113° (lit. m.p. 110° (30)). Found: C, 79.81; H, 6.39%. Calc. for $C_{15}H_{14}O_2$: C, 79.62; H, 6.24%.

Oxidation of the benzoin with cupric sulphate and pyridine (31, p. 715) gave 4-methylbenzil as a yellow oil, which largely crystallized after distillation (lit. m.p. 31° (32)). Conversion to 4-methylbenzilic acid proceeded in high yield (31, p. 715), but the acid proved remarkably difficult to crystallize. The yield of white needles from chloroform–hexane, m.p. 132–134°, was only 41% (lit. m.p. 132° (32)).

Cyclization of the benzilic acid has already been reported (34) but proceeds in higher yield by a more recent procedure (33). The crude dried 3-methylfluorene-9-carboxylic acid was decarboxylated by distillation at 1 mm, giving 3-methylfluorene in 43% yield

**Primes (') are used for substituents on the ring adjacent to the carbinol group.*

based on the benzilic acid. It crystallized from methanol as colorless plates, m.p. 87–88° (lit. m.p. 88° (34)).

Prepared similarly, *benzyl p-ethylphenyl ketone* (71%) crystallized as lustrous colorless plates from methanol, m.p. 62–64°. Found: C, 85.41; H, 7.02%. Calc. for $C_{16}H_{16}O$: C, 85.67; H, 7.19%. The *2,4-dinitrophenylhydrazone* formed iridescent vermilion scales from benzene, m.p. 186–187°. Found: C, 65.10; H, 5.48%. Calc. for $C_{22}H_{20}N_4O_4$: C, 65.01; H, 5.48%.

4-Ethylbenzoin formed clusters of needles from heptane, m.p. 89–90°. Found: C, 79.91; H, 6.44%. Calc. for $C_{16}H_{16}O_2$: C, 79.97; H, 6.71%. 4-Ethylbenzil and 4-ethylbenzilic acid have failed to crystallize and have not been characterized.

ACKNOWLEDGMENTS

This work has been carried out during the tenure of a National Research Council of Canada Postdoctoral Fellowship (University of Ottawa, 1954–1956) and an I.C.I. Fellowship (the University, Hull, 1958–1960).

REFERENCES

1. P. M. G. Bavin and M. J. S. Dewar. J. Chem. Soc. 4477 (1955).
2. J. D. Loudon, A. D. B. Sloan, and L. A. Summers. J. Chem. Soc. 3814 (1957).
3. F. A. L. Anet and P. M. G. Bavin. Can. J. Chem. **34**, 991 (1956).
4. F. A. L. Anet and P. M. G. Bavin. Can. J. Chem. **36**, 763 (1958).
5. P. M. G. Bavin. Can. J. Chem. **37**, 2023 (1959).
6. F. E. Ray and W. C. Francis. J. Org. Chem. **8**, 52 (1943).
7. C. Angelini. Ann. chim. (Rome), **43**, 247 (1953).
8. E. J. Greenhow, D. McNeil, and E. N. White. J. Chem. Soc. 986 (1952).
9. E. Mosettig and J. van de Kamp. J. Am. Chem. Soc. **52**, 3704 (1930).
10. P. M. G. Bavin and M. J. S. Dewar. J. Chem. Soc. 164 (1956).
11. P. H. Gore. Chem. Revs. **55**, 229 (1955).
12. H. Shechter, D. Fishel, and L. Friedman. Abstracts of Papers, 136th Meeting of the American Chemical Society, Atlantic City, N.J. September, 1959.
13. F. L. Rose. J. Chem. Soc. 2360 (1932).
14. R. Paul and N. Joseph. Bull. soc. chim. France, 758 (1953).
15. J. Kollonitsch, O. Fuchs, and V. Gábor. Nature, **173**, 125 (1954).
16. A. J. Nunn, K. Schofield, and R. S. Theobald. J. Chem. Soc. 2797 (1952).
17. P. M. G. Bavin. Can. J. Chem. **36**, 238 (1958).
18. R. G. Shuttleworth, W. S. Rapson, and E. T. Stewart. J. Chem. Soc. **72** (1944).
19. C. Courtot. Ann. chim. (Paris), **14**, (10), 5 (1930).
20. J. Von and E. C. Wagner. J. Org. Chem. **9**, 162 (1944).
21. A. Jeannes and R. Adams. J. Am. Chem. Soc. **59**, 2608 (1937).
22. W. S. Rapson. J. Chem. Soc. 15 (1941).
23. J. W. Cook and C. L. Hewett. J. Chem. Soc. 401 (1933).
24. J. R. Dice and P. A. S. Smith. J. Org. Chem. **14**, 181 (1949).
25. J. Schultz, M. A. Goldberg, E. P. Ordas, and G. Carsch. J. Org. Chem. **11**, 309 (1946).
26. R. A. Barnes and R. T. Gottesman. J. Am. Chem. Soc. **74**, 35 (1952).
27. C. F. H. Allen and W. E. Barker. *In* Organic syntheses. Collective Vol. II. John Wiley and Sons, New York. 1943. p. 156.
28. K. Isimura. Bull. Chem. Soc. Japan, **16**, 196 (1941).
29. W. S. Ide and J. S. Buck. Organic reactions. Vol. IV. John Wiley and Sons, New York. 1948. p. 296.
30. R. T. Arnold and R. C. Fuson. J. Am. Chem. Soc. **58**, 1295 (1936).
31. A. I. Vogel. A text-book of practical organic chemistry. Longmans, Green and Co., London. 1957. p. 715.
32. H. H. Hatt, A. Pilgrim, and W. J. Hurran. J. Chem. Soc. 93 (1936).
33. H. J. Richter. Org. Syntheses, **33**, 37 (1953).
34. D. Vörlander and C. Pritzsche. Ber. **46**, 1793 (1913).

ALIPHATIC CHEMISTRY OF FLUORENE

PART IV. PREPARATION AND ALKYLATION OF SOME SULPHIDES AND SULPHONES[1]

P. M. G. BAVIN[2]

ABSTRACT

The preparations are described of some 9-fluorenyl sulphides which have been oxidized with peracetic acid to the corresponding sulphones.

9-Fluorenyl *p*-tolyl sulphone has been alkylated with a range of alkyl halides; other sulphones, including 2-nitro-9-fluorenyl *p*-tolyl sulphone, have been methylated.

Methyl fluorene-9-carboxylate anion was reduced by *p*-toluenesulphonyl chloride to dimethyl 9,9′-difluorenyl-9,9′-dicarboxylate.

The acidity of methylene hydrogen activated by the sulphone group has been known for some time, but opinions have been divided on the reasons. Recent studies by Doering and his co-workers (1, 2, 3) have established that anions of type I are resonance stabilized by overlap between carbon 2*p* and sulphur 3*d* orbitals. The spectroscopic studies of Fehnel and Carmack (4) lend strong support to these conclusions. The latter workers found no evidence for the formation of anions from methylene activated only by a sulphone group, but Grignard derivatives of dialkyl sulphones (5, 6) and aralkyl sulphones (7, where references are given to prior publications) are well known. Field, Holsten, and Clark (7) have recently examined some reactions of phenylsulphonylmethyl magnesium bromide (II) and shown that it was alkylated in modest yield by benzyl chloride and

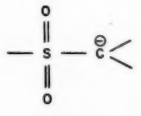

I

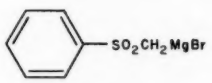

II

hexyl *p*-toluenesulphonate, in low yield by benzhydryl chloride, and not at all by *t*-butyl chloride and hexyl iodide, results which prompted its formulation as a weakly nucleophilic Grignard reagent rather than as a carbanion salt.

Nitrobenzyl sulphones are more acidic than the unsubstituted sulphones, and 2,4-dinitrobenzyl *p*-tolyl sulphone (III) has been methylated (8) using potassium ethoxide as base. The only simple sulphone to have been alkylated under comparable conditions is ethyl 9-fluorenyl sulphone (IV) (9).

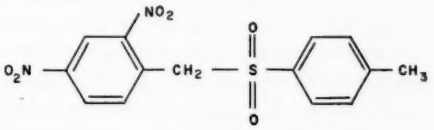

III

The remarkable facility with which methyl fluorene-9-carboxylate anion reacts with a wide range of alkyl halides (10, 11, 12) has prompted an examination of other 9-substituted fluorenes. Some experiments with 9-benzoylfluorene have already been reported (13). The present paper describes the alkylation of 9-fluorenyl *p*-tolyl sulphone (VII),

[1]*Manuscript received February 5, 1960.*
Contribution from the Chemistry Department, the University, Hull, East Yorkshire, England.
[2]*I.C.I. Fellow.*

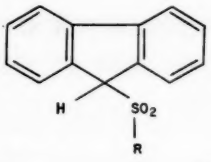

IV, R = CH_3CH_2 VI, R = C_6H_5

V, R = CH_3 VII, R = p-$CH_3 \cdot C_6H_4$

prompted by the work on ethyl 9-fluorenyl sulphone mentioned above (9), together with miscellaneous experiments on related systems.

9-Fluorenyl *p*-tolyl sulphone dissolved in warm ethanol containing sodium ethoxide with formation of a yellow solution. Under similar conditions 2-nitro-9-fluorenyl *p*-tolyl sulphone gave a purple-brown solution, similar to those reported for methyl 2-nitrofluorene-9-carboxylate (14) and 2,4-dinitrobenzyl *p*-tolyl sulphone (8). These solutions undoubtedly contained the organic anions and, in confirmation of this, 9-methyl-, -ethyl-, -isopropyl-, -allyl-, -benzyl-, and -cyclohexyl-9-fluorenyl *p*-tolyl sulphones (VIII,

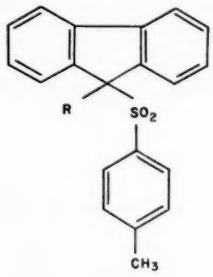

VIII

R = alkyl) were prepared by reaction with appropriate alkyl halides. In a similar manner were prepared 9-methyl-2-nitro-9-fluorenyl *p*-tolyl sulphone, 9-methyl-9-fluorenyl phenyl sulphone, and the methyl and isopropyl derivatives of 9-fluorenyl methyl sulphone. Comparison of these results with those reported for phenylsulphonylmethyl magnesium bromide (7) shows that anions of the type X are powerful nucleophiles which behave as true anion metal salts.

Fluorene has not been alkylated using ethanolic sodium ethoxide as base, so the reactions described above establish that fluorene anion is stabilized by a sulphone group. Although the anions derived from 9-fluorenyl *p*-tolyl sulphone, methyl fluorene-9-carboxylate, and 9-benzoylfluorene show many similar reactions, there are important differences. The sulphone (VII) was recovered unchanged after attempted bromination in acetic acid in the presence of sodium acetate, conditions which gave good yields of methyl 9-bromofluorene-9-carboxylate (11). From the reaction between *t*-butyl chloride and the anion of VII, only unreacted sulphone (30%) was isolated in a pure state. However, examination of the infrared spectrum of the crude product showed the presence of one or more additional compounds, with bands in the positions reported (15) for the *t*-butyl group (cf. methyl 9-*t*-butylfluorene-9-carboxylate (11)). Prolonged reaction times

led to the formation of fluorenone, probably by anionic oxidation (16). It follows that the ester anion (IX) is more nucleophilic than the sulphone anion (X), differences in their behavior towards *t*-butyl chloride being of degree rather than kind.

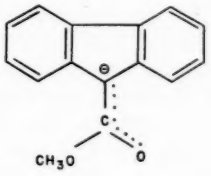

IX

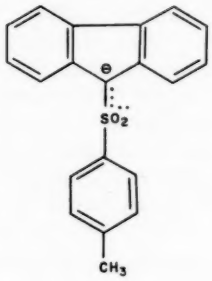

X

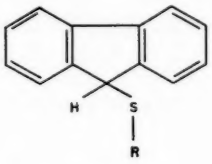

XI, R = CH_3
XII, R = C_6H_5
XIII, R = *p*-$CH_3C_6H_4$

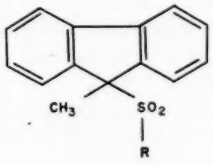

XIV, R = CH_3
XV, R = C_6H_5
XVI, R = *p*-$CH_3C_6H_4$

The sulphides (XI, XII, and XIII) have been prepared, the first from 9-fluorenylmercaptan and the others from thiophenol and thio-*p*-cresol, respectively. Methylation with ethereal methyl lithium – methyl iodide (cf. fluorene (17)) gave the tertiary sulphides (XIV, XV, and XVI), the mild conditions employed precluding the rearrangement observed for some 9-fluorenyl ethers (18). All six sulphides were oxidized with peracetic acid to the corresponding sulphones, confirming the structures of the methylation products of sulphones (V, VI, and VII). Attempts were made to oxidize 9-fluorenyl *p*-tolyl sulphide to the sulphoxide but mixtures were always obtained, consisting of the desired sulphoxide together with the sulphone and fluorenone, as shown by infrared spectra.

9-Methyl-9-fluorenyl *p*-tolyl sulphone was not cleaved by sodium piperidide (19, 20), although 9-methylfluorene was slowly formed by reaction with caustic soda in boiling diethylene glycol (cf. 21).

Characteristic sulphone bands have been recorded for the compounds reported in this paper but, being more complex than those reported for other sulphones (15), are being discussed elsewhere (22).

Although keto-esters have been prepared from fluorene-ester anion with acetyl (10) and benzoyl (28) chlorides, the similar reaction with *p*-toluenesulphonyl chloride gave dimethyl 9,9′-difluorenyl-9,9′-dicarboxylate by reductive dimerization of the anion.

EXPERIMENTAL

Sulphides

9-Fluorenylmercaptan (9) was prepared from 9-bromofluorene (23) via the thiouronium salt. Methylation with methyl iodide – methanolic sodium methoxide gave *9-fluorenyl methyl sulphide*, which crystallized from methanol as large colorless blades (77%), m.p. 47–48°. Found: C, 79.42; H, 5.92%. Calc. for $C_{14}H_{12}S$: C, 79.20; H, 5.65%.

9-Fluorenyl phenyl sulphide was prepared by warming 9-bromofluorene (1 mole) and thiophenol (1.1 moles) with methanol containing sodium methoxide (1 mole).* The reaction was complete in 10 minutes. The product crystallized as blades (69%) from methanol, m.p. 48–49°. Found: C, 83.10; H, 4.97%. Calc. for $C_{19}H_{14}S$: C, 83.17; H, 5.14%.

Prepared in a similar way, *9-fluorenyl p-tolyl sulphide* formed laths or dense prisms from ethanol (88%), m.p. 85–86°. Found: C, 83.20; H, 5.43%. Calc. for $C_{20}H_{16}S$: C, 83.29; H, 5.59%.

The foregoing sulphides were methylated with ethereal methyl lithium – methyl iodide, as described for fluorene (17), giving the following:

Methyl 9-methyl-9-fluorenyl sulphide crystallized as rhombohedral plates from methanol (71%), m.p. 63–65°. Found: C, 79.47; H, 6.19%. Calc. for $C_{15}H_{14}S$: C, 79.60; H, 6.23%.

9-Methyl-9-fluorenyl phenyl sulphide formed colorless needles from ethanol after cooling to and keeping at 0° (65%), m.p. 39.5–41.5°. Found: C, 83.30; H, 5.49%. Calc. for $C_{20}H_{16}S$: C, 83.26; H, 5.59%.

9-Methyl-9-fluorenyl p-tolyl sulphide formed well-defined prisms from acetone–methanol, m.p. 72–73° (82%). Found: C, 83.08; H, 5.83%. Calc. for $C_{21}H_{18}S$: C, 83.40; H, 5.60%.

Sulphones

The six sulphides described in the preceding section were oxidized with 50% hydrogen peroxide (1 volume) in acetic acid (3 volumes). The reactions, which were exothermic, were complete in a few minutes at 50°. Yields varied from 72 to 88% (24, 25).

9-Fluorenyl methyl sulphone formed long white needles from methanol or acetic acid, m.p. 188–189°. Found: C, 68.76; H, 5.09%. Calc. for $C_{14}H_{12}O_2S$: C, 68.87; H, 4.95%.

Methyl 9-methyl-9-fluorenyl sulphone crystallized from hexane as colorless prisms or needles, m.p. 136–137°. Found: C, 69.85; H, 5.77%. Calc. for $C_{15}H_{14}O_2S$: C, 69.74; H, 5.46%.

9-Fluorenyl phenyl sulphone formed colorless prisms from acetone–heptane, m.p. 182–183°. Found: C, 74.34; H, 4.45%. Calc. for $C_{19}H_{14}O_2S$: C, 74.48; H, 4.61%.

9-Methyl-9-fluorenyl phenyl sulphone crystallized as plates from ethanol, m.p. 165–167°. Found: C, 74.30; H, 4.94%. Calc. for $C_{20}H_{16}O_2S$: C, 74.97; H, 5.03%.

9-Fluorenyl p-tolyl sulphone crystallized as plates from benzene, m.p. 226–228°, identical with an authentic sample (21).

9-Methyl-9-fluorenyl p-tolyl sulphone formed colorless prisms from benzene–heptane, m.p. 151–152°. Found: C, 75.34; H, 5.26%. Calc. for $C_{21}H_{18}O_2S$: C, 75.42; H, 5.42%.

Attempts to oxidize 9-fluorenyl *p*-tolyl sulphide to the sulphoxide by standard techniques (25, 26) gave mixtures, not resolved by chromatography.

9-Fluorenyl *p*-tolyl sulphone, used in the alkylation experiments described below, was obtained from the reaction between 9-bromofluorene and sodium *p*-toluenesulphinate (21, 29). Prepared similarly, *2-nitro-9-fluorenyl p-tolyl sulphone* (from 9-bromo-2-nitrofluorene (27)) formed almost colorless plates from benzene, m.p. 217–219° with de-

**It is important to have present a slight excess of thiophenol over alkoxide to prevent formation of difluorenylidene.*

composition. The first crystallization required judicious separation from traces of dinitrodifluorenylidenes. Found: C, 65.70; H, 4.16%. Calc. for $C_{20}H_{15}NO_4S$: C, 65.74; H, 4.14%.

9-Fluorenyl *p*-tolyl sulphone (1 g) was dissolved in ethanol (200 ml) containing sodium ethoxide (from sodium, 0.5 g). The alkyl halide (2–3 g) was added and the mixture was left at room temperature overnight.

9-Methyl-9-fluorenyl p-tolyl sulphone, prepared in this way (81%), crystallized as prisms from hexane, m.p. 150–151°, identical with the sample described above.

9-Ethyl-9-fluorenyl p-tolyl sulphone (76%) formed clusters of long blades from methanol, m.p. 168–169°. Found: C, 75.73; H, 5.81%. Calc. for $C_{22}H_{20}O_2S$: C, 75.83; H, 5.79%.

9-isoPropyl-9-fluorenyl p-tolyl sulphone (75%) crystallized as needles from heptane, m.p. 181–182°. Found: C, 76.27; H, 6.04%. Calc. for $C_{23}H_{22}O_2S$: C, 76.21; H, 6.12%.

9-Allyl-9-fluorenyl p-tolyl sulphone (89%) formed prisms from heptane, m.p. 175–176°. Found: C, 76.78; H, 5.54%. Calc. for $C_{23}H_{20}O_2S$: C, 76.63; H, 5.59%.

9-Benzyl-9-fluorenyl p-tolyl sulphone (86%) formed well-defined prisms from heptane, m.p. 201–202°. Found: C, 78.99; H, 5.51%. Calc. for $C_{27}H_{22}O_2S$: C, 78.99; H, 5.40%.

9-cycloHexyl-9-fluorenyl p-tolyl sulphone (77%) crystallized as small colorless prisms from heptane, m.p. 209–210°. Found: C, 77.87; H, 6.82%. Calc. for $C_{26}H_{26}O_2S$: C, 77.57; H, 6.51%.

The following were also prepared:

9-Methyl-2-nitro-9-fluorenyl p-tolyl sulphone (81%) formed pale yellow prisms from benzene–hexane, m.p. 187–188°. Found: C, 66.28; H, 4.46%. Calc. for $C_{21}H_{17}NO_4S$: C, 66.47; H, 4.52%. (The solution of the starting sulphone in ethanolic sodium ethoxide was filtered to remove traces of dinitrodifluorenylidenes.)

9-Methyl-9-fluorenyl phenyl sulphone (76%) crystallized as plates from ethanol, m.p. 164–166°, identical with the sample described above.

Methyl 9-methyl-9-fluorenyl sulphone (69%) formed colorless prisms from hexane, m.p. 134–136°, identical with the sample described above.

Methyl 9-isopropyl-9-fluorenyl sulphone (72%) crystallized as almost colorless prisms from hexane, m.p. 122–124°. Found: C, 71.24; H, 6.10%. Calc. for $C_{17}H_{18}O_2S$: C, 71.30; H, 6.33%.

Dimethyl 9,9'-Difluorenyl-9,9'-dicarboxylate

Methyl fluorene-9-carboxylate (2.3 g) was dissolved in methanol (50 ml) containing sodium methoxide (from sodium, 0.5 g). Addition of *p*-toluenesulphonyl chloride (3.5 g) resulted in the rapid separation of a microcrystalline solid. Recrystallization from chloroform–hexane gave small needles (1.7 g), m.p. 240–242°, identical with an authentic specimen of the above-named ester (10, 17). Found: C, 79.92; H, 4.81%. Calc. for $C_{30}H_{22}O_4$: C, 80.70; H, 4.97%.

REFERENCES

1. W. von E. Doering and L. K. Levy. J. Am. Chem. Soc. **77**, 509 (1955).
2. W. von E. Doering and K. C. Schreiber. J. Am. Chem. Soc. **77**, 514 (1955).
3. W. von E. Doering and A. K. Hoffmann. J. Am. Chem. Soc. **77**, 521 (1955).
4. E. A. Fehnel and M. Carmack. J. Am. Chem. Soc. **71**, 231 (1949).
5. W. E. Truce and K. R. Buser. J. Am. Chem. Soc. **76**, 3577 (1954).
6. L. Field and J. W. McFarland. J. Am. Chem. Soc. **75**, 5583 (1953).
7. L. Field, J. R. Holsten, and R. D. Clark. J. Am. Chem. Soc. **81**, 2572 (1959).
8. R. L. Shriner and S. O. Greenlee. J. Org. Chem. **4**, 242 (1939).
9. M. M. Klenk, C. M. Suter, and S. Archer. J. Am. Chem. Soc. **70**, 3846 (1948).
10. W. Wislicenus and W. Mocker. Ber. **46**, 2778 (1913).
11. F. A. L. Anet and P. M. G. Bavin. Can. J. Chem. **34**, 991 (1956).

12. P. M. G. BAVIN. Unpublished data.
13. P. M. G. BAVIN. Can. J. Chem. **37**, 2023 (1959).
14. P. M. G. BAVIN. Can. J. Chem. This issue.
15. L. J. BELLAMY. The infrared spectra of complex molecules. Methuen and Co. Ltd., London. 1954.
16. Y. SPRINZAK. J. Am. Chem. Soc. **80**, 5449 (1958).
17. P. M. G. BAVIN. Can. J. Chem. This issue.
18. G. WITTIG, H. DOSER, and I. LORENZ. Ann. **562**, 192 (1949).
19. W. BRADLEY. J. Chem. Soc. 1091 (1937).
20. W. BRADLEY. J. Chem. Soc. 458 (1938).
21. G. W. FENTON, C. K. INGOLD and J. A. JESSOP. J. Chem. Soc. 705, 708 (1930).
22. P. M. G. BAVIN, G. W. GRAY, and A. STEPHENSON. In preparation.
23. N. BUU-HOI and J. LECOCQ. Compt. rend. **226**, 87 (1948).
24. S. HUNIG and O. BOES. Ann. **579**, 23 (1953).
25. M. GAZDAR and S. SMILES. J. Chem. Soc. **93**, 1834 (1908).
26. R. KNOLL. J. prakt. Chem. **113**, 40 (1926).
27. E. D. HUGHES and S. V. ANANTAKRISHNAN. J. Chem. Soc. 1607 (1935).
28. W. SCHLENK, H. HILLEMANN, and I. RODLOFF. Ann. **487**, 135 (1931).
29. F. ADICKES. J. prakt. Chem. **145**, 235 (1936).

CARBON-13 KINETIC ISOTOPE EFFECTS IN THE SOLVOLYSIS OF 1-BROMO-1-PHENYLETHANE[1]

J. B. STOTHERS[2] AND A. N. BOURNS

ABSTRACT

Carbon-13 kinetic isotope effects have been measured for the solvolysis in methanol and ethanol of 1-bromo-1-phenylethane of natural isotopic abundance. Methanolysis of the bromide at 25° C gave a kinetic isotope effect (k^{12}/k^{13}) of 1.0065±0.0006, and ethanolysis at 45° C gave 1.0064±0.0010. These surprisingly low effects for a bond-rupture process have been interpreted in terms of a model for the transition state in which the bonding of the isotopic carbon is strengthened by conjugation of the electron deficient center with the ring. The results are considered to provide support for the mass fragment model for evaluation of the effective mass term of the Bigeleisen expression for the theoretical calculation of kinetic isotope effects.

INTRODUCTION

It has been known for many years that molecules differing only in the isotopic mass of a component atom may react at different rates (1, 2, 3). These kinetic isotope effects are largest when some bond associated with the isotopic atom is undergoing rupture in the rate-determining step of the process. Consequently, isotope effect studies have played an important role in the elucidation of reaction mechanisms (1, 4).

Following the discovery (5, 6, 7) of carbon kinetic isotope effects of considerable magnitude, Bigeleisen (8, 9) proposed equations for the theoretical evaluation of kinetic isotope effects using spectroscopic data. In applying these equations to the rather complex molecular systems for which kinetic isotope effects had been studied experimentally, it was usually found necessary to make the simplifying assumption that the vibrational frequencies of all bonds other than the bond undergoing rupture remain unaltered in the transition state (3, 9). Notwithstanding this and other approximations, surprisingly good agreement has been obtained between calculated and experimental isotope effects in a number of reactions.

Since, in principle, kinetic isotope effects provide information concerning the nature of the transition state, it was decided to undertake a carbon isotope effect study of the reaction of nucleophilic substitution at a saturated carbon atom, a reaction which is one of the most important in organic chemistry and which has been the subject of detailed mechanistic study for over 25 years. At the outset of the investigation it was thought that kinetic isotope effects might provide a useful criterion of mechanism since, on the basis of a simplified theoretical treatment, one might expect that reaction by the unimolecular, or S_N1, mechanism, in which the main covalency change in the rate-determining step is the rupture of a bond associated with the isotopic atom, would give rise to a larger effect than reaction by the bimolecular, or S_N2, mechanism, in which bond formation and bond rupture are synchronous. It was hoped, also, that the investigation might serve as a test for the theoretical equations and, in particular, might help in deciding between the Slater and mass fragment methods for evaluation of the temperature-independent term of these equations.

While this work was in progress two papers by Bender appeared (10, 11) reporting

[1]*Manuscript received February 5, 1960.*
Contribution from the Charles E. Burke Laboratories, Department of Chemistry, Hamilton College, McMaster University, Hamilton, Ontario.
[2]*Graduate student and a recipient of National Research Council Studentships (1954–57). Present address: Department of Chemistry, University of Western Ontario, London, Ontario.*

the results of a carbon-14 isotope effect study of the displacement reactions of methyl iodide and *tert*-butyl chloride. In the S_N2 reaction of methyl iodide with hydroxide ion and with several tertiary amines k^{12}/k^{14} ratios ranging from 1.09 to 1.14 were observed. Solvolysis of methyl iodide in aqueous ethanol in the presence of silver ion, which was considered to be a borderline case between a S_N2 and S_N1 reaction, gave an isotope effect which was essentially no different from effects found in the pure S_N2 processes. These large effects are of the same magnitude as many effects observed in reactions involving only bond rupture and agree with the predictions of the Bigeleisen equation based on a model for the transition state in which only the bond undergoing fission is considered to have changed in the activation process. Hydrolysis of *tert*-butyl chloride in aqueous dioxane, somewhat surprisingly, gave rise to a smaller effect, $k^{12}/k^{14} = 1.03$, than did the reactions proceeding by the bimolecular mechanism. From these results, Bender concluded that kinetic isotope effect studies are of very limited value in differentiating between S_N1 and S_N2 reactions.

The present paper is concerned with a carbon-13 study of the solvolysis of 1-bromo-1-phenylethane in methanol and ethanol. Carbon-13 was chosen as the heavier isotope rather than carbon-14 since, using mass spectrometry, a higher order of precision in evaluation of the isotope effect is possible (± 0.001 in this study, compared with ± 0.005 to ± 0.015 in Bender's work), contamination of samples is less likely to give rise to spurious effects, and isotopic labelling is unnecessary. The choice of 1-bromo-1-phenylethane as the reactant was dictated by two considerations. First, depending upon the conditions, the compound may be made to undergo reaction either exclusively by the S_N1 or by the S_N2 mechanism (12, 13); under solvolytic conditions in solvents of high ionizing power the reaction exhibits characteristics of a unimolecular process, while pure second-order kinetics are observed for reaction in ethanol using ethoxide concentrations of 1.5 *M* or higher. Secondly, the compound and its reaction products, 1-methoxy- and 1-ethoxy-1-phenylethane, may be degraded so as to furnish, in good yield for mass spectrometer analysis, carbon dioxide derived exclusively from the carbon at the seat of displacement.

EXPERIMENTAL

Materials

Absolute methanol and ethanol were prepared from commercial "absolute" products using magnesium, followed by distillation through a 20-in. Vigreux column.

1-Bromo-1-phenylethane was prepared by passing dry hydrogen bromide into 1-phenylethanol maintained at 0° C (14). The product, purified by fractional distillation, was obtained in 85–93% yields (b.p. 83–84° C (10 mm), n_D^{25} 1.5592).

1-Methoxy-1-phenylethane and 1-ethoxy-1-phenylethane, products of the solvolysis reactions, were required for testing the degradation procedures. These were prepared in approximately 75% yield by heating a solution of 1-bromo-1-phenylethane in the anhydrous alcohol for 24 hours at reflux temperatures. The physical constants of the ethers were: 1-methoxy-1-phenylethane, b.p. 55–56° C (10 mm), n_D^{25} 1.4900; 1-ethoxy-1-phenylethane, b.p. 65–66° C (11 mm), n_D^{25} 1.4821.

To test for possible isotopic exchange between the ether product and 1-bromo-1-phenylethane it was necessary to prepare 1-ethoxy-1-phenylethane-1-C^{13}. Acetophenone-carbonyl-C^{13} (8.6 g, 0.072 mole), prepared from sodium acetate-1-C^{13} by the method of Shantz and Rittenberg (15), was reduced to the carbinol using lithium aluminum hydride

(2.0 g, 0.053 mole) in anhydrous ether (50 ml). The complex was decomposed with 20% sulphuric acid and the product isolated by ether extraction. The crude carbinol was dissolved in carbon tetrachloride (25 ml) and treated with anhydrous hydrogen bromide until there was no further absorption of gaseous halide. The reaction mixture was poured into water and extracted with carbon tetrachloride. The combined extracts were dried, concentrated, and taken up in absolute ethanol (100 ml). This solution was heated under reflux for 24 hours while small amounts of a solution of sodium ethoxide in ethanol were added periodically to neutralize the hydrogen bromide formed. At the end of this period the solution was poured into cold water and extracted with ether. Fractional distillation gave 1-ethoxy-1-phenylethane-1-C^{13} (b.p. 64–65° C (10 mm), n_D^{25} 1.4821) in 65% yield, based on the acetophenone.

Kinetic Measurements

The rates of solvolysis of 1-bromo-1-phenylethane in absolute methanol and ethanol were followed by acid–base titration of the product, hydrogen bromide. Reaction temperatures were chosen such that there was approximately 5% reaction in 15 minutes. This was a convenient rate for the partial reactions in the subsequent isotope effect experiments. A solution of the bromide in the alcohol was maintained to within ±0.02° C of the desired temperature and at appropriate time intervals accurately measured aliquots were removed and quickly placed in a cold mixture of benzene and water. The resulting mixture was immediately titrated with standard sodium hydroxide using phenolphthalein as indicator. The rate constants were obtained from a least-squares plot of reaction time versus log[RBr].

Isotope Effect Experiments

In the determination of the carbon-13 isotope effect, 1-bromo-1-phenylethane of normal isotopic abundance was solvolyzed to some small known extent of reaction, the ether product separated from unreacted bromide and degraded so as to furnish carbon dioxide derived exclusively from the alkoxy-bearing carbon. The isotopic ratio for this carbon dioxide and that of the carbon dioxide formed from the original reactant by a similar degradation procedure were measured mass spectrometrically. The rate constant ratios, k^{12}/k^{13}, were calculated from the isotopic ratios using an expression derived by Stevens and Attree (16), which takes into account the extent of reaction.

The detailed procedure was as follows. One liter of the appropriate alcohol was equilibrated to the desired reaction temperature and a weighed sample of 1-bromo-1-phenylethane was added. The resulting solution, approximately 0.5 *M* in organic bromide, was allowed to stand in the constant-temperature bath for an accurately measured time corresponding to approximately 5% reaction, and then was quickly poured into a mixture of 3–4 liters of cold water and 600 ml of benzene. The quenched reaction mixture was vigorously shaken, the layers separated, and the aqueous layer extracted with three 300-ml portions of fresh benzene. The combined extracts were thoroughly washed with water and dried over calcium chloride, and the benzene then removed by distillation under reduced pressure. The small amount of product was separated from the large amount of unreacted bromide by careful fractional distillation under reduced pressure using a 50-cm tantalum-wire column described by Cason and Rapoport (17). One such distillation was sufficient to separate the methyl ether; a second distillation was required for 1-ethoxy-1-phenylethane. Trial experiments on synthetic mixtures of 1-ethoxy-1-phenylethane and the organic bromide showed that ether of 93–95% purity could be separated with

better than 90% recovery. The impurity, which was mainly bromide, would not be expected to affect significantly the isotopic ratios subsequently determined.

Under the normal solvolytic conditions, hydrogen bromide concentration builds up as the reaction proceeds and, as a result, there might be some tendency for ether cleavage with the regeneration of starting bromide. If this were to happen, the measured isotopic fractionation would not be that resulting from a strictly unidirectional process but rather from a process tending toward equilibrium. Since, in all experiments, the reaction was stopped before more than 10% of organic halide had been consumed, the back reaction, if it occurred at all, would be expected to make only a very minor contribution to the measured effect. Nevertheless, to establish this point, two isotope effect experiments in methanol were carried out in which sodium methoxide was present in a concentration which was sufficient to neutralize the hydrogen bromide formed in the partial reaction but not sufficient to induce any significant amount of bimolecular reaction (12, 13). The isotope effects obtained in the presence and in the absence of methoxide ion differed only very slightly, if at all.

It was also necessary to establish that no isotopic exchange occurred during the separation of the ether product from the large amount of unreacted organic bromide. This was accomplished by subjecting a mixture of 1-ethoxy-1-phenylethane-1-C^{13} and unlabelled 1-bromo-1-phenylethane to the usual separation procedure and determining the loss of label in the recovered ether. It was found that an upper limit for the exchange, if it occurred at all, was 5%. This would have no measurable effect on the results.

Degradation Method

Since the isotopic ratio for the carbon atom at the center of displacement must be determined for the reactant and for the product of partial reaction, it was necessary to develop a degradation procedure whereby this atom could be removed from the rest of the molecule and converted in high yield to carbon dioxide for mass spectrometric analysis. The method consisted of oxidation of the bromide and ether to benzoic acid followed by decarboxylation using the Schmidt reaction.

Oxidation to Benzoic Acid

Best over-all yields of benzoic acid were obtained by a two-stage oxidation procedure. In the first stage, the compounds were oxidized with alkaline permanganate in a pyridine–water solvent to give a mixture of benzoic acid and benzoylformic acid. This acid mixture was then further oxidized with hydrogen peroxide whereby the benzoylformic acid was quantitatively converted to benzoic acid.

1-Bromo-1-phenylethane (1.65 g, 0.0089 mole) was placed in pyridine (50 ml) and water (100 ml) and potassium hydroxide (5 g, 0.089 mole) was added. The mixture was heated under reflux for 15 minutes with vigorous stirring. Solid potassium permanganate (8 g, 0.051 mole) was then added slowly at reflux temperature to the stirred solution over a period of 15 minutes and the reaction mixture heated for an additional 30 minutes with vigorous stirring. The mixture was cooled to about 50° C and excess potassium permanganate destroyed by the addition of ethanol. The inorganic solids were removed by filtration and washed thoroughly with hot water. The filtrate was cooled, acidified with concentrated hydrochloric acid, and extracted four times with ether. Ether was removed and the residue stirred vigorously for 2 to 3 hours with 5% hydrogen peroxide (30 ml). The reaction mixture was allowed to stand overnight and then heated under reflux to destroy excess peroxide, additional water being added to

effect complete solution of the benzoic acid. The solution was allowed to cool and the benzoic acid collected. Additional acid was recovered by ether extraction of the filtrate. Total yield of pure acid was 0.909 g (84%), m.p. 121.5°–121.8° C (corr.).

A similar procedure using, however, 50% more oxidizing agent was followed for the two ether products. Yields of benzoic acid were generally slightly higher than those obtained from the bromide.

Decarboxylation of Benzoic Acid

An apparatus similar to that described by Phares (18) was used. A solution containing approximately 1 millimole of benzoic acid in 3–4 ml of concentrated sulphuric acid was placed in the reaction flask and cooled to 0° C. Approximately 80 mg of sodium azide was added and the flask connected to the absorption traps. The reaction mixture was maintained at about 40° C for 2 hours while the carbon dioxide was swept by means of a slow stream of purified nitrogen into 0.2 *M* carbonate-free sodium hydroxide. The trapped gas was precipitated as barium carbonate (19). Great care was taken in all operations to avoid contamination with atmospheric carbon dioxide. Yields of barium carbonate were in the range 91–93%.

Tests for Rearrangement and Isotopic Fractionation in the Degradation Reactions

There is a possibility, albeit an unlikely one, that rearrangement might occur during the two-stage oxidation of bromide and ether to benzoic acid, with the result that the carbon atom in the carboxyl group of the acid would not be the atom originally joined to the benzene ring. To test for this, some labelled ether, 1-ethoxy-1-phenylethane-1-C^{13}, was subjected to the usual alkaline oxidation while another sample was oxidized by chromic anhydride to acetophenone, which was then converted to benzoic acid by means of the haloform reaction. Carbon dioxide samples were prepared in the usual way from each benzoic acid sample and analyzed mass spectrometrically. The isotopic ratios obtained for the two samples were identical within the precision limits of the measurements and they corresponded closely to the ratio expected on the basis of the carbon-13 content of the barium carbonate used in the synthesis of the labelled ether. From this result it may be concluded that no rearrangement occurred during the degradation.

Although the yields in each of the degradation steps were good, the possibility remained that isotopic fractionation during the conversion of bromide or ether to carbon dioxide might affect, to a measurable extent, the isotopic abundance of this gas. To test for this possibility the following interconversions were carried out: (1) 1-phenylethanol of normal isotopic abundance to 1-bromo-1-phenylethane using dry hydrogen bromide; (2) a sample of this bromide to 1-methoxy-1-phenylethane by methanolysis; and, (3) a further sample of the 1-phenylethanol to 1-methoxy-1-phenylethane using methyl sulphate. Since conversion (3) involved no change in the bonding of the carbon atom alpha to the ring, the isotopic abundance for this carbon should be identical in the alcohol and the ether product. Furthermore, since conversion (1) proceeded in better than 90% yield the isotopic ratio of the bromide should correspond very closely to that of the alcohol. One or more samples of the alcohol, ether, and bromide were oxidized in the usual way to benzoic acid, samples of which were then converted in duplicate or triplicate to carbon dioxide for mass spectrometric analysis. The fourteen carbon dioxide samples prepared in this way gave C^{12}/C^{13} ratios which were the same within the limits of the mass spectrometric analysis. These results definitely establish that either there was no isotopic fractionation in the degradation reactions or that any small fractionation

that did occur was the same for the ether and the bromide. In either case, the degradations were entirely suitable for the isotope effect studies in which an intercomparison of isotopic ratios was being made.

Preparation of Carbon Dioxide Samples for Mass Spectrometric Analysis

Carbon dioxide was liberated from the barium carbonate samples by means of concentrated sulphuric acid using standard high vacuum techniques. The gas was trapped at liquid nitrogen temperatures, distilled at −78° C through an "anhydrone" drying tube, and condensed into a standard mass spectrometer sample tube.

Mass Spectrometry

All carbon dioxide samples were analyzed in a 180° direction-focussing mass spectrometer. The C^{12}/C^{13} ratios were obtained from the mass 44 / mass 45 ion current ratio after applying a suitable correction for the contribution to mass 45 of the molecule species $C^{12}O^{16}O^{17}$. Each carbon dioxide sample in a given series of experiments was analyzed relative to a standard, the standard being one of the samples of carbon dioxide prepared from the reactant used in that series. An arbitrary value of 85.00 for the mass 44/45 ratio was assigned to these standards. The procedure was to analyze the standard, the unknown, and the standard again all in the shortest possible time. A single analysis consisted of a series of at least six double spectrograms, each double spectrogram being obtained from a scan of the masses in the order 44, 45, 45, 44. A single analysis was considered satisfactory if the mean deviation of the 44/45 ratios was less than 0.1%, and the mean for the unknown was accepted if the mean for the standard, before and after analysis of unknown, differed by no more than this value.

RESULTS

The results of the kinetic measurements for the solvolysis of 1-bromo-1-phenylethane in absolute methanol and in absolute ethanol are summarized in Table I.

TABLE I

Kinetic results for solvolyses of 1-bromo-1-phenylethane

Solvent	Temp., °C	Concn. of RBr, *M*	$k_1 \times 10^5$ sec^{-1}
Methanol	25.0	0.112	5.70
		0.114	5.72
		0.303	5.57
			Average 5.67
Ethanol	45.0	0.486	5.87
		0.525	6.07
		0.512	6.07
			Average 6.00

The results of the isotope effect experiments on the methanolysis and the ethanolysis of 1-bromo-1-phenylethane are given in Tables II and III, respectively. Each individual experiment consisted of a partial reaction of bromide to ether followed by parallel degradations to carbon dioxide of a sample of the original reactant and of the product. The rate constant ratios, k^{12}/k^{13}, were calculated from the C^{12}/C^{13} ratios and the percentage of reaction (16).

TABLE II

C^{12}/C^{13} ratios and kinetic isotope effects in the methanolysis of 1-bromo-1-phenylethane at 25° C

Expt. No.	Compound degraded	Reaction, %	C^{12}/C^{13} ratios	k^{12}/k^{13}
1	RBr		91.16	1.0063
	$ROCH_3$	5.1	91.72	
2	RBr		91.13	1.0070
	$ROCH_3$	5.1	91.75	
3	RBr		90.95	1.0061
	$ROCH_3$	4.7	91.49	
4	RBr		91.00	1.0068
	$ROCH_3$	4.8	91.60	
5	RBr		90.94	1.0070
	$ROCH_3$	4.8	91.56	
6	RBr		90.87	1.0076
	$ROCH_3$	4.7	91.54	
7[a]	RBr		91.07	1.0054
	$ROCH_3$	5.0	91.54	
8[a]	RBr		90.99	1.0060
	$ROCH_3$	5.0	91.52	
		Mean value of isotope effect		1.0065[b]

[a]Experiments carried out in the presence of ~0.03 *M* $NaOCH_3$.
[b]Standard deviation 0.0007; 95% confidence limit 0.0006.

TABLE III

C^{12}/C^{13} ratios and kinetic isotope effects in the ethanolysis of 1-bromo-1-phenylethane at 45° C

Expt. No.	Compound degraded	Reaction, %	C^{12}/C^{13} ratios	k^{12}/k^{13}
1	RBr		90.86	1.0067
	ROC_2H_5	4.9	91.45	
2	RBr		90.88	1.0054
	ROC_2H_5	4.9	91.35	
3	RBr		90.97	1.0070
	ROC_2H_5	5.8	91.59	
4	RBr		91.02	1.0065
	ROC_2H_5	5.6	91.59	
		Mean value of isotope effect		1.0064[a]

[a]Standard deviation 0.0007; 95% confidence limit 0.0011.

DISCUSSION

It seems reasonable to assume on the basis of the results of extensive kinetic and stereochemical studies (12, 13, 20, 21) that the solvolysis of 1-phenylethyl halides in good ionizing solvents, including methanol and ethanol, proceeds by a S_N1 mechanism in the sense that some type of carbonium ion intermediate is involved. Winstein and co-workers (22, 23) have recently proposed that the ionization process for a compound RX can involve two discrete ion pair intermediates, as well as dissociated carbonium ions, and that one or all of these ion types may interact with solvent to form product.

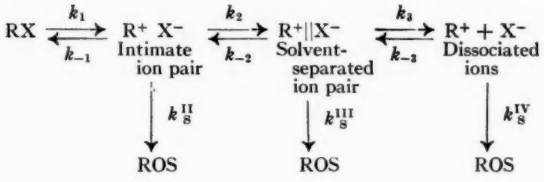

Grunwald and co-workers (24) have presented cogent arguments in support of the idea that for 1-phenylethyl compounds the ratio k_2/k_S^{II} is small and, therefore, that substitution occurs mainly at the intimate ion pair stage. This seems reasonable since the 1-phenylethyl carbonium ion should be very reactive, particularly in the moderately nucleophilic solvents, methanol and ethanol, used in the present investigation.

There remains the question of the relative rates of reaction of the intimate ion pair with solvent and its collapse to re-form RX (internal return). Winstein (25) has reported that in the acetolysis of 1-bromo-1-phenylethane the true ionization rate is about seven times greater than the titrimetric solvolysis rate. Assuming that product is formed mainly by interaction of solvent with the intimate ion pair, the ratio k_{-1}/k_S^{II} in acetolysis is therefore 6. In methanol and ethanol, which are more nucleophilic solvents (26), there should be a smaller tendency for internal return. One cannot assume, however, that the alcoholysis rates will be determined solely by the ionization step.

On the basis of these considerations the mechanism of solvolysis of 1-phenylethyl bromide may be formulated as follows:

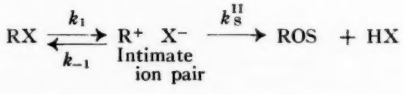

For a theoretical evaluation of the carbon isotope effect in this reaction, it is useful to examine two limiting cases, one in which the ionization step is rate determining ($k_S^{II} \gg k_{-1}$), and the other in which the intimate ion pair is in equilibrium with the organic halide ($k_S^{II} \ll k_{-1}$). In the former case, the observed isotope effect will be the kinetic isotope effect associated with the ionization process. In the latter case, the observed effect will be the result of two fractionation processes, that associated with the equilibrium between substrate and intimate ion pair and that associated with the interaction of intimate ion pair with solvent. It may be readily shown in this case that the over-all isotope effect is given by the expression

$$[1] \qquad k/k' = K_{exch} \cdot \frac{k_S^{II}}{k_S^{II'}}$$

where k and k' are the specific reaction rate constants for solvolysis of the light and heavy isotopic organic halides, RX and R′X, respectively, k_S^{II} and $k_S^{II'}$ are the corresponding rate constants for interaction of the intimate ion pairs, R^+X^- and $R^+{}'X^-$, with solvent, and K_{exch} is the equilibrium constant for the isotopic exchange process

$$RX + R^+{}'X^- \rightleftarrows R'X + R^+X^-.$$

Bigeleisen and Mayer (27) have shown that the equilibrium constant for an isotopic exchange process can be expressed as the ratio of the so-called isotopic partition functions ratios, f, for the reacting species. For the exchange process given above,

[2] $$K_{\text{exch}} = \frac{f_{RX}}{f_{R^+X^-}}$$

where f_{RX} is the isotopic partition function ratio for organic halide and $f_{R^+X^-}$ the ratio for the intimate ion pair. For a rate process, the ratio of the rate constants for the isotopic molecules is given by an expression developed by Bigeleisen (8), which, for the present case of the interaction of solvent molecules with the intimate ion pair, takes the form

[3] $$\frac{k_s^{II}}{k_s^{II'}} = \frac{K}{K'} \cdot \left[\frac{m_{ROS}^{\ddagger'}}{m_{ROS}^{\ddagger}}\right]^{\frac{1}{2}} \cdot \frac{f_{R^+X^-}}{f_{ROS}^{\ddagger}}$$

where the K's are transmission coefficients, the ratio of which may be taken as unity, $m_{ROS}^{\ddagger}$ and $m_{ROS}^{\ddagger'}$ are, respectively, the effective masses of the light and heavy transition states in the direction of the reaction co-ordinate, and $f_{ROS}^{\ddagger}$ is the isotopic partition function ratio for these states.

The over-all isotope effect for solvolysis proceeding through an intimate ion pair in equilibrium with undissociated organic halide is, therefore,

[4] $$\frac{k}{k'} = K_{\text{exch}} \cdot \frac{k_s^{II}}{k_s^{II'}} = \left[\frac{m_{ROS}^{\ddagger'}}{m_{ROS}^{\ddagger}}\right]^{\frac{1}{2}} \cdot \frac{f_{RX}}{f_{ROS}^{\ddagger}}.$$

If, on the other hand, there is little or no internal return, the rate of solvolysis will be equal to the rate of ionization and, therefore, the istope effect will be given by

[5] $$\frac{k}{k'} = \left[\frac{m_{RX}^{\ddagger'}}{m_{RX}^{\ddagger}}\right]^{\frac{1}{2}} \cdot \frac{f_{RX}}{f_{RX}^{\ddagger}}$$

where the m's and $f_{RX}^{\ddagger}$ refer to the isotopic transition states for the ionization step.

The f functions appearing in these equations depend upon molecular vibrations only (27) and are of the form

[6] $$f = 1 + \sum_{1}^{3n-6} G(u_1)\Delta u_1$$

where

$$G(u_1) = \frac{1}{2} - \frac{1}{u_1} - \frac{1}{e^{u_1}-1}$$

$$u_1 = h\nu/kT$$

$$\Delta u_1 = h/kT(\nu_1 - \nu_1').$$

The ν and ν' quantities are fundamental vibrations of the light and heavy isotopic species, respectively.

The rate constant ratio, k/k', for the solvolysis reaction proceeding through an intimate ion pair in equilibrium with RX now becomes

[7] $$k/k' = \left[\frac{m_{ROS}^{\ddagger'}}{m_{ROS}^{\ddagger}}\right]^{\frac{1}{2}} \left[1 + \sum_{1}^{3n-6} G(u_{RX_1})\Delta u_{RX_1} - \sum_{1}^{3n-6} G(u_{ROS_1}^{\ddagger})\Delta u_{ROS_1}^{\ddagger}\right]$$

whereas this rate ratio for solvolysis in which the ionization step is rate determining takes the form

$$[8] \qquad k/k' = \left[\frac{m^{\ddagger'}_{RX}}{m^{\ddagger}_{RX}}\right]^{\frac{1}{2}}\left[1+\sum_{1}^{3n-6} G(u_{RX_1})\Delta u_{RX_1} - \sum_{1}^{3n-6} G(u^{\ddagger}_{RX_1})\Delta u^{\ddagger}_{RX_1}\right].$$

It can be seen that equations [7] and [8] differ in the effective mass term and in the second summation of the free energy term. In equation [7] these quantities refer to the transition state for covalent bond formation between carbonium ion and solvent; in equation [8] they refer instead to the transition state of the ionization process. It is, therefore, important to compare the nature of these transition states.

Since the intimate ion pair formed from 1-bromo-1-phenylethane is a high-energy intermediate, the energy of activation both for its reaction with solvent and for internal return to organic halide will be very small. Both transition states, therefore, will resemble the intimate ion pair (28). In other words, the carbon–bromine bond of the halide should be almost completely broken in the transition state for the first step and the carbon–oxygen bond should be only starting to form in the transition state of the second step. As a result, the change in vibrational energy resulting from the substitution of carbon-13 for carbon-12 will be much the same for the two transition states and will correspond closely to the change in energy resulting from isotopic substitution in the intermediate itself. The only significant difference then in the magnitude of the isotope effect for reaction in which the intimate ion pair is in equilibrium with RX and for reaction in which it is not, should arise from a difference in the effective mass factor.*

For calculation of the effective mass term Bigeleisen (8) originally applied a theorem of Slater (29) which in effect considers the reaction to be simply the formation or dissociation of a hypothetical diatomic molecule consisting of the two atoms between which the bond change is taking place. Each value of $m^{\ddagger}$ is then the reduced mass, μ, of the corresponding diatomic molecule and the effective mass term is the square root of the ratio of the reduced masses of the two isotopic molecules,

$$[9] \qquad \left[\frac{m^{\ddagger'}}{m^{\ddagger}}\right]^{\frac{1}{2}} = \left[\frac{\mu'}{\mu}\right]^{\frac{1}{2}} = \left[\left(\frac{1}{m_A}+\frac{1}{m_B}\right)\Big/\left(\frac{1}{m'_A}+\frac{1}{m_B}\right)\right]^{\frac{1}{2}}.$$

For rupture of a C—Br bond $m_A = 12$, $m'_A = 13$, and $m_B = 80$; for formation of a C—O bond $m_A = 12$, $m'_A = 13$, and $m_B = 16$.

Recently Bigeleisen (9) has suggested that since the reaction path for a polyatomic molecule involves not merely motion of individual atoms A and B, but rather motion of whole reacting fragments α and β, a more reasonable formulation of the mass term is

$$[10] \qquad \left[\frac{m^{\ddagger'}}{m^{\ddagger}}\right]^{\frac{1}{2}} = \left[\left(\frac{1}{M_\alpha}+\frac{1}{M_\beta}\right)\Big/\left(\frac{1}{M'_\alpha}+\frac{1}{M_\beta}\right)\right]^{\frac{1}{2}}.$$

For ionization of 1-bromo-1-phenylethane $M_\alpha = 105$, $M'_\alpha = 106$, and $M_\beta = 80$; for bond formation between 1-phenylethyl carbonium ion and methanol $M_\alpha = 105$, $M'_\alpha = 106$, and $M_\beta = 32$. In ethanol, M_β equals 46.

The effective mass terms for each transition state of the solvolytic reaction, calculated both from the Slater and the mass fragment models, are given in Table IV. It is of interest

**Since the vibrational stretching frequency of a carbon–oxygen bond is higher than that of a carbon–bromine bond, the summation for the transition state for covalent bond formation might be slightly higher than that for ionization.*

TABLE IV

Effective mass and free energy values for the transition-states of 1-bromo-1-phenylethane solvolysis

Reaction[a]	Effective mass term		$(k^{12}/k^{13})_{expt}{}^{b}/(m^{*12}/m^{*13})^{\frac{1}{2}}$	
	Slater	Mass fragment	Slater	Mass fragment
R—Br → R^+Br^-	1.0352	1.0021	0.972	1.004
R^+Br^- → $ROCH_3$	1.0227	1.0011	0.984	1.005
R^+Br^- → ROC_2H_5	1.0227	1.0014	0.984	1.005

[a] R = $C_6H_5\dot{C}HCH_3$. [b] $(k^{12}/k^{13})_{expt}$ taken as 1.006.

to calculate from these mass terms the values of the free energy terms,

$$\left[1+\sum_{1}^{3n-6} G(u_1)\Delta u_1-\sum_{1}^{3n-6} G(u_1^{\ddagger})\Delta u_1^{\ddagger}\right],$$

which would be required to produce the experimentally observed isotope effect of 1.006. These are shown in the last two columns of the Table IV.

The values of less than unity for the free energy term, which are obtained by dividing the experimental isotope effect by mass terms calculated from the Slater model, require that the difference in the vibrational energies for the isotopic transition states be greater than the corresponding difference for the isotopic RX molecules,

$$\sum_{1}^{3n-6} G(u_1^{\ddagger})\Delta u_1^{\ddagger} > \sum_{1}^{3n-6} G(u_1)\Delta u_1.$$

This could only come about if the isotopic atom were considerably more "tightly bound" in the transition state than in the initial state (8), a situation which would seem most unlikely in the present reaction system in which the transition state in both the ionization step and the bond formation step closely resembles the carbonium ion intermediate.

The low isotope effect observed in the solvolysis of 1-bromo-1-phenylethane, therefore, lends support to the mass fragment method of evaluating the effective mass term.

A common procedure in calculating from vibrational frequency data the free energy term of the Bigeleisen equation is to assume a model for the transition state in which the force constant for the bond being broken is equal to zero and the vibrational frequencies of all other bonds are the same as those for the initial state (3). The summations for the transition state in equations [7] and [8] then become zero and the initial state term can be readily calculated from the vibrational stretching frequency of the isotopic bond which is undergoing rupture in the reaction. To the extent that the bond in question is less than completely broken in the transition state, or other bonds associated with the isotopic atom are formed or strengthened, the over-all free energy term, calculated on the assumption of a zero value for the transition state summation, will be too high.

Using this very approximate method, one obtains a theoretical value of 1.018 for the free energy term in equations [7] and [8] at 25° C.* Comparison with the values given in the last two columns of Table IV shows that this value is much too high to account for the observed isotope effect. Even when combined with the low mass term given by the mass fragment theory it leads to an isotope effect of about 2%, and when combined with a mass term calculated on the basis of the Slater theorem it gives an effect of over 4%.

An even larger value is given by a more recent equation which makes use of the theorem of the trace (9).

It is suggested that the origin of this discrepancy arises mainly from the complete neglect of the transition state term.

Of the two simplifying assumptions upon which neglect of this term was based, that involving the assignment of a zero force constant to the carbon–bromine bond in the transition state of the ionization step and to the carbon–oxygen bond in the transition state of the second step would seem justified since, for reasons already given, the two transition states must closely resemble the intimate ion pair intermediate. What undoubtedly is not justified is the assumption that the vibrational frequencies of all other bonds associated with the isotopic carbon will remain unchanged in the transition state. Indeed, the bonding of this carbon to the benzene ring will be considerably strengthened as a result of overlap of its fairly well-developed vacant p orbital with the π orbitals of the benzene ring. Added to this, but of lesser importance, will be hyperconjugative interaction with the attached methyl group. The low isotope effect observed in the reaction would suggest that this conjugation in the transition state compensates to a considerable degree for the loss of the carbon–bromine vibration.

Some support for this interpretation of the low isotope effect is found in a recent study by Magee and Daniels (30) of the carbon-13 isotope effect in the unimolecular decomposition of substituted ureas, the results of which are summarized in Table V. Given also in

TABLE V

Unimolecular decomposition of substituted ureas

Reactant	$(k^{12}/k^{13})_{expt}$	$(k^{12}/k^{13})_{expt}/(m^{\pm 13}/m^{\pm 12})^{\frac{1}{2}}$
sym-Dimethylurea	1.027	1.024
Phenylurea	1.016	1.015
sym-Diphenylurea	1.008	1.006
3,3′-Dimethylcarbanilide	1.007	1.005

this table are the $(k^{12}/k^{13})_{expt}/(m^{\pm 13}/m^{\pm 12})^{\frac{1}{2}}$ values calculated using the mass fragment model for evaluation of the effective mass term. These authors attribute the effect of phenyl substitution on the magnitude of the isotope effect to resonance stabilization of the transition state resulting in a strengthening of a bond associated with isotopic carbon. This would tend to increase the $G(u_1^{\pm})\Delta u_1^{\pm}$ term and result in a lowering of the over-all free energy term.

It may be noted also that the carbon-14 isotope effect observed by Bender and Buist (11) in the hydrolysis of *tert*-butyl chloride is lower than would be predicted on the assumption of a zero transition state term. Using a mass term calculated from the mass fragment hypothesis one obtains a value for $(k^{12}/k^{14})_{expt}/(m^{\pm 14}/m^{\pm 12})^{\frac{1}{2}}$ of 1.014 ± 0.015, whereas the free energy term calculated on the assumption of complete carbon–chlorine bond rupture and no change in other vibrational frequencies is 1.045. It has been suggested that the low effect may be due in part to the electron-releasing effect of the three methyl groups which would tend to loosen the carbon–chlorine bond in the initial state resulting in a lower free-energy term. Another possibility is that hyperconjugative interaction of the three methyl groups with the isotopic carbon tends to strengthen the bonding of this atom in the transition state, hence increasing the free energy term for this state.

ACKNOWLEDGMENTS

The authors are indebted to Dr. J. Bigeleisen for a helpful discussion and to the National Research Council of Canada for financial assistance.

REFERENCES

1. K. B. WIBERG. Chem. Revs. **55**, 713 (1955).
2. J. G. LINDSAY, A. N. BOURNS, and H. G. THODE. Can. J. Chem. **29**, 192 (1951).
3. J. BIGELEISEN. J. Phys. Chem. **56**, 823 (1952).
4. E. GROVENSTEIN, JR. and G. A. ROPP. J. Am. Chem. Soc. **78**, 2560 (1956).
5. O. BEECK, J. W. OTVOS, D. P. STEVENSON, and C. D. WAGNER. J. Chem. Phys. **16**, 255 (1948).
6. P. E. YANKWICH and M. CALVIN. J. Chem. Phys. **17**, 109 (1949).
7. J. G. LINDSAY, D. E. MCELCHERAN, and H. G. THODE. J. Chem. Phys. **17**, 589 (1949).
8. J. BIGELEISEN. J. Chem. Phys. **17**, 675 (1949).
9. J. BIGELEISEN and M. WOLFSBERG. Advances in Chem. Phys. **1**, 15 (1958).
10. M. L. BENDER and D. F. HOEG. J. Am. Chem. Soc. **79**, 5649 (1957).
11. M. L. BENDER and G. J. BUIST. J. Am. Chem. Soc. **80**, 4304 (1958).
12. E. D. HUGHES, C. K. INGOLD, and A. D. SCOTT. J. Chem. Soc. 1201 (1937).
13. E. D. HUGHES, C. K. INGOLD, S. MASTERMAN, and B. J. MCNULTY. J. Chem. Soc. 899 (1940).
14. J. B. CONANT and A. H. BLATT. J. Am. Chem. Soc. **50**, 554 (1928).
15. E. M. SHANTZ and D. RITTENBERG. J. Am. Chem. Soc. **68**, 2109 (1946).
16. W. H. STEVENS and R. W. ATTREE. Can. J. Research, B, **27**, 807 (1949).
17. J. CASON and H. RAPOPORT. Laboratory text in organic chemistry. Prentice-Hall, New York. 1954.
18. E. F. PHARES. Arch. Biochem. Biophys. **33**, 173 (1951).
19. M. CALVIN, C. HEIDELBERGER, J. C. REID, B. M. TOLBERT, and P. E. YANKWICH. Isotopic carbon. J. Wiley and Sons, New York. 1949.
20. L. WILPUTTE-STEINERT and P. J. C. FIERENS. Bull. soc. chim. Belges, **64**, 287 (1955).
21. A. H. FAINBERG and S. WINSTEIN. J. Am. Chem. Soc. **79**, 1602 (1957).
22. S. WINSTEIN, E. CLIPPINGER, A. H. FAINBERG, R. HECK, and G. C. ROBINSON. J. Am. Chem. Soc. **78**, 328 (1956).
23. S. WINSTEIN and G. C. ROBINSON. J. Am. Chem. Soc. **80**, 169 (1958).
24. E. GRUNWALD, A. HELLER, and F. S. KLEIN. J. Chem. Soc. 2604 (1957).
25. S. WINSTEIN, A. H. FAINBERG, and E. GRUNWALD. J. Am. Chem. Soc. **79**, 4146 (1957).
26. H. L. GOERING, T. D. NEVITT, and E. F. SILVERSMITH. J. Am. Chem. Soc. **77**, 5026 (1955).
27. J. BIGELEISEN and M. G. MAYER. J. Chem. Phys. **15**, 261 (1947).
28. G. S. HAMMOND. J. Am. Chem. Soc. **77**, 334 (1955).
29. N. B. SLATER. Proc. Roy. Soc., A, **194**, 112 (1948).
30. E. M. MAGEE and F. DANIELS. J. Am. Chem. Soc. **79**, 829 (1957).

THE DIFFERENTIAL THERMAL ANALYSIS OF NATURAL AND SYNTHETIC HYDRATES OF CALCIUM SULPHATE[1]

W. E. P. Fleck, M. H. Jones, R. A. Kuntze, and H. G. McAdie

ABSTRACT

A variety of naturally occurring forms of calcium sulphate dihydrate produce substantially identical differential thermograms under conditions of uniform heating rate and particle size. These thermograms closely resemble those for synthetic dihydrate and β-hemihydrate, showing four endothermic effects and one exothermic effect below 500° C. Two of these endothermic effects, at about 170° and 300° C, respectively, which have not been reported previously, were found to be easily masked by changes in heating rate or sample concentration. Resolution of the several effects was improved by using different heating rates at different stages of the thermogram. Thermograms of the α-hemihydrate were similar, except that the endothermic effect at 300° C was not evident and the exothermic effect occurred at a much lower temperature than for the dihydrate. No conspicuous differences were found in the temperatures corresponding to the various endothermic and exothermic effects which might be correlated with the general dehydration behavior of the particular material. The endothermic effect at about 170° C appears to be associated with part of the hemihydrate to soluble anhydrite transition, possibly arising during the removal of the last traces of water.

In the differential thermograms reported for many natural and synthetic gypsums of widely different origin (1–7), two large endothermic effects occurring below 200° C have been attributed to the formation of the hemihydrate and its subsequent decomposition to soluble anhydrite. The exact temperatures at which these effects appear depend on a variety of experimental conditions, the resolution of the two endotherms being improved at slow rates of heating (2). In the region of 400° C an exothermic effect, not found when natural anhydrite is heated from room temperature, has been attributed to the conversion of β-soluble anhydrite to insoluble or natural anhydrite (3). A contradiction exists in the literature regarding the presence (8) or absence (4, 5) of a similar exothermic effect in the case of the α-soluble anhydrite. No further thermal effects have been reported below about 1200° C where a high-temperature modification of anhydrite is formed (1, 6, 7).

It has been recorded that the above exothermic effect appears at different temperatures, depending upon the origin of the gypsum sample (2, 3), and in the gypsum industry it is known that natural gypsums of different origin produce hemihydrates of widely differing properties. Hence an examination of several natural gypsums, as well as the pure hydrates of calcium sulphate, was undertaken by differential thermal analysis to investigate the possibility that some correlation might exist between both the endothermic and exothermic effect temperatures and the dehydration behavior of the particular gypsum. The natural gypsums selected represented several mineralogical forms and attention was focused on thermal effects appearing below 500° C.

EXPERIMENTAL

The instrument used contained a horizontal furnace, wound with 15-gauge Kanthal A wire, having a maximum operating temperature of 1300° C. No attempt was made to control the atmosphere within this furnace except in cases where a sample was cooled in a stream of dry nitrogen, after determination of a thermogram, prior to determination of a second thermogram on the same sample.

[1]*Manuscript received February 23, 1960.*
Contribution from the Department of Chemistry, Ontario Research Foundation, 43 Queen's Park Crescent, Toronto 5, Ontario. This paper was presented at the 137th Meeting of The American Chemical Society, Cleveland, April 5–14, 1960. Published with the permission of The American Chemical Society.

Can. J. Chem. Vol. 38 (1960)

For measurement of temperature above 200° C, and control of heating rate over the entire temperature range, a Leeds and Northrup Model S Speedomax G indicating and recording temperature-program controller was used. Heating rates up to 20° C min^{-1} were possible, and above 200° C the sample temperature could be read to 1–2° C. Below 200° C another recorder, calibrated for 0–200° C with an iron–constantan thermocouple, was used to measure sample temperature to within 0.5° C. The differential temperature of a pair of Pt–Pt/13% Rh thermocouples was measured with a Speedomax G millivolt recorder fed from a stabilized microvolt amplifier. Differential temperatures of the order of 0.2 μv, corresponding to 0.03° C and about 2-mm deflection on the recorder chart, could be detected.

Below 200° C a heating rate of 3° C min^{-1} was found to give the best combination of peak definition and resolution. Smaller peaks occurring above 200° C were found to be better defined at higher heating rates, so that above this temperature the heating rate was increased to 12° C min^{-1}. The sample was contained in a palladium block having separate cavities for sample and reference material. At 3° C min^{-1} the difference between block and bulk sample temperature was found to be 2–4° C, while at 12° C min^{-1} this difference was 10–12° C. Since the temperature-measuring thermocouples were always in contact with the block, the peak temperatures to be reported are those of the sample block at the particular maximum differential temperature.

Ignited reagent grade α-alumina, having an average particle diameter, by the Fisher Sub-Sieve Sizer, of about 12 μ, was used as reference material and as diluent for the sample. With this material in both cavities of the palladium block, no significant differential temperature could be measured over the temperature range of interest.

A preliminary study of the effect of particle size on peak temperature showed that lower and more reproducible peak temperatures were obtained as the particle size of the sample was decreased. Some variation in relative peak heights with particle size was also noted. The most satisfactory results were obtained with a −325-mesh sample diluted to 20% concentration in ignited alumina.

The materials investigated are listed in Tables III and IV. The synthetic materials were prepared as follows. Calcium sulphate dihydrate was precipitated from 0.5 *M* solutions of calcium nitrate and sulphuric acid at room temperature, thoroughly washed and air-dried. The α-hemihydrate was precipitated from a boiling 50% nitric acid solution of the dihydrate. The β-hemihydrate was obtained by dehydrating dihydrate at 100° C in a stream of nitrogen containing water vapor until the theoretical hemihydrate composition was reached. These two hemihydrates were identified by measuring their heats of solution in 2 *N* hydrochloric acid (9), and their analyses, together with that of the synthetic dihydrate, are given in Table I. The agreement of experimental heats of solution with accepted values (9) provides sufficient identification of the hemihydrates.

TABLE I

Analysis of synthetic calcium sulphates

Material	% Ca		% H_2O		ΔH soln. (298° K) (cal $mole^{-1}$)	
	Exptl.	Theor.	Exptl.	Theor.	Exptl.	Accepted (9)
$CaSO_4 \cdot 2H_2O$	23.31	23.28	20.88	20.93	—	—
$CaSO_4 \cdot \frac{1}{2}H_2O(\alpha)$	27.59	27.61	6.24	6.21	+1580	+1600
$CaSO_4 \cdot \frac{1}{2}H_2O(\beta)$	27.57	27.61	6.25	6.21	+1085	+1100

RESULTS

For convenience, the peaks corresponding to the various endothermic and exothermic effects are numbered from the low-temperature end of the differential thermogram. Thus, peak No. 1 corresponds to the endothermic transition from dihydrate to hemihydrate, peak No. 2 to the endothermic transition from hemihydrate to soluble anhydrite, peaks Nos. 3 and 4 to further endothermic transitions to be discussed below, and peak No. 5 to the exothermic transition to insoluble anhydrite.

Natural Gypsums

The results shown in Table II are typical of the various samples studied. These data

TABLE II

Peak temperatures in the differential thermograms of selenite (Windsor, N.S.)

Particle size	Concn. (%)	Heating rate (°C min^{-1})	Final temp. (°C)	Endotherm peak temperature (°C)				Exotherm peak temperature (°C)
				No. 1	No. 2	No. 3	No. 4	No. 5
60–80 mesh	20	3	190	147	161	170	—	—
−325 mesh	10	3	180	124	140	155	—	—
−325 mesh	20	3	177	135	157	170	—	—
−325 mesh	20	3	197	137	158	169	—	—
−325 mesh	20	12	500	157	189	202	300	410
−325 mesh	100	3	215	144	191	202	—	—

show that the reproducibility of peak temperatures at constant concentration and heating rate was satisfactory, and that peak temperatures were displaced upwards when sample concentration, heating rate, or particle size was increased.

Representative results for the various natural forms of calcium sulphate studied are given in Table III and some typical differential thermograms are shown in Fig. 1. Small

TABLE III

Peak temperatures in the differential thermograms of natural forms of calcium sulphate dihydrate

Sample	Concn. (%)	Heating rate (°C min^{-1})	Final temp. (°C)	Endotherm peak temp. (°C)				Exotherm peak temp. (°C)
				No. 1	No. 2	No. 3	No. 4	No. 5
Alabaster Hillsborough, N.B.	20	3, 12	500	130	149	162	300	395
Alabaster Pomaia, Italy	20	3, 12	500	129	154	169	300	410
Massive gypsum Caledonia, Ont.	20	3, 12	500	131	151	166	310	400
Massive gypsum Grand Rapids, Mich.	20	3, 12	500	129	156	169	300	410
Massive gypsum Halifax County, N.S.	20	3, 12	500	132	151	166	310	390
Massive gypsum Hillsborough, N.B.	20	3, 12	505	126	149	163	300	430
Massive gypsum Nappan, N.S.	20	3, 12	500	126	149	163	310	400
Satinspar Amarillo, Texas	20	3, 12	500	132	155	169	300	410
Satinspar Windsor, N.S.	20	3, 12	500	133	151	165	300	395
Selenite Penfield, N.S.	20	3, 12	500	134	154	169	310	400
Selenite Windsor, N.S.	20	3, 12	500	137	158	169	300	410

differences in the size and shape of peaks may be due to packing of the sample within the block as well as to differences in its dihydrate content. In all cases the samples were heated to about 200° C at 3° C min^{-1}, and at 12° C min^{-1} thereafter to give better definition to the smaller high-temperature peaks. The broken lines in Fig. 1 indicate the region in which the heating rate, and hence the base line, was changing. Independent experiments at both 3° C and 12° C min^{-1} showed no thermal effects occurring in the 200° to 300° C region.

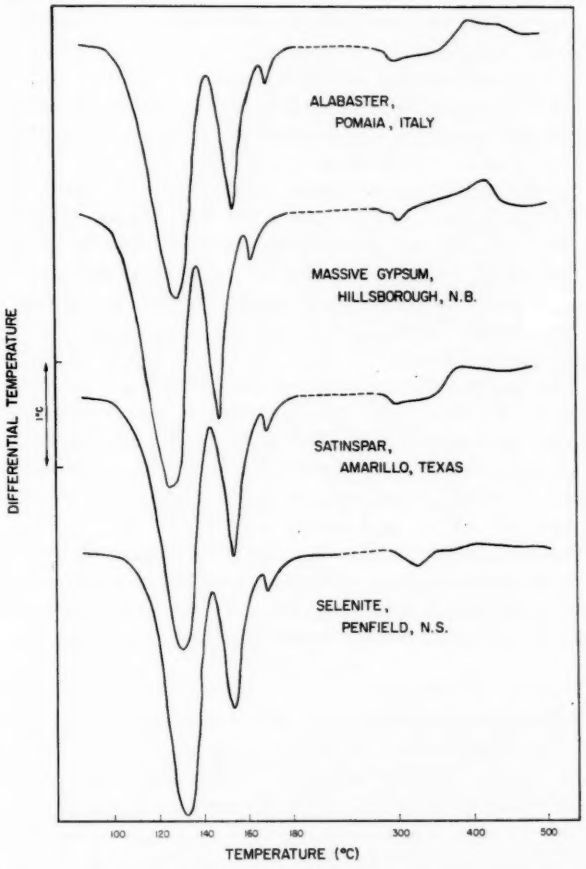

FIG. 1. Differential thermograms of natural calcium sulphate dihydrate.

In addition to the two endothermic peaks below 200° C (Nos. 1 and 2), another endothermic peak (No. 3) was consistently found associated with the dehydration of the hemihydrate (peak No. 2). Although peak No. 3 was observed under all conditions, there was a tendency for it to be masked by the larger peak No. 2 at both higher heating rates and sample concentrations. The occurrence of peak No. 3 was found to be independent of the particle size of the sample, the type or origin of the gypsum (natural or synthetic), the ambient humidity, and the diluent used. The fact that it was found when either

ignited alumina or powdered nickel metal was used as diluent and reference indicates that it is unlikely to be due to any sample–diluent interaction.

When a sample was heated at 12° C min^{-1} a further small endothermic peak (No. 4) was indicated in the vicinity of 300° C, appearing often as a doublet. This effect appeared to be independent of the origin of the sample and the diluent used, and was too small to be detected in samples heated to 500° C at 3° C min^{-1}. It was not possible to isolate this effect further at present.

The exothermic peak (No. 5) was moderately well defined at heating rates of 12° C min^{-1}. Throughout the variety of natural dihydrates studied, it was not possible to obtain large differences in the temperature at which this exothermic effect occurred (2, 3), although the shape of the peak varied between samples.

To ascertain if peak No. 3 could be associated with the transition to insoluble anhydrite, a series of experiments were carried out on samples of a massive gypsum whose differential thermograms had previously been obtained up to 250°, 300°, 350°, and 440° C. Since it is possible to hydrate a soluble anhydrite to the corresponding hemihydrate by moistening it with 80% ethanol and evaporating off the residual liquid (10), whereas if pure water is used the hydration will proceed completely to the dihydrate, these samples were each treated with 80% ethanol, the residual liquid evaporated off at 46° C until a uniform base line was again obtained on the thermogram, and the differential thermogram redetermined. The samples heated initially to 250°, 300°, and 350° C all produced second differential thermograms comparable to their initial ones, except for the absence of peak No. 1, indicating that no dihydrate was formed under the conditions of rehydration. The areas under peaks Nos. 2 and 3 were somewhat reduced and the temperatures corresponding to these peaks were slightly lower than in the initial thermograms, possibly due to changes in particle size and sample porosity resulting from the technique. The sample heated initially to 440° C lacked any peaks in the second differential thermogram, as did a sample heated to 500° C and cooled in a stream of dry nitrogen before the differential thermogram was redetermined. These results support the suggestion that the exothermic peak in the vicinity of 400° C is associated with the soluble to insoluble anhydrite transition (2, 3, 8), so that peak No. 3 occurs well below this temperature and does not appear to be associated with this particular transition.

Synthetic Hydrates

Table IV gives representative results of the differential thermal analysis of synthetic calcium sulphates, the thermograms appearing in Fig. 2. No significant differences between the thermograms of natural and synthetic varieties of calcium sulphate dihydrate were found.

TABLE IV

Peak temperatures in the differential thermograms of synthetic forms of calcium sulphate

Sample	Concn. (%)	Heating rate (°C min^{-1})	Final temp. (°C)	Endotherm peak temp. (°C)				Exotherm peak temp. (°C)
				No. 1	No. 2	No. 3	No. 4	No. 5
$CaSO_4 \cdot 2H_2O$	20	3, 12	500	134	154	169	305	390
$CaSO_4 \cdot \frac{1}{2}H_2O$ (α)	20	3, 12	500	—	156	172	—	177
$CaSO_4 \cdot \frac{1}{2}H_2O$ (β)	20	3, 12	500	—	154	172	310	400

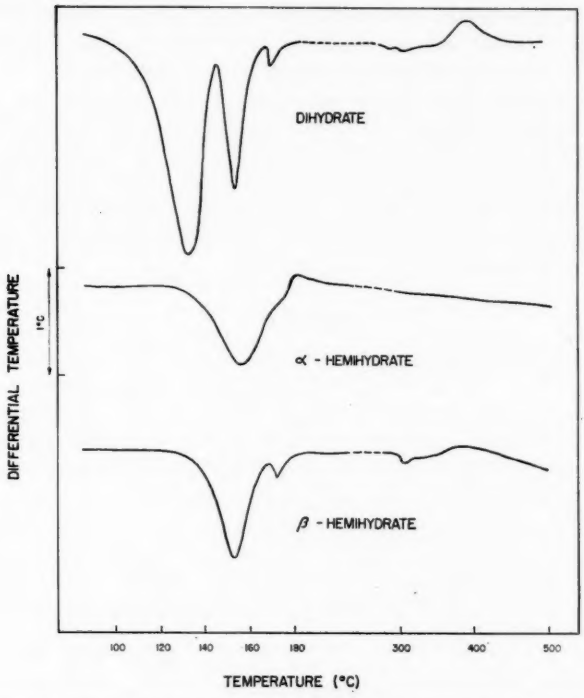

FIG. 2. Differential thermograms of synthetic hydrates of calcium sulphate.

With the α-hemihydrate, endothermic peak No. 3 was found, associated again with peak No. 2, at about the same temperature as in the case of the dihydrate. However, it was very much smaller than for the dihydrate or the β-hemihydrate (Fig. 2), appearing only as a shoulder on the high-temperature side of peak No. 2. An effort to resolve these peaks further at heating rates of the order of 1° C min^{-1} was unsuccessful. There was some indication that endothermic peak No. 4 might be present in the thermograms of α-hemihydrate, but its magnitude approached the sensitivity of the instrument.

The exothermic peak (No. 5) appeared at a considerably lower temperature with the α-hemihydrate than with the dihydrate or the β-hemihydrate, and was smaller and relatively sharper. Samples of α-hemihydrate, heated to 250°, 300°, and 350° C initially, were treated with 80% ethanol as described earlier and second differential thermograms were obtained. The sample initially heated to 250° C showed a small but definite peak No. 2 (transition of hemihydrate to soluble anhydrite) but no evidence of other peaks. The relative magnitudes of peak No. 2 in the first and second thermograms in this case indicated that any other peaks in the second thermogram would be beyond the sensitivity of the instrument. Samples heated initially to 300° and 350° C gave no clear indication of any peaks in the second thermogram. Such behavior would be expected if the α-soluble anhydrite is not completely converted to insoluble anhydrite at the exothermic peak temperature, as reported by Powell (8). Contrary to some reports (4, 5) there seems to be no doubt that this exothermic effect also exists in the case of the α-hemihydrate.

The differential thermogram of the β-hemihydrate closely resembled those of the various dihydrates, both natural and synthetic, indicating that the dehydration of these materials proceeded via the β-series of products as expected (9).

In an effort to identify peak No. 3 more fully, synthetic dihydrate was heated to 190° C, peak No. 3 being recorded at 169° C in this case, and slowly cooled to room temperature in a stream of dry nitrogen. The differential thermogram obtained on reheating this sample gave no indication of any peaks below 200° C suggesting that peak No. 3 is not due to some reversible, temperature-dependent phase change within the dehydrated sample, but rather appears to be associated directly with the loss of water during the dehydration of the hemihydrate.

COMMENT

Peaks Nos. 1 and 2 agree with those already reported in the literature for the dehydration of calcium sulphate dihydrate to hemihydrate and thence to soluble anhydrite at moderate heating rates, and need not be commented on further. Exothermic peak No. 5 has been confirmed as arising from the transition of soluble to insoluble anhydrite, and this process occurs when either α- or β-soluble anhydrite is heated, a much lower temperature being observed in the case of the α-soluble anhydrite.

Of the two further endothermic effects found, peak No. 4 in the vicinity of 300° C appears to be a reality when β-hemihydrate is heated, and not due to instrumentation, although it has not been possible to isolate this effect further. It is uncertain whether the same effect exists when α-hemihydrate is heated, and an instrument of higher sensitivity might resolve this point.

It has been found that the remaining endothermic effect (peak No. 3) cannot be ascribed to some interaction between sample and diluent, and that it is present only under conditions where the hemihydrate and corresponding soluble anhydrite can be interconverted. The transition of the sample to insoluble anhydrite erases both peaks Nos. 2 and 3. Heating of a sample to just above the conclusion of peak No. 3, cooling under anhydrous conditions, and reheating results in the absence of all of the first three endothermic peaks in the second thermogram, independent of the length of the initial heating. It is therefore reasonable to suggest that peak No. 3 is not due to some reversible temperature-dependent phase change occurring in the absence of water vapor within the calcium sulphate lattice.

An attempt has been made to estimate the enthalpy change associated with peak No. 3 by comparison with peak No. 2. The enthalpy change associated with this latter peak was calculated from the data of Kelley *et al.* (9), who consider the first reaction taking place on the dehydration of β-hemihydrate to be

$$CaSO_4 \cdot \tfrac{1}{2}H_2O(\beta)_s = CaSO_4(\beta)^*_s + \tfrac{1}{2}H_2O_g.$$

The product $CaSO_4(\beta)^*$ may contain up to 0.07 mole H_2O, which appear to be considerably more difficult to remove than the remainder of the 0.5 mole H_2O originally present. The corrected enthalpy equation for the above process (9) gives $\Delta H_{427°K} = +7.4$ kcal mole^{-1}. Comparison of areas under peaks Nos. 2 and 3, by means of a compensating planimeter, indicates that on this basis the enthalpy change associated with peak No. 3 is $\Delta H_{445°K} = +0.7$ kcal mole^{-1} $CaSO_4(\beta)^*$, equivalent to about 10 kcal mole^{-1} of residual H_2O.

In the case of the α-hemihydrate, dehydration produces a virtually water-free soluble

anhydrite containing perhaps 0.002 to 0.004 mole H_2O (9). The enthalpy change for the process

$$CaSO_4 \cdot \tfrac{1}{2}H_2O(\alpha)_s = CaSO_4(\alpha)_s + \tfrac{1}{2}H_2O_g$$

is $\Delta H_{427°K} = +6.9$ kcal mole^{-1}. As seen from Fig. 2, the area under peak No. 3 in this case, although too small to estimate with any degree of accuracy, may be roughly an order of magnitude less than in the case of the β-hemihydrate. Since the residual H_2O in the α-soluble anhydrite is also roughly an order of magnitude less than in the $CaSO_4(\beta)$*, it is possible that the enthalpy change associated with peak No. 3, per mole of residual H_2O, is about the same as that in the case of the β-hemihydrate. Thus, it may be speculated that the beginning of release of these last traces of water gives rise to the observed small endothermic effect, and that just as the conversion of soluble to insoluble anhydrite is not completed until temperatures above the end of the exothermic peak associated with this change, so these last traces of water continue to be removed over a wide temperature range as reported by Powell (8).

Another possible explanation for the presence of peak No. 3 might be as a "false peak" similar to those reported by Borchardt and Daniels (11) in the dehydration of several salt hydrates, and due to the vaporization of liquid water released from a previous dehydration reaction. Under this interpretation, peak No. 3 would be due to vaporization of liquid water produced from the dehydration of the hemihydrate (peak No. 2). However, in the cases reported (11) these "false peaks" were of a magnitude comparable to the peak associated with the original dehydration process producing the liquid water and the magnitudes of peaks Nos. 2 and 3 are sufficiently different as to suggest another explanation must be sought for the appearance of peak No. 3.

ACKNOWLEDGMENTS

The authors wish to express their gratitude to Mr. L. J. Chapman, Department of Physiography, Ontario Research Foundation, for placing the required instrumentation at their disposal. Two of them (R. A. K., H. G. M.) also thank Gypsum, Lime and Alabastine, Canada, Ltd., for permission to devote some of their time to the direction of this work.

REFERENCES

1. R. M. Gruver. J. Am. Ceram. Soc. **34**, 353 (1951).
2. J. A. Schedling and J. Wein. Österr. Akd. Wiss. Math. naturw. Kl. Sitzber. Abt. II. **164**, 175 (1955).
3. J. A. Schedling and J. Wein. Acta Phys. Austriaca, **10**, 247 (1956).
4. L. G. Berg and V. N. Sveshnikova. Izvest. Akad. Nauk S.S.S.R., Otdel. Khim. Nauk, 19 (1946).
5. P. P. Budnikov and Z. S. Kosyreva. Voprosy Petrog. i. Mineral. Akad. Nauk S.S.S.R. **2**, 342 (1953).
6. E. S. Newman. J. Research Natl. Bur. Standards, **22**, 191 (1941).
7. W. Grahmann. Z. anorg. Chem. **81**, 257 (1913).
8. D. A. Powell. Nature, **182**, 792 (1958).
9. K. K. Kelley, J. C. Southard, and C. T. Anderson. U.S. Bureau of Mines, Tech. Paper No. 625, 1941.
10. National Gypsum Co., Buffalo, N.Y. Private communication.
11. H. J. Borchardt and F. Daniels. J. Phys. Chem. **61**, 917 (1957).

THE SYNTHESIS OF 2-*O*-β-D-GLUCOPYRANOSYL-D-XYLOSE[1]

J. K. N. JONES AND P. E. REID

ABSTRACT

A synthesis of the disaccharide named in the title is described. Some aspects of the periodate oxidation of this sugar and of analogous sugar derivatives have been examined.

INTRODUCTION

Aldobiouronic acids containing D-glucuronic acid or 4-*O*-methyl-D-glucuronic acid and D-xylose have been isolated from a number of xylans. We are attempting the synthesis of oligosaccharides which may occur in nature and as part of this program we have synthesized 2-*O*-β-D-glucopyranosyl-D-xylose. This compound provides a possible route to the aldobiouronic acid 2-*O*-β-D-glucuronosidyl-D-xylose and its 4-*O*-methyl-D-glucuronosidyl isomer, which have recently been synthesized by Timell and Bowering (1).

3,5-*O*-Isopropylidene-α + β-methyl-D-xylofuranosides were condensed with acetobromglucose (2,3,4,6-tetra-*O*-acetyl-α-D-glucopyranosyl bromide) under standard Koenigs–Knorr conditions (2). After removal of the blocking groups the mixture of monosaccharides and oligosaccharides was fractionated by chromatography on a charcoal column and yielded a white crystalline disaccharide fraction in small yield. The use of argentic oxide (3) instead of the more usual argentous oxide in the Koenigs–Knorr condensation apparently made very little difference to the course of the reaction.

Hydrolysis and paper chromatography of the hydrolyzate showed that the compound contained glucose and xylose only. The theoretical results to be expected from the periodate oxidation of the possible reducing disaccharides containing glucose and xylose where (*a*) xylose is the reducing group and (*b*) the xylose residue has been reduced to a pentitol are shown in Tables I and II. In Table I the assumption is made that the rate-determining steps in the oxidation of the reducing disaccharide are, first, the rate of hydrolysis of the hemiacetal group, which is present in the product of oxidation of the 1,2-linked disaccharide, and, second, the rate of hydrolysis of any formyl esters produced.

TABLE I

Oxidation at acid pH – unbuffered conditions

Linkage	Moles of periodate taken up per mole of disaccharide	Moles of formic acid (as free acid) released per mole of disaccharide	Moles of formic acid per mole disaccharide as formyl ester	Overoxidation expected
1 → 2	3	1	—	Yes
1 → 3	3	1	1	Yes (see ref. 7)
1 → 4	4	2	1	No
1 → 5	4	2	1	No

Periodate oxidation of the disaccharide at 4° C proceeded rapidly and at 20 hours the periodate consumption was 5.4 moles and the formic acid released 4.1 moles. When the results obtained were plotted graphically and the flattened portion of the curve extrapolated to zero time the results obtained were 3.07±.13 moles of sodium metaperiodate consumed and 1.09±.11 moles of formic acid released per mole of disaccharide.

[1]*Manuscript received December 1, 1959.*
Contribution from the Department of Chemistry, Queen's University, Kingston, Ontario.

TABLE II

Oxidation at acid pH – unbuffered conditions

Linkage	Moles of periodate consumed per mole of disaccharide	Moles of formic acid released per mole disaccharide	Overoxidation expected
1 → 2	4	2	No
1 → 3	4	1	Yes
1 → 4	4	2	No
1 → 5	5	3	No

When the oxidation was carried out at 23°±2° C the oxidation was extremely rapid in the initial stages. After 3 hours 5 moles of periodate was consumed and 2.85 moles of formic acid was released, while after 20 hours the totals were 7.15 moles periodate consumed and 5.35 moles of formic acid released. It was evident that in both these cases extensive overoxidation had occurred. Overoxidation is known to occur with 1 → 2 linked disaccharides (4, 5). For example, periodate oxidation of 2-*O*-α-D-glucopyranosyl-D-glucose (5) resulted in a periodate uptake of 6.1 moles of periodate and a formic acid yield of 3.1 moles per mole after 22 hours at room temperature.

From Table I it will be seen that a 1 → 2 linked disaccharide should take up 3 moles of periodate and produce 1 mole of formic acid providing the first assumption is correct. To test this the periodate oxidation of 2-*O*-methyl-D-xylose and 2-*O*-β-D-glucopyranosyl-D-glucose* as models for 2-*O*-β-D-glucopyranosyl-D-xylose was examined.

Schwarz and MacDougall (6) have investigated the periodate oxidation of 2-*O*-benzyl-D-arabinose at 15–18° C. They found that the oxidation proceeded in three stages. One mole of periodate was consumed rapidly (ca. 5 minutes) and after 14 hours the uptake was 4 moles of periodate, oxidation then proceeded slowly. The fact that they were able to isolate benzyloxymalondialdehyde from the reaction mixture after 5 minutes suggests that the hydrolysis of the intermediary hemiacetal must be rapid. Mitchell (6*a*) has examined the periodate oxidation of 2-*O*-methyl-D-arabinose at 5° C and has isolated after a short time interval of oxidation the bisphenyl hydrazone of methoxymalondialdehyde. Methyl glyoxylate and glycollic aldehyde were also detected as products of oxidation. This work indicates that the hydrolysis of the hemiacetal is rapid and that overoxidation of methoxymalondialdehyde then occurs, as would be expected from the results of Schwarz and MacDougall (6).

Periodate oxidation of 2-*O*-methyl-D-xylose at 4° C was initially rapid and then became slow: 1.28 moles per mole (25 minutes); 3.1 moles (12 hours). The release of formic acid was relatively slow, 0.23 mole per mole (25 minutes); 1.1 moles (12 hours). These results are explicable on the basis of rapid hydrolysis of the hemiacetal linkage followed by oxidation of the glycollic aldehyde and methoxymalondialdehyde so formed (7, 8).

When the oxidation was carried out at 23°±2° C there was a rapid initial uptake of periodate and release of formic acid followed by a slower oxidation. (Periodate uptake: 0.9 mole (5 minutes); 3.4 moles (25.5 hours). Formic acid released: 0.22 mole (5 minutes); 2.02 moles (25.5 hours).) The high apparent yield of formic acid is not readily explicable on the basis of the above mechanism. If the rate of hydrolysis of the hemiacetal is a rate-limiting step it might be expected that a break in the rate curve would occur such that extrapolation to zero time would, in the case of 2-*O*-methyl-D-xylose, give a consumption of 1 mole of periodate and a release of no formic acid. When the figures obtained

*The authors thank Professors A. Thompson and M. L. Wolfrom for a gift of this material.

were plotted graphically no such results were obtained. Similarly 2-*O*-β-D-glucopyranosyl-D-glucose would be expected to take up 3 moles of periodate and release 1 mole of formic acid. However, this result was not obtained when the experimental results were plotted graphically. In agreement with previous results (4, 5) extensive overoxidation was observed.

These results indicate that the rate of the hydrolysis of the hemiacetal is rapid and that the satisfactory results obtained from the extrapolation to zero time in the case of the oxidation of the disaccharide must be viewed with caution and indeed are probably fortuitous, particularly as the apparent final quantity of formic acid produced is higher than would be expected from the apparent periodate consumption (6). A substituted malondialdehyde would be expected to neutralize 1 mole of alkali.

Nevertheless the results of the periodate oxidations follow the same pattern as those expected of a synthetic 2-*O*-β-D-glucopyranosyl-D-xylose.

Table I shows that the disaccharides expected to overoxidize are those containing $1 \rightarrow 2$ and $1 \rightarrow 3$ linkages. The absence of a $1 \rightarrow 3$ type linkage in the synthetic disaccharide is indicated because 3-*O*-β-D-glucopyranosyl-D-xylose has been synthesized (7) and the physical constants differ from those of the synthetic disaccharide reported here.

Table II shows that a reduced $1 \rightarrow 2$ linked disaccharide on reduction followed by periodate oxidation would be expected to take up 4 moles of periodate and to release 2 moles of formic acid. The results actually obtained (periodate consumption: 4.05 moles; formic acid released: 2.15 moles) are in good agreement with those expected from theoretical considerations. Observed overoxidation was very low.

Periodate oxidation of 2-*O*-methyl-D-xylitol as a model for the oxidation of the reduced disaccharide resulted in the consumption of 1.97 moles of periodate and the release of 0.92 mole of formic acid. No overoxidation was observed. This result is in good agreement with theoretical predictions (periodate consumption: 2 moles; formic acid released: 1 mole).

Table II indicates that a $1 \rightarrow 4$ linked disaccharide would be expected to give the same result as a $1 \rightarrow 2$ linked compound, but since the $1 \rightarrow 4$ linked compound does not overoxidize when in a non-reduced form it is distinguished from a $1 \rightarrow 2$ linked compound.

EXPERIMENTAL

Optical rotations were measured in water at 23°±2° C and in water unless otherwise indicated. Solutions were concentrated at reduced pressure below 50° C. The following solvent systems were used to separate sugars on paper chromatograms: (*a*) ethyl acetate, acetic acid, formic acid, water (18:3:1:4); (*b*) butan-1-ol, ethanol, water (3:1:1); and (*c*) butan-1-ol, pyridine, water (10:3:3) (all volume/volume).

Reducing sugars were detected with the *p*-anisidine spray (9) and non-reducing sugars were detected by the alkaline silver nitrate spray (10). Rates of movement of sugars on paper chromatograms are quoted relative to the rate of movement of D-galactose (R_{gal}).

Acetobrom-glucose (2,3,4,6-Tetra-O-acetyl-α-D-glucopyranosyl Bromide)

This was prepared by the method of Barczai-Martos and Korosy (11). 3,4-*O*-Isopropylidene methyl-α + β-D-xylosides were prepared by the methods of Baker, Schaub, and Williams (12).

Condensation of Acetobrom-glucose and 3,5-O-Isopropylidene-methyl-α + β-D-xyloside

3,4-*O*-Isopropylidene methyl-α + β-D-xylosides (11.1 g) in pure dry chloroform (170 ml) was shaken for 30 minutes with Drierite (67.5 g), glass beads (51 g), argentic oxide (33.75 g), and iodine (3.38 g). Acetobrom-glucose (48 g) in pure dry chloroform (142 ml) was then added and the mixture shaken until a test for ionizable bromine was negative. The mixture was shaken for a further 2 days and filtered, and the filtrate concentrated to a syrup. The syrup was boiled under reflux with methanolic sodium hydroxide (400 ml) (4% w/v) for 3 hours and the cations removed by passage down a bed of Amberlite IR-120 (H-form) ion exchange resin. The resulting acidic solution was heated at 70–80° C for 5 hours, cooled, deionized by passage down a bed of Duolite A4 (OH-form) ion exchange resin, and concentrated to a syrup (14 g). Chromatography (solvent (*a*)) indicated the presence of glucose, xylose, a red spot R_{gal} 0.55, and a trace of yellow spot, R_{gal} 0.142. The syrup was dissolved in water and fractionated on a column of charcoal (Darco-G-60). Elution with water (2 l.) removed all the monosaccharides and the disaccharide was recovered by elution with varying concentrations of alcohol up to 50%. The solution was concentrated to a syrup (2 g). Attempts to prepare a crystalline acetate were unsuccessful. The syrup (1.4 g) was set aside when it crystallized in part. The crystalline material was recrystallized from a mixture of methanol and butan-1-ol and ran as a single discrete spot in solvents (*a*), (*b*), and (*c*). Microanalysis of this compound indicated the presence of ash (5%) and the results of the periodate oxidations carried out on this sample have been adjusted accordingly. The material was dissolved in water, the solution deionized by use of IR 120 (H-form) and IR-45 (OH-form) Amberlite ion exchange resins, concentrated, and the residue dissolved in boiling ethanol. The crystalline material so obtained had a melting point of 200°–202° C, $[\alpha]_D$ ±0° (equil.). Calc. for $C_{11}H_{20}O_{10}$: C, 42.3%; H, 6.4%. Found: C, 42.51%; H, 6.56%. The infrared spectrum was determined in potassium bromide at 0.4% concentration. The spectrum showed the following absorption maxima recorded as frequency cm^{-1}: 3340 (s), 2900 (m), 2860 (m), 1410 (m), 1385 (m), 1360 (m), 1345 (m), 1300 (w), 1280 (m), 1260 (m), 1230 (m), 1163 (m), 1143 (m), 1105 (s), 1078 (s), 1030 (s), 930 (w), 915 (m), 900 (m), 800 (m), 755 (w), 715 (w), 650 (w). (Intensity: s = strong, m = medium, w = weak.)

Hydrolysis of Disaccharide

The disaccharide (10 mg) was hydrolyzed with sulphuric acid (*N*) in a sealed tube for 11 hours at 100°. The hydrolyzate was neutralized with barium carbonate, filtered, and passed down a small bed of IR 120 (OH-form) ion exchange resin, and then concentrated to a syrup. Chromatographic examination in solvent (*a*) indicated the presence of glucose and xylose only.

Preparation of the Reduced Disaccharide

The disaccharide (18.2 mg) was dissolved in water (10 ml) and sodium borohydride (37 mg) was added. After 24 hours the solution was acidified with glacial acetic acid passed through a bed of IR 120 (H-form) Amberlite ion exchange resin and concentrated to a syrup. Boric acid was removed as methyl borate by codistillation with methanol (×20) and the residual syrup was dried over phosphorus pentoxide under reduced pressure (yield, 17.5 mg). Chromatographic examination in solvent (2) indicated the absence of reducing sugar (no reaction was observed with the *p*-anisidine hydrochloride spray). When the chromatogram was sprayed with alkaline silver nitrate a positive reaction resulted indicating the disaccharide had been reduced to the D-xylitol derivative.

Preparation of 2-O-Methyl-D-xylitol

2-*O*-Methyl-D-xylitol was prepared by the reduction of 2-*O*-methyl-D-xylose by the same procedure as described above.

Periodate Oxidations

The periodate oxidations of 2-*O*-methyl-D-xylose and 2-*O*-β-D-glucopyranosyl-D-glucose were carried out on accurately weighed samples (ca. 10 mg) with 0.3 *M* sodium metaperiodate (2 ml) made up to 25 ml with distilled water. The reactions were carried out in the dark at room temperature or at 4° C. Aliquots (1 ml) were used for analysis. The periodate was estimated by the method of Neumüller and Vasseur (13). The formic acid by that of Andrews *et al.* (14).

Oxidation of 2-O-Methyl-D-xylose

Moles of periodate consumed and moles of formic acid produced per mole at stated time intervals *at 4° C*: 0.67, 0.045 (10 minutes); 1.28, 0.23 (25 minutes); 2.25, 0.27 (1 hour); 2.47, 0.36 (2 hours); 2.67, 0.43 (4 hours); 2.92, 0.82 (6 hours, 10 minutes); 3.1, 1.1 (12 hours).

At room temperature (ca. 20° C): 0.84, 0.072 (5 minutes); 1.24, 0.072 (10 minutes); 1.75, 0.192 (20 minutes); 1.75, 0.51 (40 minutes); 2.39, 1.20 (2 hours); 2.69, 1.75 (3 hours); 3.02, 1.99 (7.5 hours); 3.1, 1.99 (15 hours); 3.22, 2.03 (28 hours).

Oxidation of 2-O-β-D-Glucopyranosyl-D-glucose

Moles of periodate consumed and formic acid produced at the time intervals stated at 4° C: 0.26, 0.07 (15 minutes); 0.75, 0.2 (30 minutes); 1.72, 0.46 (1 hour); 2.14, 0.57 (3 hours); 2.32, 0.62 (5 hours); 2.75, 1.02 (8 hours); 3.16, 1.08 (10 hours); 4.2, 1.92 (24 hours); 4.9, 2.04 (27 hours).

Oxidation of 2-O-β-D-Glucopyranosyl-D-xylose

Oxidations were carried on accurately weighed samples (ca. 10 mg) with 0.3 *M* sodium metaperiodate (1 ml made up to 10 ml with distilled water). Moles of periodate consumed and moles of formic acid released at stated time intervals *at room temperature*: 3.38, 0.75 (30 minutes); 3.82, 1.54 (1.5 hours); 5.07, 2.88 (3 hours); 6.35, 4.7 (7 hours); 7.15, 5.35 (20 hours).

At 4° C: 1.35, 0.75 (30 minutes); 2.4, 1.0 (1 hour); 2.7, — (2 hours); 3.0, 1.6 (3 hours); 3.25, 1.6 (4 hours); 3.7, 1.6 (5 hours); 3.95, — (3.95 hours); 5.4, — (21 hours); and 4.1, — (20 hours).

The periodate oxidations of the reduced disaccharide and of 2-*O*-methyl-D-xylose were carried out on weighed samples (ca. 10 mg) as described above.

Reduced Disaccharide

Moles of periodate consumed and moles of formic acid produced at the time intervals stated: 2.38, 1.15 (20 minutes); 2.7, — (40 minutes); 2.7, 1.15 (1 hour); 3.18, 1.6 (2 hours, 10 minutes); 3.82, 1.6 (3 hours, 10 minutes); 3.93, 1.6 (4 hours, 10 minutes); 4.27, 2.3 (5 hours); 4.45, 2.6 (21 hours).

2-O-Methyl-D-xylitol

Periodate consumption and moles of formic acid produced at the time intervals stated: 1.83, 0.78 (10 minutes); 2.02, 0.82 (30 minutes); 2.01, 0.92 (60 minutes); 2.02, 0.88 (165 minutes); 2.02, 0.92 (540 minutes).

ACKNOWLEDGMENTS

The authors thank the National Research Council of Canada and the Ontario Research Foundation for financial assistance.

REFERENCES

1. T. E. TIMELL and W. D. S. BOWERING. Am. Chem. Soc. 136th Meeting, Atlantic City, September, 1959.
2. W. KOENIGS and E. KNORR. Ber. **34**, 957 (1901).
3. INORG. SYNTHESES, **4**, 12 (1953).
4. A. J. CHARLSON and A. S. PERLIN. Can. J. Chem. **34**, 1805 (1956).
5. R. W. BAILEY, S. A. BARKER, E. Y. BOURNE, P. M. GRANT, and M. STACEY. J. Chem. Soc. 1895 (1958).
6. J. C. P. SCHWARZ and M. MACDOUGALL. J. Chem. Soc. 3065 (1956).
6*a*. P. W. D. MITCHELL. Proc. Roy. Irish Acad. B, **59**, 43 (1958).
7. A. R. ARCHIBALD, D. J. MANNERS, and J. L. THOMPSON. Biochem. J. **73**, 295 (1959).
8. J. C. P. SCHWARZ. Chem. & Ind. (London), 1000 (1954).
9. L. HOUGH, J. K. N. JONES, and W. H. WADMAN. J. Chem. Soc. 1702 (1950).
10. W. E. TREVELYAN, D. D. PROCTOR, and J. S. HARRISON. Nature, **166**, 444 (1950).
11. M. BÁRCZAI-MARTOS and F. KŐRÖSY. Nature, **165**, 369 (1950).
12. B. R. BAKER, R. E. SCHAUB, and J. H. WILLIAMS. J. Am. Chem. Soc. **77**, 9 (1955).
13. G. NEUMÜLLER and E. VASSEUR. Arkiv Kemi, **2**, 235 (1953).
14. P. ANDREWS, L. HOUGH, and J. K. N. JONES. J. Chem. Soc. 806 (1959).

GRISEOVIRIDIN: THE C_6 FRAGMENT[1]

P. DE MAYO[2] AND A. STOESSL

ABSTRACT

The structure of a hydrolytic degradation product from griseoviridin, isolated as the 2,4-dinitrophenylhydrazone, has been shown, by synthesis, to be IV. A by-product of the synthesis was the stereoisomeric 2,4-dinitrophenylhydrazone. This establishes IX as a part structure of griseoviridin. Evidence is provided that the previously proposed structural environment of the sulphur atom is incorrect, and that the sulphur may, in fact, be attached to the C_6 fragment.

The antibiotic griseoviridin, isolated from cultures of a strain of *Streptomyces griseus* (1) has been studied by Ames, Bowman, and their collaborators (2, 3, 4), who were able to establish the empirical formula $C_{22}H_{29\pm2}O_7N_3S$. In their extended investigations they provided evidence for the presence, in this molecule, of three moieties.

First, the existence of a C_{10} fragment was established by the isolation, after reduction and hydrolysis, of ω-amino-decanoic acid. For this portion of the molecule the part structure I was tentatively proposed (4). Secondly, they showed by hydrolysis the presence of two alanine residues (4) in octahydrodesthiogriseoviridin diacetate, a reduced substance from which the sulphur had been removed by Raney nickel. Griseoviridin itself, on the other hand, gave no alanine on hydrolysis, but yielded cystine and some serine together with 1 mole ammonia. From this and other evidence, they deduced the part structure II, the sulphur being part of a ring since removal of the sulphur did not cause the disruption of the molecule. Finally some indication of the disposition of the remaining carbon atoms was obtained from the following experiments (3).

Ozonolysis of griseoviridin (or its diacetate) followed by decomposition of the ozonide and mild treatment with acid or base and steam distillation gave crotonaldehyde, characterized as its 2,4-dinitrophenylhydrazone. The hydrochloride,[3] obtained from griseoviridin by the action of concentrated hydrochloric acid, in contrast, gave crotonaldehyde *directly* after ozonolysis, whilst hexahydrogriseoviridin diacetate gave no aldehyde at all. The facts were construed to indicate the part structure III.

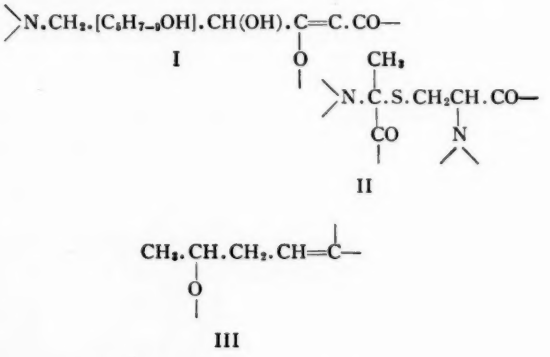

I

II

III

[1]*Manuscript received February 9, 1960.*
Contribution from the Departments of Chemistry, Imperial College, London, S.W.7, England, and the University, Glasgow, Scotland.
[2]*Present address: Department of Chemistry, University of Western Ontario, London, Ontario.*
[3]*The hydrochloride was reported to have an anomalous analysis. Satisfactory analyses for it, and derivatives, are reported in the Experimental section.*

Such formulations accounted for all but one of the 22 carbon atoms in griseoviridin, and since some evidence, derived from infrared spectra, was adduced for the presence of a diacylimide the remaining carbon atom was conjecturally attached to the fragment represented by III. The present communication is mainly concerned with this fragment.

Although griseoviridin itself does not yield a 2,4-dinitrophenylhydrazone, Ames and Bowman (3) reported that after acid hydrolysis such a derivative, $C_{14}H_{14}O_7N_4$, was obtained, corresponding to a fragment $C_8H_{10}O_3$. Re-examination of this substance, purified by chromatography on bentonite–celite, showed that it had, in fact, the formula $C_{12}H_{12}O_6N_4$, corresponding to a derivative of a compound $C_6H_8O_3$. The material was optically active and so contained at least one asymmetric carbon, whilst Kuhn–Roth oxidation indicated the presence of one C-methyl group. The ultraviolet spectrum (λ_{max} 365 mμ) suggested the derivative of a saturated ketone and precluded the presence of any other high intensity chromophore in the molecule. The infrared spectrum, however, showed a band at 1680 cm^{-1} to be attributed to a remaining carbonyl function. Since the empirical formula required the presence, in the original substance, of three double-bond equivalents, and, since the remaining oxygen was not a hydroxyl group, a cyclic structure seemed inevitable. Bearing in mind the implications of the part structure III the formulation IV appeared attractive. Such a structure with the appropriate geometry would, by hydrogen bonding and conjugation, be expected to lower the normal δ-lactone frequency to that actually found. Furthermore, a band at 3154 cm^{-1}, to be attributed to the N—H stretch, was lower, as would be expected for hydrogen bonding, than is usual for such bonds in these derivatives: the accepted region is in the vicinity of 3300 cm^{-1}. Since the amounts of material available did not allow of chemical degradation the racemate of IV was, accordingly, synthesized by the following steps.

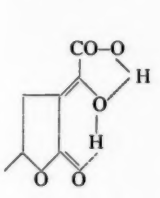

V

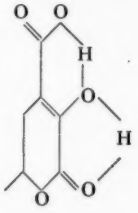

VI

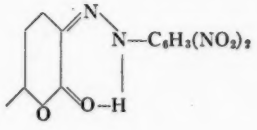

IV

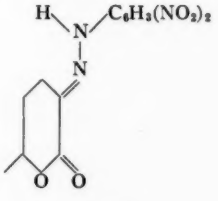

VIII

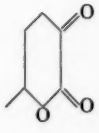

VII*a*

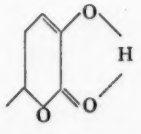

VII*b*

γ-Valerolactone was condensed with ethyl oxalate to give, after hydrolysis, an acid, $C_7H_8O_5$, corresponding to one or more of the tautomers of V or VI. It liberated carbon dioxide from sodium hydrogen carbonate, titrated as a monobasic acid, and gave an intense purple color with ferric chloride.

The acid was decarboxylated (with the evolution of one molecule of carbon dioxide) to give VII*a*, $C_6H_8O_3$, which appeared to exist largely as the enol (VII*b*). This substance also titrated sharply as a monobasic acid, and although it could be obtained pure by recrystallization after sublimation it rapidly decomposed on exposure to air, as do the corresponding γ-lactones (5).

The preparation of the 2,4-dinitrophenylhydrazone was accomplished in the usual way, the acidic material isolated then being cyclized to the lactone by refluxing in chloroform. Chromatography on bentonite–celite then afforded racemic IV, m.p. 230–231°. The ultraviolet spectrum, and the infrared spectra, both in chloroform and methylene dichloride solution, were superposable on that of IV from hydrolytic degradation.

Concomitant with the formation of IV, a second, isomeric, 2,4-dinitrophenylhydrazone was isolated. This absorbed at somewhat shorter wavelength in the ultraviolet, and, in the infrared spectrum showed bands at 3300 (free N—H) and 1724 cm^{-1}. This substance is accordingly attributed the structure VIII. Such pairs of isomers have been previously separated and our interpretation has ample analogy (6).

The structural identification of IV indicated the presence, in griseoviridin, of the six-carbon fragment (IX) which, with I and II, or their equivalents, accounts for all the carbon atoms. The formulation (IX) is supported by the fact that whilst both griseoviridin and hexahydrodeoxygriseoviridin (obtained by hydrogenation of the hydrochloride) give iodoform (35 and 48% respectively) when treated with iodine and base, griseoviridin gives acetaldehyde merely on refluxing with 4 *N* sodium hydroxide. This process, presumably involving a dealdolization, occurs also in the hydrochloride but not in the reduced hydrochloride where one of the requisite structural features, the double bond, is no longer present as is shown by the non-formation of crotonaldehyde on ozonolysis. Formic and acetic acids are formed, in addition to acetaldehyde, in the hydrolysis of griseoviridin.

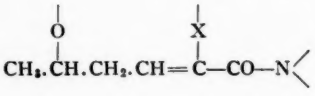

IX

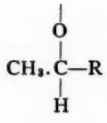

X

The atom (X) in IX may be oxygen, or, less probably, nitrogen. Evidence is available that, in fact, sulphur cannot be excluded and that the part structure II is incorrect. First, Kuhn–Roth oxidation of griseoviridin suggests (2) the presence of 1 C—Me group which is surely that present in IX. Secondly, the n.m.r. spectrum in deuterochloroform of griseoviridin diacetate and several other derivatives showed a doublet at 8.55 p.p.m. (relative to tetramethylsilane as 10) ($J \sim 7$ c.p.s.) attributable to the system X: no other bands (other than acetate) attributable to C—Me could be detected. We are much indebted to Dr. L. M. Jackman for the determination of these spectra.

Finally although modification of II to XI would circumvent these difficulties, evidence is available that the situation is more subtle. Thus, griseoviridin reacts with perbenzoic acid (2) to give an "oxide" which does not show sulphone bands in the infrared (7) and which gives cystine and traces of serine on acid hydrolysis, as does griseoviridin itself.

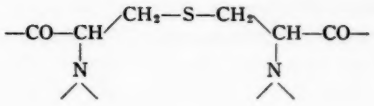

XI

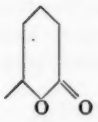

XII

Since sulphides are, in general, rapidly oxidized by peracids this observation appears incompatible with II or XI. But, by contrast, hexahydrodeoxygriseoviridin rapidly gives a sulphone further characterized by a number of derivatives. The implication is, therefore, that reduction or hydrogenolysis in the vicinity of the sulphur atom renders it open to oxidation, a fact not readily interpretable in terms of II and XI. If the sulphur is not assigned to the two alanine molecules it then becomes available for inclusion in part formula IX. Consistent with this is the fact that basic hydrolysis of octahydrodethiogriseoviridin diacetate readily affords δ-caprolactone (XII) whereas hexahydrodeoxygriseoviridin, in which the sulphur link remains, does not. In this case some second hydrogenolysable function is required to mask the second potential alanine moiety.

EXPERIMENTAL

Melting points were taken on the Kofler Hot Stage. Rotations were determined in chloroform and ultraviolet spectra in 95% ethanol. Except where otherwise indicated the phrase 'petroleum ether' refers to the fraction of boiling range 60–80°; unless otherwise stated infrared spectra were determined as Nujol mulls.

Preparation of the 2,4-Dinitrophenylhydrazone (IV)

Griseoviridin (200 mg) was hydrolyzed with 6 *N* hydrochloric acid and the crude 2,4-dinitrophenylhydrazone was prepared as described by Ames and Bowman (3). The crude, dried product (40 mg) was dissolved in chloroform and applied to a short column of bentonite–celite (1:1 by volume). Elution with ethanol–chloroform (1:6) gave, after evaporation and crystallization from ethanol–chloroform, the almost pure 2,4-dinitrophenylhydrazone (7.6 mg), m.p. 223–226° (Ames and Bowman record 220–222°), $[\alpha]_D$ +84 (*c*, 0.20); λ_{max} 258, 365 mμ and log ε 3.91 and 4.35 respectively. The compound has maxima in the infrared at 3154, 3090, 1680, and 1615 cm^{-1}. Found: C, 46.78%; H, 4.12%; N, 18.09%; C—Me, 4.38%. $C_{12}H_{12}N_4O_6$ requires: C, 46.75%; H, 3.92%; N, 18.18%; C—Me, (1), 4.88%.

2-Oxalyl-γ-valerolactone

A mixture of diethyl oxalate (100 ml) and γ-valerolactone (10 g) was added to a solution of sodium (2.3 g) in absolute ethanol (40 ml) and the mixture heated under reduced pressure (10 cm Hg) at 55° for 1 hour, the pressure lowered (2 cm Hg), and heating continued for a further 2 hours. After the mixture was cooled the precipitated solid was collected, washed with ether, and just acidified with *N* hydrochloric acid. Extraction with ether and evaporation under reduced pressure then gave the crude required, 2-oxalyl-γ-valerolactone (16.2 g).

The crude ester (8.0 g) was dissolved in sodium hydroxide solution (125 ml, 1.1 *N* NaOH) and set aside overnight. Acidification followed by repeated extraction with ether gave the crude lactone (5.9 g). Crystallization from ether, extraction with benzene to remove small amounts of oxalic acid, and recrystallization from carbon tetrachloride gave the γ-lactone, m.p. 93–102° (variable, dependent on rate of heating and solvent).

Found: C, 48.7%; H, 4.80%; equiv. 90. $C_7H_8O_5$ requires: C, 48.85%; H, 4.69%; equiv. 86. The substance had λ_{max} 276 mμ (log ϵ 3.54) and bands in the infrared at 3546, 3460, 3300, 1718, 1698, 1669, and 1631 cm^{-1}.

2-Oxo-δ-caprolactone

The γ-lactone (840 mg) was refluxed in water for 2 hours. The solution was then cooled and evaporated under reduced pressure at 40° to give a yellow oil (760 mg) which crystallized after sublimation. The crystals liquefied after brief exposure to the atmosphere, but could be purified by crystallization from petroleum ether to give the δ-lactone, m.p. 56–59°. Found: C, 56.18%; H, 6.33%; equiv. 130. $C_6H_8O_3$ requires: C, 56.24%; H, 6.29%; equiv. 128. The substance had λ_{max} 256 mμ (log ϵ 3.70) (neutral) and λ_{max} 246 (log ϵ 3.64) (.001 *N* NaOH), and bands in the infrared spectrum at 3068, 1675 (broad), and 1613 cm^{-1}.

The 2,4-Dinitrophenylhydrazones of (±)-2-Oxo-1,5-hexanolide

The δ-lactone (400 mg) in water (25 ml) was added to 2,4-dinitrophenylhydrazone (1.2 g) in sulphuric acid (10 ml) and water (75 ml). After 24 hours the precipitate formed was extracted into chloroform containing 10% ethanol, and the acidic material isolated, in the usual manner, by extraction with a saturated solution of sodium hydrogen carbonate (100 ml), followed by acidification and re-extraction with chloroform. Evaporation gave the crude acid (733 mg) which was cyclized by refluxing in chloroform and partial removal of solvent by distillation. After removal of acidic contaminants with sodium hydrogen carbonate solution the remaining neutral material (305 mg) was crystallized from benzene to give fraction A (90 mg). This was retained. The mother liquors were added to a bentonite (10 g) – celite column (equal volumes). Elution with ethyl acetate – benzene (1:9) gave fraction B, whilst ethanol – ethyl acetate (1:9) gave material identical with fraction A.

(*a*) The trans (±)-2,4-dinitrophenylhydrazone was obtained by crystallization of fraction A from benzene. It melted unsharply at 200–210°, but the ultraviolet spectrum and melting point were unchanged on repeated crystallization. Found: C, 47.01%; H, 4.15%; N, 17.96%. $C_{12}H_{12}N_4O_6$ requires: C, 46.75%; H, 3.92%; N, 18.18%. The compound had λ_{max} 255, 350 mμ; log ϵ 4.38 and 3.90 respectively.

(*b*) The cis (±)-2,4-dinitrophenylhydrazone was obtained by crystallization of fraction B from ethanol–chloroform and from benzene, m.p. 230–231°. Found: C, 46.96%; H, 4.08%; N, 18.36%. The infrared spectrum in chloroform and methylene dichloride were superposable on that of the active material.

The Hydrolysis of Griseoviridin

(*a*) A solution of griseoviridin (505 mg) in aqueous sodium hydroxide (4 *N*, 50 ml) was distilled at constant volume in a nitrogen atmosphere, the distillate being collected in an aqueous sulphuric acid solution of 2,4-dinitrophenylhydrazone. The precipitate was collected (176 mg) and the absorption curve in the ultraviolet accurately paralleled that of the acetaldehyde derivative, indicating the absence of any crotonaldehyde. Chromatography of the crude product or alumina (Brockman Grade III, 20 g) gave, on elution with benzene – petroleum ether (1:5) followed by crystallization from methanol–chloroform, acetaldehyde 2,4-dinitrophenylhydrazone, melting point and melting point on admixture with an authentic specimen of the same melting point, 163–166°.

(*b*) The alkaline hydrolyzate was acidified with 6 *N* sulphuric acid, the gummy precipitate removed by filtration, and the volatile acids isolated by distillation at constant

volume under nitrogen. Qualitative paper chromatography showed the presence of both acetic and formic acids. Treatment after concentration to 20 ml of an aliquot (150 ml of a total of 250) at room temperature with sodium hydrogen carbonate (1 g) and a few drops of bromine (8) destroyed the formic acid and after removal of the excess bromine in a stream of air the aqueous acid was distilled. Titration showed the presence of 0.4 mole of acid. Paper chromatography confirmed the presence of acetic acid only and identity was confirmed by the infrared spectrum of the residue of sodium acetate on evaporation, and by conversion to *p*-phenyl – phenacyl acetate identical in every respect with an authentic specimen.

In another aliquot (100 ml) the carbon dioxide evolved by oxidation of the formic acid with orange mercuric oxide (250 mg) (9) was collected in barium hydroxide. Titration of the barium carbonate produced indicated the presence in the original solution of 0.9 mol. formic acid. The identity of the acid was confirmed by extraction of the salts (138 mg) from the hydrolysis of griseoviridin (1 g) with 95% ethanol and crystallization from absolute ethanol. The sodium formate so obtained had a melting point of 251–256°; its infrared spectrum could be superimposed on that of an authentic specimen. Found: Na, 34.08%; Calc. for CHO_2Na: Na, 33.81%.

Alkaline Hydrolysis of Octahydrodethiogriseoviridin Diacetate

The diacetate (213 mg) was refluxed in solution in aqueous sodium hydroxide (4 *N*, 20 ml) under nitrogen for 30 minutes. No precipitate was obtained by distillation into 2,4-dinitrophenylhydrazine solution. The hydrolyzate was acidified and distilled at constant volume until the titer was negligible. Addition of excess alkali and backtitration indicated the presence of 0.8 mol. lactone. Repeated extraction of the acidified solution with ether gave, after evaporation, an oil (12 mg) which was distilled at 100°/3 mm to give (+)-δ-caprolactone (5.4 mg), m.p. ca. 15°, $[\alpha]_D$ +39 (*c*, 0.54). The infrared spectrum in chloroform was superposable on that of synthetic (±)-δ-caprolactone, and the two substances behaved in the same way on partition chromatography in a propanol–ammonia system (10).

In another experiment the crude alkaline titration solution was mixed with a solution of chromic acid in 2 *N* sulphuric acid (0.4 *N*, 4 ml) and set aside for 16 hours. The excess oxidant was then destroyed (sulphur dioxide) and the mixture treated with Brady's reagent. The resultant precipitate, after collection, was chromatographed on bentonite–celite (1:1 by volume) the fraction eluted with ethanol–chloroform (1:4) then being crystallized from benzene to give 5-oxocaproic acid 2,4-dinitrophenylhydrazone, m.p. 137–139°, unchanged on admixture with an authentic specimen (11) of the same melting point. The infrared spectra in Nujol mull were superposable.

Hexahydrodeoxygriseoviridin

Griseoviridin hydrochloride was prepared as described by Ames and Bowman. Crystallized from ether–methanol it had $[\alpha]_D$ −177° (*c*, 0.53 in MeOH). Found: C, 50.87%; H, 5.86%; Cl, 7.07%. $C_{22}H_{29}O_7N_3S.HCl$ requires: C, 51.20%; H, 5.86%; Cl, 6.87%.

The hydrochloride (3 g) was hydrogenated in ethanol solution in the presence of palladized charcoal (9 g). The filtered solution was evaporated and the glassy residue was crystallized from ethanol. The product had a melting point of 246–248°, $[\alpha]_D$ −55°. Found: C, 56.62%; H, 6.93%; O, 20.75%; N, 8.92%; S, 6.85%. $C_{22}H_{33}O_6N_3S$ requires: C, 56.49%; H, 7.11%; O, 20.53%; N, 8.99%; S. 6.85%. The substance had λ_{max} 212 mμ (log ε 4.29) in neutral solution. In ethanol containing .01 *N* sodium hydroxide it had λ_{max} 255 mμ (log ε 3.89). No crotonaldehyde was obtained by ozonolysis and distillation.

Hydrolysis with 6 *N* hydrochloric acid and distillation of the residue from citrate buffer and ninhydrin (4) gave no volatile carbonyl compounds. No acetaldehyde was formed on alkaline hydrolysis.

Acetylation (pyridine – acetic anhydride at room temperature) gave the monoacetate which, after crystallization from ethanol, had a melting point of 226–228°. Found: C, 56.92%; H, 7.02%; N, 8.34%; S, 6.11%; $C_{24}H_{35}O_7N_3S$ requires: C, 56.54%; H, 6.92%; N, 8.25%; S, 6.28%. The compound has $[\alpha]_D$ −53° (*c*, 1.89).

Benzoylation (pyridine–benzoyl chloride at room temperature for 4.5 hours) afforded the monobenzoate which, after crystallization from ethanol, had a melting point of 193–196°. Found: C, 61.22%; H, 6.38%; N, 7.25%. $C_{29}H_{37}O_7N_3S$ requires: C, 60.92%; H, 6.52%; N, 7.35%. The compound had λ_{max} 227 mμ (log ε 4.14).

Hexahydrodeoxygriseoviridin Sulphone

The deoxy compound (70 mg) in chloroform (10 ml) was added to a solution of perbenzoic acid in benzene (2 ml, 0.4 *N*) and the mixture was left overnight. The solution was then diluted with chloroform and washed with sodium hydrogen carbonate solution and water, and the solution concentrated to give the sulphone, m.p. 205–220° (dec.) unchanged by repeated crystallization from chloroform–ethanol. Found: C, 52.91%; H, 6.74%; O, 25.32%; N, 8.31%. $C_{22}H_{33}O_8N_3S$ requires: C, 52.87%; H, 6.60%; O, 25.63%; N, 8.41%. In neutral solution it showed λ_{max} 212 mμ (log ε 4.21) λ_{inf} 258 mμ (log ε 3.85). The infrared spectrum showed bands at 1295 and 1126 cm^{-1}. A similar, but quantitative, experiment showed that the uptake of oxidant ceased at 2 moles perbenzoic acid.

Similar oxidation of the monoacetate gave the corresponding sulphone, m.p. 220–230° (from ethanol–chloroform). Found: C, 53.33%; H, 6.59%; O, 26.37%; N, 7.78%. $C_{24}H_{35}O_9N_3S$ requires: C, 53.21%; H, 6.51%; O, 26.59%; N, 7.76%. It had bands in the infrared spectrum at 1290 and 1124 cm^{-1}. This compound was also prepared by acetylation of the sulphone (acetic anhydride – pyridine at room temperature). Oxidation of the benzoate gave the corresponding sulphone, m.p. ca. 200° (from ethanol–chloroform). Found: C, 57.81%; H, 6.38%; N, 6.41%. $C_{29}H_{37}O_9S$ requires: C, 57.70%; H, 6.18%; N, 6.96%. The compound had $[\alpha]_D$ +25 (*c*, 2.0) and showed bands in the infrared at 1294 and 1121 cm^{-1}.

Dehydrohexahydrodeoxygriseoviridin Sulphone

Hexahydrodeoxygriseoviridin sulphone (50 mg) was dissolved in acetic acid (glacial, 5 ml) and a solution of chromic acid in acetic acid (1.05 ml, 0.2 *N*) was added. The mixture was set aside for 5 hours, after which the product was isolated with chloroform. Crystallized from methanol–chloroform the substance had a melting point of approximately 230° (with previous sintering), unchanged by further crystallization. Found: C, 53.37%; H, 6.34%; N, 8.85%. $C_{22}H_{31}O_8N_3S$ requires: C, 53.09%; H, 6.28%; N, 8.44%. The substance in neutral solution had λ_{max} 220 mμ (log ε 4.17) and in .01 *N* ethanolic hydroxide λ_{max} 299 mμ (log ε 4.30). The compound had $[\alpha]_D$ −4° (*c*, 0.85) and showed bands in the infrared at 1709, 1282, and 1119 cm^{-1}.

Iodoform Reaction

Griseoviridin (26 mg) in aqueous potassium hydroxide (10%, 0.5 ml) was warmed until dissolved, cooled to 60°, and iodine – potassium iodide solution added. Iodoform (melting point and mixed melting point with an authentic specimen 119°) (7.2 mg) was isolated equivalent to 0.35 mole per molecule of griseoviridin. A similar experiment on the hexahydrodeoxygriseoviridin gave 0.48 mole iodoform.

ACKNOWLEDGMENTS

We wish to thank Mr. J. M. L. Cameron (Glasgow) and Miss J. Cuckney (Imperial College) and their associates for the microanalyses. We are also very grateful to Dr. R. E. Bowman (Parke, Davis, England) and to Dr. L. M. Long (Parke, Davis, Detroit) for making the material available to us.

REFERENCES

1. Q. R. Bartz *et al.* Second Annual Symposium on Antibiotics, Washington. 1954.
2. D. E. Ames, R. E. Bowman, J. F. Cavalla, and D. D. Evans. J. Chem. Soc. 4260 (1955).
3. D. E. Ames and R. E. Bowman. J. Chem. Soc. 4264 (1955).
4. D. E. Ames and R. E. Bowman. J. Chem. Soc. 2925 (1956).
5. H. Schinz and M. Hinder. Helv. Chim. Acta, **30**, 1349 (1947).
6. F. A. Isherwood and R. L. Jones. Nature, **175**, 419 (1955).
7. K. C. Schreiber. Anal. Chem. **21**, 1168 (1949).
8. I. M. Kolthoff and R. Belcher. Volumetric analysis. Vol. III. Interscience, N.Y. 1957. p. 567.
9. W. L. Evans and H. B. Hass. J. Am. Chem. Soc. **48**, 2703 (1926).
10. F. A. Isherwood and C. S. Hanes. Biochem. J. **55**, 824 (1953).
11. A. Eschenmoser and A. Frey. Helv. Chim. Acta, **35**, 1660 (1952).

THE FREEZING OF WATER AND BENZENE IN POROUS VYCOR GLASS[1]

C. HODGSON[2] AND R. MCINTOSH

ABSTRACT

Freezing has been detected in the adsorbed water and benzene of porous Vycor glass at temperatures below that at which the bulk phases freeze. The evidence presented by equilibrium pressure measurements and dimensional changes of the systems is considered in terms of theories of capillary condensation and freezing in cements and soil. Although not all the results can be explained, it is concluded that the freezing process is a gradual one for both adsorbate–adsorbent systems. The evidence further suggests that hysteresis is absent in isotherms if the solid phase has formed.

INTRODUCTION

In a note from this laboratory (1) the detection of the freezing of water in porous Vycor glass was reported. The method of detection was the observation of the change of linear dimension of the adsorbate–adsorbent system using an extensometer of a type previously described (2). At approximately $-22°$ C a large expansion of the system occurred, in striking contrast with the gradual contraction found as the temperature was lowered in a range above $-22°$ C.

A qualitative explanation of the finding was suggested as either or both of the following possibilities. As in the case for the bulk phases, the solid adsorbate may have a larger molar volume than the liquid adsorbate. Or, since the contractive force due to concave menisci has been demonstrated (3), it is possible that the destruction of concave menisci by the formation of solid adsorbate might also allow a large expansion. To try to distinguish between these possibilities and to establish a broader basis for discussion of the phenomena associated with adsorption hysteresis in general, experiments using benzene as the adsorbate were undertaken. Differences in the behavior of the two adsorbates are marked, and some of the differences are undoubtedly due to the unusual molar volume change in the transition of water. However, insufficient understanding of all the phenomena has been achieved, and it is necessary to compare the results for the two systems in detail. It is also pertinent to analyze the theories so far advanced to rationalize the known transition phenomena and to comment upon claims made by Puri, Singh, and Myer (4) of excellent agreement between the predictions of capillary condensation theory and observation.

One advantage of the experimental method employed in this investigation is that it reveals that the freezing phenomenon does not occur at a single temperature as may be seen from Figs. 1A, 2A. The observation of a sudden change in the rate at which the equilibrium pressure changes with temperature need not mean a sharp phase transition, but it has apparently been interpreted in this way, and a transition temperature, rather than a transition range, has been discussed by many authors. Other evidence against the occurrence of sharp transitions is contained in the work of Jones and Gortner (5), and Patrick and Kemper (6). The evidence obtained using benzene also points to a gradual freezing. The behavior of the two substances differs,

[1]*Manuscript received November 30, 1959.*
Contribution from the Department of Chemistry, University of Toronto. Based upon a thesis by Hodgson submitted in partial fulfillment of the requirements for the degree of Ph.D.
[2]*Holder of the Union Carbide Fellowship (1957–58) and National Research Council Studentship (1958–59). Present address: Canadian Industries Limited, Textiles Fibres Division, Kingston, Ontario.*

however, in that water begins to freeze at a temperature which is insensitive to the quantity adsorbed, while the initial freezing temperature of benzene varies in a readily discernible manner with quantity adsorbed. In the case of benzene, since the higher equilibrium pressures were more readily measured, it was possible to show that there is no hysteresis in that part of the isotherm where solid benzene may exist. This fact supports the suggestion made earlier (1) that meniscus effects of the liquid phase may be the fundamental cause of hysteresis.

Because of the very large amount of data involved, most of the information will be presented in graphical form.

EXPERIMENTAL

As the extensometer and system for temperature control have been described previously (2), only the form of pressure gauge and the minor modification made to the injector for the adsorbates will be discussed. The pressure gauge was a form suggested by Pearson (7) and in this case butylphthalate was used rather than mercury, so that a magnification of 179 relative to readings of a U-tube type of mercury manometer was obtained. In practice the manometer was not free from error. Difficulty was experienced in measuring the low pressures of water because of degassing of the butylphthalate.

The injector holding the adsorbate was arranged with a heating wire around connecting metal valves and tubing, so that after allowing adsorbate to distill from the capillary to the adsorbent chamber, the slow drift in the level of adsorbate in the capillary tube of the injector due to adsorption on metal valves and walls was eliminated. This difficulty has been noted by Amberg (8), but had not been corrected.

The temperature was varied by increments usually less than 10 degrees. Before length and pressure measurements were taken at a new temperature, the system was allowed to come to apparent equilibrium, a process which took between 8 and 12 hours.

RESULTS

1. Water. Length Changes and Equilibrium Pressures

The results of a typical cooling and heating experiment for water at an initial content of 0.175 g/g, established as an adsorption point at 9° C, is given in Fig. 1A. It should be noted that the temperature range over which the expansion (i.e. freezing) occurs on the cooling curve differs from the temperature range over which contraction (i.e. melting) occurs on the heating curve. An important displacement of the two curves is evident, showing a difference of the absolute lengths of the rod. Repeated cycles did not eliminate this behavior. By contrast, it is seen that the equilibrium pressure values of Fig. 1B lie on the same curve for both heating and cooling.

2. Benzene. Length Changes and Equilibrium Pressures

Two typical sets of curves showing length changes as a function of temperature for both heating and cooling and the corresponding equilibrium pressure data are given in Figs. 2, 3, and 4. The contents of benzene are respectively 0.233 g/g, 0.162 g/g, and 0.170 g/g. The reason for giving these figures is that comparison shows the shift of the temperature at which freezing begins with quantity adsorbed. It should also be noted that the sudden change of slope of the equilibrium pressure curves occurs at the same temperature as the change of slope of the length versus temperature plots. Table I contains a further comparison.

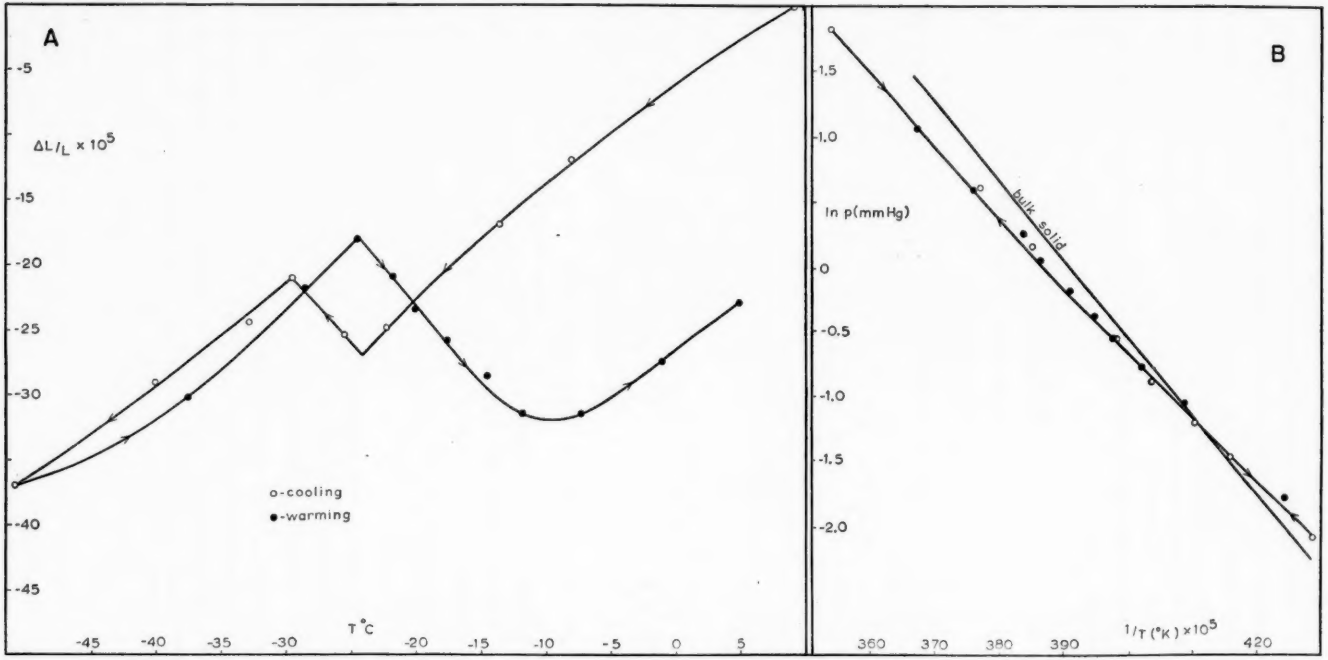

FIGS. 1A, 1B. Typical plots of length variation and equilibrium pressure as functions of temperature for the system water – Vycor glass. Amount of water adsorbed 0.175 g/g.

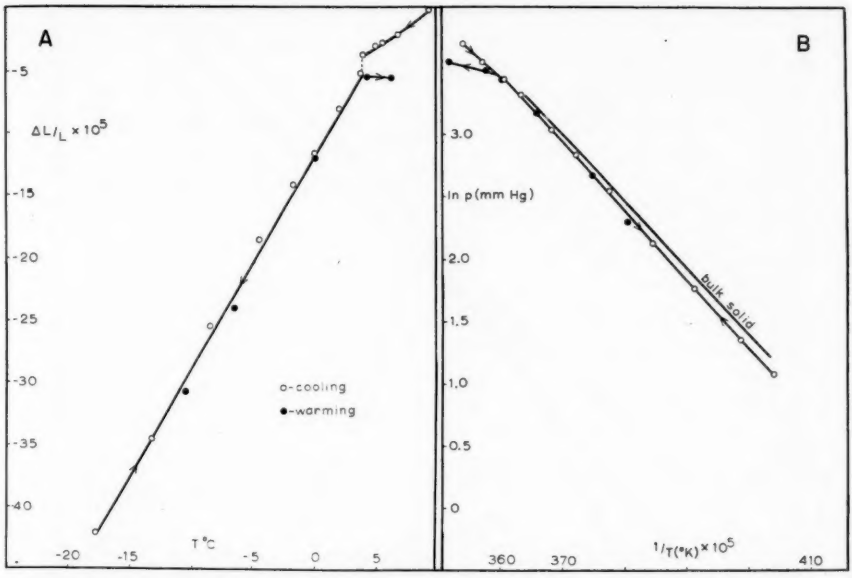

FIGS. 2A, 2B. Length variation and equilibrium pressure as functions of temperature for the system benzene – Vycor glass. Amount of benzene adsorbed 0.233 g/g.

TABLE I

The freezing and melting point depressions of benzene–Vycor systems

Benzene content, g/g	Depression of freezing point from pressure data	Depression of freezing point from length data
0.233	1.6° (f.p.)	1.6°
0.210	4.1 (f.p.)	4.1
0.179	11.5 (f.p.)	11.1
0.170	25.6 (f.p.)	27.3 (f.p.)
	19.4 (m.p.)	19.1 (m.p.)
0.162	28.1 (f.p.)	28.2 (f.p.)
	20.4 (m.p.)	20.8 (m.p.)

There are many points of difference between the behavior of benzene, as exhibited in these graphs, and of water, the behavior of which was depicted earlier. First, no sudden expansion occurs at the start of the transition, which fact therefore supports the view that the increase of the molar volume of the adsorbate rather than a meniscus effect is of primary importance in causing expansion. Second, the gradual transition of benzene is revealed by the persistence of the changed rate of contraction, rather than by the range of temperature over which an expansion occurs. Third, in the case of benzene, the length as a function of temperature does not show hysteresis below the temperature at which transition begins on the initial cooling. Fourth, the equilibrium pressure of benzene for a heating run follows the same curve as for a cooling run below the temperature at which the transition begins, and the rate of variation persists for some degrees above this temperature on heating. This persistence suggests that melting is incomplete,

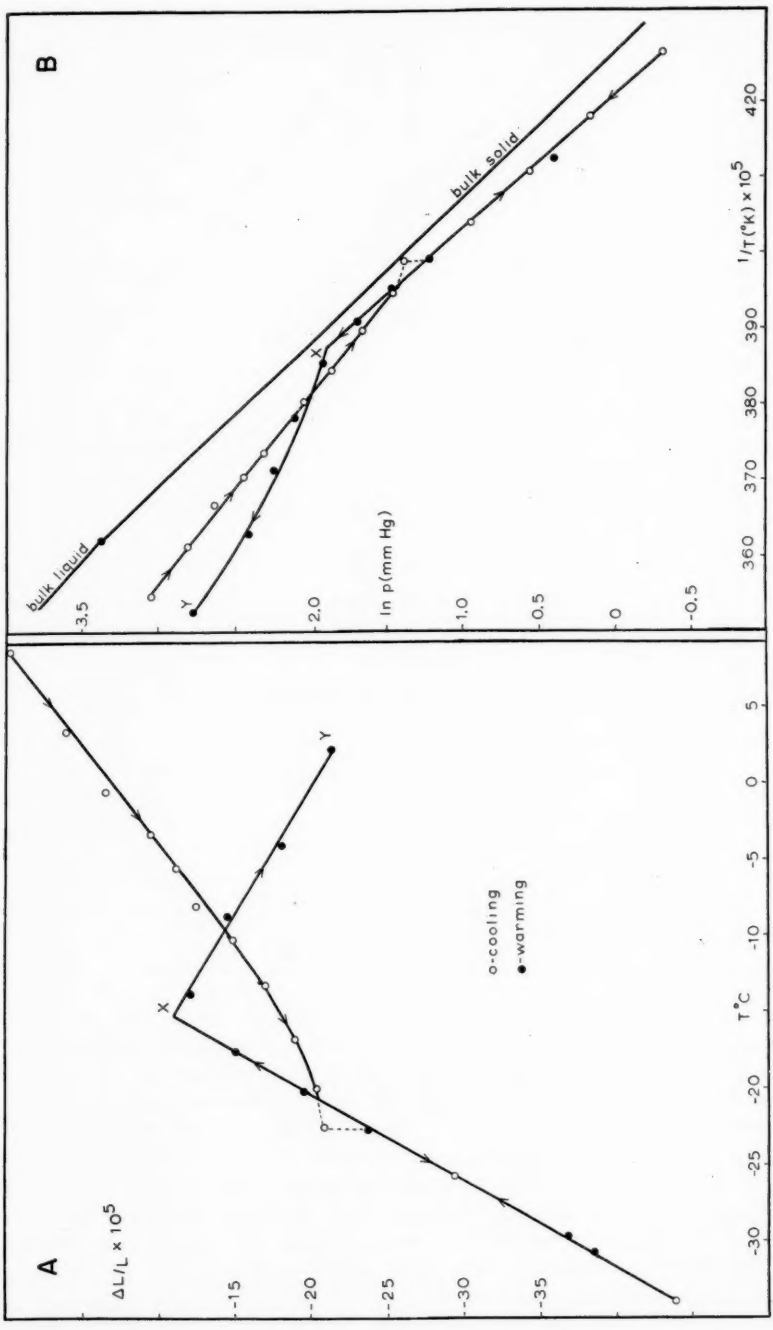

FIGS. 3A, 3B. Length variation and equilibrium pressure as functions of temperature for the system benzene – Vycor glass. Amount of benzene adsorbed 0.162 g/g.

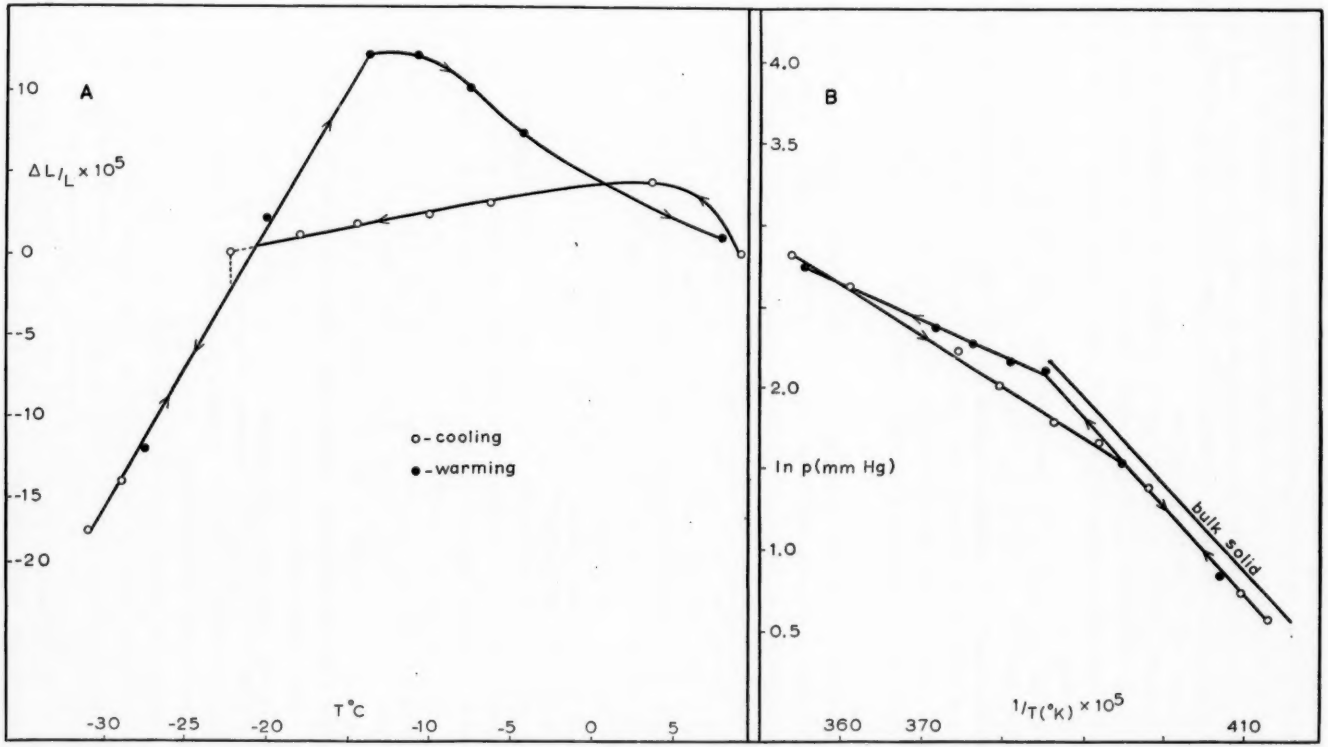

FIGS. 4A, 4B. Length variation and equilibrium pressure as functions of temperature for the benzene – Vycor glass system. Amount of benzene adsorbed 0.170 g/g.

and that heating and cooling would show a common reversible curve in this region. The separation of the curves at the point at which melting is complete is believed to be due to transfer of adsorbate in the gas phase, and consequent change in the curvature of the menisci. Fifth, the equilibrium pressure of the solid adsorbate is lower than for bulk benzene at the same temperature, whereas the (less reliable) data for water suggest a reversal of this at the lower temperatures.

There are, however, two important points of similarity in the behavior of water and benzene: (*a*) both adsorbates show a gradual transition to the solid form; (*b*) both adsorbates complete their melting processes at higher temperatures than those for the inception of freezing.

Finally, it should be stated that throughout the upper temperature range for many conditions using benzene, complicating effects existed due to the adsorption from the gas phase. For example, in cooling a system with 0.170 g/g of adsorbed benzene (see Fig. 4) an initial expansion occurred and this was followed by the normal type of contraction. Such complications emphasize the desirability of restricting the volume of the gaseous phase and maintaining isosteric conditions when possible.

3. Isotherms for Benzene

In Fig. 5 are shown isotherms of benzene and the concomitant length changes. Only one isotherm has been investigated fully, that at +9° C. It is similar in shape to those for water, ethyl chloride, ammonia, and butane on the same adsorbent (2, 3). The closure of the hysteresis loop occurs, however, at an appreciably lower pressure. The length variations are noteworthy for two observations: (*a*) a contraction below the initial length occurs; (*b*) the first approximately horizontal region of the length change versus weight adsorbed plot ceases to be horizontal as temperature is lowered. Observation (*a*) has not previously been made for Vycor systems although Haines and McIntosh (9) observed this for the charcoal–water system. Presumably it occurs because the contraction due to the concave menisci exceeds the spreading force in the adsorbed layers due to interaction with the solid.

In these graphs it is clearly shown that the relative pressure approaches a value of 1.0 asymptotically when p_s^0 is employed as the reference value for those temperatures below the normal freezing point of benzene. Because of the experimental arrangement, the pressure cannot exceed p_s^0. Nevertheless, it is suggestive of freezing of the benzene that the approach to this value is asymptotic. If, for example, the adsorbed phase consisted of a physical arrangement resembling bulk liquid, the equilibrium pressure should approach p_l^0 at the temperature of the isotherm as the amount adsorbed is increased. Experimentally it cannot approach more closely than the value p_s^0. In this event the experimental curve would tend to the ordinate at the value p_s^0 at a finite angle rather than asymptotically. But since the approach is asymptotic it is deduced that solid adsorbate has formed by a condition represented as point *B*. It is to be noted that the region *BC* begins at values of relative pressure progressively farther removed from the value 1.0 as the temperature is lowered.

A second observation which may support the view that freezing has occurred at the situation designated by point *B* is the following. Point *B* for isotherms above the bulk transition temperature has been interpreted as marking the condition that all pores are filled and menisci exist of the curvature appropriate to the relative pressure. Since it is known from the dimensional variation of the adsorbent alone that pore volume does not change appreciably with temperature, and since one would normally expect the

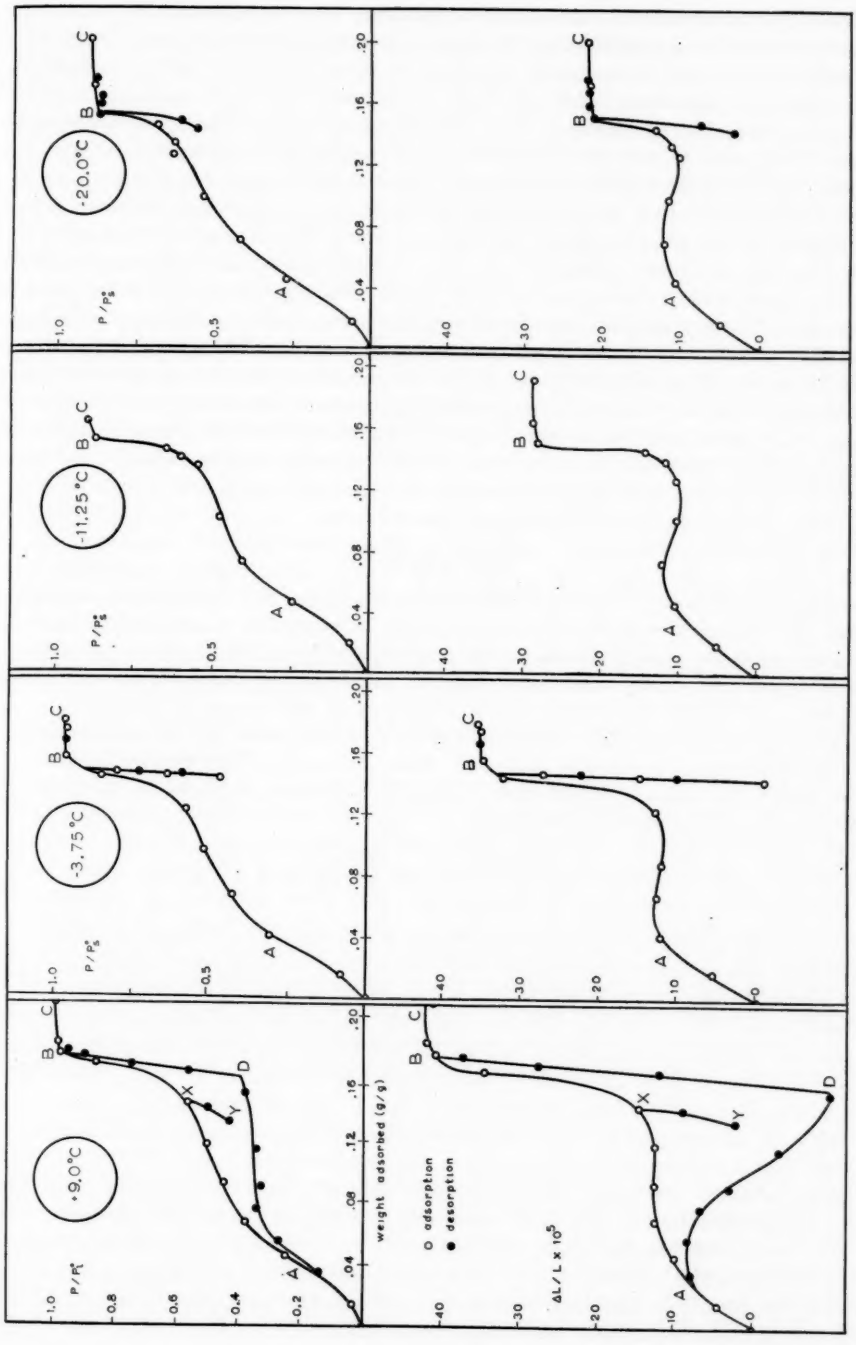

FIG. 5. Isotherms of benzene on Vycor glass at various temperatures.

density of the adsorbate to increase as temperature is reduced, one would expect the amount adsorbed at the condition of filled pores to increase with decreasing temperature. The experimental fact is the opposite of this. It is concluded, therefore, that point B has a different significance below the bulk transition temperature, namely, that solid has formed, and that this is the reason that hysteresis is not observed for adsorptions greater than point B. For temperatures above the transition temperature the filling of pores would end the region of hysteresis, but as argued above, the situation does not conform with expectation on this basis alone, and another cause for the reversible isotherm above point B is required. The best evidence that hysteresis is absent above point B is obtained from cooling and heating curves, such as those represented in Fig. 3A. Once solid phase has disappeared from the system, further increase of temperature brings about more desorption, and presumably because all menisci are now liquid, irreversible phenomena are observed (see region XY of Fig. 3A).

For the present it is sufficient to state that the behavior of the benzene–Vycor system at constant temperature is consistent with its behavior when temperature is changed. Further, it is noteworthy that even some 25 degrees below the normal triple point, hysteresis still persists in the isotherms. If the suggestion of the cause of hysteresis, namely the existence of liquid-like menisci and no solid present, is valid, then such conditions may persist to relatively low temperatures.

DISCUSSION

1. *Capillary Condensation Theory Applied to the Prediction of a Transition Temperature*

Most theoretical discussions are based upon the concept of condensed liquid in capillaries, with the liquid existing under concave menisci of the appropriate radius of curvature, and thus under negative hydrostatic pressure. On this basis the free energy per mole of the liquid adsorbate may be predicted as a function of temperature, and always lies below that for bulk liquid. If concave menisci exist for the solid adsorbate, a similar evaluation is possible provided that the surface free energy of the solid vapor interface is known. Stated first in terms of relative pressures of the solid and liquid adsorbates, the relation becomes

$$RT' \ln \frac{p_l^0 p_s}{p_s^0 p_l} = \frac{(T'-T_t)\overline{\Delta H}_{l,s}}{T_t} - T' \int_{T_t}^{T'} \frac{\Delta C}{T}\, dT + \int_{T_t}^{T'} \Delta C\, dT$$

where T' is the temperature of the transition; p_l^0, p_s^0 refer to the vapor pressures over bulk phases; p_s and p_l over the adsorbate; T_t the normal freezing point of bulk; $\overline{\Delta H}_{l,s}$ the molar heat of fusion for the bulk phases; and ΔC is the difference of specific heats of the solid and liquid bulk materials. The two integrals are normally ignored, and the relative pressures of the left-hand side calculated by employment of the Kelvin equation in the form $RT \ln p^0/p = 2\sigma\tilde{V}/r$ for the appropriate interface, so that one obtains $\Delta T = 2T_t(\sigma_{lv}\tilde{V}_l - \sigma_{sv}\tilde{V}_s)/r\Delta H_{ls}$, where $\Delta T = T_t - T'$. Some authors, e.g. Puri, Myer, and Singh (4), assume that $p_s/p_s^0 = 1.0$ although from their published graph this situation is not exhibited, in agreement with our data for benzene shown earlier. Had Puri, Myer, and Singh actually employed the equilibrium pressure data for the solid adsorbate, agreement between theory and experiment would not have been good. However, they used the Kelvin relation and data obtained well above the transition range and extrapolated to obtain the value of p_l/p_l^0 at the initial temperature of the transition, a procedure which results in too high values and reduces the predicted value of ΔT and brings it into closer agreement with experiment (10).

If freezing is, indeed, a process occurring over a range of temperature, this is a fact which is in disagreement with the use of the Kelvin concepts. At a given relative pressure, all menisci must have the same value of the radius of curvature, and a sharp transition should be observed. Appeal to equilibrium pressure data might appear to support a sharp transition, as a sudden change in the slope of pressure–temperature curves is found. In itself, however, this means nothing, since the situation is akin to the freezing of a macroscopic two-component system. Deposition of solid will begin at some temperature dependent upon the composition, and more solid will be deposited as the temperature is lowered. Over this range of temperature the equilibrium partial pressure of the component which has formed the solid phase must be identical with that of the solid. Similarly, if a solid adsorbate phase forms, since equality of chemical potential must exist for the two phases, the equilibrium pressure as a function of temperature must be that for the solid phase.

This realization is useful in connection with other observations. It was noted earlier that no hysteresis is observed for vapor pressure data until melting is complete. Evidence was also presented which showed that for temperatures, and over ranges of pressure, where there appears to be solid benzene, no hysteresis loop is discerned in the isotherms. If one presumes, therefore, that adsorbed solid benzene does not form menisci, and if meniscus effects are the basic cause of hysteresis, none will be observed when solid benzene is present. This argument should be of general application to all adsorbates.

One concludes, therefore, that appeal to capillary condensation theory will not suffice to explain observation. The points of disagreement are (*a*) the freezing of both water and benzene occurs over a range of temperature; (*b*) the inception of freezing for benzene is a function of amount adsorbed, but that for water is not; (*c*) hysteresis between cooling and heating curves is observed for both adsorbates.

2. Prediction of the Freezing Point by the Theory of Liquid-like Layers due to Frenkel (11), Halsey (12), and Hill (13)

As pointed out by Hill (14), one of the major criticisms which may be levelled at the B.E.T. multilayer theory is the fact that ϕ, the spreading force of the film, does not remain finite for the infinite adsorption permitted at $p/p^0 = 1.0$. The thick layer theory, giving an isotherm of the form $\ln p/p^0 = -a/\Gamma^3$ does not suffer from this disadvantage, and moreover agrees quite well with experimental isotherms on certain non-porous adsorbents in the region of high relative pressure. Due to the model upon which the theory is based, it is possible to calculate explicitly values of $\ln p/p^0$ for both liquid- and solid-adsorbed layers. In the case of the systems studied here, the form of the isotherm does not agree with experiment, and it is not very meaningful to attempt its use. This fact also forbids the evaluation of "a" from the experimental isotherm and therefore the empirical determination of the parameters e_1, r_1, e, and r^* in the equation

$$a = \frac{\pi\rho^3}{6kT}(\rho_1 e_1 r_1^6 - \rho e r^{*6}).$$

Here ρ and ρ_1 are the densities of the adsorbate and adsorbent in molecules per cubic centimeter, e and e_1 the depths of the potential wells for the pure liquid and the liquid–adsorbent interaction, and r_1 and r^* the distances of closest approach of the liquid–adsorbent and bulk liquid molecules, respectively. Estimates of these parameters were therefore made. From the value of the heat of adsorption of water at zero coverage obtained from the data of Amberg and McIntosh (3), a value of 20,000 cal mole^{-1} was

obtained. Assuming a value of r_1 of 1 Å, it was possible to obtain $\rho_1 e_1 r_1^6$ from the equation

$$\frac{q_0 - RT}{N} = -\frac{\pi \rho_1 e_1 r_1^3}{6}$$

which gives the interaction energy between the liquid layer and the underlying adsorbent. Similarly $\rho e r^6$ was evaluated from the equation

$$\frac{\lambda - RT}{N} = -\frac{2}{3}\frac{\pi \rho e r^{*3}}{}.$$

The bulk density was assigned to the adsorbed water, and a cubic packing arrangement in evaluating r^*. Similar calculations were made for ice using parameters for bulk ice where that is appropriate and assuming that $\rho_1 e_1 r_1^6$ remains the same for adsorbate in the temperature range where bulk solid would be stable. By evaluating $\mu_{ads} - \mu_{bulk\ liq}$ at +20 and +10° C, and $\mu_{ads} - \mu_{bulk\ sol}$ for −10 and −20° C, a freezing point lowering of about 1.5° was predicted for an adsorbate content of 0.20 g/g of water. This procedure cannot be accurate since the expression was found to be very sensitive to values of r_1, but would be more useful if "a" could be obtained from experimental data. Our object here has been to show that the theory does not predict a depression of transition temperature of the magnitude found, and to suggest that transition temperatures, if known, may form another basis for testing the validity of an explicit adsorption theory.

3. Theory of Jackson and Chalmers

In dealing with the concave meniscus theory, interfaces between liquid and vapor or solid and vapor were considered to form. Jackson and Chalmers (15) have considered the conditions in a capillary pore in which liquid has a zero wetting angle with the wall and a stable interface of solid and liquid is presumed to form in the capillary pore. As the meniscus is concave to the liquid and convex to the solid, the liquid is under a negative pressure and the solid under a positive pressure. At some temperature these two phases may be in equilibrium, and this must be at a temperature below the normal transition temperature. The temperature of coexistence will vary with the radius of the tube and become less for smaller tubes, thus explaining a gradual transition. The quantitative relation for fluids of zero wetting angle (e.g. benzene and glass, Richards and Carver (16)) is approximately $\Delta T = -\sigma_{l,s} T_t / \overline{\Delta H}_{l,s} r$. It should be noted particularly that at the transition temperature, the molar free energy of liquid adsorbate is below that of the bulk liquid but that the molar free energy of solid is above that of bulk solid. Such would appear to be the case according to the supposed equilibrium pressure values for water in Fig. 1B, but is certainly not the case for benzene. That such a situation might obtain in impermeable soils or cements may be possible, but that it could obtain for equilibrium conditions in the porous Vycor glass system, where distillation into and out of the adsorbent is relatively easy, does not appear possible. Bulk solid would form on the walls by condensation from the vapor phase and transfer from adsorbent to the walls of the cell would proceed. The theory therefore does not seem applicable to the systems investigated and the apparent confirmation from the data for water could merely reflect the inaccuracy of the data.

Actually, this theory and the theory due to Powers (17) need not be dismissed, provided that equilibrium conditions do not exist in the systems under study. Before amplifying this statement the theory due to Powers will be briefly outlined.

4. Theory of Freezing due to Powers

In a porous material, such as cement, Powers assumes the existence of (*a*) large voids, (*b*) cavity spaces of narrower dimensions, and (*c*) a matrix of cement which is porous and thus permeable to water, but which is of very fine porosity and through which adsorbed water would diffuse as molecules. On lowering temperature water can freeze as bulk water in the large voids if these are present. At lower temperatures (because of the influence of the force field from the solid) nucleation may next occur in cavities. When nucleation occurs in these regions, there is expansion of adsorbate in a confined space and large hydrostatic stresses are established. Water will then begin to diffuse from regions where its chemical potential is greater than that of bulk solid at that temperature to the regions where bulk solid may exist. After appreciable freezing has occurred and some period of time has elapsed, the location of the adsorbed water throughout the mass will have altered. If, during this period of time, a measurement of pressure of the water vapor could be made, the pressure would presumably be greater than that of bulk ice at the same temperature. It should be noted that this theory, in common with that given by Jackson and Chalmers (15), predicts this situation which is anomalous if equilibrium conditions are assumed. It should also be recalled that this situation is observed for water if the pressure data are accurate. As pressure data within this same temperature range were obtained for lower water contents which were below the value at which freezing was observed, and these data did not reveal values greater than those for bulk solid, there is some reason to suppose that these data are meaningful. In conjunction with this observation, the form of the warming curve for water should be recalled, which reveals that the melting range persists to higher temperatures than the inception of freezing. On Powers' theory this can be explained by some of the water having migrated to regions where stress was less and freezing point higher. In fact, as already pointed out, distillation could occur to the wall of the cell where bulk solid would be formed and the water content of the rod thus be diminished. In this event the rod should be shorter (see Fig. 1A) than when cooling was begun, unless sufficient time is allowed for the system to return to its original state. It is possible that the system might not be restored in any event, since the presence of a hysteresis loop in the isotherm implies that the previous history of the starting system may have to be repeated.

In the case of benzene, as contraction rather than expansion is to be expected when adsorbed solid forms, large hydrostatic stresses are presumably not established. Thus the condition for equilibrium pressure greater than that for the bulk solid would not obtain. It could arise from the mechanism visualized in the Jackson and Chalmers' theory, but according to experimental observation, it does not occur. The data for water thus support Powers' theory while the data for benzene contradict the Jackson and Chalmers theory.

Two important facts remain unexplained. Melting of benzene is not complete until temperatures are reached which are higher than those at which freezing began. No explanation of this superheating has become evident, nor would the rate of cooling employed in the experiments suggest any marked departure from equilibrium conditions.

The second observation is that the initial freezing temperature for water is independent of the water content of the adsorbent over the range investigated. Until these observations are accounted for, any understanding of the transition phenomena must be considered as very incomplete.

APPENDIX

As shown in Fig. 6, the apparent temperature coefficient for the water–Vycor system diminishes in a regular way with increasing water content up to water contents at

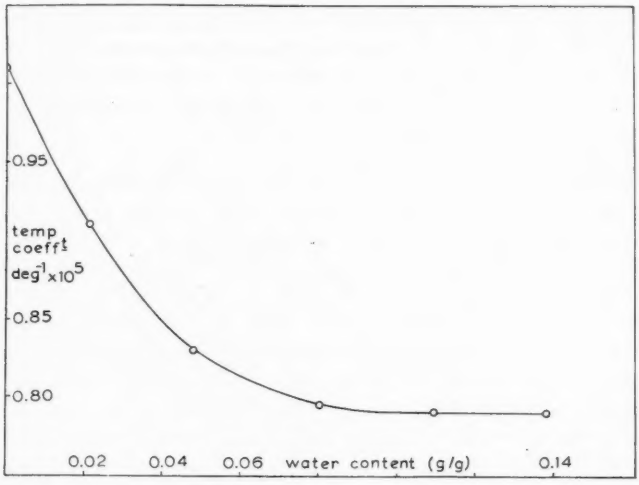

FIG. 6. The temperature coefficient of Vycor glass as a function of initial water content.

which complications due to freezing or adsorption from the vapor phase prevent further observation. The same fact has been established in the case of benzene. A straightforward analysis of the situation has been given by Hermans (18) and is set out below.

As the reasonable assumption of isotropic structure of the rod may be made, a length change may be interpreted as directly proportional to a volume change. The experimental fact is, therefore, that

$$\frac{\partial}{\partial n_T}\left(\frac{\partial V}{\partial T}\right)_{ex} < 0.$$

The subscript "ex" signifies experimental conditions. As pressure varies little in the experiments, the result is for constant hydrostatic pressure, and this restriction is to be understood throughout. Since, however, condensation from the gas phase may be important, it should be emphasized that n, the quantity of adsorbate is not constant.

The treatment assumes, in addition to the assumption that the properties are single-valued in n and T, that the sign of the volume changes, resulting from variations of adsorbate content and temperature, is revealed by the experimental measurements. The true magnitudes are doubtful because of the fact that the actual volume of the solid–adsorbate system is never measured for the porous system.

We have

$$\left(\frac{\partial V}{\partial T}\right)_{ex} = \left(\frac{\partial V}{\partial T}\right)_{n} + \left(\frac{\partial V}{\partial n}\right)_{T}\left(\frac{\partial n}{\partial T}\right)_{ex}$$

$$0 > \frac{\partial}{\partial n_T}\left(\frac{\partial V}{\partial T}\right)_{ex} = \left(\frac{\partial \bar{V}}{\partial T}\right)_{n} + \left(\frac{\partial \bar{V}}{\partial n}\right)_{T}\left(\frac{\partial n}{\partial T}\right)_{ex} + \bar{V}\frac{\partial}{\partial n_T}\left(\frac{\partial n}{\partial T}\right)_{ex}$$

where $\bar{V}$ is the partial molal volume of adsorbate. Of the terms on the right-hand side of the equation $(\partial \bar{V}/\partial T)_n$ is positive, and $(\partial \bar{V}/\partial n)_T$ is negative because the length plotted against n is concave towards the n axis in the appropriate range of n. Obviously $(\partial n/\partial T)_{ex}$ is negative. It follows that $\bar{V}(\partial/\partial n_T)(\partial n/\partial T)_{ex}$ must be negative. This conclusion has been confirmed by means of the data from three runs, and at 0° C $(\partial/\partial n_T)(\partial n/\partial T)_{ex}$ has a value of -6×10^{-4} deg^{-1} for water. Qualitatively the finding merely states that the effect of temperature on the population of a surface is greater if the surface concentration is high than if it is low. Thus the experimental observation is simply explained.

ACKNOWLEDGMENT

Grateful acknowledgment is hereby made to the National Research Council of Canada for financial support of this investigation.

REFERENCES

1. C. HODGSON and R. McINTOSH. Can. J. Chem. **37**, 1278 (1959).
2. H. W. QUINN and R. McINTOSH. Proc. Intern. Conf. of Surface Activity. 2nd Conf. Butterworth Scientific Publications, London. 1957.
3. C. H. AMBERG and R. McINTOSH. Can. J. Chem. **30**, 1012 (1952).
4. B. R. PURI, Y. P. MYER, and D. D. SINGH. Trans. Faraday Soc. **53**, 530 (1957).
5. I. D. JONES and R. A. GORTNER. J. Phys. Chem. **36**, 387 (1932).
6. W. A. PATRICK and W. A. KEMPER. J. Phys. Chem. **42**, 369 (1938).
7. T. G. PEARSON. Z. physik. Chem. (Leipzig), A, **156**, 86 (1931).
8. C. H. AMBERG. Ph.D. thesis, University of Toronto, Toronto, Ont. 1952.
9. R. HAINES and R. McINTOSH. J. Chem. Phys. **15**, 28 (1947).
10. M. H. PANCKHURST. Private communication.
11. Y. I. FRENKEL. Kinetic theory of liquids. Oxford University Press, London. 1946. p. 407.
12. G. D. HALSEY. J. Chem. Phys. **16**, 931 (1948).
13. T. L. HILL. J. Chem. Phys. **17**, 590 (1949).
14. T. L. HILL. Advances in catalysis. Vol. IV. Academic Press Inc., New York. 1952. p. 230.
15. K. A. JACKSON and B. CHALMERS. J. Appl. Phys. **29**, 1178 (1958).
16. T. W. RICHARDS and E. K. CARVER. J. Am. Chem. Soc. **43**, 827 (1921).
17. T. C. POWERS. J. Am. Concrete Inst. **16**, 245 (1944).
18. J. J. HERMANS. State University of Forestry, Syracuse, N.Y. Private communication.

STEROIDS

PART I. THE SYNTHESIS OF SOME HETEROCYCLIC STEROID DERIVATIVES[1]

BARBARA G. KETCHESON[2] AND ALFRED TAURINS

ABSTRACT

Cyanoacetamide reacted with 3β-hydroxy-16-hydroxymethylene-5-androsten-17-one to form 1-cyano-2-hydroxy-2(16′-3′β-hydroxy-17′-oxo-5′-androstenyl) propionamide or 3-cyano-4,5-dehydro-6-hydroxy-5,6(16′,17′-3′β-hydroxy-5′-androstenyl)-2-piperidone depending on whether a catalytic or a molecular amount of piperidine was used as the basic condensing agent. Carboxamidoacetamidine, and acetamidine hydrochlorides, were condensed with the sodium salt of 3β-hydroxy-16-hydroxymethylene-5-androsten-17-one, and 3β-chloro-16-chloromethylene-5-androsten-17-one yielding 2-amino-3-carboxamido-5,6(16′,17′-3′β-hydroxy-5′-androstenyl) pyridine and 2-methyl-5,6(16′,17′-3′β-chloro-5′-androstenyl) pyrimidine respectively.

DISCUSSION

The elucidation of the structure of a number of steroidal alkaloids (1), combined with their well-established physiological activity, has stimulated efforts to synthesize a variety of nitrogen-containing steroids. In many instances, the synthetic products have not displayed the anticipated physiological properties, but in several cases, the nitrogen derivatives of steroids have exhibited pharmacological properties of the same type and order of magnitude as some of the steroidal alkaloids (2, 3, 4).

With this in mind, the present investigation, concerned with the attachment of six-membered nitrogen-containing rings to the 16,17-positions of the steroid nucleus, was undertaken. As a first approach to the problem, the piperidine-catalyzed Knoevenagel condensation of 3β-hydroxy-16-hydroxymethylene-5-androsten-17-one (I) (5) with cyanoacetamide was considered. In the cyclopentane (6), cyclohexane (7), and tetrahydrophenanthrene (8) series, the reaction of hydroxymethylene ketones with cyanoacetamide had given rise to pyridine, quinoline, and azachrysene derivatives respectively.

In the preliminary attempt to accomplish the condensation, cyanoacetamide and I were allowed to stand in ethanolic solution in the presence of a catalytic amount of piperidine for 8 days at 40°. Only starting materials were obtained under these conditions. However, when an identical reaction mixture was heated at the reflux temperature for 2 days, two products were obtained. The major product proved to be the aldol addition product 1-cyano-2-hydroxy-2(16′-3′β-hydroxy-17′-oxo-5′-androstenyl) propionamide (II). On heating II with a 10% potassium hydroxide solution in methanol, ammonia was given off. The infrared spectrum of the alkaline hydrolysis product confirmed the presence of a carboxylic group in the molecule. The isolation of II from the reaction was surprising, since generally in the Knoevenagel condensation of cyanoacetamide with hydroxymethylene ketones, the initially formed aldol addition products readily lose a molecule of water, and ring closure to dehydropiperidone structure occurs (9, 10, 11). However, instances have been reported (12, 13) in which the aldol addition products analogous to II have been isolated.

[1]*Manuscript received February 8, 1960.*

Contribution from the Department of Chemistry, McGill University, Montreal, Que., with financial assistance from the National Research Council, Ottawa, Canada. Presented in part before the Division of Organic Chemistry, Chemical Institute of Canada, Toronto, Ontario, May 26, 1958. Abstracted from a portion of the thesis submitted by Barbara G. Ketcheson to the Department of Chemistry, McGill University, Montreal, Que., August 1958, in partial fulfilment of the requirements for the Ph.D. degree.

[2]*Holder of a National Research Council Studentship, 1956–57, and of Canadian Industries (1954) Limited Fellowships, 1955–56 and 1957–58.*

The second product obtained from the reaction was a condensation product of piperidine and I and, in agreement with the well-established reactivity of hydroxymethylene ketones with secondary amines, was formulated as 3β-hydroxy-16-piperidinomethylene-5-androsten-17-one (III*a*). An identical product was obtained quantitatively by refluxing an ethanolic solution of the hydroxymethylene ketone (I) and piperidine for several hours. On warming III*a* with aqueous acetic acid, 3β-acetoxy-5-androsten-17-one was obtained. The formation of the piperidinomethylene ketone (III*a*) during the reaction of cyanoacetamide and 3β-hydroxy-16-hydroxymethylene-5-androsten-17-one (I) was unexpected, and no previous instance of the formation of an analogous piperidinomethylene derivative from the corresponding hydroxymethylene compound during a Knoevenagel

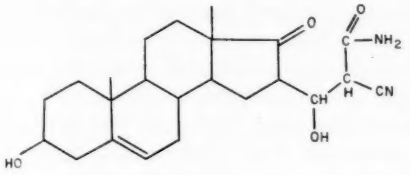

(II)

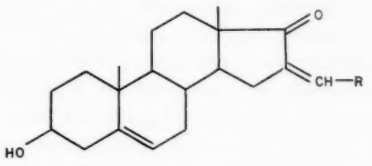

(I), R = OH

(IIIa), R = N

(IIIb), R = N O

(IIIc), R = $N(C_2H_5)_2$

(IIId), R = $NHCH_3$

(IIIe), R = NH

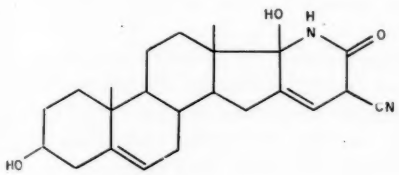

(IV)

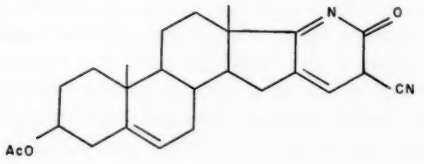

(V)

reaction could be found. However, Dev (14) had reported that when the Knoevenagel condensation of ethyl cyanoacetate with ethyl 2(2′-1′-oxo-cyclopentano)-*n*-butyrate was carried out using ammonium acetate or benzylamine as catalysts, condensation of the catalyst with the keto-ester occurred.

Subsequently it was found that morpholine, diethylamine, methylamine, and aniline also condensed readily with the hydroxymethylene ketone (I) to form the corresponding aminomethylene ketones (III_{b-e}) in high yields.

In a later attempt to effect the condensation of cyanoacetamide with I, an ethanolic solution of the reactants was refluxed in the presence of an equimolecular amount of piperidine for 3 days. Two products were isolated. They were identified as 3β-hydroxy-16-piperidinomethylene-5-androsten-17-one (III*a*), and 3-cyano-4,5-dehydro-6-hydroxy-5,6(16′,17′-3′β-hydroxy-5′-androstenyl)-2-piperidone (IV). As expected, treatment of IV with excess acetic anhydride in pyridine at room temperature led to the elimination of a molecule of water and formation of a monoacetate, 3-cyano-5,6(16′,17′-3′β-acetoxy-5′-androstenyl)-2-pyridone (V).

It appeared, from a consideration of the experimental results obtained, that this Knoevenagel reaction proceeded by different paths depending on whether a catalytic or molecular proportion of piperidine was used as the condensing agent. The formation of the piperidinomethylene ketone (III*a*) in the reactions indicated that two simultaneously proceeding reactions were occurring, or that III*a* was being formed as an intermediate product. To investigate the latter possibility, an ethanolic solution of III*a* and cyanoacetamide was refluxed for 3 days. A 20% yield of the dehydropiperidone (IV) was obtained. This result provided evidence that when the condensation of the hydroxymethylene ketone (I) and cyanoacetamide was carried out in the presence of a molecular proportion of piperidine, reaction proceeded via the formation of the stable intermediate 3β-hydroxy-16-piperidinomethylene-5-androsten-17-one (III*a*). When the reaction was performed using a catalytic amount of piperidine, apparently two separate processes occurred with the formation of the aldol addition product (II) and the piperidinomethylene compound (III*a*).

To account for the reaction occurring in the presence of a molecular amount of piperidine a mechanism is proposed in Fig. 1.

Initially there is a nucleophilic attack by the piperidine at the hydroxymethylene carbon atom. The addition product thus formed loses a molecule of water and the piperidinomethylene compound is produced. Then the carbanion of cyanoacetamide attacks at the piperidinomethylene atom forming an addition product from which the piperidine moiety is expelled. Ring closure to the dehydropiperidone structure is the final step.

Other investigators had found that the Michael reaction of cyanoacetamide and hydroxymethylene ketones led to the production of condensation products identical with those obtained by the Knoevenagel procedure (7, 9). However, when attempts were made to condense cyanoacetamide with the hydroxymethylene ketone (I) using sodium ethylate as the basic condensing agent, the product isolated was 3β-hydroxy-5-androsten-17-one (VI). On one occasion, a very small quantity of a substance whose infrared spectrum was identical with that of the aldol addition product (II) was obtained. The formation of VI in this reaction was believed to occur by a base-catalyzed reverse aldol reaction which brought about the loss of an anion from the initial aldol addition product of cyanoacetamide and I.

As another approach to accomplishing the synthesis of steroids with a nitrogen-containing ring attached to the 16,17-positions of the molecule, an effort was made to condense carboxamidoacetamidine hydrochloride (15, 16) with the sodium salt of 3β-hydroxy-16-hydroxymethylene-5-androsten-17-one (I). Dornow and Neuse (17, 18) had reported that condensation of certain hydroxymethylene ketones with carboxamidoacetamidine hydrochloride resulted in the formation of nicotinamide derivatives. In the present case, two products were obtained. One of these had a molecular formula $C_{23}H_{31}O_2N_3$, and was formulated as 2-amino-3-carboxamido-5,6(16′,17′-3′β-hydroxy-5′-androstenyl) pyridine (VII). The infrared absorption spectrum affirmed the presence of

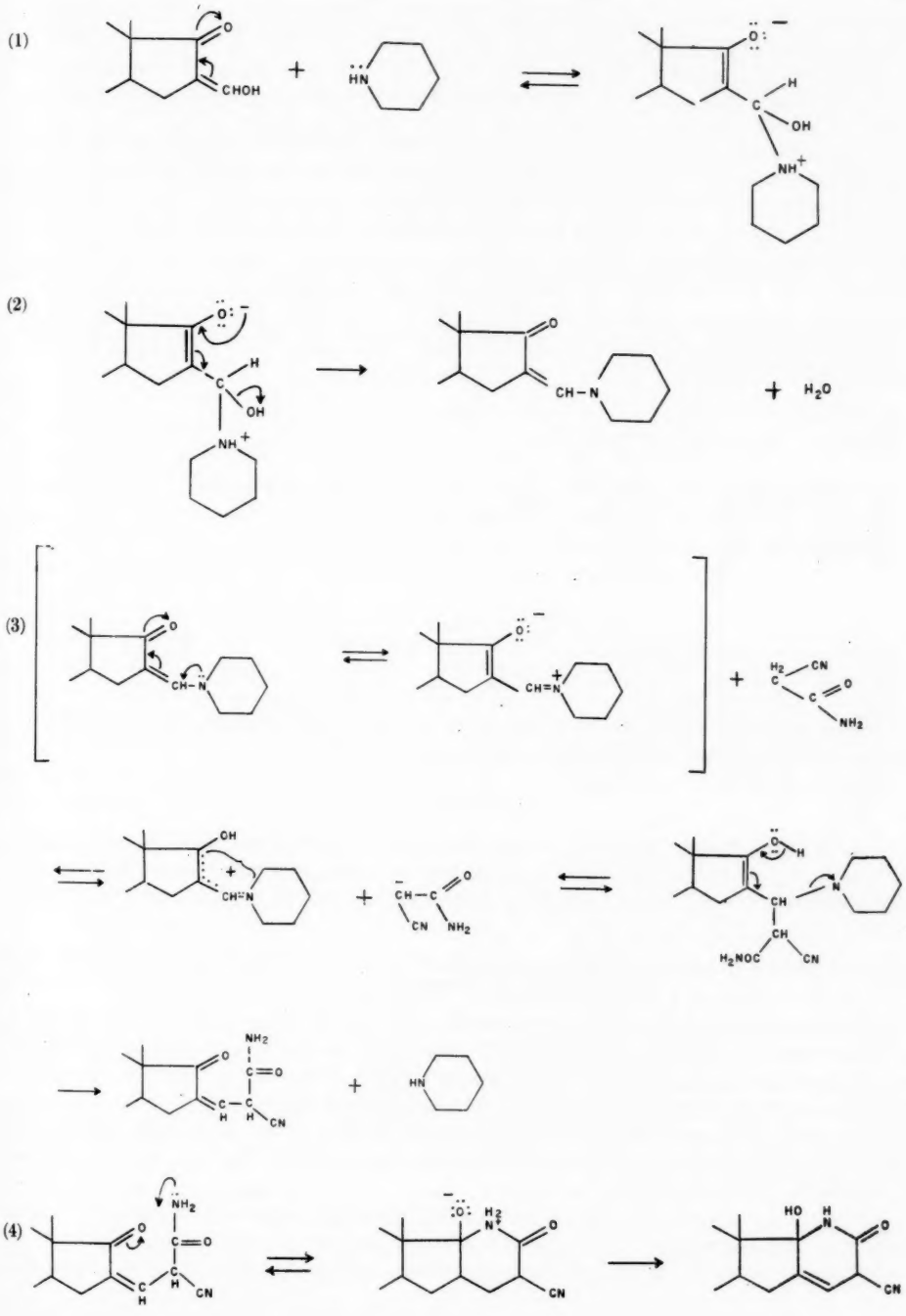

FIG. 1

a primary amide group, a primary amine function, and a pyridine ring in the molecule. The second product proved to be identical with the hydroxy ketone (VI). A reverse aldol condensation was considered responsible for the formation of VI in the reaction.

In another endeavor to achieve the synthesis of heterocyclic steroids, an attempt was made to attach a pyrimidine ring to the 16-, 17-positions of the nucleus. Since in the tetrahydrophenanthrene series, acetamidine hydrochloride had condensed with a chloromethylene ketone to form a pyrimidine derivative (8), the hydroxymethylene ketone (I) was converted to 3β-chloro-16-chloromethylene-5-androsten-17-one (VIII) by means of thionyl chloride, and allowed to react with acetamidine hydrochloride in absolute ethanol in the presence of sodium. The only product which could be isolated from the reaction mixture, melted at 145–148°, had the formula $C_{22}H_{29}ClN_2$, and in the infrared displayed absorption bands characteristic of a pyrimidine ring, and of the C—Cl stretching frequency. The product was formulated as 2-methyl-5,6(16′,17′-3′β-chloro-5′-androstenyl) pyrimidine (IX).

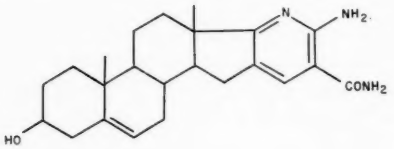

(VII)

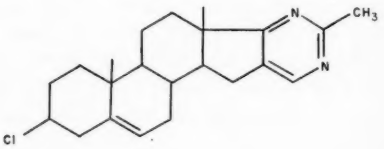

(IX)

The investigation of these and related compounds is continuing, and it is hoped that a report on their physiological activity can be issued shortly.

EXPERIMENTAL

The analyses were carried out in the W. Manser Laboratory, Zurich, Switzerland. Infrared spectra were determined in potassium bromide, unless otherwise stated, on a Perkin–Elmer Model 21 double-beam instrument equipped with a sodium chloride prism.

Reaction of Cyanoacetamide with 3β-Hydroxy-16-hydroxymethylene-5-androsten-17-one (I) *in the Presence of a Catalytic Amount of Piperidine*

A mixture of I (2.0 g) and cyanoacetamide (680 mg) in ethanol (70 ml) was refluxed in the presence of piperidine (0.1 ml) for 2 days. A yellow solid material (930 mg) which was formed during the reaction was filtered and dried. Recrystallization from dimethylformamide–water provided 1-cyano-2-hydroxy-2(16′-3′β-hydroxy-17′-oxo-5′-androstenyl) propionamide (II), m.p. 221–223°. ν_{max}^{Nujol} 3420, 3330 (sh), 3220, 1718, 1700, 1665, 1648 (sh), 1623, 1040 cm^{-1}. Anal. Calc. for $C_{22}H_{32}O_4N_2.H_2O$: C, 66.01; H, 8.19; N, 6.70. Found: C, 66.28; H, 8.04; N, 6.67%.

The filtrate was concentrated and chromatographed on alumina (80–200 mesh). Elution with methanol–ether (1:9) yielded a crystalline product (320 mg) which, after recrystallization from dimethylformamide–water, afforded 3β-hydroxy-16-piperidino-

methylene-5-androsten-17-one (III*a*), m.p. 218–224°. ν_{max} 3360, 1683, 1580 cm^{-1}. Anal. Calc. for $C_{25}H_{37}O_2N$: C, 78.25; H, 9.72; N, 3.65. Found: C, 78.12; H, 9.69; N, 3.67%. Acetyl derivative, m.p. 221–222° (from methanol). ν_{max} 1735, 1685, 1585, 1250, 1030 cm^{-1}. Anal. Calc. for $C_{27}H_{39}O_3N$: C, 76.19; H, 9.24; N, 3.29. Found: C, 76.15; H, 9.28; N, 3.26%.

Condensation of Amines with 3β-Hydroxy-16-hydroxymethylene-5-androsten-17-one (I)

A solution of I (300 mg) and a slight excess of amine in ethanol was refluxed for several hours. Dilution with water precipitated the aminomethylene steroid. The solid product was isolated by filtration and purified (refer to Table I).

Reaction of Cyanoacetamide and 3β-Hydroxy-16-hydroxymethylene-5-androsten-17-one (I) *in the Presence of a Molecular Amount of Piperidine*

A mixture of I (2.0 g), cyanoacetamide (680 mg), and piperidine (0.6 ml) was refluxed in ethanol for 3 days. On cooling, crystalline material (300 mg) precipitated out of solution. Recrystallization of the material from acetic acid gave 3-cyano-4,5-dehydro-6-hydroxy-5,6(16′,17′-3′β-hydroxy-5′-androstenyl)-2-piperidone (IV), m.p. 348–352° (dec.). ν_{max} 3480, 3150, 3040 (sh), 2230, 1660, 1580 cm^{-1}. Anal. Calc. for $C_{23}H_{30}O_3N_2$: C, 72.22; H, 7.91; N, 7.32. Found: C, 72.79; H, 7.83; N, 7.26%.

The filtrate was concentrated and a solid material precipitated. The product (1.79 g), purified by recrystallization from dimethylformamide–water, was identified by its infrared absorption spectrum, and a mixed melting point determination with the authentic sample, as 3β-hydroxy-16-piperidinomethylene-5-androsten-17-one (III*a*).

3-Cyano-5,6(16′,17′-3′β-hydroxy-5′-androstenyl)-2-pyridone (V)

A solution of 3-cyano-4,5-dehydro-6-hydroxy-5,6(16′,17′-3′β-hydroxy-5′-androstenyl)-2-piperidone (IV) (100 mg) in pyridine – acetic anhydride (1:1, 10 ml) was allowed to stand overnight at room temperature. It was then poured into water (150 ml) and solid material (100 mg) settled. Recrystallization of the product from dioxane provided 3-cyano-5,6(16′,17′-3′β-hydroxy-5′-androstenyl)-2-pyridone (V), m.p. 351–353° (dec.). ν_{max} 2230, 1730, 1665, 1580, 1245 cm^{-1}. Anal. Calc. for $C_{25}H_{30}O_3N_2$: C, 73.87; H, 7.44; N, 6.90. Found: C, 73.90; H, 7.39; N, 6.79%.

3-Cyano-4,5-dehydro-6-hydroxy-5,6(16′,17′-3′β-hydroxy-5′-androstenyl)-2-piperidone (IV)

An ethanolic solution of 3β-hydroxy-16-piperidinomethylene-5-androsten-17-one (III*a*) (1.0 g) and cyanoacetamide (340 mg) was refluxed for 3 days. The crystalline material (200 mg) which formed on cooling was identified by its infrared spectrum, and by a mixed melting point determination with an authentic sample, as 3-cyano-4,5-dehydro-6-hydroxy-5,6(16′,17′-3′β-hydroxy-5′-androstenyl)-2-piperidone (IV).

Attempted Condensation of 3β-Hydroxy-16-hydroxymethylene-5-androsten-17-one (I) *with Cyanoacetamide Using Sodium Ethylate as the Condensing Agent*

A solution of sodium (75 mg) in absolute ethanol (20 ml) was prepared in a nitrogen atmosphere. A slurry of I (300 mg) and cyanoacetamide (100 mg) in absolute ethanol (10 ml) was added, and the reaction mixture was refluxed for 17 hours in a nitrogen atmosphere. The solvent was evaporated under reduced pressure and the residue was chromatographed on alumina (80–200 mesh). Elution with petroleum ether (30–60°) afforded a product (160 mg) which was identified by its infrared absorption spectrum, and a mixed melting point determination with an authentic sample as 3β-hydroxy-5-androsten-17-one (VI). In one instance, a very small amount of a solid material, m.p.

TABLE I

Reaction of amines with 3β-hydroxy-16-hydroxymethylene-5-androsten-17-one

No.	3β-Hydroxy-5-androsten-17-one	Reflux time (hours)	Method of purification	Yield %	Melting point	Empirical formula	Analyses						Infra-red ν_{max} in cm^{-1}
							Calculated (%)			Found (%)			
							C	H	N	C	H	N	
III*a*	16-Piperidino-methylene	22	Recrystn. from dimethylformamide–water	99	215–220°	$C_{25}H_{37}O_2N$	78.25	9.72	3.65	78.12	9.69	3.67	3360 1683 1580
III*b*	16-Morpholino-methylene	24	Recrystn. from acetone	91.6	239–242°	$C_{24}H_{35}O_3N$	74.77	9.15	3.63	74.85	9.14	3.68	3460 1680 1580
III*c*	16-Diethyl-aminomethylene	24	Recrystn. from acetone	90.8	167–169°	$C_{24}H_{37}O_2N$	77.58	10.03	3.77	77.49	10.13	3.76	3400 1678 1575
III*d*	16-Methylamino-methylene	48	Recrystn. from dimethylformamide–water	90.2	204–206°	$C_{21}H_{31}O_2N.$ H_2O			4.03			4.10	3360 1680 1607– 1525
III*e*	16-Anilinomethylene	48	Elution with benzene – petroleum ether (30–60°) (1:9) from alumina; recrystn. from methanol–water	90.5	127–129°	$C_{26}H_{33}O_2N$			3.58			3.56	3400 3320 3040 1692 1622 1602 1585 1500 1267 750 690

227–232°, was isolated from the reaction mixture. The infrared spectrum of this product coincided in all respects with that of 1-cyano-2-hydroxy-2(16′-3′β-hydroxy-17′-oxo-5′-androstenyl)propionamide (II).

Reaction of 3β-Hydroxy-16-hydroxymethylene-5-androsten-17-one, Sodium Salt, with Carboxamidoacetamidine Hydrochloride

A solution of the sodium salt of 3β-hydroxy-16-hydroxymethylene-5-androsten-17-one (1.0 g) and carboxamidoacetamidine hydrochloride (420 mg) in absolute ethanol was refluxed in a nitrogen atmosphere for 17 hours. The solvent was evaporated under reduced pressure, and the residue was chromatographed on alumina (80–200 mesh). Elution with petroleum–ether (30–60°) provided crystalline material (170 mg), m.p. 142–144°. A mixed melting point determination with an authentic sample of 3β-hydroxy-5-androsten-17-one (VI) showed no depression. Further elution with methanol–ether (1:5) yielded another crystalline product (480 mg). Recrystallization of this material from methanol–benzene gave 2-amino-3-carboxamido-5,6(16′,17′-3′β-hydroxy-5′-androstenyl)pyridine (VII), m.p. 281–284° (dec.). ν_{max} 3400, 3330, 3200, 1650, 1615, 1597, 1538 cm^{-1}. Anal. Calc. for $C_{23}H_{31}O_2N_3$: C, 72.41; H, 8.19; N, 10.98. Found: C, 72.27; H, 8.35; N, 10.88%.

3β-Chloro-16-chloromethylene-5-androsten-17-one (VIII)

Thionyl chloride (3 ml) was added to 3β-hydroxy-16-hydroxymethylene-5-androsten-17-one (I) (1.0 g). A vigorous effervescence ensued, and the reaction mixture changed to a dark red liquid. The reaction was allowed to continue for 1 hour, then the liquid was poured into ice-cold 2 *N* sodium hydroxide solution (200 ml), and allowed to stand for 2 hours. The solid material (1.05 g), m.p. 199–207°, which formed, on recrystallization from benzene–methanol afforded 3β-chloro-16-chloromethylene-5-androsten-17-one (VIII), m.p. 204–210° (dec.). ν_{max} 1725, 1630, 890–666 cm^{-1}. Anal. Calc. for $C_{20}H_{26}OCl_2$: C, 67.98; H, 7.42. Found: C, 68.21; H, 7.47%.

2-Methyl-5,6(16′,17′-3′β-chloro-5′-androstenyl)pyrimidine (IX)

To a solution of sodium (235 mg) in absolute ethanol (50 ml) was added, in a nitrogen atmosphere, a slurry of 3β-chloro-16-chloromethylene-5-androsten-17-one (VIII) (1.0 g) and acetamidine hydrochloride (245 mg) in absolute ethanol (10 ml). The reaction mixture was refluxed for 1.5 hours, then was allowed to stand overnight at room temperature in a nitrogen atmosphere. The mixture was filtered, and the filtrate concentrated *in vacuo*. The residue was chromatographed on alumina (80–200 mesh). Elution with ether gave a crystalline product (200 mg). Recrystallization of the product from dioxane–water furnished 2-methyl-5,6(16′,17′-3′β-chloro-5′-androstenyl)pyrimidine (IX), m.p. 145–148°. ν_{max} 1598, 1560, 763 cm^{-1}. Anal. Calc. for $C_{22}H_{29}ClN_2$: C, 74.05; H, 8.19; N, 7.85. Found: C, 73.87; H, 8.08; N, 7.86.

REFERENCES

1. L. F. Fieser and M. Fieser. Steroids. Reinhold. 1959. p. 847.
2. F. C. Uhle. J. Am. Chem. Soc. **73**, 883 (1951).
3. D. Gould, E. L. Shapiro, and E. B. Hershberg. J. Am. Chem. Soc. **76**, 5567 (1954).
4. D. Gould, E. L. Shapiro, L. E. Finckenor, F. Gruen, and E. L. Hershberg. J. Am. Chem. Soc. **78**, 3158 (1956).
5. L. Ruzicka, V. Prelog, and J. Battegay. Helv. Chim. Acta, **31**, 1296 (1948).
6. W. C. Thompson. J. Am. Chem. Soc. **53**, 3160 (1931).
7. H. K. Sen-Gupta. J. Chem. Soc. **107**, 1347 (1915).

8. J. W. COOK and W. H. S. THOMSON. J. Chem. Soc. 395 (1945).
9. U. BASU. J. Indian Chem. Soc. **7**, 481 (1930).
10. C. BARAT. J. Indian Chem. Soc. **8**, 801 (1931).
11. H. HENECKA. Ber. **82**, 36 (1949).
12. C. BARAT. J. Indian Chem. Soc. **7**, 321 (1930).
13. E. P. KOHLER and B. L. SOUTHER. J. Am. Chem. Soc. **44**, 2903 (1922).
14. S. DEV. J. Indian Chem. Soc. **30**, 443 (1953).
15. S. M. MCELVAIN and J. W. NELSON. J. Am. Chem. Soc. **64**, 1825 (1942).
16. S. M. MCELVAIN and B. E. TATE. J. Am. Chem. Soc. **73**, 2760 (1951).
17. A. DORNOW and E. NEUSE. Arch. Pharm. **287**, 361 (1954).
18. A. DORNOW and E. NEUSE. Ber. **84**, 296 (1951).

STEROIDS

PART II. 6-AMINO STEROIDS[1]

BARBARA G. KETCHESON[2] AND ALFRED TAURINS

ABSTRACT

Reduction of methyl 3β-acetoxy-6-oximinodinorcholanate using sodium in *n*-propyl alcohol, and acetylation, gave 6α-acetamido-3β-acetoxydinorcholanic acid; treatment with lithium aluminum hydride in tetrahydrofuran provided 3β,22ξ-dihydroxydinorcholan-6-one. High-pressure hydrogenation of methyl 3β-acetoxy-6-nitro-5-dinorcholenate, using palladium black as catalyst in acetic acid medium, afforded methyl 6ξ-acetamido-3β-acetoxy-5α-dinorcholanate. Under identical conditions, catalytic hydrogenation of 3β-acetoxy-6-nitro-5-cholestene resulted in the formation of 6β-acetamido-3β-acetoxy-5α-cholestane and 6ξ-acetamido-3β-acetoxy-5β-cholestane.

DISCUSSION

A variety of amino steroids have been synthesized and tested for biological activity (1–10). In view of the fact that 6-aminocholestan-3β-ol (1), and several amino derivatives of 3β-acetoxy-5-dinorcholenic acid (5), had been found to possess appreciable antibacterial properties, the present investigation dealing with the preparation of 6-amino steroids of the dinorcholenic acid and cholestane series was undertaken.

When 3β-acetoxy-5-dinorcholenic acid (I) was nitrated by the procedure of Anagnostopoulos and Fieser (11), an oil was obtained which crystallized only after standing at room temperature for several weeks. However, conversion of I to its methyl ester (II) (12, 13), and treatment of the latter with fuming nitric acid resulted in the formation of

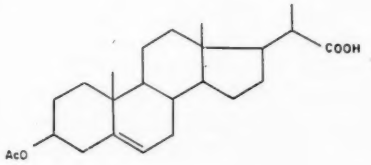

(I)

a crystalline nitration product. The product was formulated as methyl 3β-acetoxy-6-nitro-5-dinorcholenate (III), since it is well-established that nitration of a Δ^5-steroid leads to the production of the corresponding 6-nitro-Δ^5 compound (14).

When 6-nitro-Δ^5-steroids are treated with zinc dust and acetic acid, the corresponding saturated 6-oxosteroids are formed (14). However, when methyl 3β-acetoxy-6-oxodinorcholanate (IV) was prepared by this method, a very low yield was obtained. An alternative procedure was developed which involved refluxing a methanolic solution of the nitro compound (III) for several hours with iron filings in the presence of a small amount of hydrochloric acid. In this way, a 58% yield of IV was obtained.

[1]*Manuscript received March 9, 1960.*

Contribution from the Department of Chemistry, McGill University, Montreal, Que., with financial assistance from the National Research Council, Ottawa, Canada. Abstracted from a portion of the thesis submitted by Barbara G. Ketcheson to the Department of Chemistry, McGill University, Montreal, Que., August 1958, in partial fulfilment of the requirements for the Ph.D. degree.

[2]*Holder of a National Research Council Studentship, 1956–57, and of Canadian Industries (1954) Limited Fellowships, 1955–56 and 1957–58.*

Methyl 3β-acetoxy-6-oximinodinorcholanate (V) was prepared, and reduced with sodium in *n*-propyl alcohol. Although Vanghelovici (15) had reported that similar reductions of the ethyl esters of 3,7,12-trihydroxycholanic, 3,12-dihydroxycholanic, and cholenic acids had brought about the transformation of the ester group to a primary alcoholic function, James *et al.* (2) had not observed the Bouveault–Blanc effect in the reduction of ethyl 3,12-dihydroxy-7-oximinocholanate. Since the 22 position of the steroid molecule is definitely hindered, sodium–alcohol treatment of V was not expected to bring about the reduction of the ester group. The infrared spectrum provided confirmatory evidence that the reduction product was in fact 6α-amino-3β-hydroxydinorcholanic acid (VI). Acetylation of VI with acetic anhydride – pyridine at room temperature provided 6α-acetamido-3β-acetoxydinorcholanic acid (VII). The α-configuration was assigned to the amino group on the basis of mode of preparation (16, 17).

The oxime (V) also was reduced by means of lithium aluminum hydride in tetrahydrofuran. A ratio of 1:10 of V to the reducing agent was used. From the reaction, a single product was isolated in 86% yield. It contained no nitrogen, and had a molecular formula $C_{22}H_{36}O_3$. In the infrared spectrum there was a strong broad band at 3300 cm^{-1}

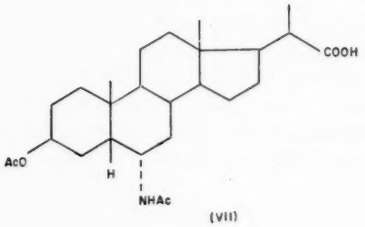

(VII)

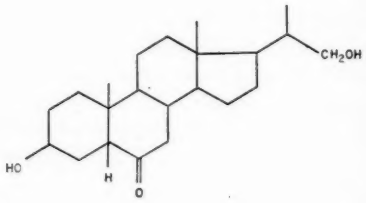

(VIII)

indicating the presence of an associated hydroxyl group or groups. A single narrow peak at 1712 cm^{-1} could be attributed to absorption by a 6-ketone of the normal series (18). The product was postulated as 3β,22ξ-dihydroxydinorcholan-6-one (VIII). In order to substantiate the formulation of VIII, the compound was acetylated, and the oxime derivative was prepared. The infrared spectrum of the oxime derivative demonstrated the presence of associated hydroxyl groups and an oxime group, but there was no indication of any carbonyl absorption. Analysis and the infrared spectrum were in agreement with the product of acetylation being 3β, 22ξ-diacetoxydinorcholan-6-one (IX). The formation of VIII by the lithium aluminum hydride reduction of the oximinoester (V) was unexpected. It was felt that the oxime group was converted to the ketone under the alkaline hydrolytic conditions of the reaction mixture when wet solvent was added to destroy the unreacted excess lithium aluminum hydride.

Catalytic hydrogenation of 3β-substituted-Δ^5-steroids is known to provide mainly saturated steroids of the A/B trans series. In some cases, the principal product may be accompanied by small quantities of saturated steroids of the A/B cis series (19).

3β-Acetoxy-6-nitro-5-cholestene (X) (11) was hydrogenated using palladium black as the catalyst in an acetic acid medium at 53 atmospheres pressure and 150° for 6 hours. Previously, X had been catalytically hydrogenated at 40 atmospheres pressure and a temperature of 100–180°, and a saturated amine $C_{29}H_{51}O_2N$, m.p. 122°, or its acetyl derivative had been obtained as the product (20). However, in the present investigation, two products were isolated, the main one in the form of dense rhombic crystals, and the

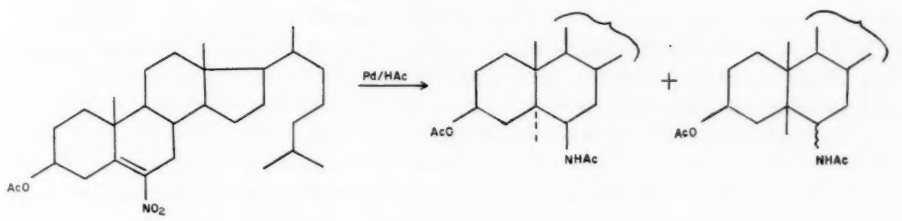

(X) (XI) (XII)

other as slender needles. Both compounds had a molecular formula $C_{31}H_{53}O_3N$. The main product melted at 167°, and the other substance at 94–96°. The compounds were postulated as 6-acetamido-3β-acetoxycholestane (XI) and 6-acetamido-3β-acetoxy-5β-cholestane (XII). A comparison of the infrared spectra of XI and 6β-acetamido-3β-acetoxycholestane (16), m.p. 166–168°, revealed that the two were identical in all respects. A mixed melting point determination of these substances showed no depression. On the basis of mode of preparation, it would be expected that the acetamido group in XII would be β-oriented.

In connection with the preparation of 6β-aminocholestan-3β-ol (XIII) from 3β-acetoxy-6-oximinocholestane (XIV) by reduction using lithium aluminum hydride, it was noted that Shoppee *et al.* (16) encountered considerable difficulty with the analysis of the hydroxy amine XIII, m.p. 128–130° (methanol). He attributed the unsatisfactory analytical values obtained to the rapid absorption of water and (or) carbon dioxide. No yield of product was reported for the reaction. In the present case, the reduction was carried out in tetrahydrofuran rather than ether, and the product was isolated in a 57% yield. No difficulty was experienced in obtaining entirely satisfactory analytical results for 6β-aminocholestan-3β-ol (XIII), m.p. 129–132° (dimethylformamide–water).

It was thought that the main product resulting from the high-pressure hydrogenation of methyl 3β-acetoxy-6-nitro-5-dinorcholenate (III) would be methyl 6-acetamido-3β-acetoxy-5α-dinorcholanate (XV). The hydrogenation was carried out under the same conditions as had been used in the α series. A single substance was isolated from the

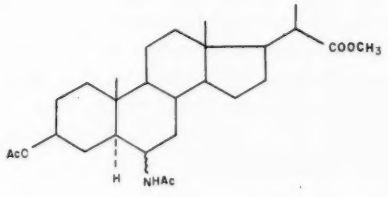

(XV)

reaction in a 67% yield. On the basis of its infrared spectrum and analysis, the product was designated as methyl 6ξ-acetamido-3β-acetoxy-5α-dinorcholanate (XV). No configuration was assigned to the acetamido group, although on the basis of mode of preparation it would be expected that the group would have the axial conformation and thus be β-oriented.

EXPERIMENTAL

The melting points were determined in a Thiele–Dennis melting point tube containing Dow Corning silicone fluid No. D.C. 550. All melting points are uncorrected. Microanalyses were carried out in the W. Manser Laboratory, Zurich, Switzerland, and in the Schwarzkopf microanalytical laboratory, Woodside, N.Y., U.S.A. The infrared absorption spectra were determined in potassium bromide by means of a Perkin–Elmer Model 21 double-beam spectrophotometer equipped with a sodium chloride prism.

Methyl 3β-Acetoxy-6-nitro-5-dinorcholenate (III)

A solution of methyl 3β-acetoxy-5-dinorcholenate (II) (25.0 g) in absolute ether (300 ml) was cooled to −20°. Fuming nitric acid (150 ml) was added, with stirring, at such a rate that the temperature did not rise above −10°. When the addition had been completed, the reaction mixture was stirred for 1½ hours, while the temperature slowly rose to 0–5°. The ethereal solution was neutralized by washing with a 2.5% sodium hydroxide solution (600 ml), and with a saturated solution of sodium chloride. The ether was removed *in vacuo* and a solid crystalline residue remained. After recrystallization from methanol, the material (22.9 g) melted at 145–147°. Further purification from methanol provided methyl 3β-acetoxy-6-nitro-5-dinorcholenate (III), m.p. 147–149°. ν_{max} 1735, 1527, 1240 cm^{-1}. Anal. Calc. for $C_{25}H_{37}O_6N$: C, 67.08; H, 8.33; N, 3.13. Found: C, 67.10; H, 8.31; N, 3.21%.

Methyl 3β-Acetoxy-6-oxodinorcholanate (IV)

To a mixture of iron filings (40 mesh, 20.0 g) and methyl 3β-acetoxy-6-nitro-5-dinorcholenate (III) (10.0 g) were added methanol (300 ml) and concentrated hydrochloric acid (3 ml). The reaction mixture was refluxed with stirring for 17 hours, then filtered hot. The residue on the filter was washed thoroughly with hot methanol. The methanolic filtrate and washings were concentrated and set aside for crystallization. The crystalline product (5.42 g) obtained melted at 160–162°. Purification by recrystallization from methanol afforded methyl 3β-acetoxy-6-oxodinorcholanate, m.p. 164.5–166.5°. ν_{max} 1745, 1730 (sh), 1718, 1280 (sh), 1263, 1248 cm^{-1}. Anal. Calc. for $C_{25}H_{38}O_5$: C, 71.72; H, 9.50. Found: C, 71.78; H, 9.31%.

Methyl 3β-Acetoxy-6-oximinodinorcholanate (V)

An ethanolic solution of methyl 3β-acetoxy-6-oxodinorcholanate IV (0.4 g), sodium acetate (0.5 g), and hydroxylamine hydrochloride (0.4 g) was refluxed for 24 hours. Water was added to the solution until a slight permanent cloudiness was observed. On standing, crystalline material (0.34 g) was deposited and isolated. It melted at 202–205°. Recrystallization from ethanol provided methyl 3β-acetoxy-6-oximinodinorcholanate (V), m.p. 207–209°. ν_{max} 3300, 1735, 1720, 1655, 1245 cm^{-1}. Anal. Calc. for $C_{25}H_{39}O_5N$: C, 69.25; H, 9.06; N, 3.23. Found: C, 69.73; H, 9.02; N, 3.29%.

6α-Acetamido-3β-acetoxydinorcholanic Acid (VII)

In a nitrogen atmosphere, small pieces of sodium (2.0 g) were added over a period of 1½ hours to a solution of methyl 3β-acetoxy-6-oximinodinorcholanate (V) (500 mg) in dry *n*-propyl alcohol (35 ml) at 70°. When the sodium had been added, the solution was refluxed for 9 hours. Then it was poured into distilled water (500 ml), and allowed to stand at room temperature for several days. Solid material precipitated out of solution and was isolated. Recrystallization of the product afforded 6α-amino-3β-hydroxydinorcholanic acid (VI), m.p. 176–178°. ν_{max} 3420,1640, 1568 cm^{-1}.

A solution of VI (100 mg) in acetic anhydride (5 ml) and pyridine (5 ml) was allowed to stand at room temperature overnight. The solution was poured into water (200 ml). The solid material (90 mg) which formed on standing was isolated and melted at 161–165°. Recrystallization from ethanol–water gave 6α-acetamido-3β-acetoxydinorcholanic acid (VII), m.p. 158–159°. ν_{max} 3340, 1735, 1663, 1540, 1245 cm^{-1}. Anal. Calc. for $C_{26}H_{41}O_5N$: N, 2.86. Found: N, 2.75%.

3β,22ξ-Dihydroxydinorcholan-6-one (VIII)

In a nitrogen atmosphere was added, dropwise, and with stirring, a solution of methyl 3β-acetoxy-6-oximinodinorcholanate (V) (1.0 g) in dry tetrahydrofuran, to a refluxing suspension of lithium aluminum hydride (1.0 g) in anhydrous tetrahydrofuran (20 ml). The resulting reaction mixture was refluxed under these conditions for 18 hours. After cooling to room temperature, wet tetrahydrofuran was carefully added to the mixture with vigorous stirring. The suspension was filtered with suction, and the filter cake was washed thoroughly with ether. The filtrate was evaporated *in vacuo* leaving a solid product (690 mg). Recrystallization from dioxane–water yielded 3β,22ξ-dihydroxydinorcholan-6-one (VIII), m.p. 190–194°. ν_{max} 3300, 1712, 1062 cm^{-1}. Anal. Calc. for $C_{22}H_{36}O_3$: C, 75.80; H, 10.41. Found: C, 75.52; H, 10.39%.

3β,22ξ-Diacetoxydinorcholan-6-one (IX)

A solution of 3β,22ξ-dihydroxydinorcholan-6-one (VIII) (140 mg) in acetic anhydride (5 ml) and pyridine (5 ml) was allowed to stand at room temperature overnight. Then it was poured into water (200 ml). Solid material (90 mg) separated from solution was isolated, and on recrystallization from dimethylformamide–water gave 3β,22ξ-diacetoxydinorcholan-6-one (IX), m.p. 115–117°. ν_{max} 1737, 1255 cm^{-1}. Anal. Calc. for $C_{26}H_{40}O_5$: C, 72.19; H, 9.32. Found: C, 72.25; H, 9.25%.

High-pressure Hydrogenation of 3β-Acetoxy-6-nitro-5-cholestene (X)

A solution of X (2.0 g) in glacial acetic acid (30 ml) was hydrogenated in a Parr high-pressure hydrogenation apparatus for 6 hours at 150° and 53 atmospheres pressure using 10% palladium on charcoal (1.0 g) as catalyst. The reaction mixture was filtered, and the residue on the filter was washed thoroughly with acetic acid. The solvent was removed *in vacuo*, and the residue was taken up in ethanol. On standing, small rhombic crystals were formed. The product (1.15 g) was purified by recrystallization from dioxane–water yielding 6β-acetamido-3β-acetoxycholestane (XI), m.p. 167°. ν_{max} 3375, 3320, 1733, 1645, 1550, 1250 cm^{-1}. Anal. Calc. for $C_{31}H_{53}O_3N$: C, 76.33; H, 10.95; N, 2.87. Found: C, 76.33; H, 10.91; N, 2.85%.

On standing, crystalline material in the form of slender needles separated from the filtrate. This product (200 mg) melted at 80–84°. Recrystallization from methanol–water gave 6ξ-acetamido-3β-acetoxy-5β-cholestane (XII), m.p. 94–96°. ν_{max} 3380, 1737, 1655, 1243 cm^{-1}. Anal. Calc. for $C_{31}H_{53}O_3N$: C, 76.33; H, 10.95. Found: C, 76.59; H, 10.93%.

6β-Aminocholestan-3β-ol (XIII)

In a nitrogen atmosphere, and with stirring, a solution of 3β-acetoxy-6-oximinocholestane (XIV) (500 mg) in anhydrous tetrahydrofuran (25 ml) was added dropwise to a refluxing suspension of lithium aluminum hydride (500 mg) in dry tetrahydrofuran (20 ml). The reaction was allowed to continue under these conditions for 18 hours. Wet tetrahydrofuran was added dropwise with vigorous stirring, then the mixture was filtered, and the filter cake was washed thoroughly with wet tetrahydrofuran. The filtrate was concentrated under reduced pressure, and the solid material which precipitated out of

solution was isolated. A yield of 250 mg of product melting at 123–129° was obtained. Further purification by recrystallization from dimethylformamide–water yielded 6β-aminocholestan-3β-ol (XIII), platelets, m.p. 129–132°. ν_{max} 3400 (sh), 3300 (sh), 3200, 1600 cm^{-1}. Anal. Calc. for $C_{27}H_{49}ON$: C, 80.33; H, 12.24; N, 3.47. Found: C, 80.21; H, 12.19; N, 3.44%.

6β-Acetamido-3β-acetoxycholestane (XI)

A solution of 6β-aminocholestan-3β-ol (XIII) (100 mg) in acetic anhydride (5 ml) and pyridine (5 ml) was allowed to stand overnight at room temperature. The reaction mixture was poured into water (150 ml), and the solid material (80 mg) which formed on standing was isolated. Recrystallization from ethyl acetate furnished 6β-acetamido-3β-acetoxycholestane (XI), m.p. 166–168°. ν_{max} 3375, 3320, 1733, 1645, 1550, 1250 cm^{-1}. Anal. Calc. for $C_{31}H_{53}O_3N$: N, 2.87. Found: N, 2.71%.

Methyl 6ξ-Acetamido-3β-acetoxy-5α-dinorcholanate (XV)

Methyl 3β-acetoxy-6-nitro-5-dinorcholenate (III) (2.0 g) in glacial acetic acid (30 ml) was hydrogenated in a Parr high-pressure hydrogenation apparatus using a 10% palladium on charcoal catalyst (1.0 g). The hydrogenation was carried out for 6 hours at 150° and 53 atmospheres pressure. The mixture was filtered, and the filter cake was washed thoroughly with acetic acid. The solvent was removed *in vacuo* and the residue taken up in ethanol. The ethanolic solution was heated to boiling and water was added until a faint cloudiness persisted. On cooling, a solid (1.41 g) separated from solution and was isolated. Recrystallization from benzene – petroleum ether (30–60°) yielded methyl 6ξ-acetamido-3β-acetoxy-5α-dinorcholanate (XV), m.p. 236–238° (dec.). ν_{max} 3290, 3070, 1737, 1655, 1558, 1242 cm^{-1}. Anal. Calc. for $C_{27}H_{43}O_5N$: N, 3.05. Found: N, 3.06%.

ACKNOWLEDGMENTS

The authors wish to thank Frank W. Horner Ltd. of Montreal for the use of their high-pressure hydrogenation equipment, and Dr. G. Frangatos for his valuable technical assistance.

REFERENCES

1. J. Barnett, B. Ryman, and F. Smith. J. Chem. Soc. 524, 526, 528 (1946).
2. S. P. James, F. Smith, M. Stacey, and M. Webb. J. Chem. Soc. 665 (1946).
3. A. S. Jones, M. Webb, and F. Smith. J. Chem. Soc. 2164 (1949).
4. R. A. Micheli and C. K. Bradsher. J. Am. Chem. Soc. **77**, 4788 (1955).
5. H. L. Herzog, C. C. Payne, and E. B. Hershberg. J. Am. Chem. Soc. **77**, 5324 (1955).
6. D. Gould, E. L. Shapiro, L. E. Finckenor, F. Gruen, and E. B. Hershberg. J. Am. Chem. Soc. **78**, 3158 (1956).
7. D. P. Dodgson and R. D. Haworth. J. Chem. Soc. 67 (1952).
8. F. C. Uhle. J. Am. Chem. Soc. **73**, 883 (1951).
9. L. F. Fieser and W. Huang. J. Am. Chem. Soc. **75**, 6306 (1953).
10. D. Gould, E. L. Shapiro, and E. B. Hershberg. J. Am. Chem. Soc. **76**, 5567 (1954).
11. C. E. Anagnostopoulos and L. F. Fieser. J. Am. Chem. Soc. **76**, 532 (1954).
12. E. Fernholz. Ann. **507**, 128 (1933).
13. A. Butenandt and G. Fleischer. Ber. **70**B, 96 (1937).
14. L. F. Fieser and M. Fieser. Steroids. Reinhold. 1959. p. 43.
15. M. Vanghelovici. Bul. soc. chim. România, **18**, 103 (1936); Chem. Zentr. II, 2533 (1937).
16. C. W. Shoppee, D. E. Evans, and G. H. R. Summers. J. Chem. Soc. 97 (1957).
17. C. W. Shoppee, R. J. W. Cremlyn, D. E. Evans, and G. H. R. Summers. J. Chem. Soc. 4364 (1957).
18. R. N. Jones and F. Herling. J. Org. Chem. **19**, 1252 (1954).
19. J. R. Lewis and C. W. Shoppee. J. Chem. Soc. 1365 (1955).
20. I. G. Farbenindustrie. Fr. Patent No. 885,439 (1943); Chem. Zentr. II, 563 (1944).

STEROIDS

PART III. REDUCTION OF OXIMINOCHOLANIC ACIDS[1]

TED H. WAID[2] AND ALFRED TAURINS

ABSTRACT

The reduction of 12-oximino-, 3,12-dioximino-, and 7,12-dioximino-cholanic acids using sodium in alcohol resulted in the formation of 12β-amino-, 3α,12β-diamino-, and 7β,12β-diamino-cholanic acids respectively. The reaction of 3,12-dioximinocholanic acid with lithium aluminum hydride provided cholane-3ξ,12ξ,24-triol, while similar treatment of 7,12-dioximinocholanic acid afforded 7ξ-amino-12-oximinocholan-24-ol.

DISCUSSION

Basic derivatives of bile acids and esters, having amino functions located in positions 3 (1, 2), 6 (3), 7 (2, 4, 5), 11 (6), and 12 (2, 5, 7) of the steroidal nucleus, have been described. Their synthesis has been accomplished for the most part by reduction of the corresponding oximes with sodium in alcohol, and has been prompted primarily by the possibility of such compounds being physiologically active.

In the present investigation, a study has been made of the reduction of 12-oximino- (I) (8), 3,12-dioximino- (II) (9), and 7,12-dioximino-cholanic acids (III) (10), using sodium in alcohol and lithium aluminum hydride. In the reductions using sodium, *n*-propyl and *n*-butyl alcohols gave the best yields of purest products. The color of reaction mixtures in isoamyl alcohol was darker, and the crude products contained appreciable amounts of tarry impurities. Since reductions of oximes with alkali metals and proton donors are known to give predominantly the equatorial conformation (11, 12), the conformation of amino groups in the steroidal amino acids synthesized by reductions with sodium in alcohol were assigned on the basis of mode of preparation. Preliminary experiments of oxime reductions using lithium aluminum hydride in tetrahydrofuran showed that two- to five-fold molar excesses of lithium aluminum hydride led to the formation of mixtures of products. When a 10-fold excess of the reagent was used, definite reaction products could be isolated in all cases.

12-Oximinocholanic acid (I) was prepared from 3α,12α-dihydroxycholanic acid (IV) by oxidation of IV to 3,12-dioxocholanic acid (V) (13), Clemmensen reduction of V to 12-oxocholanic acid (VI) (14, 15, 16), and preparation of the oxime (I). The oxidation of the dihydroxy acid (IV) to the dioxo derivative (V) was carried out using the procedure described by Heilbron (17) for the oxidation of acetylenic carbinols. This method gave consistent yields of over 90% of pure product as compared with the 70% yield obtained by Wieland's method (13) of oxidation in acetic acid. As expected, the reduction of the oximino acid (I) with sodium in alcohol provided 12β-aminocholanic acid (VII) in good yield. That VII existed as a dipole ion was confirmed by the infrared spectrum which showed bands characteristic of the carboxylate ion at 1550 cm^{-1} and of the NH_3^+ group at 1625 cm^{-1}. Several treatments of VII with concentrated hydrochloric acid resulted in the formation of the corresponding hydrochloride. The infrared spectrum of the latter showed suppression of the band due to the carboxylate ion and release of the carboxyl

[1]*Manuscript received March 9, 1960.*

Contribution from the Department of Chemistry, McGill University, Montreal, Que., with financial assistance from the National Research Council, Ottawa, Canada. Abstracted from a portion of the thesis submitted by Waid to the Department of Chemistry, McGill University, Montreal, Que., April 1957, in partial fulfilment of the requirements for the Ph.D. degree.

[2]*Holder of a National Research Council Studentship 1955–56. Present address: Monsanto Canada Ltd., Montreal, Que.*

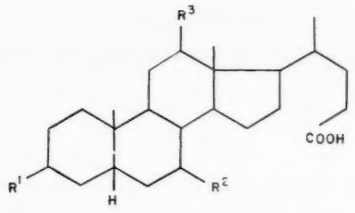

(VII) $R^1 = R^2 = H$; $R^3 = NH_2$

(VIII) $R^2 = H$, $R^1 = R^3 = NH_2$

(XII) $R^1 = H$; $R^2 = R^3 = NH_2$

band at 1705 cm^{-1}. Treatment of the oximino acid (I) with 3% sodium amalgam resulted in the transformation of the oxime group to the keto group. The keto acid (VI) was identified by a mixed melting point determination with an authentic sample.

3,12-Dioximinocholanic acid (II) was prepared from 3α,12α-dihydroxycholanic acid (IV) by oxidation of IV to 3,12-dioxocholanic acid (V) and oximation of V to the dioxime (II). The reduction of II with sodium in alcohol resulted in the formation of 3α,12β-diaminocholanic acid (VIII) in good yield. Possessing one carboxyl and two amino groups, this diaminocarboxylic acid behaved as a base and formed a dihydrochloride. The infrared spectrum confirmed the presence of the NH_2 group (1660 cm^{-1}), the NH_3^+ ion (1623 cm^{-1}), and the carboxylate ion (1575 cm^{-1}).

A product containing no nitrogen and insoluble in both acids and bases was formed in the reaction of the oximino acid (II) with lithium aluminum hydride. The infrared spectrum had a very strong band at 3340 cm^{-1}, which was attributed to absorption by associated OH groups, and a series of high intensity bands in the region 1075–1011 cm^{-1}. The latter could be assigned to C—O stretching vibrations in a steroid alcohol. On the basis of the infrared spectrum and the analytical results, the compound was formulated as cholane-3ξ,12ξ,24-triol (IX). The steric course of reductions with lithium aluminum hydride being uncertain, the conformations of the hydroxyl groups at 3- and 12-positions were not assigned.

The formation of IX was quite unexpected, although a somewhat similar result had been obtained by Redel and his co-workers (2) in their attempts to reduce methyl 3α,12α-diformoxy-7-oximinocholanate in ethanolic solution by catalytic hydrogenation under pressure using Raney nickel. Mignonac (18, 19) and Paul (20) also had observed the formation of secondary alcohols on reductions of oximes. It was considered that the reaction of the oximino acid (II) with lithium aluminum hydride proceeded via an unstable imine, which, under hydrolytic conditions, was transformed into the corresponding ketone. The latter was, in turn, reduced to the secondary alcohol (IX) by the lithium aluminum hydride still present in the reaction mixture.

Clemmensen reduction of 3,7,12-trioxocholanic acid (X) to 7,12-dioxocholanic acid (XI) and oximation provided 7,12-dioximinocholanic acid (III). The reduction of III with sodium in *n*-propyl or *n*-butyl alcohol produced 7β,12β-diaminocholanic acid (XII) in high yields, as anticipated. When the reduction of III was carried out under similar conditions to those used for the reduction of the dioximino acid (II) with lithium

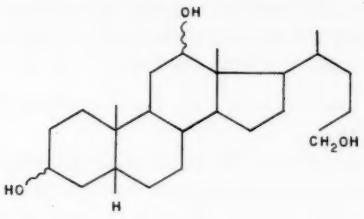

(X)

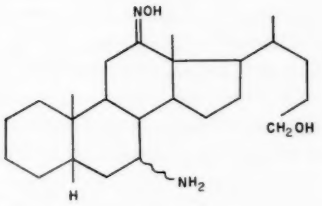

(XIII)

aluminum hydride, a nitrogen-containing product was obtained. In the infrared spectrum there was no carbonyl absorption, but the band at 3300 cm^{-1} indicated the presence of an alcoholic function. The medium intensity band at 1660 cm^{-1} could be due to absorption by an amine, an oxime, or both. Acidic hydrolysis of the reaction product gave a material which contained nitrogen, and in the infrared exhibited a carboxyl band at 1700 cm^{-1}, and bands at 3300 cm^{-1} and 1655 cm^{-1}. The hypothesis of an amino, oximino carbinol fully agreed with the analytical results. Since the 12-position is more sterically hindered than the 7-position, the reaction product was postulated as 7ξ-amino-12-oximinocholan-24-ol (XIII) and its hydrolysis product as 7ξ-amino-24-hydroxycholan-12-one (XIV).

EXPERIMENTAL

The melting points were determined in a Thiele–Dennis melting point tube containing Dow Corning silicone fluid No. D.C. 550, and are uncorrected. The analyses were carried out in the W. Manser laboratory, Zurich, Switzerland. Infrared spectra were determined in potassium bromide on a Perkin–Elmer Model 21 double-beam instrument equipped with a sodium chloride prism.

3,12-Dioxocholanic Acid (V)

To a solution of chromium trioxide (13.35 g) in water (20 ml) concentrated sulphuric acid (11.5 ml) was added dropwise, with stirring so as to avoid the formation of any precipitate. The cold solution was diluted to 50 ml. 3α,12α-Dihydroxycholanic acid (IV) (30 g) was dissolved in acetone (2.2 l.), and the resulting solution was cooled to 20° in an ice-water bath. The oxidizing solution was then added dropwise from a microburette until an orange-brown color persisted (about 45 ml of reagent was required). The solution

was decanted from the inorganic residue, and was diluted with water to a volume of 6 l. The product (23.4 g) precipitated immediately, and was isolated. A second crop (5.35 g) was obtained by diluting the filtrate with another 2 l. of water. The 3,12-dioxocholanic acid (V) melted at 184–185°.

12β-Aminocholanic Acid (VII)

In a nitrogen atmosphere, sodium (2.5 g), in small pieces, was added over a period of 3.5 hours to a refluxing solution of 12-oximinocholanic acid (I) (0.5 g) in dry *n*-propyl alcohol (58 ml) with stirring. Then the reaction mixture was cooled in an ice-water bath, and made slightly acidic with 4% sulphuric acid. The propyl alcohol was distilled off *in vacuo* in a nitrogen atmosphere, and some precipitation occurred. The precipitation was made complete by adjusting the pH to 5.6–5.8 with 1% sulphuric acid. The yellow solid (0.48 g) was isolated. It melted at 122–126° to an opaque viscous liquid which cleared at 138–140°. The product was dissolved in hot acetone (20 ml), and the yellow solution filtered with suction through celite and carbon Nuchar C190-N. The colorless filtrate was concentrated under reduced pressure to a 10-ml volume, and heated to boiling. Hot water was added dropwise until the solution became slightly turbid. Upon cooling to room temperature, needles were deposited from solution. Recrystallization from acetone–water provided 12β-aminocholanic acid (VII) melting at 115–116° to a liquid which became transparent at 120°. ν_{max} 3440 (O—H), 3040 (sh) ($\overset{+}{N}H_3$), 1625 ($\overset{+}{N}H_3$), 1550 cm^{-1} (COO^-). Anal. Calc. for $C_{24}H_{41}O_2N \cdot 3H_2O$: C, 67.13; H, 10.95; N, 3.24. Found: C, 67.20; H, 10.88; N, 3.53%. Hydrochloride: Addition of concentrated hydrochloric acid (0.5 ml) to VII (0.4 g) and evaporation to dryness under reduced pressure was repeated 5 times. The white residue obtained, on recrystallization from methanol–water, gave the hydrochloride as a white powder, m.p. 257–258°. ν_{max} 1705 (C=O), 1610 cm^{-1} ($\overset{+}{N}H_3$).

Attempted Reduction of 12-Oximinocholanic Acid (I) *with Sodium Amalgam in Absolute Ethanol*

Sodium amalgam (3%, 26.6 g) was added in a nitrogen atmosphere to a refluxing solution of I (0.2 g) in absolute ethanol (20 ml), and the mixture was stirred for 6 hours. The major part of the amalgam seemed to have reacted. The supernatant solution was decanted, allowed to cool, diluted with water to 50 ml, and neutralized with 4% sulphuric acid. A white product (0.18 g) which precipitated was isolated. It melted at 178–179° to a milky liquid which cleared completely at 198–201°. Recrystallization from ethanol provided platelets, m.p. 180–182°, which were identified as 12-oxocholanic acid (VI) by a mixed melting point determination (183–184°) with an authentic sample of the keto acid. An oxime derivative of the reaction product was prepared, and a mixed melting point determination with an authentic sample of I showed no depression.

3α,12β-Diaminocholanic Acid (VIII)

To a refluxing solution of 3,12-dioximinocholanic acid (II) (0.4 g) in dry *n*-propyl alcohol (60 ml) were added, with stirring in a nitrogen atmosphere, small pieces of sodium (4.0 g) over a period of 4 hours. The reaction mixture was cooled in an ice-water bath, and treated with 4% sulphuric acid until pH 9 was reached. The propyl alcohol was evaporated under reduced pressure and the pH of the aqueous solution was further adjusted with 1% sulphuric acid to 8.6–8.8. A yellow product (0.25 g) precipitated and was isolated. Recrystallization from methanol–water gave 3α,12β-diaminocholanic acid

(VIII), m.p. 244–245°. ν_{max} 3380 (O—H, NH_2), 1660 (sh) (NH_2), 1623 ($\overset{+}{N}H_3$), 1575 cm^{-1} (COO^-). Anal. Calc. for $C_{24}H_{42}O_2N_2 \cdot H_2O$: C, 70.58; H, 10.78; N, 6.86. Found: C, 70.35; H, 10.63; N, 6.59%.

Reduction of 3,12-Dioximocholanic Acid (II) *with Lithium Aluminum Hydride in Tetrahydrofuran*

To a refluxing suspension of lithium aluminum hydride (0.37 g) in dry tetrahydrofuran (20 ml) in a nitrogen atmosphere was added dropwise, and with stirring, a solution of II (0.3 g) in dry tetrahydrofuran (30 ml). The resulting mixture was stirred and refluxed for a further period of 2 hours, then was cooled to room temperature. A saturated solution (50 ml) of sodium potassium tartrate was added dropwise with stirring. The tetrahydrofuran was removed by evaporation under reduced pressure, and a semisolid material separated in the aqueous phase. It was extracted with three 40-ml portions of *n*-butyl alcohol. The alcoholic extract was washed with 1% sulphuric acid, and with water, then was dried over anhydrous magnesium sulphate. After filtration, the solvent was removed *in vacuo* leaving an amorphous residue (0.23 g), which contained no nitrogen. The product was dissolved in 2 ml of boiling ethanol, and hot water was added dropwise until a slight cloudiness was observed. The solution was seeded with crystals obtained by cooling a few drops of the solution in a dry ice – acetone mixture for 2–3 minutes, and keeping the resulting solid in a refrigerator overnight, and long needles were obtained. Recrystallization from acetone–water yielded cholane-3ξ,12ξ,24-triol (IX), m.p. 166–169°. ν_{max} 3340 cm^{-1} (H—O), 1075, 1055, 1042, 1011 cm^{-1} (C—O). Anal. Calc. for $C_{24}H_{42}O_3$: C, 76.19; H, 11.11. Found: C, 75.86; H, 11.45%.

7β,12β-Diaminocholanic Acid (XII)

In a nitrogen atmosphere, sodium (2.0 g) was added in small pieces, with stirring, to a refluxing solution of 7,12-dioximinocholanic acid (III) (0.2 g) in dry *n*-propyl alcohol (40 ml) over a period of 3 hours. The reaction mixture was cooled in an ice-water bath, and adjusted to pH 9 with 4% then 2% sulphuric acid. The propyl alcohol was removed under reduced pressure, and 1% sulphuric acid was added until precipitation occurred at pH 8.3–8.6. The crude product (0.16 g) was dissolved in 8 ml of ethanol, and the yellow solution was filtered through celite and carbon Nuchar C190-N. The filtrate was concentrated to 4 ml and, when it was left to stand at room temperature, needles were deposited and isolated. Recrystallization from acetone–water afforded 7β,12β-diaminocholanic acid (XII), m.p. 128–130°. ν_{max} 3400 cm^{-1} (O—H), 1635, 1560, 1630 cm^{-1} (NH_2, $\overset{+}{N}H_3$), 1550 cm^{-1} (COO^-). Anal. Calc. for $C_{24}H_{42}N_2O_2 \cdot 1.5H_2O$: C, 69.06; H, 10.31; N, 6.71. Found: C, 68.52; H, 10.32; N, 6.57%.

7ξ-Amino-12-oximinocholan-24-ol (XIII)

A solution of 7,12-dioximinocholanic acid (III) (0.60 g) in dry tetrahydrofuran (80 ml) was added in a nitrogen atmosphere to a refluxing suspension of lithium aluminum hydride (0.73 g) in dry tetrahydrofuran (50 ml), with stirring, over a period of 40 minutes. The reaction mixture was stirred under reflux for a further 2.5 hours. When the suspension had cooled to room temperature, it was hydrolyzed by the dropwise addition of 100 ml of a saturated sodium potassium tartrate (Rochelle salt) solution. The tetrahydrofuran was removed under reduced pressure, and a white precipitate separated from the aqueous solution. The product was extracted with four 50-ml portions of *n*-butanol, and the extract was washed once with 1% sulphuric acid, twice with water, and then was dried over anhydrous magnesium sulphate. The solution was filtered, and the butanol was removed

under reduced pressure leaving a crystalline residue (0.45 g) which melted at 203–209° and became transparent at 215°. Recrystallization from ethanol gave 7ξ-amino-12-oximinocholan-24-ol (XIII) in shiny plates, m.p. 234–236°. ν_{max} 3300 cm^{-1} (O—H), 1660 cm^{-1} (C═N, NH_2). Anal. Calc. for $C_{24}H_{38}O_2N_2$: C, 71.79; H, 9.74; N, 7.17. Found: C, 71.15%; H, 10.17; N, 7.15%.

7ξ-Amino-12-oxocholan-24-ol (XIV)

7ξ-Amino-12-oximinocholan-24-ol (XIII) (15 mg) was dissolved in ethanol (3 ml), and one drop of 4% hydrochloric acid was added to the solution. The reaction mixture was refluxed for 20 minutes, then was concentrated to a volume of 1 ml *in vacuo*, and the needles which separated when the mixture was left to stand at room temperature were isolated; the needles melted at 180–183°. Recrystallization from ethanol–water provided 7ξ-amino-12-oxocholan-24-ol (XIV) in the form of needles, m.p. 183–184°. ν_{max} 3300 cm^{-1} (O—H); 1700 cm^{-1} (C═O); 1655 cm^{-1} (NH_2). Anal. Calc. for $C_{24}H_{37}ON \cdot 1.5H_2O$: C, 71.39; H, 9.95. Found: C, 70.83; H, 9.98%.

REFERENCES

1. A. S. Jones, M. Webb, and F. Smith. J. Chem. Soc. 2164 (1949).
2. J. Redel, A. Bouteville, B. Gauthier, and Nguyen Hun Quy. Bull. soc. chim. France, (5) **16**, 877 (1949).
3. B. G. Ketcheson and A. Taurins. Can. J. Chem. This issue.
4. S. P. James, F. Smith, M. Stacey, and M. Webb. J. Chem. Soc. 665 (1946).
5. J. Hadacek and B. Duchoslav. Publs. fac. sci. Univ. Masaryk, **357**, 251 (1954); Chem. Abstr. **49**, 14015 (1954).
6. J. Barnett and T. Reichstein. Helv. Chim. Acta, **22**, 75 (1939).
7. H. B. MacPhillamy and C. R. Scholz. J. Org. Chem. **14**, 643 (1949).
8. M. Schenck and H. Kirchhof. Z. physiol. Chem. **163**, 120 (1927).
9. M. Schenck and H. Kirchhof. Z physiol. Chem. **180**, 115 (1929).
10. M. Schenck and H. Kirchhof. Z. physiol. Chem. **180**, 107 (1929).
11. D. H. R. Barton and C. H. Robinson. J. Chem. Soc. 3045 (1954).
12. D. H. R. Barton. J. Chem. Soc. 1029 (footnote 23) (1953).
13. H. Wieland. Z. physiol. Chem. **194**, 257 (1931).
14. H. Wieland and O. Schlicting. Z. physiol. Chem. **150**, 267 (1925).
15. H. Wieland and E. Boersche. Z. physiol. Chem. **106**, 190 (1919).
16. H. Wieland and E. Dane. Z. physiol. Chem. **210**, 281 (1932).
17. I. Heilbron, E. R. H. Jones, and G. F. Woods. J. Chem. Soc. 461 (1953).
18. G. Mignonac. Bull. soc. chim. France, (4) **27**, 387 (1921).
19. G. Mignonac. Ann. chim. (Paris), **2**, 255 (1934).
20. R. Paul. Bull. soc. chim. France, (5) **4**, 1121 (1937).

THEORETICAL STUDIES ON SOLVATION

PART II. NEW THEORY FOR EVALUATION OF IONIC SOLVATION NUMBER FOR DIVALENT IONS AT 25° C[1]

A. M. AZZAM

ABSTRACT

The concepts of ionic solvation are discussed and the definition of four types are suggested. Utilizing Webb's theory, values of the dielectric constant of water in terms of distance from a divalent ion are evaluated. The statistical mechanics of the distribution of solvent molecules round a divalent ion in aqueous solution has been worked out.

The present theory shows that all divalent ions with radius less than 1.6 Å can have a saturated envelope of eight water molecules in excess of the Goldschmidt co-ordination number have to be accounted for as inner primary solvation number. The concept of catonium is suggested for such a stable aquo-complex entity. The catonium entity is further hydrated electrostatically in the normal way by primary and secondary solvation types. The conditions governing all types of solvation and their possible termination boundaries are discussed and evaluated.

The theoretically calculated values of the ionic solvation numbers are in good agreement with the experimental results.

1. INTRODUCTION

Solvation plays an extremely important part in most solution phenomena (1, 2, 4). Most investigations have dealt with aqueous solutions and several experimental methods (1, 4) have been used to find out the degree of hydration of ions but they give widely divergent results as shown in Table I.

TABLE I

Values of the hydration number of alkaline earth metal ions in dilute solution at room temperature by various experimental methods

Method	Reference	Be^{++}	Mg^{++}	Ca^{++}	Sr^{++}	Ba^{++}
Mobility (Ulich)	(16)		10.5–13	7.5–10.5		5–9
Entropy (Ulich)	(1)		13	10		8
Compressibility (Passynski)	(1)	8	16	16		
Cryoscopic (Bourin *et al.*)	(1)		22.3	21.6	21.3	20.1
Cryoscopic (Van Ruynen)	(11)	30	15	10.5	10	9
Dialysis (Brintzinger)	(1)		37.5	33.4	29.1	25.1
Partial molar volume (Darmoir)	(1)		6.6	5.2		4
Solubility of gases (Manchot)	(1)		13	14.6		16.8

The most outstanding problem connected with solvation lies in the need of theoretical calculations to supply definite quantitative knowledge of the nature of the solvation sheath and the structure of the solvated ion. Such information may also throw light on the general problem of the interionic attraction theory of electrolytes (7, 8, 9) which has reached a quasi-static position. No further essential advances in the field of more concentrated solution appears possible without the concept of ion–solvent interaction (5, 6, 7, 8, 9, 11).

In a previous paper (3), the present author worked out the basis of a statistical mechanical method for the calculation of solvation number of ions and the following equation was developed:

$$[1] \qquad ds = 4\pi n_0 e^{-(w/kt)} r^2 dr$$

[1]*Manuscript received January 28, 1960.*
Contribution from the Department of Chemistry, Faculty of Science, A'in Shams University, Cairo, Egypt.

where ds = the number of solvent molecules associated with the ion in the spherical shell between r and $r+dr$ from the center of the ion;

n_0 = the number of solvent molecules per cubic centimeter in the bulk of the solution;

w = net potential energy of a solvent molecule in the solvation sheath. This energy is the algebraic sum of energies of ion–dipole and dipole–dipole interactions;

k = Boltzman's constant;

t = temperature.

The theoretically calculated values of primary solvation number (for definition see Discussion) for alkali metal and halide ions are in good agreement with those obtained by four mutually self-consistent experimental methods (3).

The purpose of the present paper is to verify the above-mentioned theory by applying it to the calculation of solvation number for alkaline earth metal and divalent transition metal ions.

2. CONCEPTS OF IONIC SOLVATION

In spite of much experimental work (1), the significance of the term solvation has remained somewhat vague. Considering the former concepts of ionic solvation (13, 14, 15, 16, 17), together with conclusions derived from the present author's theory (3), a possible classification and definition of the different types of solvation can be given as follows:

(a) Permanent Solvation (Chemical Bonds)

This term refers to solvent molecules which are firmly associated with the ion through the formation of chemical bonds. These forces between ions and solvent molecules are so strong that an ion can retain this type in crystals. In other words, this type of solvation persists in the solid as well as in its solutions (e.g. co-ordinated water of crystallization).

(b) Primary Solvation (Physical Forces)

This term refers to solvent molecules which are firmly associated with the ion by electrostatic attraction. They have lost their translational degree of freedom and move as one entity with the ion during its Brownian motion. In other words, they cannot be dislodged by thermal motion.

(c) Secondary Solvation (Physical Forces)

This term refers to solvent molecules which undergo electrostatic attraction with the primary solvated ions. These molecules are much more weakly held but the electrostatic attraction predominates over the separating action of thermal motion sufficiently to affect solvation-dependent quantities, e.g. salting out.

(d) Hydrodynamical Solvation (Streaming Effect)

This term refers to solvent molecules which could be transferred hydrodynamically as the hydrated ion moves *under* the influence of an applied electrostatic field. This effect is mainly due to change in momentum between the solvated ion and the solvent molecules.

These different types of solvation play parts of different order or degree in the various experimental phenomena depending on specific factors (2, 3, 4, 18).

However, the number of solvent molecules in both the permanent and the primary solvation sheaths have definite values, moving with the ion as a single entity without exchange with bulk solvent. On the other hand, the number of solvent molecules in the secondary solvation sheath have variable values dependent on the phenomena observed. Ions continuously exchange these solvent molecules as they wander about in solution.

Hydrodynamical solvation is relevant only in dynamic experiments such as in measurements of transport number. This explains the fact that hydrodynamical methods for the determination of solvation number give much too high values (2, 3, 4, 18).

This scheme of classification gives a clear understanding of the reason for the large discrepancy between the results obtained by various experimental methods (1, 2, 3, 4, 18).

3. PROPOSED STRUCTURE OF HYDRATED DIVALENT IONS

Divalent metals such as Be, Mg, Ca, Sr, Ba, Zn, Cd, Fe, Co, Ni, Cu, . . . form a very large number of hydrated salts of definite constitution in the solid state (19, 20, 21, 24, 28, 29, 32, 33, 34). X-Ray crystallography has confirmed that definite hydrated cation complexes such as $[Be(H_2O)4]^{2+}$, $[Cu(H_2O)_4]^{2+}$, $[Mg(H_2O)_6]^{2+}$, $[Ni(H_2O)_6]^{2+}$ . . . are components of the corresponding polar lattices. $[M(H_2O)_n]^{2+}$ is the general formulation of such a stable hydrated entity in the solid state. These entities thus persist in the solid as well as in aqueous solution and have as much right (18, 34) to be considered complex ions as $[PtCl_4]^{2-}$ and $[Fe(CN)_6]^{4-}$.

The conclusion which follows is that divalent cations, which are hydrated in the solid state $[M(H_2O)_n]^{2+}$, never exist in very dilute aqueous solution as the bare ion M^{2+} but as a stable hydrated form. It is not known whether the number of water molecules in the nearest layer around the ion in dilute aqueous solution will remain "n" (as in the solid state) or whether and to what extent primary solvation will contribute in this first layer. To overcome this difficulty, it will be assumed that "x" (where $x \geqslant n$) is the number of water molecules in the first layer around the ion in very dilute aqueous solution.* Accordingly the formulation of the stable hydrated entity in dilute aqueous solution is $[M(H_2O)_x]^{2+}$ or more generally $\left[M\begin{matrix}(H_2O)_n\\(H_2O)_{x-n}\end{matrix}\right]^{2+}$. It is suggested that this entity be called "*a catonium*".

This terminology is the more correct form and should be more often used, but for simplicity the symbol M^{2+} may be accepted.†

The catonium entity is further hydrated in the normal way (see section on concept of ionic solvation) by purely electrostatic forces depending on the field strength at the surface of the catonium. The new situation arising on the dissolution of a hydrated salt with a co-ordinated hydrated cation is depicted as follows:

$$\underset{\text{(hydrated cation in crystal)}}{[M(H_2O)_n]^{2+}} \underset{\text{crystallization}}{\overset{\text{dissolution}}{\rightleftharpoons}} \underset{\text{(hydrated catonium in very dilute aqueous solution)}}{\left[M\begin{matrix}(H_2O)_n\\(H_2O)_{x-n}\end{matrix}\right]^{2+} \cdot (H_2O)_p(H_2O)_s(H_2O)_h} \qquad [2]$$

where x represents the permanent solvation number,

$(x - n)$ represents the inner primary solvation number,

$[M(H_2O)_n]^{2+}$ represents the hydrated cation in crystal,

$\left[M\begin{matrix}(H_2O)_n\\(H_2O)_{x-n}\end{matrix}\right]^{2+}$ represents the catonium entity in solution,

p represents the primary solvation number of the catonium or outer primary solvation,

s represents the secondary solvation number of the catonium,

h represents the hydrodynamical solvation number of the catonium.

This proposed structure is diagrammatically shown in Fig. 1.

**Some authors (18) seem to be of the opinion that n and x are the same, but there is no evidence for such a statement.*

†In analogy with the use of (H^+) *for the hydroxonium ion* $(H_3O)^+$.

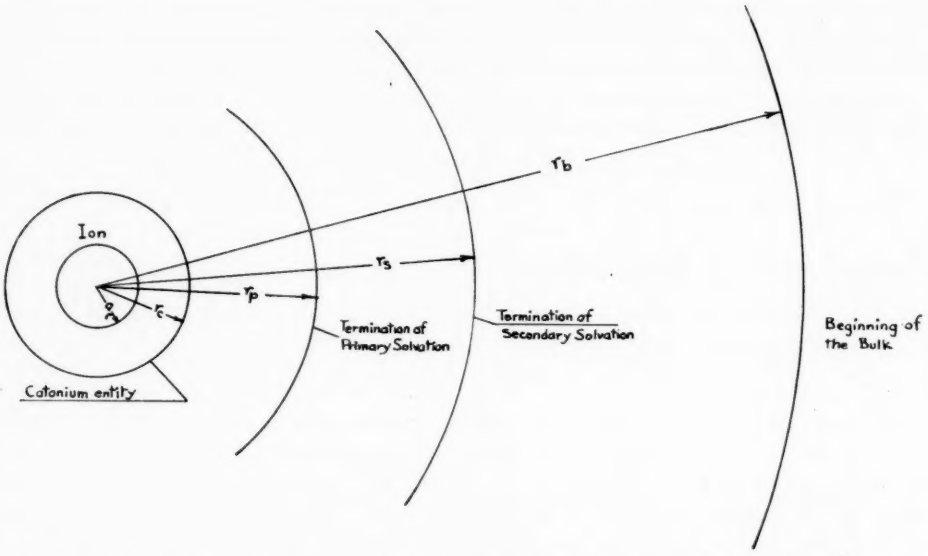

FIG. 1. The proposed structure of a solvated divalent ion in dilute aqueous solution.

4. METHOD OF CALCULATION

A serious difficulty, which occurs generally in the evaluation of ion–dipole interaction, is the lack of knowledge of the values of the dielectric constant near an ion. The only values reported in the literature (10, 12) are those near a monovalent ion. Utilizing Webb's theory (10), values of the dielectric constant of water in terms of distance from a divalent ion could be evaluated (see Fig. 2). Knowing this relation, the solvation number

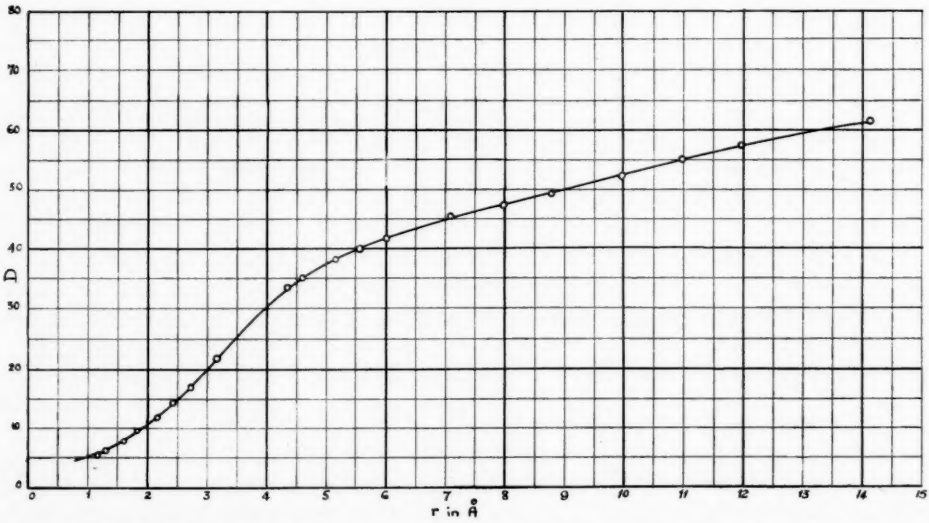

FIG. 2. Variation of the dielectric constant of water D in the vicinity of a divalent ion.

of divalent ions can be calculated by following the method of calculation previously given for monovalent ions (3). All data which are needed in the present calculation are recorded in Table II. The corresponding relation $[e^{-(w/kt)}r^2 - r]$, which is required for the graphical evaluation of solvation numbers (3), is shown plotted in Fig. 3. The curve is of

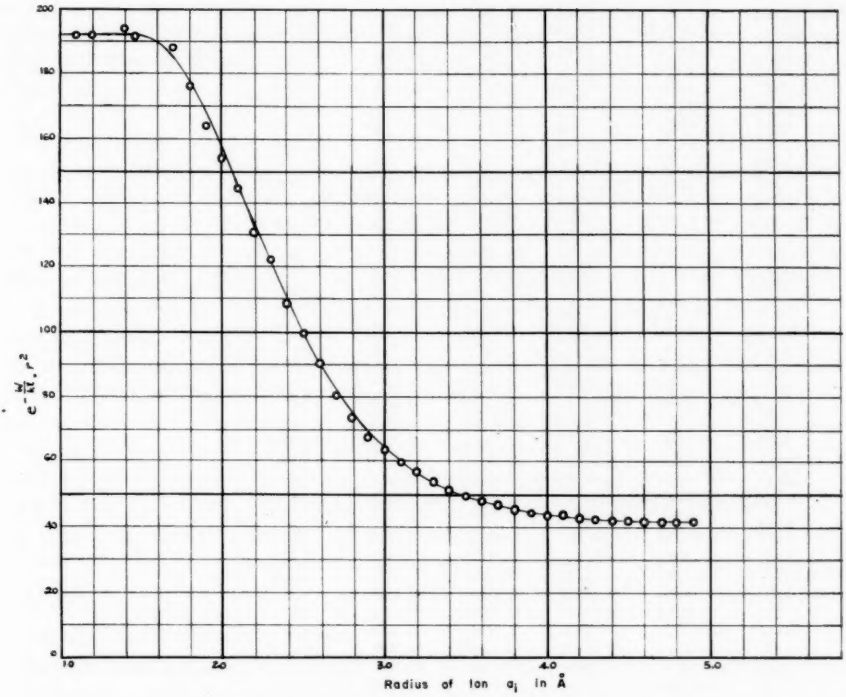

FIG. 3. Relation between $e^{-w/kt}$. r^2 and radius of ions.

the sigmoid type. It shows a horizontal portion at first extending to a distance $r = 1.6$ Å (from the center of the ion), followed by a rapid decrease which extends up to a distance $r = 3.2$ Å and finally a steady insignificant decrease.

5. DISCUSSION

Permanent and primary solvations are the only types involving definite solvent molecules in association with the ion (see section on concepts of ionic solvation). Each experiment measures the above-mentioned types plus some contribution from the other types of solvation depending on the phenomenon observed. Accordingly, Part I of this discussion is devoted to permanent and primary solvation types. Possible termination boundaries of the different types of solvation are given in Part II. In Part III, values of the ionic radii are discussed.

(I) Permanent and Primary Solvation Numbers

Examination of the present analysis (see Table II and Fig. 3) shows that the statistical possible number of water molecules which could be accommodated in the first layer

TABLE II

Data needed for the present statistical analysis

a_i	U_1	U_2	U_3	$(U_1-U_2-U_3)$	w/kt	$e^{-(w/kt)r^2}$	
1.0	0.4189	0.0213	0.2488	0.1487	3.3751	194.5	
1.1	0.3767	0.0196	0.2122	0.145	3.284	191.5	
1.2	0.3474	0.018	0.1796	0.142	3.212	191.7	
1.3	0.312	0.0169	0.1560	0.1391	3.142	192.0	Approximately constant value
1.4	0.278	0.0168	0.1244	0.1369	3.087	193.9	
1.5	0.2567	0.0152	0.1080	0.1335	3.004	191.4	
1.6	0.2325	0.015	0.0870	0.1305	2.932	189.8	
1.7	0.2123	0.014	0.0708	0.1275	2.859	187.7	
1.8	0.1928	0.0135	0.0571	0.1225	2.736	176.3	
1.9	0.1755	0.0131	0.0456	0.1169	2.6	163.0	
2.0	0.1603	0.0127	0.0352	0.1122	2.486	154.0	
2.1	0.1468	0.0124	0.0271	0.1073	2.367	144.5	
2.2	0.1334	0.0121	0.0203	0.1009	2.212	130.5	
2.3	0.1228	0.0119	0.0150	0.0958	2.089	121.9	
2.4	0.1124	0.0117	0.0113	0.0894	1.931	109.3	
2.5	0.1037	0.0115	0.0088	0.0835	1.788	99.6	
2.6	0.0958	0.0113	0.0069	0.0776	1.646	90.6	
2.7	0.0875	0.0111	0.0054	0.0709	1.483	80.7	
2.8	0.0809	0.0109	0.0046	0.0655	1.35	74.0	
2.9	0.0748	0.0108	0.0038	0.0603	1.223	68.2	
3.0	0.0698	0.0106	0.0032	0.0559	1.118	64.1	A possible boundary of primary solvation
3.1	0.0649	0.0105	0.0028	0.0515	1.01	60.1	
3.2	0.0631	0.0104	0.0024	0.0475	0.913	57.0	
3.3	0.0562	0.0103	0.0021	0.0438	0.823	54.2	
3.4	0.0521	0.0102	0.0018	0.0401	0.732	51.6	
3.5	0.0487	0.0101	0.0016	0.0370	0.657	49.8	
3.6	0.0453	0.0100	0.0014	0.0339	0.58	47.9	
3.7	0.0425	0.0099	0.0012	0.0313	0.518	46.8	
3.8	0.0396	0.0098	0.0011	0.0287	0.454	45.6	
3.9	0.0370	0.0097	0.0010	0.0262	0.395	44.6	
4.0	0.0347	0.0096	0.0009	0.0230	0.316	43.0	
4.1	0.0325	0.0095	0.0008	0.0222	0.318	44.0	
4.2	0.0305	0.0095	0.0008	0.0202	0.248	42.8	
4.3	0.0287	0.0094	0.0007	0.0185	0.207	42.5	A possible boundary of secondary solvation
4.4	0.0270	0.0093	0.0007	0.0169	0.169	42.3	
4.5	0.0255	0.0093	0.0007	0.0155	0.133	42.3	
4.6	0.0239	0.0092	0.0006	0.0140	0.098	42.3	
4.7	0.0225	0.0092	0.0006	0.0127	0.066	42.1	Approximately constant value
4.8	0.0212	0.0091	0.0006	0.0116	0.039	42.3	
4.9	0.020	0.0091	0.0005	0.0104	0.010	42.6	
5.0	0.0188	0.0090	0.0005	0.0092			

around a divalent ion is 8.06 water molecules. This could be considered as a possible value of "x" provided that the mode of association is purely electrostatic. On the other hand, several lines of evidence (18, 19, 21, 24, 32, 33, 34) combine to show that the value of "n", which is a measure of the tendency of an ion to co-ordinate in the solid state, is given by the Goldschmidt co-ordination number. According to Sidgwick (21), the value of "n" for an element depends upon its position in the periodic classification, but the co-ordination number can only assume these values (2, 4, 6, or 8). The values 4 and 6 are the most usual. Following these lines of discussion, it could be concluded that in very dilute aqueous solution, the number of water molecules in the first shell around an ion is 8 irrespective of the mode of association. It seems very probable that when the binding capacity of a cation (as given by the value of n) appears exhausted, it can link up with other water molecules by physical forces and build up a more complex structure to an upper limit which is given by the average value 8.06 water molecules. In other words, the 8.06 water molecules in the first layer around an ion constitute a mixture of both permanent and primary solvation types.

The values of these two types are given by "n" and "$8.06-n$" respectively. As this

primary solvation number of the ion $(8.06-n)$ is within the catonium entity, it is better to refer to this number as the "*inner primary solvation number*".

The catonium entity as stated before is further hydrated in the normal way (primary, secondary) by electrostatic forces depending on the field strength at the surface of the catonium (see equation 2 and Fig. 1). The most important fact which results from the present theory is that primary solvation of the catonium entity exists for only one layer of water molecules. This result follows from the application of the concept of screening effect (3, 30). The calculated values of "p" are shown in Table IV. This number of water molecules attached to the catonium can be called the "*outer primary solvation number*".

(II) The Termination Boundaries of the Different Types of Solvation of the Catonium Entity

It could be postulated that for primary solvation, as qualitatively defined above, the interaction of the catonium with dipole is such that the net interaction energy in the solvation sheath minus the solvent–solvent interactions in the bulk is greater than the kinetic thermal energy. The possible termination of primary solvation can thus be regarded as the point at which $w/kt \geqslant 1$. This condition is reached at $r \simeq 3.1$ Å (see Table II and see Fig. 1). This indicates that all catoniums of radius less than 3.1 Å are primary hydrated.

After the termination of primary solvation, the ion and dipoles from the bulk of the solution compete and where the energy of the catonium–dipole interaction is equal and opposite to that of dipole–dipole interaction, $w = 0$, so that the secondary solvation may be regarded as terminated. This condition is reached at r about 4.4 Å. It is also characterized by an approximately constant value of ds as shown in Table II. This indicates that all *primary solvated catoniums* of radius less than 4.4 Å are secondary hydrated.

The beginning of the bulk can be recognized as the critical radius inside which no water molecule has the normal dielectric properties. This is reached for r about 22 Å (see Fig. 2).

(III) Crystal Radii and Univalent Radii

With regard to ionic radii, in general, no unique radius can be ascribed to the ion. Comprehensive assignment of fixed radii to ions has frequently been attempted, notably by Lande (23), Wasestjerna (23), Goldschmidt (24), and Pauling (22). Most of the ionic radii values adopted by these authors are different (see Table III). The difference is mainly due to the arbitrary nature of the allotment of fixed extension to ions. However, Pauling formulated a semi-empirical set of ionic radii. These radii are known as univalent radii of the ions and are shown in Table III. These radii are the radii the multivalent ions would possess if they were to retain their electron distributions and enter into coulomb interaction as if they were univalent. It seems very probable that these univalent radii are in harmony and more suitable for use than the crystal radii. The following simple arguments can be given in support of this:

1. The univalent radii are very accurate to about 1% and form a complete set under comparable conditions.

2. These radii represent correctly the relative sizes of the outer electron shells of the ions compared with those for the alkali and halogen ions.

3. They have absolute values such as to cause their sums to be equal to the equilibrium interionic distance in standard crystals.

4. In ionic crystals, the crystal radii sums decrease about 10% for the change from *a crystal* M^+X^- to its *isoelectronic* $M^{++}X^{--}$. This decrease is not due to lack of compensation of the charges in the electron distribution but results rather from the effect of doubling

the electric charges on the ions. On the other hand, the univalent radius sums remain nearly constant.

5. If both univalent radii and crystal radii are represented graphically as functions of the atomic number, it will be seen that there is great regularity in the univalent radii sequences (22).

TABLE III

Crystal ionic radii and univalent crystal radii

Ion	Crystal ionic radii					Univalent crystal radii (Pauling (22))
	Pauling (22)	Wasestjerna (23)	Wyckoff (29)	Zachariasen (31)	Goldschmidt (24)	
Be^{++}	0.31		0.3	0.55	0.34	0.44
Mg^{++}	0.65	0.75	0.75	0.89	0.78	0.82
Ca^{++}	0.99	1.02	1.06	1.17	1.06	1.18
Sr^{++}	1.13	1.2	1.18	1.34	1.27	1.32
Ba^{++}	1.35	1.4	1.38	1.49	1.43	1.53
Zn^{++}	0.74		0.83		0.83	0.88
Cd^{++}	0.97		0.99		1.03	1.14
Hg^{++}	1.10		0.66		1.12	1.25
Mn^{++}			0.83		0.91	
Fe^{++}			0.80		0.87	
Co^{++}			0.78		0.82	
Ni^{++}			0.74		0.78	
Sn^{++}						
Pb^{++}			1.18		1.32	
Ti^{++}					0.76	
Cu^{++}					0.80	
Pt^{++}					0.52	
Pd^{++}					0.50	

The list of univalent radii, however, is incomplete while a complete list of crystal radii is available (see Table III).

For this reason, and for testing the significance of this new concept, the primary solva-

TABLE IV

Permanent and primary solvation numbers $(x+p)$

Ion	Outer primary solvation number (p)		Permanent and inner primary solvation number (x)	$(x+p)$
	Using Pauling univalent crystal radii	Using Goldschmidt crystal ionic radii		
Be^{++}	7.2	7.56	8.06	15.62
Mg^{++}	5.3	5.5	8.06	13.56
Ca^{++}	3.78	4.26	8.06	12.32
Sr^{++}	3.25	3.4	8.06	11.46
Ba^{++}	2.79	3.02	8.06	11.08
Zn^{++}	5.04	5.27	8.06	13.33
Cd^{++}	3.9	4.37	8.06	12.43
Hg^{++}	3.4	3.99	8.06	12.05
Mn^{++}		4.89	8.06	12.95
Fe^{++}		5.08	8.06	13.14
Co^{++}		5.3	8.06	13.36
Ni^{++}		5.5	8.06	13.56
Sn^{++}		4.85	8.06	12.91
Pb^{++}		3.25	8.06	11.31
Ti^{++}		5.65	8.06	13.71
Cu^{++}		5.38	8.06	13.44
Pt^{++}		6.66	8.06	14.72
Pd^{++}		6.91	8.06	14.97

NOTE: (*a*) Goldschmidt's values of crystal ionic radii are used in the present calculation of $(x+p)$.

(*b*) Pauling's value of univalent crystal radii are not complete and have been used to demonstrate the effect of this new concept on solvation number.

tion number "p" was calculated using Pauling's univalent radii and the Goldschmidt crystal ionic radii. As can be seen from Table IV, the difference between the two cases is less than 0.5, and this is insignificant.

CONCLUSIONS

1. Concepts of ionic solvation are discussed and the definition of the following four types is suggested: "permanent, primary, secondary, and hydrodynamic".

2. The variation of the dielectric constant of water in the vicinity of divalent ion is evaluated.

3. The dissolution process of a co-ordinated cation is depicted as

$$[M(H_2O)_n]^{2+} \underset{\text{crystallization}}{\overset{\text{dissolution}}{\rightleftharpoons}} \left[M\begin{matrix}(H_2O)_n \\ (H_2O)_{x-n}\end{matrix}\right]^{2+} . (H_2O)_p . (H_2O)_s .$$

4. The permanent solvation type "n", which persists in solid state and in solution, is given by Goldschmit co-ordination number (4 or 6) and its mode of association has been assumed not to be purely physical.

5. Divalent cations in solution are not simply cations corresponding to the symbol M^{2+} but rather catonium entities $\left[M\begin{matrix}(H_2O)_n \\ (H_2O)_{x-n}\end{matrix}\right]^{2+}$.

6. All divalent ions with radius less than 1.6 Å can have an envelope of 8.06 water molecules ($x = 8.06$). This is a mixture of both permanent solvation type "n" and inner primary solvation type $(x-n)$.

7. All catonium ions with radius less than 3.1 Å are primary solvated "p". This is called the outer primary solvation number.

8. The outer primary solvation number exists for only one layer of water molecules around the catonium entity. This result follows from the application of the concept of screening effect.

9. The following critical radii have been calculated:

(*a*) Inner primary solvation types exist inside the critical radii 1.6 Å.

(*b*) Outer primary solvation types exist inside the critical radii 3.1 Å.

(*c*) Secondary solvation types exist inside the critical radii 4.7 Å.

(*d*) Water does not have the normal dielectric properties inside the critical radius of about 22 Å.

10. The present theory demonstrates

(*a*) Azzam's theory of ionic solvation which was previously given in Part I,

(*b*) Fuoss's theory of the screening effect,

(*c*) Webb's theory of the variation of the dielectric constant of water near an ion,

(*d*) Pauling univalent radii concept.

11. The theoretically calculated values of ionic solvation of divalent ions are in good agreement with those obtained by mutually self-consistent experimental methods.

TABLE V

Comparison between the theoretically calculated values and values of the self-consistent experimental methods

Method	Be^{++}	Mg^{++}	Ca^{++}	Sr^{++}	Ba^{++}	Zn^{++}	Cd^{++}	Hg^{++}	Mn^{++}	Fe^{++}	Co^{++}	Ni^{++}	Sn^{++}	Pb^{++}	Ti^{++}	Cu^{++}	Pt^{++}	Pd^{++}
The present method	15.6	13.5	12.3	11.4	11	13.3	12.4	12	13	13.1	13.3	13.5	12.9	11.3	13.7	13.4	14.7	15
Average of: Mobility (16), Entropy (1), Compressibility (1)		14	12.2		9	12.2	12			12.2						12.2		

REFERENCES

1. J. BABOROVSKY. Rec. trav. chim. **42**, 229 (1923); Collection Czechoslov. Chem. Commun. **11**, 542 (1938).
   H. BRINTZINGER. Z. anorg. u. allgem. Chem. **223**, 101 (1935).
   E. H. RIESENFELD. Z. physik. Chem. **66**, 672 (1909).
   H. REMY. Z. physik. Chem. **126**, 161 (1927).
   N. BJERRUM. Z. anorg. u. allgem. Chem. **109**, 275 (1920).
   H. ULICH. Z. Elektrochem. **36**, 497 (1930).
   A. PASSYNSKI. Acta Physicochim. U.R.S.S. **8**, 385 (1938).
   E. DARMOIR. J. phys. radium, **2**, 2 (1941).
   F. BOURIN and E. ROUYER. Compt. rend. **204**, 1420 (1937).
   M. CORDIER. J. chim. phys. **43**, 345 (1946).
   H. FREUNLICH and A. SCHNELL. Z. physik. Chem. **133**, 151 (1928).
   W. MANCHOT *et al.* Z. anorg. Chem. **141**, 38 (1924).
2. A. M. AZZAM. Ph.D. Thesis. University of London, London, 1949.
3. A. M. AZZAM. Part I. Z. Elektrochem. **58**, 889 (1954).
4. J. O'M. BOCKRIS. Quart. Rev. **3**, 173 (1949).
5. N. BJERRUM. Z. anorg. u. allgem. Chem. **109**, 275 (1920).
6. G. SCATCHORD. J. Am. Chem. Soc. **17**, 2098 (1925).
7. H. S. F. FRANK. J. Am. Chem. Soc. **63**, 1789 (1941).
8. R. STOKE and R. ROBINSON. J. Am. Chem. Soc. **70**, 1870 (1948).
9. O. HALPERN and P. GRESS. J. Chem. Phys. **2**, 136 (1934).
10. T. J. WEBB. J. Am. Chem. Soc. **48**, 2589 (1926).
11. B. H. VAN PUYNEN. Chem. Weekblad. **53**, 461 (1957).
12. P. DEBYE. Marx handbuch der radiologie. Leipzig. 1925. Vol. VI, pp. 618, 680.
    C. H. COLLIE, J. B. HASTED, and D. M. RITSON. J. Chem. Phys. **16**, 1 (1948).
    G. SCHWARTZENBACK. Z. physik. Chem. **176**, A, 133 (1936).
13. S. ASCHKANASI. Z. Elektrochem. **36**, 504 (1930).
14. K. FAJANS. Verb. Dtsch. Physik Ges. **21**, 709 (1919).
    K. FAJANS. Z. Elektrochem. **34**, 502 (1928).
15. M. BORN. Z. Physik, **1**, 45 (1920).
16. H. ULICH. Hand-u. Jahrb. Chem. Physik, **6**, 186 (1933).
    H. ULICH. Z. physik. Chem. **168**, 141 (1934).
    H. ULICH. Trans. Faraday Soc. **23**, 392 (1927).
17. R. LINDEMAN. Z. physik. Chem. **23**, 387 (1927).
18. J. BERNAL and R. FOWLER. J. Chem. Phys. **1**, 515 (1933).
19. R. FRICKS and H. SCHITZDELLOR. Z. anorg. chem. **131**, 132 (1923).
    R. SCHURTZ *et al.* Z. anorg. Chem. **226**, 33 (1935).
    H. J. EMELÉUS and J. S. ANDERSON. Modern aspects of inorganic chemistry. London. 1943.
20. J. LANGMIUR. J. Am. Chem. Soc. **41**, 868 (1919).
    L. CAMBI, A. CAGNASSO *et al.* Gazz. chim. ital. **64**, 758 (1938).
21. N. V. SIDGWICK. Ann. Rept. Chem. Soc. **30**, 110 (1933); Electronic theory of valency. Oxford. 1927.
22. L. PAULING. J. Am. Chem. Soc. **49**, 765 (1927); Proc. Roy. Soc. A, **114**, 181 (1927).
23. H. BRÜCK. Z. Physik, **51**, 707 (1928).
    W. E. BLEICH *et al.* J. Chem. Phys. **2**, 252 (1934).
    J. A. WASESTJERNA. Soc. Sci. Fennica Commentationes Phys. Math. **6**, 22 (1932).
    B. O. GRONBLOW. Soc. Sci. Fennica Commentationes Phys. Math. **8**, 13 (1935).
    A. LANDÉ. Z. Physik, **1**, 191 (1920).
24. V. M. GOLDSCHMIDT. Trans. Faraday Soc. **25**, 253 (1929); Geochemische verteilungsgestze der element. Oslo. 1926; Ber. **60**, 1263 (1927).
25. M. VOLMER. Ann. **200**, 440 (1924).
26. A. E. VAN ARKEL *et al.* Chemical binding. Leipzig. 1931.
27. E. J. W. VERWEY. Rec. trav. chim. **61**, 127 (1942).
28. G. T. MORGAN. J. Chem. Soc. **117**, 1639 (1920).
29. R. W. G. WYCKOFF. The structure of crystals. 2nd ed. Chemical Catalogue Co., New York. 1931.
30. R. M. FUOSS. Trans. Faraday Soc. **30**, 970 (1934).
    R. H. FOWLER. Statistical mechanics. The University Press, Cambridge, Eng. 1936.
31. W. ZACHARIASEN. Z. Krist. **80**, 137 (1931).
32. H. J. EMELÉUS and J. S. ANDERSON. Modern aspects of inorganic chemistry. London. 1943.
33. A. WERNER. Komplexverbindungen. 1924.
    O. SCHMITZ and DUMONT. Z. anorg. Chem. **226**, 33 (1935).
    A. WERNER. Ber. **41**, 345 (1908).
34. G. WAGNER. Z. anorg. Chem. **124**, 289 (1922).
    F. J. GARRICK. Phil. Mag. VII, **9**, 131 (1930).

ACID ACTIVATION OF MONTMORILLONITE[1]

R. D. HEYDING, R. IRONSIDE, A. R. NORRIS,[2] AND R. Y. PRYSIAZNIUK[3]

ABSTRACT

A Pembina montmorillonite clay has been activated with sulphuric acid at various dosages by the conventional wet process and by the new "dry" process. The products are compared with respect to the fractions of the metal ion components remaining after leaching, the hydrated silica content, the bleaching capacity, and the B.E.T. nitrogen and water surface areas which they exhibit. Surface areas were also determined after calcining the products *in vacuo*. The surface areas are discussed with reference to the removal of metal ions occupying octahedral lattice sites in a model clay particle.

INTRODUCTION

Montmorillonite clays are employed extensively as bleaching agents for mineral and vegetable oils, and as cracking catalysts in the petroleum industry. Often the capacity of a particular montmorillonite with respect to either of these functions is enhanced by "activation", that is, by the removal of basic constituents in the clay lattice by leaching with acid. In the conventional activation procedure the clay is refluxed with relatively dilute sulphuric (or hydrochloric) acid, filtered, and washed. The acid concentration is limited by the consistency of the clay/water/acid system, while the temperature attainable in open vats is limited by atmospheric pressure. A new procedure developed by Puddington and Farnand (1) permits higher concentrations of acid for a given dosage (acid-to-clay ratio) since only sufficient water is used to produce a reasonably free-flowing crumb on mixing, and this may be heated to about 200° C to promote rapid reaction. Subsequent treatment is similar to the conventional process. It is convenient to describe these two methods as the "wet" process and the "dry" process, respectively.

The dry process embodies obvious technical advantages as far as production of activated clay is concerned. The present study was designed to evaluate the products of dry activation by comparison of some of their physical characteristics with those of wet activated clays. The physical properties were chosen on the assumption that their variation would indicate the nature of the degradation of the clay lattice on activation.

The montmorillonite lamina or pseudo unit cell consists of partially hydrated silica/alumina/silica layers in which some of the octahedral aluminum sites are occupied by trivalent iron or divalent magnesium. The substitution of trivalent ions by divalent metal ions implies an electrostatic inequality within each lamina which is cancelled by the inclusion of hydrogen, alkali metal, or alkaline earth ions (the exchangeable ions) between adjacent laminae in the lattice. In the presence of water vapor, water is included in the interlaminar space resulting in an expansion of lattice along the *c* axis. It is not certain whether the water is adsorbed or chemisorbed by hydration of the interlaminar ions, or by hydration of the silica forming the faces of the interlaminar area. The last possibility is the basis of the montmorillonite model proposed by Edelman and Favejee (2), in which the tetrahedral silica units point into the interlaminar space. This model is not as generally accepted as the Hoffman–Endell–Wilm–Marshall–Hendricks model (3) in which the silica units point into the lattice and away from the interlaminar region.

[1]*Manuscript received December 4, 1959.*
Contribution from the Division of Applied Chemistry, National Research Council, Ottawa, Canada. Issued as N.R.C. No. 5663.
[2]*N.R.C. Summer Student, 1958. Present address: Graduate School, University of Chicago, Chicago, Illinois.*
[3]*N.R.C. Summer Student, 1959. Present address: Graduate School, Iowa State College, Ames, Iowa.*

Although these models differ considerably in detail, the existence of silica/alumina/silica structural layers separated by exchangeable ions is not disputed. In what follows, either model will serve as the basis for the argument, and the data do not serve to distinguish between them.

According to Bradley and his co-workers (3), water is adsorbed in monomolecular layers between the silicate laminae as are many polar but otherwise neutral molecules. This water is accommodated reversibly regardless of heat treatment below ca. 300° C; above 500° C water of hydration is removed, and the laminae are bound together irreversibly. After calcination at 600° C, that is, after the conversion of the clay to a silica/alumina catalyst, no water is adsorbed in the interlaminar areas. Nitrogen, on the other hand, is not adsorbed in the interlaminar region even in non-calcined montmorillonite. These phenomena have been exploited by Mooney, Keenan, and Wood (4), who have reasoned that while B.E.T. nitrogen surface areas can represent external particle area only, B.E.T. water surface areas must indicate the interlaminar area as well. The interlaminar area obtained by difference in the two B.E.T. areas is quite consistent with the crystal model.

On leaching with acid, the metal ions in the middle layer of the silicate lamina are dissolved, according to Mills *et al.* (5), in essentially the same proportions in which they were present in the original clay. With the removal of these ions, the surface area can be expected to increase, and there is ample proof of this in the literature (5, 6, 7, 8, 9, 10). Usually intercorrelation of data obtained by various workers is difficult, as a result of differences in the raw clays and in the many variables associated with the activation and the subsequent treatment of the product. It is apparent, however, that the ability of a clay to decolorize mineral and vegetable oils is directly proportional to the B.E.T. nitrogen surface area of the clay, other factors, such as heat treatment, water content, and exchangeable ion, remaining constant. On the other hand, no direct relation between area and catalytic activity is observed (5); clays with similar activation and calcination histories and similar nitrogen areas need not necessarily exhibit similar catalytic properties.

The quantitative comparison of B.E.T. nitrogen and water surface areas as applied to natural montmorillonites by Mooney and his co-workers is a convenient means of studying the clay lattice before and after acid activation. We have activated a montmorillonite by both wet and dry processes at several acid dosages, and have measured the B.E.T. nitrogen and water surface areas of the products. These data, together with the total analyses of the clays, permit a self-consistent interpretation of the activation process. Redetermination of these surface areas after calcining the clays indicates in turn the extent of the modification of the lattice on irreversible dehydration. The decolorizing characteristics of the clays were measured, but no attempt was made to evaluate the calcined clays as catalysts.

EXPERIMENTAL PROCEDURE

The montmorillonite was supplied by Pembina Mountain Clays, Ltd., Manitoba. X-ray diffraction patterns showed no crystalline impurities in measurable amounts. The raw clay was ground to 80% −200 mesh and stored in airtight glass containers until used. Separate batches were used in the wet and dry activation experiments. The water content of the raw clay was determined by drying specimens at 110° C, and allowance was made for this adsorbed water in calculating the quantities of water and acid required by the activation procedure.

To activate by the wet method, 100 g (110° C dry basis) of clay was mixed with weighed amounts of 98% reagent grade sulphuric acid corresponding to 0 to 50% of the clay by weight, and sufficient water, including the water adsorbed by the clay, to bring the total liquid content to 400 g. This mixture was refluxed at 100° C for 6 hours with mechanical stirring. The product was filtered and washed to a pH of 3.0–3.5, at which point the washings were in all instances free of sulphate ion. The liquor and washings were recovered for analysis. The filter cake was dried overnight at 90° C and reground to −80 mesh. The fraction with particle sizes in the −80 to 100 mesh range was retained for surface area determinations.

The clay designated by the number 7A was subjected to two 50% acid leaches each of 6-hour duration, while clay 7B was leached three times in a similar manner.

To activate by the dry method, 454 g of clay (110° C dry basis) was mixed in a small muller for 30 minutes with 0–50% acid based on the dry clay and sufficient water to bring the total liquid content to 454 ml. After mixing, a 100- to 200-g portion was heated for 4 hours at 150° C in a drying oven, mixed with water while hot, filtered, and washed to a pH of 3.0–3.2. Subsequent treatment was identical with that of the wet activated clays. Since there was no means of determining weight changes during the mulling operation, the washings were not recovered for analysis.

The bleaching power of the activated clays was determined by adding 1 g of clay (−200 mesh material equilibrated overnight in a moisture cabinet) to 33 g of a semi-finished test oil kindly supplied by Imperial Oil Limited. The mixture was stirred mechanically while the temperature was increased in 5 to 7 minutes to 142° C. After cooling in air to 100° C, the oil was filtered and the percentage of transmittance measured in a Lumetron colorimeter equipped with red (6500 Å), green (5300 Å), and blue (4200 Å) filters. All transmissions were determined relative to Stanolax, a water-white medicinal oil produced by Standard Oil of Indiana.

Conventional procedures were used in analyzing the clays.* An estimate of "hydrated silica" was included in the analysis, although the precise significance of the determination is problematical. The difference in solubility of crystalline and amorphous silica in weak sodium carbonate solution, established by Lunge and Millberg (15), has been made the basis of several procedures for estimating the degree of chemical decomposition of clay minerals (9, 16). The fraction of the silica in the clay which dissolves in a sodium carbonate solution under certain conditions is defined as "hydrated silica" and presumably represents the amorphous silica contained in the mineral. Since the conditions are essentially empirical, the details of the method used in these analyses are given below.†

The activated clays were calcined *in vacuo* at 600°±5° C. Approximately 30 minutes

**The major components, viz.* SiO_2, Al_2O_3, MgO, *and* CaO, *were determined by the conventional gravimetric and volumetric procedures appropriate to samples of this nature (11, 12).* Na_2O *and* K_2O *were determined by flame photometry using methods adapted from well-established techniques for siliceous materials (13). The determination of sulphate ion was complicated by the presence in these samples of silicon and iron. The determination was made, finally, by a method based on the chromatographic separation of the sulphate ion from perchloric acid solution according to Nydahl (14).*

†To estimate "hydrated silica" content, 1.000±0.001 g of clay and 2.00 g Na_2CO_3 *were weighed into a stainless steel beaker. 100 ml of water was added and the solution heated to boiling within 6 minutes. Boiling was continued for 10 minutes, and the steel beaker was then removed from the heat. After settling for 4 minutes, the clear liquid was decanted into a filter of paper pulp supported on a perforated steel filter plate. The filter was sucked dry. 25 ml of 2% w/v hot solution of* Na_2CO_3 *was added and the liquid boiled for 2 minutes. After settling for 4 minutes, the clear liquid was again decanted into the filter funnel which was again sucked dry. This was repeated once more with a further 25-ml portion of* Na_2CO_3 *solution. 25 ml of hot 2% w/v* NaCl *solution was then added to the residue in the steel beaker, and the suspension poured into the filter funnel. Another 25 ml of hot* NaCl *solution was used to rinse the beaker and this too was added to the filter funnel when it had sucked dry. The filtrate was made up to 500 ml and a 5-ml aliquot taken for the determination of silica by the usual colorimetric method using ammonium molybdate and reading the yellow color developed on a filter photometer.*

were required to bring the sample to temperature if "boiling" was to be avoided, and the total heating time was 2.5 hours. The volatile products were collected in a liquid nitrogen cooled trap. Loss in weight was determined, and the volatile products examined qualitatively.

Nitrogen sorption isotherms were determined in a volumetric system in the usual manner. Water adsorption isotherms to 94% of saturation at 25° C were determined gravimetrically using Worden quartz springs of 2 g maximum capacity and 100 mg/cm sensitivity. The water vapor pressure in the system was controlled by a liquid water reservoir maintained at constant temperatures between −19° and 25° C. The clay samples were brought to constant weight in the system by repeated sorption/evacuation cycles before determination of the isotherm was begun.

RESULTS AND DISCUSSION

1. *Analyses*

For convenience, the activated clays have been designated W-1, W-2, . . . , W-6, the wet activated series, with 0%, 10%, . . . , 50% acid, and D-1, D-2, . . . , D-6, the dry activated series, with comparable acid concentrations. Clays W-1 and D-1 constitute "blanks", and represent the products obtained by the leaching process in the absence of sulphuric acid. As mentioned earlier, clays D-7A and D-7B were the products of two and three consecutive 50% acid leaches, respectively.

TABLE I

Analysis of activated clays

Basis, clay dried at 105° C; ignition temperature, 950° C. Series W, wet activated; series D, dry activated

Clay No.	% H_2SO_4 in activation	Ignition loss, %	$SO_4^{=}$, %	H_2O, %	SiO_2, %	Fe_2O_3, %	Al_2O_3, %	MgO, %	CaO, %	Na_2O, %	K_2O, %	Hydrated silica, %
Raw clay	—	8.86	3.66	5.81	61.30	3.82	19.59	4.36	0.97	0.16	0.15	0.58
W-1	0	9.46	2.07	7.74	60.85	3.53	20.31	4.62	1.02	0.40	0.14	0.60
W-2	10	8.90	1.11	7.98	63.21	3.02	20.24	4.22	—	—	—	0.82
W-3	20	8.52	0.64	7.99	64.08	2.66	20.00	4.66	0.38	0.26	0.07	1.66
W-4	30	8.15	0.35	7.86	66.40	1.85	19.44	4.89	—	—	—	3.16
W-5	40	7.85	0.12	7.75	68.08	1.42	18.40	4.76	0.36	0.02	0.04	4.98
W-6	50	7.92	0.50	7.49	70.62	1.25	16.75	3.38	—	—	—	8.35
W-7A	2×50	6.76	1.46	5.54	80.93	0.82	9.53	1.67	—	—	—	22.1
W-7B	3×50	5.56	1.07	4.67	88.18	0.48	4.53	0.56	—	—	—	28.8
D-1	0	7.94	2.69	5.70	64.21	3.58	18.92	4.36	0.97	0.61	0.16	0.81
D-2	10	7.92	1.14	6.98	65.82	2.94	18.89	4.07	—	—	—	1.84
D-3	20	7.20	1.41	6.03	69.57	1.88	17.48	3.79	0.16	0.04	0.09	5.05
D-4	30	6.64	1.45	5.43	71.27	1.47	17.73	3.30	—	—	—	9.98
D-5	40	6.30	0.55	5.85	75.02	1.30	14.02	2.82	0.20	0.05	0.05	15.0
D-6	50	6.27	0.68	5.71	77.81	1.26	11.80	2.23	0.22	0.04	0.06	16.0

The analyses of the activated clays are given in Table I, and the analyses of the wet activation leach liquors in Table II. To be comparative, these quantities must be reduced with reference to some invariant component to a common basis. It will be seen in Table II that the dissolution of silica during the wet activation process is less than 0.7% of the total silica, and can be regarded as negligible. Similarly, semiquantitative estimates of the silica removed from the clay by the dry activation process were of the same order of magnitude. The assumption can be made, therefore, that the silica content of the clays is a constant for each series, and the analyses can be expressed in terms of the "blanks", W-1 and D-1. The residual compositions calculated on this basis are recorded in Table III.

TABLE II

Analysis of wet activation liquor
Basis: clay as activated, 110° C dry

Clay No.	SiO_2, %	Fe_2O_3, %	Al_2O_3, %	MgO, %	CaO, %
W-1	0.07	0.03	0.10	0.11	0.22
W-2	0.38	0.50	1.23	0.41	0.68
W-3	0.31	1.03	2.15	0.53	0.76
W-4	0.37	1.79	3.36	0.78	0.84
W-5	0.25	1.70	5.28	1.05	0.84
W-6	0.34	2.12	7.21	1.46	0.86
W-7A	0.34	2.33	13.85	2.71	0.94
W-7B	0.43	2.52	17.55	3.45	0.96

TABLE III

Residual composition of activated clays
Assumption: No silica removed by activation process

	(1)	(2)	(3) Fe_2O_3		(4) Al_2O_3		(5) MgO		(6)	(7)
Clay No.	$SO_4^{=}$, g	H_2O, g	g	% rem.*	g	% rem.*	g	% rem.*	$M^{2+, 3+}$, % rem.†	Hydrated SiO_2, g
					Wet activated clays					
					Basis, 100 g clay W-1; SiO_2 content, 60.85 g					
W-1	2.07	7.74	3.53		20.31		4.62			0.60
W-2	1.07	7.68	2.91	(82.6)	19.49	(96.0)	4.06	(87.9)	(93.2)	0.79
W-3	0.61	7.58	2.53	(71.8)	18.99	(93.5)	4.43	(95.9)	(92.2)	1.57
W-4	0.32	7.20	1.70	(48.3)	17.81	(87.7)	4.48	(97.0)	(86.4)	2.90
W-5	0.11	6.93	1.27	(36.1)	16.44	(81.0)	4.25	(92.0)	(79.6)	4.45
W-6	0.43	6.45	1.08	(30.7)	14.43	(71.1)	2.91	(63.0)	(66.3)	7.20
W-7A	1.10	4.17	0.62	(17.6)	7.17	(35.3)	1.26	(27.3)	(32.4)	16.6
W-7B	0.74	3.22	0.33	(9.4)	3.13	(15.4)	0.39	(8.4)	(13.4)	19.9
					Dry activated clays					
					Basis, 100 g clay D-1; SiO_2 content, 64.21 g					
D-1	2.69	5.70	3.58		18.92		4.36			0.81
D-2	1.11	6.81	2.87	(80.2)	18.43	(97.4)	3.97	(91.1)	(94.7)	1.79
D-3	1.30	5.57	1.74	(48.6)	16.13	(85.2)	3.50	(80.3)	(81.1)	4.66
D-4	1.31	4.89	1.32	(36.9)	15.97	(84.4)	2.97	(68.1)	(77.3)	8.99
D-5	0.47	5.00	1.11	(31.0)	11.20	(59.2)	2.41	(55.2)	(56.1)	12.8
D-6	0.56	4.71	1.04	(29.0)	9.74	(51.5)	1.84	(42.2)	(47.8)	13.2

*Percentage of component remaining in the clay.
†Percentage of metal ions remaining in the clay.

Summations of the quantities of the various components found in the leach liquor and the clay residues are consistent within the limits of uncertainty in analysis and homogeneity of the clay samples.

The sulphate contents (Table III, column 2), particularly of the blanks and the dry activated clays, are abnormally large. Indeed, during the calcining of these clays, SO_2 as well as water was recovered in the gaseous products. In the montmorillonite deposit from which the raw clay was obtained, the clay strata are bounded by sulphide bearing deposits. It is generally accepted that the sulphates produced by natural oxidation of the sulphides and carried in solution into the clay deposits dissolve metal ions and produce, *in situ*, a semiactivated clay. Consequently an appreciable sulphate content in the raw clay is to be expected. The refluxing and washing operations which produced clays W-1 and D-1 might be expected to remove essentially all of the metal sulphates which might

be present with the exception of $CaSO_4$. Now if most of the sulphur in these clays is present as $CaSO_4$, appreciable quantities of SO_2 would not be produced on heating *in vacuo* at 600° C. It appears logical to propose that some sulphate ions are associated with the montmorillonite lattice itself, and this suggestion is substantiated by the relatively high sulphate content of clays W-7A and W-7B.

The natural leaching of these clays is responsible for the variation in composition from batch to batch. The difference in composition of clays W-1 and D-1 is unfortunate, but not significant in what follows.

Metal ions are removed by the activation process, but in these clays the fractions dissolved are not in proportion to the quantities present in the unactivated clays. Iron is removed to a much greater extent than aluminum or magnesium, while aluminum is the least removed of the three. It may be that the concentration of iron (and, to a lesser extent, magnesium) in the octahedral sites is greater near the surfaces of the particles than in the bulk of the crystal.

For a given acid dosage, the metal ions are removed to a greater extent by dry activation than by wet activation (Table III, column 6). However, a more notable variation in the two series is the greater "hydrated silica" content of the dry activated clays (Table III, column 7), even though the constitutional water content is consistently less than that of the wet activated clays. In view of the rather arbitrary nature of the quantity, it is rather doubtful that any structural argument explaining the difference could be supported.

The decolorizing capacities of the activated clays are recorded in Table IV. The results

TABLE IV

Decolorizing characteristics of activated montmorillonite
Transmissions relative to Stanolax. Red, 6500 Å;
green, 5300 Å; blue, 4200 Å

Wet activated				Dry activated			
Clay No.	% transmission			Clay No.	% transmission		
	Red	Green	Blue		Red	Green	Blue
W-1	91.5	67.3	25.8	D-1	90.5	65.5	25.0
W-2	95.0	75.0	32.0	D-2	95.0	78.3	36.3
W-3	98.0	87.0	46.0	D-3	99.0	92.0	54.5
W-4	99.7	91.8	52.5	D-4	99.5	94.0	58.5
W-5	100	95.8	61.0	D-5	99.0	94.0	58.0
W-6	100	96.5	61.4	D-6	99.0	93.3	55.3
W-7A	100	97.5	65.0				
W-7B	99.0	89.0	45.3				
S*	100	94.0	55.5	S*	99.0	92.5	54.0

*Control using the commercial decolorizing agent Superfiltrol.

are consistent with the conclusions drawn by Farnand and Peterson (17) based on the examination of a great number of activated clays obtained under a wide variety of experimental conditions: Dry activated clays produced with 0 to 35% acid are more efficient bleaching agents than are wet activated clays obtained with comparable acid dosages. Above 40% acid dosages, the capacity of the dry activated clays decreases and in the 35–50% region dry activated clays are inferior to wet activated clays. The maximum in decolorizing capacity of wet activated clays occurs at acid dosages in excess of 50%; nevertheless, a dry activated clay obtained with 20% acid is equivalent in capacity to a wet activated clay obtained with 30% acid.

2. Sorption Isotherms

Typical nitrogen sorption isotherms are reproduced in Fig. 1, and typical water sorption isotherms in Figs. 2 and 3.

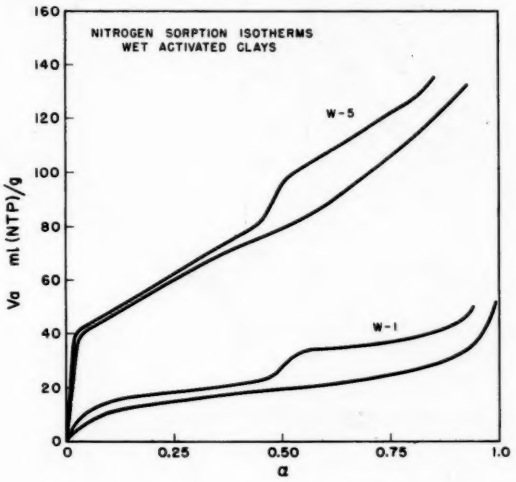

FIG. 1. Typical nitrogen sorption isotherms, wet activated clays.

The water isotherms are of characteristic form, although we could detect no inflections normally attributed to the completion of one and two water layers in the interlaminar region of the lattice. The curves were reproducible, although it should be reiterated that these isotherms were determined only after constant clay weight had been obtained by adsorption/evacuation cycles. The D-1 and W-1 isotherms are essentially identical. For strict comparison, the isotherms of the activated clays W-6 and D-6 should lie some 10% closer to the abscissa since the experimental data are expressed in terms of the product rather than the unactivated clay; nevertheless the decreased adsorption at low relative pressures and increased adsorption near saturation is quite evident. On the other hand, the adsorption capacity of the clay with respect to nitrogen is increased at all relative pressures by activation.

The hysteresis exhibited in the nitrogen isotherms is not uncommon among montmorillonites, but is not always observed. The "break" in the desorption loop was observed at relative pressures between 0.43 and 0.53 in all of the clays for which complete isotherms were obtained.

On calcining the clays at 600° C, the water isotherms are altered as shown in Fig. 4, and become quite similar in form to the nitrogen isotherms of the uncalcined clays. Since the calcined clays can no longer sorb water in the interlaminar regions, adsorption can occur only on surfaces which are also available for nitrogen adsorption, and the similarity in isotherms is to be expected. Presumably these isotherms are inherent in the water isotherms of the uncalcined clays, but are masked by the greater volumes adsorbed in the interlaminar spaces.

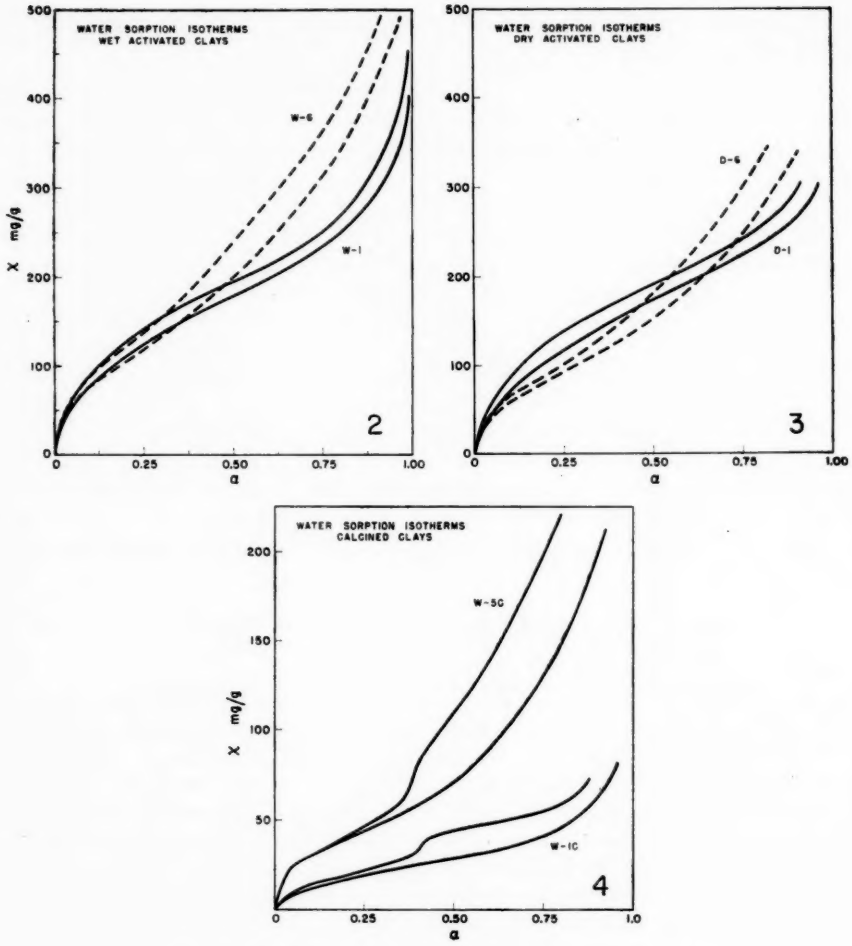

FIG. 2. Typical water sorption isotherms, wet activated clays.
FIG. 3. Typical water sorption isotherms, dry activated clays.
FIG. 4. Typical water sorption isotherms, calcined clays.

3. B.E.T. Surface Areas

The classical B.E.T. function has been applied to the desorption arms of the nitrogen and water isotherms as indicated in Fig. 5. The results are compiled in Tables V and VI. Again these data have been expressed in terms of the common denominators W-1 and D-1 on the assumption that the loss of SiO_2 from the lattice has been negligible.

A comparison of surface areas as a function of acid dosage is given in Fig. 6. Water surface areas decrease with increasing acid dosage more rapidly for the dry activated clays. The initial increase in nitrogen area is greater for the dry activated clays, but the

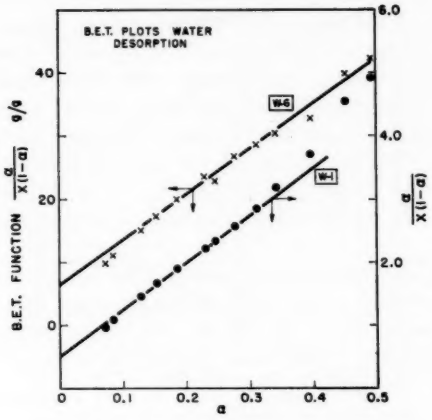

FIG. 5. Typical B.E.T. plots obtained from desorption isotherms.

TABLE V

B.E.T. nitrogen and water surface areas, wet and dry activated clays

Clay No.	N_2, m^2/g	H_2O, m^2/g	Area relative to W-1: N_2, m^2/g W-1	Area relative to W-1: H_2O, m^2/g W-1
W-1	60	454	60	454
W-2	94	—	90	—
W-3	138	444	132	426
W-4	205	492	188	451
W-5	225	—	201	—
W-6	269	467	231	402
W-7A	367	296	276	223
W-7B	366	238	253	164

Clay No.	N_2, m^2/g	H_2O, m^2/g	Area relative to D-1: N_2, m^2/g D-1	Area relative to D-1: H_2O, m^2/g D-1
D-1	61	444	61	444
D-2	110	425	107	415
D-3	185	393	171	363
D-4	215	391	193	352
D-5	229	—	196	—
D-6	239	352	197	290

areas of the wet activated clays are greater at high acid dosage. Maximum areas are attained at 33% and >50% acid for the dry and wet procedures, respectively.

The decolorizing capacity of each series as a function of nitrogen area is illustrated in Fig. 7. For areas below 220 m^2/g the bleaching capacity appears to be a function of area alone; however, above this point the capacity of the dry activated clays decreases. The corresponding decrease in wet activated clay capacity occurs at ca. 360 m^2/g.

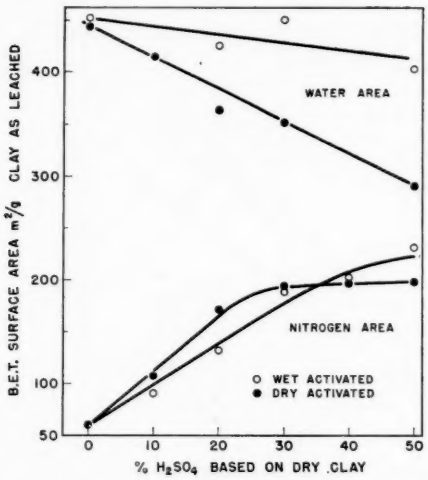

FIG. 6. B.E.T. water and nitrogen surface areas of wet and dry activated clays as a function of acid dosage.

TABLE VI

B.E.T. nitrogen and water surface areas, calcined clays

Clay No.	Weight loss, %	N_2, m^2/g	H_2O, m^2/g	Areas relative to W-1 and D-1	
				N_2, m^2/g	H_2O, m^2/g
W-1C	8.7	46	76	50	83
W-3C	7.7	97	98	100	101
W-5C	7.5	181	150	175	145
W-6C	—	240	—	—	—
W-7AC	—	367	—	—	—
W-7BC	4.6	360	—	259	—
D-1C	9.3	56	78	62	86
D-3C	7.3	154	124	153	123
D-5C	6.3	203	160	179	141

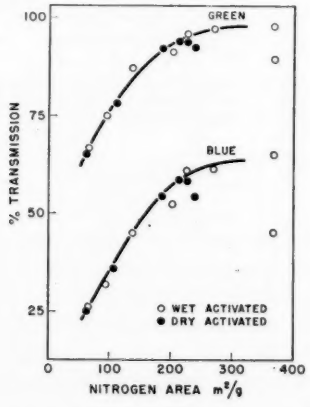

FIG. 7. Bleaching capacity of wet and dry activated clays as a function of nitrogen surface area.

It has been observed (17) that decolorizing capacity is a function of adsorbed water content. In general, the capacity increases with increasing water content, with the upper limit dictated by the degree of frothing of the oil/clay mixture which can be tolerated during bleaching. One might reasonably assume that adsorption of color bodies occurs on the interlaminar faces of the clay, and that water is required to expand the lattice and facilitate penetration by the color groups. However, since the capacity is a function of the nitrogen surface area rather than the water surface area, the interlaminar areas appear to be relatively unimportant. It may be that the adsorbed water is responsible for a modification in the silicate surface which facilitates the chemisorption of the color groups in the oil.

The reduction in nitrogen surface areas on calcining is less than 30%, but water surface areas decrease from ca. 400 m^2/g to values equal to or less than the nitrogen areas. Insofar as comparison of the two activation processes are concerned, the calcined dry activated clays exhibit higher surface areas, particularly at intermediate acid dosages.

4. Surface Areas and Structure

On the basis of the analysis, the quasi-unit cell of clay W-1 contains

$$Si_8^{IV}(Al_{3.2}Fe_{0.3}Mg_{0.9})^{VI}O_{20}(OH)_4(SO_4)_{0.2}\,.$$

Assuming the dimensions of this cell are $5\times10\times10$ Å, the interlaminar area is approximately 410 m^2/g. The observed water surface area is 454 m^2/g, and the nitrogen area 60 m^2/g. According to Mooney, Keenan, and Wood, the interlaminar area is the difference in these two values, i.e. 393 m^2/g. In this argument it is implied that the external surface is indifferent to both nitrogen and water vapor, and the B.E.T. external surface areas are identical for both adsorbates.

The disintegration of the montmorillonite lattice on leaching can be considered in the following way. For the model clay particle illustrated in Fig. 8, we shall assume p silicate

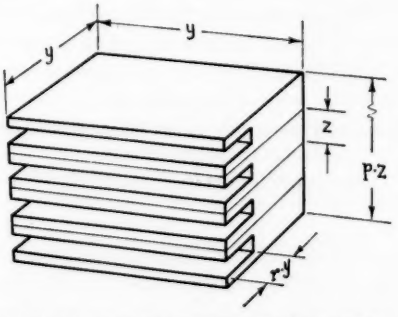

FIG. 8. Model activated montmorillonite particle.

laminae z Å thick, and y Å in length and width. If n is the number of such particles per gram of clay, the density, ρ, in grams per cubic angstrom, is given by

$$\rho = 1/npzy^2. \qquad [1]$$

When the lattice is attacked by acid, metal ions in the intralaminar octahedral sites are removed. This can be represented in an idealized manner as indicated in Fig. 8; the increase in nitrogen area per gram, ΔA_N, is given by

$$\Delta A_N = nmpry^2 \qquad [2]$$

in which r is the fraction of metal ions removed from the lattice, and m is the number of layers of nitrogen which can be accommodated in the intralaminar pores, and can have the values $1 \leqslant m \leqslant 2$.

Substituting for n in eq. 2 in terms of eq. 1,

$$\Delta A_N = mr/\rho z (\text{Å}^2/\text{g}). \quad [3]$$

Assuming a lattice dimension z of 10 Å, and a density of 2.5 g/cc,

$$\Delta A_N = 400mr \ (\text{m}^2/\text{g}). \quad [4]$$

This expression can be obtained simply by extension of the interlaminar water area argument given earlier, but the development from the model shows that the increase in nitrogen area is quite independent of particle size and shape. Unfortunately it is not likely that m will be independent of r. For low values of r, that is, when the lattice is not seriously attacked, the intralaminar pores will likely admit only one layer of nitrogen which will be adsorbed by both upper and lower silica surfaces. For intermediate values of r, the silica layers may be distorted to such an extent that almost two layers can be admitted. For higher values of r, the silica lattice may be expected to collapse on itself, and m will decrease. When the metal ions have been removed to such an extent that the montmorillonite lattice can not be considered to exist, the model and the equation will not apply.

There is reason to suspect that clays W-1 and D-1 have already been subjected to natural leaching processes, because of their high sulphate content and high nitrogen surface areas. Most natural montmorillonites exhibit nitrogen areas of 10 to 30 m^2/g, although some hydrogen montmorillonites may have areas of 40 m^2/g. Assuming that clays W-1 and D-1 would exhibit areas of 30 m^2/g had natural leaching not occurred, and assuming m is unity, then by eq. 4, r equals 0.075, and 0.925 of metal ions are still retained in the lattice. The fraction of metal ions remaining in the artificially activated clays can then be obtained directly using the analyses in Table III, column 6, and the increase in area to be expected calculated using eq. 4. The results are given in Table VII.

TABLE VII

Observed and calculated nitrogen area increments equation 4
(areas in m^2/g)
Assumption: r for W-1, D-1 = 0.075

Clay No.	$1-r$	r	$\Delta A_{N\ calc}$	$\Delta A_{N\ obs}$	Clay No.	$1-r$	r	$\Delta A_{N\ calc}$	$\Delta A_{N\ obs}$
W-1	0.925	0.075	30	30	D-1	0.925	0.075	30	30
W-2	0.86	0.14	56	60	D-2	0.875	0.125	50	67
W-3	0.85	0.15	60	102	D-3	0.75	0.25	100	141
W-4	0.80	0.20	80	158	D-4	0.715	0.285	114	163
W-5	0.74	0.26	104	170	D-5	0.52	0.48	192	166
W-6	0.61	0.39	156	200	D-6	0.44	0.56	224	167
W-7A	0.30	0.70	280	246					
W-7B	0.12	0.88	350	223					

In spite of the simplicity of the model, the agreement in observed and calculated nitrogen area increments is satisfactory. In no instance is ΔA_N observed greater than twice ΔA_N calculated, and consequently the discrepancies are within the limits of m. For the wet activated clays, m attains a maximum value of 1.98 at W-4 (30% acid, 20% ion

removal); beyond this point the silicate layers appear to collapse reducing the value of m. For clays W-7A and W-7B the clay lattice is destroyed to the extent that the equation is no longer tenable. In the dry activated series, the maximum value of m is only 1.4, and the collapse of the lattice begins at slightly lower acid concentrations. For clay D-6 (50% acid) the model is not valid.

As metal ions are removed, the water sorbed in the interlaminar spaces will decrease, particularly if they are associated with the exchangeable ions in the formation of hydrates. The interlaminar area can then be estimated by multiplying the idealized interlaminar area, 410 m²/g, by the factor $(1-r)$. The total water surface area should then be the sum of this area plus the nitrogen surface area of the sample. The results of the approximation are given in Table VIII.

TABLE VIII

Observed and calculated water areas
(areas in m²/g)

Clay No.	$410(1-r)$	A_{N_2}	$A_{H_2O\ calc}$	$A_{H_2O\ obs}$	Clay No.	$410(1-r)$	A_{N_2}	$A_{H_2O\ calc}$	$A_{H_2O\ obs}$
W-1	380	60	440	454	D-1	380	61	441	444
W-2	352	90	442	—	D-2	358	107	465	415
W-3	349	132	481	426	D-3	307	171	478	363
W-4	328	188	516	451	D-4	293	193	486	352
W-5	304	201	505	—	D-5	213	196	409	—
W-6	250	231	481	402	D-6	180	197	377	290
W-7A	123	276	399	223					
W-7B	48	253	301	164					

With the exception of W-1 and D-1, the agreement is poor, particularly for heavily leached samples. The major source of error may lie in the equation of water and nitrogen external surface areas. For clays W-7A, W-7B, and the calcined clays W-5C, D-3C, and D-5C, the observed total water areas are less than the observed nitrogen areas. In all of these samples the interlaminar adsorption will be negligible; hence it appears that the external water areas are less than the nitrogen areas by a factor of 0.67 to 0.80. For clays with relatively low nitrogen areas the correction is small; but the subtraction of nitrogen areas from total water areas as a measure of the interlaminar area of activated clays is not generally valid unless some correction factor is introduced.

5. Summary

1. In this particular montmorillonite, metal ions in octahedral sites are not removed by acid activation in the proportions in which they are originally present. On both wet and dry activation, the rates of removal are in the order Fe > Mg > Al.

2. At any given acid dosage, the extent of removal of metal ions, the formation of "hydrated silica", and the general degradation of the lattice is greater by the dry process than by the wet process.

3. The bleaching capacity with respect to mineral oil is a function of nitrogen surface area up to 220 m²/g for dry activated clays, and 360 m²/g for wet activated clays.

4. The nitrogen areas and the bleaching capacities of clays activated with 30% acid by the dry process are superior to the analogous wet activated clays.

5. On calcining, water isotherms become similar in form to nitrogen isotherms. Nitrogen areas are decreased slightly, water surface areas, drastically. At comparable acid dosages

surface areas of calcined dry activated clays are larger than the areas of calcined wet activated clays.

6. External silicate surfaces do not appear to give equivalent B.E.T. nitrogen and water surface areas.

7. According to the model presented, the montmorillonite lattice is essentially intact even after removal of 25% of the metal ions. With greater removal the residual silica layers collapse, and above 50% removal, the product no longer behaves as montmorillonite towards the adsorption of nitrogen and water vapor.

ACKNOWLEDGMENTS

We are indebted to Mr. A. E. McIlhinney and Mr. L. Pageau for assistance in the preparation of the dry activated clays, and for the determination of bleaching capacities.

REFERENCES

1. I. E. PUDDINGTON and J. R. FARNAND. Can. Patent No. 583,497 (1959).
2. C. H. EDELMAN and J. CH. L. FAVEJEE. Z. Krist. **100**, 417 (1940).
3. G. W. BRINDLEY. The X-ray identification and crystal structures of clay minerals. The Mineralogical Soc., London. 1951.
4. R. W. MOONEY, A. G. KEENAN, and L. A. WOOD. J. Am. Chem. Soc. **74**, 1367 (1952).
5. G. A. MILLS, J. HOLMES, and E. B. CORNELIUS. J. Phys. & Colloid Chem. **54**, 1170 (1950).
6. J. ESCARD. J. chim. phys. **51**, 638 (1954).
7. S. TEICHNER. Compt. rend. **227**, 392, 427 (1948).
8. W. T. GRANQUIST and G. G. SUMNER. Proceedings of the Sixth National Conference on Clays and Clay Minerals. Pergamon Press. 1959. p. 292.
9. J. DE D. LOPEZ-GONZALEZ and V. R. DEITZ. J. Research Natl. Bur. Standards, **48**, 325 (1952).
10. K. YAMAMOTO and Y. MORITA. J. Chem. Soc. Japan, Ind. Chem. Sect. **55**, 745 (1952).
11. Am. Soc. Testing Materials. Chemical analysis of refractory materials, Method C18–52. Book of Standards, Part 3. 1955.
12. W. F. HILDEBRAND, G. E. F. LUNDELL, H. A. BRIGHT, and J. I. HOFFMAN. Applied inorganic analysis. 2nd ed. John Wiley. 1953.
13. Am. Soc. Testing Materials. Spec. Tech. Publ. No. 116. 1952.
14. F. NYDAHL. Anal. Chem. **26**, 580 (1954).
15. G. LUNGE and C. MILLBERG. Z. angew. Chem. **393**, 425 (1897).
16. U.S.A. Dept. of the Interior, Geological Survey Professional Paper 205-B. Minerals of the montmorillonite group. Washington. 1945. p. 36.
17. J. R. FARNAND and W. S. PETERSON. National Research Council, Canada. Private communication.

NOTES

MOLECULAR COMPLEXES DERIVED FROM 1,3,6,8-TETRANITROPYRENE

P. M. G. BAVIN*

The low solubility and particularly the ready availability of 1,3,6,8-tetranitropyrene (I) (1) suggested its use as a complexing agent for the isolation of traces of polycyclic hydrocarbons. Molecular complexes are indeed formed (Table I) but are valueless for

TABLE I

Hydrocarbon	Complex	Solvent	Formula	Calculated (%) C	Calculated (%) H	Found (%) C	Found (%) H
Naphthalene	Crimson needles[e]	[a, b]	$C_{36}H_{22}N_4O_8$	67.71	3.47	67.77	3.84
Indole	Purple needles[e]	[a]	$C_{32}H_{20}N_6O_8$	62.34	3.27	63.91	2.92
Fluorene	Bright red needles[e]	[a]	$C_{29}H_{16}N_4O_8$	63.50	2.94	65.79	3.46
Carbazole	Dark blue needles	[a]	$C_{28}H_{15}N_5O_8$	61.20	2.75	61.36	2.84
Phenanthrene	Brick red needles[c, e]	[a]	$C_{30}H_{16}N_4O_8$	64.29	2.88	66.61	3.49
Anthracene	Very dark green needles	[a, b]	$C_{30}H_{16}N_4O_8$	64.29	2.88	64.96	2.98
9,10-Dimethylphenanthrene	Purple needles[d, e]	[a, b]	$C_{32}H_{20}N_4O_8$	65.30	3.43	63.73	3.66
Benz[a]anthracene	Olive-green needles	[a]	$C_{34}H_{18}H_4O_8$	66.88	2.97	67.54	3.05
Pyrene	Very dark green needles	[a, b]	$C_{32}H_{16}N_4O_8$	65.75	2.76	65.61	2.61
Benzidine	Black needles	[a]	$C_{28}H_{18}N_6O_8$	59.36	3.20	59.44	3.07
4,4″-Diamino-*p*-terphenyl	Black needles	[e]	$C_{34}H_{22}N_6O_8$	63.55	3.45	63.91	3.12

[a]Xylene. [b]Acetic acid. [c]M.p. 222–224° (decomp.), rapid heating in sealed capillary. [d]M.p. 262–264° (decomp.), rapid heating in sealed capillary. [e]Crystals decomposed by washing with fresh solvent.

purposes of characterization or isolation (except, perhaps, in the cases of benzidine and 4,4″-diamino-*p*-terphenyl), as their isolation in a crystalline state requires the presence of a large excess of the hydrocarbon. This may be due to the very low solubility of the tetranitropyrene which, in solution, is in equilibrium with hydrocarbon and complex:

$$\text{tetranitropyrene} + \text{hydrocarbon} \rightleftharpoons \text{complex.}$$

Whether complex or tetranitropyrene crystallizes from a given system depends on their relative solubilities and the position of the equilibrium.

Some of the crystalline complexes are decomposed by washing with fresh solvent. All of them can be recrystallized only in the presence of added hydrocarbon so that the microanalyses in Table I refer to crude preparations. Only naphthalene and indole form 2:1 complexes, the others being 1:1.

The complexes decompose when heated, only those of phenanthrene and 9,10-dimethylphenanthrene melting reasonably sharply. Indole and naphthalene sublime from their complexes below 100°; those of pyrene, anthracene, and benz[a]anthracene decompose above 320°.

*I.C.I. Fellow.

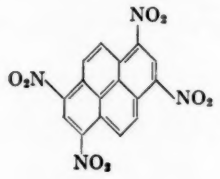

I

EXPERIMENTAL

Microanalyses are by Drs. Weiler and Strauss of Oxford.

Reagent

1,3,6,8-Tetranitropyrene was prepared as described in the literature (1). The hydrocarbons, etc. were mostly available samples but the author is indebted to I. Ungar for a very pure sample of carbazole and to Dr. D. Lewis for the 4,4″-diamino-*p*-terphenyl.

Preparation of the Complexes

Approximately 0.1 g tetranitropyrene was dissolved in the minimum of boiling xylene (occasionally acetic acid was used) and the volume increased by one-fourth to prevent crystallization. The hydrocarbon was added and the solution decanted from any impurities. The complexes slowly separated on cooling and were collected before crystallization of tetranitropyrene occurred. The crystals were sucked free of mother liquor, washed with fresh solvent (unless this decomposed them), and dried at 100° and 1–2 mm (40° in the cases of naphthalene and indole).

Some idea of the difficulties encountered in obtaining pure crystalline complexes may be gathered from the fact that almost 20 g naphthalene was necessary to obtain 0.1 g complex whereas little more than the theoretical amount of benzidine gave a good yield of complex.

Complex formation is largely dependent on the electron acceptor properties of the tetranitropyrene and the donor properties of the hydrocarbons. Consequently benzidine, which is a much stronger base than naphthalene, will form complexes more readily than the latter and should be more stable. The solubilities of the complexes will be determined primarily by their ionic character. Complexes with the amines would have more ionic character than those with polycyclic hydrocarbons and would therefore be less soluble in solvents such as xylene.

1. H. Vollmann, H. Becker, M. Corell, and H. Streeck. Ann. **531**, 1 (1937).

Received December 1, 1959.
Chemistry Department,
The University,
Hull, East Yorkshire, England.

O—H STRETCHING FREQUENCIES FOR SOME PHENOLS AND THEIR RELATIONSHIPS TO THE THERMODYNAMICS OF IONIZATION

William J. Canady

The O—H stretching frequencies of a large number of phenols have been studied by Ingraham, Corse, Bailey, and Stitt (1). The results were correlated with the Hammett

sigma values for these compounds. Some phenols were also studied by Stone and Thompson (2), Flett (3), and Brown (4).

Goulden (5) studied the O—H stretching frequencies of a large number of acid substances and found that they could be correlated with the pK values of the compounds in aqueous solution. The results showed that separate plots were obtained, depending upon the type of acid under consideration.

Bavin and Canady (6) demonstrated the same type of behavior with a number of phenols. It was shown that the failure to obtain a single plot with a number of substituted benzoic acids could not be ascribed to variations in electrostatic contributions, but was probably due to structural factors. No correlation was attempted with ortho constituents which could bring about appreciable hydrogen bonding.

Since the pK of an acid, and hence the free energy of ionization, may be related to the O—H stretching frequency, the question arises as to whether any similar relationships may exist for the changes in heat content and entropy of ionization.

At the time of the last-mentioned work, insufficient precise data were available to test this possibility. Recently, however, precise measurements of ΔH and ΔS for all of the mono- and dimethyl-substituted phenols have become available (7).

Table I shows the values for ΔF, ΔH, and ΔS as well as the O—H stretching frequencies for this series of phenols.

TABLE I

	Compound	ΔF (kcal)	ΔH (kcal)	ΔS cal/mole deg	Stretching frequency, cm^{-1}
1	Phenol	13.63	5.60	−27.0	3600
2	*d*-Cresol	14.03	7.13	−23.2	3606
3	*m*-Cresol	13.76	4.90	−30.7	3605
4	*p*-Cresol	14.00	4.23	−32.8	3604
5	2,3-Xylenol	14.14	6.61	−25.3	3608
6	2,4-Xylenol	14.29	7.68	−22.1	3610
7	2,5-Xylenol	13.90	6.22	−25.7	3606
8	2,6-Xylenol	14.46	4.95	−31.9	3618
9	3,4-Xylenol	13.86	8.24	−18.9	3605
10	3,5-Xylenol	13.67	7.51	−20.7	3602

The O—H stretching frequencies for the phenols are those of Bavin and Canady (6) and were measured in carbon disulphide. The instrument used was a Beckman DK-2. Since the frequencies measured are close to the cutoff point of the prism, resolution is very good.

The thermodynamical quantities are taken from the work of Papeé, Canady, Zawidzki, and Laidler (7).

The plot of stretching frequency vs. ΔF of ionization for phenol and methyl-substituted phenols can be seen in Fig. 1A. It may be noted that reasonably linear results are obtained.

Figures 1B and 1C show the O—H stretching frequencies plotted against ΔH and ΔS respectively for the phenols.

Figures 1B and 1C indicate that no particular relationship between stretching frequency and the heat and entropy of ionization can be demonstrated.

These findings tend to support the contention of Laidler (8), who has suggested that while the free energies of ionization of a particular series may be related to the vibrational frequencies involved, the effects on ΔH and ΔS are masked by solute–solvent interactions.

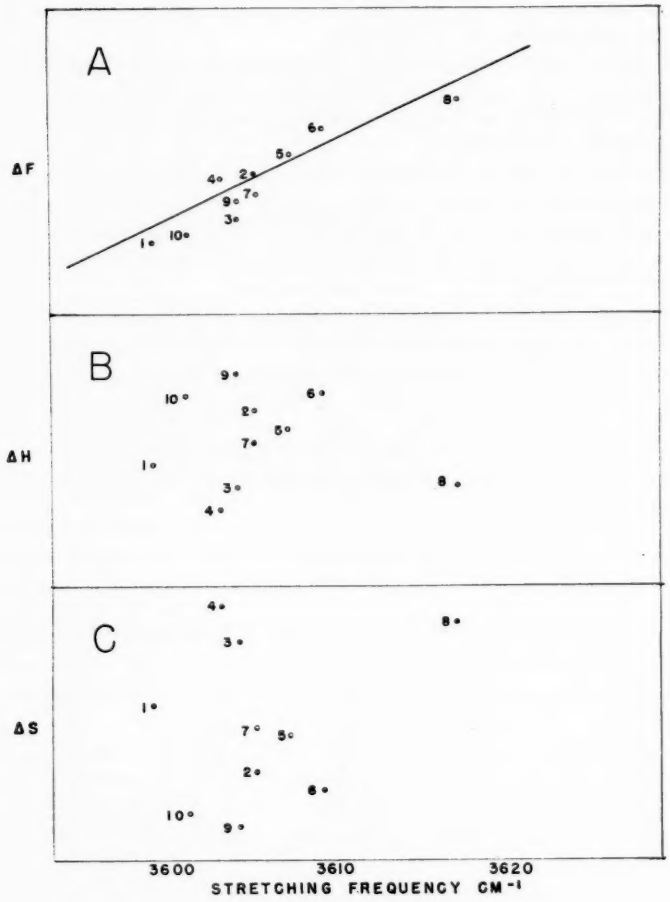

FIG. 1.

1. L. L. INGRAHAM, J. CORSE, G. F. BAILEY, and F. STITT. J. Am. Chem. Soc. **74**, 2297 (1952).
2. P. J. STONE and H. W. THOMPSON. Spectrochim. Acta, **10**, 17 (1957).
3. M. StC. FLETT. Spectrochim. Acta, **10**, 21 (1957).
4. T. L. BROWN. J. Phys. Chem. **61**, 820 (1957).
5. J. D. S. GOULDEN. Spectrochim. Acta, **6**, 129 (1953–54).
6. P. M. G. BAVIN and W. J. CANADY. Can. J. Chem. **35**, 1555 (1957).
7. H. M. PAPÉE, W. J. CANADY, T. W. ZAWIDZKI, and K. J. LAIDLER. Trans. Faraday Soc. **55**, 1734 (1959).
8. K. J. LAIDLER. Trans. Faraday Soc. **55**, 1725 (1959).

RECEIVED FEBRUARY 29, 1960.
DEPARTMENT OF BIOCHEMISTRY,
WEST VIRGINIA UNIVERSITY SCHOOL OF MEDICINE,
MORGANTOWN, WEST VIRGINIA,
U.S.A.

THE SYNTHESIS OF 10-SUBSTITUTED PHENOXAZINES

GERASSIMOS FRANGATOS, GEZA KOHAN, AND FRANCIS L. CHUBB

The recent publication by Muller, Buu Hoi, and Rips (1) describing the cyanoethylation of phenoxazine, and the issuing of a Belgian patent (2) describing the preparation of a series of 10-dialkylaminoalkyl phenoxazines, prompt us to report some work on the chemistry of phenoxazine, which has been in progress in these laboratories for some time. Dialkylaminoalkyl chlorides reacted with phenoxazine in the presence of freshly prepared sodamide to yield a series of 10-dialkylaminoalkyl phenoxazines which are listed in Table I. Some differences in the physical constants of these compounds from those reported by the Belgian workers are noted.

The addition of phenoxazine to acrylonitrile (1) and ethyl acrylate yielded 3-(10-phenoxazinyl)propionitrile (I) and ethyl 3-(10-phenoxazinyl)propionate (II) respectively and they were both hydrolyzed to 3-(10-phenoxazinyl)propionic acid (III). Lithium aluminum hydride reduction of II and III yielded 10-(3-hydroxypropyl)phenoxazine (IV). Attempts to prepare the corresponding chloride by treatment of IV with either thionyl chloride or phosphorus pentachloride only resulted in extensive polymerization. However, IV reacted smoothly with phosphorus tribromide to yield 10-(3-bromopropyl)phenoxazine (V). When V was allowed to react with 1-methylpiperazine, 10-(3-(3-methyl-1-piperazinyl)propyl)phenoxazine (VI) was formed.

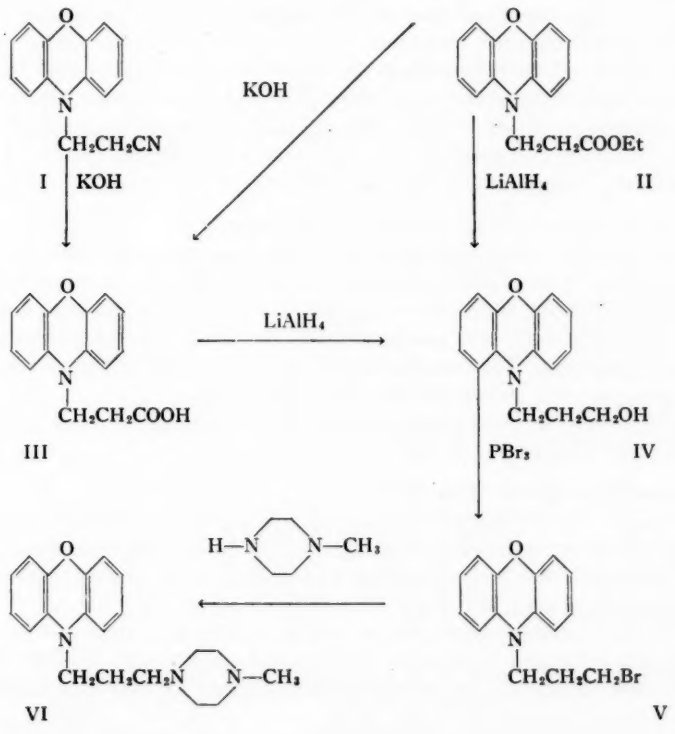

3-(10-Phenoxazinyl)propionic acid (III) underwent cyclization with phosphorus pentoxide to give a yellow ketone, assumed to be 2,3-dihydro-1H-pyrido(3,2,1-*kl*) phenoxazine-3-one (VII), m.p. 104–105°. Muller, Buu Hoi, and Rips have reported a melting point of 144° for this compound.

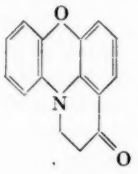

VII

EXPERIMENTAL

10-(3-Dimethylaminopropyl)phenoxazine

The procedure for the synthesis of 10-(3-dimethylaminopropyl)phenoxazine is a general one and has been followed for the synthesis of all 10-dialkylaminoalkyl phenoxazines listed in Table I.

A suspension of sodamide in 100 ml of xylene was prepared from 100 ml of liquid ammonia and 3.04 g of sodium according to the procedure of Hauser, Swamer, and Adams (3). To this stirred and refluxing mixture a solution of 22 g of phenoxazine in 150 ml of xylene was slowly added. During the addition the reaction mixture turned a greenish color. It was stirred and refluxed for another hour. To this mixture a solution of dimethylaminopropyl chloride (obtained from 19 g of the corresponding hydrochloride treated with 18 g of sodium hydroxide in 66 ml of H_2O and extracted with 75 ml of xylene and dried over sodium sulphate) was added. The reaction mixture thus obtained was stirred and refluxed for 6 hours. After this mixture was cooled and filtered, the xylene was distilled under reduced pressure. The oily residue was distilled *in vacuo*. Twenty-six grams (80.5%) of a yellow oil was obtained distilling at 178°/2 mm.

Addition of Phenoxazine to Ethyl Acrylate or Acrylonitrile

To a stirred and ice-cooled mixture of 20 g phenoxazine and 33 ml ethyl acrylate (or 50 ml acrylonitrile), 2 ml of 35% methanolic benzyltrimethylammonium hydroxide was added dropwise. After the addition was completed the reaction was heated overnight (or 1 hour) on the steam bath. The excess of ethyl acrylate (or acrylonitrile) was distilled under reduced pressure. The residual ethyl 3-(10-phenoxazinyl)propionate (II) was distilled *in vacuo* to yield 20.6 g (66.5%), b.p. 187°/1 mm.

The residual 3-(10-phenoxazinyl)propionitrile was recrystallized from aqueous ethanol to yield 19.5 g (72.9%), m.p. 121–122°.

3-(10-Phenoxazinyl)propionic Acid (III)

(*a*) A mixture of 4 g of 3-(10-phenoxazinyl)propionitrile, 4 g sodium hydroxide, 12 ml of water, and 40 ml of methanol was refluxed for 15 hours. The hydrolysis product was poured into ice water, acidified with dilute hydrochloric acid, filtered, and recrystallized from aqueous ethanol. 2.3 g of III was obtained, m.p. 136–138°.

(*b*) Ethyl-3-(10-phenoxazinyl)propionate (14.15 g, 0.05 mole) was dissolved in 300 ml of 10% ethanolic potassium hydroxide and refluxed for 2 hours. To this mixture after being cooled, 300 ml of water was added. The alcohol (300 ml) was distilled and the

TABLE I

10-Substituted phenoxazines

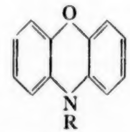

No.	R	Yield %	B.p.	M.p.	Carbon Calc.	Carbon Found	Hydrogen Calc.	Hydrogen Found	Nitrogen Calc.	Nitrogen Found
1	$(H_3C)_2NCH_2CH_2$	60.2	168°/2.5 mm[a]		75.54	75.75	7.08	7.01	11.02	11.11
2	$(H_3C)_2NCH_2CH_2CH_2$	80.5	178°/2 mm		76.07	75.80	7.46	7.75	10.44	10.59
3	$(H_5C_2)_2NCH_2CH_2$ hydrochloride	54.8		241–242°[b]	67.79	67.72	7.24	6.88	8.81	8.88
4	$(H_3C)_2NCH(CH_3)CH_2$	55.9	168°/2.5 mm		76.07	75.47	7.46	7.69	10.44	11.03
5	$H_5C_2OC(=O)—CH_2CH_2$	66.5	187°/1 mm[c]		72.08	71.73	6.00	5.98	4.95	5.07
6	$HOOCCH_2CH_2$	57		138°[d]	70.59	70.45	5.09	5.27	5.49	4.93
7	$HOCH_2CH_2CH_2$	65.5		68°[e]	74.68	74.76	6.22	6.49	5.81	5.79
8	$BrCH_2CH_2CH_2$	48		55°	59.21	59.00	4.60	4.62	4.60	4.73
9	$H_3C—N(CH_2CH_2)_2N—CH_2CH_2CH_2$	73.6		89–91°	74.30	74.08	7.73	7.96	13.16	12.98

[a]The hydrochloride has been reported to melt at 241° (7).
[b]Lit. value (2) 167–169°.
[c]Lit. value (2) 210°/2 mm.
[d]Lit. value (1) 138°.
[e]Only a boiling point of 200°/0.8 mm is reported (2).

remaining mixture was acidified with 6 *N* hydrochloric acid. 3-(10-Phenoxazinyl)propionic acid (III) precipitated and was recrystallized from aqueous ethanol; 7.3 g (57%) of the acid (III) was obtained melting at 137–138°.

10-(3-Hydroxypropyl)phenoxazine (IV)

A solution of 14 g of ethyl 3-(10-phenoxazinyl)propionate in 100 ml of ether was added slowly to a mixture of lithium aluminum hydride (2 g) in 100 ml of ether at such a rate as to maintain gentle refluxing. The reaction mixture was stirred and refluxed for 45 minutes. The excess hydride was destroyed with 2 ml of water. The reaction mixture was poured into ice water, acidified cautiously with 2 *N* sulphuric acid, and the ether layer was separated. The aqueous layer was saturated with ammonium sulphate and further extracted with ether. The combined ether extracts were washed with water and dried over sodium sulphate. The solvent was distilled and the residue recrystallized from a mixture of benzene ligroin. Eight grams (65.5%) of IV was obtained, m.p. 68°. 10-(3-Hydroxypropyl)phenoxazine was also obtained in a similar yield when 3-(10-phenoxazinyl)propionic acid (III) was reduced by lithium aluminum hydride in ether according to the procedure of Dahlbom (4) for the phenothiazine analogue.

10-(3-Bromopropyl)phenoxazine (V)

Freshly redistilled phosphorus tribromide (4.2 ml) was added to 15 g of 10-(3-hydroxypropyl)phenoxazine with cooling. The reaction mixture was heated on the steam bath for 1 hour and then poured onto crushed ice. The bromide (V) separated as an oil which solidified on standing overnight. It was filtered, washed with water on the filter, and after recrystallization from ethanol melted at 55–56°. The yield was 9 g (48%).

10-(3-(4-Methyl-1-piperazinyl)propyl)phenoxazine (VI)

A mixture of 9 g of 10-(3-bromopropyl)phenoxazine and 18 ml of 1-methylpiperazine was heated on the steam bath for 4 hours. Eighty milliliters of 10% sodium hydroxide solution was added to the reaction mixture which was then thoroughly extracted with ether. The ether extracts were combined and dried over Na_2SO_4. The ether was distilled and the residue was recrystallized from ligroin. Seven grams (73.6%) of VI was obtained, m.p. 89–91°.

2,3-Dihydro-1H-pyrido(3,2,1-kl)phenoxazine-3-one

The procedure of Smith (5) and Buu Hoi (6) for the phenothiazine and phenoselenazine analogue was followed in principle.

Fifty grams of phosphorus pentoxide was suspended in 200 ml of benzene and 10 g of 3-(10-phenoxazinyl)propionic acid was added to the stirred and heated reaction mixture. The mixture was stirred and refluxed for 1 hour and then left at room temperature overnight. It was filtered and the material remaining on the filter was washed thoroughly with an additional quantity (100 ml) of benzene. The benzene was removed from the filtrate by distillation and the residue was recrystallized from a minimum amount of ethanol; 4.5 g (48.4%) of a yellow ketone was obtained, m.p. 104°. Anal. for $C_{15}H_{11}NO_2$. Calc.: C, 75.95; H, 4.64; N, 5.91%. Found: C, 75.50; H, 4.68; N, 5.90%.

The corresponding semicarbazone was prepared and melted at 232°. Anal. for $C_{16}H_{14}N_4O_2$. Calc.: C, 65.3; H, 4.76%. Found: C, 65.13; H; 4.92%.

1. P. Muller, N. P. Buu Hoi, and R. Rips. J. Org. Chem. **24**, 1699 (1959).
2. Belg. Patent No. 569,697 (January, 1959): Chem. Abstr. **54**, 586 (1960).

3. C. R. HAUSER, F. W. SWAMER, and J. T. ADAMS. *In* Organic reactions. Vol. VIII. R. Adams. John Wiley & Sons Inc., New York. 1954. p. 122.
4. R. DAHLBOM. Acta Chem. Scand. **6**, 310 (1952).
5. N. L. SMITH. J. Org. Chem. **15**, 1125 (1950).
6. P. MULLER, N. P. BUU HOI, and R. RIPS. J. Org. Chem. **24**, 37 (1959).
7. U.S. PATENT No. 2,687,414 (August, 1954): Chem. Abstr. **50**, 1092 (1956).

RECEIVED FEBRUARY 8, 1960.
RESEARCH LABORATORIES,
FRANK W. HORNER LIMITED,
MONTREAL, QUE.

NOTES TO CONTRIBUTORS

Canadian Journal of Chemistry

MANUSCRIPTS

General.—Manuscripts, in English or French, should be typewritten, double spaced, on paper 8½×11 in. **The original and one copy are to be submitted.** Tables and captions for the figures should be placed at the end of the manuscript. Every sheet of the manuscript should be numbered. Style, arrangement, spelling, and abbreviations should conform to the usage of recent numbers of this journal. Greek letters or unusual signs should be written plainly or explained by marginal notes. Characters to be set in bold face type should be indicated by a wavy line below the characters. Superscripts and subscripts must be legible and carefully placed. Manuscripts and illustrations should be carefully checked before they are submitted. Authors will be charged for unnecessary deviations from the usual format and for changes made in the proof that are considered excessive or unnecessary.

Abstract.—An abstract of not more than about 200 words, indicating the scope of the work and the principal findings, is required, except in Notes.

References.—These should be designated in the text by a key number and listed at the end of the paper, with the number, in the order in which they are cited. The form of the citations should be that used in this journal; in references to papers in periodicals, titles should not be given and only initial page numbers are required. The names of periodicals should be abbreviated in the form given in the most recent *List of Periodicals Abstracted by Chemical Abstracts.* All citations should be checked with the original articles and each one referred to in the text by the key number.

Tables.—Tables should be numbered in roman numerals and each table referred to in the text. Titles should always be given but should be brief; column headings should be brief and descriptive matter in the tables confined to a minimum. Vertical rules should not be used. Numerous small tables should be avoided.

ILLUSTRATIONS

General.—All figures (including each figure of the plates) should be numbered consecutively from 1 up, in arabic figures, and each figure referred to in the text. The author's name, title of the paper, and figure number should be written in the lower left corner of the sheets on which the illustrations appear. Captions should not be written on the illustrations.

Line drawings.—Drawings should be carefully made with India ink on white drawing paper, blue tracing paper, or co-ordinate paper ruled in blue only; any co-ordinate lines that are to appear in the reproduction should be ruled in black ink. Paper ruled in green, yellow, or red should not be used. All lines must be of sufficient thickness to reproduce well. Decimal points, periods, and stippled dots must be solid black circles large enough to be reduced if necessary. Letters and numerals should be neatly made, preferably with a stencil (**do NOT use typewriting**), and be of such size that the smallest lettering will not be less than 1 mm high when the figure is reduced to a suitable size. Many drawings are made too large; originals should not be more than 2 or 3 times the size of the desired reproduction. Wherever possible two or more drawings should be grouped to reduce the number of cuts required. In such groups of drawings, or in large drawings, full use of the space available should be made; the ratio of height to width should conform to that of a journal page (5½×7⅞ in.) but allowance must be made for the captions. **The original drawings and one set of clear copies (e.g. small photographs) are to be submitted.**

Photographs.—Prints should be made on glossy paper, with strong contrasts. They should be trimmed so that essential features only are shown and mounted carefully, with rubber cement, on white cardboard, with no space between those arranged in groups. In mounting, full use of the space available should be made. **Photographs are to be submitted in duplicate; if they are to be reproduced in groups one set should be mounted, the duplicate set unmounted.**

REPRINTS

A total of 100 reprints of each paper, without covers, are supplied free. Additional reprints, with or without covers, may be purchased at the time of publication.

Charges for reprints are based on the number of printed pages, which may be calculated approximately by multiplying by 0.5 the number of manuscript pages (double-space typewritten sheets, 8½×11 in.) and including the space occupied by illustrations. Prices and instructions for ordering reprints are sent out with the galley proof.

Contents

Printed in Canada by University of Toronto Press